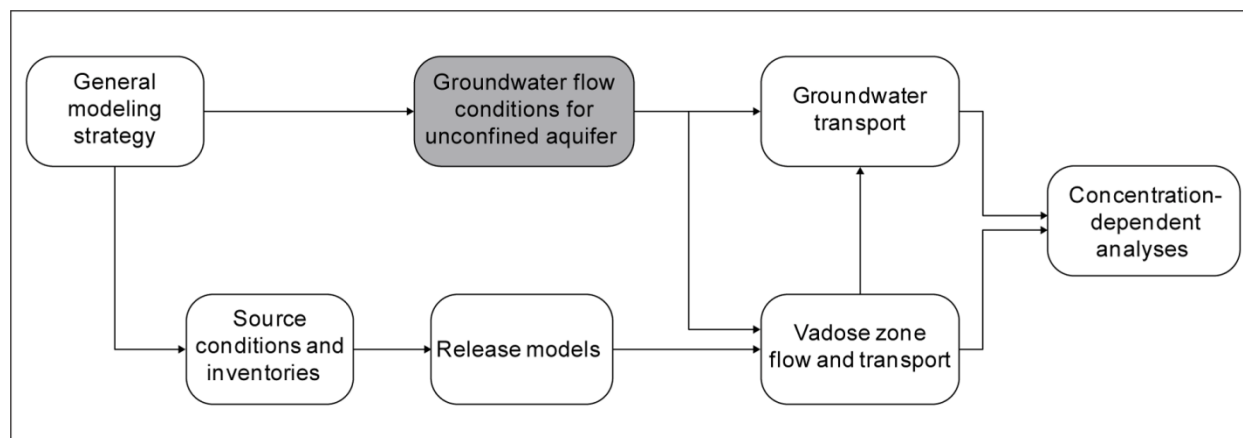# APPENDIX L
GROUNDWATER FLOW FIELD DEVELOPMENT

This appendix describes the development of the regional-scale groundwater flow field used for the groundwater modeling that supports assessment of the groundwater quality impacts discussed in the *Draft* and *Final Tank Closure and Waste Management Environmental Impact Statement for the Hanford Site, Richland, Washington (TC & WM EIS),* Chapters 5 and 6 and Appendices O and V. Included are an overview of groundwater flow at the site; the purpose and scope of the groundwater flow field development in the context of the overall groundwater modeling effort; changes in the groundwater flow field between the *Draft* and *Final TC & WM EIS*; model design variants to address uncertainty and sensitivity of the groundwater flow field; specifications of the model framework and inputs; the strategy and process of groundwater flow model calibration to head data; and sensitivity of the model to changes in input parameters. A thorough summary of the groundwater flow field results is also provided.

L.1 INTRODUCTION

This *Tank Closure and Waste Management Environmental Impact Statement for the Hanford Site, Richland, Washington (TC & WM EIS)* is being prepared in accordance with the National Environmental Policy Act (NEPA) of 1969, as amended (42 U.S.C. 4321 et seq.); U.S. Department of Energy (DOE) implementing procedures for NEPA (10 CFR 1021); and Council on Environmental Quality (CEQ) regulations for implementing the procedural provisions of NEPA (40 CFR 1500–1508). These regulations require that an environmental impact statement evaluate short- and long-term environmental impacts of the alternatives and the cumulative environmental impacts. This *TC & WM EIS* evaluates the impacts of Tank Closure, FFTF Decommissioning, and Waste Management alternatives on land resources, infrastructure, noise, air quality, geology and soils, water resources, ecological resources, cultural resources, socioeconomics (e.g., employment, regional demographics, housing and community services), public and occupational health and safety, environmental justice, and waste management activities. Contaminants in groundwater at the Hanford Site (Hanford) could potentially impact water resources, ecological resources, cultural resources, public health and safety, and environmental justice over the long term. In particular, the Columbia River and its associated ecological resources are highly valued resources that could be impacted by contaminants transported from Hanford through groundwater.

This *TC & WM EIS* quantifies impacts on the human and natural environment to the extent practicable, consistent with DOE's sliding-scale approach, taking into account available project information and design data. This approach to NEPA analysis implements CEQ's instruction to "focus on significant environmental issues and alternatives" (40 CFR 1502.1) and discuss impacts "in proportion to their significance" (40 CFR 1502.2(b)). This *TC & WM EIS* acknowledges uncertainty and incompleteness in the data and, where the uncertainty is significant or a major factor in understanding the impacts, explains how the uncertainty affects the analysis. Thus, this *TC & WM EIS* balances the dual goals of accuracy and comparability against the available information and the need for timely decisions.

Figure L–1 shows the components of the *TC & WM EIS* groundwater modeling system that was used to predict the long-term impacts on groundwater quality, human health, and ecological resources. This appendix specifically discusses the representation of the flow field used to support the long-term impact analyses. Topics discussed include the development of the flow field conceptualization, the groundwater flow observed at Hanford and predicted by the model, the model calibration process, and model sensitivities and uncertainties.

Figure L–1. Groundwater Modeling System Flowchart

L.1.1 Purpose

This appendix describes the development of a regional-scale groundwater flow field for Hanford. A groundwater flow field is a time-dependent, spatially varying representation of the direction and magnitude of groundwater flow. The Hanford groundwater flow field was critical to the evaluation and comparison of the potential long-term impacts of the *TC & WM EIS* alternatives, and evaluation of the long-term cumulative impacts on resources related to groundwater.

The groundwater flow field was calculated prior to simulation of contaminant transport in the vadose zone (the area of unsaturated soil and rock between the ground surface and the water table) and unconfined aquifer. The groundwater flow field provided the numerical representation of water table elevations and velocities that were necessary inputs to the vadose zone transport model, STOMP [Subsurface Transport Over Multiple Phases] (see Appendix N of this *TC & WM EIS*), and the saturated zone transport model (see Appendix O). A well-calibrated groundwater flow field provided connection and consistency between the vadose zone and saturated zone transport models that were used to evaluate alternative and cumulative impacts.

Three key criteria were considered in the development of the *TC & WM EIS* groundwater flow field based on NEPA requirements, as follows:

- The flow field must provide a basis for an unbiased evaluation of the impacts of the *TC & WM EIS* alternatives for the 10,000-year period of analysis (calendar years [CY] 1940–11,940).

- The flow field must provide a basis for understanding the *TC & WM EIS* alternatives in the context of cumulative impacts.

- The effects of uncertainties and gaps in input data (e.g., spatial distribution of well borings across the study area), modeling assumptions (e.g., conceptualization of the top of basalt [TOB] as a no-flow boundary), and numerical error (e.g., head and water balance residuals) must be evaluated and discussed.

This appendix describes how the *TC & WM EIS* groundwater flow field was developed to meet these requirements.

L.1.2 Scope

In describing the development of the *TC & WM EIS* groundwater flow field for Hanford, this appendix presents the following information:

- The fundamental features of the regional-scale flow field model specific to Hanford

- The data sources, data, and representation (encoding) of the data in the flow field model

- Model parameters and settings

- Algorithms selected for the model

- Calibration to existing water-level data and the results of calibration runs to check model sensitivity to varying boundary conditions

The model simulating the flow field for this *Final TC & WM EIS* was built by modifying the model used for the *Draft TC & WM EIS* groundwater analysis. Changes were made to the material types assigned in selected areas, and updates were made to the head observation data set.

L.1.3 Technical Guidance

The *Technical Guidance Document for Tank Closure Environmental Impact Statement Vadose Zone and Groundwater Revised Analyses (Technical Guidance Document)* (DOE 2005) specifies technical assumptions, model input parameters, and methods for proceeding with *TC & WM EIS* vadose zone and groundwater analyses. The technical bases supporting many of the assumptions result from various multiyear field- and science-based activities consistent with the Hanford Federal Facility Agreement and Consent Order, also known as the Tri-Party Agreement (Ecology, EPA, and DOE 1989); the Record of Decision for the *Tank Waste Remediation System, Hanford Site, Richland, Washington, Final Environmental Impact Statement (TWRS EIS)* (62 FR 8693); and the National Research Council's review of the *Draft TWRS EIS* (National Research Council 1996). This appendix indicates where design features or input data used in the development of the flow field are specified by the *Technical Guidance Document*.

The *Technical Guidance Document* specifies five key requirements for development of the *TC & WM EIS* groundwater flow field, as follows:

1. The flow field should be transient (i.e., change with time).

2. The factor driving the transient behavior should be operational recharge to the aquifer rather than time-changing boundary conditions.

3. The sitewide natural recharge rate should be 3.5 millimeters per year.

4. Both a Base Case and a Sensitivity (Alternate) Case should be investigated, and the difference between the two cases should take into account the uncertainty in the TOB elevation in the Gable Mountain–Gable Butte Gap (Gable Gap). The Sensitivity Case was presented in the *Draft TC & WM EIS* and is not presented again. Only the Base Case modifications and results are presented in this *Final TC & WM EIS*.

5. Flow field development should be consistent with the frameworks for vadose zone and contaminant transport modeling.

The *TC & WM EIS* groundwater flow model and simulated flow field meet these specifications.

L.1.4   Groundwater at the Hanford Site

Groundwater at Hanford is modeled on a regional scale. This regional-scaled approach results in, for analysis purposes, a single representation of the saturated zone beneath the site. This single representation requires some simplifying assumptions and does not allow for inclusion of all detailed site characterization data that may be available at particular areas of interest across the site. One example of a simplifying assumption used is that the Columbia and Yakima River stages are modeled as unchanging with time, although field observations show frequent river stage fluctuations for both. This and other simplifying assumptions incorporated into the regional-scaled groundwater model reflect a balance between representing the interaction of complex natural systems on a regional scale and the bounds of computational limitations in a production environment.

The conceptualization of groundwater flow at Hanford is that of an unconfined, heterogeneous aquifer bounded at the bottom by an impermeable basalt surface. Water enters the aquifer from the highlands on the southern and western sides of the region, from the Yakima River, and via natural and anthropogenic areal recharge (water applied at or near the ground surface). Water enters the groundwater and moves across Hanford to the east and north, discharging into the Columbia River. As groundwater flows across the site from the south and west, it encounters a groundwater divide in the 200 Areas. The location of this divide is uncertain as it is not well defined by field data; however, it dictates flow direction either to the north or to the east from the 200 Areas. Groundwater north and west of this divide moves to the north through Gable Gap (or Umtanum Gap) and then to the Columbia River north of Gable Mountain and Gable Butte. Groundwater south and east of this divide stays south of Gable Mountain and Gable Butte and continues generally eastward to the Columbia River. Refer to Figure L–2 for an overview of groundwater flow at Hanford.

Groundwater hydraulic head observation wells are dispersed across Hanford. Hydraulic head data have been collected over time starting in the 1940s. This database includes over 136,000 head observations from approximately 1,900 discrete locations. The field data indicate that the groundwater potentiometric surface changes over time, that it has continued to change up to the present day, and that it is higher and steeper in the western regions of the site and relatively flat in the eastern regions (CHPRC 2009a). The transient nature of the water table is due primarily to planned and unplanned discharges to the ground surface and directly to the water table during the Hanford operational period. The variable steepness in the potentiometric surface is due to the occurrence of materials with lower hydraulic conductivity in the west, causing a steeper water table; and materials of higher hydraulic conductivity in the east, resulting in a flatter surface.
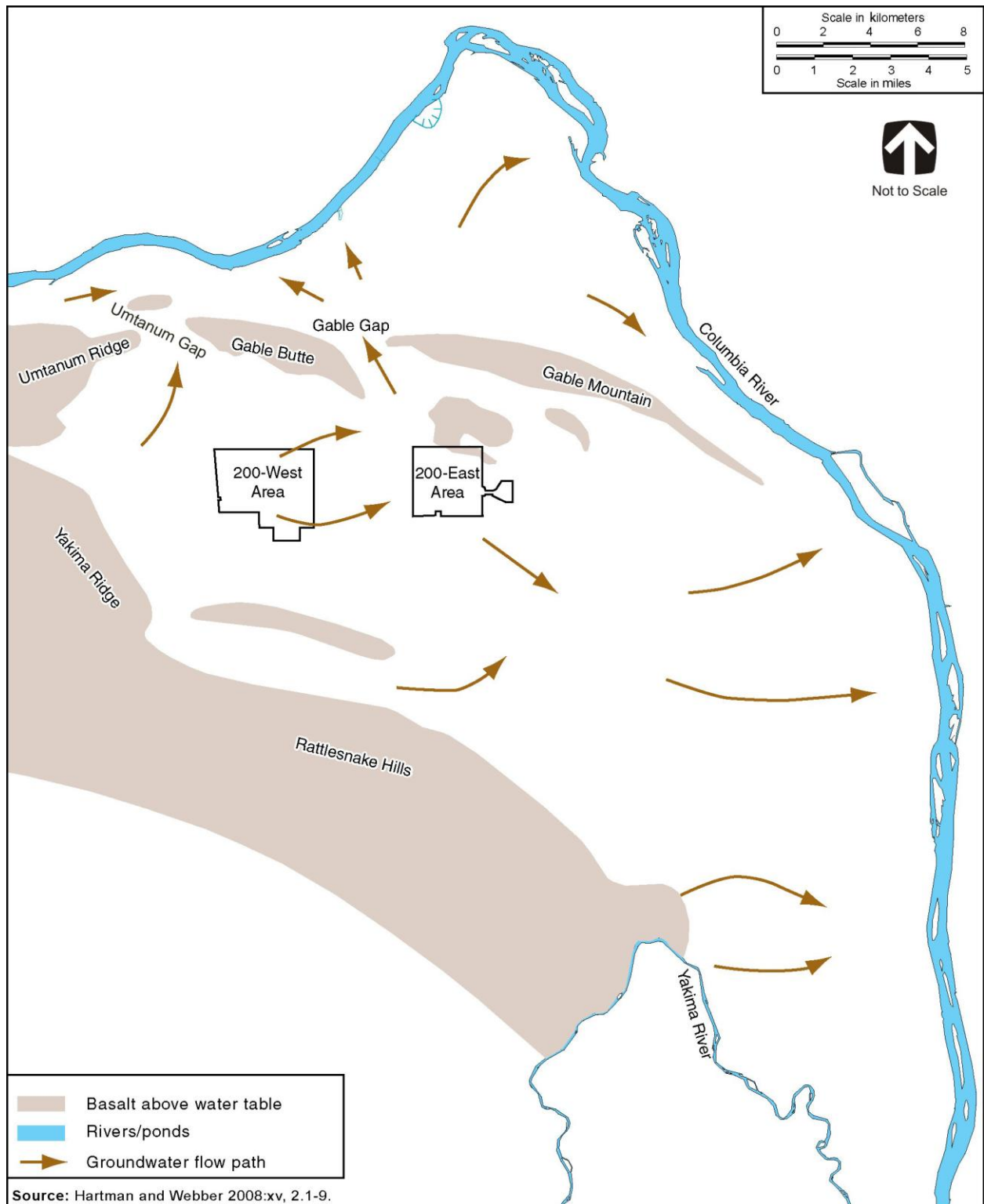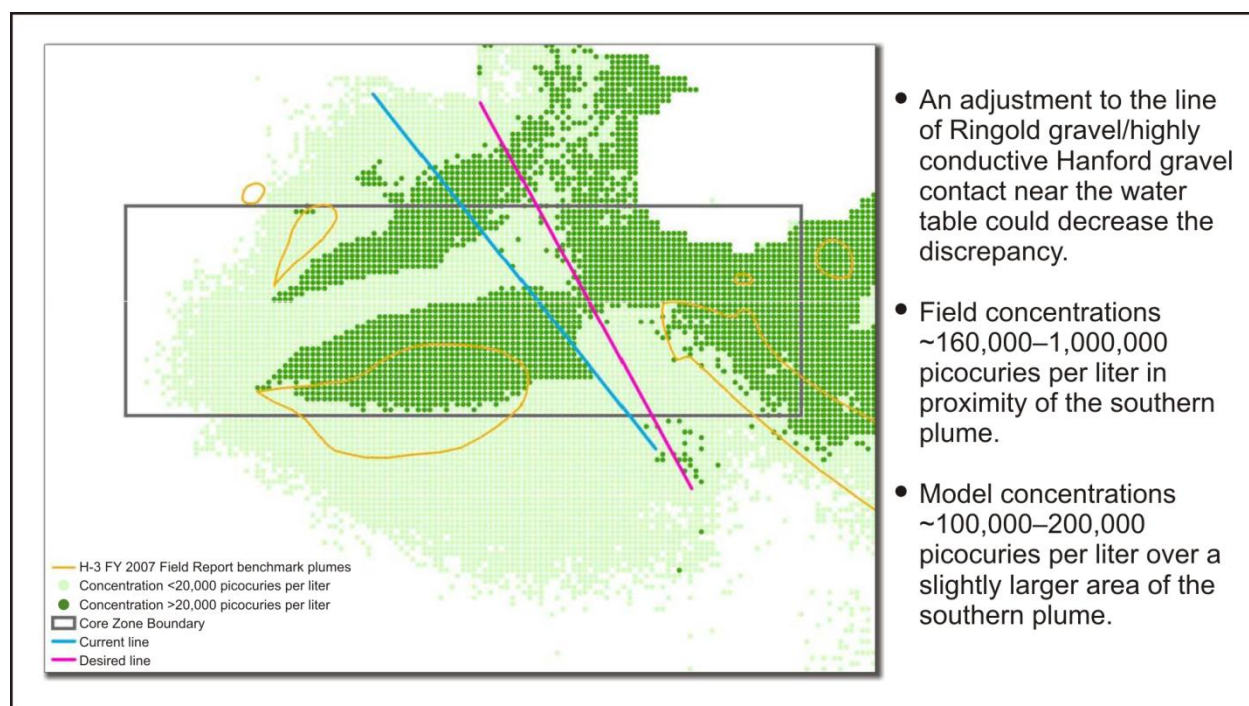
Figure L–2. Groundwater Flow at the Hanford Site

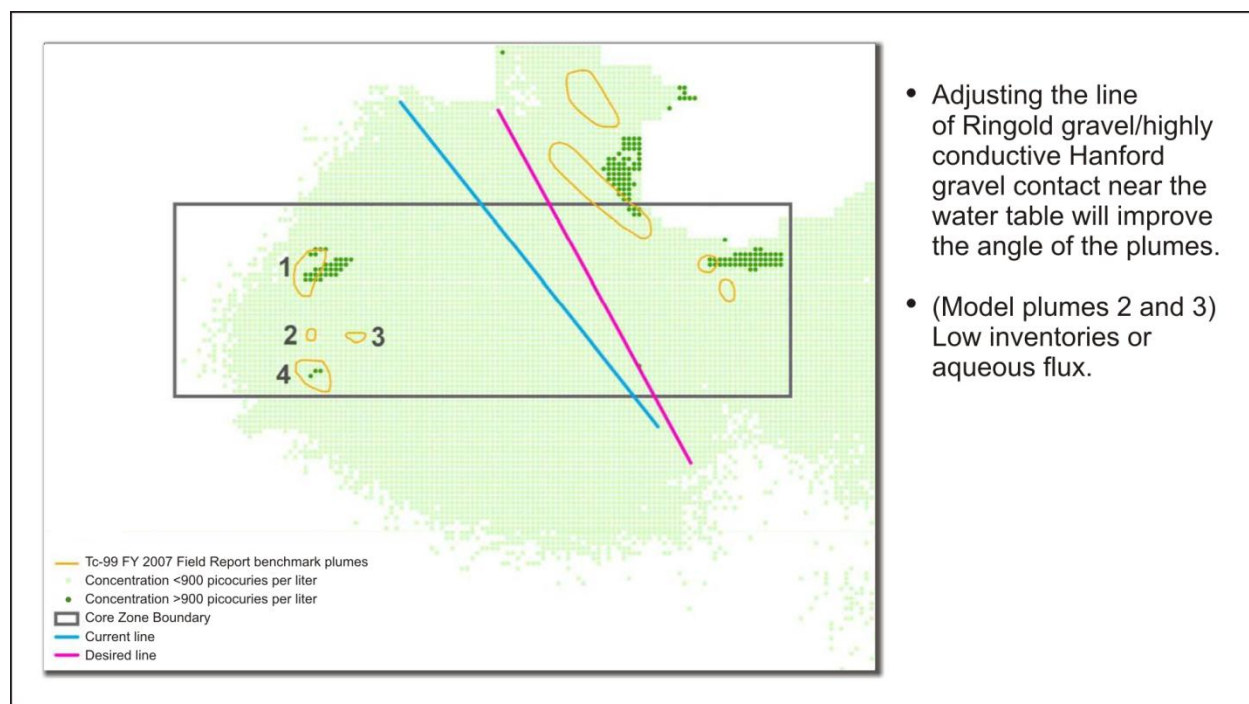**L.1.5   Summary of the *Draft TC & WM EIS* Groundwater Flow Model Results**

The primary metric used to judge the acceptability of the groundwater flow model is the hydraulic head root mean square (RMS) error. RMS error is the result of a comparison of simulated hydraulic heads across the site and over time with the field-observed hydraulic heads at those same locations and times. The differences, or residuals, for all times and all locations are aggregated into a single RMS error for the groundwater flow model. For the *Draft TC & WM EIS* groundwater flow model, this error is between 2 and 3 meters (6.6 and 9.8 feet). The model residuals are reasonably well distributed with no obvious temporal or spatial biases (see the *Draft TC & WM EIS*, Appendix L, Section L.10.1).

As discussed in Section L.1.4 and shown in Figure L–2, groundwater flow across Hanford is generally from west to east, with some flow to the north through Gable Gap and Umtanum Gap. Additionally, it was hypothesized that adjusting the TOB surface cutoff elevation in Gable Gap within the uncertainty of the TOB well-boring log data may influence whether or not groundwater flows through Gable Gap. To test this hypothesis, the *Draft TC & WM EIS* included analysis of a flow model design variant (Alternate Case flow model). This model adjusted the TOB cutoff elevation in Gable Gap downward by 3 meters (9.8 feet) relative to the Base Case model. This lower cutoff elevation is the lowest reasonable elevation at which the cutoff can be expected based on the uncertainty in the available data. The results of the Alternate Case flow model evaluation in the *Draft TC & WM EIS* showed that although flow through Gable Gap can be affected by changes to the TOB cutoff elevation in this region, this cutoff elevation does not exclusively control flow direction. The analysis also showed that variations within the uncertainty of hydraulic conductivity values of the suprabasalt sediments have an influence on flow direction. Further, models with different cutoff elevations in Gable Gap could behave similarly during the historical timeframe with respect to their easterly versus northerly flow behavior yet diverge in the long-term future. This conclusion is supported by concentration-versus-time curves and concentration maps for a variety of contaminants as presented in Appendix O of the *Draft TC & WM EIS*. In summary, the *Draft TC & WM EIS* analysis of the uncertainty in the TOB cutoff elevation in the Gable Gap region found that this uncertainty does not affect the important features of the predicted flow field.

All contaminants of potential concern that were released to groundwater, as determined by the STOMP (vadose zone) analysis were analyzed for groundwater transport. Representative results of this groundwater transport analysis are published in the *Draft TC & WM EIS*. As with all modeling efforts, the modeled results vary from observations in the field. Figures L–3, L–4, and L–5 compare the *Draft TC & WM EIS* modeled contaminant plumes (2005) with the subsequent (2007) field-observed contaminant plumes for hydrogen-3 (tritium), technetium-99, and iodine-129, respectively. These figures are modified from isopleths produced in the *Draft TC & WM EIS*. The dark-green shading in the figures represents areas with higher modeled contaminant concentrations; the light-green shading, lower modeled contaminant concentrations. The beige lines representing the field-observed contaminant plumes from the 2007 Groundwater Monitoring Report (Hartman and Webber 2008) are included for comparison specifically with the areas of higher contaminant concentration (the dark-green areas). The comparisons show that, in terms of their modeled angles and extents, the modeled plumes vary from the field-observed plumes. Analysis of these variances shows that the modeled plumes could be made to more closely match field observations by making an eastward adjustment to the line where lower-conductivity sediments in the west transition to higher-conductivity sediments in the east. The red and blue lines running from the northwest to the southeast in each figure are schematic representations of changes made to the hydraulic conductivity zones in the *Final TC & WM EIS* groundwater flow model.
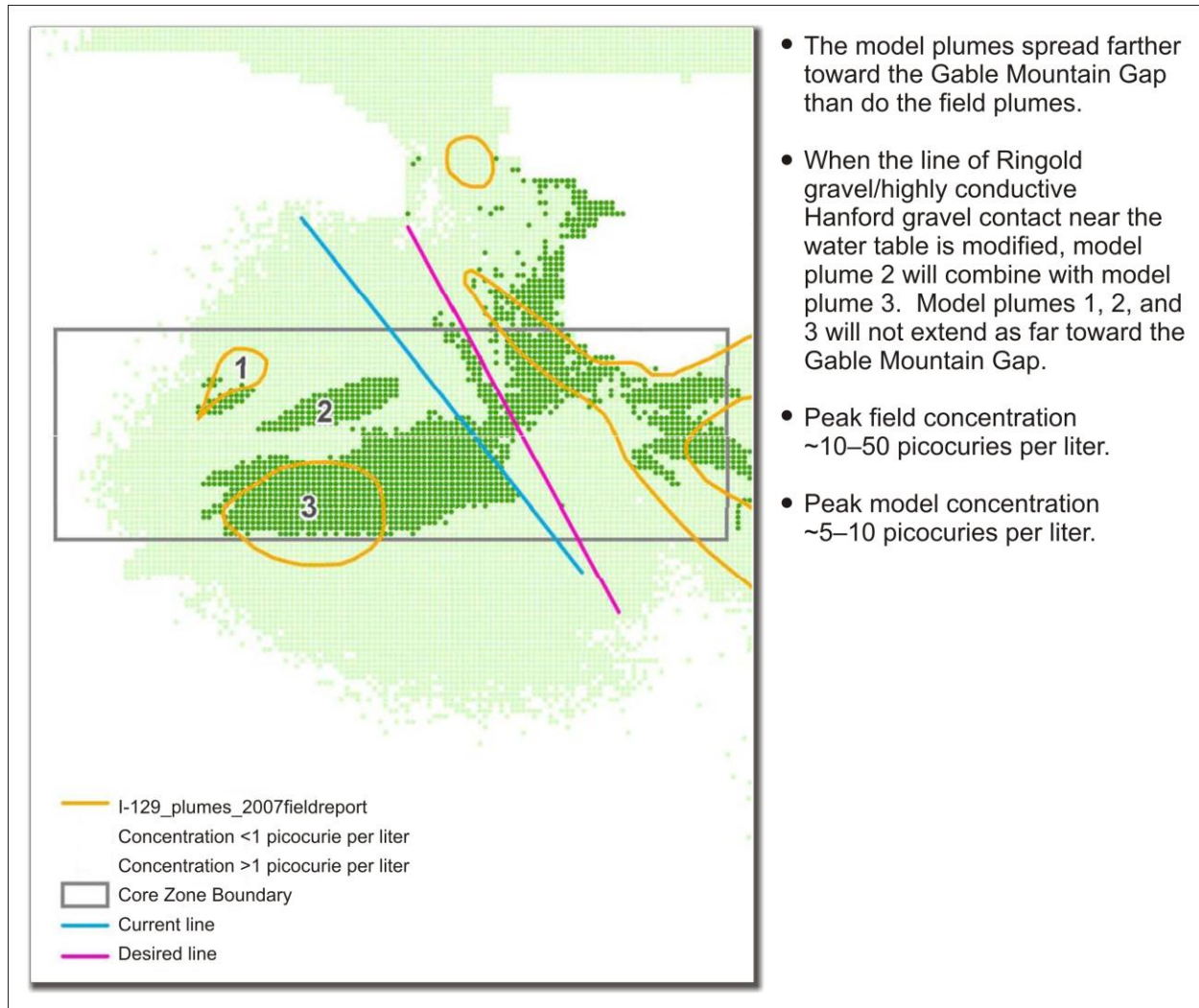
- An adjustment to the line of Ringold gravel/highly conductive Hanford gravel contact near the water table could decrease the discrepancy.

- Field concentrations ~160,000–1,000,000 picocuries per liter in proximity of the southern plume.

- Model concentrations ~100,000–200,000 picocuries per liter over a slightly larger area of the southern plume.

Figure L–3. Comparison of *Draft TC & WM EIS* Modeled Tritium Plumes to Field Observations in the 200-West Area

- Adjusting the line of Ringold gravel/highly conductive Hanford gravel contact near the water table will improve the angle of the plumes.

- (Model plumes 2 and 3) Low inventories or aqueous flux.

Figure L–4. Comparison of *Draft TC & WM EIS* Modeled Technetium-99 Plumes to Field Observations in the Core Zone

The model plumes spread farther toward the Gable Mountain Gap than do the field plumes.

When the line of Ringold gravel/highly conductive Hanford gravel contact near the water table is modified, model plume 2 will combine with model plume 3. Model plumes 1, 2, and 3 will not extend as far toward the Gable Mountain Gap.

Peak field concentration ~10–50 picocuries per liter.

Peak model concentration ~5–10 picocuries per liter.

I-129_plumes_2007fieldreport
Concentration <1 picocurie per liter
Concentration >1 picocurie per liter
Core Zone Boundary
Current line
Desired line

**Figure L–5. Comparison of *Draft TC & WM EIS* Modeled Iodine-129 Plumes to
Field Observations in the Core Zone**

L.1.6 Significant Changes from the *Draft TC & WM EIS* to This *Final TC & WM EIS*

The groundwater flow model used to complete the analysis met the calibration acceptance criteria as described in the *Draft TC & WM EIS*, Appendix L, Table L–19. However, as described in the preceding section, the simulation of contaminant plumes could be improved by moving eastward the line that separates the lower-conductivity sediments in the west from the higher-conductivity sediments in the east. Figure L–6 shows the *Draft TC & WM EIS* model's hydraulic conductivity zones at model layer 11 (120 to 121 meters [394 to 397 feet] above mean sea level [MSL]); Figure L–7 shows the *Final TC & WM EIS* model's hydraulic conductivity zones at this same layer. A black line has been added to each figure to highlight the separation of the zones of lower hydraulic conductivity in the west from the zones of higher hydraulic conductivity in the east. Note that this black line is moved eastward in the *Final TC & WM EIS* model. This change in the hydraulic conductivity zones between the draft and this final environmental impact statements (EISs) is within the uncertainty of the interpretations made using the available borehole log data (CHPRC 2009b, 2010; Ecology 2003).
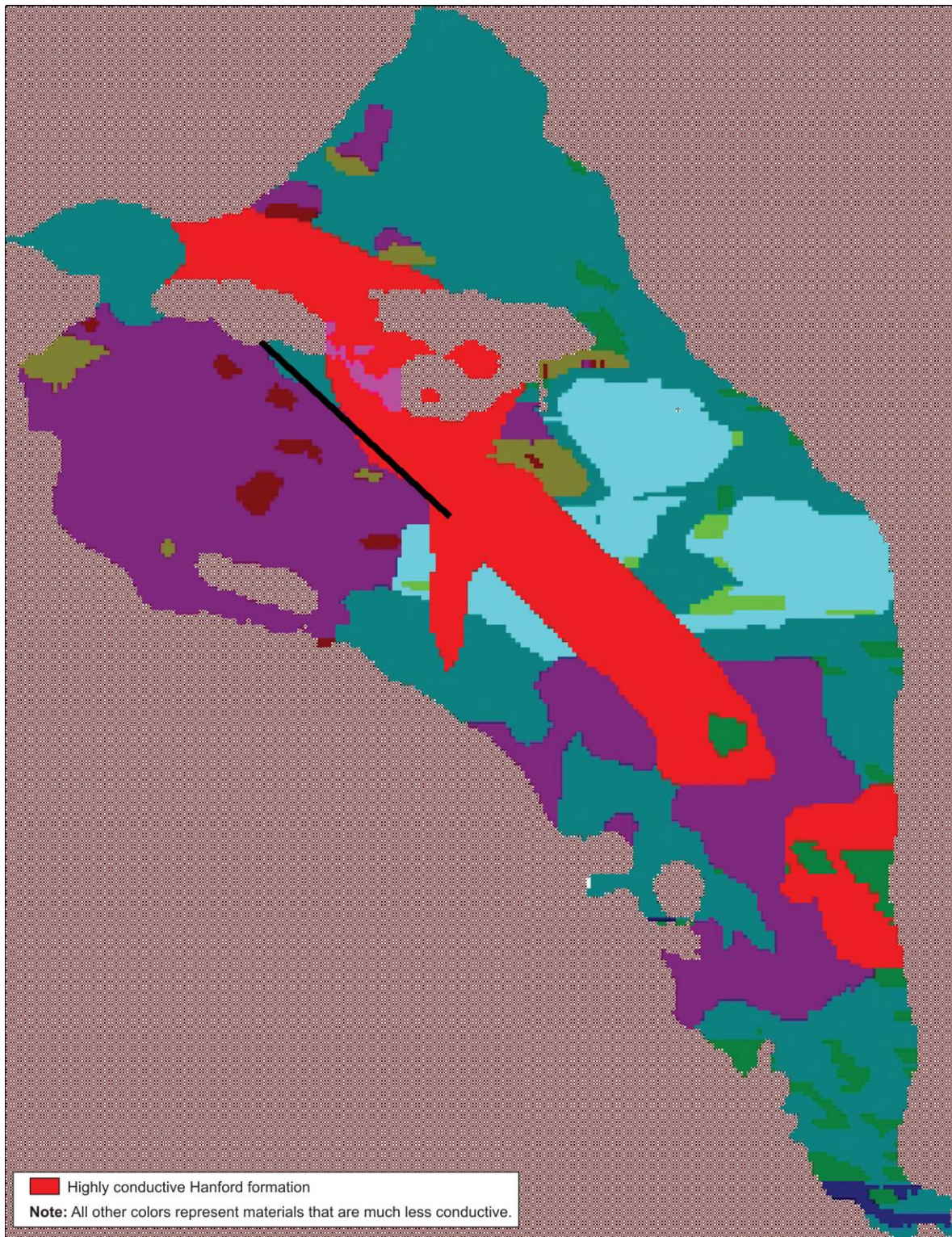
Figure L–6. *Draft TC & WM EIS* **Flow Model Conductivity Zones –
Layer 11 (120–121 meters above mean sea level)**
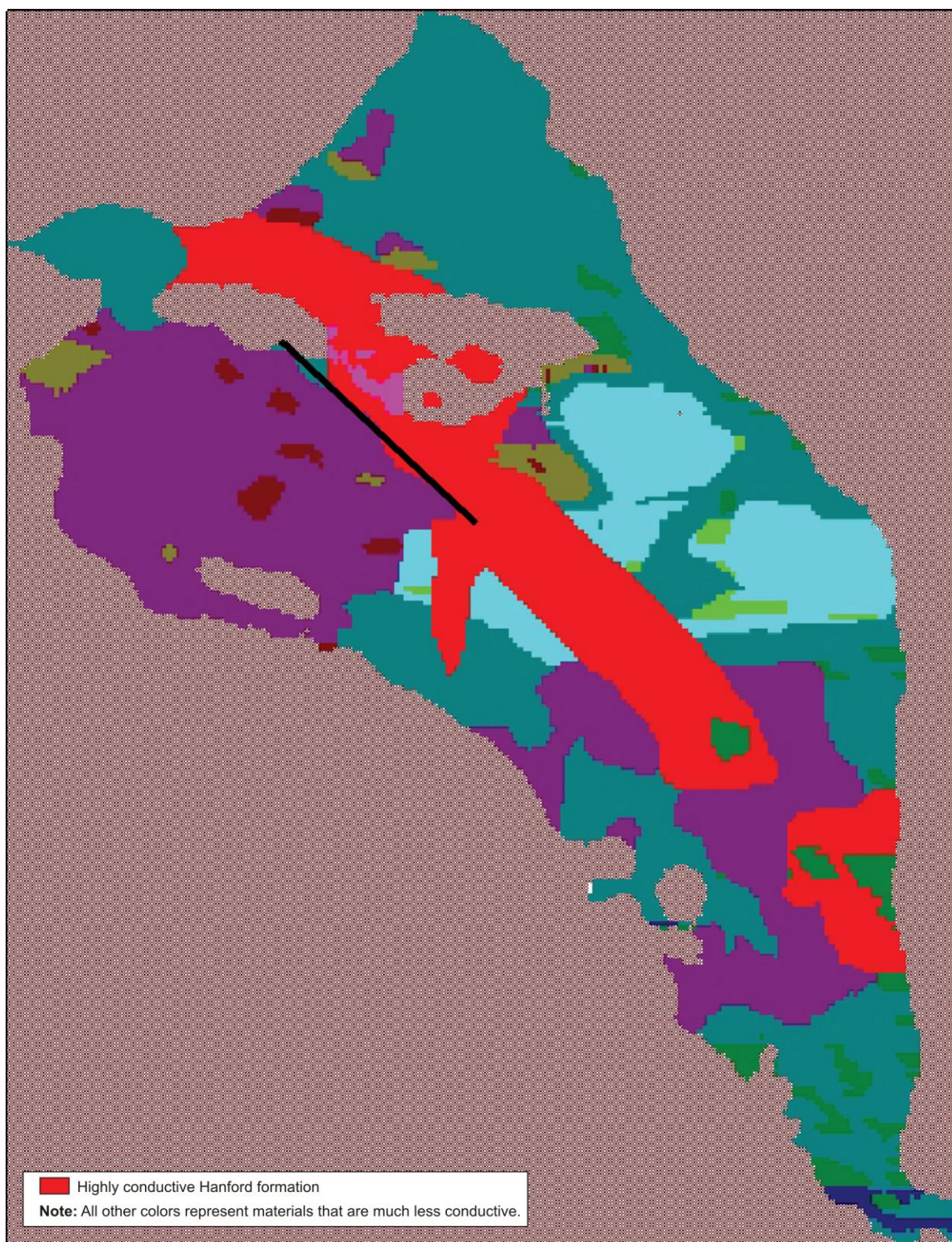
Figure L–7. *Final TC & WM EIS* **Flow Model Conductivity Zones –**
Layer 11 (120–121 meters above mean sea level)

The other changes made to the *Draft TC & WM EIS* groundwater flow model include an update to the head observation data set and a change to the methodology used to process this updated data set for use in the *Final TC & WM EIS* groundwater flow model. The update to the data set included all quality-assurance-complete head observation records available as of December 2008. The head observation data set used in the *Draft TC & WM EIS* included head data available as of August 2006. In addition to updating the head data set, this *Final TC & WM EIS* used a different methodology for processing the data. In the *Draft TC & WM EIS*, the available data were partitioned into three calibration data sets and one validation data set. This methodology is described in the *Draft TC & WM EIS*, Appendix L, Section L.6.1. For this *Final TC & WM EIS*, a single data set was used for calibration. Since the data were not divided as they were for the *Draft TC & WM EIS*, more data points are present in this *Final TC & WM EIS* than were included in the *Draft TC & WM EIS*. This change in methodology tests the robustness of the data set by grouping it differently and checking to see if it produces a significantly different calibration error. The RMS error for the *Final TC & WM EIS* groundwater model, using this larger calibration data set, is between 2 and 3 meters (6.6 and 9.8 feet)—about the same as the RMS error for the *Draft TC & WM EIS* groundwater model.

Although not a significant change, Visual MODFLOW [modular three-dimensional finite-difference groundwater flow model], the graphic interface used to run MODFLOW 2000, was updated from Version 4.2 to Version 2009.1 (SWS 2009). Also not significant, the number of time steps used to solve the first stress period in the flow model was changed from 5 to 100. This time-stepping change was required because the model's conductivity zones were changed slightly from those used in the *Draft TC & WM EIS* groundwater model, as described above; however, no change was made to the initial head distribution. Therefore, additional time steps were needed to solve the first stress period in the simulation.
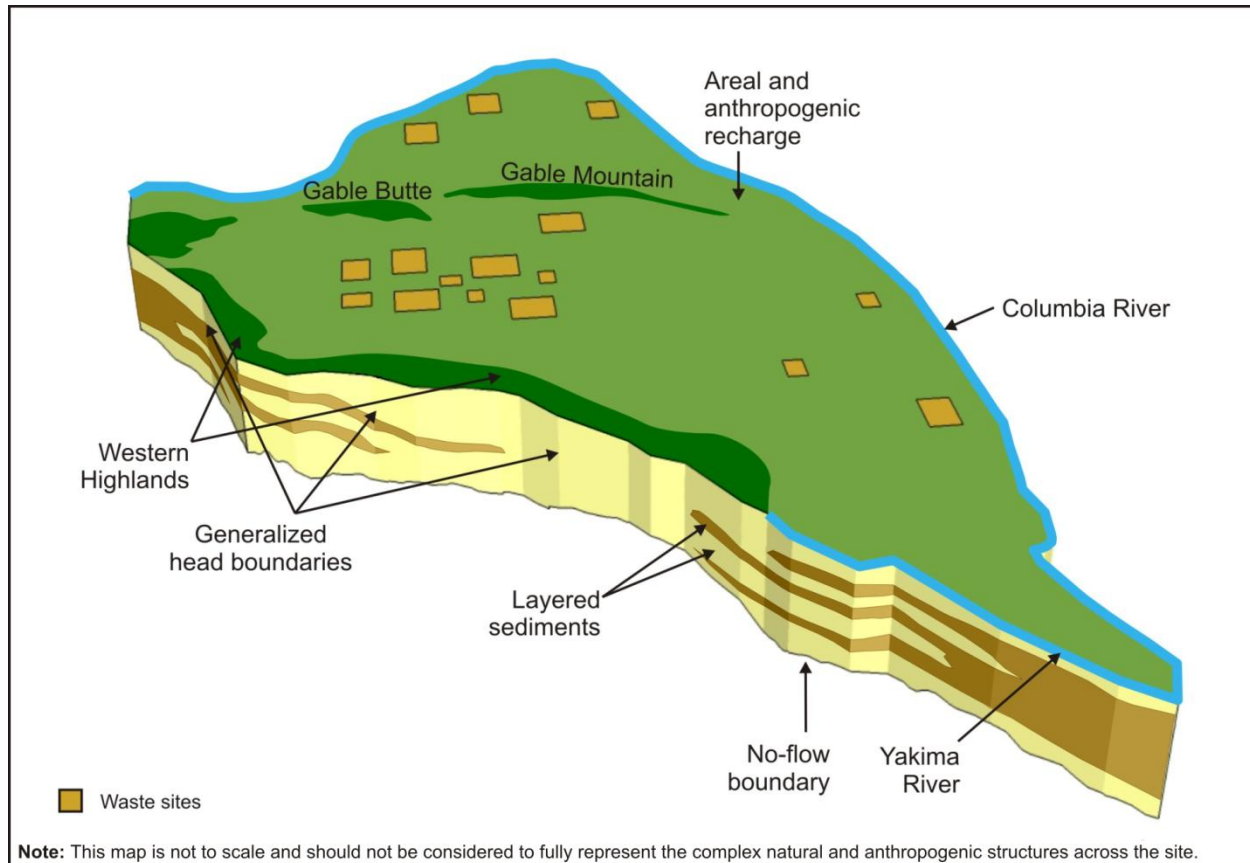
The following parameters/settings are unchanged in the *Final TC & WM EIS* groundwater flow model:

- Columbia River and Yakima River boundaries
- Background (natural) and anthropogenic recharge boundaries
- Generalized head boundaries (GHBs)
- Basalt surface boundary
- Horizontal and vertical model extents, including gridding
- Material properties
- Initial head distribution
- Rewetting methods
- Numerical engine and parameterization

Appendix O, Section O.2, contains a discussion of the changes in the groundwater transport model between the *Draft TC & WM EIS* and this *Final TC & WM EIS*. The most significant changes were adjustments to the dispersivity parameters to better match plume shapes. Appendix U contains a discussion of the correspondence between the model results and field data at the regional and subregional scales in light of changes to the groundwater flow field and transport parameters. Overall, shapes and extents of plumes originating in the eastern part of the Core Zone are in good agreement with field data. Groundwater velocities may be slightly too high for plumes originating in the northeastern part of the 200-West Area. These results are qualitatively similar to those of the *Draft TC & WM EIS*. Section L.8 contains a discussion of the uncertainty in the calibration, particularly with respect to the amount of flow north through Gable Gap and the effect on predicted technetium-99 concentrations versus time for Tank Closure Alternative 2B and Waste Management Alternative 2, Disposal Group 1, Subgroup 1-A. These results demonstrate that the differences in long-term groundwater impacts among the alternatives are discernible in light of the uncertainties in the calibration.

L.2   GROUNDWATER FLOW CONCEPTUAL MODEL

Figure L–8 provides a representation of the Hanford conceptual groundwater flow model. Water enters the region from the highlands in the west and the Yakima River in the south, and discharges into the Columbia River to the north and east. As modeled, aqueous recharge from anthropogenic and natural sources enters from the surface, and the basement is bounded by impermeable basalt. The geologic materials within the vertical and horizontal extents of the model consist of cataclysmic and quiescent deposits of well to poorly sorted sediments, resulting in highly variable hydraulic conductivity zones across the region.

Note: This map is not to scale and should not be considered to fully represent the complex natural and anthropogenic structures across the site.

Figure L–8. Hanford Site Conceptual Groundwater Flow Model

L.2.1   Site Geometry

The Hanford groundwater flow model covers an area of approximately 152,000 hectares (375,000 acres). The Columbia River bounds the region to the north and east, stretching approximately 80 kilometers (50 miles) along the Hanford border. The Yakima River and western highlands border the region to the south and west.

The hydrogeologic boundaries of the site include the Columbia River to the north and east, the Yakima River to the south, and western highlands of outcropping basalt above the water table along the Rattlesnake, Yakima, and Umtanum ridgelines. The highlands along the western boundary of the model domain are basalt outcrops above the water table and provide sources of groundwater flux into the model domain from ephemeral surface-water runoff, underground streams, and agricultural activities in these areas. The Columbia River is a groundwater sink, providing the location of eventual discharge for all

water entering the model domain. The Yakima River, due to its higher elevation and proximity to the Columbia River, is a source of water influx to the model.

The top of the aquifer is a phreatic surface bounded by highlands to the south and west and the Columbia River to the north and east. The site's water table is higher and steeper in the west, with hydraulic heads ranging between 125 and 160 meters (410 and 525 feet) above MSL. The water table gradient in this part of the site is the result of materials with low hydraulic conductivity. Horizontal hydraulic conductivities in the west range from less than 1 to around 20 meters (66 feet) per day. Highly conductive material zones in the central region of the site from Gable Gap through the eastern part of the 200-East Area, then south and east for several kilometers, result in an essentially flat water table in this area. Hydraulic heads here range between 120 and 122 meters (394 and 400 feet) above MSL. Horizontal hydraulic conductivity values in this region are around 4,000 meters (13,124 feet) per day. Moderately conductive material zones are typical of the northern, eastern, and southern portions of the site, resulting in a more gently sloping water table as groundwater moves to the Columbia River. Hydraulic heads in these regions range from 104 and 122 meters (341 and 400 feet) above MSL. Horizontal hydraulic conductivity values in these areas are less than 200 meters (656 feet) per day. Hydraulic heads in areas near the Columbia River are heavily influenced by its river stage, which is conceptualized as a constant head that ranges from 122 meters (400 feet) above MSL in the northwest to 104 meters (341 feet) above MSL in the southeast.

The aquifer thickness across the region ranges from 0 meters in areas where basalt is above the water table to as much as 180 meters (591 feet) due to the highly irregular topology of the TOB across the region. The areas where basalt is above the water table include the highlands along the western boundary and areas on and around Gable Mountain and Gable Butte. Gable Gap, the area between Gable Mountain and Gable Butte, has an uncertain TOB elevation, but data suggest that its elevation is near the water table and, therefore, the aquifer thickness here is estimated to be about 1 meter (3.3 feet) at its shallowest. North of Gable Mountain and Gable Butte the aquifer thicknesses reach up to 180 meters (591 feet). In the western region between Gable Gap and the western highlands the aquifer thicknesses approach 160 meters (525 feet), in part due to the higher water table in the west. The region southeast of Gable Gap, between the 200 Areas and the Columbia River, has aquifer thickness up to 200 meters (656 feet). Figure L–9 provides a graphic representation of the aquifer thickness across the region. This highly variable aquifer thickness is primarily due to the highly variable basalt surface in the region.

The basalt bounding the bottom of the aquifer is conceptualized as an impermeable layer. This basalt surface is highest along the western highlands, reaching elevations up to 1,000 meters (3,281 feet) above MSL. North and east of these highlands, the TOB dips to elevations as low as 80 meters (262 feet) below MSL, then rises again at Gable Mountain and Gable Butte to elevations up to around 200 meters (656 feet) above MSL. North of Gable Mountain and Gable Butte the basalt surface drops off abruptly, again reaching elevations as low as 60 meters (197 feet) below MSL. Figure L–10 provides a graphic representation of the basalt surface across the region.
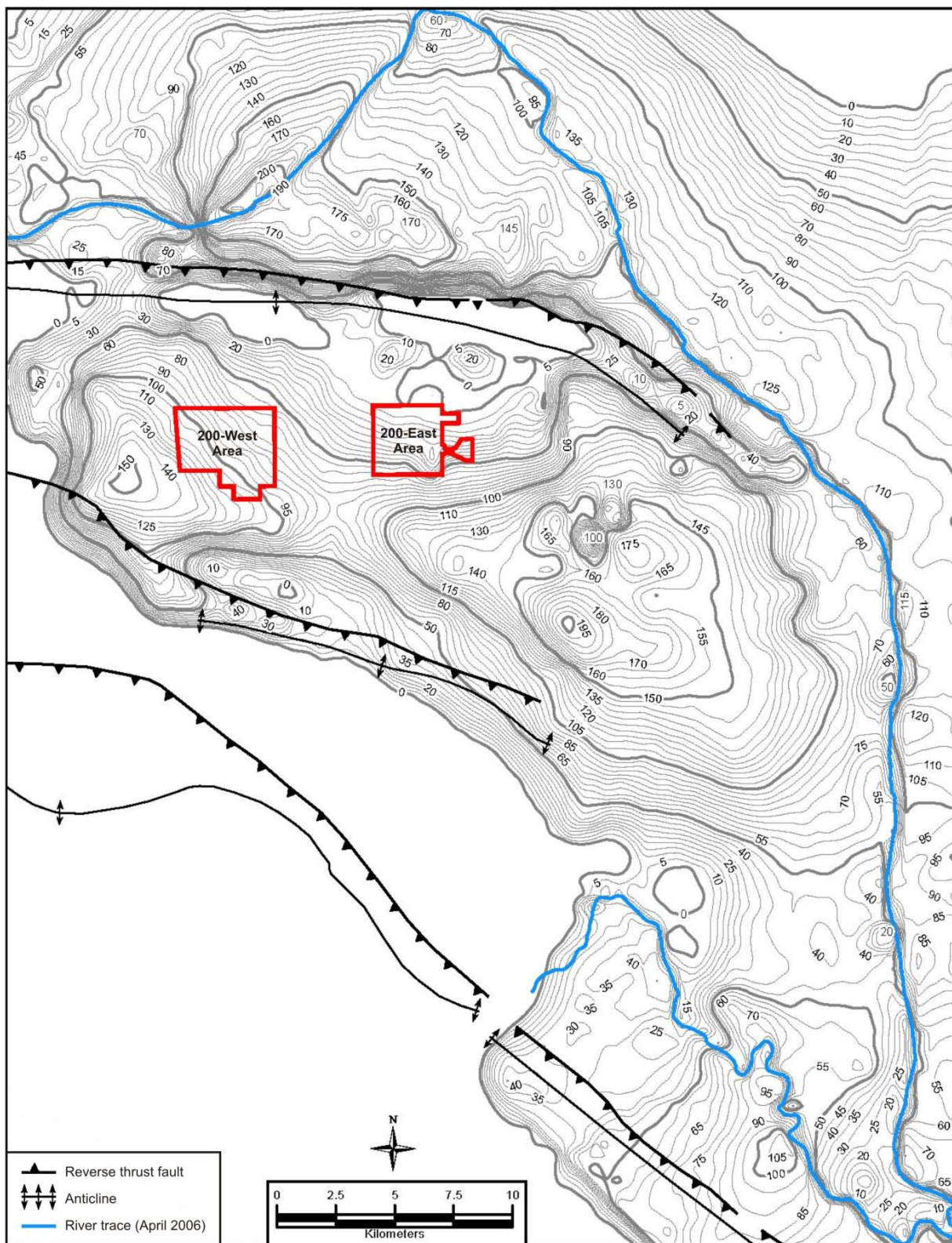
Note: Contour units are in meters.

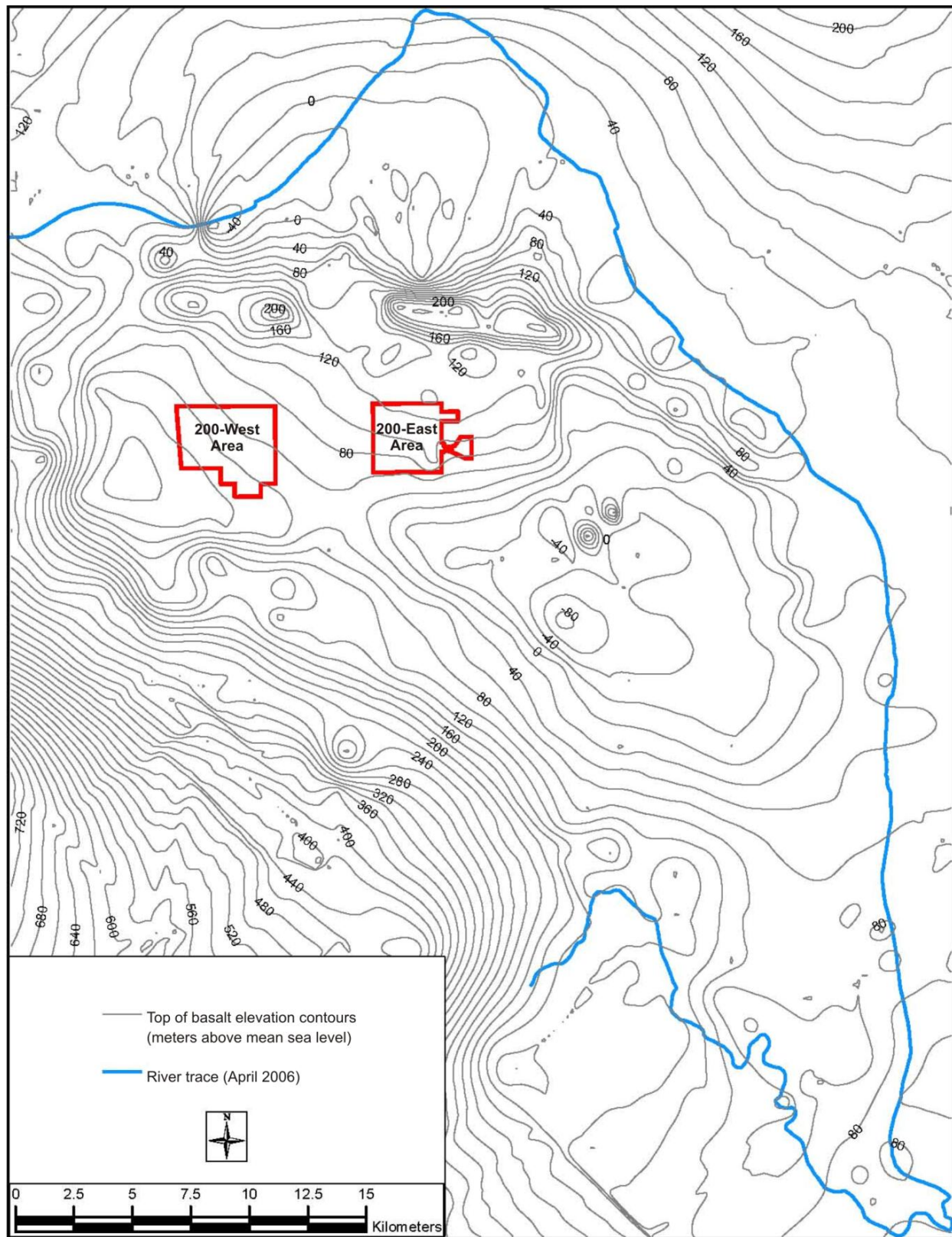**Figure L–9. Representation of Aquifer Thickness (meters) Across the Hanford Site**

Figure L–10. Representation of the Basalt Surface Across the Hanford Site

L.2.2   Boundary Conditions

Water moves into the groundwater from the western and southern portions of the region, including Cold Creek Valley, Dry Creek Valley, Rattlesnake Mountain (runoff), and the Yakima River. Water also enters the model through natural and anthropogenic recharge to the ground surface. Water exits the model at the Columbia River, which bounds the model on its northern and eastern sides. Evapotranspiration is not explicitly modeled, but is taken into account as part of the natural areal recharge boundary condition.

Cold Creek Valley, Dry Creek Valley, and Rattlesnake Mountain runoff are modeled as GHB inputs to the model. Conceptually, a GHB represents a reservoir of water at a constant hydraulic head at some distance outside the model domain with a hydraulic conduction to the regional aquifer being modeled. GHBs allow water to move into and out of the modeled domain depending upon the difference between the time-varying hydraulic heads simulated inside the model and the constant heads at these simulated reservoirs outside the model.

The Yakima River and Columbia River are both modeled as constant hydraulic heads that vary with the elevation of the rivers. The Columbia River is a gaining stream, and it acts in the model as a groundwater sink, drawing water out of the model and forcing hydraulic heads in nearby modeled areas to be near its constant head value. Due to the Yakima River's elevation relative to the Columbia River, the Yakima River is a losing stream that acts in the model as a groundwater source.

Basalt, conceptualized and modeled as impermeable, bounds the bottom of the model. The TOB is a complex surface of variable depth that outcrops above the water table at the western and southern boundaries of the model and again rises above the water table in the Gable Mountain and Gable Butte area. Otherwise, basalt is generally below the water table and provides an impermeable surface through which water is not allowed to enter or exit the model.

The top of the model is open to the atmosphere and subject to natural recharge (precipitation) and anthropogenic recharge. Anthropogenic recharge has been applied both at the ground surface and directly to the aquifer as a result of planned and unplanned releases at Hanford during the operational period. Significant anthropogenic water extractions from the aquifer are also modeled. In the model, all recharge is applied directly to the top of the aquifer. No vadose zone attenuation is considered.

Groundwater pump-and-treat activities are not considered in the *TC & WM EIS* groundwater model. The planned duration of these activities is short (DOE 2010) compared with the *TC & WM EIS* 10,000-year period of analysis. In addition, the final configuration of the groundwater pump-and-treat system was not established prior to the *Final TC & WM EIS* data cutoff date. Appendix U does contain a mass-removal sensitivity analysis illustrating the changes in concentration of carbon tetrachloride resulting from various degrees of removal from the aquifer system.

L.2.3   Geologic Materials

Hanford is located in south-central Washington in the Pasco Basin, which is part of the Columbia Plateau. The site is located in the Yakima Fold Belt and is characterized by a series of east–west-oriented anticlinal ridges and synclinal valleys (Lindsey 1995; Reidel and Chamness 2007). The general structure of the Pasco Basin includes bedrock composed of Miocene-aged tholeiitic flood basalts that are part of the Columbia River Basalt Group overlain by sedimentary materials of the Miocene-Pliocene Ringold Formation, Cold Creek Unit (Plio-Pleistocene Unit), and the Pleistocene Hanford formation. The basalt anticlinal structures have steeply dipping north flanks and gently dipping south flanks. In the 200 Areas located within the Hanford Central Plateau, basalt bedrock dips approximately 5 degrees to the south (Reidel and Chamness 2007).

The sedimentary materials overlying basalt bedrock form the suprabasalt aquifer system that contains the Hanford unconfined aquifer. Figure L–11 shows the locations of the geologic data points and two transects that illustrate the distribution of materials in the unconfined aquifer. The transects themselves (A-A' and B-B') are shown in Figures L–12 and L–13 at a vertical exaggeration of 5:1.   The Ringold Formation, the oldest of the suprabasalt sediments deposited on top of the Columbia River Basalt Group, represents fluvial and lacustrine materials of the migrating, ancestral Columbia River and its tributaries (Reidel et al. 2006). Ringold material types range from coarser gravel and sand deposited in former river channels to finer overbank deposits of silt and mud that formed during periods of quiescence. Felsic minerals such as quartz and feldspar typically dominate Ringold sediments, and the sediment texture varies from moderately well- to well-sorted. The Hanford unconfined aquifer is found in Ringold sediments predominantly in the western and southern portions of Hanford west of the 200-East Area, and also to the north along the Columbia River near the 100-K, 100-N, and 100-D Areas.

Note: To convert meters to feet, multiply by 3.281.
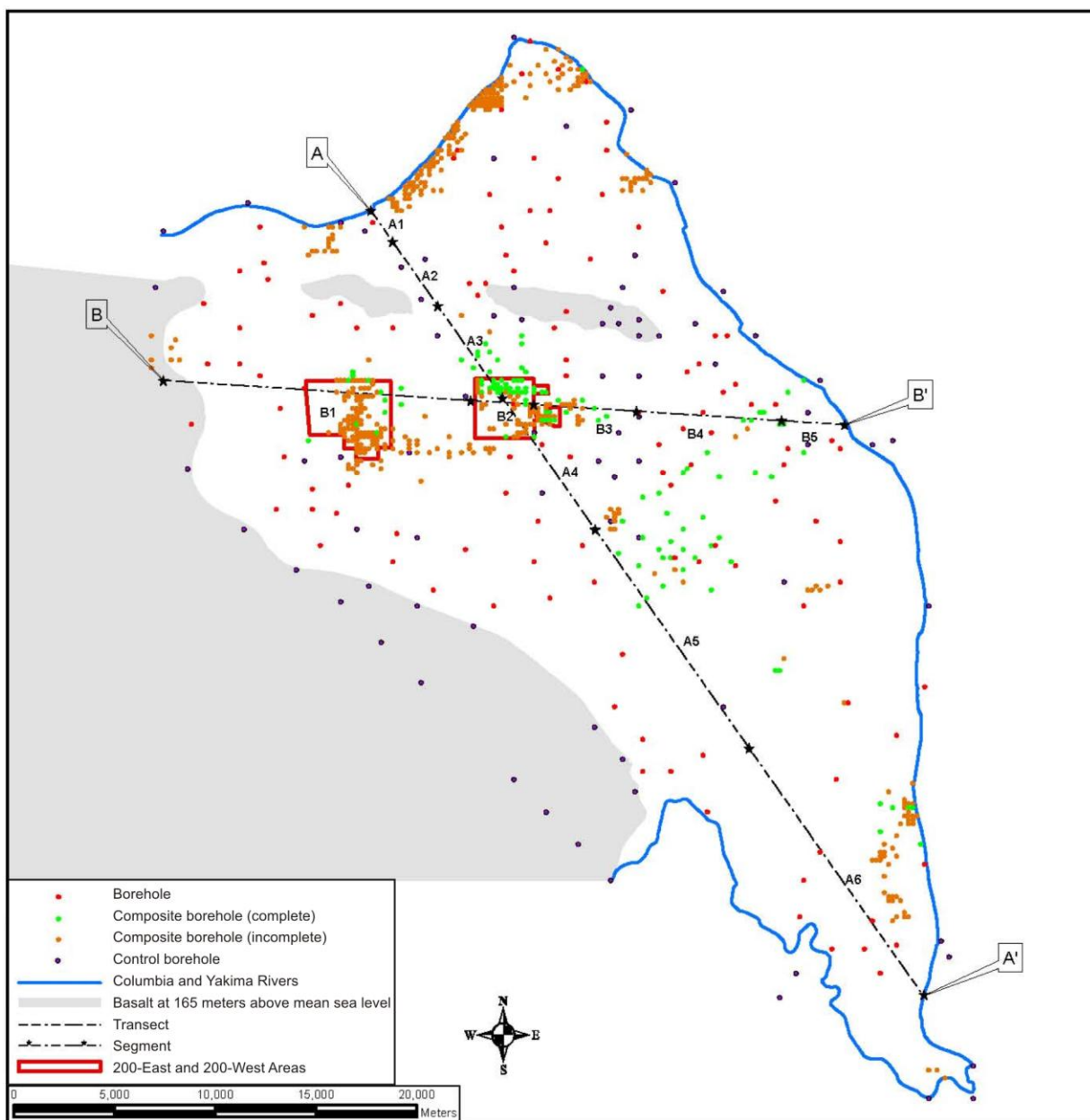
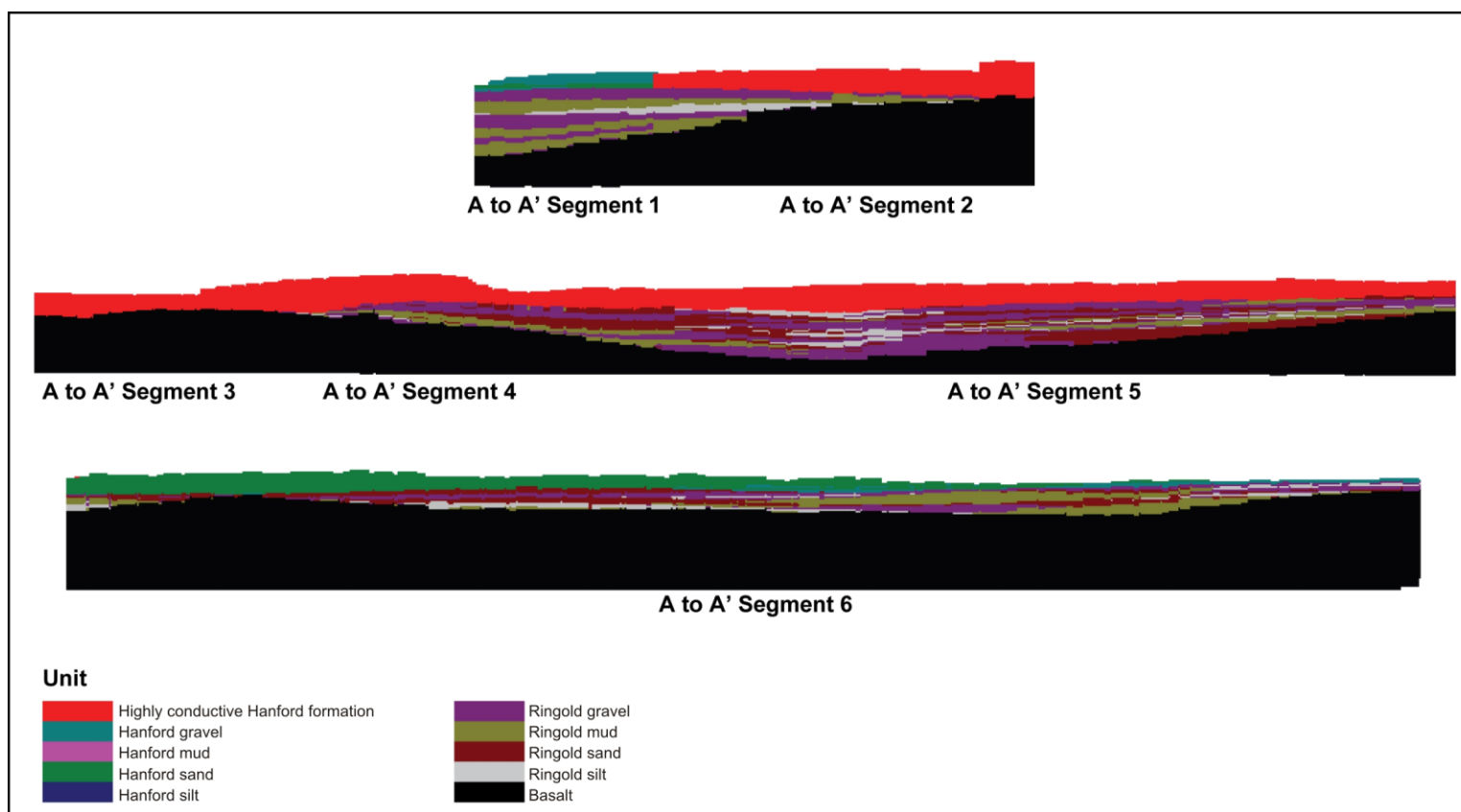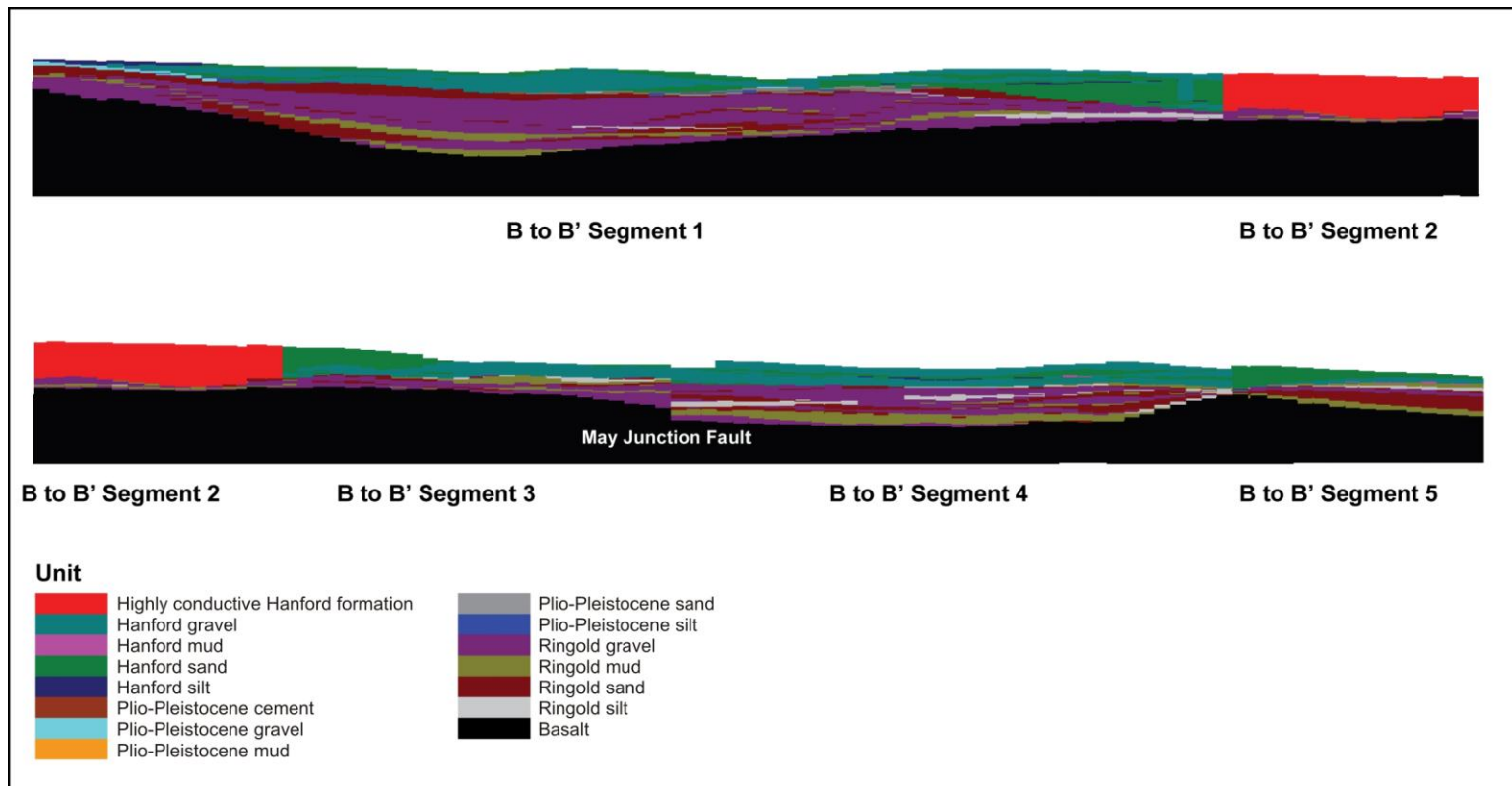**Figure L–11. Geologic Materials – Borehole and Transect Locations**

**Figure L–12. Geologic Materials – Transect A–A'**

**Figure L–13. Geologic Materials – Transect B–B'**

The Hanford formation consists of glaciofluvial sediments resulting from high-energy cataclysmic flood events during the Pleistocene period from glacial Lake Missoula (Bjornstad and Lanigan 2007; Lindsey 1995; Serne et al. 2010). Hanford sediments tend to be dominated by mafic basaltic minerals rather than the felsic counterparts characterizing Ringold sediments and generally are poorly sorted to moderately well sorted. Hanford formation sediments are typically sand- or gravel-dominated and constitute most of the vadose zone on Hanford (Bjornstad and Lanigan 2007). Hanford formation sediments also constitute much of the saturated zone in the northern and eastern portions of Hanford.

The Cold Creek Unit represents fluvial and eolian sediments deposited during the late Pliocene to early Pleistocene period (Bjornstad and Lanigan 2007) between the Hanford formation and Ringold Formation. The Cold Creek Unit was deposited after the period of Columbia River incision that resulted in the deposition of the Ringold Formation and before the Pleistocene Missoula floods that deposited the Hanford formation (Reidel and Chamness 2007). The Cold Creek Unit in the 200-West Area is dominated by carbonate-rich paleosols and fine-grained sediments that represent eolian and flood materials found in the vadose zone. These sediments are also referred to as the "Plio-Pleistocene Unit" (e.g., Lindsey 1995). The spatial distribution of these fine-grained sediments in the 200-West Area below elevation 165 meters (541 feet) above MSL is shown in Figure L–14. Coarser Cold Creek gravels and sand, also referred to as "pre-Missoula gravels," are the dominant material type at the water table across much of the east-central part of Hanford.

The contrast in the paleoenvironments responsible for the sedimentary deposition of materials ranging from boulders to mud results in a wide range of hydraulic properties across Hanford that span many orders of magnitude and are variable locally and regionally. The distribution of sediments at the water table interface is shown in Figure L–15. Higher hydraulic conductivities have been measured for the coarser gravel and sand materials relative to the lower-conductivity silt and mud lithologies. Typically, Hanford formation materials have much higher conductivities than either the Ringold Formation or Cold Creek Unit materials (Bjornstad et al. 2010; Thorne et al. 2006). The hydraulic conductivity of the three-dimensional mosaic of Hanford sediments and their spatial distribution is a major factor controlling the vertical moisture movement and contaminant transport in the vadose zone and the horizontal groundwater flow and contaminant transport in the saturated zone.
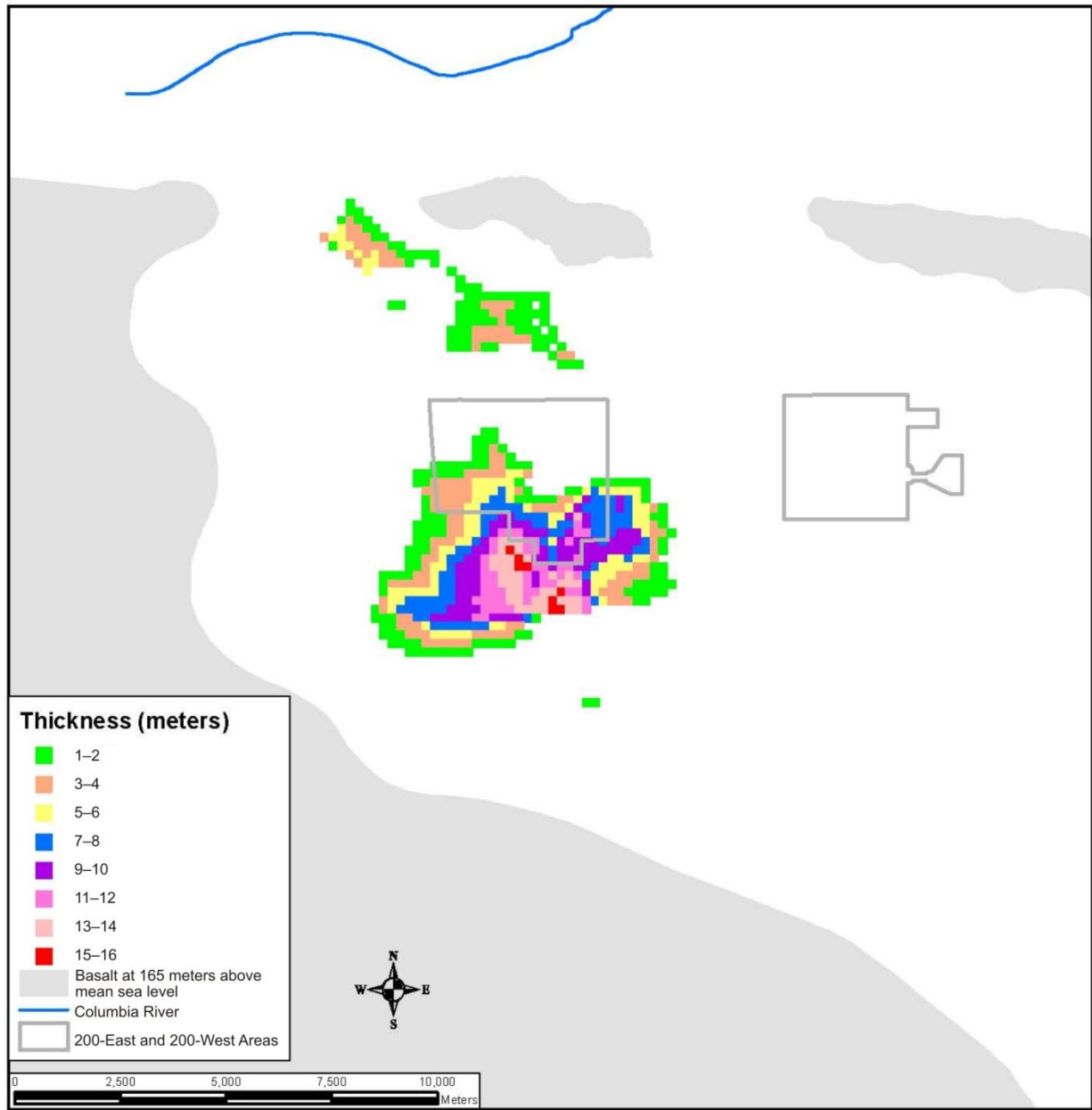
Figure L–14. Geologic Materials – Plio-Pleistocene Isopach Map
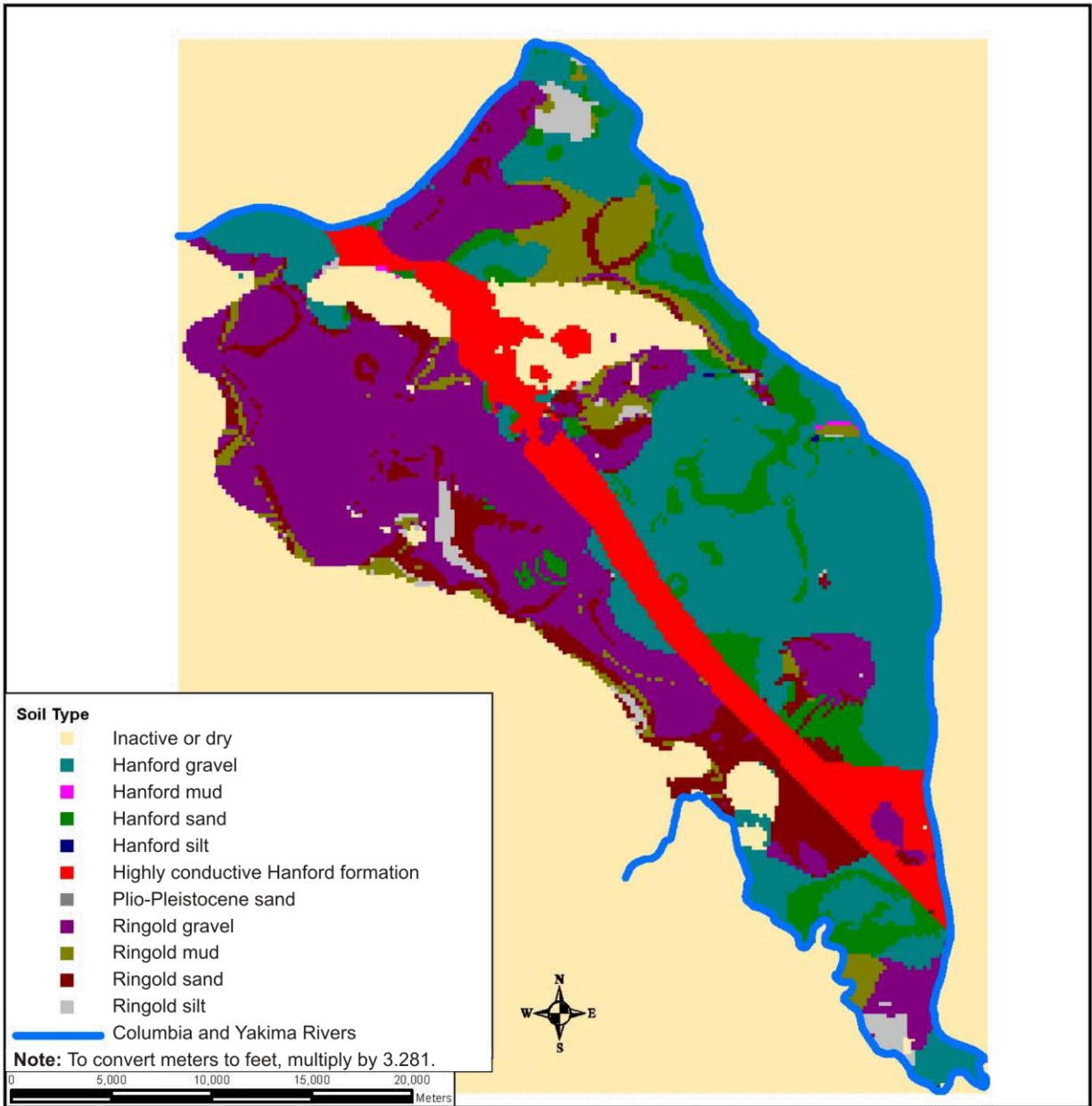
Figure L–15. Geologic Materials – Distribution of Sediments at the Water Table

L.2.4   Conclusion

The conceptual groundwater flow model was developed to solve the multidimensional problem of simulating groundwater elevations and movement over time across Hanford. Determining groundwater elevations and movement includes calculating the head, direction, and magnitude of groundwater at every location within the modeled domain consistent with the model's gridding structure. Calculations for these heads, directions, and magnitudes were based on the site geometry, the site boundary conditions, and the site geology as described in the preceding paragraphs. The following section describes the implementation of these concepts into the Hanford groundwater flow model.

L.3   MODEL DEVELOPMENT FRAMEWORK

The *TC & WM EIS* groundwater flow model simulates the time-varying spatial distribution of the rate and direction of water movement in the unconfined aquifer. Groundwater flow through the unconfined aquifer is simulated using the U.S. Geological Survey (USGS) MODFLOW 2000 Engine, Version 1.15.00 (USGS 2004). The commercial version used in this *TC & WM EIS* is Visual MODFLOW, Version 2009.1 (SWS 2009). The resulting time-varying groundwater flow field is then used to simulate the transport of contaminants from their points of contact with the groundwater at various times in the history of the site to various receptor locations, including the Columbia River (see Appendix O).

The *TC & WM EIS* groundwater flow model was built using the best-available information for Hanford. The development of the groundwater flow model was based, in part, on the Site-Wide Groundwater Model (e.g., Thorne et al. 2006), when features of the work were adequately documented, traceable, and independently verifiable. Previously compiled site data were used when they could be traced to a source and were judged to be adequate. When compiled site data were unavailable or inadequate for the development methodology used, historical primary data were obtained and processed for use or additional data were collected. Published conceptualizations informed some modeling decisions when neither compiled site data nor historical primary data were available for direct use or as input to associated models. When the above sources did not provide the necessary information, the required inputs were derived through engineering judgment or became model calibration parameters. MODFLOW groundwater flow model inputs derived both directly and indirectly from site data and knowledge are described in Section L.4. Model calibration and uncertainty data are described in Section L.7.

The *Draft TC & WM EIS* MODFLOW groundwater flow model was developed in an incremental fashion, proceeding through a preliminary two-layer, steady-state realization to the final transient, multilayered, calibrated, and parameterized model. This appendix presents the *Final TC & WM EIS* flow model, updated as described in Section L.1.6, describing the technical bases for model modifications as well as the calibration and uncertainty analysis (see Section L.7).

L.3.1   MODFLOW 2000

Per direction from the DOE Office of River Protection, the numeric engine selected for simulating groundwater flow was MODFLOW 2000, Version 1.15.00 (USGS 2004). A numeric engine performs the calculations to solve the equations describing water flow through the unconfined aquifer. MODFLOW 2000, a modular three-dimensional finite-difference groundwater flow model, describes the flow of groundwater into and out of every active finite model cell for each discrete time step and along all three dimensions: two horizontal and the vertical.

L.3.2   Visual MODFLOW

Per direction from the DOE Office of River Protection, the MODFLOW interface software selected for this *TC & WM EIS* was Visual MODFLOW, Version 2009.1 (SWS 2009), a product that supports MODFLOW 2000 by providing tools for data input, model control, and presentation of model output. The MODFLOW 2000 numerical engine and its parameter settings in Visual MODFLOW, Version 2009.1, are discussed further in Section L.5.

L.4   MODEL INPUTS – CONCEPTUALIZATION, CHARACTERIZATION, AND ENCODING

This section describes the model inputs for defining the model grid design, cell properties, and flow boundary conditions. The encoding of these features of the *TC & WM EIS* groundwater flow model captures a conceptualization of the unconfined aquifer, its geomorphology, the hydrogeostratigraphic structure of the unconsolidated sediments, and its gross water budget based on underlying principles, data, and interpretation.

L.4.1   Discretization

"Discretization" of the groundwater flow model refers to the specification of the model domain (extent) and the compartmentalization (gridding) of the model domain in three dimensions: two horizontal and the vertical. Defining the model extent and the model grid is a matter of convenience informed by model purpose and computational considerations.

L.4.1.1   Extents

The *TC & WM EIS* groundwater flow model extents are determined by the Columbia and Yakima Rivers and by the top of the uppermost layer of basalt beneath the unconfined aquifer at Hanford.

The horizontal extents of the MODFLOW groundwater flow model are defined on the north, east, and south by the Columbia and Yakima Rivers. Review of hydrographs from wells along the river and comparison with river stage showed that the Columbia River is a reasonable hydrologic boundary. Coordinates for the Columbia and Yakima Rivers within the model domain were collected offshore within 25 meters (82 feet) of the nearshore bank using a global positioning system device in April 2006. The resulting river trace is shown in Figure L–16. The model extent on the west side is arbitrarily set at easting 557000, which is west of the Hanford boundary and the basalt ridge, Rattlesnake Mountain.

The minimum vertical extent is set at 90 meters (295 feet) below MSL, based on the lowest observed TOB elevation from boring logs for Hanford boreholes (CHPRC 2009b, 2010; Ecology 2003).   The deepest estimated TOB elevation is 91 meters (299 feet) below MSL, which is rounded to –90 meters (–295 feet) in the model, given the uncertainties in elevation estimates. The maximum extent in the vertical direction is set at 165 meters (541 feet) above MSL, which is arbitrarily set above the maximum water table elevation (150 meters [492 feet] above MSL) for Hanford (Thorne et al. 2006:Figure 7.23).
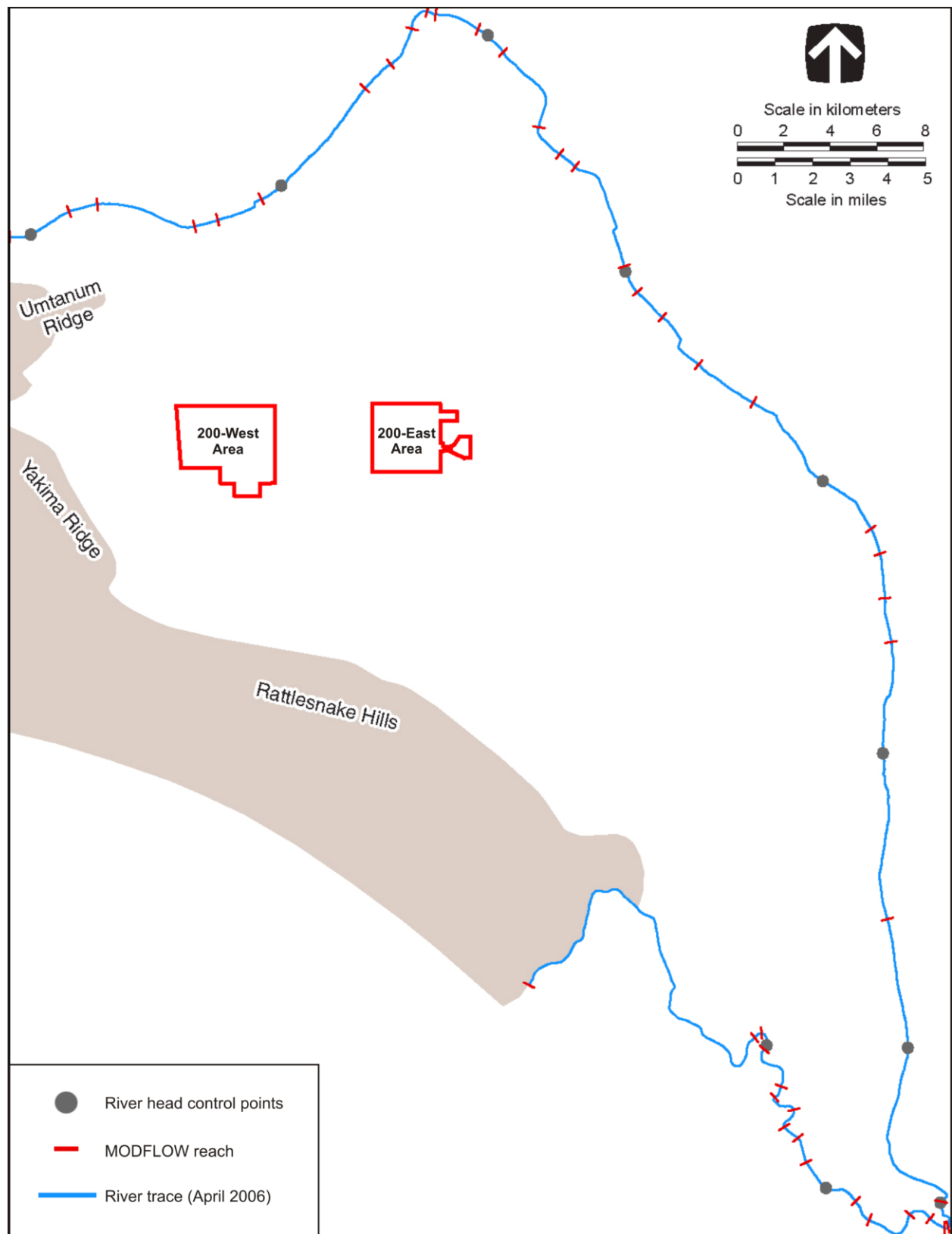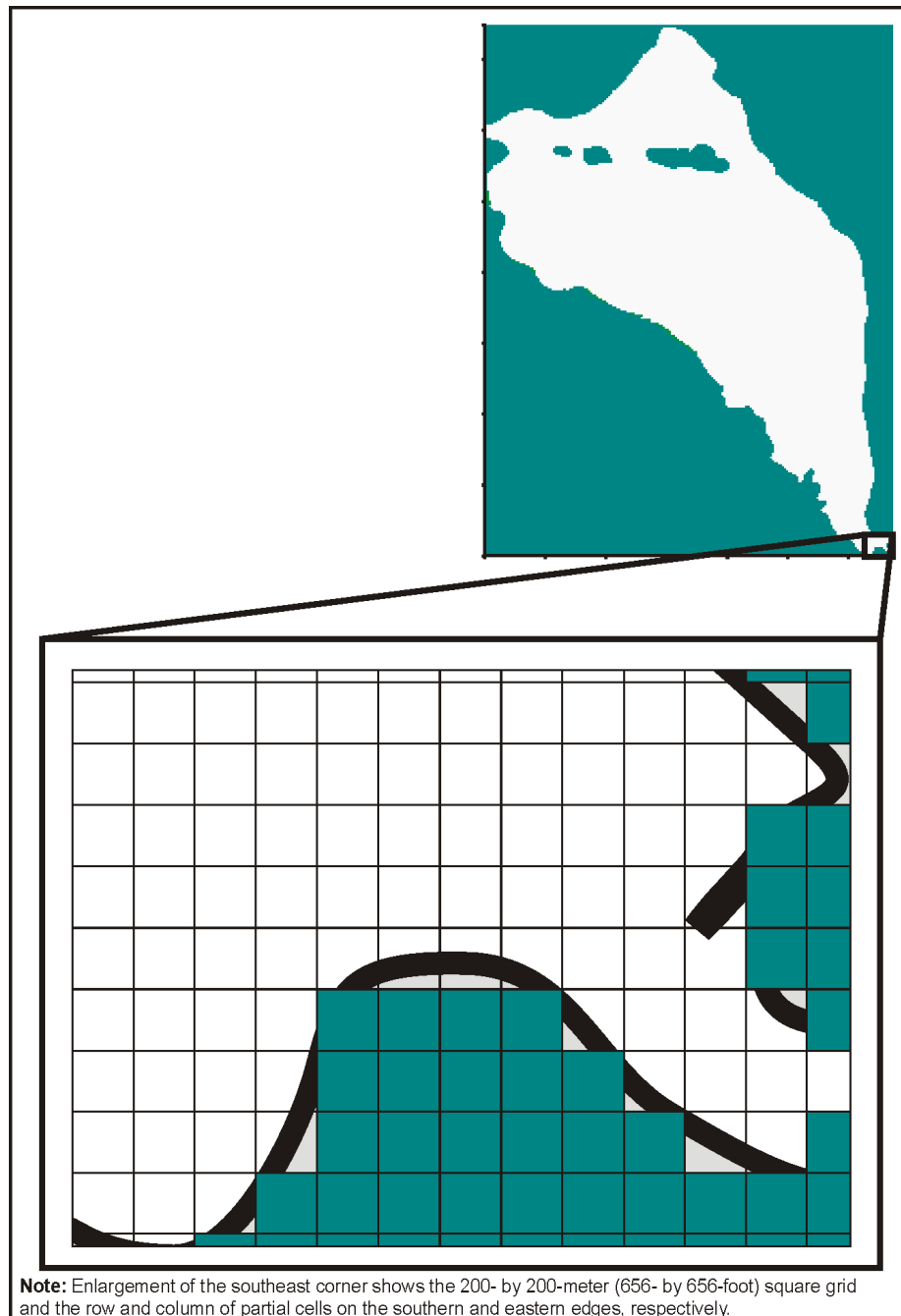
Figure L–16. MODFLOW Groundwater Flow Model Domain,
Columbia and Yakima River Reaches, and River Head Control Points

L.4.1.2   Gridding

The *TC & WM EIS* MODFLOW groundwater flow model divides Hanford within the model domain into three-dimensional blocks or cells. The model domain is divided into a 200- by 200-meter (656- by 656-foot) horizontal grid, with a "fringe" of partial cells on the northern, eastern, and southern sides. The sizes of the partial cells are defined by the distance between the last full-size row and column and the model extent. The horizontal grid and the fringe on the eastern and southern edges of the *TC & WM EIS* MODFLOW groundwater flow model are depicted in Figure L–17.

Note: Enlargement of the southeast corner shows the 200- by 200-meter (656- by 656-foot) square grid and the row and column of partial cells on the southern and eastern edges, respectively.

Figure L–17. Plan View of MODFLOW Horizontal Gridding

The horizontal grid size of 200 by 200 meters (656 by 656 feet) was selected based on two primary criteria: (1) a grid of such size that the heterogeneity of the hydrogeologic material types can be encoded to reasonably represent the suprabasalt sediments on a regional scale; and (2) a grid of such size that a reasonable flow mass balance (in the range of plus or minus 2 percent discrepancy) can be achieved. The horizontal grid size of 200 by 200 meters (656 by 656 feet) was initially selected to meet Criteria 1 because two grid cells cover approximately 0.5 kilometers, which can reasonably represent the minimum area of a particular material type to be encoded for a regional-scaled model. This grid size also achieved an acceptable flow mass balance discrepancy as discussed in Section L.8. No consideration was given to groundwater transport when selecting the grid size for the flow model because the groundwater transport model is not constrained by the flow model grid. See Appendix O for additional information on the groundwater transport model.

The interpolated elevation of the TOB surface in Gable Gap is not sensitive to the cell size of the horizontal grid. The lowest TOB elevation in Gable Gap (i.e., the "cutoff" elevation) determines the water level at which flow through the gap is possible. A comparison of 31 variants of the interpolated TOB surface for both a 200- by 200-meter (656- by 656-foot) grid and a 100- by 100-meter (328- by 328-foot) grid found that the elevation of the TOB surface in Gable Gap was not sensitive to grid size (see Table L–1).

Table L–1. Top-of-Basalt "Cutoff"[a] Elevation in Gable Mountain–Gable Butte Gap
by Grid Size and Aggregation Mean

		Elevation (meters)	
Run	**Description**	**100- by 100-meter grid[b]**	**200- by 200-meter grid[c]**
Default	Geostatistical Analyst (Johnston et al. 2001) default settings.	121	121
Variant 1	Reduce major range from default (22,580 m) to 22,354 m.	121	121
Variant 1a	Reduce major range from default (22,580 m) to 21,451 m.	121	121
Variant 2	Reduce minor range to 22,354 m; model direction = 0 degrees.	121	121
Variant 2a	Reduce minor range to 21,451 m. Major range = 22,580 m and model direction = 0 degrees.	120	120
Variant 3	Minor range = 22,354 m; model direction = 356 degrees.	121	121
Variant 3a	Reduce minor range to 21,451 m and change model direction to 352 degrees (or 172 degrees).	121	121
Variant 4	Reduce partial sill from default (12,519 m) to 12,394 m.	121	121
Variant 4a	Reduce partial sill from default (12,519 m) to 11,893 m.	121	121
Variant 5	Increase nugget from default (0 m) to 15 m.	121	121
Variant 5a	Increase nugget from default (0 m) to 150 m.	121	120
Variant 6	Partial sill = 12,394 m; increase nugget to 125 m; constant sill.	121	120
Variant 6a	Reduce partial sill from default (12,519 m) to 11,893 m and increase nugget to 626 m.	120	120

**Table L–1. Top-of-Basalt "Cutoff"[a] Elevation in Gable Mountain–Gable Butte Gap
by Grid Size and Aggregation Mean** *(continued)*

Run	Description	Elevation (meters)	
		100- by 100-meter grid[b]	200- by 200-meter grid[c]
Variant 7	Increase number of neighbors to include per sector from default (5) to 6, "Include at Least" 2.	120	120
Variant 7a	Increase number of neighbors to include per sector from default (5) to 7, "Include at Least" 2.	120	120
Variant 8	Reduce lag size from default (4,859.2 m) to 4,810.7 m.	121	121
Variant 8a	Reduce lag size from default (4,859.2 m) to 4,616 m.	121	121
Variant 9	Increase number of lags to 13.	121	121
Variant 9a	Increase number of lags to 14.	121	121
Variant 10	Lag size 4,810.7 m; number of lags 13.	121	121
Variant 10a	Reduce lag size from default (4,859.2 m) to 4,616 m and increase number of lags to 14.	121	121
Random 1	Random Realization No. 1.	121	120
Random 2	Random Realization No. 2.	121	121
Random 3	Random Realization No. 3.	120	120
Random 4	Random Realization No. 4.	121	121
Random 5	Random Realization No. 5.	121	121
Random 6	Random Realization No. 6.	120	120
Random 7	Random Realization No. 7.	120	120
Random 8	Random Realization No. 8.	122	122
Random 9	Random Realization No. 9.	118	118
Random 10	Random Realization No. 10.	121	120

[a] Lowest maximum elevation along MODFLOW flow path through Gable Mountain–Gable Butte Gap.
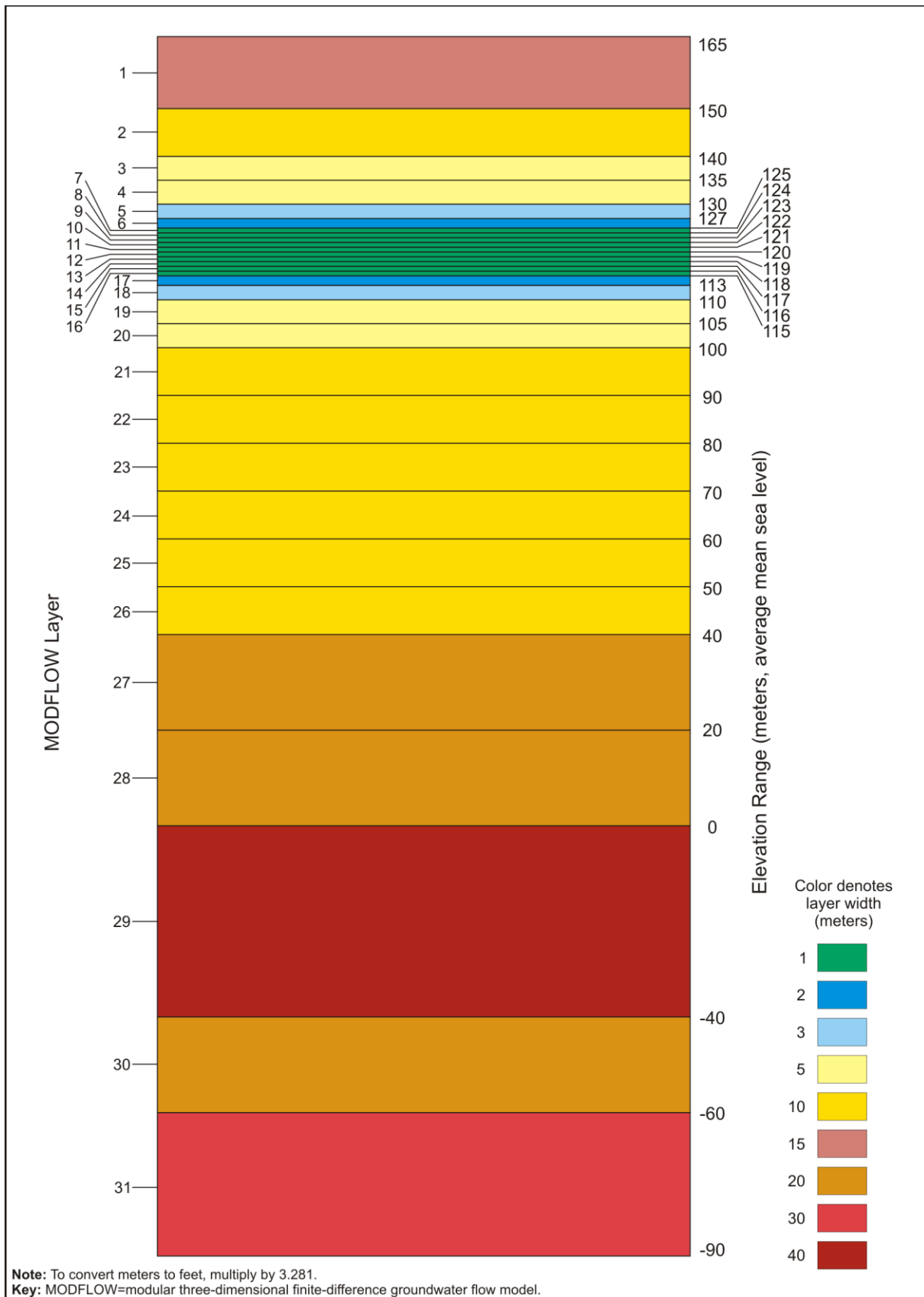[b] Environmental Systems Research Institute default mean.
[c] Harmonic mean.
Note: To convert meters to feet, multiply by 3.281.
Key: m=meters; MODFLOW=modular three-dimensional finite-difference groundwater flow model.

The *TC & WM EIS* MODFLOW groundwater flow model is divided into 31 layers in the vertical direction. Each layer is a uniform (constant) thickness across the entire model domain in the horizontal directions. The layers range in thickness from 1 meter (3.281 feet) to 40 meters (131 feet). The layering of the *TC & WM EIS* MODFLOW groundwater flow model is depicted in Figure L–18. The model has 1-meter-thick (3.281-feet-thick) layers at depths between 115 and 125 meters (377 and 410 feet) above MSL, where the TOB surface is near the water table. These high-resolution layers span the TOB elevations simulated to occur in Gable Gap. Water levels fluctuate between these depths during the model simulation period. The thickest layers, which are greater than 15 meters (49 feet) thick, occur deep in the aquifer, where less resolution is required.

Figure L–18. Cross-Sectional View of MODFLOW Vertical Grid

Note: To convert meters to feet, multiply by 3.281.
Key: MODFLOW=modular three-dimensional finite-difference groundwater flow model.

L.4.2 Boundary Conditions

The boundary conditions for the *TC & WM EIS* groundwater flow model are defined by the Yakima and Columbia Rivers, the subsurface influx of water into the unconfined aquifer along Rattlesnake Mountain, the basalt layer beneath the unconfined aquifer, and recharge (anthropogenic and natural) at the ground surface. The Columbia and Yakima Rivers and naturally occurring subsurface influxes of groundwater to the unconfined aquifer at three discrete locations along the western boundary are modeled as GHBs. Except for the discrete GHB-encoded areas along the western boundary where mountain-front recharge is thought to occur (see Section L.4.2.3), the basalt layer beneath the unconfined aquifer is assumed to be a no-flow boundary, that is, no water enters the unconfined aquifer from the underlying basalt. For the *TC & WM EIS* groundwater flow model, the rivers, subsurface influx, basalt "basement," and natural recharges are taken as constant. The only time-varying fluxes of water across the model boundary are anthropogenic areal recharges. These boundary conditions are discussed below.

L.4.2.1 Basalt Surface (No-Flow Boundary)

Massive basalts beneath the unconfined aquifer at Hanford define a no-flow boundary (aquiclude) in the *TC & WM EIS* groundwater flow model. A no-flow boundary represents a limit to flow within the unconfined aquifer. In this MODFLOW groundwater flow model, no water enters the unconfined aquifer from the underlying basalt. Except for a ridge of basalt in Gable Gap, the model cell in which the TOB surface is assigned and all lower cells are encoded in the model as "inactive." Inactive cells do not allow water to flow to neighboring cells and do not accept flow coming from neighboring cells. For the ridge of basalt in Gable Gap, only cells at 115 meters (377 feet) above MSL and below are encoded as inactive; these elevations correspond to MODFLOW Layers 16 through 31. Cells above 115 meters (377 feet) above MSL that are encoded as basalt are made active, with a hydraulic conductivity 500 times lower than that of Hanford and Ringold muds (0.001 meters [0.00328 feet] per day). Active status prevents the MODFLOW cells from drying out during fluctuations of the water table; cells going dry cause model instabilities (see Section L.5.1.1).

L.4.2.2 Columbia and Yakima Rivers (River Package)

The *TC & WM EIS* groundwater flow model uses the Visual MODFLOW river package to encode the Columbia and Yakima Rivers. This package encodes surface-water/groundwater interaction via a seepage layer (riverbed) separating the surface-water body from the groundwater aquifer. The portions of the Columbia and Yakima Rivers in the *TC & WM EIS* MODFLOW groundwater flow model domain (see Figure L–16) are encoded in the model as an unbroken sequence of cells sharing a face or vertex. Each 200- by 200-meter (656- by 656-foot) cell encoded as river is assigned to a reach, and each reach is assigned a conductance, which is an inverse measure of the resistance to flow between the streambed and the underlying aquifer. For the *TC & WM EIS* groundwater flow model, conductance is a calibration parameter.

In the MODFLOW river package, conductance is a function of the length and width of a reach and the thickness and conductivity of the streambed. The *TC & WM EIS* MODFLOW groundwater flow model sets streambed thickness at 2 meters (6.6 feet) and conductivity at 0.0004 meters (0.0013 feet) per second. Reach width is a uniform 200 meters (656 feet). Reaches of different lengths are defined on the basis of slope. The river conductance parameter values in the *TC & WM EIS* MODFLOW groundwater flow model were varied to determine the model's sensitivity to changes in these parameter values (see Section L.7). Because the length and width of each reach are fixed, adjusting conductance during calibration implies an adjustment of the ratio of streambed conductivity to streambed thickness.

In the *TC & WM EIS* MODFLOW groundwater flow model domain, 27 reaches, each with a relatively constant slope, are defined on the Columbia River, and 14 reaches are defined on the Yakima River

(see Figure L–16). Elevations were assigned to coordinates along the trace by interpolating from existing river elevation data developed by Pacific Northwest National Laboratory (PNNL) (Thorne et al. 2006). Elevations were assigned assuming constant slope between PNNL data points. The PNNL data set contains 700 data points for the Columbia River and 44 points for the Yakima River within the model extent. The entire Yakima River within the model domain is not modeled because the river upstream of Horn Rapids is assumed to be separate and distinct from (not connected to) the unconfined aquifer at Hanford.

The specified river stages, river bed thicknesses, and river bed conductances govern the interactions of the Columbia and Yakima Rivers with the unconfined aquifer. When the river stage is greater than the head in the aquifer immediately below, water flows from the river into the aquifer. The flow is reversed when the river stage is lower than the head in the aquifer immediately below. The former condition is described as a losing reach of the river, and the latter as a gaining reach. In general, the Columbia River gains throughout the modeled domain, and the Yakima River loses.

L.4.2.3   Mountain-Front Recharge (Generalized Head Boundary)

Groundwater is thought to enter the unconfined aquifer at Hanford from the underlying basalt layer in defined areas along the western boundary—Cold Creek Valley, Dry Creek Valley, and Rattlesnake Mountain (Thorne et al. 2006). Well-documented springs occur in Cold Creek Valley and Dry Creek Valley. Runoff from the eastern face of Rattlesnake Mountain is the third source of subsurface influx of groundwater along Hanford's "upstream" boundary.

These three examples of mountain-front recharge are encoded in the *Final TC & WM EIS* groundwater flow model using the Visual MODFLOW GHB package (see Figure L–19). Figure L–19 provides the locations of the model-encoded GHB cells overlain onto a pictorial view of Hanford to show these encoded locations relative to the land features that they represent. With the GHB package, one defines groups of cells (zones) with specific values for head and parameters affecting conductance, the resistance to water flow into the cells of the zone. The head and conductance parameter values for each of the three GHB zones in the *TC & WM EIS* MODFLOW groundwater flow model were varied to determine the model's sensitivity to changes in these parameter values (see Section L.7).

The Base Case groundwater flow model includes a simplifying assumption that mountain-front recharge does not vary with time. Field observations indicate that recharge, possibly from agricultural activities to the west of Hanford, is increasing with time. See Appendix V for an analysis of the model's sensitivity to this and other features related to increased water fluxes into the model.
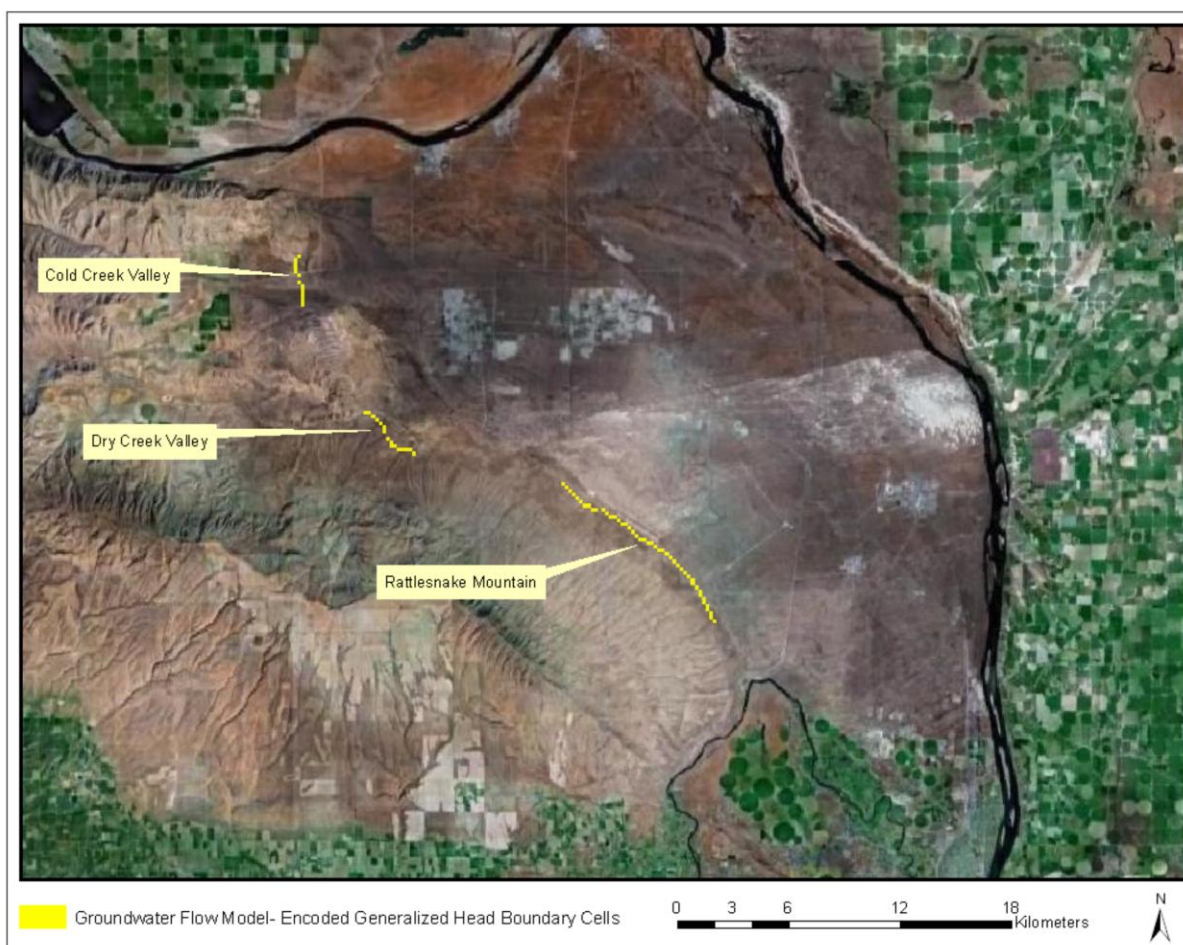
Figure L–19. Mountain-Front Recharge Zones

L.4.2.4   Natural Areal Recharge (Recharge Boundary)

The *TC & WM EIS* groundwater flow model incorporates natural recharge at the rates specified in the *Technical Guidance Document* (DOE 2005).   Cribs and trenches (ditches) receive 50 millimeters (2 inches) of natural recharge per year, and tank farms receive 100 millimeters (4 inches) of natural recharge per year. Fifty millimeters per year is equivalent to 50 liters (13.2 gallons) per square meter per year. For situations where a particular facility does not completely cover a 200- by 200-meter (656- by 656-foot) MODFLOW grid cell, the full recharge value (e.g., 100 millimeters per year for tank farms) is applied across the entire MODFLOW cell that contains all or part of the facility. A fixed infiltration rate, 3.5 millimeters (0.14 inches) per year, representing precipitation on natural surfaces, is applied to the remaining areas not otherwise specified. These natural infiltration rates are also used in the STOMP vadose zone models (see Appendix N). The City of Richland and the sitewide recharge parameter values in the *TC & WM EIS* MODFLOW groundwater flow model were varied to determine the model's sensitivity to changes in these parameter values (see Section L.7).

L.4.2.5   Artificial Recharge (Recharge Boundary)

Anthropogenic recharge associated with Hanford operations and, to a lesser extent, extraction (water withdrawal) and irrigation beyond the Hanford boundary represents the important time-varying fluxes of water into and out of the aquifer during the model period of analysis (CYs 1940–11,940). Water originally taken from the Columbia River was discharged onto the ground surface during operations.

These anthropogenic recharge sources are the time-varying inputs that drive the transient behavior of the *TC & WM EIS* groundwater flow model.

Values for over 200 sources (or sinks) of water were taken from the Cumulative Impacts Inventory Database (SAIC 2006) and encoded into the model. These fluxes were encoded as constant flux boundary conditions in the MODFLOW cells that contain the sources and release sites. These recharge fluxes were also modeled using STOMP to simulate transport of contaminants through the vadose zone to the groundwater.

Of all the anthropogenic liquid sources identified in the Hanford inventory database, eight sites account for 88 percent of the total site recharge (see Table L–2). The volumes released at these sites range from 41 billion liters (10.8 billion gallons) at the 216-S-16P Pond to 300 billion liters (79.3 billion gallons) at the 116-K-2 Trench. All eight sites combined released roughly 1.43 trillion liters (0.38 trillion gallons). Five of these sites are located in the 200 Areas, and they were major contributors to the mounds of water that built up beneath the 200-East and 200-West Areas during operations from 1945 through the mid-1990s (SAIC 2006).

Table L–2. Major Total Recharge Sources on the Hanford Site (1940–Present)

WIDS ID	Site Type	Source Type	Centroid Easting	Centroid Northing	Volume (liters)	Cumulative Fraction
116-K-2	Trench	Liquid	569801	147701	300,000,000,000	0.21
216-A-25	Pond	Liquid	574970	139650	293,899,037,982	0.42
216-B-3	Pond	Liquid	576898	136687	282,689,367,700	0.61
216-U-10	Pond	Liquid	566318	134602	159,859,250,966	0.73
116-N-1	Crib	Liquid	571534	149782	83,700,000,000	0.78
316-1	Pond	Liquid	594283	116106	51,116,602,319	0.82
216-T-4A	Pond	Liquid	566475	137133	42,826,720,640	0.85
216-S-16P	Pond	Liquid	565412	133192	40,723,265,275	0.88

**Note:** To convert liters to gallons, multiply by 0.26417.
Key: WIDS ID=Waste Information Data System identification.

Anthropogenic areal recharge is encoded in the model in 1-year stress periods beginning in 1944. The model applies the estimated annual flux to the water table from each site in the appropriate 1-year stress periods, beginning in the first year of operations at the site and ending in the final year of operations. The total recharge applied to the water table in a given stress period fluctuates from year to year as the number of contributing sites and their fluxes vary. For example, Figures L−20 and L−21 show the timing and magnitude of flux from the dominant anthropogenic recharge sources in the 200-East and 200-West Areas, respectively.
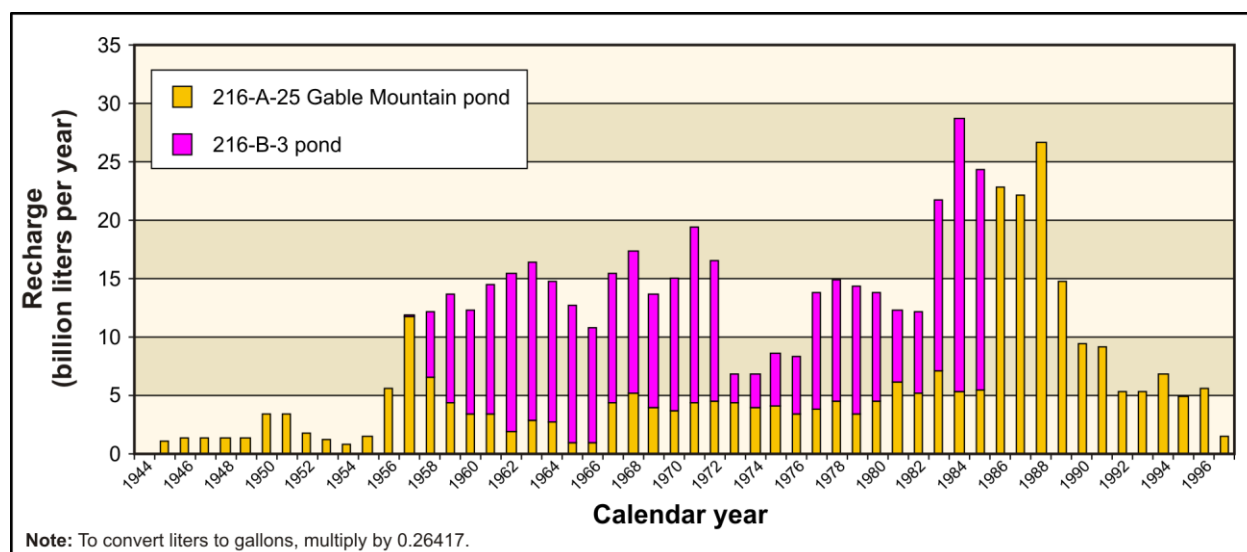
Figure L–20. Major Anthropogenic Recharge Sources in the 200–East Area
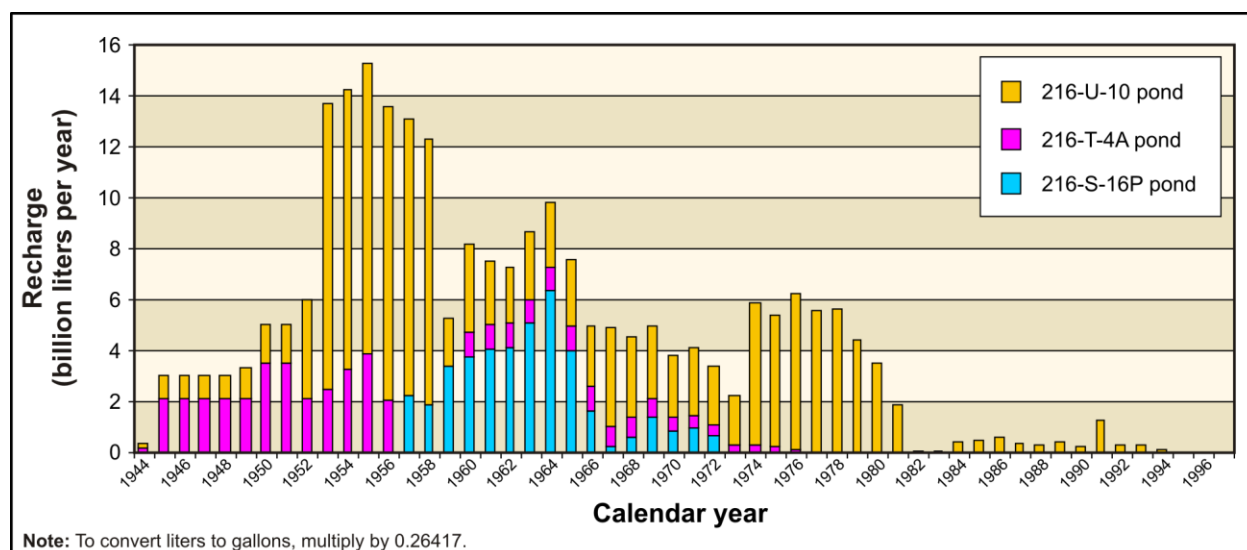
Figure L–21. Major Anthropogenic Recharge Sources in the 200–West Area

In addition to the liquid inventory sources, the model boundaries encompass three City of Richland water system well fields: North Richland, 1100B, and Wellsian Way. The pump houses at the North Richland and 1100B fields were constructed in 1978. Retention basins at these sites received Columbia River water, which was allowed to infiltrate to groundwater. Reference data for recharge from the retention basins and production wells were obtained from City of Richland water system reports dating from 1981 to 2006 (see Table L–3). Based on information provided in the water system reports, a 95th percentile upper confidence limit on mean net recharge was calculated and used for the time period from 1978 to 1981. For analysis purposes, future anthropogenic recharges were estimated based on past usage. The 95th percentile upper confidence limit on the mean was used for the CYs 2006 through 11,940 for all three City of Richland well field locations. The anthropogenic recharge parameter values in the *TC & WM EIS* MODFLOW groundwater flow model were varied to determine the model's sensitivity to changes in these parameter values (see Section L.7).

Table L–3. City of Richland Water Supply Data – Annual Summary Report

Year	Extraction North Richland (Mgal)	Extraction 1100B (Mgal)	Positive Recharge (Mgal)[a]	Positive Recharge/ Extraction	Net Recharge (Mgal)	Net Recharge (gal)
1978	9.13×10^2	6.86×10^1	3.70×10^{3b}	3.77	2.72×10^3	2.72×10^9
1979	9.13×10^2	6.86×10^1	3.70×10^{3b}	3.77	2.72×10^3	2.72×10^9
1980	9.13×10^2	6.86×10^1	3.70×10^{3b}	3.77	2.72×10^3	2.72×10^9
1981	9.13×10^2	6.86×10^1	3.66×10^3	3.73	2.68×10^3	2.68×10^9
1982	9.13×10^2	6.86×10^1	2.36×10^3	2.40	1.38×10^3	1.38×10^9
1983	9.13×10^2	6.86×10^1	2.76×10^3	2.82	1.78×10^3	1.78×10^9
1984	5.31×10^2	0.00×10	3.61×10^3	6.79	3.07×10^3	3.07×10^9
1985	5.42×10^2	0.00×10	2.72×10^3	5.01	2.17×10^3	2.17×10^9
1986	3.99×10^2	1.08×10^2	2.35×10^3	4.63	1.84×10^3	1.84×10^9
1987	5.11×10^2	1.02×10^2	2.33×10^3	3.80	1.72×10^3	1.72×10^9
1988	5.39×10^2	1.08×10^1	1.94×10^3	3.53	1.39×10^3	1.39×10^9
1989	1.08×10^3	7.19×10	2.92×10^3	2.69	1.83×10^3	1.83×10^9
1990	1.45×10^3	4.07×10	2.70×10^3	1.86	1.25×10^3	1.25×10^9
1991	1.13×10^3	1.02×10^1	2.77×10^3	2.44	1.64×10^3	1.64×10^9
1992	8.39×10^2	4.35×10^1	1.71×10^3	1.93	8.23×10^2	8.23×10^8
1993	6.01×10^2	1.57×10^1	3.30×10^3	5.35	2.68×10^3	2.68×10^9
1994	1.34×10^3	6.17×10^1	2.64×10^3	1.89	1.24×10^3	1.24×10^9
1995	5.72×10^2	6.00×10^1	1.86×10^3	2.94	1.23×10^3	1.23×10^9
1996	5.03×10^2	5.84×10^1	2.34×10^3	4.16	1.77×10^3	1.77×10^9
1997	6.23×10^2	6.84×10^1	1.90×10^3	2.75	1.21×10^3	1.21×10^9
1998	1.33×10^3	1.47×10^2	1.86×10^3	1.26	3.85×10^2	3.85×10^8
1999	7.46×10^2	1.11×10^2	1.61×10^3	1.88	7.54×10^2	7.54×10^8
2000	7.65×10^2	3.64×10^1	1.83×10^3	2.29	1.03×10^3	1.03×10^9
2001	5.34×10^2	7.47×10^1	1.48×10^3	2.44	8.76×10^2	8.76×10^8
2002	1.19×10^3	6.85×10^1	3.05×10^3	2.43	1.80×10^3	1.80×10^9
2003	5.35×10^2	1.76×10^1	2.67×10^3	4.83	2.12×10^3	2.12×10^9
2004	4.10×10^2	5.79×10^1	1.69×10^3	3.61	1.22×10^3	1.22×10^9
2005	5.39×10	1.33×10^2	2.61×10^3	18.86	2.47×10^3	2.47×10^9
2006–11,940	9.13×10^2	6.86×10^1	3.70×10^{3b}	3.77	2.72×10^3	2.72×10^9
			Count	24.00		
			SD	1.35		
			Average	3.23		
			95% UCL	3.77		

[a] Positive recharge taken from City of Richland water system reports for years 1981–2005 (Richland 1981–2005).
[b] Used the 95th percentile UCL ratio.
Note: To convert gallons to liters, multiply by 3.7854.
Key: %=percent; gal=gallon; Mgal=million gallons; SD=standard deviation; UCL=upper confidence limit.

L.4.3 Lithology

Three major lithologic units that occur beneath Hanford are encoded in the *TC & WM EIS* groundwater flow model: Elephant Mountain basalt, Ringold Formation, and Hanford formation. The Elephant Mountain basalt represents the bottom of the unconfined aquifer (see Section L.4.3.2.1). The unconsolidated sediments of the Hanford and Ringold Formations constitute the unconfined aquifer. The sediments of these two formations represent the saturated zones through which groundwater flow is modeled.

L.4.3.1 Hydrogeologic Unit Definition

The *TC & WM EIS* groundwater flow model recognizes two major lithologic formations in the unconfined aquifer above the basalt, Hanford and Ringold, and two minor geologic units, the Cold Creek and Plio-Pleistocene Units. The Ringold Formation is the lower geologic unit of the unconfined aquifer, and, where it occurs, it directly overlies basalt. The Hanford formation overlies the Ringold Formation where the latter occurs and directly above the basalt where the Ringold is missing. Between the Hanford and Ringold Formations, the Cold Creek and Plio-Pleistocene Units locally occur at Hanford. Although the Cold Creek Unit is Plio-Pleistocene in age, for the purposes of the *TC & WM EIS* groundwater flow model, the Cold Creek Unit and the Plio-Pleistocene Unit have been identified as separate encoded material types. In the groundwater flow model, the Plio-Pleistocene Unit defines the fine-grained silts and caliche sediments prevalent in the 200-West Area, and the Cold Creek Unit refers to the coarse-grained, pre-Missoula gravels found farther to the east. Both the Hanford and the Ringold Formations consist of fluvial and lacustrine sequences of mud, silt, sand, and gravel. The coarse-grained multilithic facies of the Cold Creek Unit are thought to be more like Hanford formation gravel and sand than the harder, more cemented Ringold Formation gravel and sand (Thorne et al. 2006).

L.4.3.2 Hydrogeologic Unit Encoding

The *TC & WM EIS* groundwater flow model has been encoded with hydrogeologic data for the entire model domain developed from Hanford well borings completed as of September 2009 (CHPRC 2009b, 2010; Ecology 2003). Approximately 5,000 boring logs from Hanford and its surroundings were reviewed to determine whether the geologic units and discrete hydrostratigraphic layers could be recognized from the geologic descriptions. When multiple logs existed for a borehole, higher credibility was given to those descriptions recorded by a professional geologist. Logs were reviewed for specific identification of the Elephant Mountain basalt, Hanford and Ringold Formations, and Cold Creek and Plio-Pleistocene Units. The logs were further examined to discern textural types among the sedimentary units: mud, silt, sand, and gravel. Each of the resulting hydrogeologic units is encoded with unique properties (see Section L.4.4). The development of the hydrogeologic data for use in the *TC & WM EIS* groundwater flow model is described in the following sections.

L.4.3.2.1 Basalt Surface

The TOB surface encoded in the *TC & WM EIS* groundwater flow model was derived from boring logs, surface measurements, and geostatistical interpolation. The 5,000 boring logs used for hydrogeologic unit encoding were reviewed to determine whether the geologic descriptions accompanying the boring logs indicated the depth of the uppermost basalt layer underlying the unconfined aquifer. Only boreholes whose locations (coordinates) were known with some confidence were used. The TOB surface elevations at basalt outcroppings on or near Hanford were measured using a global positioning system device. Some TOB surface elevation values were taken from USGS topographic maps of Gable Mountain, Gable Butte, and Rattlesnake Mountain, which are massive outcroppings of the Elephant Mountain basalt, the formation underlying the unconfined aquifer at Hanford. Uncertainty estimates were assigned to each TOB elevation value.

The TOB surface encoded in the *TC & WM EIS* MODFLOW groundwater flow model is a geostatistical interpolation of the basalt-elevation data points from approximately 850 Hanford boring logs and 18 control points (see Figure L–22). Of the 18 control points, 12 are "structural," representing site knowledge about TOB surface elevation where there were limited or no data available, and 6 are "visual," added to improve the depiction of the TOB surface. Nine of the 12 structural control points were added along the Columbia River where it enters Hanford to position the TOB surface beneath the river. The other three structural control points were added at borehole (well) locations where the boring did not extend completely to the basalt, but only to the Ringold Formation Lower Mud Unit, which lies atop the basalt where it occurs. At these three locations, the TOB surface was estimated from other nearby borings that went deep enough to encounter the Ringold Formation Lower Mud Unit and the underlying basalt. Four of the six visual control points were added north of Gable Butte and Gable Mountain along the known position of the Gable Mountain Fault (see Figure L–22). The visual control points along the Gable Mountain Fault do not affect the simulated elevation of the TOB surface in Gable Gap (see Table L–4). The other two visual control points were added at Yakima Ridge. These two visual control points are not expected to affect the flow field in the operational areas of the site because of their distance from the operational areas (several kilometers to the south) and the predominant direction of groundwater flow (easterly).
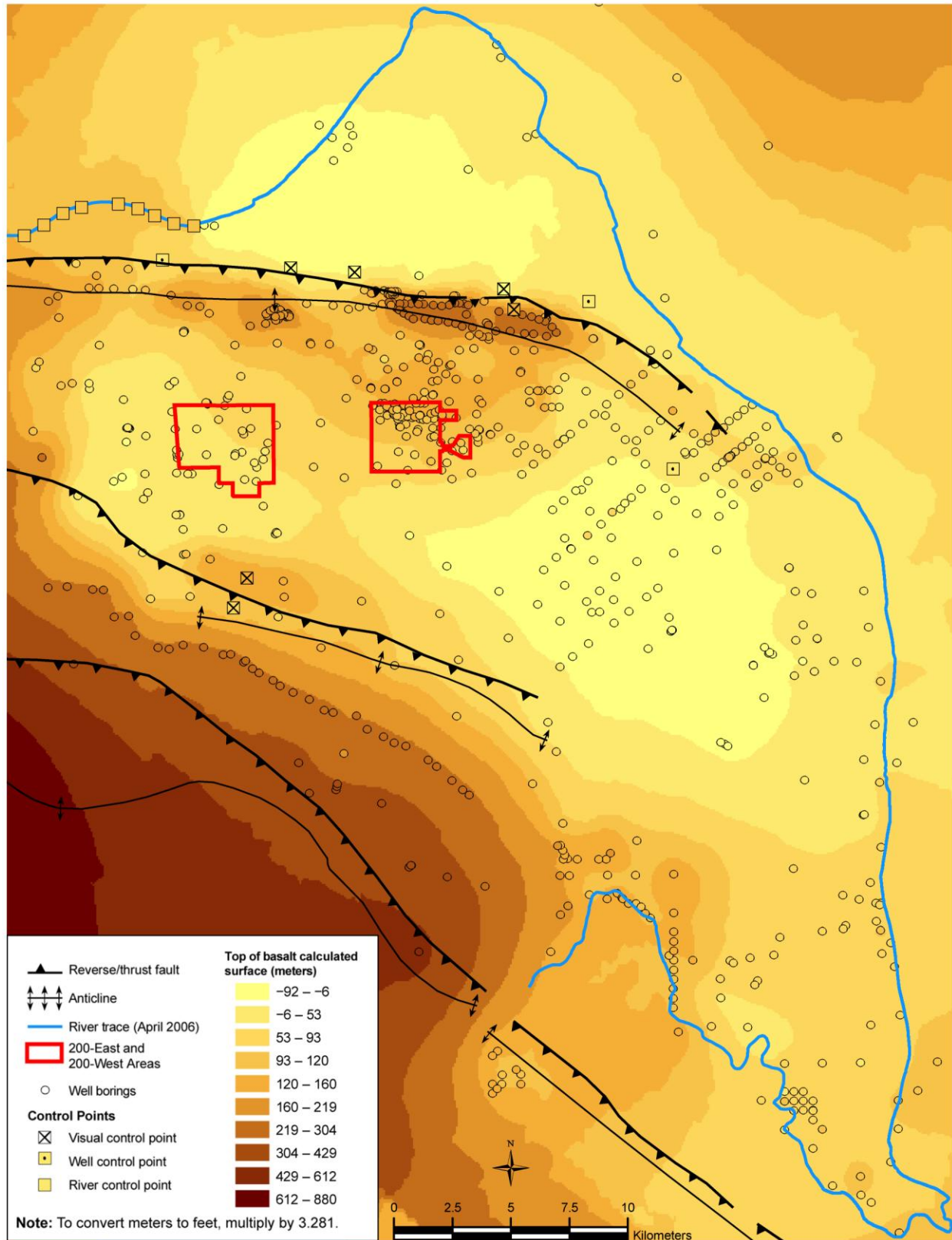
Figure L–22. Interpolated Top-of-Basalt Surface at the Hanford Site Showing Faults and Anticlines

Table L–4. Effect of Visual Control Points on Top-of-Basalt "Cutoff"[a] Elevation in Gable Gap

Visual Control Points	Gable Gap Cutoff Elevation[a] (meters)	MODFLOW Layer (elevation in meters)	Notes
None	120.8407	11 (120–121)	–
5	120.8409	11 (120–121)	Includes new visual control points YRCP-1, YRCP-2, GMFCP-1, GMFCP-2, and GMFCP-3
6	120.8412	11 (120–121)	Includes five visual control points listed above and GMFCP-4 (closest to Gable Gap)

[a] Lowest maximum elevation along MODFLOW flow path through Gable Gap.
Note: To convert meters to feet, multiply by 3.281.
Key: Gable Gap=Gable Mountain–Gable Butte Gap; MODFLOW=modular three-dimensional finite-difference groundwater flow model.

The TOB surface encoded into the *TC & WM EIS* groundwater flow model was interpolated from the data and control points using ArcGIS Version 9.1, ArcInfo Level with Geostatistical Analyst Extension (Johnston et al. 2001). The interpolated TOB surface is not sensitive to the parameter settings assigned in ArcGIS. To make this determination, the TOB surface for the MODFLOW flow field model domain was interpolated by ordinary kriging using ArcGIS for the cases listed in Table L–5. The resulting TOB Gable Gap cutoff elevations, also shown in Table L–5, indicate that the interpolated TOB surface is insensitive to the parameter settings assigned in ArcGIS.

Table L–5. Top-of-Basalt "Cutoff"[a] Elevation in Gable Mountain–Gable Butte Gap Based on ArcGIS Parameter Settings

Run	Description	Top-of-Basalt Elevation (meters)[b]
Default	Geostatistical Analyst (Johnston et al. 2001) default settings.	121
Variant 1	Reduce major range from default (22,580 m) to 22,354 m.	121
Variant 1a	Reduce major range from default (22,580 m) to 21,451 m.	121
Variant 2	Reduce minor range to 22,354 m; model direction = 0 degrees.	121
Variant 2a	Reduce minor range to 21,451 m. Major range = 22,580 and model direction = 0.	121
Variant 3	Minor range 22,354 m; model direction = 356 degrees.	121
Variant 3a	Reduce minor range to 21,451 m and change model direction to 352 degrees (or 172 degrees).	121
Variant 4	Reduce partial sill from default (12,519 m) to 12,394 m.	121
Variant 4a	Reduce partial sill from default (12,519 m) to 11,893 m.	121
Variant 5	Increase nugget from default (0 m) to 15 m.	121
Variant 5a	Increase nugget from default (0 m) to 150 m.	121
Variant 6	Partial sill 12,394; increase nugget to 125 m; constant sill.	121
Variant 6a	Reduce partial sill from default (12,519 m) to 11,893 m and increase nugget to 626 m.	120
Variant 7	Increase number of neighbors to include per sector from default (5) to 6, "Include at Least" 2.	120
Variant 7a	Increase number of neighbors to include per sector from default (5) to 7, "Include at Least" 2.	120
Variant 8	Reduce lag size from default (4,859.2 m) to 4,810.7 m.	121
Variant 8a	Reduce lag size from default (4,859.2) to 4,616 m.	121

Table L–5. Top-of-Basalt "Cutoff"[a] Elevation in Gable Mountain–Gable Butte Gap Based on ArcGIS Parameter Settings *(continued)*

| Run	Description	Top-of-Basalt Elevation (meters)[b]
Variant 9	Increase number of lags to 13.	121
Variant 9a	Increase number of lags to 14.	121
Variant 10	Lag size 4,810.7 m; number of lags 13.	121
Variant 10a	Reduce lag size from default (4,859.2 m) to 4,616 m and increase number of lags to 14.	121

[a] Lowest maximum elevation along MODFLOW flow path through Gable Mountain–Gable Butte Gap.
[b] Grid is 200 by 200 m (harmonic mean).
Note: To convert meters to feet, multiply by 3.281.
Key: m=meter; MODFLOW=modular three-dimensional finite-difference groundwater flow model.

The final TOB surface was interpolated using ordinary kriging with the default settings (see Figure L–23). The resulting TOB surface was output to a raster file containing the elevation of the center point of each cell of the 200- by 200-meter (656- by 656-foot) grid of the *TC & WM EIS* groundwater flow model. These values were used to encode the TOB surface at the proper vertical layer in the MODFLOW groundwater flow model. For each MODFLOW cell, the TOB surface was assigned to the layer containing the TOB elevation if the TOB elevation was greater than the midpoint of the layer; otherwise, the TOB surface was assigned to the next-lower layer. The cell to which the TOB surface was assigned and all lower cells were made inactive, i.e., assigned the "no-flow" condition.
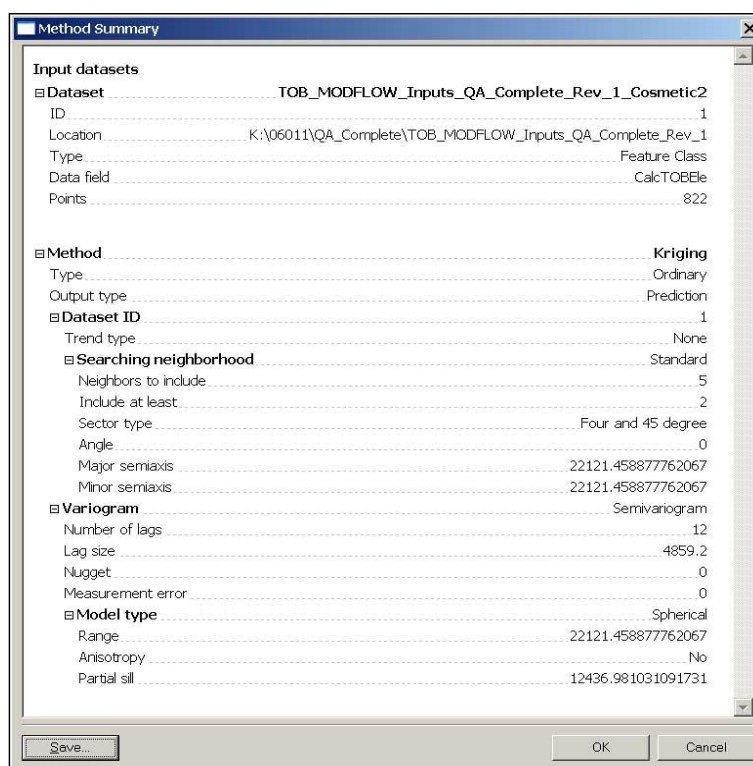
Figure L–23. Screen Print of Default Settings from Top-of-Basalt Surface Interpolation Using ArcGIS Geostatistical Analyst

The impact on the flow field of lower TOB elevations in Gable Gap is evaluated in the *Draft TC & WM EIS* (Appendix L, Sections L.2.2 and L.10.2). The lowest TOB elevation in Gable Gap, i.e., the "cutoff" elevation, determines the water level at which flow to the north through the gap is possible. One hundred TOB surfaces were created by randomly selecting the TOB elevation for each of the 849 borings and 12 structural control points from a normal distribution, with the mean equal to the reported TOB elevation and the interval size equal to twice the elevation uncertainty estimate. The results indicated that there are multiple possible locations for the gap to occur, with different elevation values. The mean elevations of the three most frequent locations correspond to cutoffs encoded in the groundwater flow model at approximately 118 meters (387 feet), 121 meters (397 feet), and 122 meters (400 feet) above MSL. Less than 5 percent of the realizations have a cutoff elevation lower than 118.5 meters (389 feet) above MSL. The TOB surface encoded in Gable Gap for the *Draft TC & WM EIS* groundwater flow model Alternate Case (Appendix L, Section L.2.2) was interpolated from a random TOB elevation data set with a cutoff value of 117.8 meters (387 feet) above MSL.

L.4.3.2.2   Suprabasalt Sedimentary Layers

Hanford boring logs were examined to discern textural layers of mud, silt, sand, and gravel within the Hanford and Ringold Formations and Cold Creek and Plio-Pleistocene Units. Individual layers were assigned to 1 of 13 material types (see Table L–6). The resulting lithological profiles—well name, well location, ground surface elevation, starting and ending depths of each layer, and each layer's assignment to the textural types—were imported into a database program that generates geologic cross sections.

Table L–6. Abundance of Textural Types in the
MODFLOW *Final TC & WM EIS* Groundwater Flow Model: Base Case

Textural Type (Model Material Type Zone)	Unweighted (Cells)	Unweighted Percent	Weighted (km³)	Weighted Percent
Hanford mud (1)	245	0.05	0.05	0.04
Hanford silt (2)	2,238	0.43	0.30	0.28
Hanford sand (3)	33,066	6.35	8.63	7.98
Hanford gravel (4)	131,826	25.30	17.69	16.37
Ringold sand (5)	27,333	5.25	10.27	9.51
Ringold gravel (6)	171,245	32.87	37.78	34.96
Ringold mud (7)	52,637	10.10	20.98	19.41
Ringold silt (8)	1,757	0.34	0.47	0.43
Plio-Pleistocene sand (9)	115	0.02	0.06	0.05
Plio-Pleistocene silt (10)	186	0.04	0.09	0.09
Cold Creek sand (11)	3,444	0.66	0.40	0.37
Cold Creek gravel (12)	31,724	6.09	2.35	2.18
Highly conductive Hanford formation (13)	64,223	12.33	8.97	8.30
Activated basalt (14)[a]	967	0.19	0.04	0.04

[a] Zone 14 (Activated basalt) was assigned to mitigate rewetting problems (see Section L.5.1.1) and was encoded over nine model layers.

Note: To convert cubic kilometers to cubic miles, multiply by 0.2399.

Key: km³=cubic kilometers; MODFLOW=modular three-dimensional finite-difference groundwater flow model.

Hydrostratigraphic cross sections were constructed using HydroGeo Analyst, Version 3.0 (WHI 2005). Transects for these cross sections are located in the exact middle of a MODFLOW grid row (or column), and have a 100-meter (328-foot) buffer on either side. Thus, each cross section represents one row (or column) of the *TC & WM EIS* groundwater flow model. Transect length varies, but generally cross sections do not span the entire model domain. Lithological profiles for boreholes located within the

buffer area are projected onto the cross section for stratigraphic interpretation and interpolation. Elevations of contacts between the discrete geologic layers are determined by the resulting cross sections. Geologic layers within the cross section are encoded into the groundwater flow model based on elevation, from 165 meters (541 feet) above MSL down to the TOB surface. If more than one geologic layer is contained within one MODFLOW cell, the cell was assigned the properties of the hydrostratigraphic type with the largest total thickness over the range of elevations represented by the MODFLOW layer. At elevations near the water table (115 to 125 meters [377 to 410 feet]), this approach allows encoding of features on the order of several meters in thickness. At elevations deeper in the aquifer, the vertical grid spacing increases, and the minimum thickness of features that can be represented in the model ranges from several to tens of meters (see Figure L–18). The overall thickness of the model domain is approximately 250 meters (820 feet). At a minimum, features with thicknesses of about 10 percent of the overall model domain (25 meters [82 feet]) are represented in the model, which is appropriate for a regional-scale representation.

The hydrostratigraphy encoded into the *TC & WM EIS* groundwater flow model on the basis of HydroGeo Analyst cross sections was fine-tuned to remove artifacts associated with the encoding of adjacent transects, thus to ensure consistency with the final TOB surface, to eliminate rewetting problems (see Section L.5.1.1), and to add zonation within textural types. Fine-tuning involved re-encoding the MODFLOW stratigraphy to achieve the following:

- Remove incongruities due to extrapolation from the borehole out to the edge of the transect (seam).

- Remove incongruities due to truncation of the lithology that should extend out to the seam.

- Remove incongruities due to extrapolation of the lowest layer of the borehole down to the TOB surface.

- Remove incongruities due to the incorrect assignment to textural types.

- Remove inconsistent assignment to mud or silt from the same formation.

- Eliminate disconnects due to the lack of a shared face at the seam (edge contact only).

- Extend the lithology laterally or vertically to the TOB surface.

- Activate the basalt in the Gable Gap area at elevations where the water table fluctuates to mitigate rewetting problems. See Section L.5.1.1 for more-detailed information.

- Add a zone of high hydraulic conductivity extending from north of Gable Gap and through the Gable Gap, as well as south and southeast through the central area of the model domain. This change was a result of Local Users' Group input, Technical Review Group input, and testing that improved the match between model-simulated hydraulic heads and field-observed hydraulic heads across the model domain. See Section L.4.3.2.3 for additional details regarding this highly conductive material type.

In this *Final TC & WM EIS*, changes were made to the hydrostratigraphy to extend eastward the line where the hydrostratigraphy transitions from lower-conductivity materials in the 200-West Area to the higher-conductivity materials in the 200-East Area. A more detailed discussion of this change is included in Section L.1.6.

L.4.3.2.3   Identification of the Highly Conductive Hanford Formation

The *TC & WM EIS* groundwater flow model requires information about the spatial distribution of the hydraulic conductivity of sedimentary materials across the 1,518-square-kilometer (586-square-mile) Hanford Site. The sedimentary materials identified at Hanford include fluvial and lacustrine materials of the Miocene-Pliocene Ringold Formation, fluvial and eolian sediments of the Plio-Pleistocene and Cold Creek Units, and the Pleistocene glaciofluvial sediments resulting from cataclysmic flood events that are characteristic of the Hanford formation (Bjornstad and Lanigan 2007; Lindsey 1995; Reidel and Chamness 2007; Reidel et al. 2006; Serne et al. 2010). Sediments that make up the Hanford unconfined water table include members of all three units and vary spatially across the site.

Measured hydraulic conductivities of the Hanford sediments range from 0.0001 meters (0.00033 feet) per day for the finer Ringold mud sediments up to about 1 million meters (3,281,000 feet) per day for the Hanford coarser flood deposits (Cole et al. 2001; DOE 1988). The conductivity of the coarser sand- and gravel-dominated Hanford sediments is generally orders of magnitude greater than either the Cold Creek or Ringold sediments (Bjornstad et al. 2010). Estimates of the hydraulic conductivity for coarse Hanford materials range from about 10 to 6,000 meters (33 to 19,686 feet) per day, with an estimated maximum of 10,000 meters (32,810 feet) per day, in contrast to Ringold Formation sediments that have hydraulic conductivities ranging from 0.1 to approximately 200 meters (0.33 to approximately 656 feet) per day (Cole et al. 2001; DOE 1988). Cold Creek sediments have conductivities intermediate between Hanford and Ringold sediments (Bjornstad et al. 2010).

Several lines of evidence suggest that the spatial distribution and range of hydraulic conductivities of aquifer materials at Hanford have an important influence on the non-uniform, potentiometric surface that defines the water potential for the Hanford unconfined aquifer. The first is the field observation that the potentiometric surface is very steep across the western part of the Central Plateau near the 200-West Area and flattens considerably through Gable Gap and across the eastern parts of the Central Plateau near the 200-East Area (see Figures L–48, L–49, and L–50). The differences in the steepness of the groundwater potential gradient has been ascribed to contrasts in the lower hydraulic conductivities of Ringold sediments dominant in the 200-West Area relative to the higher hydraulic conductivities of Hanford and Cold Creek sediments that dominate aquifer materials near Gable Gap, the 200-East Area, and areas farther east (Bjornstad et al. 2010).

The second line of evidence is field measurements of hydraulic conductivity (see Figure L–42) that indicate the range in hydraulic conductivity among the geologic materials present at the Hanford water table. As Figure L–42 shows, the conductivity of Hanford (and Cold Creek) sediments implies a much higher and broader range of saturated hydraulic conductivities relative to the Ringold sediments. The highest hydraulic conductivities measured at Hanford occur in the Hanford and Cold Creek sediments that stretch in a southeast direction from the 100 B/C Area, through Gable Gap, across the Central Plateau through the 200-East Area, and into the 300 Area. Some of this area, particularly near Gable Gap and the 200-East Area, has been mapped as buried paleochannels, where the Pleistocene flooding has deposited Hanford formation materials directly on the TOB (Bjornstad et al. 2010).

The third line of evidence is available field data showing that the calibration of all groundwater flow models developed for the Hanford unconfined aquifer has required a zone of high-conductivity material at the water table to appropriately reproduce the contrast in the groundwater potential gradient from the western to eastern portion of Hanford (Cole et al. 2001; Thorne et al. 2006; Wurstner et al. 1995). The location of those high-conductivity materials that ensure the best calibration of the models is based on the field data for hydraulic conductivity measured in aquifer pump tests (see Figure L–42).

L.4.4 Material Properties

The different textural types in the Hanford, Ringold, and other sedimentary hydrostratigraphic units are characterized by different material properties. Material properties required for the groundwater flow model include hydraulic conductivity, specific storage, and specific yield. Hydraulic conductivity is a measure of how easily water moves through pore spaces. Specific storage of a saturated aquifer is the amount of water that a given volume of aquifer material will release under a unit change in hydraulic head. Specific yield is the volumetric fraction of the bulk aquifer volume that an aquifer will yield when all the water is allowed to drain out of it under the forces of gravity.

Material properties for unconsolidated sediments below the water table are required for MODFLOW calculations. In MODFLOW, material of a given type can have only one value for a property, e.g., hydraulic conductivity. Each of the 14 material types encoded in the *TC & WM EIS* groundwater flow model (see Table L–6) has a unique combination of values for the several material properties. Material properties in the *Final TC & WM EIS* Base Case model are the same as the material properties used in the *Draft TC & WM EIS* Base Case model. The sensitivity of the *Final TC & WM EIS* Base Case model to changes in material properties, as well as to changes in other parameters, is evaluated and discussed further in Section L.7.

L.5 MODEL INPUTS – ALGORITHM SELECTION, PARAMETERS, AND SETTINGS

Some model inputs are independent of site data. These inputs include initial conditions and settings specifying how to make the calculations and how to modify the model to eliminate numerical instabilities that may arise. Some of the inputs are required by the MODFLOW software (e.g., rewetting rules), while others are common to all groundwater simulation models (e.g., time-stepping settings and initial conditions). These data-independent model inputs are discussed in the following sections.

L.5.1 Rewetting Methods

MODFLOW allows for cells to become dry (inactive) if the simulated head falls below the elevation of the cell bottom. Conversely, if the simulated head rises above the cell bottom or the laterally adjacent cells are wet, a currently dry cell can become wet. This process is called rewetting. The rewetting rules and parameters used to develop the *TC & WM EIS* groundwater flow model were generally the default parameters of MODFLOW 2000 (USGS 2004). The settings selected in Visual MODFLOW for the *TC & WM EIS* groundwater flow model are given in Table L–7.

Table L–7. Visual MODFLOW Rewetting Settings

Option	Setting
Activate cell wetting	On
Wetting threshold	0.1
Wetting interval	1 (iteration)
Wetting method	From below
Wetting head	Calculated from neighboring cells
Head value in dry cells	-1×10^{30} (meters)
Minimum saturated thickness for bottom layer	0.01 (meters)

Note: To convert meters to feet, multiply by 3.281.

Key: MODFLOW=modular three-dimensional finite-difference groundwater flow model.

L.5.1.1   Mitigation of Rewetting Problems

Rewetting problems emerged during model development that required mitigating actions. The rewetting problems were encountered in areas within the model where the water table and the TOB (inactive model cells) were at or near the same elevation and resulted in dry model cells in areas that should have been wet, based on the elevation of the water table in surrounding active model cells. Based on the model's rewetting settings, once an active model cell becomes dry, it can only be rewet from an active wet model cell below the active dry model cell. In the problem cases, the cell below the active dry model cell was an inactive cell that represented the TOB in that area within the model. This configuration would not allow the active dry model cell to rewet even though water table elevations in surrounding active wet model cells would normally result in rewetting of the problem dry model cell. This problem was significant enough that mitigation was required in the area of the model that represents Gable Gap.

To mitigate the rewetting problem in the Gable Gap area within the model, inactive cells that represented the TOB were made active and assigned hydraulic conductivity values that are more than 500 times lower than that of Hanford and Ringold muds (0.001 meters [0.00328 feet] per day). Making the inactive cell active and using a low hydraulic conductivity value allowed the active water table cells above the TOB to rewet from below, but maintained the TOB in this region as a low-permeability boundary. The TOB was activated in the Gable Gap area within the model between 124 meters (407 feet) above MSL and 115 meters (377 feet) above MSL.

L.5.2   Time-Stepping Settings

The *TC & WM EIS* groundwater flow model period of analysis is 10,000 years, from 1940—prior to the start of operations—to 11,940. In addition to the model preconditioning described in Section L.5.4, Initial Head Distribution, the model is further preconditioned by simulating CYs 1940 through 1943 (pre-Hanford) in transient mode prior to the occurrence of any anthropogenic recharge influxes (see Section L.4.2.5). The model then continues running in transient mode to capture the time-varying anthropogenic recharge influxes and the resulting water table fluctuations. Anthropogenic inputs are applied in 1-year stress periods beginning in 1944. The final stress period begins in 2022 and ends in 11,940. A stress period is defined as a period of time during the model simulation when all of the model's boundary conditions are static (i.e., unchanging).

L.5.3   Numerical Engine Selection and Parameterization

The numeric engine selected for simulating groundwater flow was MODFLOW 2000, Version 1.15.00 (USGS 2004), which is public domain software supported by Visual MODFLOW, Version 2009.1. The settings selected in Visual MODFLOW for the *TC & WM EIS* groundwater flow model are given in Table L–8.

Table L–8. Visual MODFLOW Numerical Solution Settings

Option	Setting
Simultaneous equation solver	Preconditioned conjugate-gradient (PCG2)
Preconditioning method	Modified incomplete Cholesky
Cholesky relaxation parameter	0.98
Maximum outer iterations	500
Maximum inner iterations	200
Head change criterion	0.01 (meter)
Residual criterion	5,000
Damping factor	1
Printout interval	10 (time steps)

Note: To convert meters to feet, multiply by 3.281.
Key: MODFLOW=modular three-dimensional finite-difference groundwater flow model.

The preconditioned conjugate-gradient package for solving simultaneous equations is described in USGS Water-Resources Investigations Report 90-4048 (Hill 1990). Modified incomplete Cholesky preconditioning of the hydrogeologic parameter matrix is efficient on scalar (nonvector) computers (SWS 2009). Outer iterations vary the preconditioned matrix of hydrogeologic parameters of the flow system (e.g., transmissivity, saturated thickness) in an approach toward the solution. Inner iterations continue until the user-defined maximum number of inner iterations has been executed or the final convergence criteria are met. Outer iterations continue until the final convergence criteria are met on the first inner iteration after an update. Both the head change and residual criteria determine convergence of the solver. The head change criterion is used to judge the overall solver convergence; the residual criterion is used to judge the convergence of the inner iterations of the solver. The damping factor allows the user to reduce the head change calculated during each successive outer iteration.

L.5.4   Initial Head Distribution

Pre-Hanford head observation data are not available. The *TC & WM EIS* groundwater flow model was assigned an initial arbitrarily high water table and run in transient mode for 500 years to simulate pre-Hanford (1940–1943) conditions with only natural recharges applied per the *Technical Guidance Document* (DOE 2005). This initial 500-year model run approached long-term, steady state conditions, which were assumed to represent pre-Hanford conditions.

L.5.5   Layer Properties

The layer property package used in the *TC & WM EIS* groundwater flow model is the Block-Centered Flow (BCF) package, which simulates flow in an unconfined aquifer. See Table L–9 for the BCF package run settings.

Table L–9. Visual MODFLOW BCF Package Settings

Settings	Values
CUNIT	1
Extension	.BCF
HDRY	-1×10^{30}
LUNIT	11

Key: BCF=Block-Centered Flow; MODFLOW=modular three-dimensional finite-difference flow model.

L.6   CALIBRATION STRATEGY

The *TC & WM EIS* groundwater flow model was calibrated to heads observed beginning in 1948. Artificial recharges during Hanford operations, especially those from 1944 to the mid-1990s, produced mounding of groundwater underneath the 200-East and 200-West Areas on the Central Plateau of Hanford (see Section L.4.2.5). Groundwater mounding influenced the local direction of flow and transport and consequently needed to be accurately represented in the long-term groundwater flow model.

Model calibration to head was conducted in the following three process steps:

1. Prepare a calibration data set consisting of observed groundwater (head) levels across Hanford during the calibration period of 1948–2008 and the preconditioning period of 1940–1943. This data set was updated between the *Draft* and *Final TC & WM EIS*.

2. Specify the model calibration criteria, that is, how similar model results need to be compared with the observations in the calibration data sets. The model calibration criteria are unchanged between the *Draft* and *Final TC & WM EIS*.

3. Conduct the final model calibration using structured and Monte Carlo optimization methods. This method was used when calibrating the *Draft TC & WM EIS* groundwater flow model, and the details of that calibration process are presented in the *Draft TC & WM EIS*, Appendix L, Section L.9.

For the *Final TC & WM EIS* groundwater flow model, a calibration and uncertainty analysis was conducted to determine the model's sensitivity to changes in a variety of parameter values. This sensitivity analysis was used as part of the final calibration.

The technical approach to these steps and the results are discussed in Sections L.6, L.7, and L.8.

L.6.1   Calibration Data Set

The *TC & WM EIS* groundwater flow model was calibrated to head data collected between 1948 and 2008 for a large number of selected wells scattered across the site. The data came from the HydroDat database of measured water table elevations provided by CH2M HILL and accepted by the *TC & WM EIS* team as quality assurance complete (CHPRC 2009a). This database includes approximately 136,000 observations at approximately 1,900 discrete locations. Wells were excluded from use in the head observation data set under the following conditions:

*   They were closer than 600 meters (1,969 feet) to the Columbia River to remove the periodic fluctuations in the river stage from the head observation data.

*   They were outside the active model domain because the model is not being calibrated in these areas.

*   They were screened in basalt because these observations measure head values within confined aquifers that are not part of this flow model calibration.

*   There were obvious data recording or entry errors, wells and/or observations with outlier data based on review of data in adjacent wells, or wells that were located in dry or inactive model cells.

Table L–10 details the number of well locations and observations that were removed from the original head observation data set.

Table L–10. Number of Well Locations and Head Observations Removed from Original Head Observation Data Set

Change	Number of Observations Remaining	Number of Wells Remaining
Original head observation data set	136,282	1,923
Removal of wells with data qualifiers	133,308	1,901
Removal of wells outside of the horizontal model domain	132,591	1,804
Removal of wells located within 600 meters (1,968 feet) of the Columbia River	99,224	1,430
Removal of wells screened in basalt	90,174	1,266
Removal of wells with duplicate locations	87,543	1,160
Averaging of observations for each well, screen, and year such that each well and/or screen has a single observation for each year	20,408	1,160
Edit and deletion of well locations and observations per detailed hydrograph and model review	15,996	713

The data from the remaining 713 wells were encoded into the flow model for use in the head calibration.

L.6.2   Calibration Criteria

The calibration data set was used to assess the ability of the model to accurately simulate water levels and flow direction in the past, which is an indication of its ability to accurately simulate water levels and flow direction in the future. The calibration criteria define acceptable model performance in terms of measures of similarity (difference) between observed and simulated values. The model calibration criteria are as follows:

- Residuals (differences between observed and modeled heads) should be reasonably distributed.

  - Residual distribution should be reasonably normal.

  - The mean residual should be approximately 0.

  - The number of positive residuals should approximate the number of negative residuals.

  - The correlation coefficient (calculated versus observed) should be greater than 0.9.

  - The RMS error (calculated versus observed) should be less than 5 meters (16.4 feet), approximately 10 percent of the gradient in the water table elevation.

- The residual distribution should meet the needs of this *TC & WM EIS*.

  - Residuals in the 200-East Area should be distributed similarly to those in the 200-West Area.

  - The residuals should be evenly distributed through the calibration period (1948–2008).

  - The residuals should be evenly distributed across the site.

- The calibrated parameters should compare reasonably well with field-measured values.

- Parameters should be reasonably uncorrelated. Correlation among the parameters is a symptom of a poorly posed problem with many nonunique solutions.

These criteria were used to assess the final head calibrations and are unchanged between the *Draft* and *Final TC & WM EIS*.

L.6.3   Development of Objective Function

The groundwater flow model was calibrated to observed hydraulic heads across Hanford during the calibration period (1948–2008). The objective of the head calibration was to minimize the difference between the model-simulated head values and the field-observed head values during the calibration period. All head observation data used in the head calibration were weighted equally. No concentration calibration was performed as part of the flow model development. Concentration calibration of the groundwater transport model is discussed in Appendix O.

L.7   CALIBRATION AND UNCERTAINTY ANALYSIS

The *Draft TC & WM EIS* analysis and results, along with public comments, led to a more detailed exploration of the model sensitivity to changes in the following model parameters:

- Hydraulic conductivity values
- Storage properties (specific yield [Sy])
- GHB head and conductance
- Background and anthropogenic recharge
- River conductance

RMS error was the measure of model sensitivity to each parameter.

L.7.1   Hydraulic Conductivity

No changes to hydraulic conductivity values were made in the *Final TC & WM EIS* flow model. To determine the sensitivity of the flow model to varying the hydraulic conductivity values across a reasonable range for the 13 material types used, a Monte Carlo analysis with 5,000 model realizations was developed. Table L–11 provides the range of hydraulic conductivity values applied in the analysis.

Table L–11. Range of Hydraulic Conductivity Values Used in Monte Carlo Analysis

Material Type (Model Zone)	Range of Horizontal Hydraulic Conductivity (Kh) Values (meters per day)
Hanford mud (1)	0.01 – 1.0
Hanford silt (2)	0.8 – 10.0
Hanford sand (3)	40.0 – 200.0
Hanford gravel (4)	75.0 – 300.0
Ringold sand (5)	0.5 – 5.0
Ringold gravel (6)	8.0 – 25.0
Ringold mud (7)	0.2 – 2.0
Ringold silt (8)	0.5 – 5.0
Plio-Pleistocene sand (9)	10.0 – 100.0
Plio-Pleistocene silt (10)	3.0 – 30.0
Cold Creek sand (11)	30.0 – 110.0
Cold Creek gravel (12)	0.1 – 120.0
Highly conductive Hanford formation (13)	1,500.0 – 5,000.0

Note: Vertical hydraulic conductivity = Kh × 0.1. To convert meters to feet, multiply by 3.281

In each of the 5,000 realizations, all 13 material types were varied randomly across the ranges listed in Table L–11. The results of this analysis show that the model is sensitive (in terms of the RMS error metric) to changes in hydraulic conductivity values across the ranges listed. Figure L–24 shows the range of RMS error values resulting from the approximately 4,000 converged model runs.

Note: To convert meters to feet, multiply by 3.281.
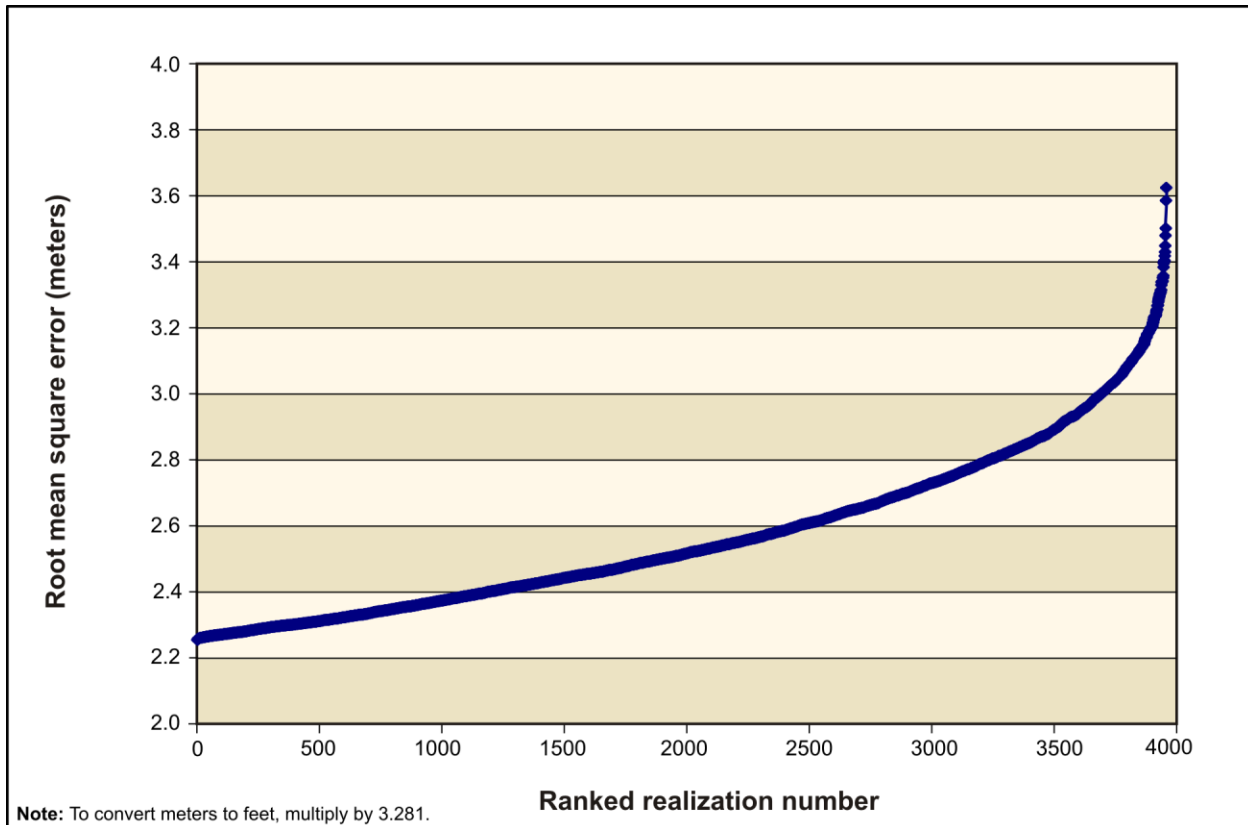
Figure L–24. Range of Root Mean Square Error for Varying Hydraulic Conductivity Values

L.7.2 Storage Properties (Specific Yield) Analysis

No changes to storage property values (expressed as Sy values) were made in the *Final TC & WM EIS* flow model. To determine the sensitivity of the model to varying the storage property values across a reasonable range for the 13 material types, a Monte Carlo analysis with 5,000 model realizations was developed. Approximately 4,700 were run to completion through the calibration period (1948 through 2008). Approximately 300 of the 5,000 runs did not converge. Table L–12 provides the range of Sy values applied in the analysis.

Table L–12. Range of Storage Property (Sy) Values Used in Monte Carlo Analysis

Material Type (Model Zone)	Range of Storage Property (Sy) Values
Hanford mud (1)	0.15 – 3.0
Hanford silt (2)	0.15 – 3.0
Hanford sand (3)	0.15 – 3.0
Hanford gravel (4)	0.15 – 3.0
Ringold sand (5)	0.15 – 3.0
Ringold gravel (6)	0.15 – 3.0
Ringold mud (7)	0.15 – 3.0
Ringold silt (8)	0.15 – 3.0
Plio-Pleistocene sand (9)	0.15 – 3.0
Plio-Pleistocene silt (10)	0.15 – 3.0
Cold Creek sand (11)	0.15 – 3.0
Cold Creek gravel (12)	0.15 – 3.0
Highly conductive Hanford formation (13)	0.15 – 3.0

Key: Sy=specific yield.

In each of the 5,000 realizations, all 13 material types were varied randomly across the ranges listed in Table L–12. The results of this analysis show that the model is not sensitive (in terms of RMS error) to changes in Sy values across the ranges listed. Figure L–25 shows the range of RMS error values resulting from the approximately 4,700 converged model runs.

Note: To convert meters to feet, multiply by 3.281.
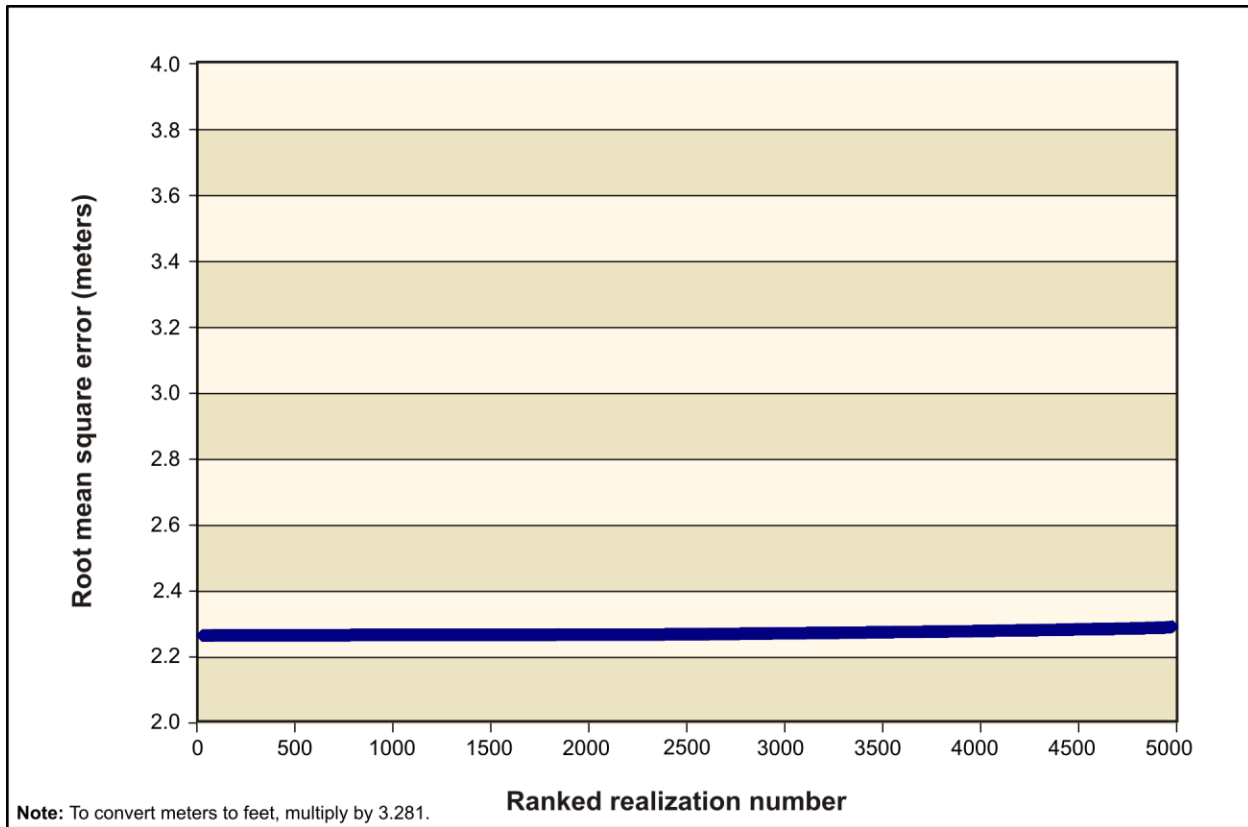
**Figure L–25. Range of Root Mean Square Error for
Varying Storage Property (Specific Yield) Values**

L.7.3   GHB Head and Conductance

L.7.3.1   GHB Head

No changes to GHB head values were made in the *Final TC & WM EIS* flow model. To determine the sensitivity of the model to varying the GHB head values across a reasonable range, head values at each of the GHB areas in the model (Cold Creek, Dry Creek, and Rattlesnake Mountain) were varied by adjusting the base values by +4, +2, 0, –2, and –4 meters. This structured approach to varying the GHB head values resulted in 125 model realizations, all of which converged. The results of this analysis show that the model was not highly sensitive (in terms of RMS error) to changes in GHB head values across the ranges listed. Figure L–26 shows the range of RMS error values resulting from the 125 converged model runs.
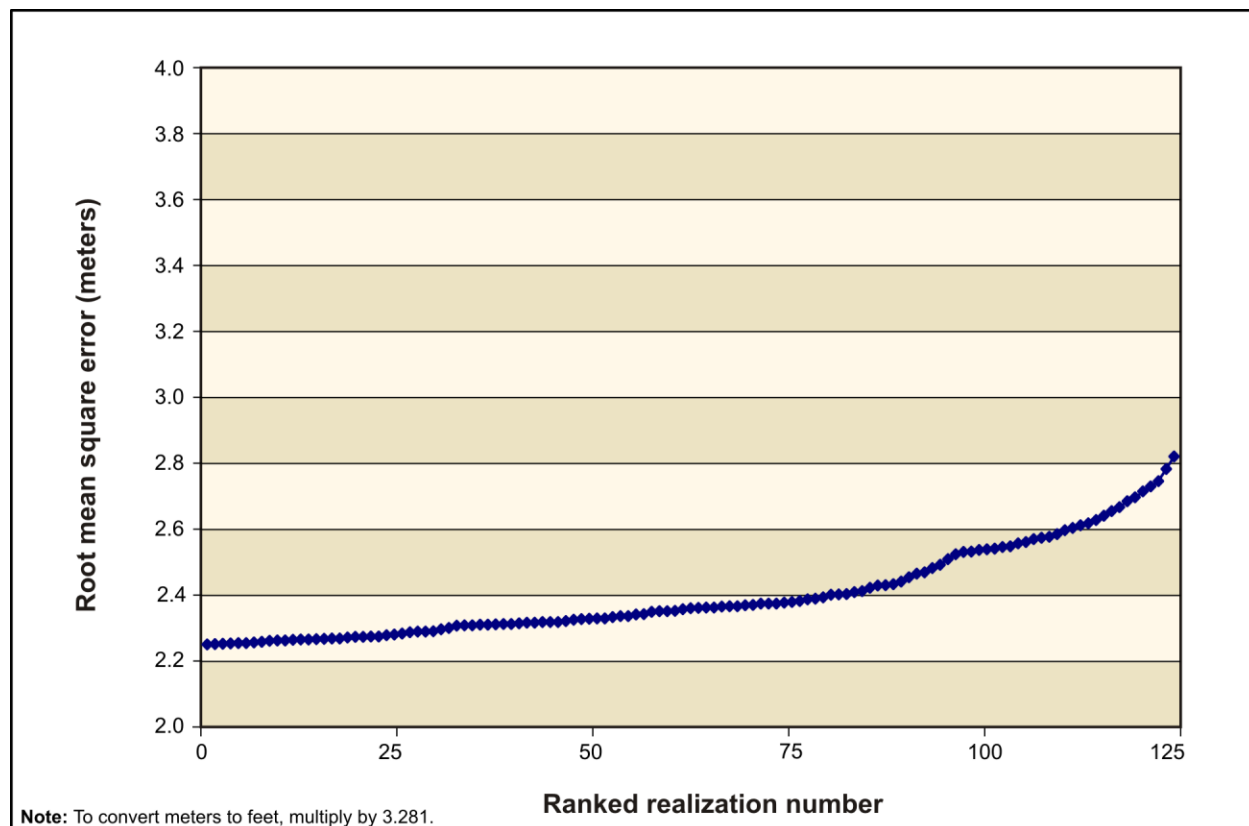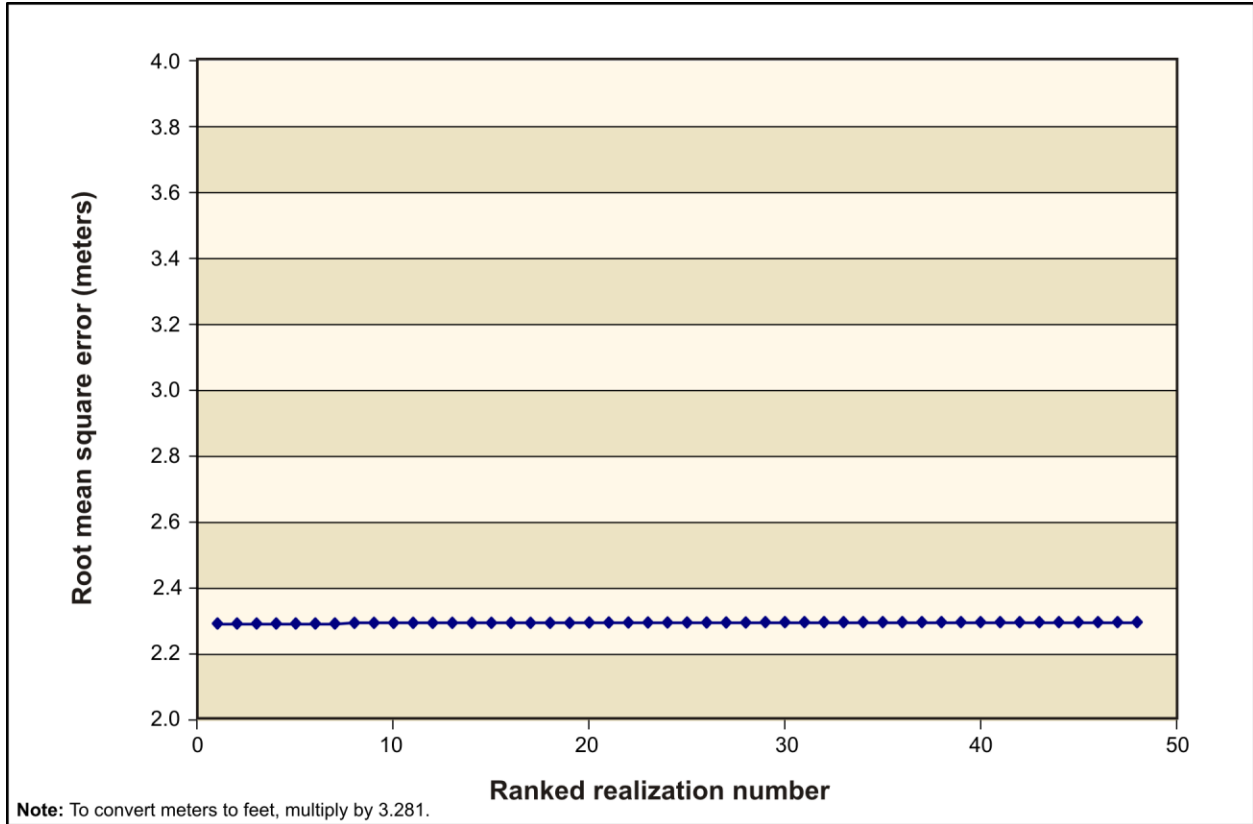
**Figure L–26. Range of Root Mean Square Error for
Varying Generalized Head Boundary Head Values**

L.7.3.2   GHB Conductance

No changes to GHB conductance values were made in the *Final TC & WM EIS* flow model. To determine the sensitivity of the model to varying the GHB conductance values across a reasonable range, conductance values at each of the GHB areas in the model (Cold Creek, Dry Creek, and Rattlesnake Mountain) were varied by multiplying the base values by 0.1, 0.5, 1.0, 5.0, and 10.0. This structured approach to varying the GHB conductance values resulted in 125 model realizations, most of which converged. The results of this analysis show that the model was not highly sensitive (in terms of RMS error) to changes in GHB head values across the ranges listed. Figure L–27 shows the range of RMS error values resulting from the 122 converged model runs.

Note: To convert meters to feet, multiply by 3.281.
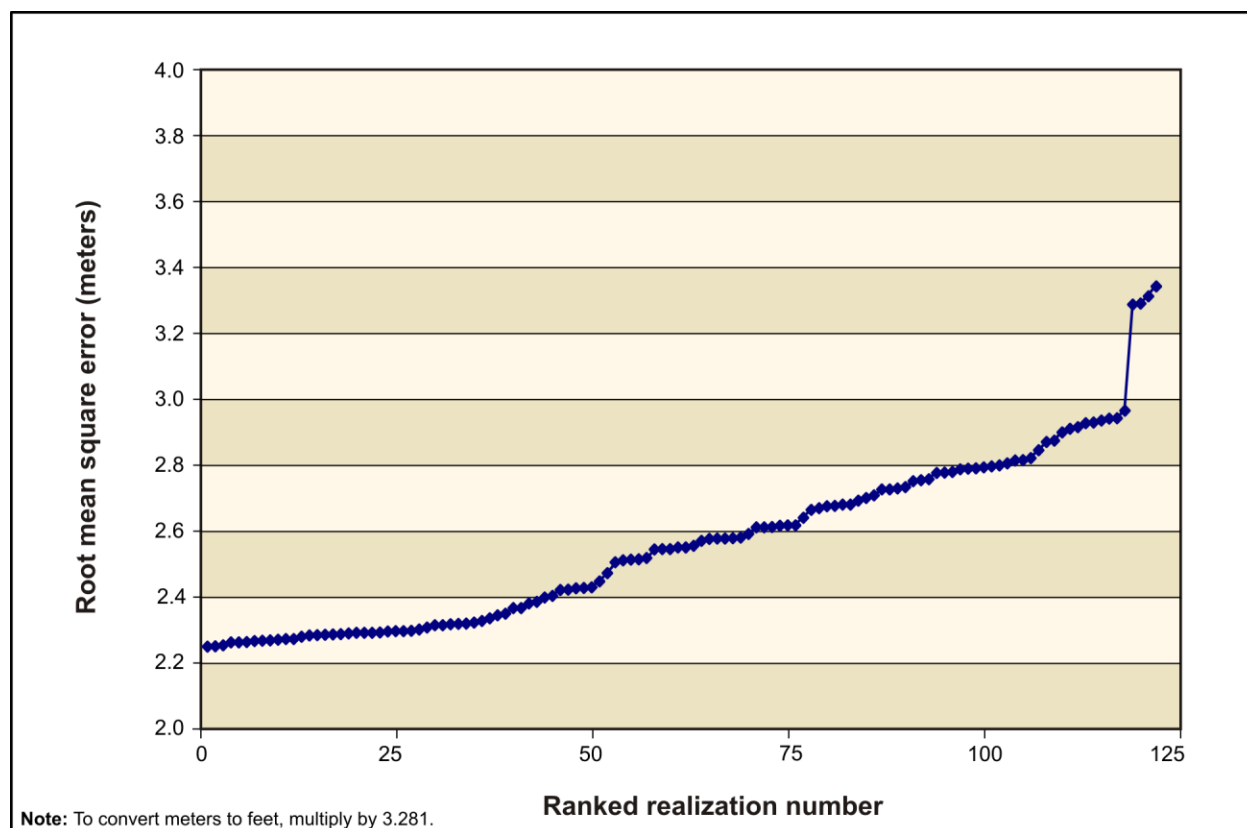
**Figure L–27. Range of Root Mean Square Error for
Varying Generalized Head Boundary Conductance Values**

L.7.4   Background and Anthropogenic Recharge

L.7.4.1   Background Recharge

No changes to background recharge values were made in the *Final TC & WM EIS* flow model. To determine the sensitivity of the model to varying the background recharge values across a reasonable range, recharge values for sitewide and City of Richland recharge zones in the model were varied as shown in Table L–13.

Table L–13. Range of Background Recharge Values Considered

Recharge Zone	Recharge Values (millimeters per year)
Sitewide	0.5
	1.5
	2.5
	3.5
	4.5
	5.5
	6.5
	7.5
	8.5
	9.5
	10.5
City of Richland	5
	15
	25
	35
	45
	55
	65
	75
	85
	95
	105

This structured approach to varying the background recharge values (including those of the Base Case) resulted in 122 model realizations, all of which converged. The results of this analysis show that the model was not sensitive (in terms of RMS error) to changes in background recharge values across the ranges listed. Figure L–28 shows the range of RMS error values resulting from the 122 converged model runs.
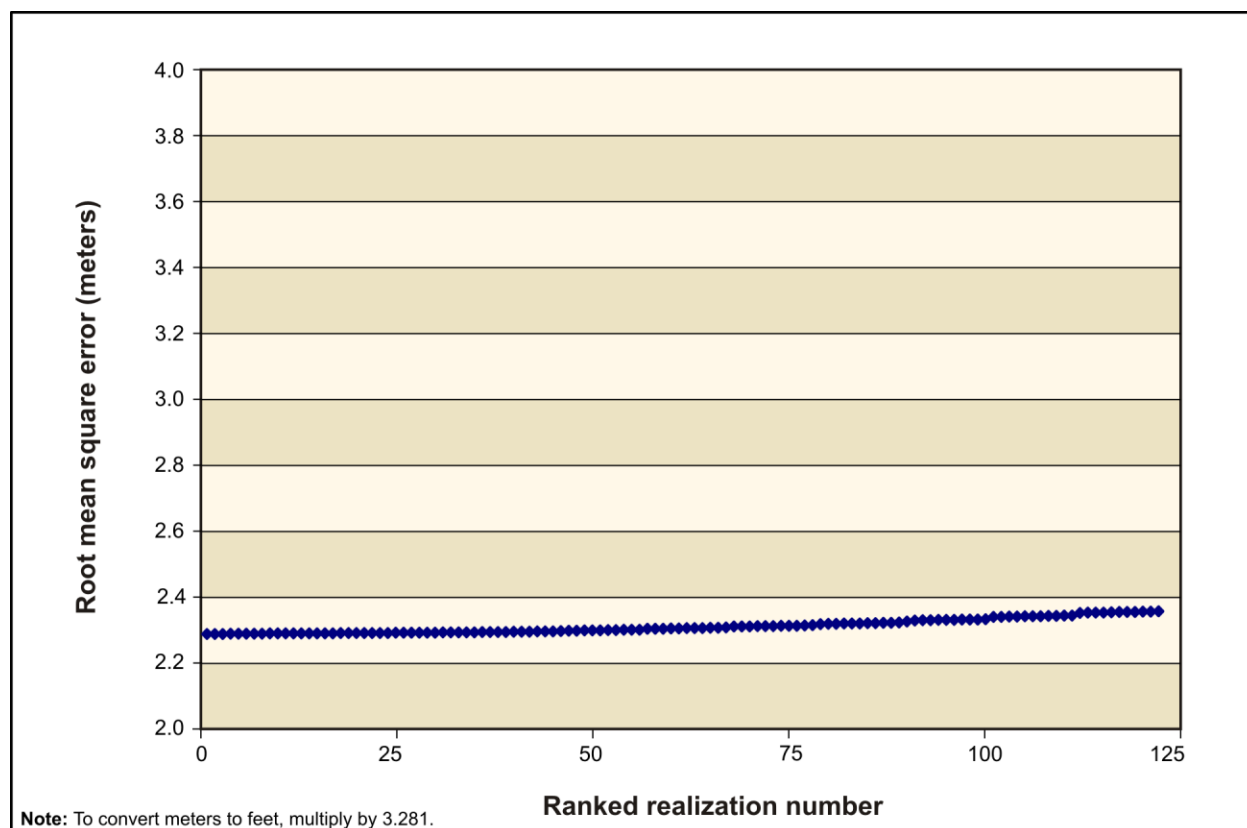
Figure L–28. Range of Root Mean Square Error for Varying Background Recharge Values

L.7.4.2   Anthropogenic Recharge

No changes to anthropogenic recharge values were made in the *Final TC & WM EIS* flow model. To determine the sensitivity of the model to varying the anthropogenic recharge values across a reasonable range, recharge values for approximately 130 recharge zones were varied randomly between 50 percent and 150 percent of the base values. Each recharge zone was varied independently from all other recharge zones in each of 5,000 model realizations, most of which converged. The results of this analysis show that the model was not sensitive (in terms of RMS error) to changes in anthropogenic recharge values across the ranges listed.   Figure L–29 shows the range of RMS error values resulting from the 4,970 converged model runs.

Note: To convert meters to feet, multiply by 3.281.
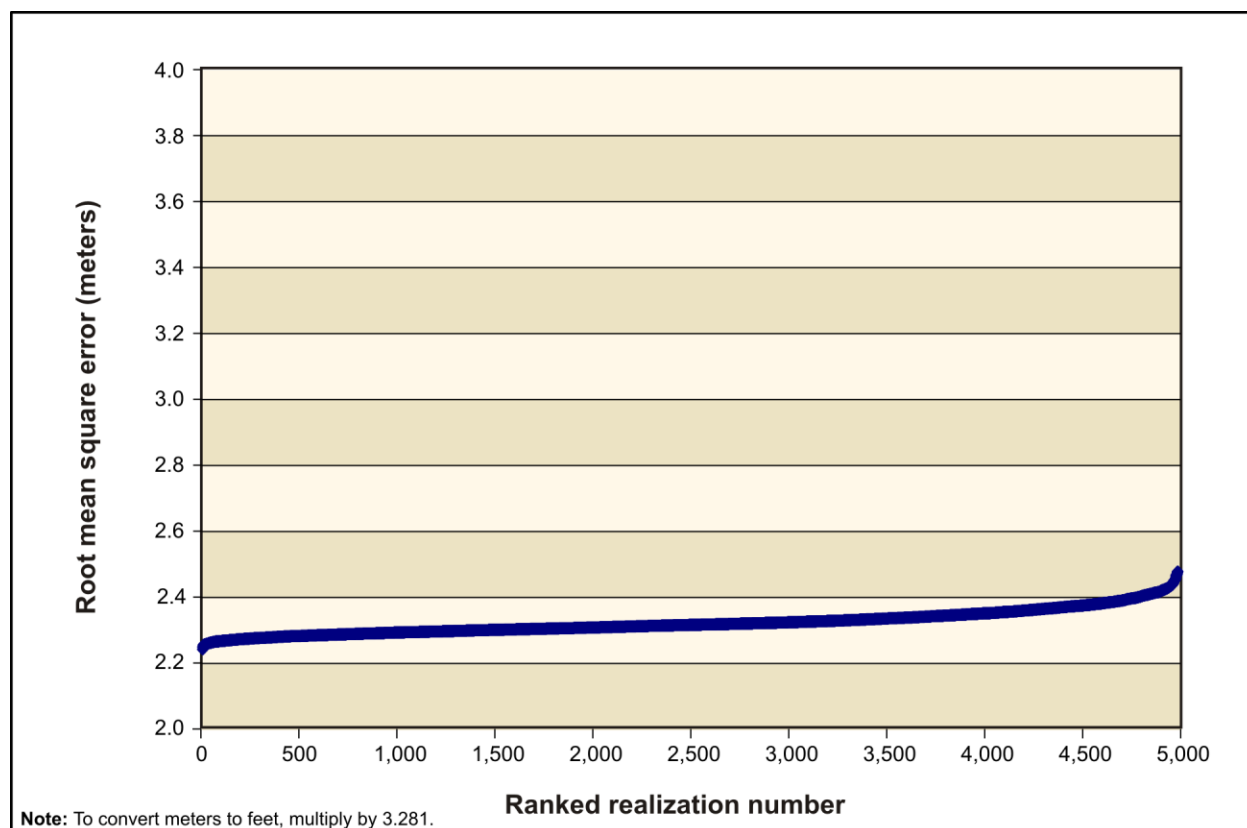
Figure L–29. Range of Root Mean Square Error for Varying Anthropogenic Recharge Values

L.7.5   River Conductance

No changes to river conductance values were made in the *Final TC & WM EIS* flow model. To determine the sensitivity of the model to varying the river conductance values across a reasonable range, river conductance values were varied using seven multipliers (0.1, 0.2, 0.5, 1.0, 2.0, 5.0, and 10.0) applied independently to the Columbia River and Yakima River reach base conductance values. Varying the conductance values in this structured way resulted in 49 model realizations, most of which converged. The results of this analysis show that the model was not sensitive (in terms of RMS error) to changes in river conductance values across the ranges listed. Figure L–30 shows the range of RMS error values resulting from the 48 converged model runs.

The above analyses demonstrated that the model was sensitive to changes in hydraulic conductivity values and not highly sensitive to the remaining parameters that were evaluated. The following section provides detailed results from three models that span the best one-third (in terms of RMS error) of models evaluated in the above hydraulic conductivity analysis.

Note: To convert meters to feet, multiply by 3.281.

Figure L–30. Range of Root Mean Square Error for Varying River Conductance Values

L.8   FLOW MODEL PERFORMANCE – TOP ONE-THIRD OF MODELS

Results from three models that are among the best one-third (in terms of RMS error) evaluated in the preceding section's sensitivity analysis for hydraulic conductivity are provided below. The ranking identifiers for each of the three models are as follows:

- 95th percentile (better than 95 percent of model realizations in terms of lowest RMS error), this being selected as the *Final TC & WM EIS* Base Case flow model.

- 100th percentile (best model realization in terms of lowest RMS error).

- 66th percentile (better than 66 percent of model realizations in terms of lowest RMS error).

The purpose of reviewing and evaluating the results of these three models is to determine whether there are significant differences in the model behavior across the top one-third of the flow models as ranked in the hydraulic conductivity sensitivity analysis.

L.8.1 Results from the 95th Percentile (Base Case) Flow Model

L.8.1.1 Calibration Acceptance

Table L–14 provides a restatement of the flow model calibration criteria discussed in Section L.6.2, along with an assessment of the 95th percentile (Base Case) flow model's performance against each criterion. Specific data illustrative of such performance are reflected in Tables L–15 and L–16 and Figures L–31 through L–42.

Table L–14. Summary of the 95th Percentile (Base Case) Flow Model
Performance Compared with the Calibration Acceptance Criteria

Flow Model Calibration Acceptance Criteria	95th Percentile (Base Case) Flow Model Performance
Residual distribution should be reasonably normal.	Residual distribution is reasonably normal (see Figure L–31).
The mean residual should be approximately 0.	Residual mean = 0.122 meters (0.400 feet) (see Figure L–32).
The number of positive residuals should approximate the number of negative residuals.	Positive residuals approximately equal negative residuals (see Figure L–31).
The correlation coefficient (calculated versus observed) should be greater than 0.9.	Correlation coefficient = 0.973 (see Figure L–32).
The root mean square (RMS) error (calculated versus observed) should be less than 5 meters (16.4 feet), approximately 10 percent of the gradient in the water table elevation.	RMS error = 2.281 meters (7.484 feet) (see Figure L–32).
Residuals in the 200-East Area should be distributed similarly to those in the 200-West Area.	Residuals in the 200-East and 200-West Areas are distributed similarly (see Figures L−33 and L−34).
The residuals should be evenly distributed over time.	Residuals are approximately evenly distributed over time (see Figures L−35, L−36, L−37, and L−38).
The residuals should be evenly distributed across the site.	Residuals are approximately evenly distributed across the site (see Figures L−39, L−40, and L−41).
The calibrated parameters should compare reasonably well with field-measured values.	Calibrated hydraulic conductivity values are listed in Table L–15 and compare reasonably with field-measured values for material types to which the model is sensitive (i.e., Hanford formation and Ringold Formation material types). Figure L–42 provides field-measured values from aquifer pumping tests (Cole et al. 2001).
Parameters should be reasonably uncorrelated.	Hydraulic conductivity parameters are reasonably uncorrelated (see Table L–15 for the key to model material type zones and Table L–16 for the correlation coefficient matrix).

**Table L–15. 95th Percentile (Base Case) Flow Model
Calibrated Hydraulic Conductivity Values**

Material Type (Model Zone)	Hydraulic Conductivity (K_x)[a]	Hydraulic Conductivity (K_y)[b]	Hydraulic Conductivity (K_z)[c]
Hanford mud (1)	0.171	0.171	0.0171
Hanford silt (2)	6.8	6.8	0.68
Hanford sand (3)	123.6	123.6	12.36
Hanford gravel (4)	156.0	156.0	15.6
Ringold sand (5)	3.57	3.57	0.357
Ringold gravel (6)	19.2	19.2	1.92
Ringold mud (7)	1.514	1.514	0.1514
Ringold silt (8)	1.51	1.51	0.151
Plio-Pleistocene sand (9)	96.8	96.8	9.68
Plio-Pleistocene silt (10)	5.81	5.81	0.581
Cold Creek sand (11)	99.13	99.13	9.913
Cold Creek gravel (12)	62.7	62.7	6.27
Highly conductive Hanford formation (13)	3982.0	3982.0	398.2
Activated basalt (14)	0.001	0.001	0.0001

[a] Hydraulic conductivity with respect to the *x* axis, meters per day.
[b] Hydraulic conductivity with respect to the *y* axis, meters per day.
[c] Hydraulic conductivity with respect to the *z* axis, meters per day.
Note: To convert meters to feet, multiply by 3.281.

Table L–16. Flow Model Hydraulic Conductivity Parameter Correlation Coefficient Matrix

Model Zone	1	2	3	4	5	6	7	8	9	10	11	12	13
1	1.00	–0.01	0.00	0.02	–0.02	0.00	0.00	0.02	0.00	0.04	0.00	0.01	0.01
2	–0.01	1.00	0.02	0.03	–0.03	0.01	–0.01	0.00	–0.03	0.02	–0.02	–0.01	–0.02
3	0.00	0.02	1.00	–0.03	0.02	0.00	0.02	–0.02	–0.02	0.01	0.01	–0.02	–0.02
4	0.02	0.03	–0.03	1.00	0.00	–0.03	–0.01	0.00	0.02	0.02	–0.01	–0.02	0.02
5	–0.02	–0.03	0.02	0.00	1.00	–0.02	0.01	–0.01	0.00	0.02	–0.02	0.00	–0.01
6	0.00	0.01	0.00	–0.03	–0.02	1.00	–0.03	–0.01	–0.01	0.01	0.03	–0.02	0.00
7	0.00	–0.01	0.02	–0.01	0.01	–0.03	1.00	0.00	0.00	0.00	0.01	0.00	–0.03
8	0.02	0.00	–0.02	0.00	–0.01	–0.01	0.00	1.00	–0.01	0.01	0.01	0.01	–0.01
9	0.00	–0.03	–0.02	0.02	0.00	–0.01	0.00	–0.01	1.00	0.02	0.01	0.00	–0.03
10	0.04	0.02	0.01	0.02	0.02	0.01	0.00	0.01	0.02	1.00	0.02	0.00	–0.03
11	0.00	–0.02	0.01	–0.01	–0.02	0.03	0.01	0.01	0.01	0.02	1.00	0.02	–0.02
12	0.01	–0.01	–0.02	–0.02	0.00	–0.02	0.00	0.01	0.00	0.00	0.02	1.00	0.01
13	0.01	–0.02	–0.02	0.02	–0.01	0.00	–0.03	–0.01	–0.03	–0.03	–0.02	0.01	1.00
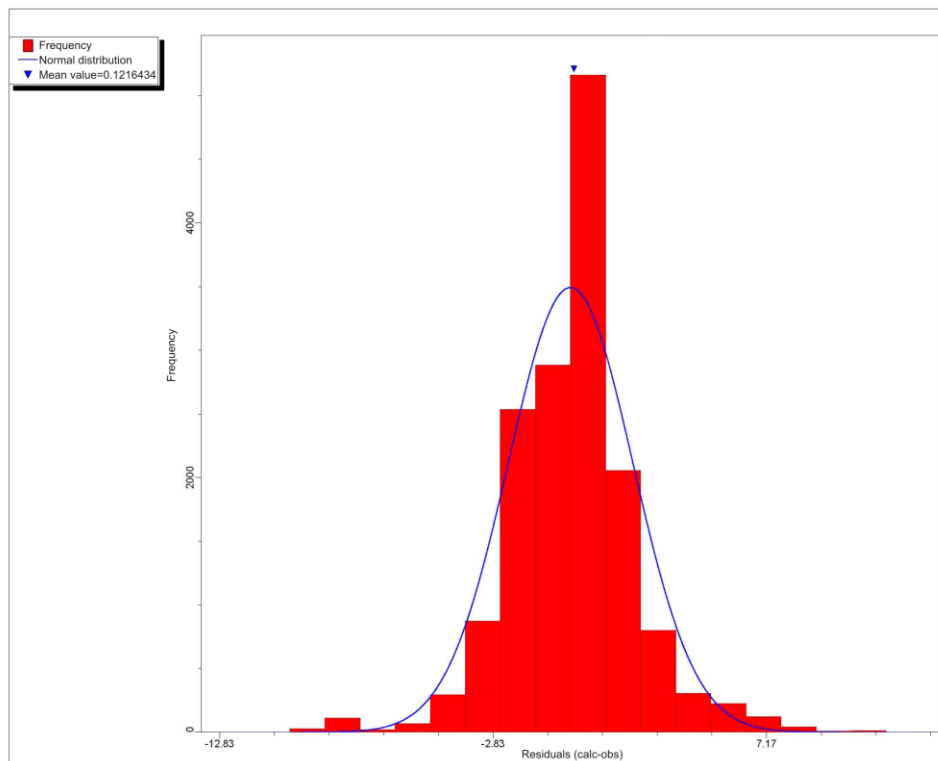
**Figure L–31. 95th Percentile (Base Case) Flow Model
Residual Distribution**
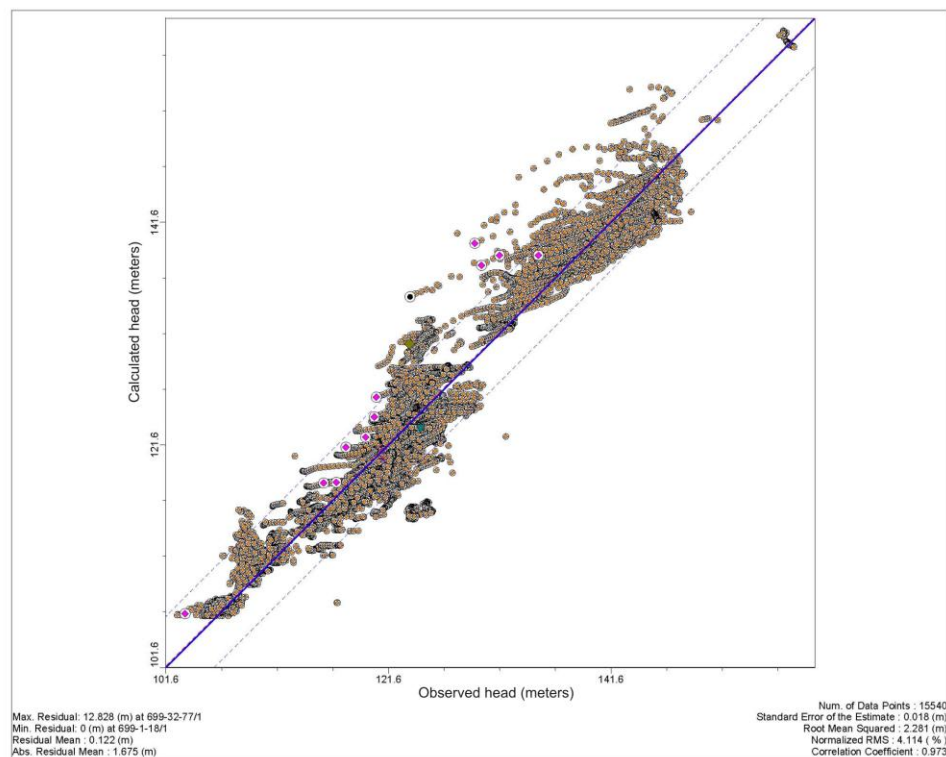
**Figure L–32. 95th Percentile (Base Case) Flow Model
Calibration Graph and Statistics**
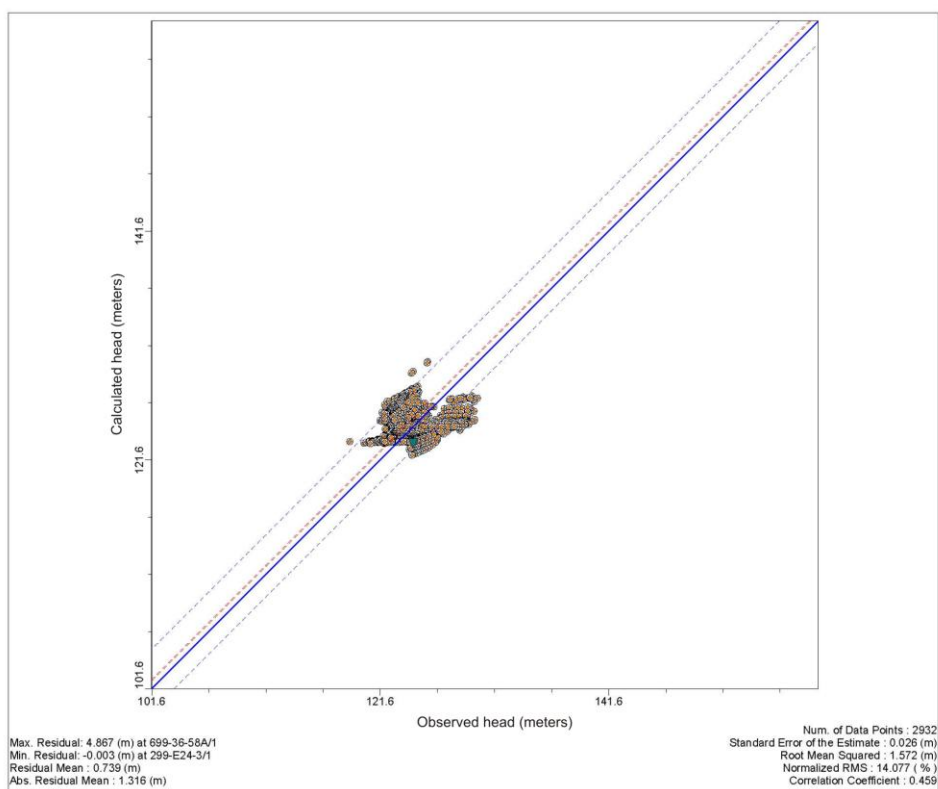
**Figure L–33. 95th Percentile (Base Case) Flow Model Residuals –
200-East Area**
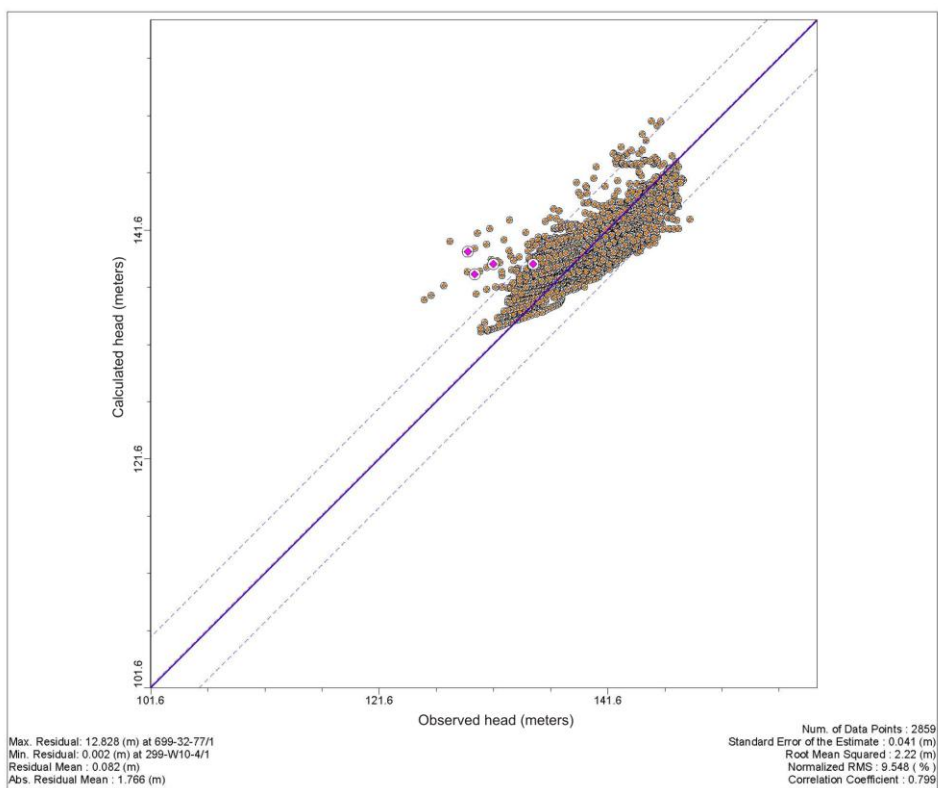
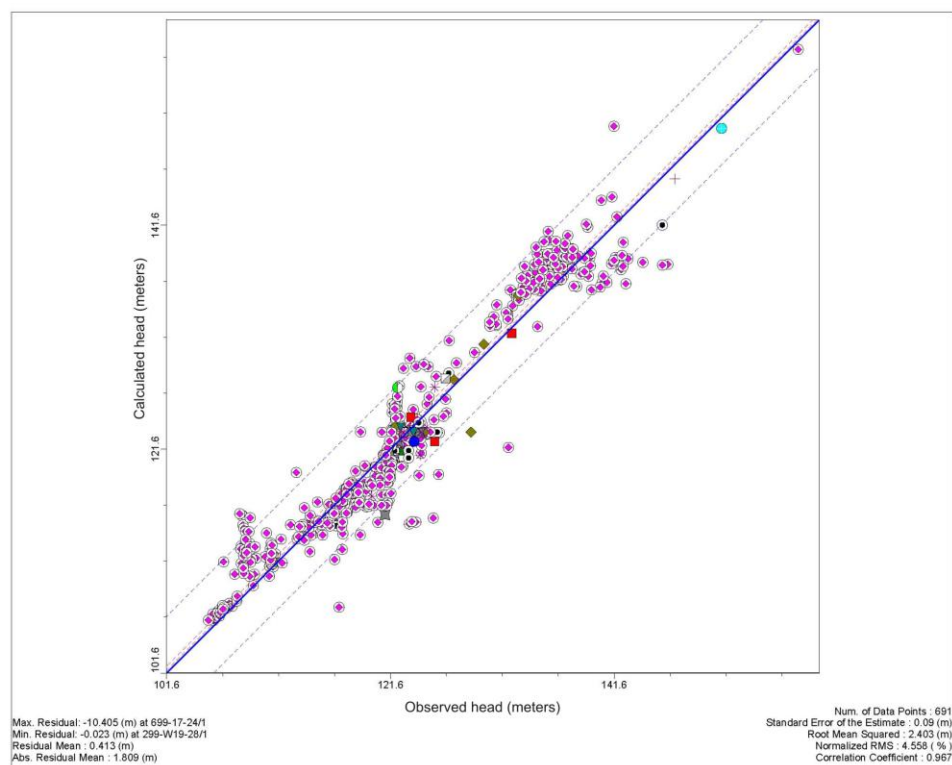**Figure L–34. 95th Percentile (Base Case) Flow Model Residuals –
200-West Area**
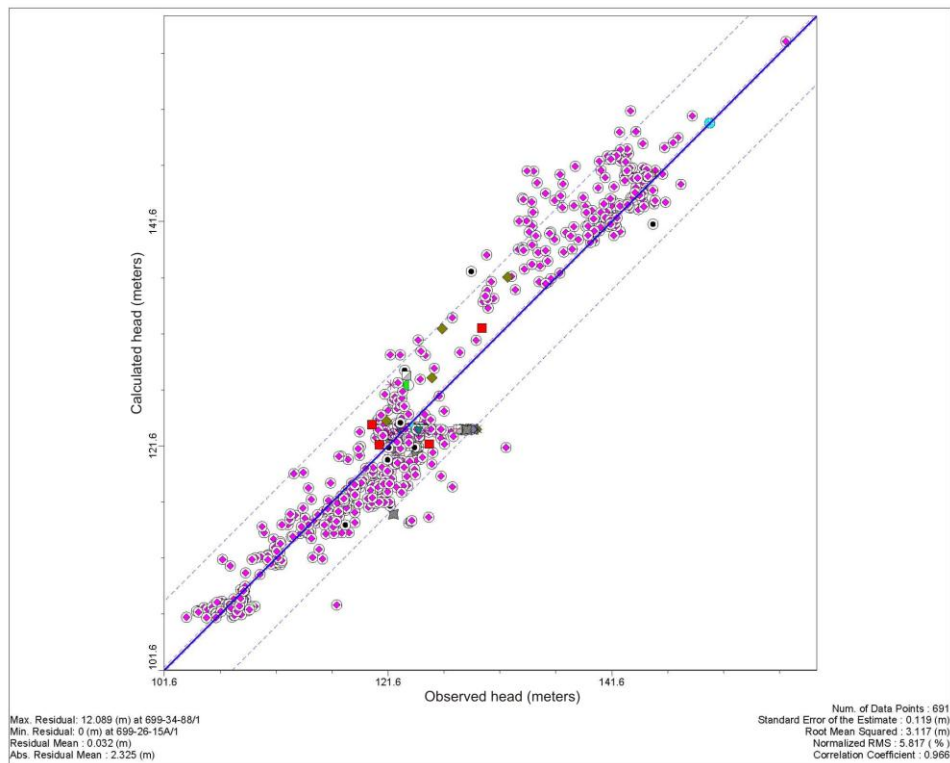
Figure L–35. 95th Percentile (Base Case) Flow Model Residuals,
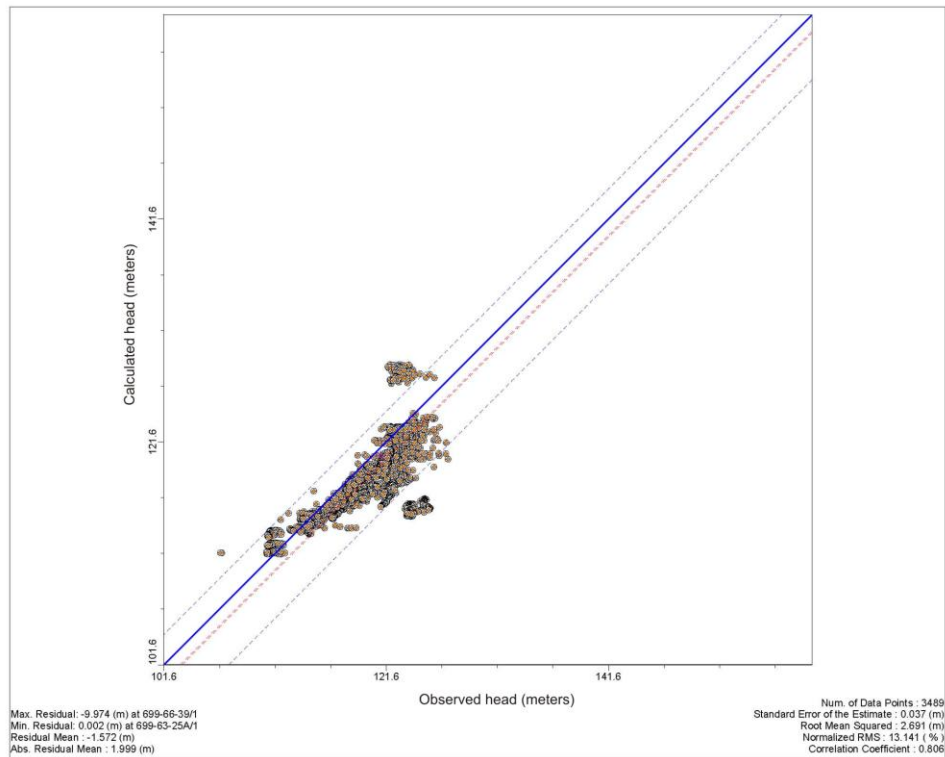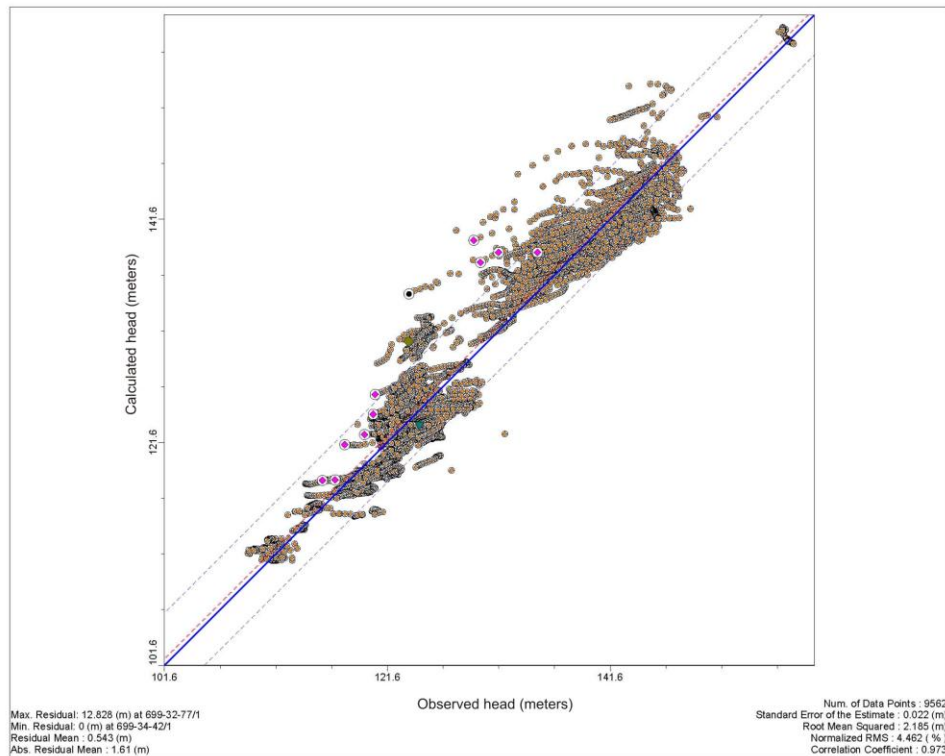**Calendar Year 1955**
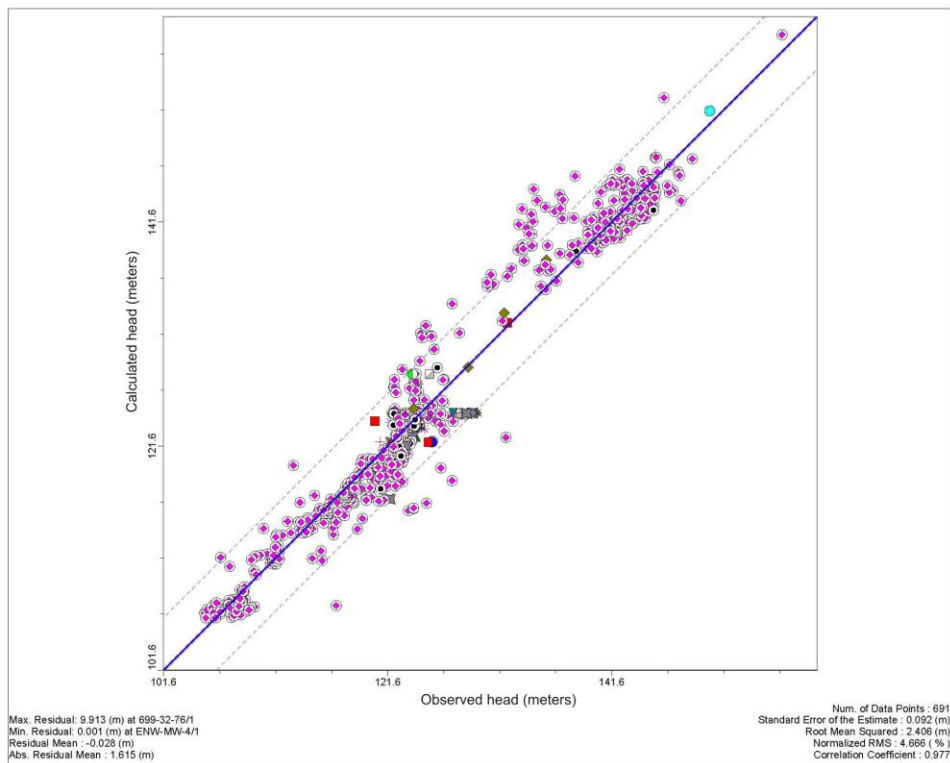
Figure L–36. 95th Percentile (Base Case) Flow Model Residuals,
Calendar Year 1975
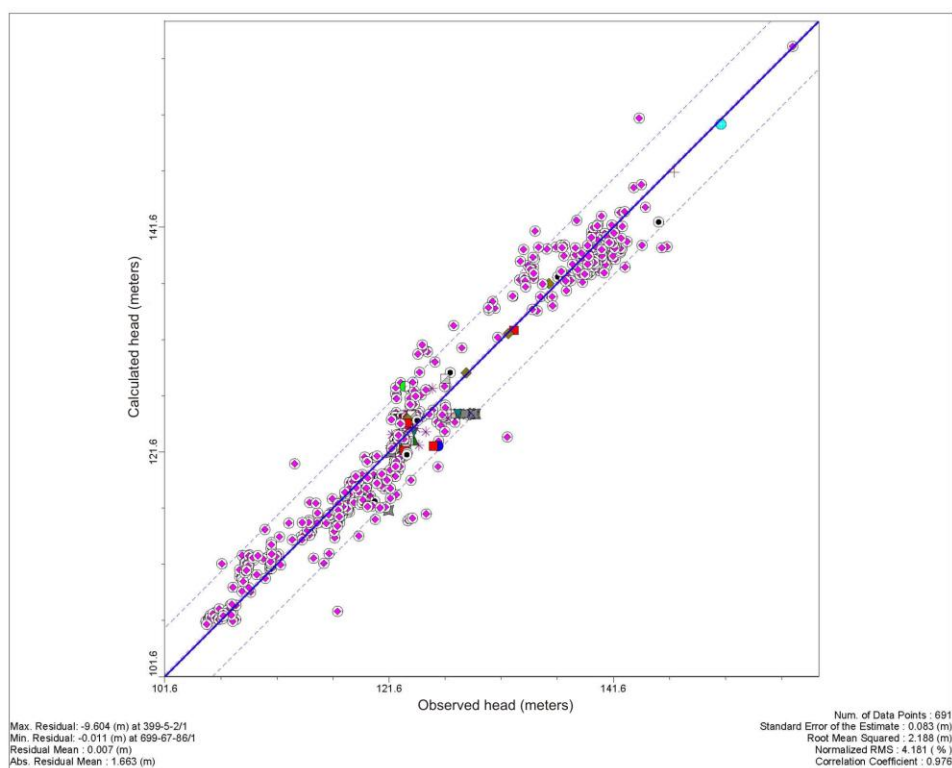
Figure L–37. 95th Percentile (Base Case) Flow Model Residuals, Calendar Year 1995

Figure L–38. 95th Percentile (Base Case) Flow Model Residuals, Calendar Year 2010

**Figure L–39. 95th Percentile (Base Case) Flow Model Residuals in
Northern Region of Model**

**Figure L–40. 95th Percentile (Base Case) Flow Model Residuals in
Central Region of Model**
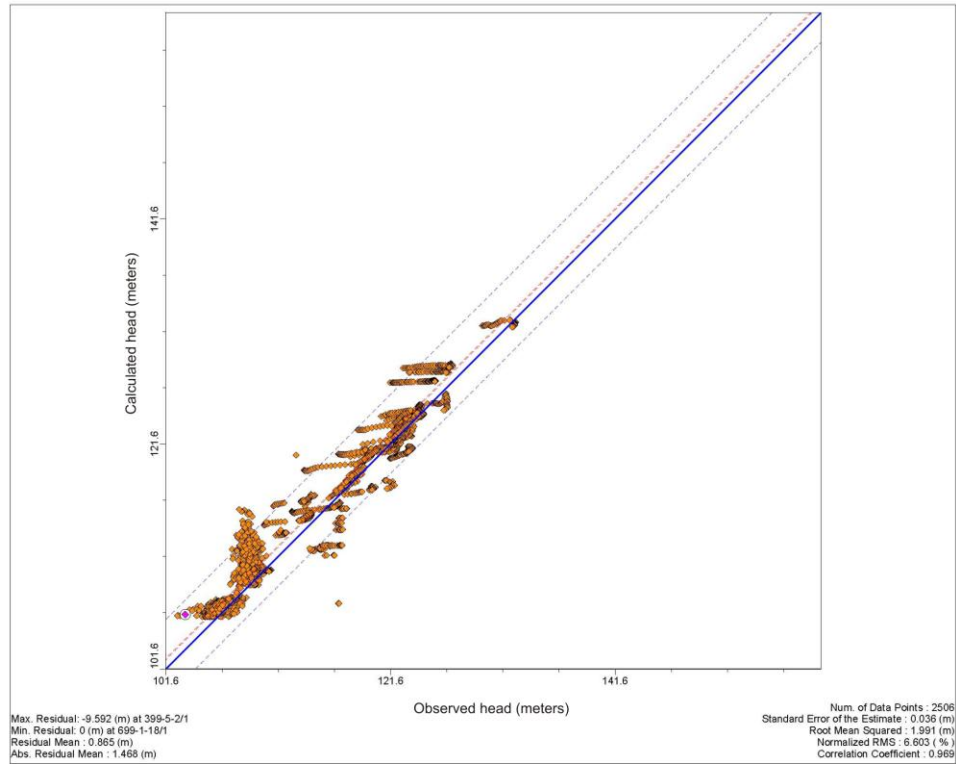
Figure L–41. 95th Percentile (Base Case) Flow Model Residuals in Southern Region of Model
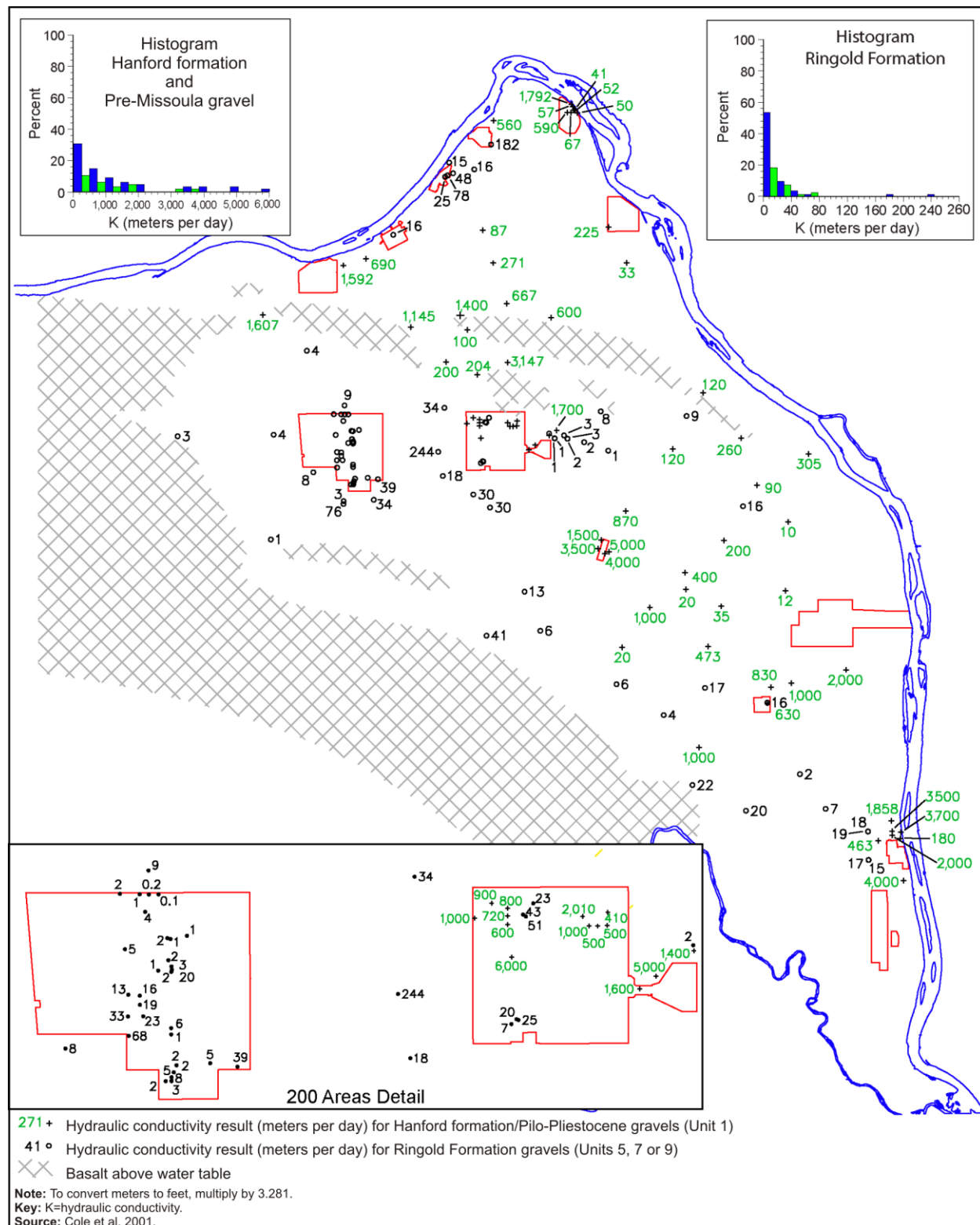
Figure L–42. Distribution of Wells with Hydraulic Conductivity Determined from Aquifer Pumping Tests

In addition to the calibration acceptance criteria, water (or mass) balance and a long-term, steady state condition must be achieved in the calibrated flow model. Cumulative mass water balance data are shown in Figure L–43, indicating a cumulative mass balance error of approximately –1.6 percent. Total water balance and storage data as a function of time are shown in Figure L–44. The Figure L–44 data show storage values relative to the total water balance and indicate that storage-in is approximately equal to storage-out in model year 261 (CY 2200). This indicates that a long-term, steady state condition is achieved. Note that, in Figure L–44, there is a spike in "storage" at model year 82. This spike is the result of a time-stepping change at the beginning of the final long-term stress period. As a result, the model is moving from a relatively long time step at the end of the previous stress period (model year 82) to a relatively short time step at the beginning of the final stress period.

Note: Year zero=calendar year 1940.
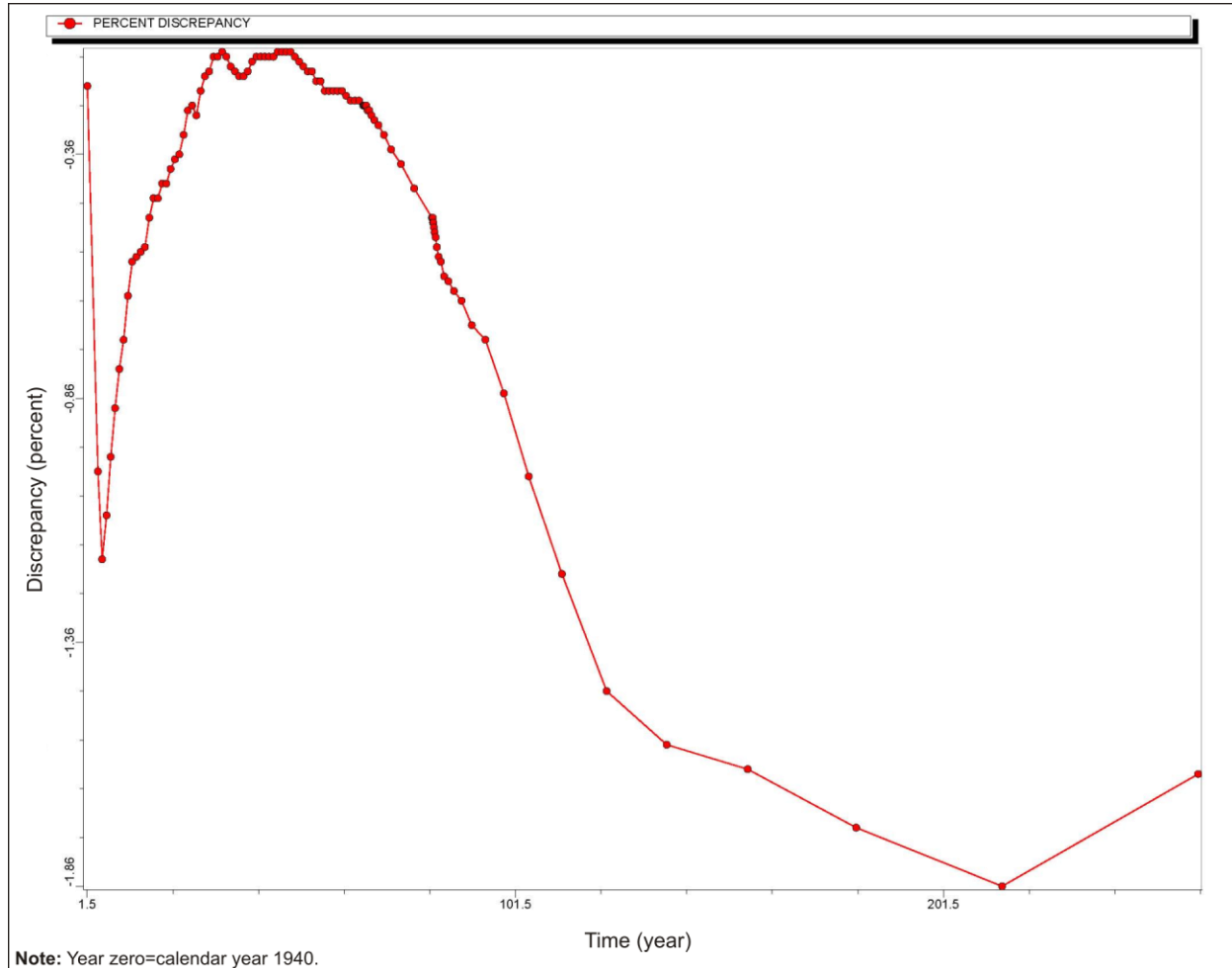
Figure L–43. 95th Percentile (Base Case) Flow Model Cumulative Water Balance Discrepancy

Note: Year zero=calendar year 1940. To convert cubic meters to cubic feet, multiply by 35.315.
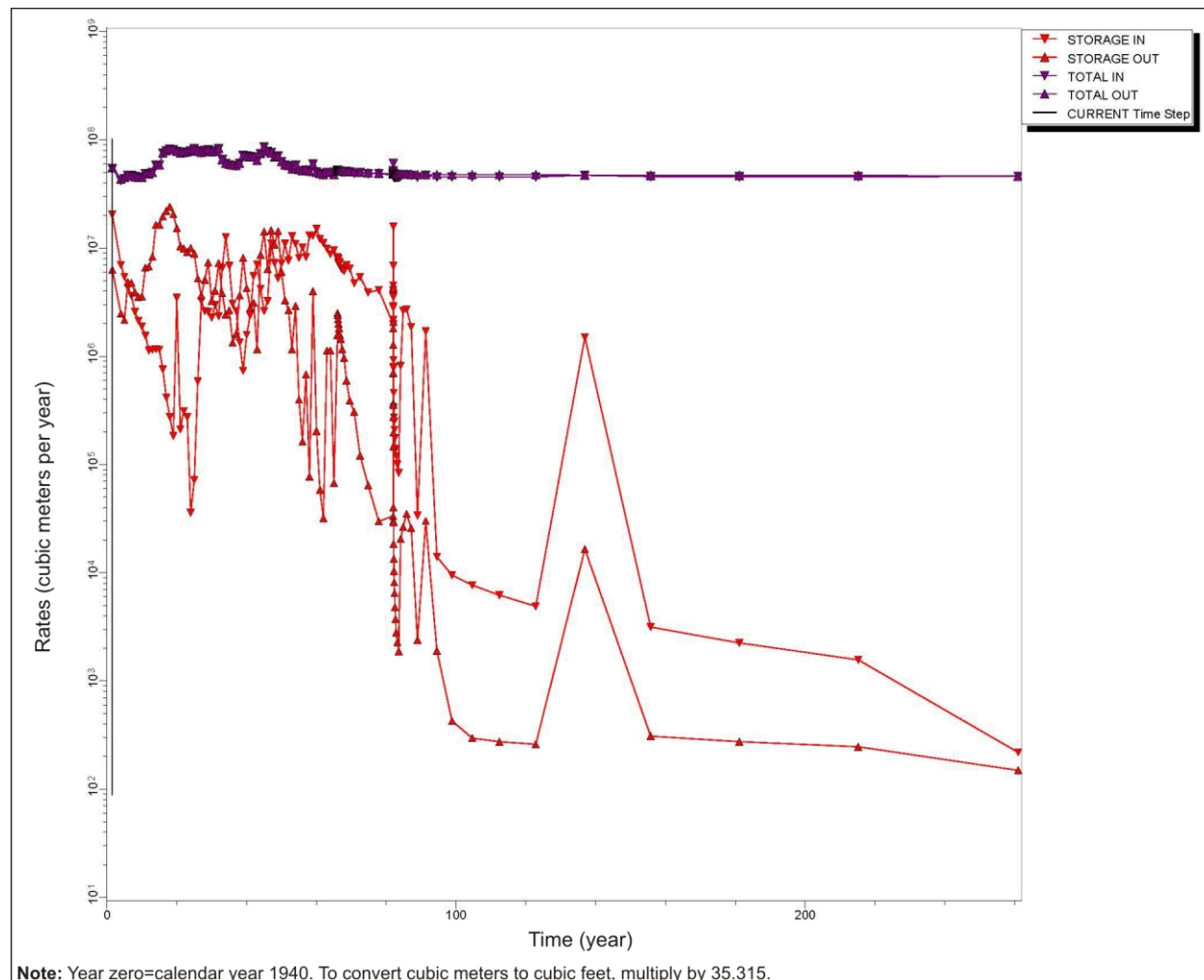
Figure L–44. 95th Percentile (Base Case) Flow Model Total Water and Storage Rates over Time

Additional water balance results for the 95th percentile (Base Case) flow model are shown in Figures L–45, L–46, and L–47 for GHBs, river boundaries, and recharge boundaries, respectively. In Figure L–47, the 'Recharge Out' value goes to zero at model year 82. This reduction occurs because the cells below the water extraction zone in the model become dry at this time during the model simulation and do not rewet for the remainder of the simulation.
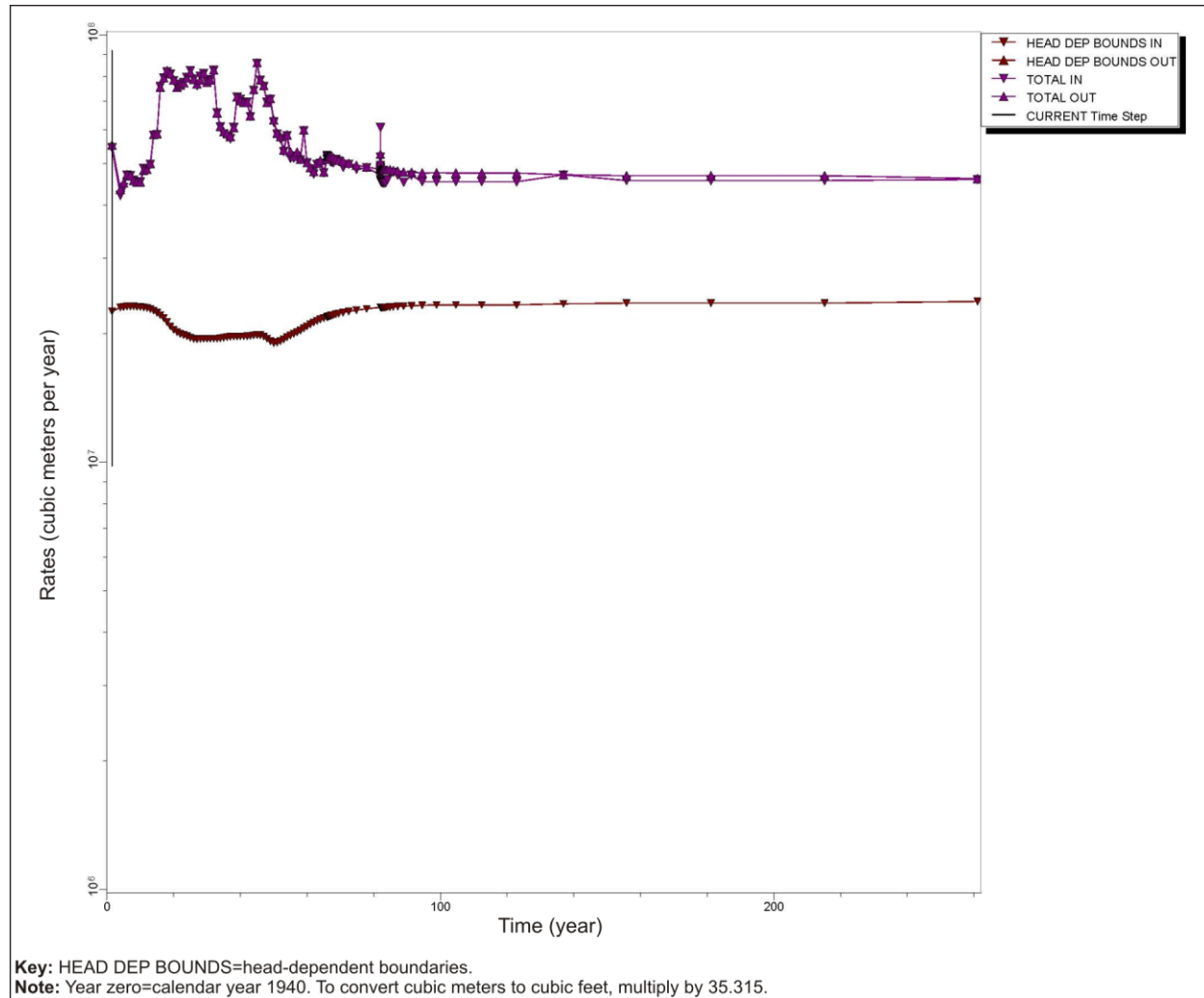
**Figure L–45. 95th Percentile (Base Case) Flow Model
Total Water and Generalized Head Boundary Rates over Time**

Note: Year zero=calendar year 1940. To convert cubic meters to cubic feet, multiply by 35.315.
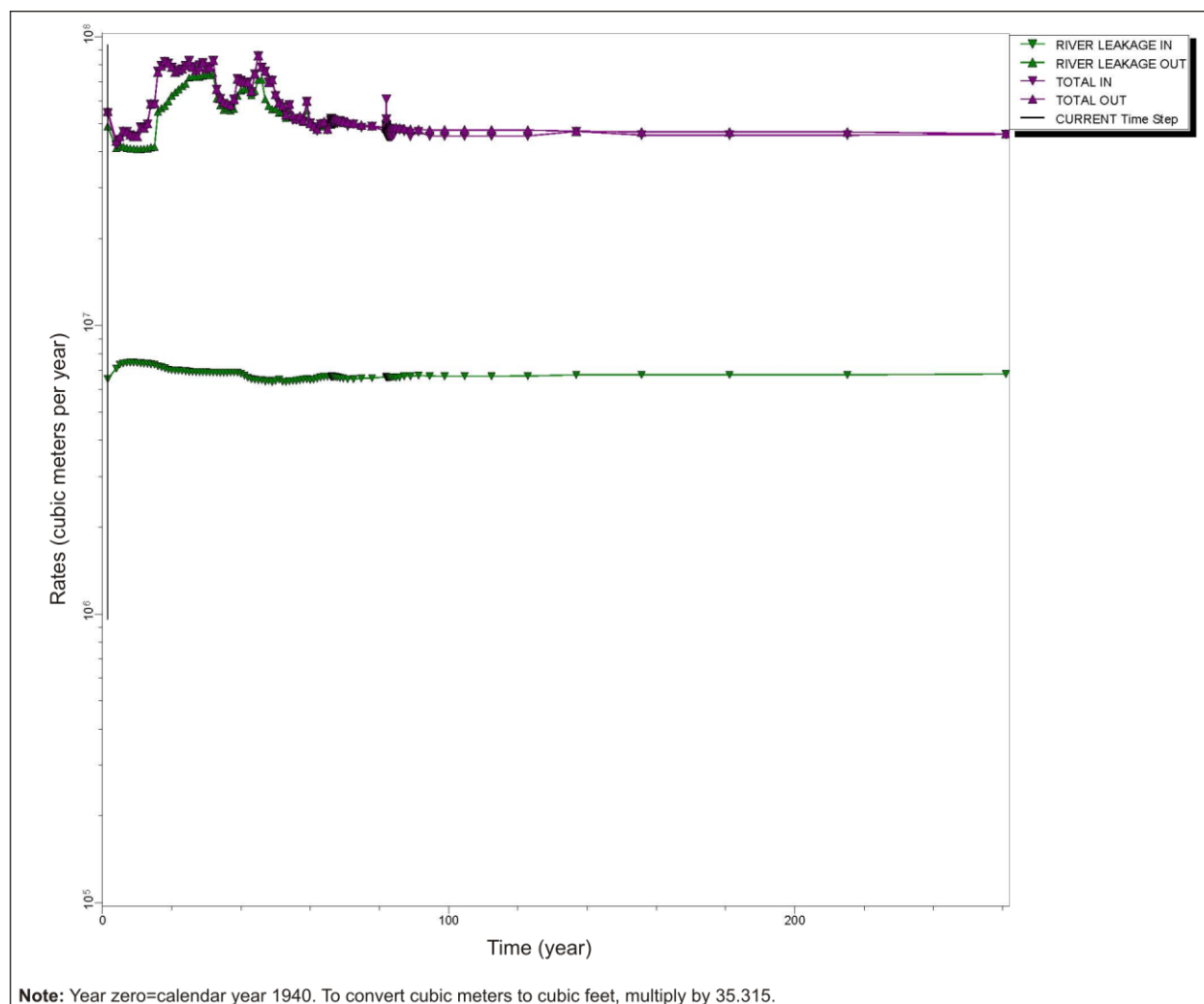
Figure L–46. 95th Percentile (Base Case) Flow Model Total Water and River Rates over Time

Note: Year zero=calendar year 1940. To convert cubic meters to cubic feet, multiply by 35.315.
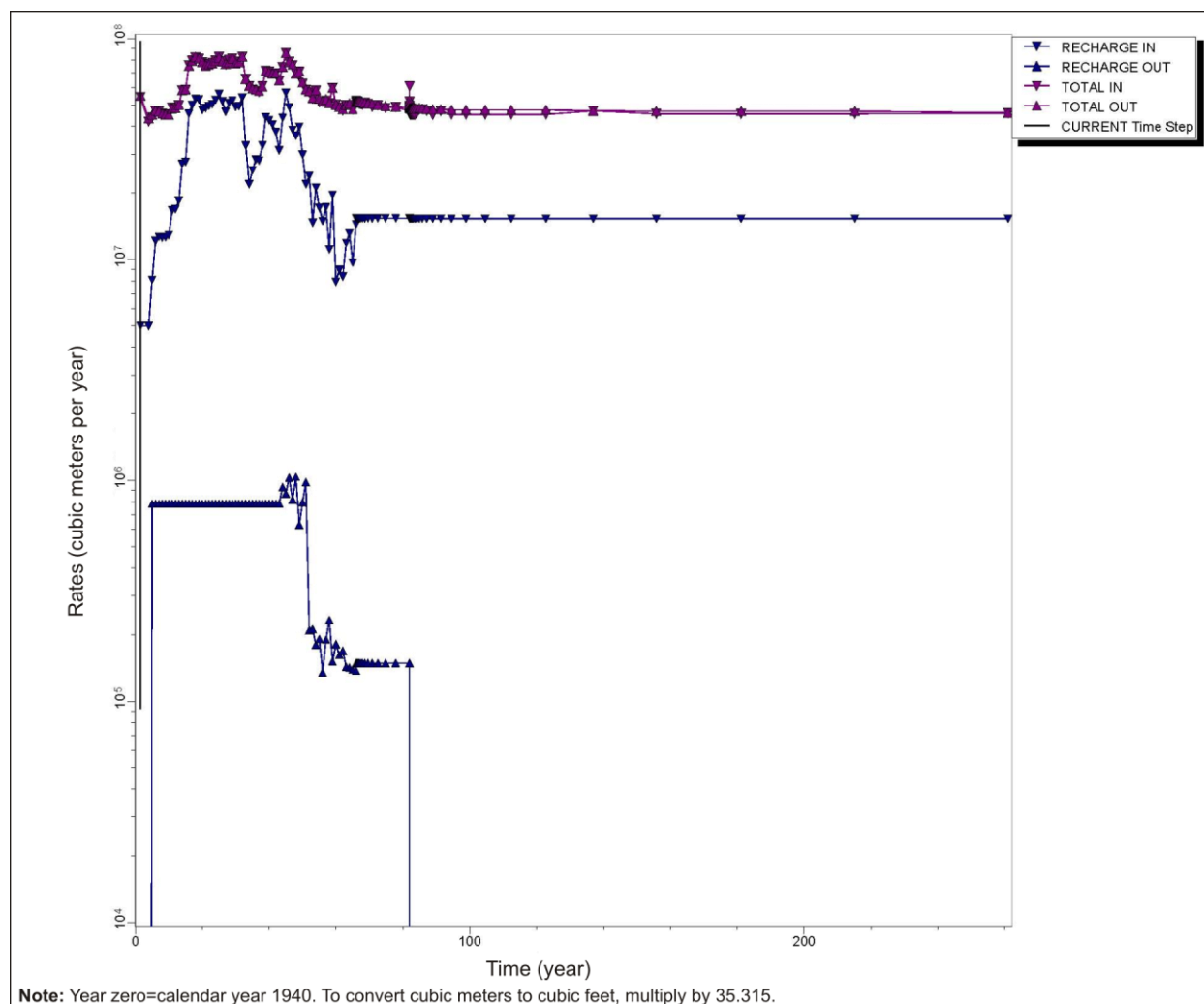
Figure L–47. 95th Percentile (Base Case) Flow Model Total Water and Recharge Rates over Time

L.8.1.2   95th Percentile (Base Case) Potentiometric Head Distribution

A goal for the Base Case flow model is to produce a potentiometric distribution of heads that shows a steep water table in the 200-West Area and a relatively flat water table in the 200-East Area. The pre-Hanford potentiometric surface is assumed to be approximately the same as the post-Hanford long-term steady state condition, with water table mounding occurring below areas where, and at times when, Hanford operational discharges were released at the ground surface. Figures L–48, L–49, and L–50 are Base Case flow model simulations of the potentiometric surface in CY 1944 (pre-Hanford), CY 1975 (Hanford operations), and CY 2200 (post-Hanford), respectively.

**Figure L–48. 95th Percentile (Base Case) Flow
Model Potentiometric Head Distribution,
Calendar Year 1944**

**Figure L–49. 95th Percentile (Base Case) Flow
Model Potentiometric Head Distribution,
Calendar Year 1975**
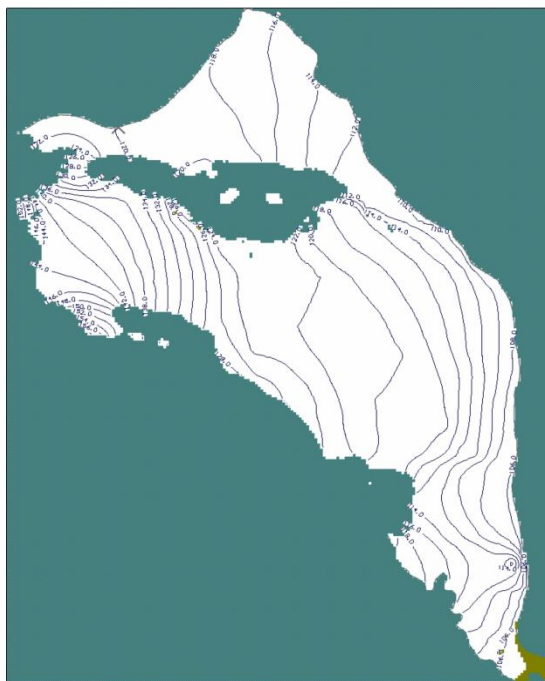
**Figure L–50. 95th Percentile (Base Case) Flow
Model Potentiometric Head Distribution,
Calendar Year 2200**

L.8.1.3   95th Percentile (Base Case) Flow Model Velocity Field

The 95th percentile (Base Case) flow model velocity field is variable in both magnitude and direction over time and across the model domain. This variability at selected locations within the model is shown in Figures L−51 through L−56. As expected, the velocities simulated in the 200-West Area are generally lower than those simulated in the 200-East Area, particularly at the 200-East Area BY Cribs. An additional observation is that the velocity directions are highly variable during the Hanford operational period, particularly at the 200-East Area BY Cribs; there the velocity directions change by approximately 180 degrees due to water table mounding, coupled with this source's proximity to Gable Gap, where water table velocity and direction are sensitive to water table elevation.

Note: To convert meters to feet, multiply by 3.281.
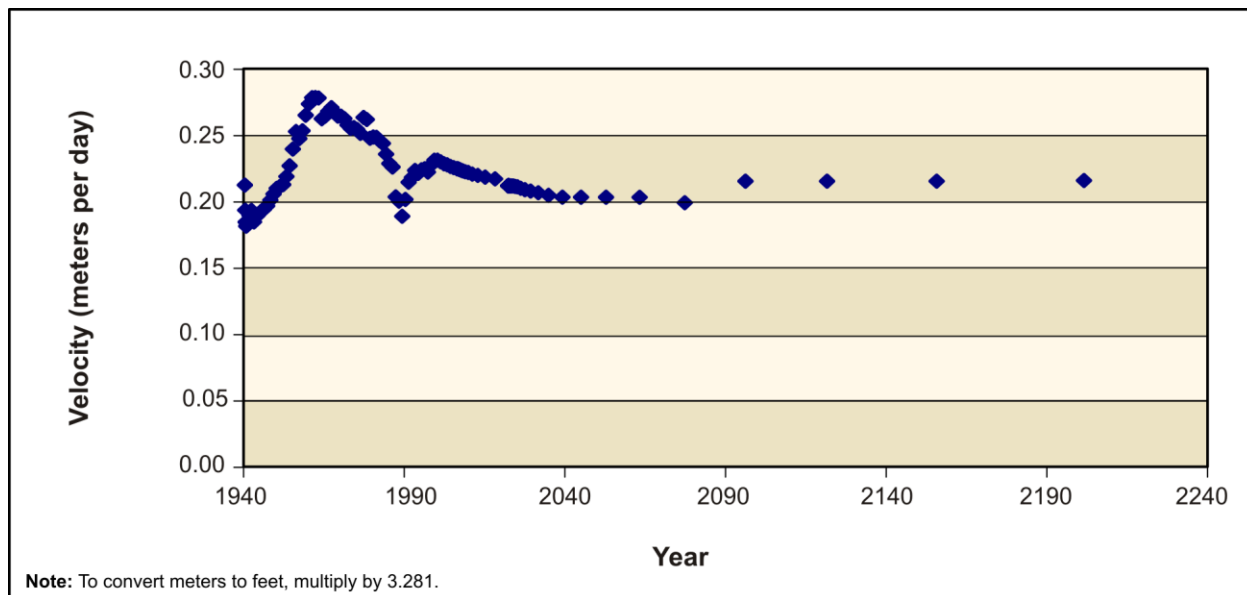
**Figure L–51. 95th Percentile (Base Case) Flow Model
Velocity Magnitude at 216-B-26 (BC Cribs in 200-East Area)**
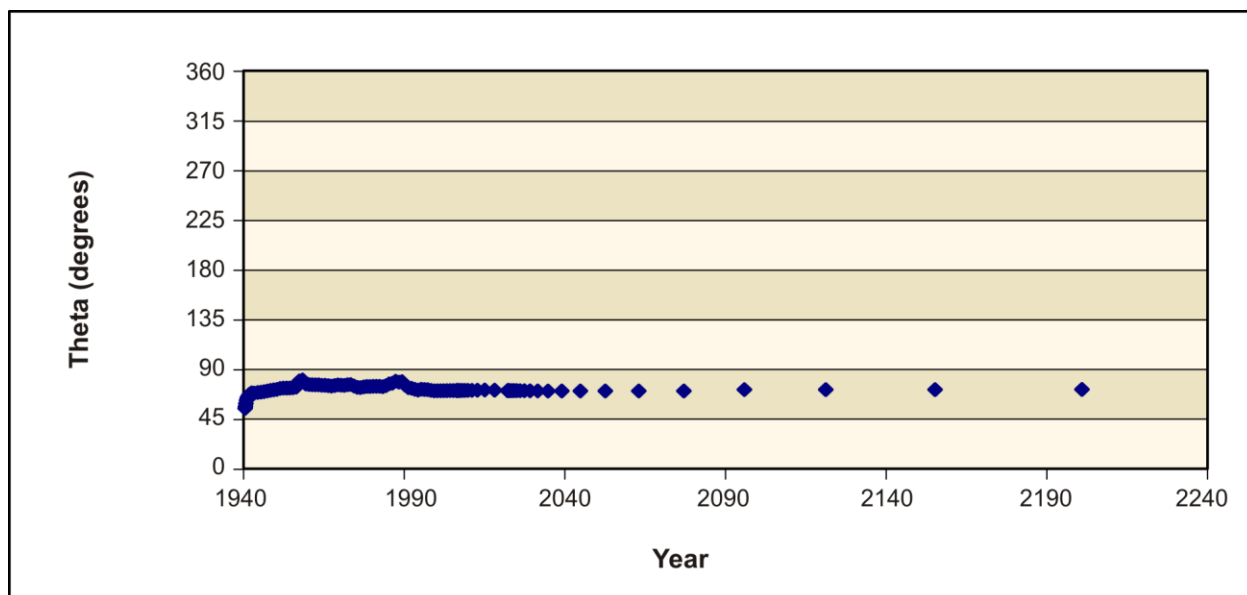
**Figure L–52. 95th Percentile (Base Case) Flow Model
Velocity Direction at 216-B-26 (BC Cribs in 200-East Area)**
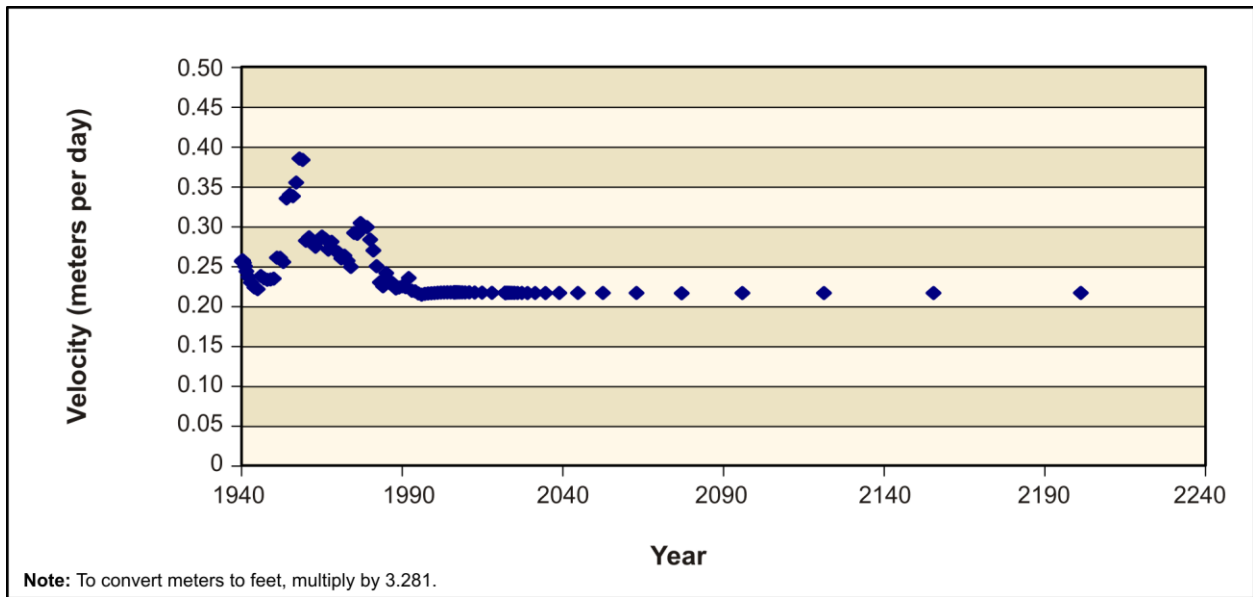
Figure L–53. 95th Percentile (Base Case) Flow Model
Velocity Magnitude at 216-T-28 (200-West Area)
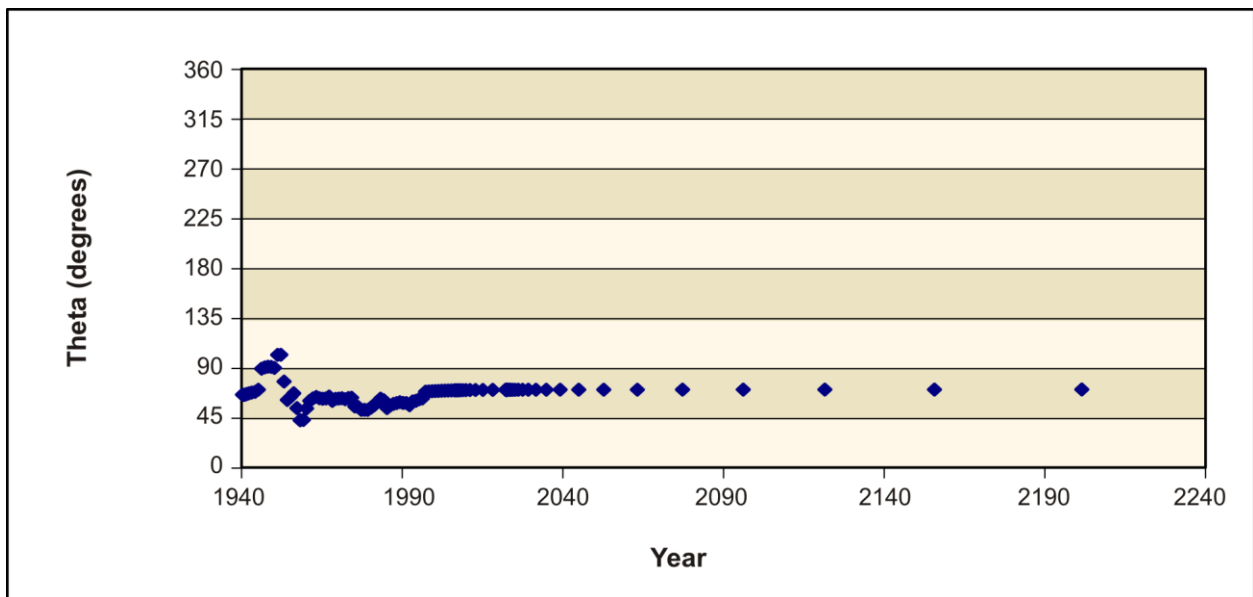
Figure L–54. 95th Percentile (Base Case) Flow Model
Velocity Direction at 216-T-28 (200-West Area)

Note: To convert meters to feet, multiply by 3.281.
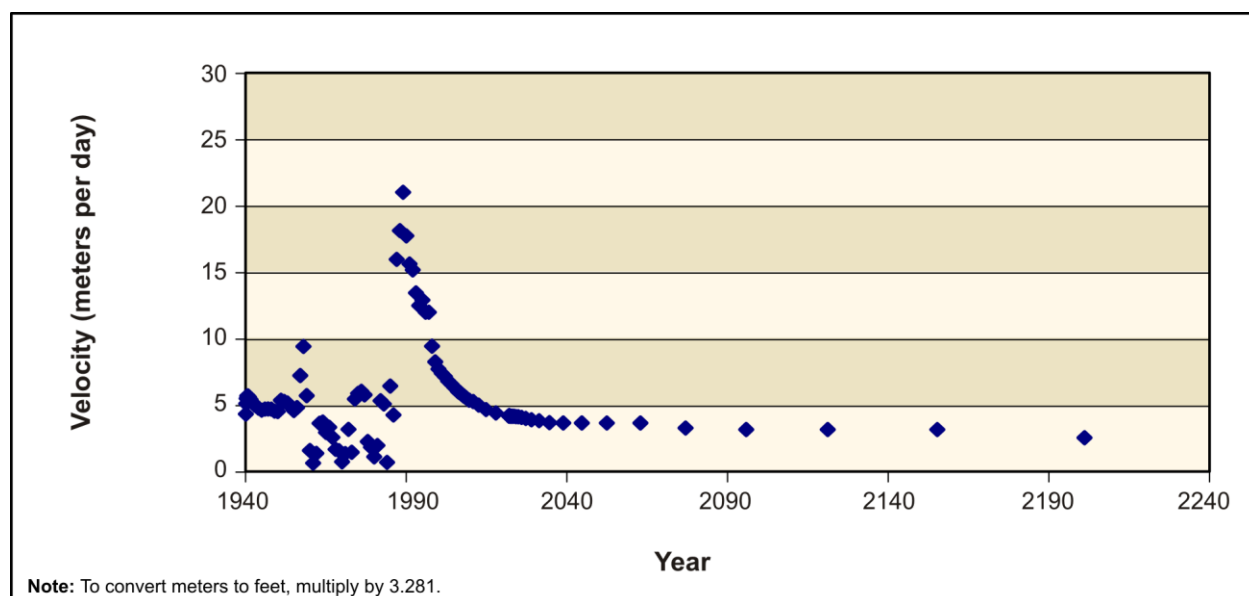
**Figure L–55. 95th Percentile (Base Case) Flow Model
Velocity Magnitude at BY Cribs (200-East Area)**
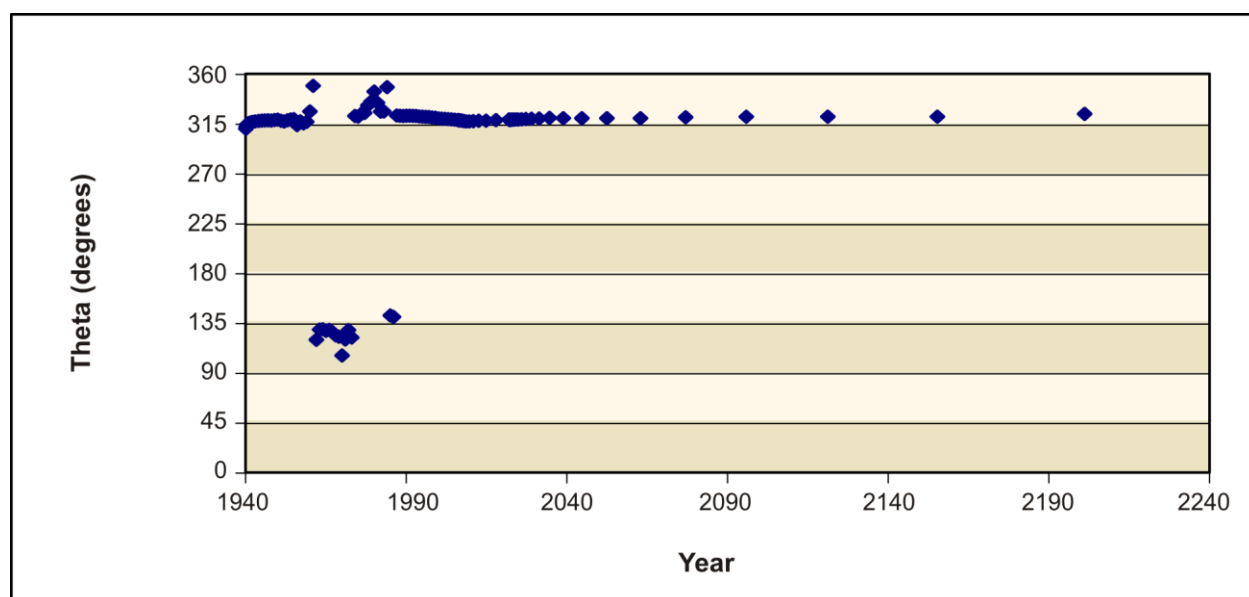
**Figure L–56. 95th Percentile (Base Case) Flow Model
Velocity Direction at BY Cribs (200-East Area)**

L.8.1.4   95th Percentile (Base Case) Flow Model Central Plateau Pathline Analysis

Pathline analysis determined the number of particles (measured in area) released in the Central Plateau area that would move to the north through Gable Gap and the number that would move to the east toward the Columbia River. As discussed in Section L.1.5, in the *Draft TC & WM EIS*, the pathline analysis to demonstrate the area of northerly versus easterly flow from the Central Plateau depended primarily on hydraulic conductivity distribution rather than on uncertainties in the TOB surface. Comparison of this analysis with the 66th and 100th percentile cases (see Sections L.8.2.4 and L.8.3.4) confirms this observation. This pathline analysis included a MODFLOW and MODPATH [MODFLOW particle-tracking postprocessing package] model run, releasing a uniformly distributed set of particles across the

Central Plateau area. The Central Plateau is depicted as a rectangular boundary that includes all of the 200-East and 200-West Areas, as well as other areas between and outside the 200 Areas. Figure L–57 shows that, in terms of area, the flow of the Base Case flow model is predominantly eastward from the Central Plateau.
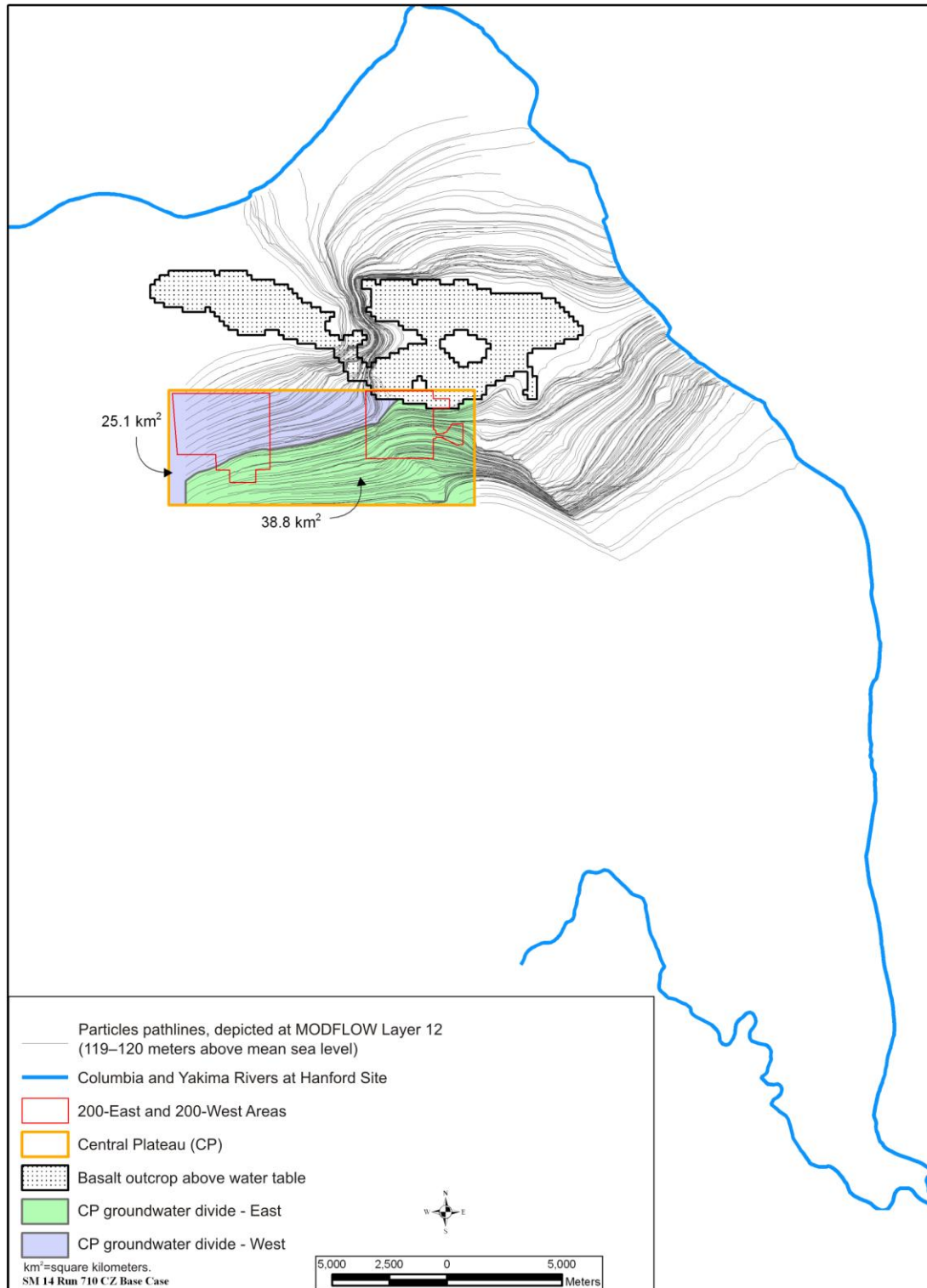
Figure L–57. 95th Percentile (Base Case) Flow Model
Central Plateau Pathline Analysis

The computer program MODPATH was developed by the USGS to calculate three-dimensional particle-tracking pathlines from steady state and transient flow simulation output obtained using MODFLOW (SWS 2009).

L.8.1.5   95th Percentile (Base Case) Flow Model Zone Budget Analysis

A zone budget analysis was completed to determine simulated water flow volumes from south of Gable Mountain and Gable Butte through Umtanum Gap, through Gable Gap, and easterly toward the Columbia River. Table L–17 provides total water flow volumes through these areas for CY 2200. These results show that about 17 percent of the total volume of water entering the Columbia River passes through Umtanum Gap, about 15 percent through Gable Gap, and about 68 percent directly east to the Columbia River. Comparison of these results with those of the 66th and 100th percentile cases shows that in terms of volumetric flow, rather than in terms of geometric position of the flow divide across the Central Plateau (see Section L.8.1.4), the model is less sensitive to variations in hydraulic conductivity.
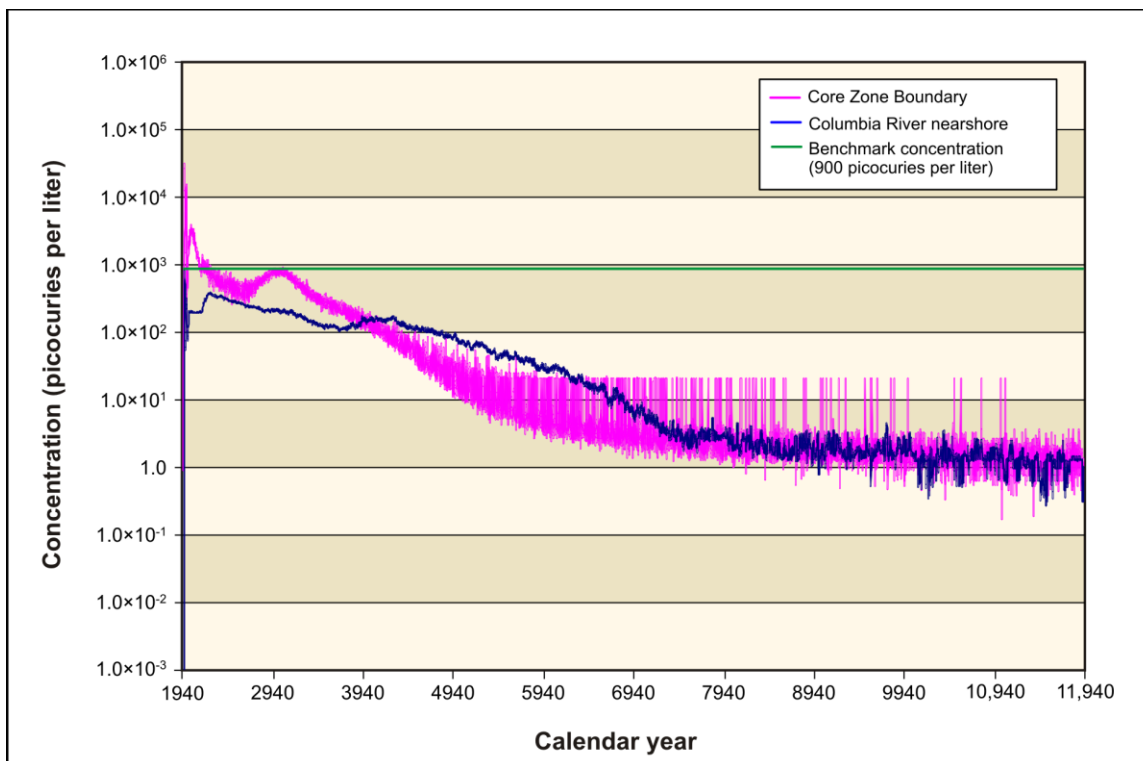
**Table L–17. 95th Percentile (Base Case) Flow Model –
Simulated Water Flow Volumes Through Selected Areas, Calendar Year 2200**

| Water Flow Through	Water Volume (cubic meters per year)
Umtanum Gap	4,332,200
Gable Gap	3,714,000
East to Columbia River	16,954,000

Note: To convert cubic meters to cubic feet, multiply by 35.315.

L.8.1.6   95th Percentile (Base Case) Flow Model – Transport Model Concentration-Versus-Time Results

Groundwater transport modeling was completed using the 95th percentile flow model. Figures L–58 and L–59 show the concentration-versus-time results measured at the Core Zone Boundary and at the Columbia River for technetium-99 under Tank Closure Alternative 2B and Waste Management Alternative 2, Disposal Group 1, Subgroup 1-A, respectively. Figures L–58 and L–59 are comparable to Figures L–86 and L–87, respectively, for the 100th percentile model, and comparable to Figures L–114 and L–115, respectively, for the 66th percentile model. These comparisons show that the three flow models result in similar technetium-99 concentrations over time for the two alternatives presented. See Chapter 2 of this *TC & WM EIS* for a description of these alternatives.

Figure L–58. Tank Closure Alternative 2B 95th Percentile (Base Case)
Flow Model Concentration-Versus-Time Results for Technetium-99
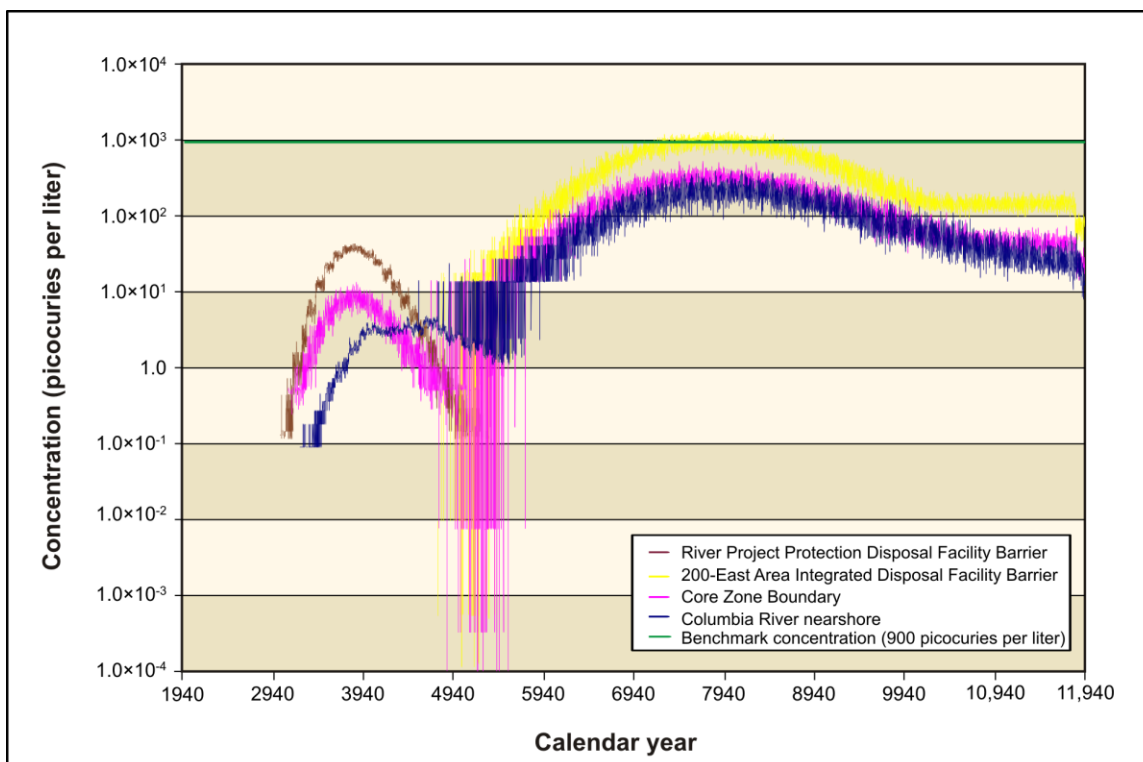
Figure L–59. Waste Management Alternative 2, Disposal Group 1, Subgroup 1-A,
95th Percentile Flow Model
Concentration-Versus-Time Results for Technetium-99

L.8.2 Results from the 100th Percentile Flow Model

L.8.2.1 Calibration Acceptance

Table L–18 provides a restatement of the flow model calibration criteria discussed in Section L.6.2, along with an assessment of the 100th percentile flow model's performance for each criterion. Specific data illustrative of such performance are reflected in Table L–19 and Figures L–60 through L–70.

Table L–18. Summary of the 100th Percentile Flow Model
Performance Compared with the Calibration Acceptance Criteria

Flow Model Calibration Acceptance Criteria	100th Percentile Flow Model Performance
Residual distribution should be reasonably normal.	Residual distribution is reasonably normal (see Figure L–60).
The mean residual should be approximately 0.	Residual mean = −0.108 meters (−0.354 feet) (see Figure L–61).
The number of positive residuals should approximate the number of negative residuals.	Positive residuals approximately equal negative residuals (see Figure L–60).
The correlation coefficient (calculated versus observed) should be greater than 0.9.	Correlation coefficient = 0.974 (see Figure L–61).
The root mean square (RMS) error (calculated versus observed) should be less than 5 meters (16.4 feet), approximately 10 percent of the gradient in the water table elevation.	RMS error = 2.25 meters (7.382 feet) (see Figure L–61).
Residuals in the 200-East Area should be distributed similarly to those in the 200-West Area.	Residuals in the 200-East and 200-West Areas are distributed similarly (see Figures L−62 and L−63).
The residuals should be evenly distributed over time.	Residuals are approximately evenly distributed over time (see Figures L−64, L−65, L−66, and L−67).
The residuals should be evenly distributed across the site.	Residuals are approximately evenly distributed across the site (see Figures L−68, L−69, and L−70).
The calibrated parameters should compare reasonably well with field-measured values.	Calibrated hydraulic conductivity values are listed in Table L–19 and compare reasonably with field-measured values for material types to which the model is sensitive (i.e., Hanford formation and Ringold Formation material types). Figure L–42 provides field-measured values from aquifer pumping tests (Cole et al. 2001).
Parameters should be reasonably uncorrelated.	Hydraulic conductivity parameters are reasonably uncorrelated (see Table L–19 for the key to model material type zones and Table L–15 for the correlation coefficient matrix).

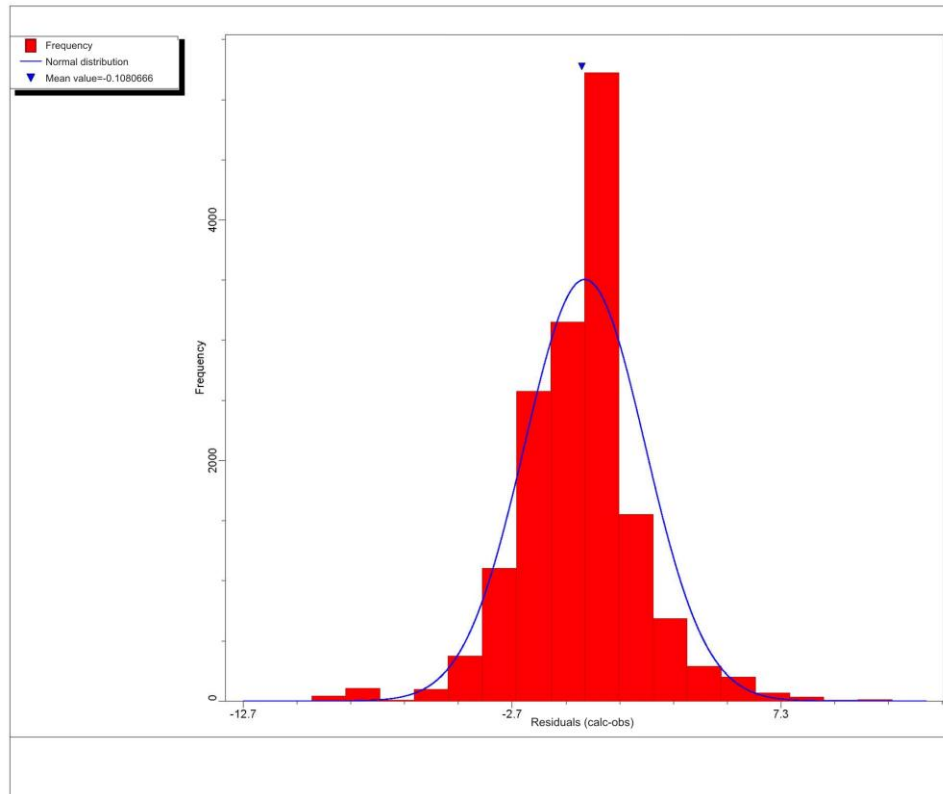**Table L–19. 100th Percentile Flow Model Calibrated Hydraulic Conductivity Values**

Material Type (Model Zone)	Hydraulic Conductivity (K_x)[a]	Hydraulic Conductivity (K_y)[b]	Hydraulic Conductivity (K_z)[c]
Hanford mud (1)	0.28	0.28	0.028
Hanford silt (2)	3.79	3.79	0.379
Hanford sand (3)	49.6	49.6	4.96
Hanford gravel (4)	223.64	223.64	22.364
Ringold sand (5)	1.89	1.89	0.189
Ringold gravel (6)	19.51	19.51	1.951
Ringold mud (7)	1.95	1.95	0.195
Ringold silt (8)	2.12	2.12	0.212
Plio-Pleistocene sand (9)	40.71	40.71	4.071
Plio-Pleistocene silt (10)	4.7	4.7	0.47
Cold Creek sand (11)	83.95	83.95	8.395
Cold Creek gravel (12)	79.7	79.7	7.97
Highly conductive Hanford formation (13)	4,793.76	4,793.76	479.376
Activated basalt (14)	0.001	0.001	0.0001

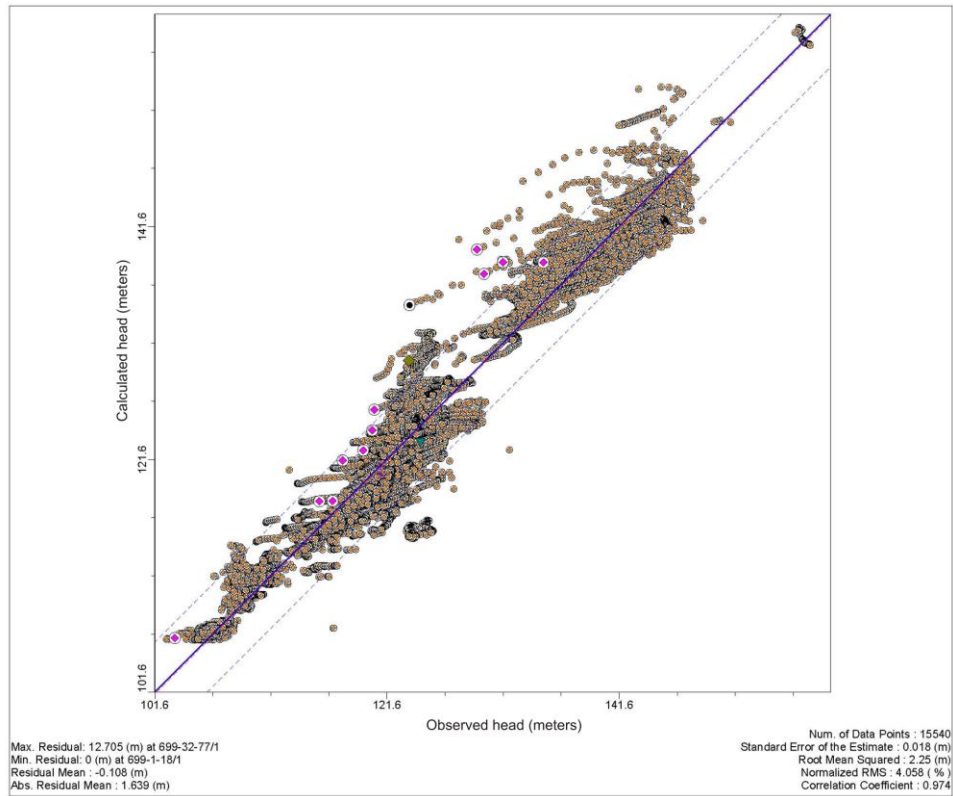[a] Hydraulic conductivity with respect to the *x* axis, meters per day.
[b] Hydraulic conductivity with respect to the *y* axis, meters per day.
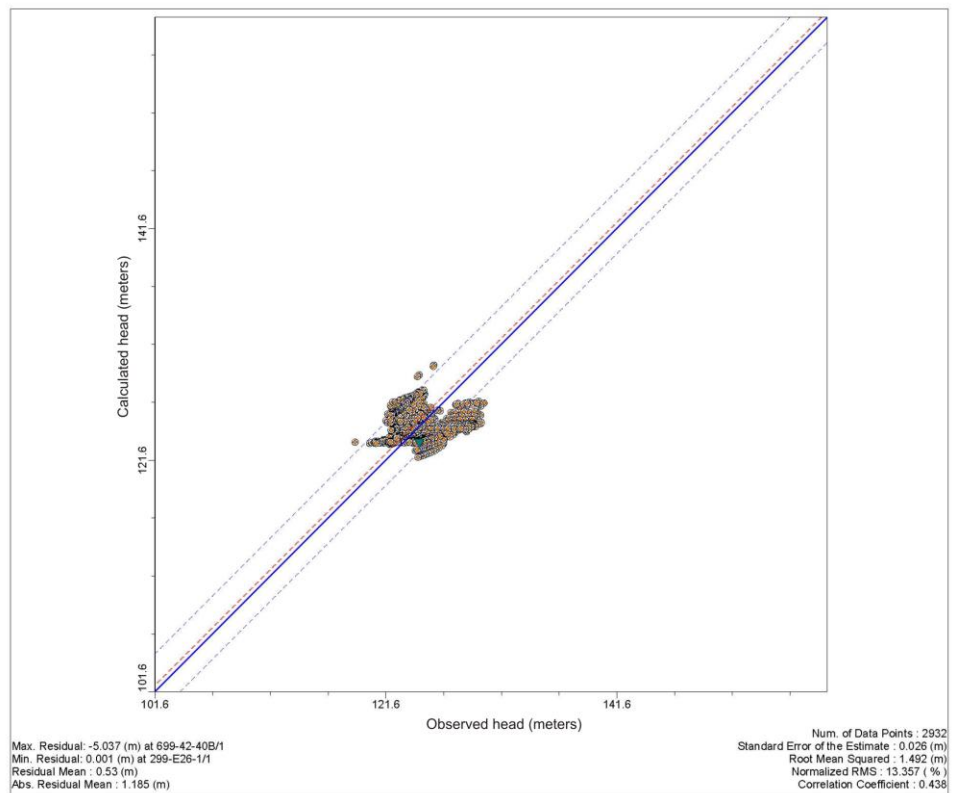[c] Hydraulic conductivity with respect to the *z* axis, meters per day.
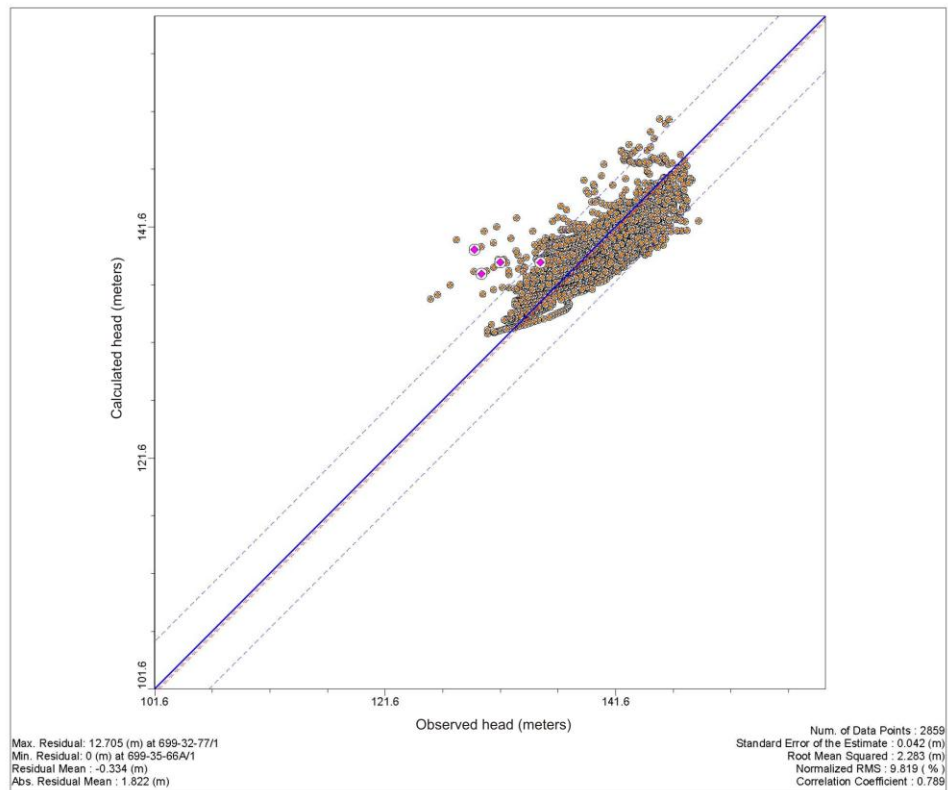**Note:** To convert meters to feet, multiply by 3.281.

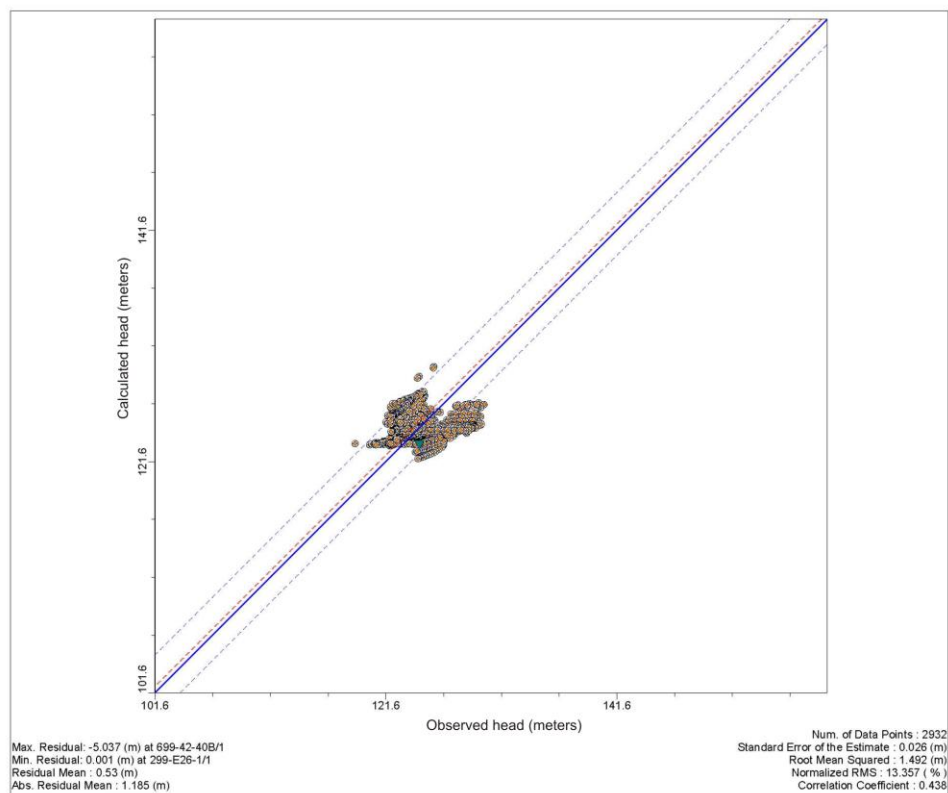**Figure L–60. 100th Percentile Flow Model Residual Distribution**

Max. Residual: 12.705 (m) at 699-32-77/1   Num. of Data Points : 15540
Min. Residual: 0 (m) at 699-1-18/1   Standard Error of the Estimate : 0.018 (m)
Residual Mean : -0.108 (m)   Root Mean Squared : 2.25 (m)
Abs. Residual Mean : 1.639 (m)   Normalized RMS : 4.058 (%)
    Correlation Coefficient : 0.974

Figure L–61. 100th Percentile Flow Model Calibration Graph and Statistics

Max. Residual: -5.037 (m) at 699-42-40B/1   Num. of Data Points : 2932
Min. Residual: 0.001 (m) at 299-E26-1/1   Standard Error of the Estimate : 0.026 (m)
Residual Mean : 0.53 (m)   Root Mean Squared : 1.492 (m)
Abs. Residual Mean : 1.185 (m)   Normalized RMS : 13.357 (%)
    Correlation Coefficient : 0.438

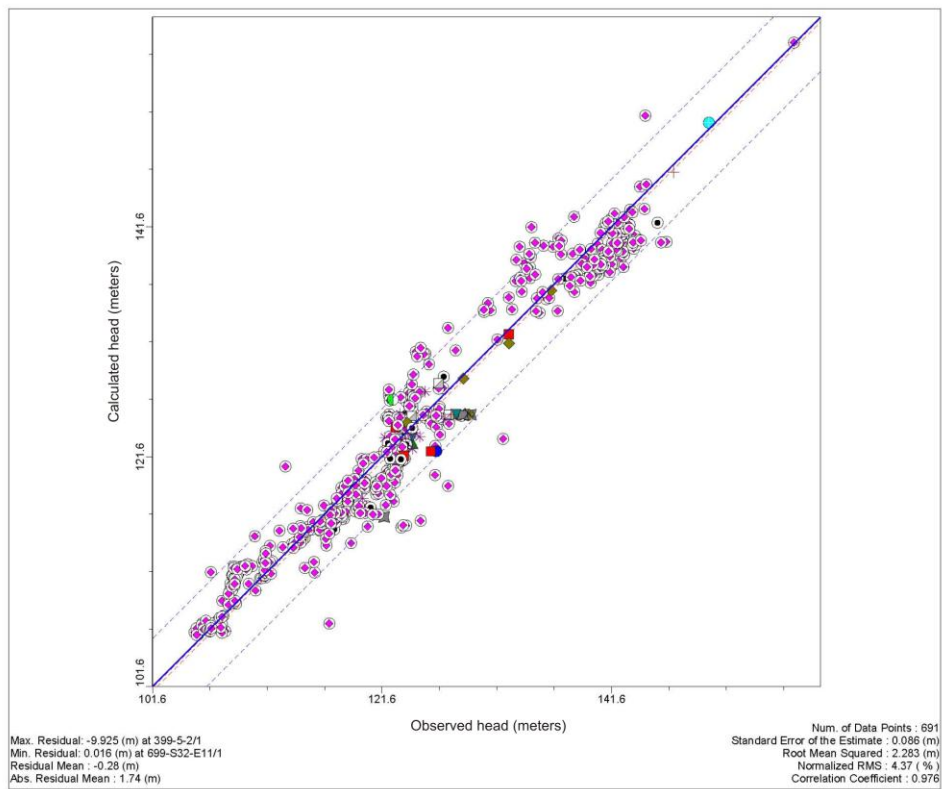**Figure L–62. 100th Percentile Flow Model Residuals – 200-East Area**

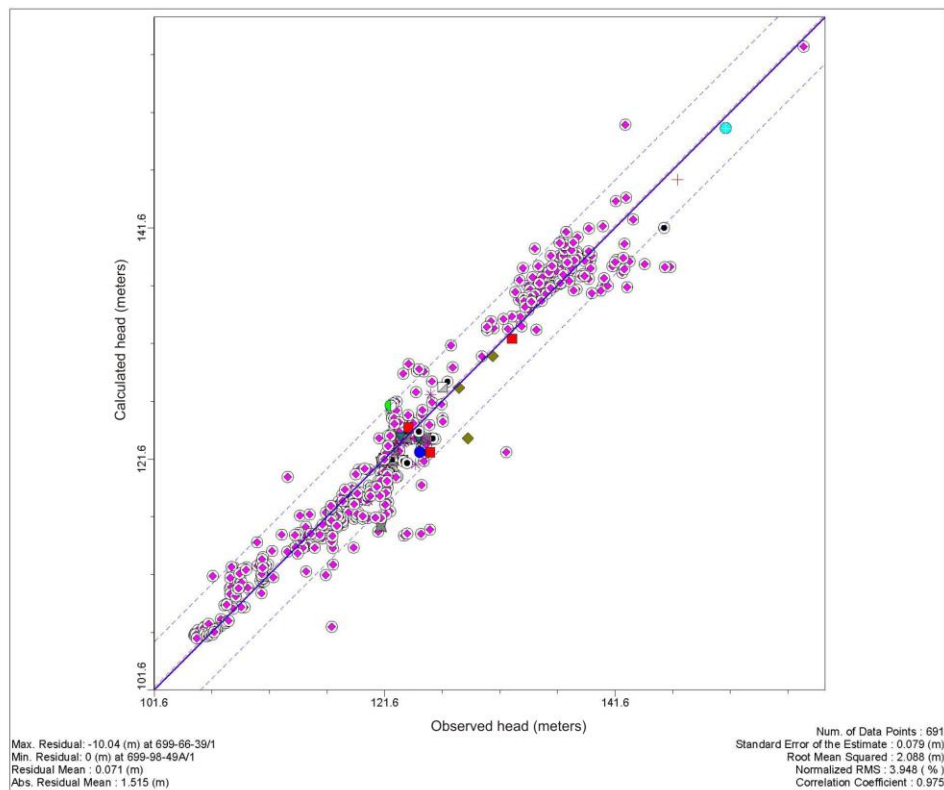**Figure L–63. 100th Percentile Flow Model Residuals – 200-West Area**

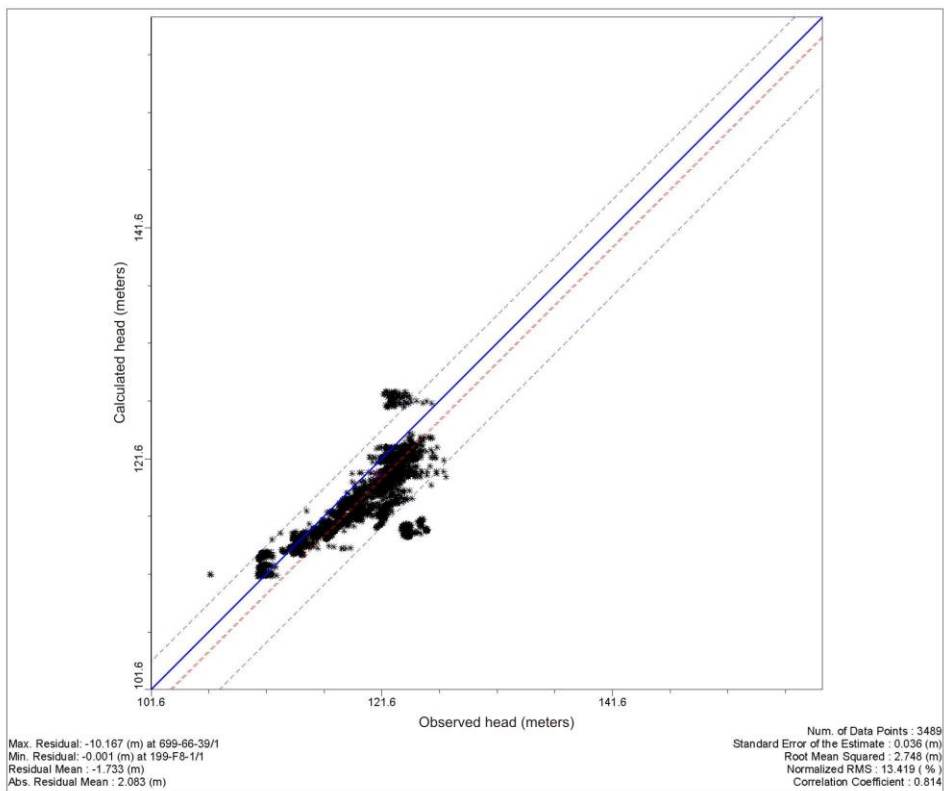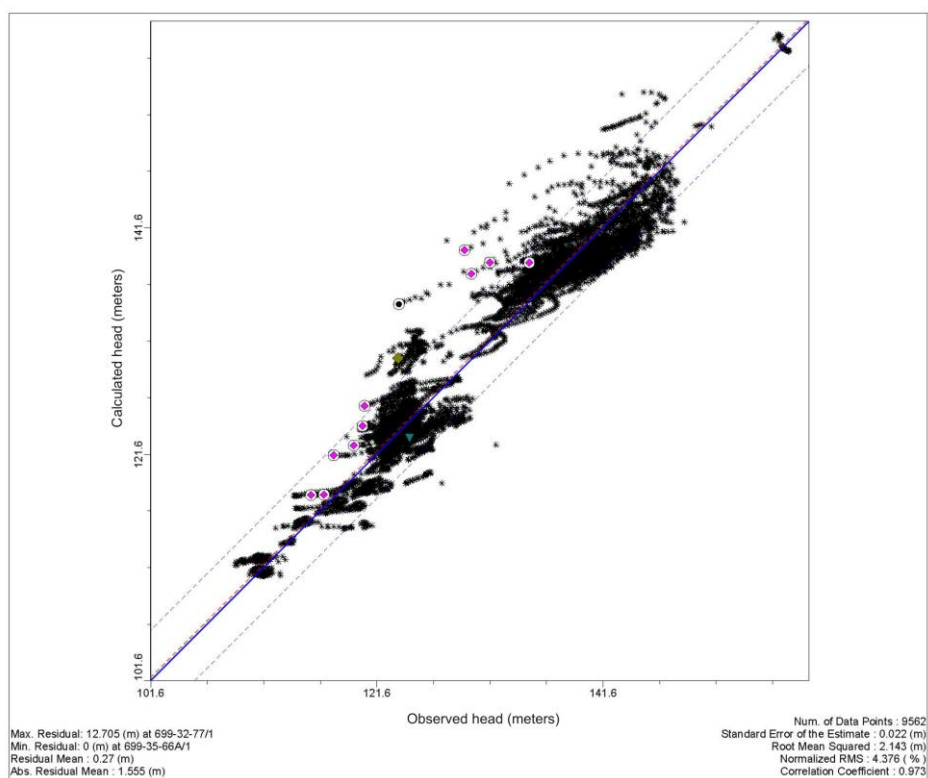**Figure L–64. 100th Percentile Flow Model Residuals, Calendar Year 1955**

Max. Residual: -9.934 (m) at 399-5-2/1
Min. Residual: -0.002 (m) at 299-E27-8/1
Residual Mean : -0.105 (m)
Abs. Residual Mean : 1.659 (m)

Num. of Data Points : 691
Standard Error of the Estimate : 0.092 (m)
Root Mean Squared : 2.424 (m)
Normalized RMS : 4.695 (%)
Correlation Coefficient : 0.976
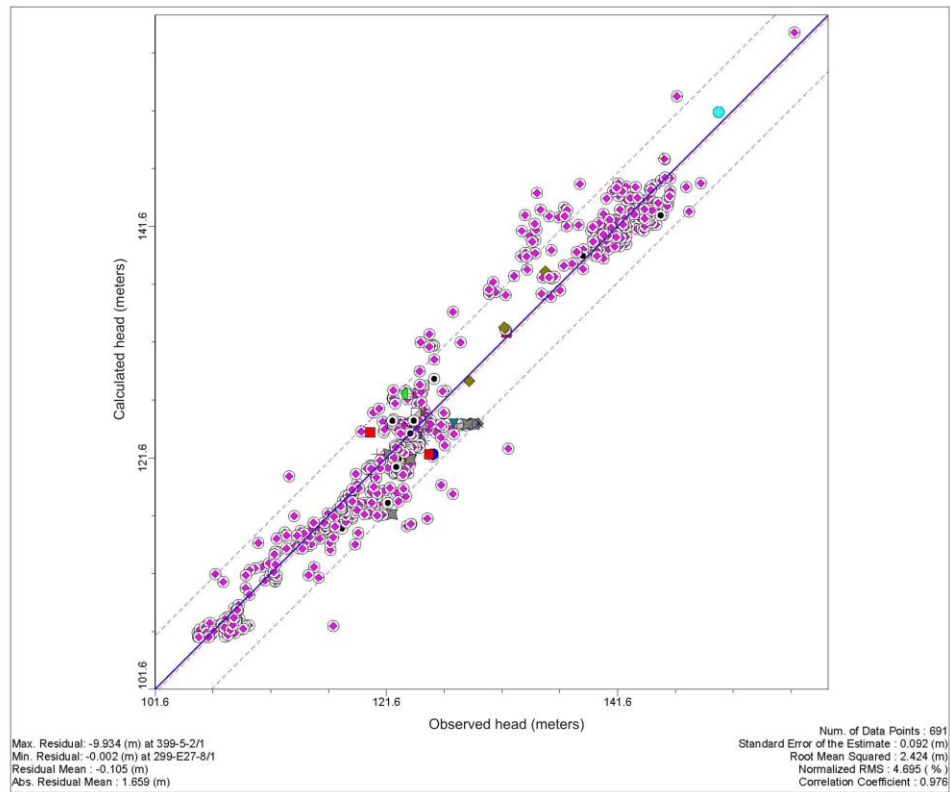
Figure L–65. 100th Percentile Flow Model Residuals, Calendar Year 1975

Max. Residual: -9.925 (m) at 399-5-2/1
Min. Residual: 0.016 (m) at 699-S32-E11/1
Residual Mean : -0.28 (m)
Abs. Residual Mean : 1.74 (m)

Num. of Data Points : 691
Standard Error of the Estimate : 0.086 (m)
Root Mean Squared : 2.283 (m)
Normalized RMS : 4.37 (%)
Correlation Coefficient : 0.976

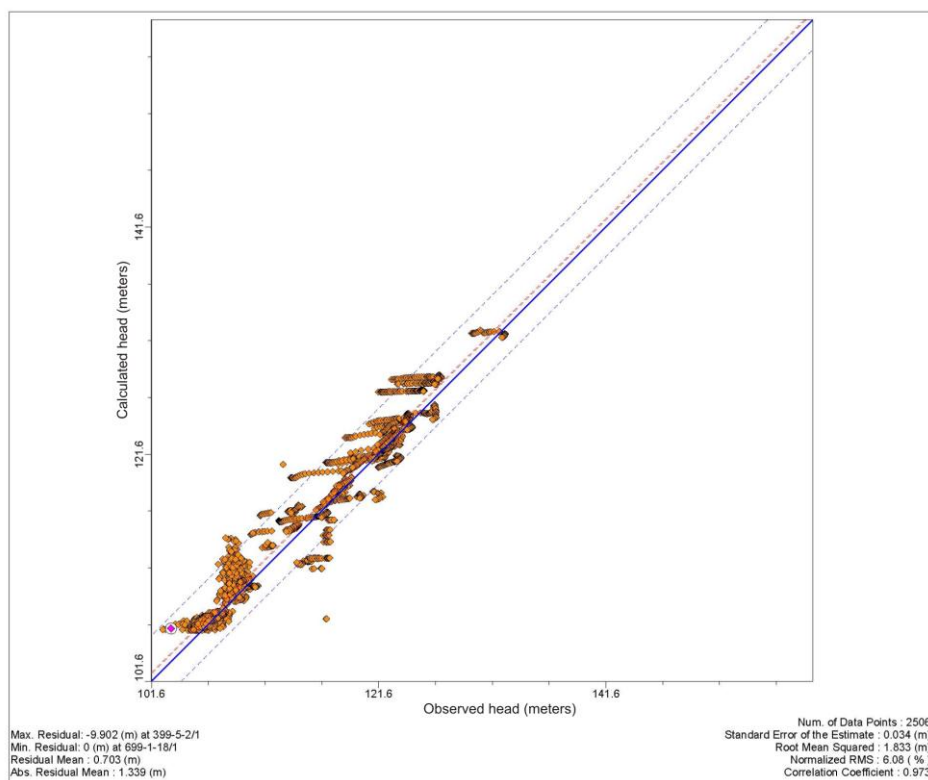**Figure L–66. 100th Percentile Flow Model Residuals, Calendar Year 1995**

Figure L–67. 100th Percentile Flow Model Residuals, Calendar Year 2010

Figure L–68. 100th Percentile Flow Model Residuals in
**Northern Region of Model**

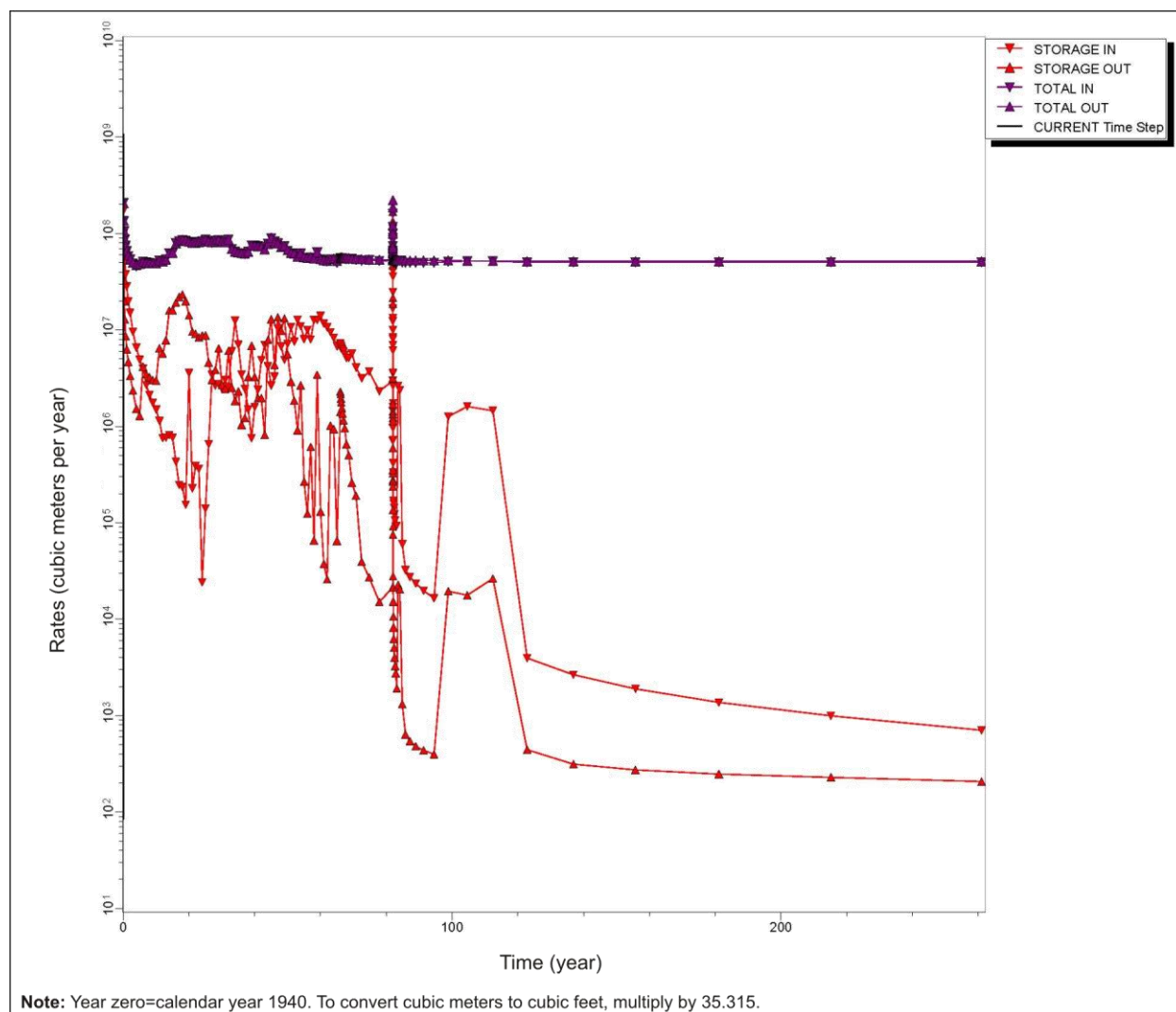**Figure L–69. 100th Percentile Flow Model Residuals in Central Region of Model**

Figure L–70. 100th Percentile Flow Model Residuals in Southern Region of Model

In addition to the calibration acceptance criteria, water (or mass) balance and a long-term, steady state condition must be achieved in the calibrated flow model. Cumulative mass water balance data are shown in Figure L–71, indicating a cumulative mass balance error of approximately –1.4 percent. Total water balance and storage data as a function of time are shown in Figure L–72. The Figure L–72 data show storage values relative to the total water balance and indicate that storage-in is approximately equal to storage-out in model year 261 (CY 2200). This indicates that a long-term steady state condition is achieved. Note that, in Figure L–72, there is a spike in "storage" at model year 82. This spike is the result of a time-stepping change at the beginning of the final long-term stress period. As a result, the model is moving from a relatively long time step at the end of the previous stress period (model year 82) to a relatively short time step at the beginning of the final stress period.
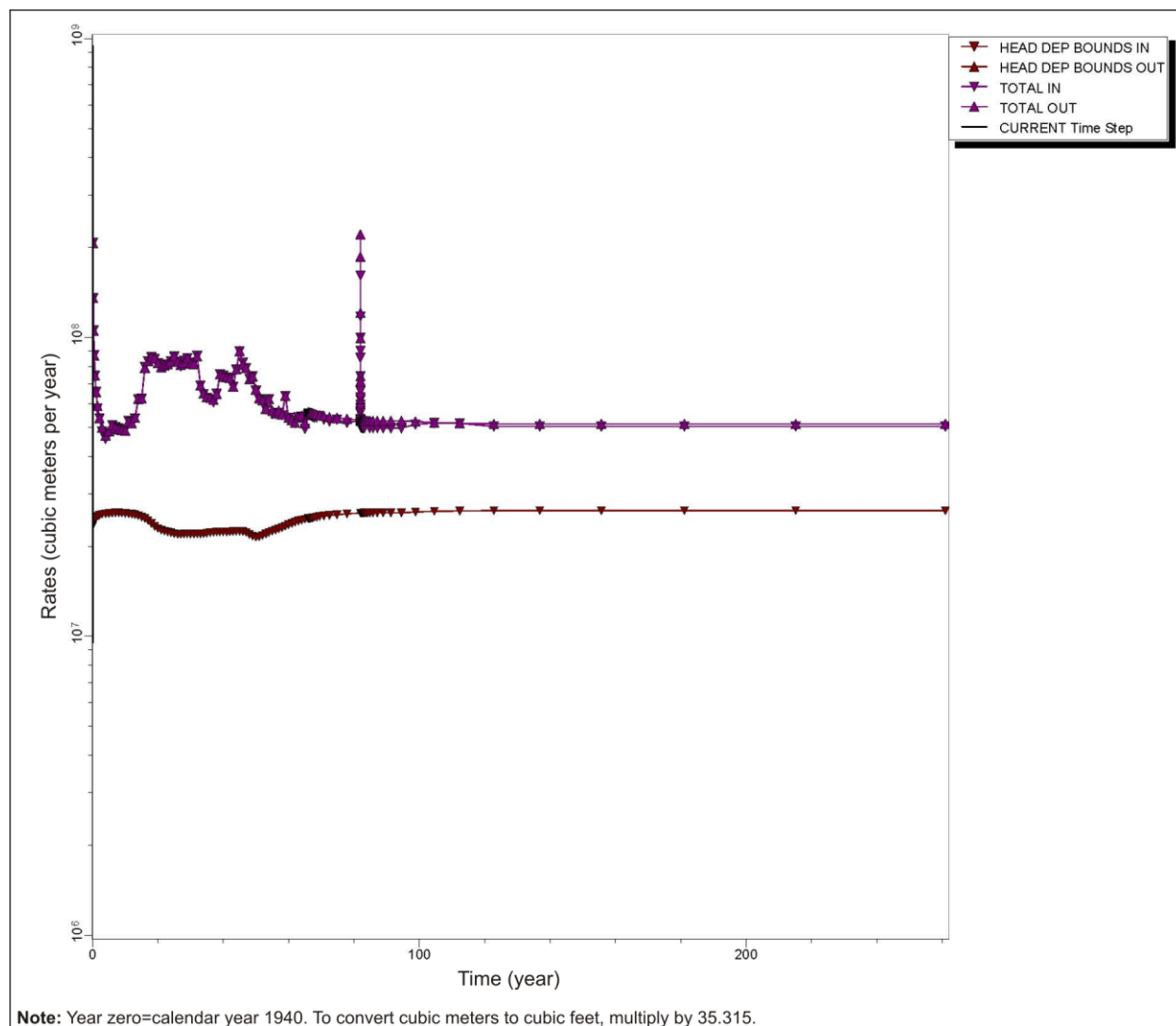

Note: Year zero=calendar year 1940.
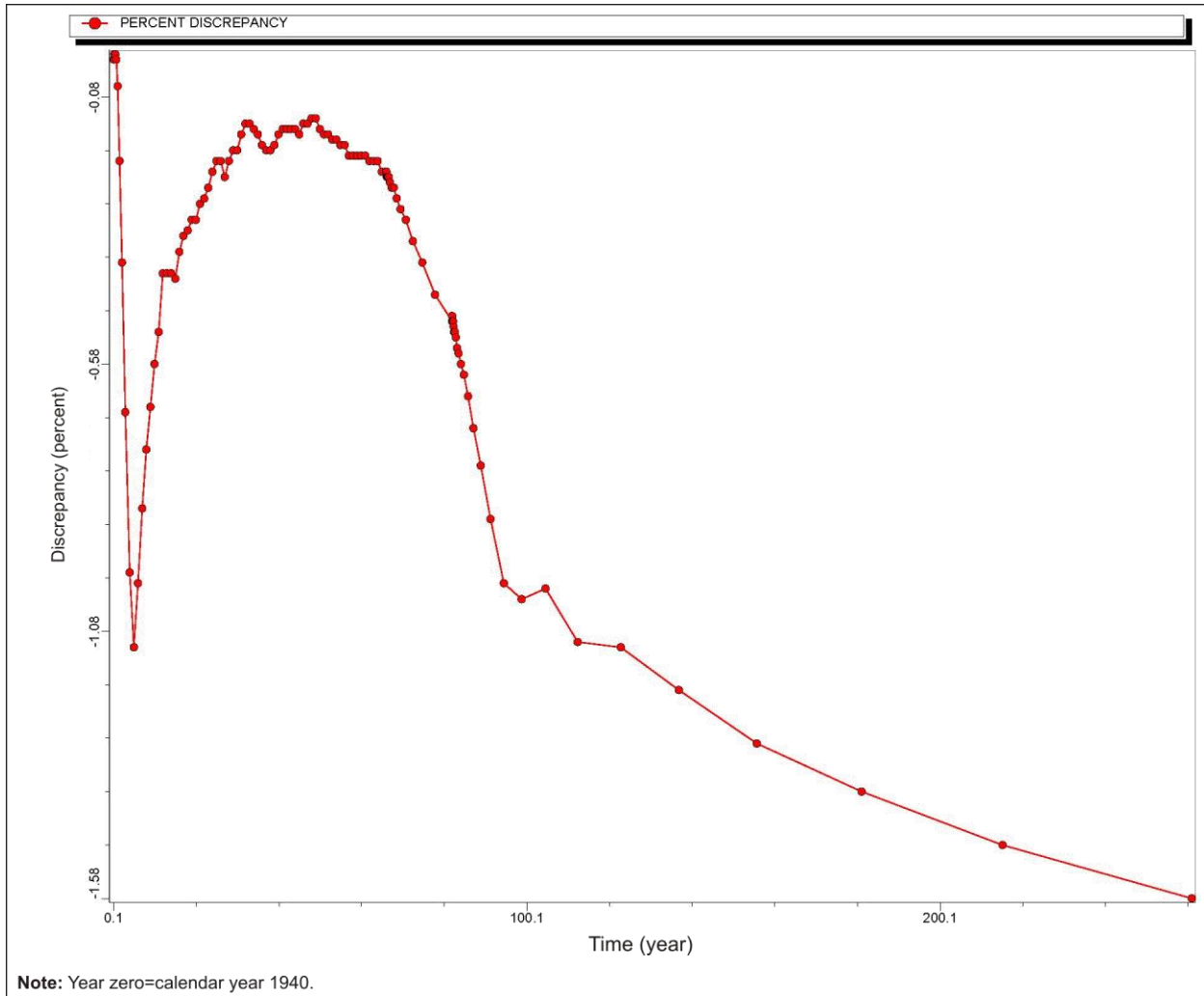
Figure L–71. 100th Percentile Flow Model Cumulative Water Balance Discrepancy
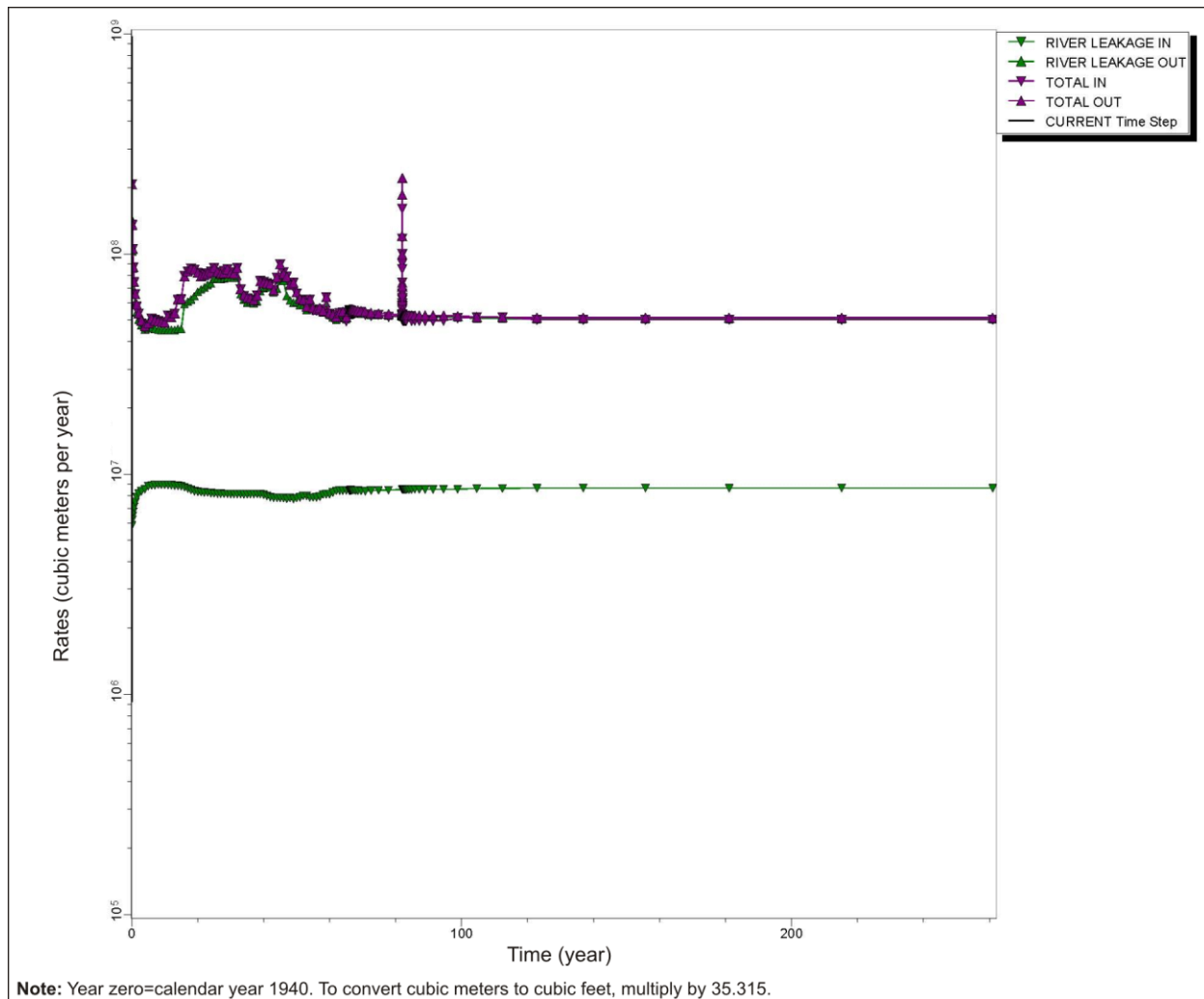
Figure L–72. 100th Percentile Flow Model Total Water and Storage Rates over Time
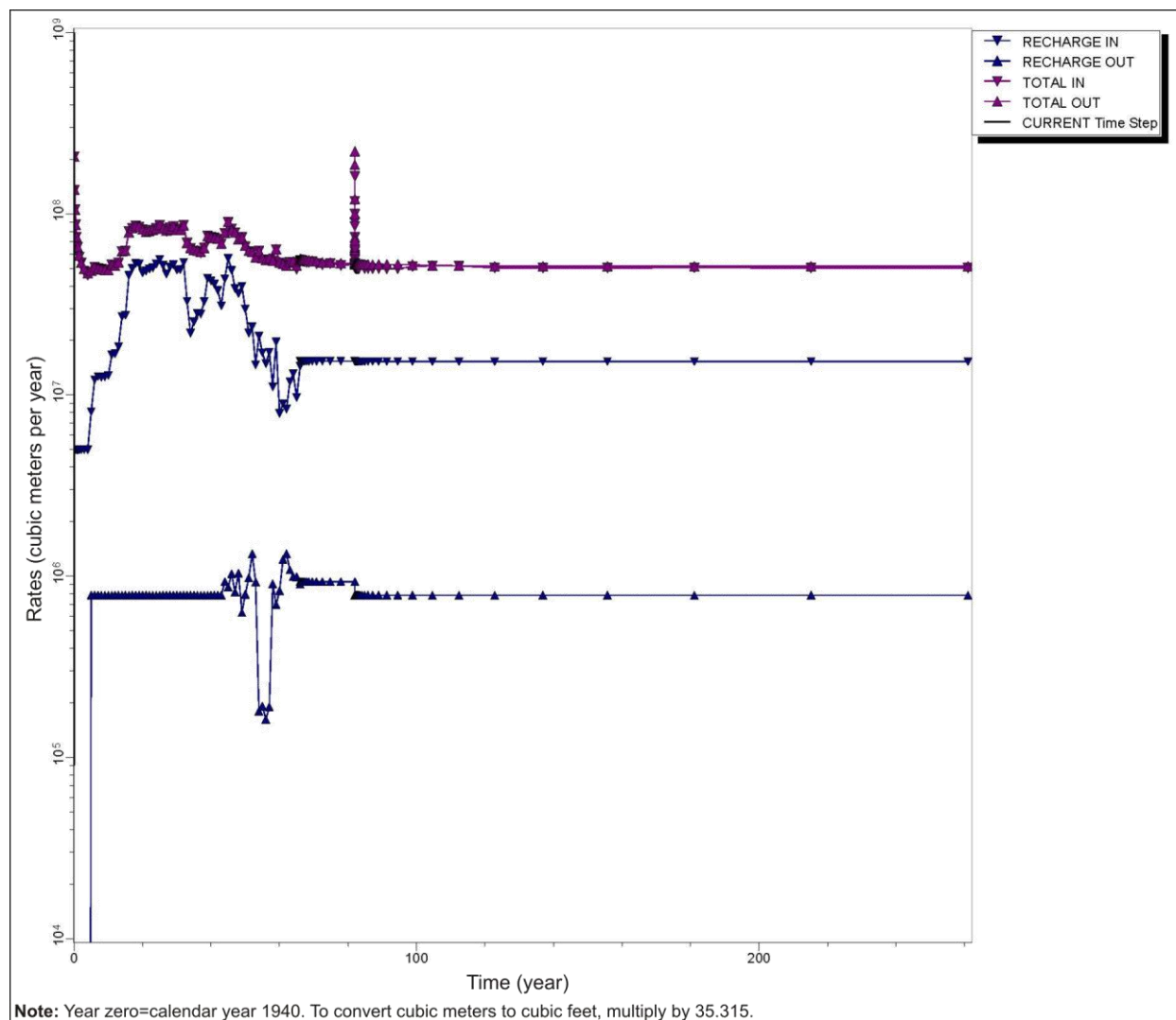
Additional water balance results for the 100th percentile flow model are shown in Figures L–73, L–74, and L–75 for GHBs, river boundaries, and recharge boundaries, respectively.

Note: Year zero=calendar year 1940. To convert cubic meters to cubic feet, multiply by 35.315.

Figure L–73. 100th Percentile Flow Model
Total Water and Generalized Head Boundary Rates over Time

Note: Year zero=calendar year 1940. To convert cubic meters to cubic feet, multiply by 35.315.

Figure L–74. 100th Percentile Flow Model Total Water and River Rates over Time

**Note:** Year zero=calendar year 1940. To convert cubic meters to cubic feet, multiply by 35.315.

Figure L–75. 100th Percentile Flow Model Total Water and Recharge Rates over Time

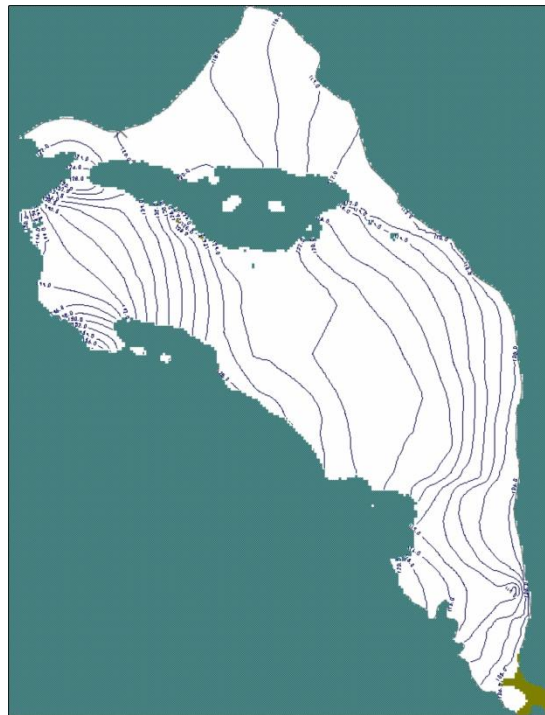## L.8.2.2   100th Percentile Potentiometric Head Distribution

A goal for the flow model is to produce a potentiometric distribution of heads that shows a steep water table in the 200-West Area due to the low-conductivity material types in that area and a relatively flat water table in the 200-East Area where high-conductivity material types are present. The pre-Hanford potentiometric surface is assumed to be approximately the same as the post-Hanford long-term, steady state condition, with water table mounding occurring below areas where, and at times when, Hanford operational discharges were released at the ground surface. Figures L–76, L–77, and L–78 are 100th percentile flow model simulations of the potentiometric surface in CY 1944 (pre-Hanford), CY 1975 (Hanford operations), and CY 2200 (post-Hanford), respectively.
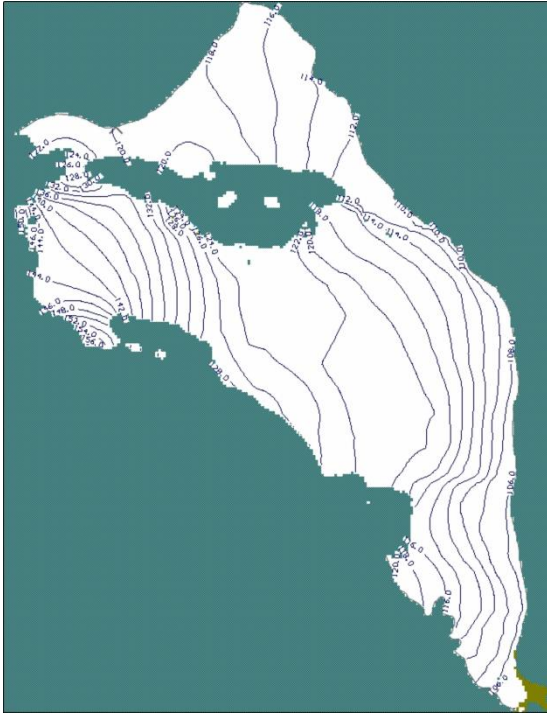
Figure L–76. 100th Percentile Flow Model Potentiometric Head Distribution, Calendar Year 1944
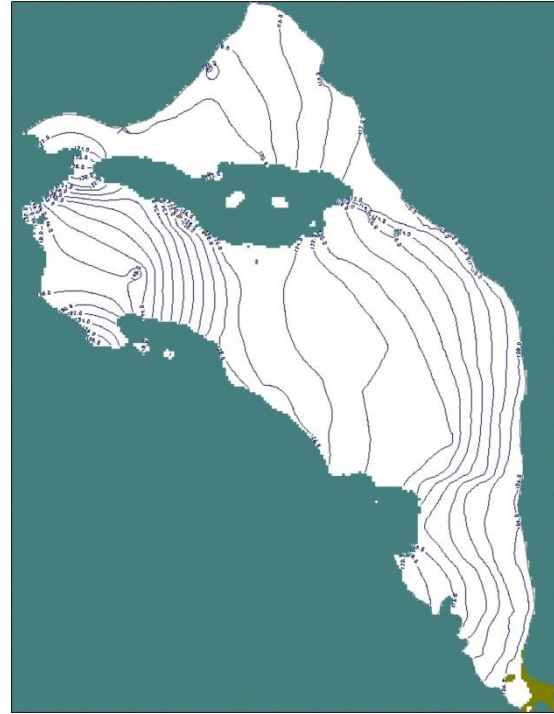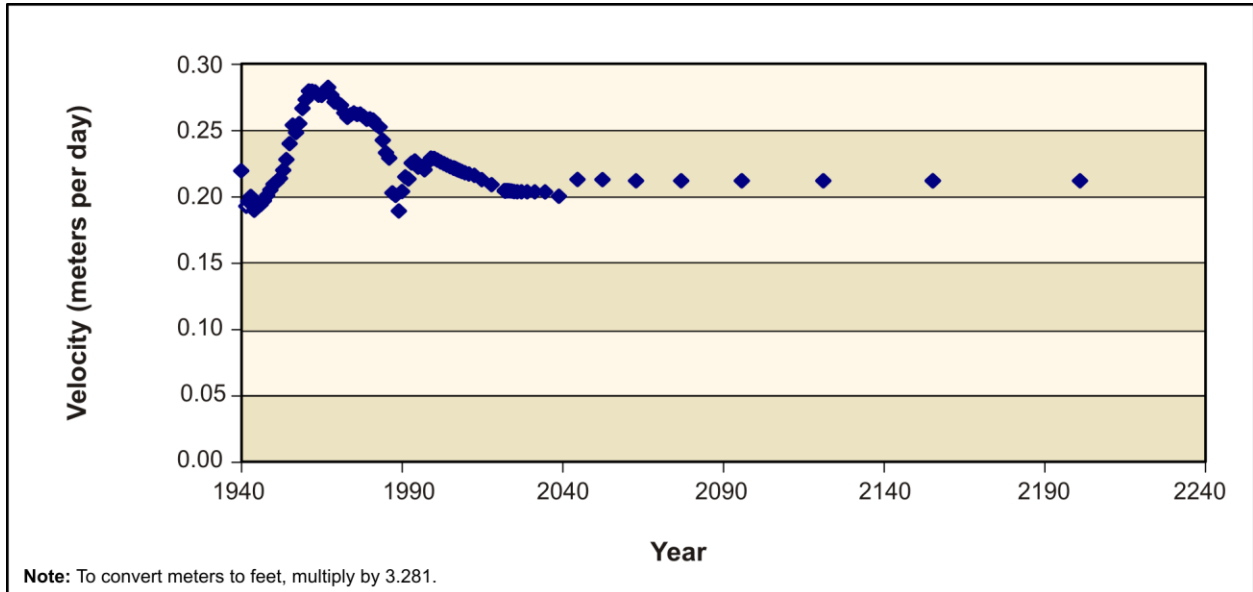

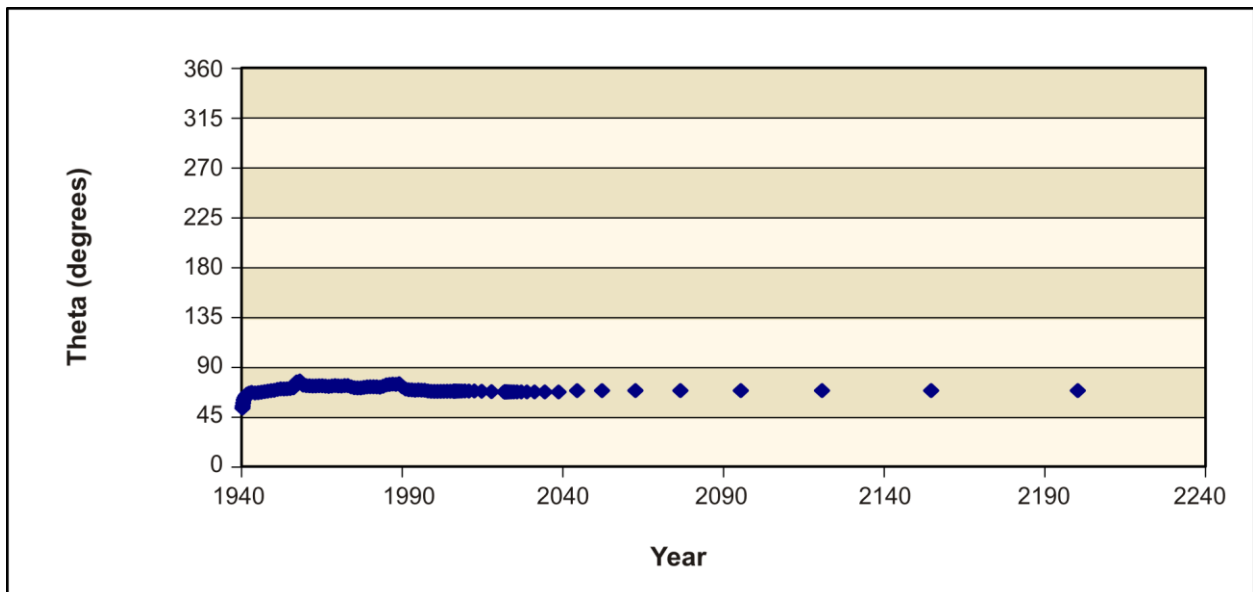**Figure L–77. 100th Percentile Flow Model Potentiometric Head Distribution, Calendar Year 1975**

Figure L–78. 100th Percentile Flow Model Potentiometric Head Distribution, Calendar Year 2200

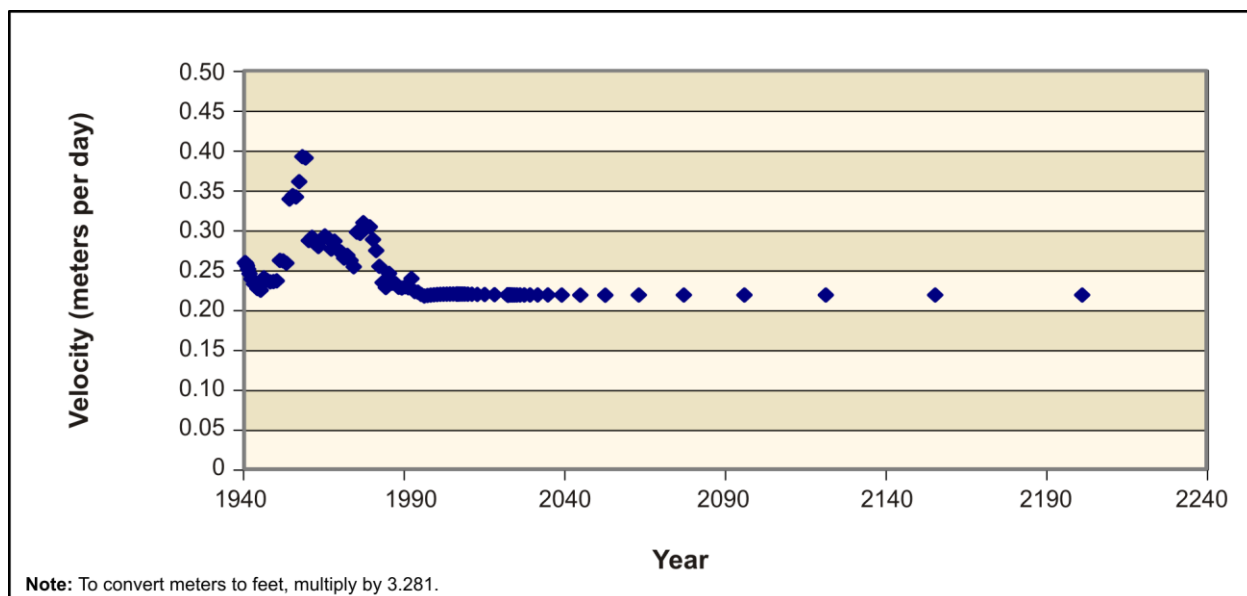## L.8.2.3 100th Percentile Flow Model Velocity Field

The 100th percentile flow model velocity field is variable in both magnitude and direction over time and across the model domain. This variability at selected locations within the model is shown in Figures L–79 through L–84. As expected, the velocities simulated in the 200-West Area are generally lower than those in the 200-East Area, particularly at the 200-East Area BY Cribs. An additional observation is that the velocity directions are highly variable during the Hanford operational period, particularly at the 200-East Area BY Cribs; there the velocity directions change by approximately 180 degrees due to water table mounding, coupled with this source's proximity to Gable Gap, where water table velocity and direction are sensitive to water table elevation.

Note: To convert meters to feet, multiply by 3.281.

Figure L–79. 100th Percentile Flow Model
Velocity Magnitude at 216-B-26 (BC Cribs in 200-East Area)

Figure L–80. 100th Percentile Flow Model
Velocity Direction at 216-B-26 (BC Cribs in 200-East Area)

Note: To convert meters to feet, multiply by 3.281.

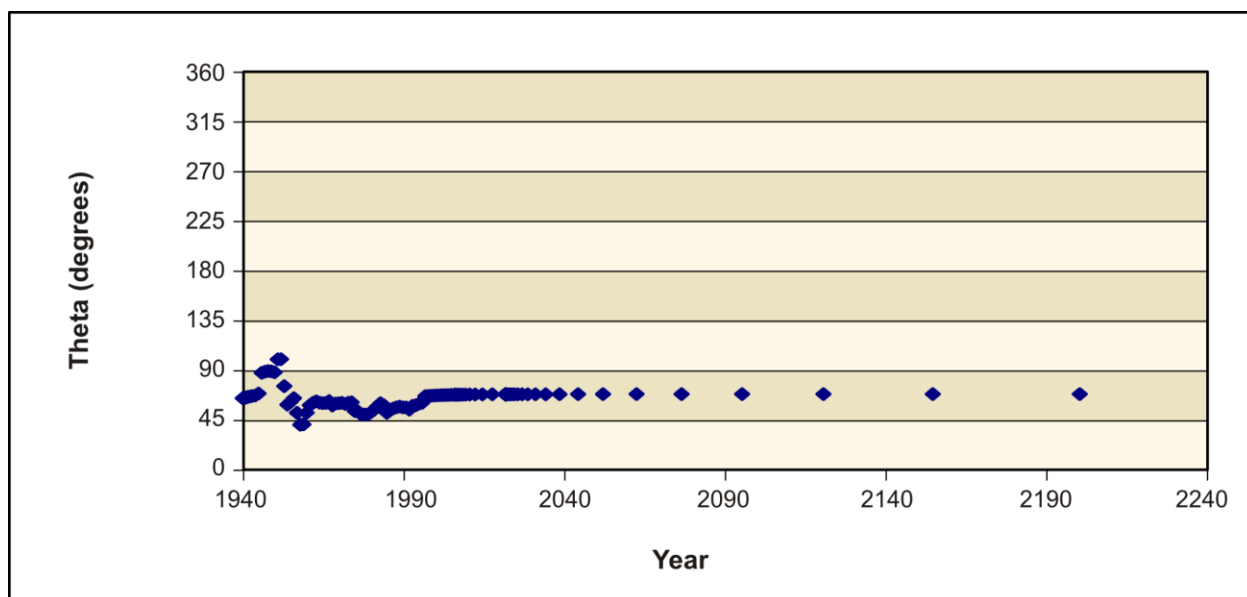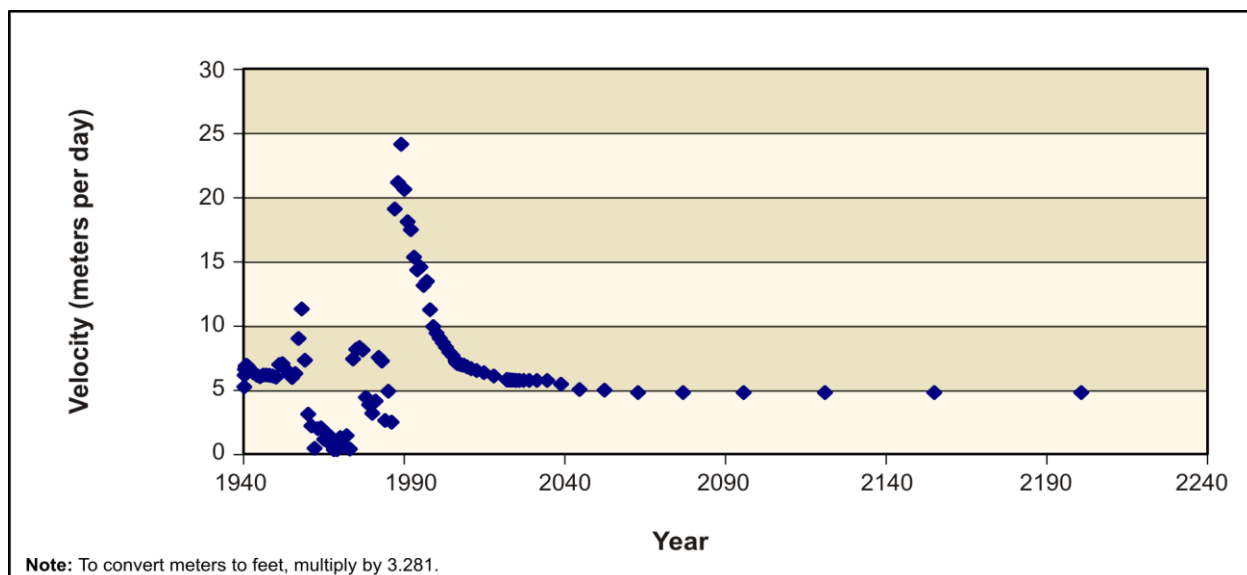**Figure L–81. 100th Percentile Flow Model Velocity Magnitude at 216-T-28 (200-West Area)**
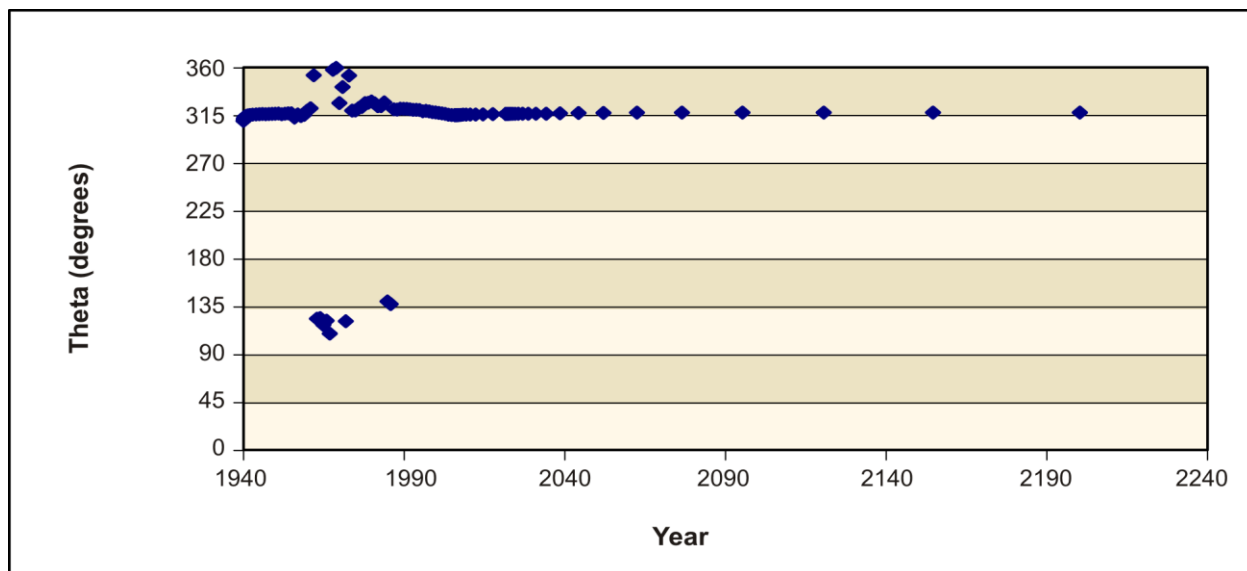

Figure L–82. 100th Percentile Flow Model Velocity Direction at 216-T-28 (200-West Area)
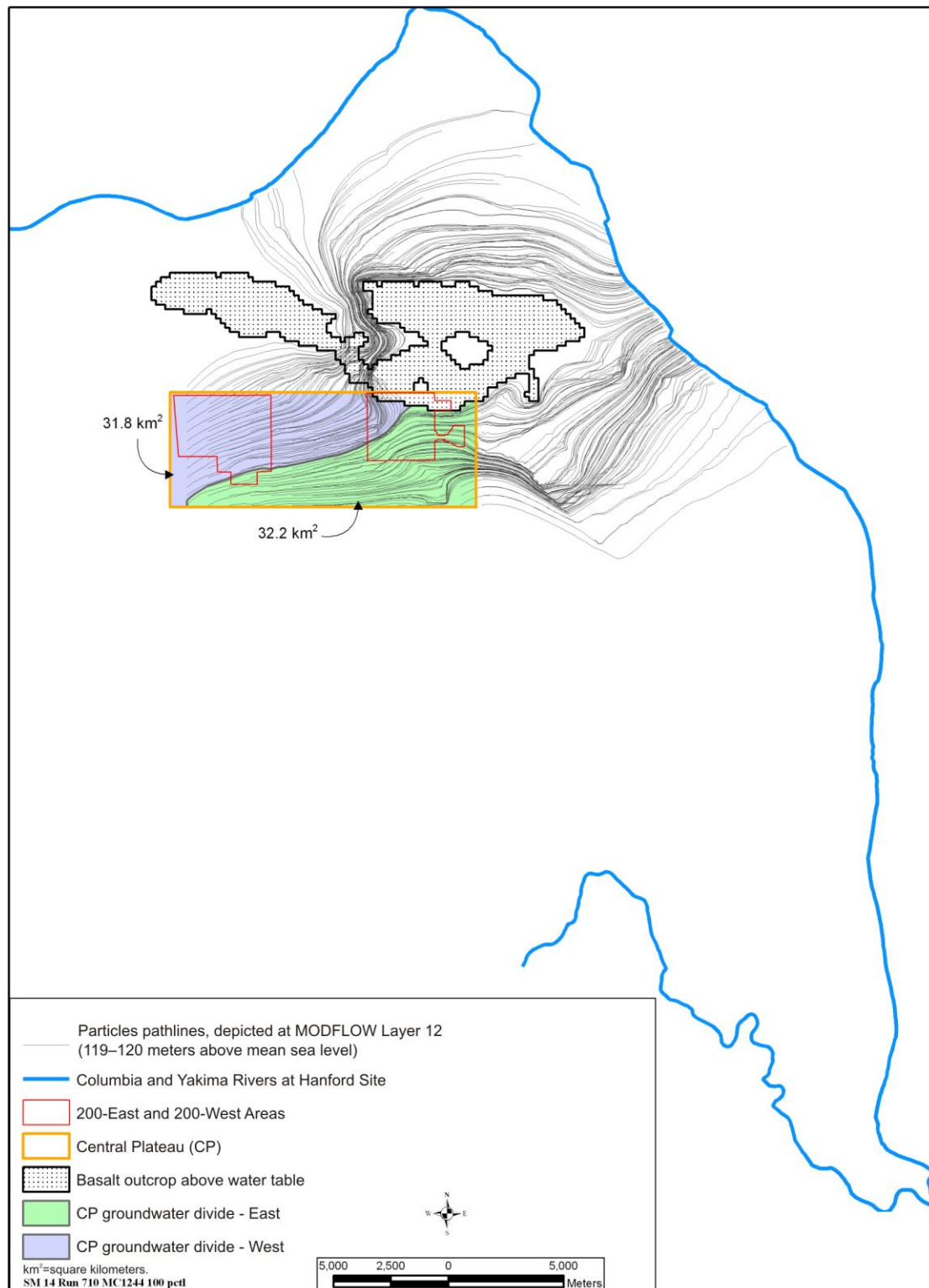
Figure L–83. 100th Percentile Flow Model Velocity Magnitude at BY Cribs (200-East Area)

Figure L–84. 100th Percentile Flow Model Velocity Direction at BY Cribs (200-East Area)

L.8.2.4   100th Percentile Flow Model Central Plateau Pathline Analysis

Pathline analysis determined the number of particles (measured in area) released in the Central Plateau area that would move to the north through Gable Gap and the number that would move to the east toward the Columbia River. As discussed in Section L.1.5, in the *Draft TC & WM EIS,* the pathline analysis to demonstrate the area of northerly versus easterly flow from the Central Plateau depended primarily on hydraulic conductivity distribution rather than on uncertainties in the TOB surface. Comparison of this analysis with the 66th and 95th percentile cases (see Sections L.8.1.4 and L.8.3.4) confirms this observation. This pathline analysis included a MODFLOW and MODPATH model run, releasing a uniformly distributed set of particles across the Central Plateau area. The Central Plateau is depicted as a rectangular boundary that includes all of the 200-East and 200-West Areas, as well as other areas between and outside the 200 Areas. Figure L–85 shows that, in terms of area, the flow of this model is predominantly eastward from the Central Plateau.

Figure L–85. 100th Percentile Flow Model Central Plateau Pathline Analysis

L.8.2.5   100th Percentile Flow Model Zone Budget Analysis

In addition to the particle pathline analysis described in the previous section, a zone budget analysis was completed to determine simulated water flow volumes from south of Gable Mountain and Gable Butte through Umtanum Gap, through Gable Gap, and easterly toward the Columbia River. Table L–20 provides total water flow volumes through these areas for CY 2200. These results show that about 17 percent of the total volume of water entering the Columbia River passes through Umtanum Gap, about 15 percent through Gable Gap, and about 68 percent directly east to the Columbia River. Comparison of these results with those of the 66th and 95th percentile cases shows that in terms of volumetric flow, rather than in terms of geometric position of the flow divide across the Central Plateau (see Section L.8.2.4), the model is less sensitive to variations in hydraulic conductivity.
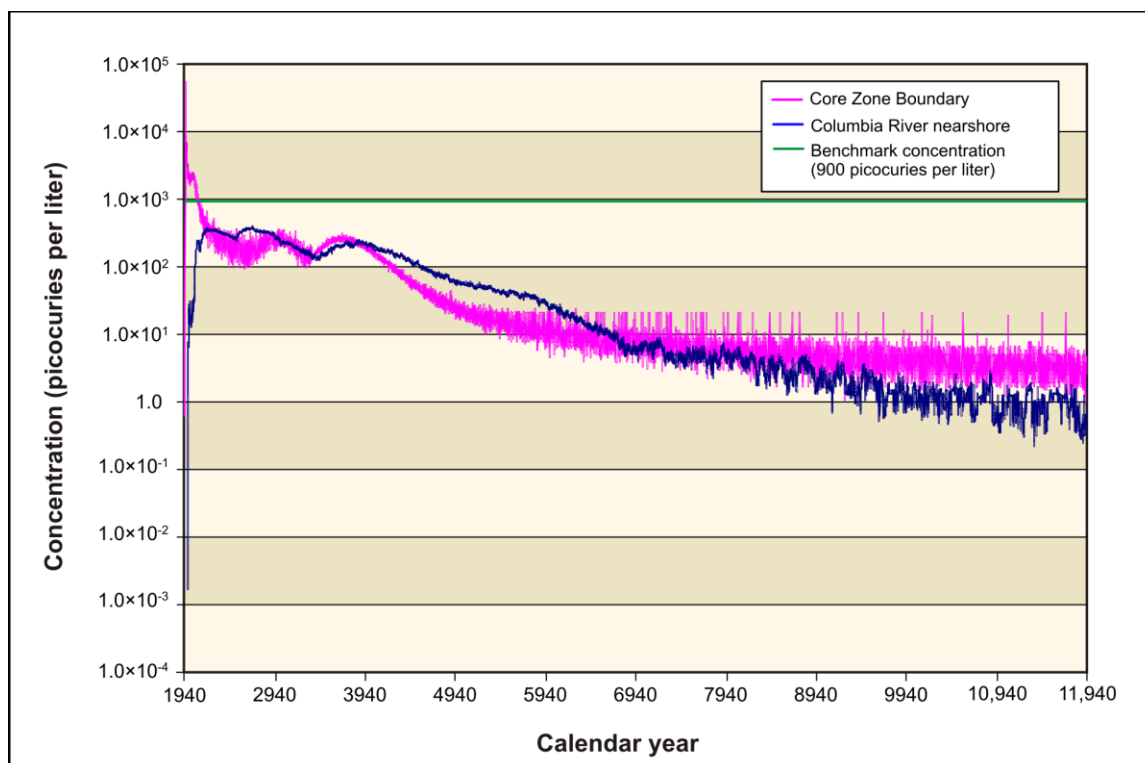
Table L–20. 100th Percentile Flow Model –
Simulated Water Flow Volumes Through Selected Areas, Calendar Year 2200

Water Flow Through	Water Volume (cubic meters per year)
Umtanum Gap	4,615,600
Gable Gap	4,294,500
East to Columbia River	18,977,000

Note: To convert cubic meters to cubic feet, multiply by 35.315.

L.8.2.6   100th Percentile Flow Model – Transport Model Concentration-Versus-Time Results

Groundwater transport modeling was completed using the 100th percentile flow model. Figures L–86 and L–87 show the concentration-versus-time results measured at the Core Zone Boundary and at the Columbia River nearshore for technetium-99 under Tank Closure Alternative 2B and Waste Management Alternative 2, Disposal Group 1, Subgroup 1-A, respectively. Figures L–86 and L–87 are comparable to Figures L–58 and L–59, respectively, for the 95th percentile flow model, and comparable to Figures L–114 and L–115, respectively, for the 66th percentile flow model. These comparisons show that the three flow models result in similar technetium-99 concentrations over time for the two alternatives presented. See Chapter 2 for a description of these alternatives.

**Figure L–86. Tank Closure Alternative 2B 100th Percentile Flow Model
Concentration-Versus-Time Results for Technetium-99**
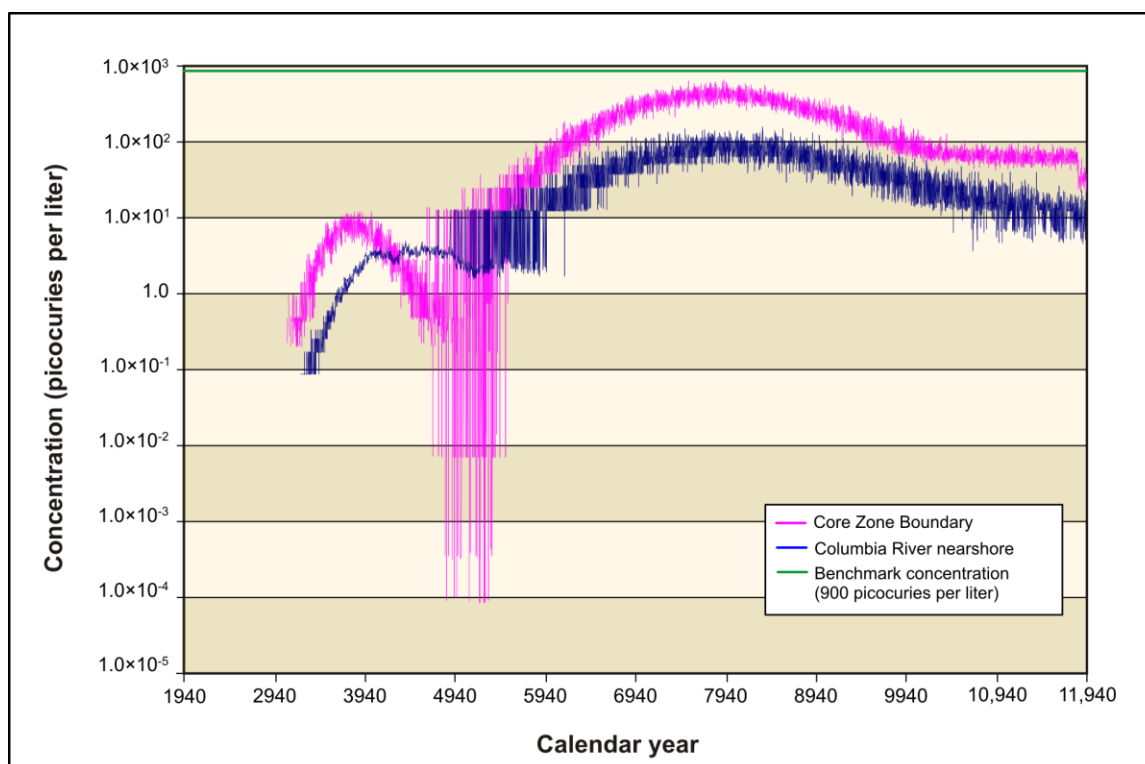
**Figure L–87. Waste Management Alternative 2, Disposal Group 1, Subgroup 1-A,
100th Percentile Flow Model
Concentration-Versus-Time Results for Technetium-99**

L.8.3   Results from the 66th Percentile Flow Model

L.8.3.1   Calibration Acceptance

Table L–21 provides a restatement of the flow model calibration acceptance criteria discussed in Section L.6.2, along with an assessment of the 66th percentile flow model's performance for each criterion. Specific data illustrative of such performance are reflected in Table L–22 and Figures L–88 through L–98.

Table L–21. Summary of the 66th Percentile Flow Model
Performance Compared with the Calibration Acceptance Criteria

Flow Model Calibration Acceptance Criteria	66th Percentile Flow Model Performance
Residual distribution should be reasonably normal.	Residual distribution is reasonably normal (see Figure L–88).
The mean residual should be approximately 0.	Residual mean = 0.462 meters (1.516 feet) (see Figure L–89).
The number of positive residuals should approximate the number of negative residuals.	Positive residuals approximately equal negative residuals (see Figure L–88).
The correlation coefficient (calculated versus observed) should be greater than 0.9.	Correlation coefficient = 0.972 (see Figure L–89).
The root mean square (RMS) error (calculated versus observed) should be less than 5 meters (16.4 feet), approximately 10 percent of the gradient in the water table elevation.	RMS error = 2.412 meters (7.913 feet) (see Figure L–89).
Residuals in the 200-East Area should be distributed similarly to those in the 200-West Area.	Residuals in the 200-East and 200-West Areas are distributed similarly (see Figures L−90 and L−91).
The residuals should be evenly distributed over time.	Residuals are approximately evenly distributed over time (see Figures L−92, L−93, L−94, and L−95).
The residuals should be evenly distributed across the site.	Residuals are approximately evenly distributed across the site (see Figures L−96, L−97, and L−98).
The calibrated parameters should compare reasonably well with field-measured values.	Calibrated hydraulic conductivity values are listed in Table L–22 and compare reasonably with field-measured values for material types to which the model is sensitive (i.e., Hanford formation and Ringold Formation material types). Figure L–42 provides field-measured values from aquifer pumping tests (Cole et al. 2001).
Parameters should be reasonably uncorrelated.	Hydraulic conductivity parameters are reasonably uncorrelated (see Table L–22 for the key to model material type zones and Table L–15 for the correlation coefficient matrix).

Table L–22. 66th Percentile Flow Model Calibrated Hydraulic Conductivity Values
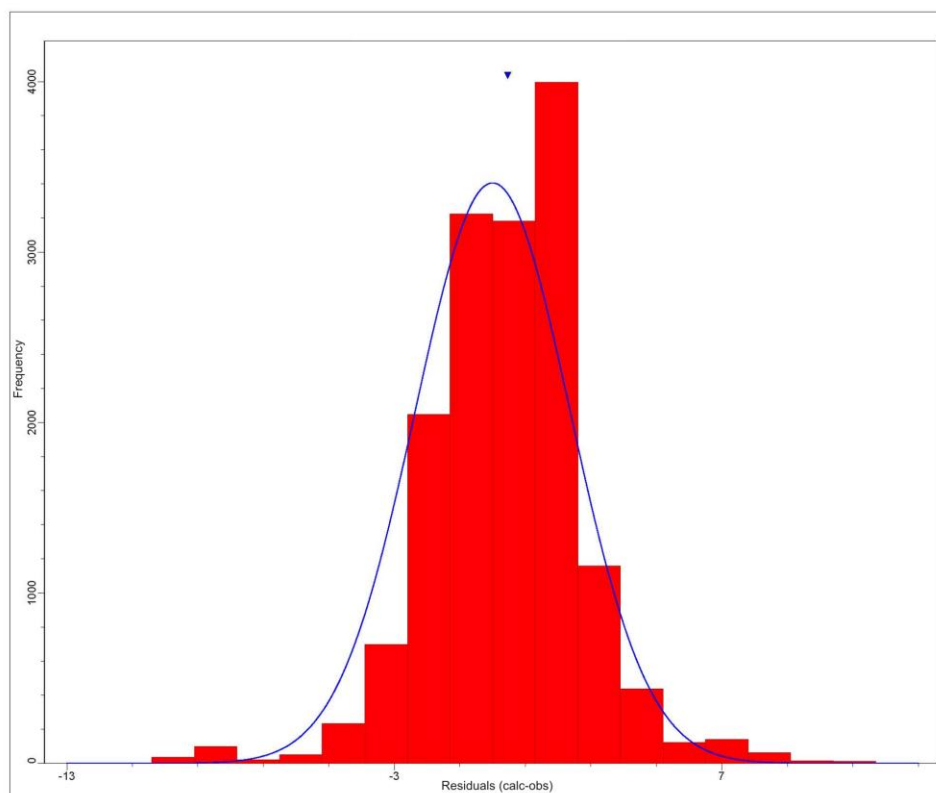
Material Type (Model Zone)	Hydraulic Conductivity (K_x)[a]	Hydraulic Conductivity (K_y)[b]	Hydraulic Conductivity (K_z)[c]
Hanford mud (1)	0.88	0.88	0.088
Hanford silt (2)	9.86	9.86	0.986
Hanford sand (3)	103.13	103.13	10.313
Hanford gravel (4)	278.63	278.63	27.863
Ringold sand (5)	3.69	3.69	0.369
Ringold gravel (6)	17.0	17.0	1.7
Ringold mud (7)	0.97	0.97	0.097
Ringold silt (8)	0.59	0.59	0.059
Plio-Pleistocene sand (9)	93.9	93.9	9.39
Plio-Pleistocene silt (10)	23.73	23.73	2.373
Cold Creek sand (11)	107.08	107.08	10.708
Cold Creek gravel (12)	43.73	43.73	4.373
Highly conductive Hanford formation (13)	2411.55	2411.55	241.155
Activated basalt (14)	0.001	0.001	0.0001

a Hydraulic conductivity with respect to the *x* axis, meters per day.
b Hydraulic conductivity with respect to the *y* axis, meters per day.
c Hydraulic conductivity with respect to the *z* axis, meters per day.
Note: To convert meters to feet, multiply by 3.281.

Figure L–88. 66th Percentile Flow Model Residual Distribution

Max. Residual: 13.001 (m) at 699-32-77/1
Min. Residual: 0 (m) at 699-44-42/1
Residual Mean : 0.462 (m)
Abs. Residual Mean : 1.843 (m)

Num. of Data Points : 15540
Standard Error of the Estimate : 0.019 (m)
Root Mean Squared : 2.412 (m)
Normalized RMS : 4.35 (%)
Correlation Coefficient : 0.972
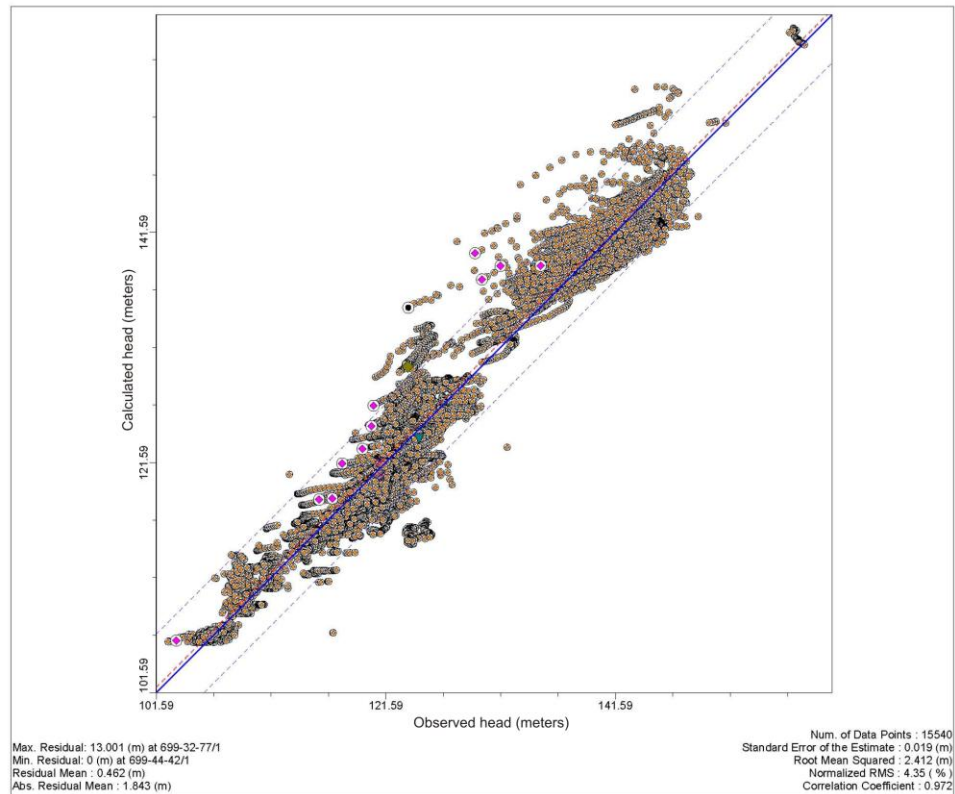
Figure L–89. 66th Percentile Flow Model Calibration Graph and Statistics

Max. Residual: 5.828 (m) at 699-36-58A/1
Min. Residual: 0 (m) at 699-44-42/1
Residual Mean : 1.873 (m)
Abs. Residual Mean : 2.144 (m)

Num. of Data Points : 2932
Standard Error of the Estimate : 0.025 (m)
Root Mean Squared : 2.312 (m)
Normalized RMS : 20.697 (%)
Correlation Coefficient : 0.52
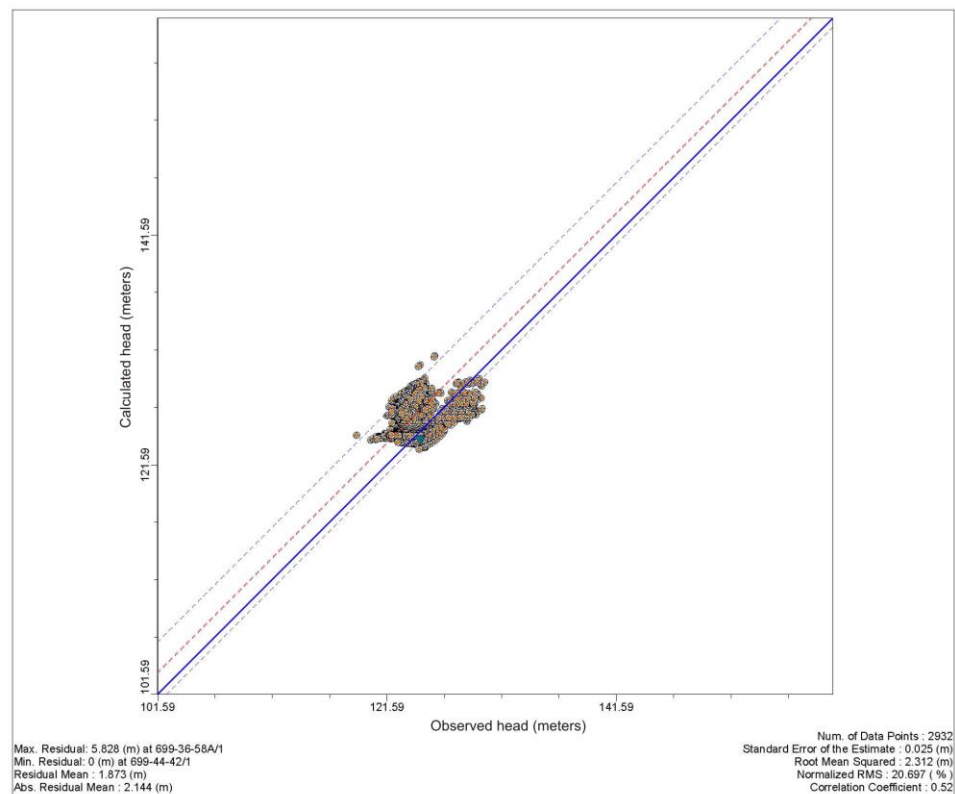
Figure L–90. 66th Percentile Flow Model Residuals – 200-East Area

Max. Residual: 13.001 (m) at 699-32-77/1
Min. Residual: -0.001 (m) at 699-49-79/1
Residual Mean : 0.322 (m)
Abs. Residual Mean : 1.754 (m)

Num. of Data Points : 2859
Standard Error of the Estimate : 0.041 (m)
Root Mean Squared : 2.226 (m)
Normalized RMS : 9.576 (%)
Correlation Coefficient : 0.8
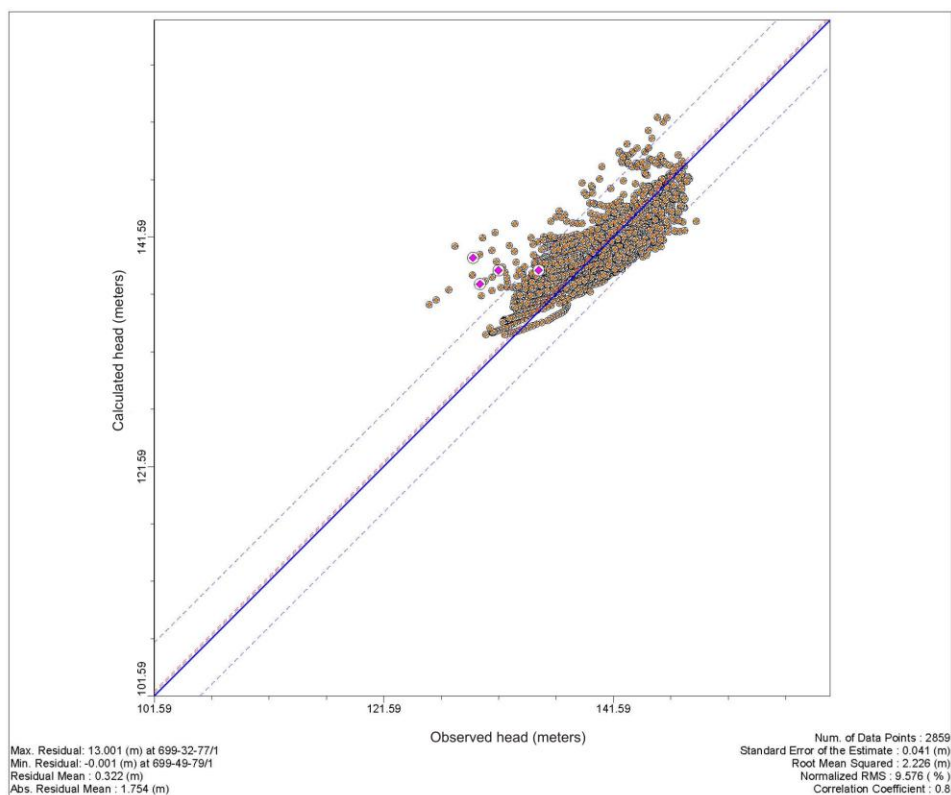
Figure L–91. 66th Percentile Flow Model Residuals – 200-West Area

Max. Residual: 11.282 (m) at 699-32-77/1
Min. Residual: 0.007 (m) at 299-E34-8/1
Residual Mean : -0.586 (m)
Abs. Residual Mean : 2.278 (m)

Num. of Data Points : 691
Standard Error of the Estimate : 0.111 (m)
Root Mean Squared : 2.986 (m)
Normalized RMS : 5.567 (%)
Correlation Coefficient : 0.959
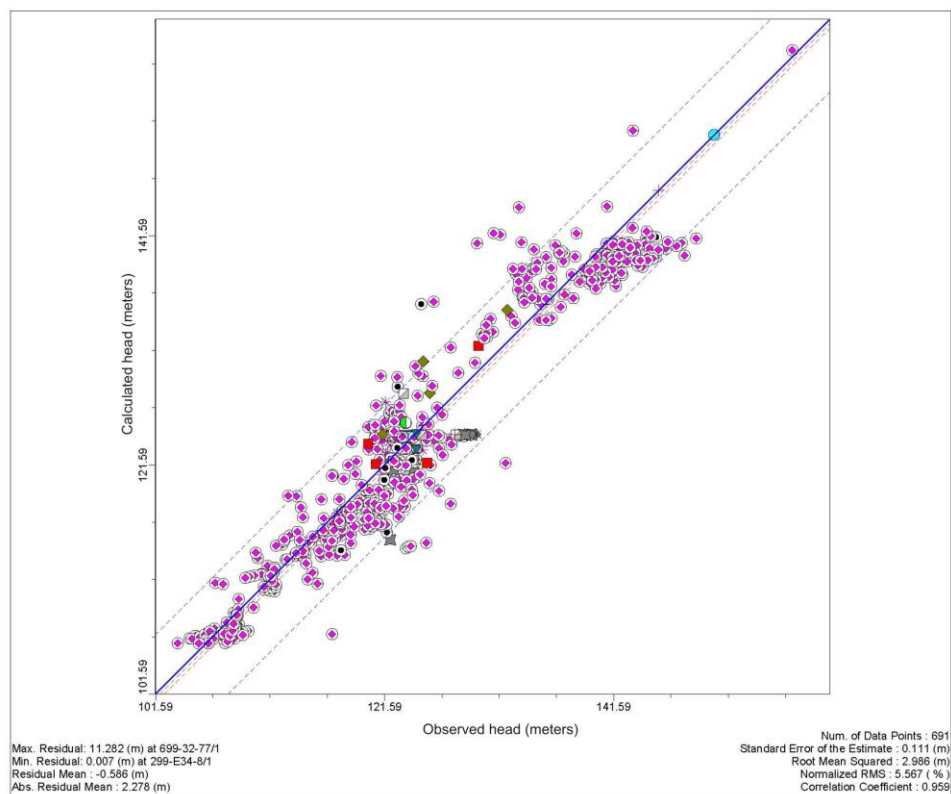
Figure L–92. 66th Percentile Flow Model Residuals, Calendar Year 1955

Figure L–93. 66th Percentile Flow Model Residuals, Calendar Year 1975
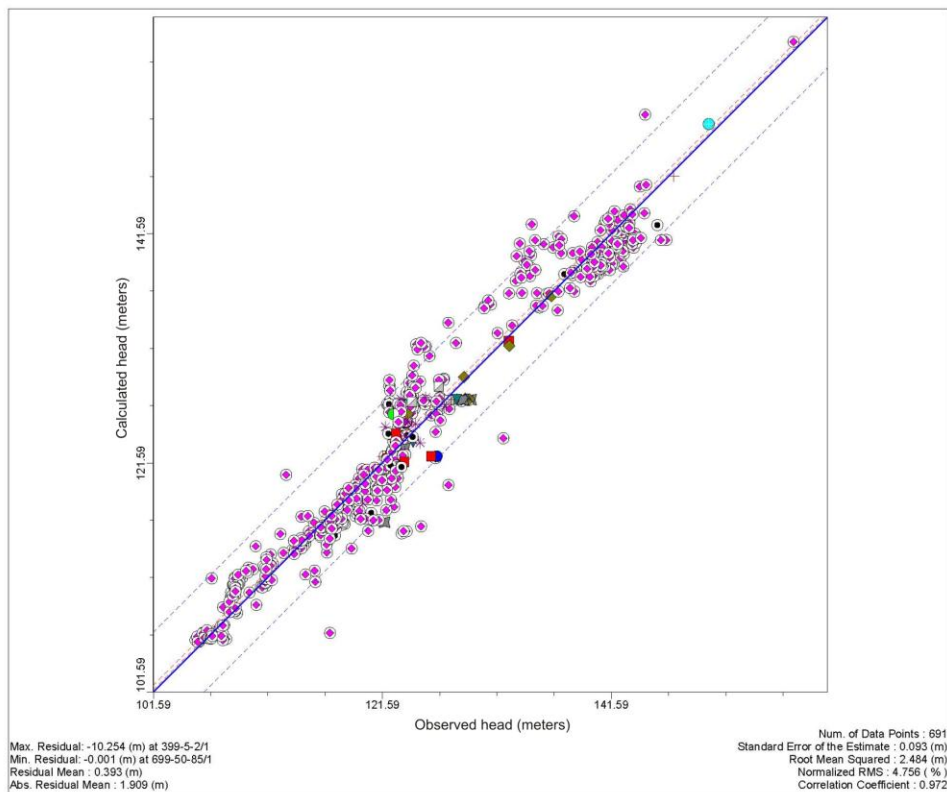
Figure L–94. 66th Percentile Flow Model Residuals, Calendar Year 1995

Figure L–95. 66th Percentile Flow Model Residuals, Calendar Year 2010

**Figure L–96. 66th Percentile Flow Model Residuals in
Northern Region of Model**
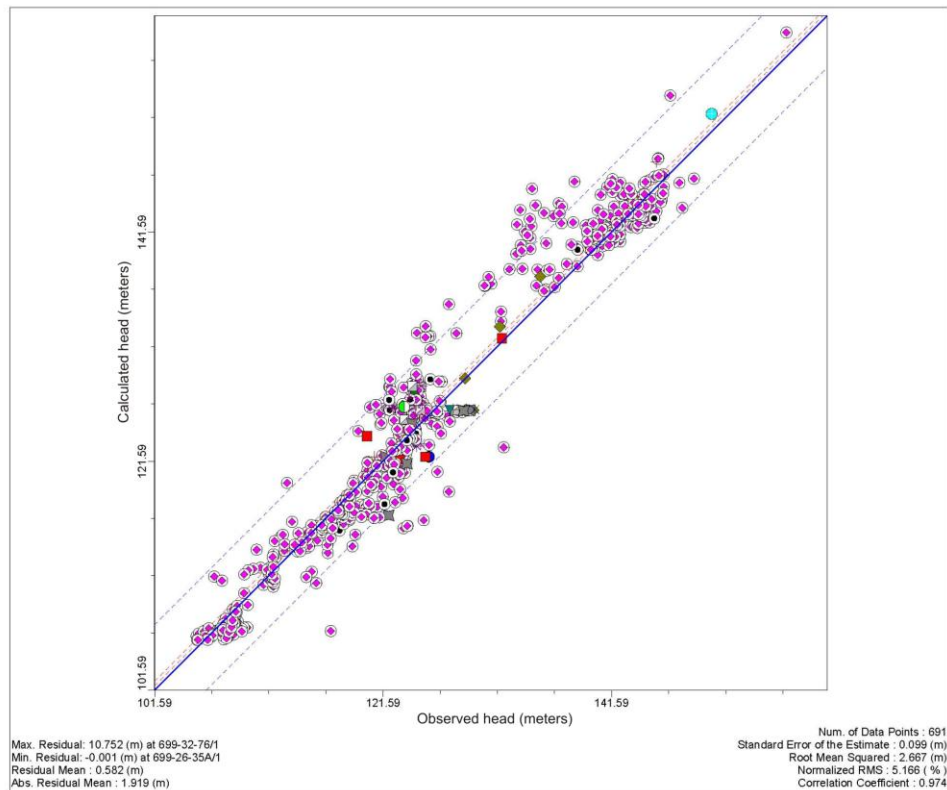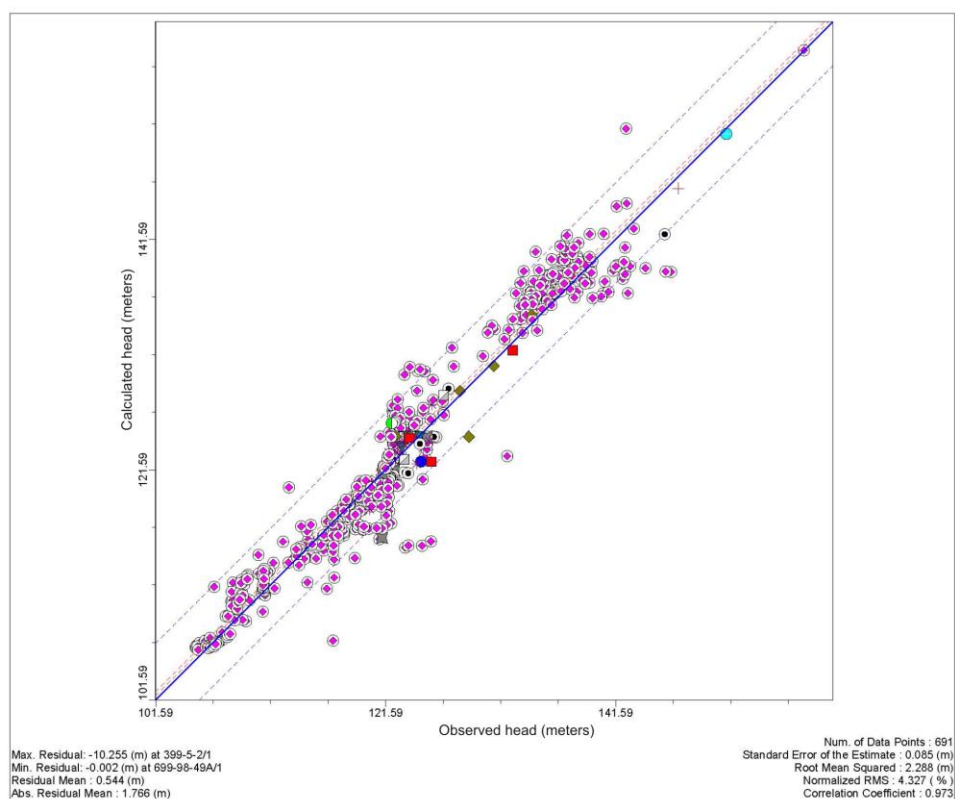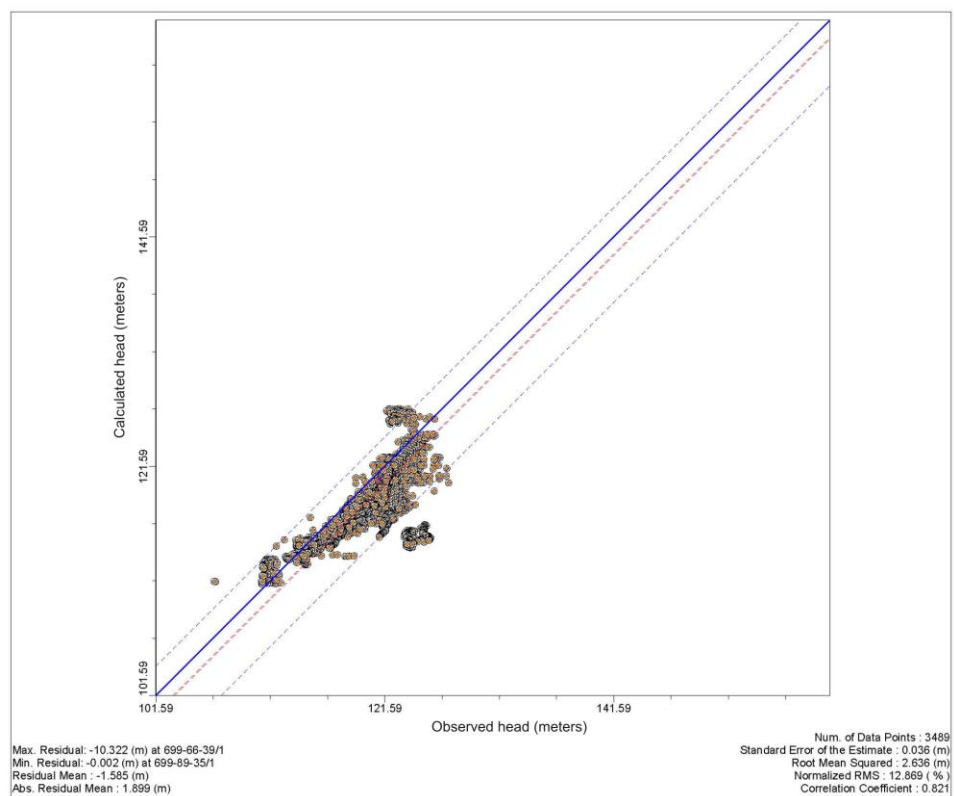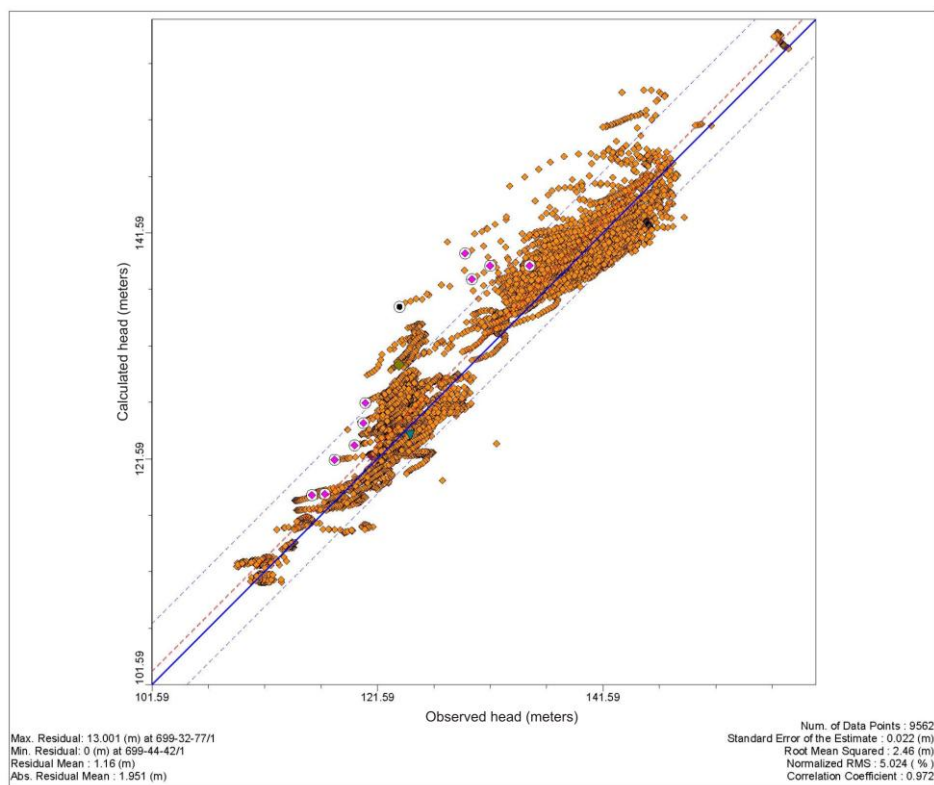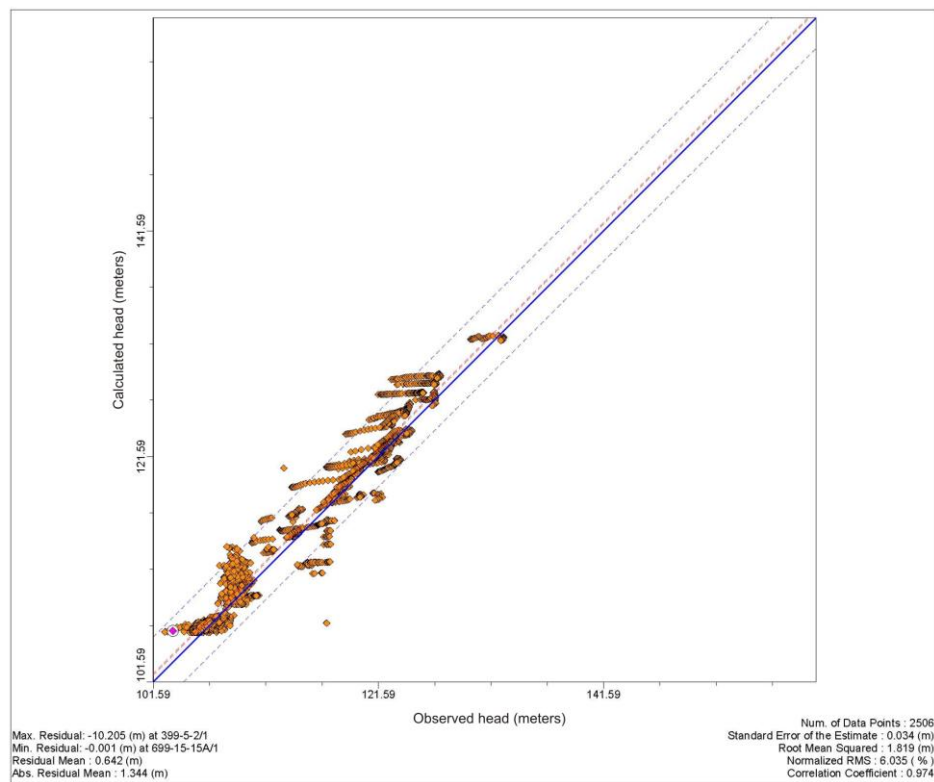
**Figure L–97. 66th Percentile Flow Model Residuals in
Central Region of Model**

**Figure L–98. 66th Percentile Flow Model Residuals in
Southern Region of Model**

In addition to the calibration acceptance criteria, water (or mass) balance and a long-term, steady state condition must be achieved in the calibrated flow model. Cumulative mass water balance data are shown in Figure L–99, indicating a cumulative mass balance error of approximately –1.4 percent. Total water balance and storage data as a function of time are shown in Figure L–100. The Figure L–100 data show storage values relative to the total water balance and indicate that storage-in is approximately equal to storage-out in model year 261 (CY 2200). This indicates that a long-term, steady state condition is achieved. Note that, in Figure L–100, there is a spike in "storage" at model year 82. This spike is the result of a time-stepping change at the beginning of the final long-term stress period. As a result, the model is moving from a relatively long time step at the end of the previous stress period (model year 82) to a relatively short time step at the beginning of the final stress period.

Note: Year zero=calendar year 1940.
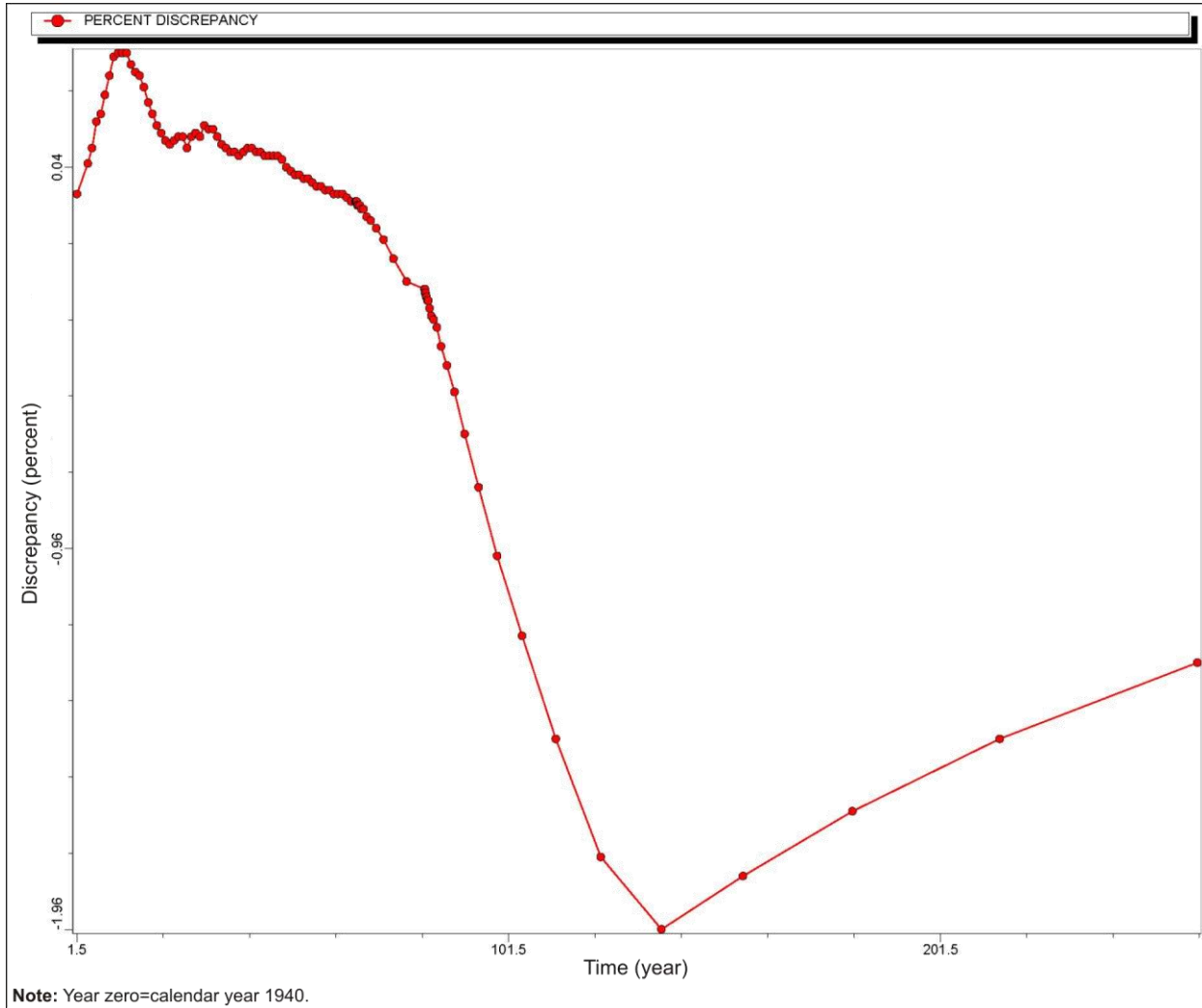
Figure L–99. 66th Percentile Flow Model Cumulative Water Balance Discrepancy

Note: Year zero=calendar year 1940. To convert cubic meters to cubic feet, multiply by 35.315.
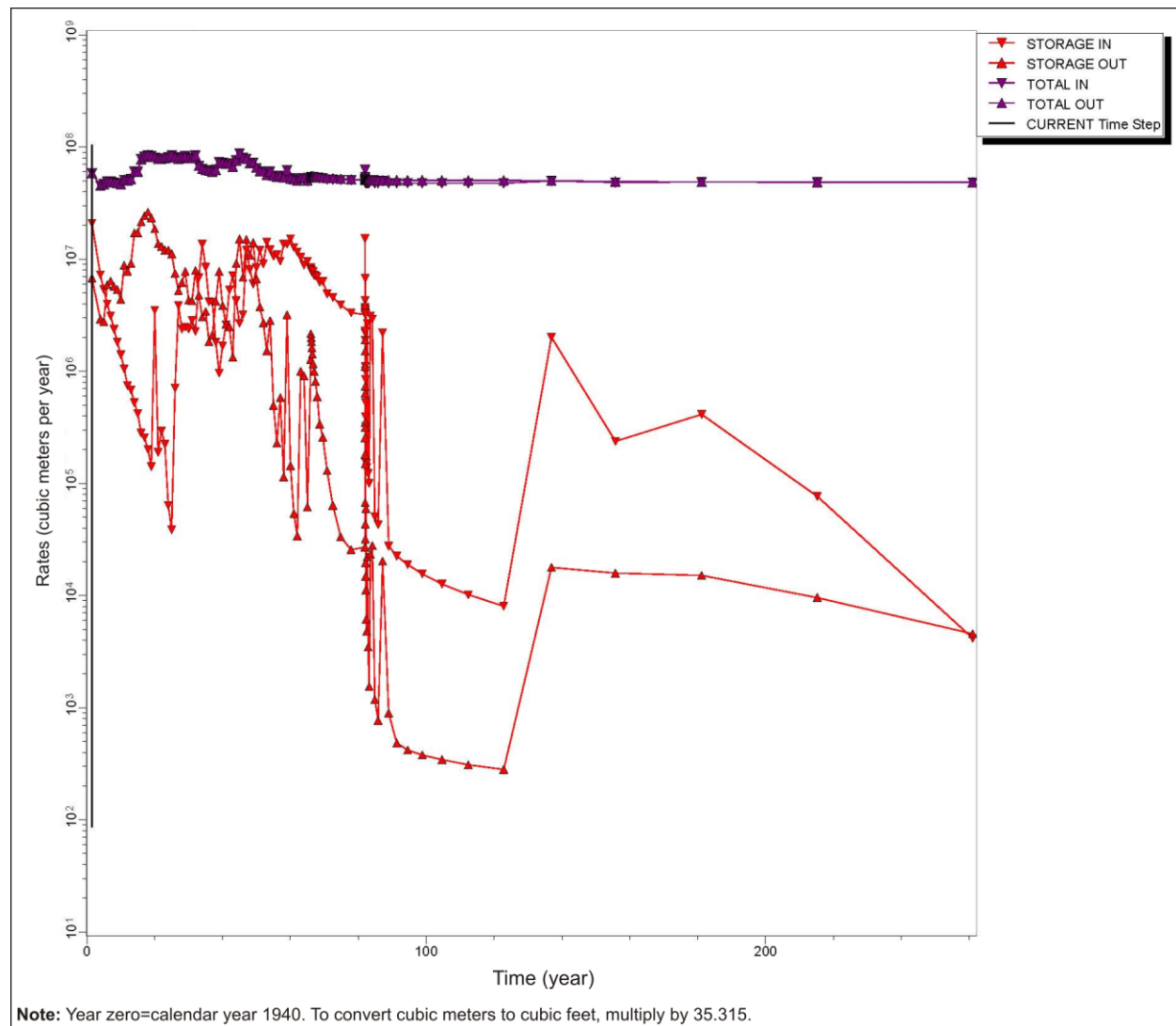
Figure L–100. 66th Percentile Flow Model Total Water and Storage Rates over Time

Additional water balance results for the 66th percentile flow model are shown in Figures L–101, L–102, and L–103 for GHBs, river boundaries, and recharge boundaries, respectively.

Key: HEAD DEP BOUNDS=head-dependent boundaries.
Note: Year zero=calendar year 1940. To convert cubic meters to cubic feet, multiply by 35.315.
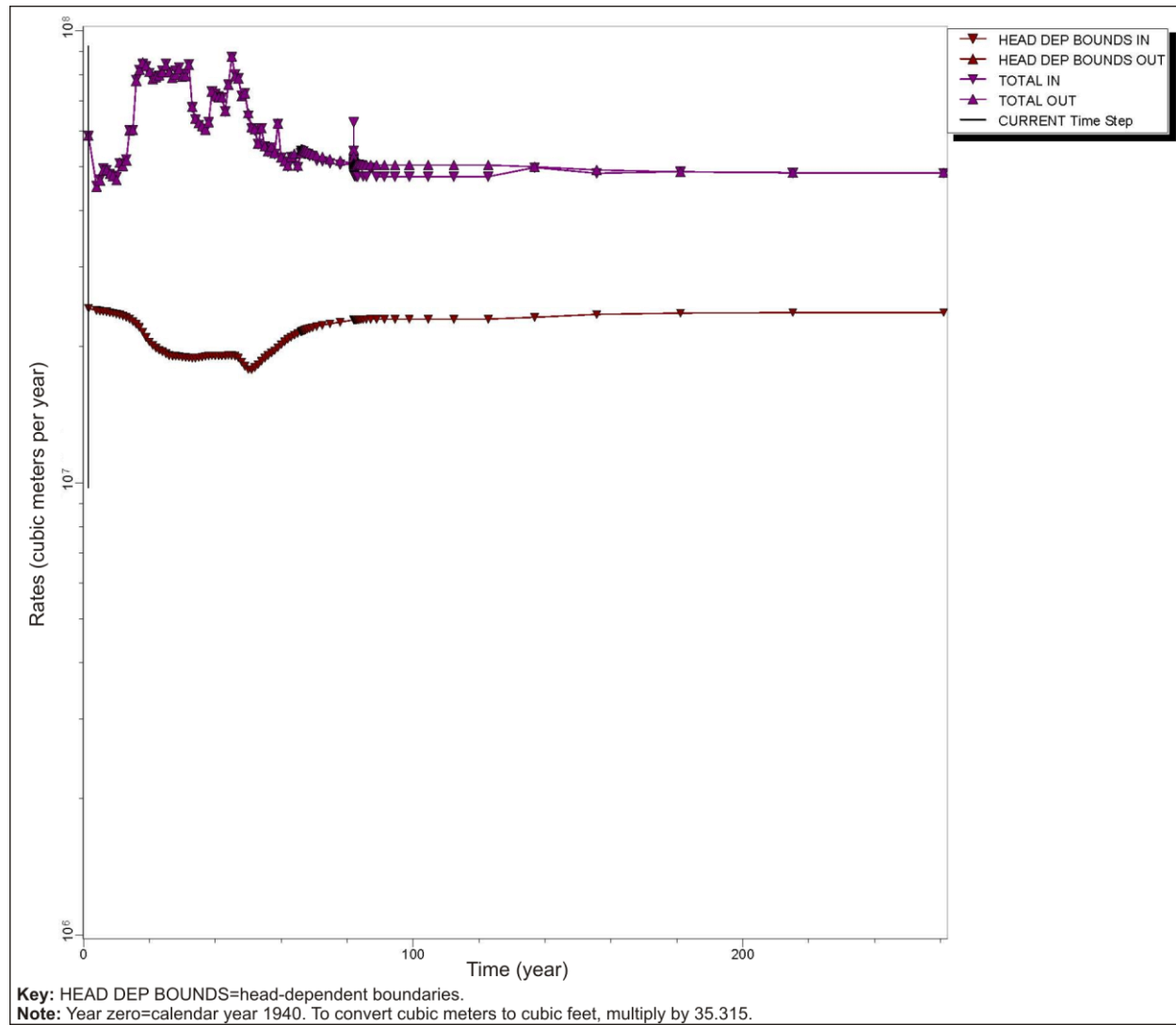
**Figure L−101. 66th Percentile Flow Model
Total Water and Generalized Head Boundary Rates over Time**

Note: Year zero=calendar year 1940. To convert cubic meters to cubic feet, multiply by 35.315.
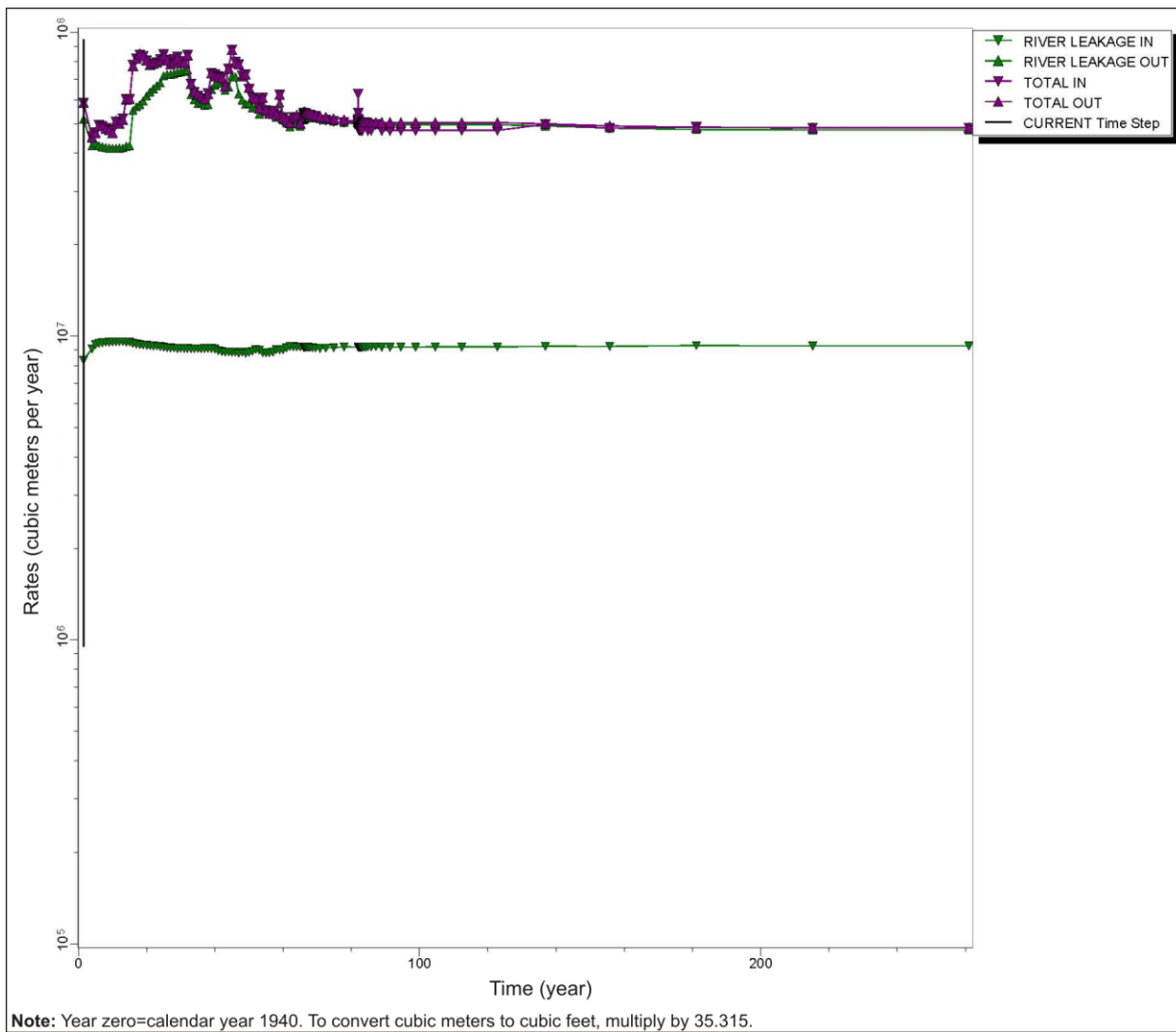
Figure L–102. 66th Percentile Flow Model Total Water and River Rates over Time
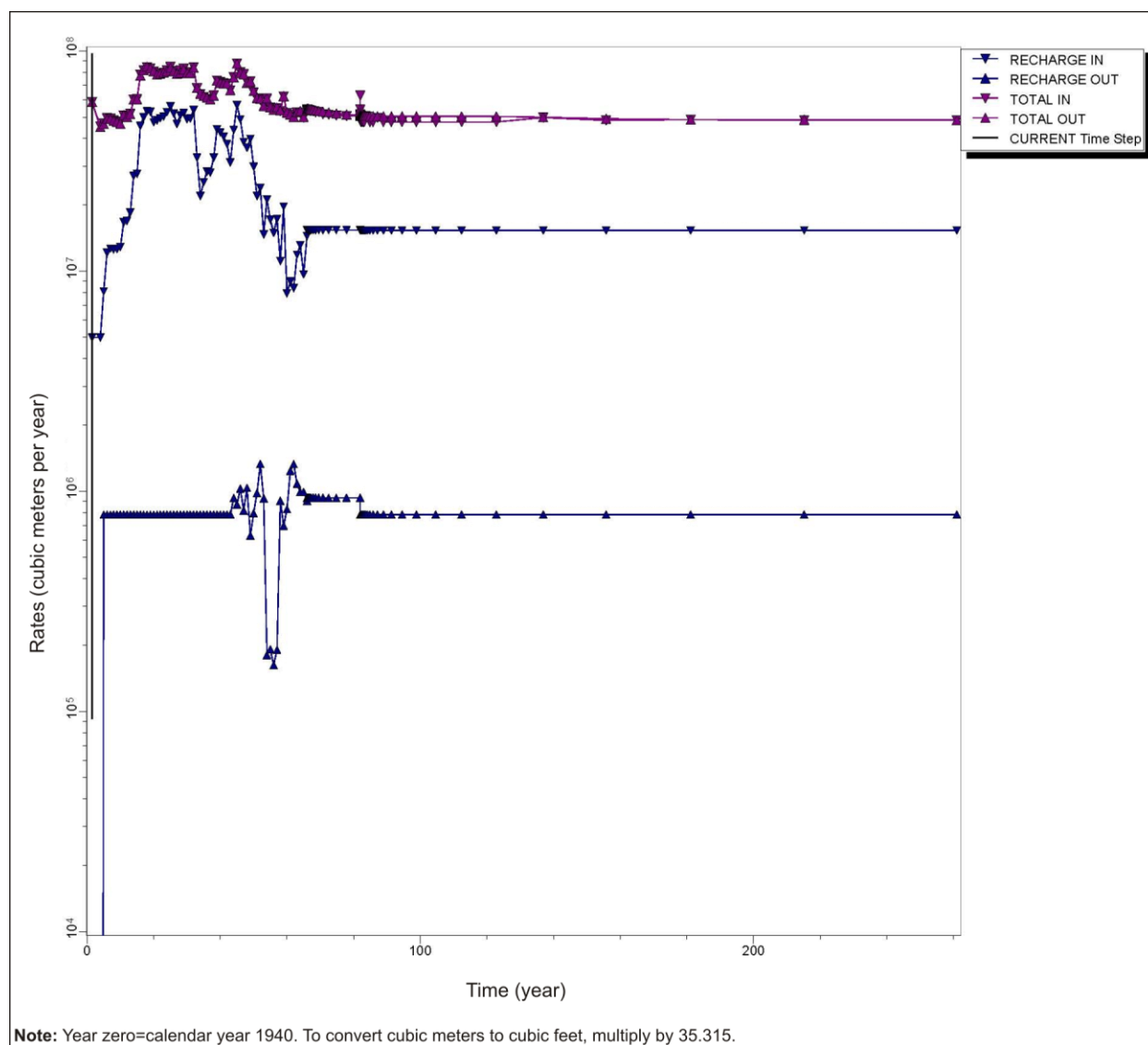
Figure L–103. 66th Percentile Flow Model Total Water and Recharge Rates over Time

L.8.3.2 66th Percentile Potentiometric Head Distribution

A goal for the flow model is to produce a potentiometric distribution of heads that shows a steep water table in the 200-West Area due to the low-conductivity material types in that area and a relatively flat water table in the 200-East Area where high-conductivity material types are present. The pre-Hanford potentiometric surface is assumed to be approximately the same as the post-Hanford long-term, steady state condition, with water table mounding occurring below areas where, and at times when, Hanford operational discharges were released at the ground surface. Figures L–104, L–105, and L–106 are 66th percentile flow model simulations of the potentiometric surface in CY 1944 (pre-Hanford), CY 1975 (Hanford operations), and CY 2200 (post-Hanford), respectively.

Figure L–104. 66th Percentile Flow Model Potentiometric Head Distribution, Calendar Year 1944

Figure L–105. 66th Percentile Flow Model Potentiometric Head Distribution, Calendar Year 1975

Figure L–106. 66th Percentile Flow Model Potentiometric Head Distribution, Calendar Year 2200

L.8.3.3   66th Percentile Flow Model Velocity Field

The 66th percentile flow model velocity field is variable in both magnitude and direction over time and across the model domain. This variability at selected locations (BC Cribs, 216-T-26 Crib, and BY Cribs) within the model is shown in Figures L–107 through L–112. As expected, the velocities simulated in 200-West Area are generally lower than those simulated in the 200-East Area, particularly at the 200-East Area BY Cribs. An additional observation is that the velocity directions are highly variable during the Hanford operational period, particularly at the 200-East Area BY Cribs; there the velocity directions change by approximately 180 degrees due to water table mounding, coupled with this source's proximity to Gable Gap, where water table velocity and direction are sensitive to water table elevation.

Note: To convert meters to feet, multiply by 3.281.
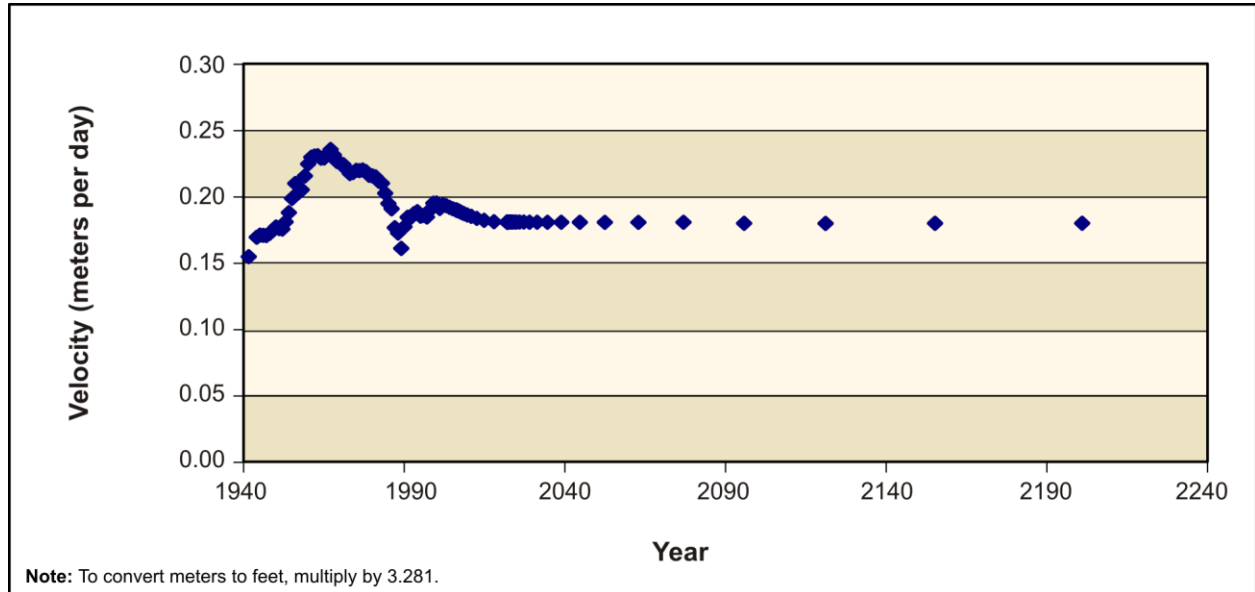
**Figure L–107. 66th Percentile Flow Model
Velocity Magnitude at 216-B-26 (BC Cribs in 200-East Area)**
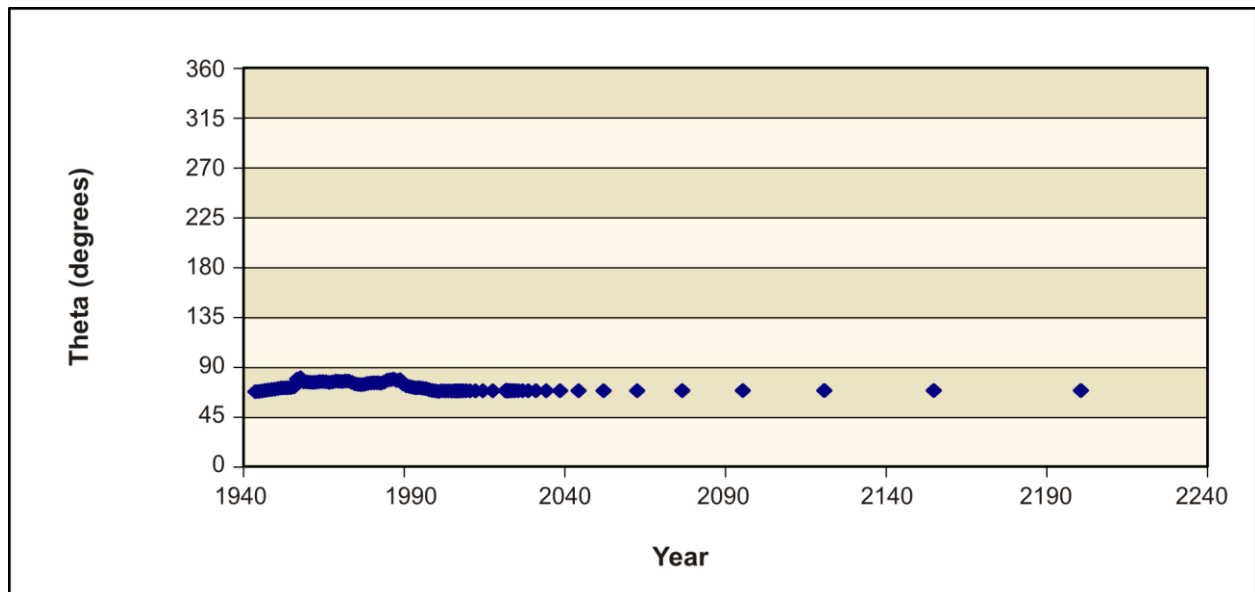
**Figure L–108. 66th Percentile Flow Model
Velocity Direction at 216-B-26 (BC Cribs in 200-East Area)**
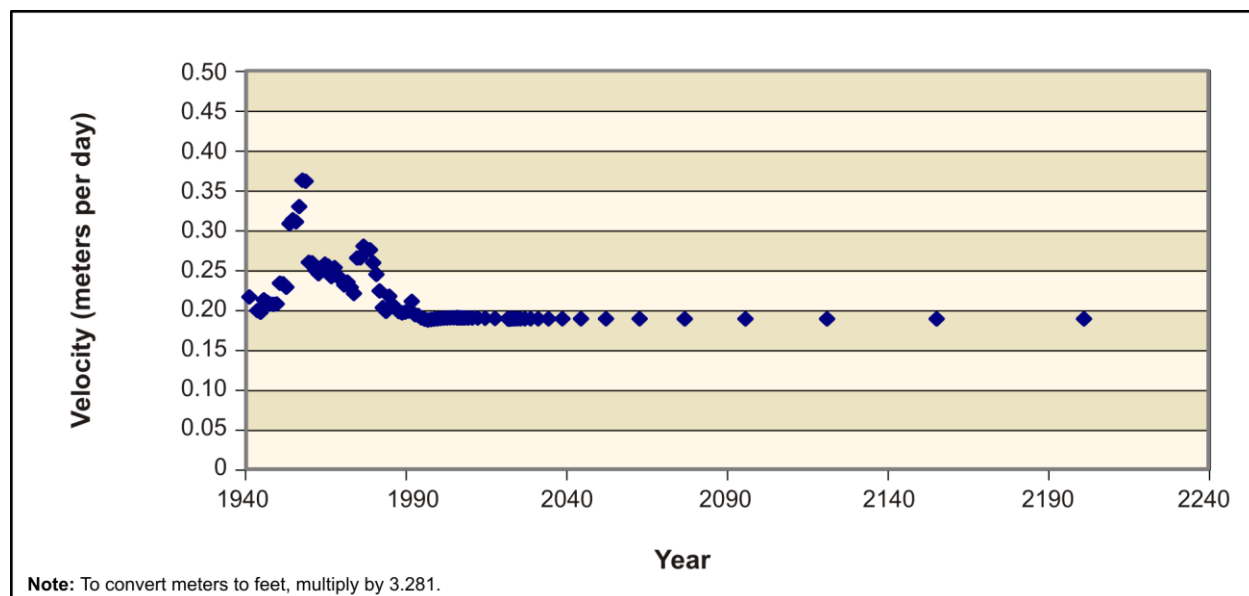
Figure L–109. 66th Percentile Flow Model
Velocity Magnitude at 216-T-28 Crib (200-West Area)
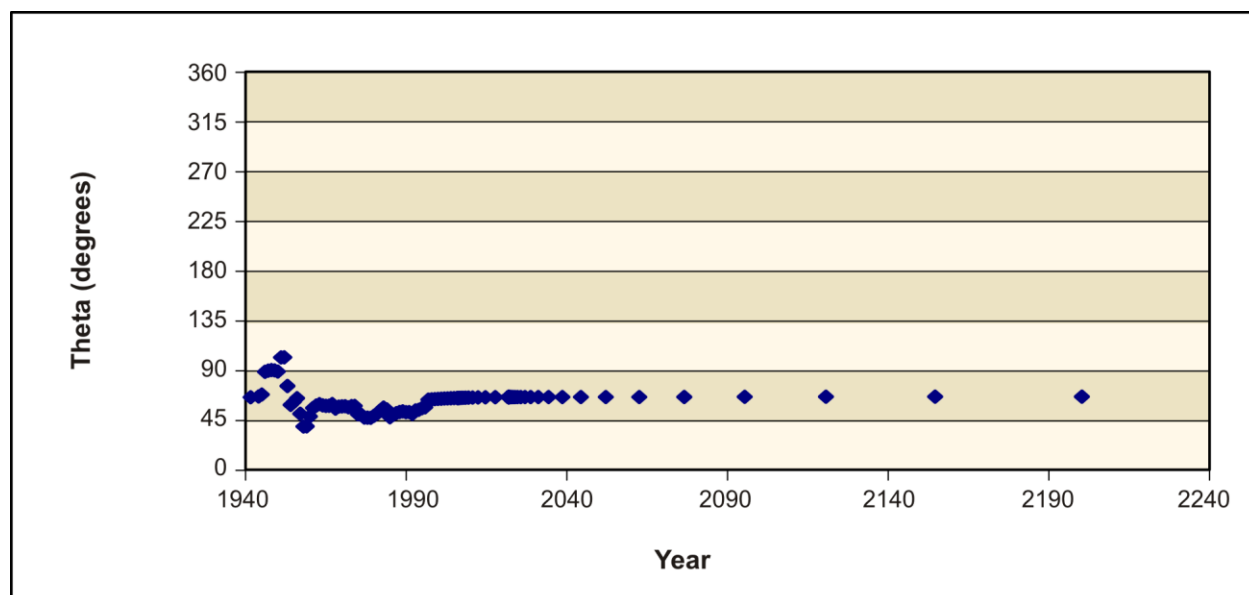
Figure L–110. 66th Percentile Flow Model
Velocity Direction at 216-T-28 Crib (200-West Area)
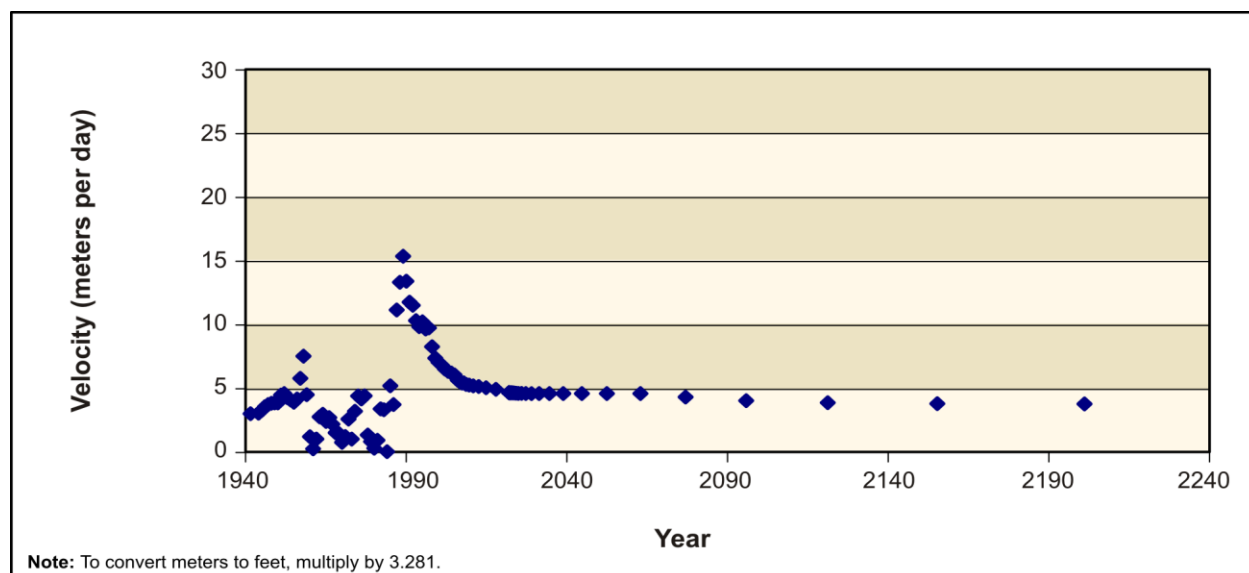
Figure L–111. 66th Percentile Flow Model Velocity Magnitude at BY Cribs (200-East Area)
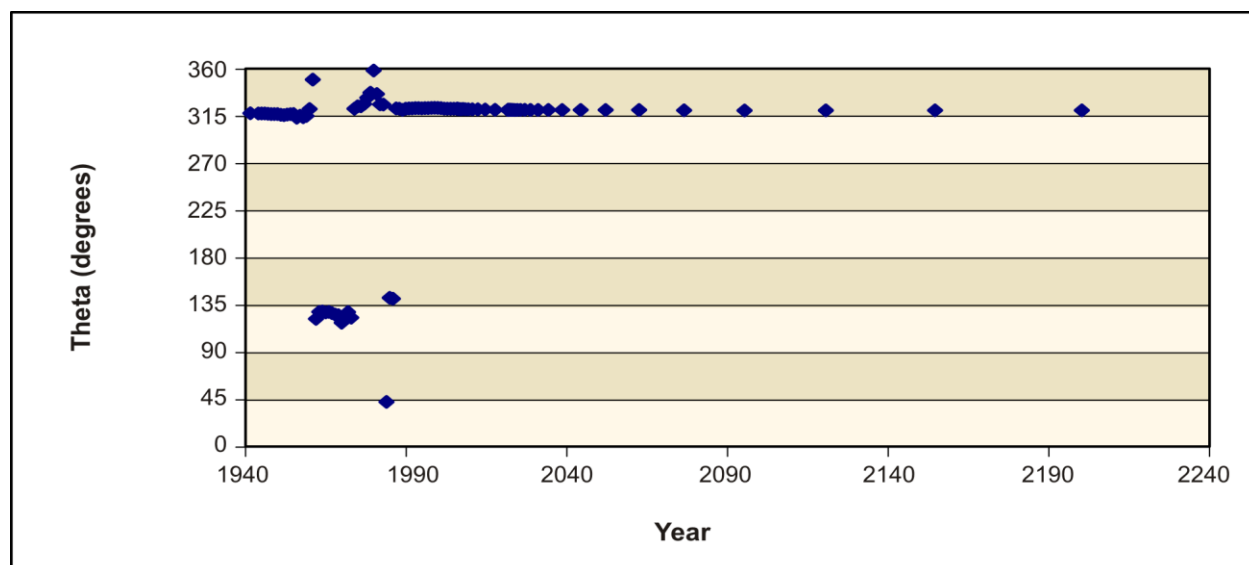
Figure L–112. 66th Percentile Flow Model Velocity Direction at BY Cribs (200-East Area)

L.8.3.4   66th Percentile Flow Model Central Plateau Pathline Analysis

Pathline analysis determined the number of particles (measured in area) released in the Central Plateau area that would move to the north through Gable Gap and the number of particles that would move to the east toward the Columbia River. As discussed in Appendix L, Section L.1.5, in the *Draft TC & WM EIS,* the pathline analysis to demonstrate the area of northerly versus easterly flow from the Central Plateau depended primarily on hydraulic conductivity distribution rather than on uncertainties in the TOB surface. Comparison of this analysis with the 95th and 100th percentile cases (see Sections L.8.1.4 and L.8.2.4) confirms this observation. This pathline analysis included a MODFLOW and MODPATH model run, releasing a uniformly distributed set of particles across the Central Plateau area. The Central Plateau is depicted as a rectangular boundary that includes all of the 200-East and 200-West Areas, as well as other areas between and outside the 200 Areas. Figure L–113 shows that, in terms of area, the flow of this model is predominantly northward from the Central Plateau.
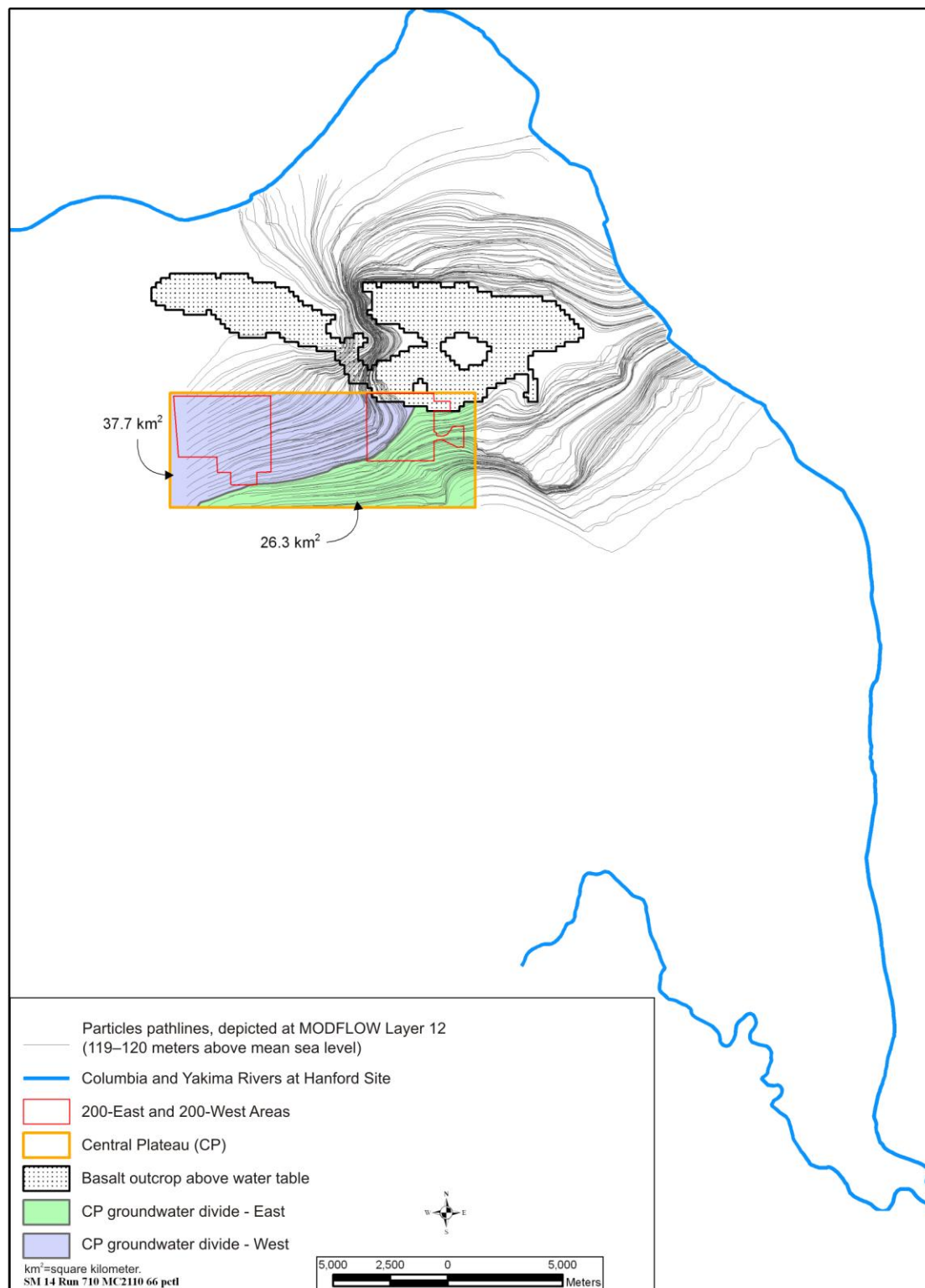
Figure L–113. 66th Percentile Flow Model Central Plateau Pathline Analysis

L.8.3.5   66th Percentile Flow Model Zone Budget Analysis

In addition to the particle pathline analysis described in the previous section, a zone budget analysis was completed to determine simulated water flow volumes from south of Gable Mountain and Gable Butte through Umtanum Gap, through Gable Gap, and easterly toward the Columbia River. Table L–23 provides total water flow volumes through these areas for CY 2200. These results show that about 18 percent of the total volume of water entering the Columbia River passes through Umtanum Gap, about 16 percent through Gable Gap, and about 66 percent directly east to the Columbia River. Comparison of these results with those of the 95th and 100th percentile cases shows that in terms of volumetric flow, rather than in terms of geometric position of the flow divide across the Central Plateau (see Section L.8.3.4), the model is less sensitive to variations in hydraulic conductivity.

Table L–23. 66th Percentile Flow Model –
Simulated Water Flow Volumes Through Selected Areas, Calendar Year 2200

Water Flow Through	Water Volume (cubic meters per year)
Umtanum Gap	4,458,400
Gable Gap	3,945,100
East to Columbia River	16,532,000

Note: To convert cubic meters to cubic feet, multiply by 35.315.

L.8.3.6   66th Percentile Flow Model – Transport Model Concentration-Versus-Time Results

Groundwater transport modeling was completed using the 66th percentile flow model. Figures L–114 and L–115 show the concentration-versus-time results measured at the Core Zone Boundary and at the Columbia River for technetium-99 under Tank Closure Alternative 2B and Waste Management Alternative 2, Disposal Group 1, Subgroup 1-A, respectively. Figures L–114 and L–115 are comparable to Figures L–58 and L–59 (respectively) for the 95th percentile flow model, and comparable to Figures L–86 and L–87 (respectively) for the 100th percentile flow model. These comparisons show that the three flow models result in similar technetium-99 concentrations over time for the two alternatives presented. See Chapter 2 of this *TC & WM EIS* for a description of these alternatives.
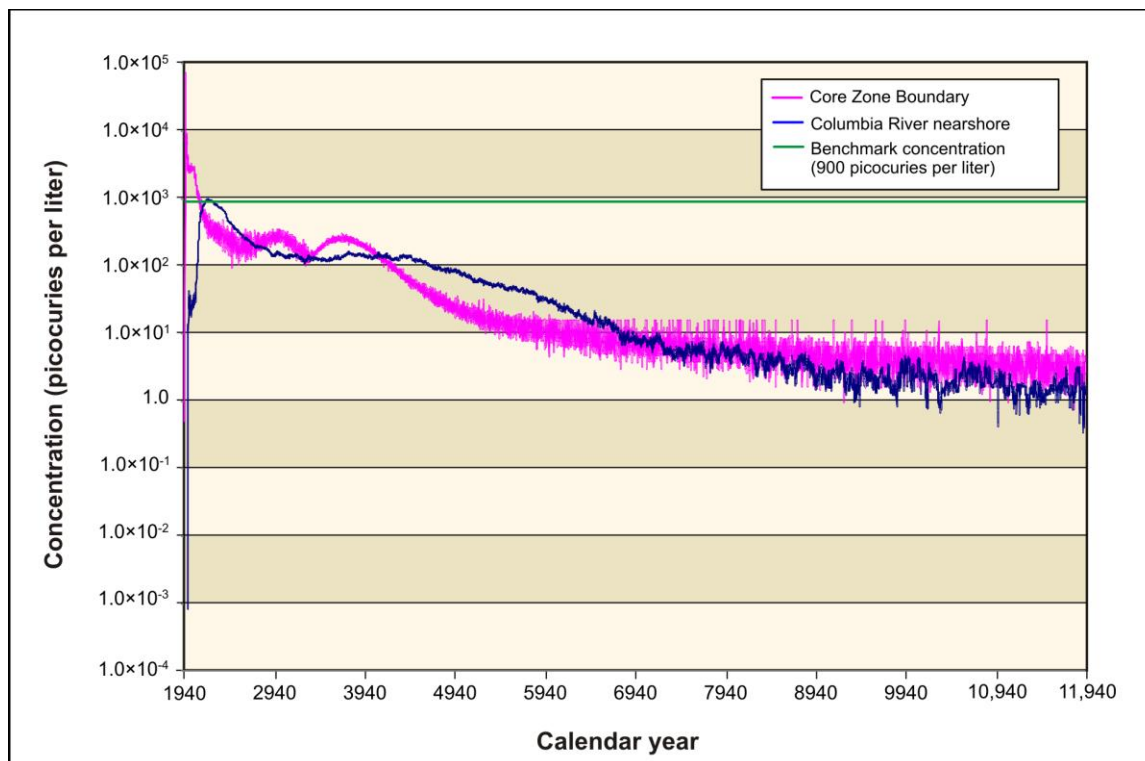
Figure L–114. Tank Closure Alternative 2B 66th Percentile Flow Model
Technetium-99 Concentration-Versus-Time Results
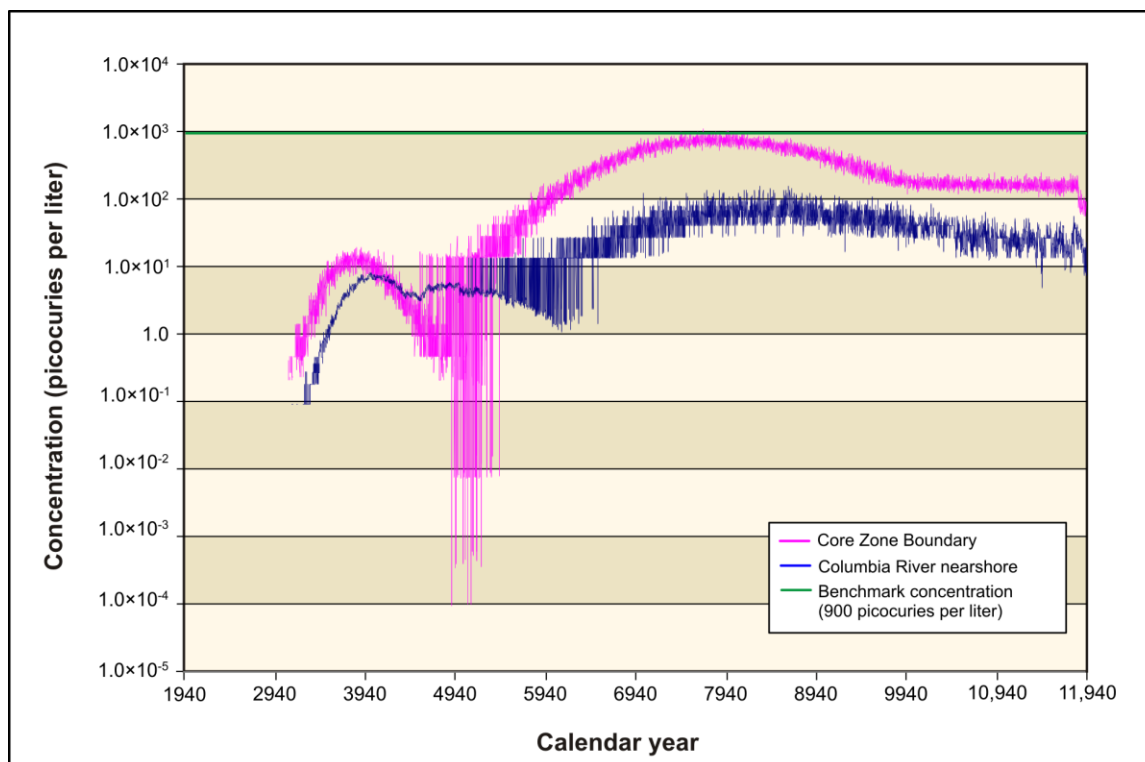
Figure L–115. Waste Management Alternative 2, Disposal Group 1, Subgroup 1-A,
66th Percentile Flow Model Technetium-99 Concentration-Versus-Time Results

L.8.4 Conclusions

Section L.10 provides a summary of the results produced by three models from the 5,000 hydraulic conductivity model runs described in Section L.7. These results show that any of the top one-third of models, as measured by RMS error when varying hydraulic conductivity values, achieves the EIS groundwater model calibration criteria. Therefore, it would be acceptable to use any of these models as the Base Case for analysis in this *Final TC & WM EIS*. The 95th percentile model was selected for analysis in this *Final TC & WM EIS* because its hydraulic conductivity values are identical to those assigned in the groundwater flow model used in the *Draft TC & WM EIS* analysis.

L.9 FLOW FIELD EXTRACTION

To support analysis of transport in the saturated zone, the MODFLOW groundwater flow model developed for this *Final TC & WM EIS* was used as the basis for particle-tracking simulations. The selected particle-tracking code does not directly read MODFLOW output files to calculate the heads and velocities required as input; instead, the MODFLOW files must be independently processed to generate these heads and velocities.

The Base Case flow model data files were processed by extracting hydraulic heads and velocities at each active cell within the model domain at selected times for use in groundwater transport modeling (see Appendix O of this *TC & WM EIS*). Table L–24 gives the times selected for extracting the head and velocity data.

Table L–24. Selected Times for Extracting the Base Case Head and Velocity Data Files

Stress Period	Time Step	Model Year	Calendar Year
1	100	4	1943
2	10	5	1944
3	10	6	1945
4	10	7	1946
5	10	8	1947
6	10	9	1948
7	10	10	1949
8	10	11	1950
9	10	12	1951
10	10	13	1952
11	10	14	1953
12	10	15	1954
13	10	16	1955
14	10	17	1956
15	10	18	1957
16	10	19	1958
17	10	20	1959
18	10	21	1960
19	10	22	1961
20	10	23	1962
21	10	24	1963
22	10	25	1964
23	10	26	1965
24	10	27	1966
25	10	28	1967
26	10	29	1968
27	10	30	1969

Table L–24. Selected Times for Extracting the Base Case Head and Velocity Data Files *(continued)*

Stress Period	Time Step	Model Year	Calendar Year
28	10	31	1970
29	10	32	1971
30	10	33	1972
31	10	34	1973
32	10	35	1974
33	10	36	1975
34	10	37	1976
35	10	38	1977
36	10	39	1978
37	10	40	1979
38	10	41	1980
39	10	42	1981
40	10	43	1982
41	10	44	1983
42	10	45	1984
43	10	46	1985
44	10	47	1986
45	10	48	1987
46	10	49	1988
47	10	50	1989
48	10	51	1990
49	10	52	1991
50	10	53	1992
51	10	54	1993
52	10	55	1994
53	10	56	1995
54	10	57	1996
55	10	58	1997
56	10	59	1998
57	10	60	1999
58	10	61	2000
59	10	62	2001
60	10	63	2002
61	10	64	2003
62	10	65	2004
63	10	66	2005
64	70	67	2006
64	90	67.9	2006.9
64	100	68.6	2007.6
64	110	69.5	2008.5
64	120	70.8	2009.8
64	130	72.5	2011.5
64	140	74.8	2013.8
64	150	77.9	2016.9
64	160	82	2021

Table L–24. Selected Times for Extracting the Base Case Head and Velocity Data Files *(continued)*

Stress Period	Time Step	Model Year	Calendar Year
65	230	83.2	2022.2
65	250	84.1	2023.1
65	270	85.8	2024.8
65	280	87.2	2026.2
65	290	88.9	2027.9
65	300	91.3	2030.3
65	310	94.5	2033.5
65	320	98.8	2037.8
65	330	104.6	2043.6
65	340	112.4	2051.4
65	350	122.8	2061.8
65	360	136.9	2075.9
65	370	155.7	2094.7
65	380	181.1	2120.1
65	390	215.2	2154.2
65	400	261	2200

L.10   SUMMARY

A three-dimensional transient flow model was developed in accordance with the *Technical Guidance Document* (DOE 2005) to support the *TC & WM EIS* analyses of alternatives and cumulative impacts. The flow model was developed using the MODFLOW 2000 engine within the Visual MODFLOW framework. The site conceptual model consists of an unconfined, heterogeneous aquifer bounded at the bottom by an impermeable basalt surface. Water enters the model from several sources: mountain-front recharge along Rattlesnake Mountain; the Yakima River; areal recharge; and operational discharges, primarily at the Central Plateau of Hanford. Water leaves the model via the Columbia River and several pumping wells. The operational discharges and pumping well withdrawals vary with time, providing the transient drivers to the model.

Standard data gathering and encoding techniques were used to develop the model extents, gridding, TOB topography, location and elevation of the Columbia and Yakima Rivers, lithology, and artificial discharges and withdrawals. These elements of the model were encoded directly from site-specific data. The background areal recharge was encoded as specified by the *Technical Guidance Document* (DOE 2005). Initial estimates for GHB heads and conductances, riverbed conductances, and material properties were encoded and refined through a flow calibration process as documented in the *Draft TC & WM EIS*, Appendix L. These parameter sets are unchanged in the *Final TC & WM EIS* model.

Internal reviews and public comment on the *Draft TC & WM EIS* motivated additional sensitivity analyses in this *Final TC & WM EIS* for a better understanding of the uncertainties in the parameter sets used for modeling. To that end, this *Final TC & WM EIS* includes a more extensive sensitivity analysis of a variety of boundary condition and material property parameter values, including the following:

- Hydraulic conductivity
- Storage properties (Sy)
- GHB head and conductance
- Background and anthropogenic recharge
- River conductance

These analyses show that the model is sensitive to changes in hydraulic conductivity values, but not highly sensitive to changes in the other parameters.

The results of the sensitivity analysis led to further evaluation of the performance of the top one-third of models, as ranked by RMS error in the hydraulic conductivity sensitivity analysis. This evaluation was completed by selecting the 66th, 95th, and 100th percentile models from this set and extracting detailed flow model results from each. These results are presented in this appendix. Evaluation of the results from these three models revealed that all achieve the calibration criteria, and thus any one of them could have been selected as the Base Case model for use in the *Final TC & WM EIS* analysis. The 95th percentile flow model was selected because it has the same parameter set values as the Base Case model used in the *Draft TC & WM EIS*.

The flow field from the 95th percentile model (Base Case) was extracted for use with contaminant transport modeling in the long-term groundwater impact analyses (see Appendix O). This flow field reflects the magnitude and direction of the pore water velocity throughout the active model domain. This Base Case model was used for additional analyses to determine the model's sensitivity to changes in recharge, GHB heads, and Columbia River heads. This analysis is presented in Appendix V.

L.11   REFERENCES

Bjornstad, B.N., and D.C. Lanigan, 2007*, Geologic Descriptions for the Solid-Waste Low-Level Burial Grounds*, PNNL-16887, Pacific Northwest National Laboratory, Richland, Washington, September.

Bjornstad, B.N., P.D. Thorne, B.A. Williams, G.V. Last, G.S. Thomas, M.D. Thompson, J.L. Ludwig, and D.C. Lanigan, 2010, *Hydrogeologic Model for the Gable Gap Area*, *Hanford Site,* PNNL-19702, Pacific Northwest National Laboratory, Richland, Washington, September.

CHPRC (CH2M HILL Plateau Remediation Company), 2009a, *Water Level Data*, Data Form 312, Richland, Washington, June 30.

CHPRC (CH2M HILL Plateau Remediation Company), 2009b, *Hanford Well Information System (HWIS),* accessed through http://prc.rl.gov/rapidweb/EDM/index.cfm?Pagenum=8, July 8.

CHPRC (CH2M HILL Plateau Remediation Company), 2010, *Soil and Groundwater Remediation Project*, accessed through http://prc.rl.gov/rapidweb/SGPR, September 29.

Cole, C.R., M.P. Bergeron, C.J. Murray, P.D. Thorne, S.K. Wurstner, and P.M. Rogers, 2001, *Uncertainty Analysis Framework – Hanford Site-Wide Groundwater Flow and Transport Model*, PNNL-13641, Pacific Northwest National Laboratory, Richland, Washington, November.

DOE (U.S. Department of Energy), 1988, *Consultation Draft, Site Characterization Plan, Reference Repository Location, Hanford Site, Washington,* DOE/RW-0164, Office of Civilian Radioactive Waste Management, Washington, D.C., January.

DOE (U.S. Department of Energy), 2005, *Technical Guidance Document for Tank Closure Environmental Impact Statement Vadose Zone and Groundwater Revised Analyses*, Final Rev. 0, Office of River Protection, Richland, Washington, March 25.

DOE (U.S. Department of Energy), 2010, *Hanford Site Cleanup Completion Framework,* DOE/RL-2009-10, Rev. 0, Richland Operations Office and Office of River Protection, Richland, Washington, July.

Ecology (Washington State Department of Ecology), 2003, *Well Logs*, accessed through http://apps.ecy.wa.gov/wellog/testsearch.asp, February 12.

Ecology, EPA, and DOE (Washington State Department of Ecology, Olympia, Washington; U.S. Environmental Protection Agency, Washington, D.C.; and U.S. Department of Energy, Richland, Washington), 1989, Hanford Federal Facility Agreement and Consent Order, 89-10, as amended, accessed through http://www.hanford.gov/tpa/tpahome.htm, May 15.

Hartman, M.J., and W.D. Webber, eds., 2008, *Hanford Site Groundwater Monitoring for Fiscal Year 2007*, DOE/RL-2008-01, Rev. 0, U.S. Department of Energy, Richland Operations Office, Richland, Washington, March.

Hill, M.C., 1990, *Preconditioned Conjugate-Gradient 2 (PCG2), A Computer Program for Solving Ground-Water Flow Equations*, Water-Resources Investigations Report 90-4048, U.S. Geological Survey, Denver, Colorado.

Johnston, K., J.M. Ver Hoef, K. Krivoruchko, and N. Lucas, eds., 2001, *Using ArcGIS Geostatistical Analyst*, Environmental Systems Research Institute, Inc., Redlands, California.

Lindsey, K.A., 1995, *Miocene- To Pliocene-Aged Suprabasalt Sediments of the Hanford Site, South-Central Washington*, BHI-00184, Rev. 00, Bechtel Hanford, Inc., Richland, Washington, July.

National Research Council, 1996, *The Hanford Tanks: Environmental Impacts and Policy Choices*, Committee on Remediation of Buried and Tank Wastes, Board on Radioactive Waste Management, Commission on Geosciences, Environment, and Resources, National Academy Press, Washington, D.C.

Reidel, S.P., D.G. Horton, Y.-J. Chen, and D.B. Barnett, 2006, *Geology, Hydrogeology, Geochemistry, and Mineralogy Data Package for the Single-Shell Tank Waste Management Areas at the Hanford Site*, RPP-23748, Rev. 0, CH2M Hanford Group, Inc., Richland, Washington, May.

Reidel, S.P., and M.A. Chamness, 2007*, Geology Data Package for the Single-Shell Tank Waste Management Areas at the Hanford Site*, PNNL-15955, Pacific Northwest National Laboratory, Richland, Washington, January.

Richland (City of Richland), 1981–2005, *Water Treatment Plant, Richland Water System Monthly Report*.

SAIC (Science Applications International Corporation), 2006, *Cumulative Impacts Analysis, Inventory Development*, Rev. 4, Germantown, Maryland, October 2.

Serne, R .J., B.N. Bjornstad, J.M. Keller, P.D. Thorne, D.C. Lanigan, J.N. Christensen, and G.S. Thomas, 2010, *Conceptual Models for Migration of Key Groundwater Contaminants Through the Vadose Zone and Into the Unconfined Aquifer Below the B-Complex*, PNNL-19277, Pacific Northwest National Laboratory, Richland, Washington, July.

SWS (Schlumberger Water Services), 2009, *Visual MODFLOW, Version 2009.1 Pro*, Waterloo, Ontario, Canada.

Thorne, P.D., M.P. Bergeron, M.D. Williams, and V.L. Freeman, 2006, *Groundwater Data Package for Hanford Assessments*, PNNL-14753, Rev. 1, Pacific Northwest National Laboratory, Richland, Washington, January.

USGS (U.S. Geological Survey), 2004, *MODFLOW 2000 Engine, Version 1.15.00*, August 6.

WHI (Waterloo Hydrogeologic, Inc.), 2005, *HydroGeo Analyst v. 3.0 User's Manual – Database Utilities*, *Borehole Logging/Reporting, 2D Mapping and Cross Sections, and 3D Visualization*, Waterloo, Ontario, Canada.

Wurstner, S.K., P.D. Thorne, M.A. Chamness, M.D. Freshley, and M.D. Williams, 1995, *Development of a Three-Dimensional Ground-Water Model of the Hanford Site Unconfined Aquifer System: FY 1995 Status Report*, PNL-10886, Pacific Northwest National Laboratory, Richland, Washington, December.

Code of Federal Regulations

10 CFR 1021, U.S. Department of Energy, "National Environmental Policy Act Implementing Procedures."

40 CFR 1500–1508, Council on Environmental Quality, "Regulations for Implementing the Procedural Provisions of the National Environmental Policy Act."

40 CFR 1502.1, Council on Environmental Quality, "Environmental Impact Statement: Purpose."

40 CFR 1502.2(b), Council on Environmental Quality, "Environmental Impact Statement: Implementation."

Federal Register

62 FR 8693, U.S. Department of Energy, 1997, "Record of Decision for the Tank Waste Remediation System, Hanford Site, Richland, WA," February 26.

United States Code

42 U.S.C. 4321 et seq., National Environmental Policy Act of 1969.

APPENDIX M
RELEASE TO VADOSE ZONE

This appendix supports Chapters 5, 6, and 7; describes the role of the release models with respect to the groundwater modeling process, the release models and the method used to estimate release rates to the vadose zone, and the release model parameters; discusses parameter sensitivity; and presents the results from the release models and the results of the sensitivity analyses.

M.1   INTRODUCTION

The assessment of human health impacts is an important element of analysis for this *Tank Closure and Waste Management Environmental Impact Statement for the Hanford Site, Richland, Washington (TC & WM EIS).* Activities associated with alternatives under consideration for tank closure and waste management include the placement of waste containing radioactive and chemical constituents in the vadose zone at the Hanford Site (Hanford). The vadose zone is the unsaturated zone that extends from the top of the ground surface to the water table. In addition, past practices resulting in spills, leaks, planned discharges, and the disposal of waste also placed such materials in the vadose zone. Major steps in assessing human health impacts are estimation of (1) rate of release to the vadose zone, (2) the rate of transport through the vadose zone, (3) the rate of transport through the unconfined aquifer, and (4) the magnitude of health impacts at the points of exposure. This appendix describes methods used to estimate rates of release to the vadose zone, summarizes the values of the parameters used in the release models, summarizes the results of the application of the models, and presents a sensitivity analysis for particular cases. The relation of the release models in the groundwater monitoring system for the *TC & WM EIS* is shown in Figure M–1. Although the best-available data and models were used to develop the analysis described in this appendix, uncertainty in the results remains. This uncertainty derives from variabilities in natural and engineered materials, such as soil and grout, as well as lack of knowledge regarding elements such as the applicability of specific models to site-specific locations or the type of climate that may be experienced in the future. The release models described in this appendix are applicable for sources defined within the *TC & WM EIS* alternatives and for sources associated with the cumulative analysis. Because of the large uncertainties involved in projection of impacts beyond a period of 1,000 years, U.S. Department of Energy (DOE) guidance recommends a period of analysis of 1,000 years for assessment of performance of low-level radioactive waste (LLW) disposal facilities (DOE Manual 435.1-1). However, the low rate of movement of water and solutes through the vadose zone at Hanford and the objective of identifying peak impacts support selection of a longer period of analysis for this *TC & WM EIS*. The analysis of travel time in the vadose zone presented in Appendix N, Section N.5.1, is appropriate for constituents that move at the velocity of water. The analysis in Appendix O, Section O.6.4, for uranium, a constituent that moves slower than groundwater, supports selection of a 10,000-year period of analysis. Thus, long-term groundwater impacts in this *TC & WM EIS* are estimated for a 10,000-year period of analysis extending over calendar years 1940 to 11,939. Further details on sources associated with the cumulative analysis are presented in Appendix S.
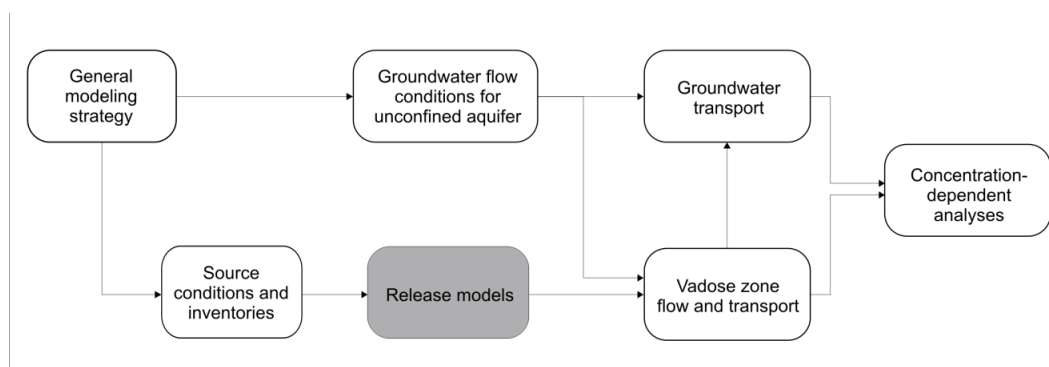

Figure M–1. Groundwater Modeling System Flowchart

M.2   DESCRIPTION OF RELEASE MODELS

A variety of sources with related release mechanisms needed to be analyzed for this *TC & WM EIS*. To provide a consistent approach and to ensure quality results, the stepwise procedure summarized in Table M–1 was applied for release model development. Releases to the vadose zone can be characterized according to the physical phase of the source and by the rate-controlling mechanism of the release. For this *TC & WM EIS*, releases to the vadose zone are characterized as occurring from the liquid- or solid-phase sources. For solid sources, release can be controlled by liquid- to solid-phase partitioning, solubility, or diffusion mechanisms. For each release model, the variation in the timing of the infiltration rate is represented as a series of pulses. The increase or decrease in the infiltration rate reflects the change in conditions, including the removal or recovery of vegetation and the placement and weathering of an engineered barrier. The form of the time dependence of the infiltration rate is presented in Figure M–2.

Table M–1. Steps in Release Model Development

Step Number	Content
1	Identify sources and characterize physical processes
2	Develop conceptual model of the release process
3	Develop mathematical description of the release
4	Develop algorithm for solution of mathematical model
5	Develop computer code implementing equations and solution algorithm
6	Verify computer code, including documentation of concepts, equations, and algorithms and execution of test cases
7	Apply release model
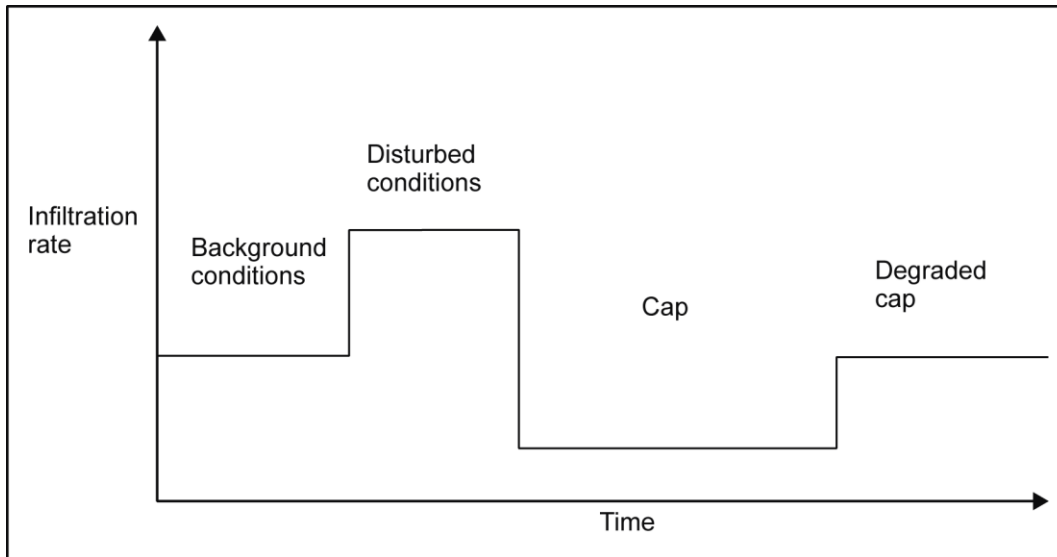
Figure M–2. Time Dependence of Infiltration Rate

The nature and level of complexity of these models is consistent with available guidance (NCRP 2005) and past site-specific analysis (Riley and Lo Presti 2004). A summary list of waste forms and associated release models is presented in Table M–2, and more-detailed descriptions of each model are presented in the following sections. Although alternative conceptual models such as constituent solubility–limited or partitioning-limited release may be applicable in given circumstances, preference is given in this analysis to the partitioning-limited mechanism due to uncertainty associated with formation of metastable, or mixed-composition, precipitation phases and the availability of site-specific measurements consistent with partitioning-limited release (Lockrem 2005; Mattigod et al. 2001).

Table M–2. Summary List of Waste Forms Evaluated in This *TC & WM EIS*

Waste Form	Material Type	Release Model
Tank Closure Alternatives		
Tank salt cake	Precipitate	Matrix solubility–limited release model
Stabilized tank residuals	Grout	Partitioning-limited, convective-flow release model
Ancillary equipment	Grout	Partitioning-limited, convective-flow release model
ILAW glass	Glass	Fractional-release-rate model
Retired ILAW melters	Glass	Fractional-release-rate model
Bulk vitrification glass	Glass	Fractional-release-rate model
Cast stone waste	Aluminosilicate	Diffusion-limited release model
Steam reforming waste	Finely divided solids	Matrix solubility–limited release model
ETF-generated secondary waste	Grout	Diffusion-limited release model
Sulfate removal grouted secondary waste	Grout	Diffusion-limited release model
FFTF Decommissioning Alternatives		
Subsurface structures	Solids, soil	Partitioning-limited, convective-flow release model
Secondary waste	Grout	Diffusion-limited release model
Waste Management Alternatives		
LLBG 218-W-5, trenches 31 and 34 waste	Solids, soil	Partitioning-limited, convective-flow release model
Onsite non-CERCLA waste	Grout	Diffusion-limited release model
Secondary waste	Grout	Diffusion-limited release model
Offsite waste	Unstabilized matrix	Diffusion-limited release model

Key: CERCLA=Comprehensive Environmental Response, Compensation, and Liability Act; ETF=Effluent Treatment Facility; FFTF=Fast Flux Test Facility; ILAW=immobilized low-activity waste; LLBG=Low-Level Radioactive Waste Burial Ground; *TC & WM EIS=Tank Closure and Waste Management Environmental Impact Statement for the Hanford Site, Richland, Washington*.

M.2.1 Liquid Sources

The set of types of sources for liquid releases include planned discharges to near-surface facilities, unplanned releases to near-surface soil, past leaks from tanks, and retrieval leaks from tanks. For a given location, the release model is defined by specification of the elevation, the area and aqueous volume of the source, the duration of the release, and inventories of constituents released during the specified time interval.

M.2.2 Solid Sources

Releases from solid sources are categorized according to the mechanism of release. Release mechanisms include partitioning from the solid to the liquid phase with convective flow through the waste form, waste form dissolution with convective flow through or around the waste form, fractional release, and partitioning from the solid to the liquid phase with diffusive transport in the waste form. The balance of this section describes details of release models for each mechanism.

M.2.2.1   Partitioning-Limited, Convective-Flow Release Model

In the partitioning-limited, convective-flow release model, the waste form of a given cross-sectional area with a constant thickness perpendicular to an infiltrating flow of water is located in the vadose zone. A schematic representation of the concept is presented in Figure M–3. This figure depicts water infiltration at a constant rate (q_{inf}) through a waste form of cross-sectional area (A_{wf}) and height (H_{wf}).
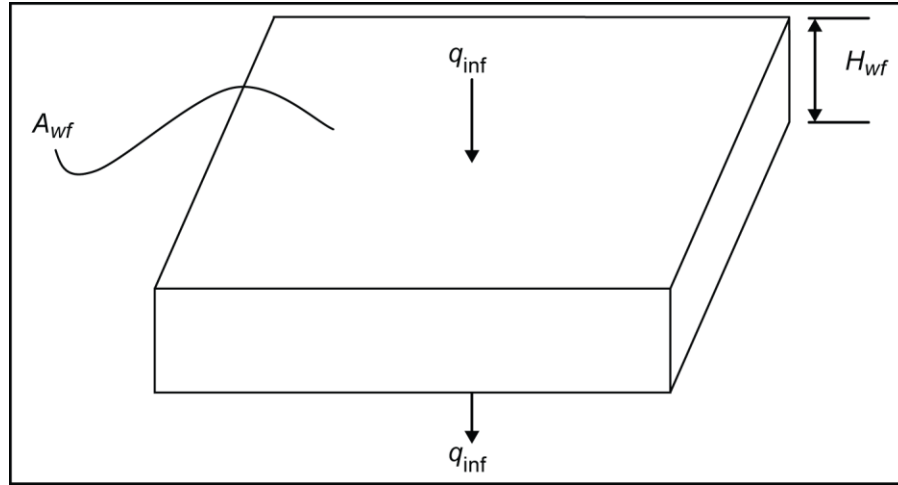
Figure M–3. Schematic of Release Concept for Partitioning-Limited,
Convective-Flow Release

A constituent bound to the solid is available for transfer to water moving through the waste form, and the release rate is determined by the extent of partitioning between the solid and liquid phases within the waste form and the rate of movement of water through the waste form. Constituents are assumed free to move within the pore space of the waste form, producing a uniform concentration of the constituent throughout the waste form. A mass balance on a constituent within the waste form provides a relation between the liquid-phase concentration and the initial mass of constituent and dimensions and properties of the waste form. The mass of the constituent within the waste form is contained within the liquid and solid phases:

$$AT = V_l\,C_l + V_s\,C_{s,v} = \varepsilon\,V_t\,C_l + (1 - \varepsilon_s)\,V_t\,C_{s,v} \tag{M–1}$$

where:

AT	=	total mass at a given time, grams
V_l	=	volume of liquid in the waste form, cubic meters
C_l	=	concentration of the constituent in the liquid phase, grams per cubic meter
V_s	=	volume of solid within the waste form, cubic meters
$C_{s,v}$	=	concentration of the constituent in the solid phase, grams per cubic meter
ε	=	volumetric moisture content of the waste form, unitless
V_t	=	total volume of the waste form, cubic meters
ε_s	=	saturated porosity of the waste form, unitless

The relationship between volumetric and mass concentration in the solid phase is as follows:

$$C_{s,v} = f_v \, \rho_s \, C_{s,m} \qquad\qquad (M–2)$$

where:

$C_{s,v}$	=	concentration of the constituent in the solid phase, grams per cubic meter
f_v	=	volumetric units conversion factor, cubic centimeters per cubic meter
ρ_s	=	particle density of the solid in the waste form, grams per cubic centimeter
$C_{s,m}$	=	concentration of constituent in the solid phase, grams per gram

The relationship between concentration of the constituent in the liquid and solid phases is represented as linear with the distribution coefficient serving as the constant of proportionality:

$$C_{s,m} = (1/f_v) \, K_d \, C_l \qquad\qquad (M–3)$$

where:

$C_{s,m}$	=	concentration of the constituent in the solid phase, grams per gram
f_v	=	volumetric units conversion factor, cubic centimeters per cubic meter
K_d	=	distribution coefficient for the constituent in the waste form, milliliters per gram
C_l	=	concentration of the constituent in the liquid phase, grams per cubic meter

Substitution of the supporting relations into the mass relation allows calculation of liquid-phase concentration for a given inventory:

$$C_l = AT \, / \, (\varepsilon_s \, V_t \, R_d) \qquad\qquad (M–4)$$

where:

C_l	=	concentration of the constituent in the liquid phase, grams per cubic meter
AT	=	total mass at a given time, grams
ε_s	=	saturated porosity of the waste form, unitless
V_t	=	total volume of the waste form, cubic meters
R_d	=	retardation factor for the constituent in the waste form, unitless

and

$$R_d = \varepsilon/\varepsilon_s + [(1 - \varepsilon_s)/\varepsilon_s] \, \rho_s \, K_d \qquad\qquad (M–5)$$

where:

R_d	=	retardation factor for the constituent in the waste form, unitless
ε	=	volumetric moisture content of the waste form, unitless
ε_s	=	saturated porosity of the waste form, unitless
ρ_s	=	particle density of the solid in the waste form, grams per cubic centimeter
K_d	=	distribution coefficient for the constituent in the waste form, milliliters per gram

In saturated flow, the retardation factor for a constituent is the ratio of the rate of movement of groundwater to the rate of movement of the constituent. A mass balance formed around the waste form during a time interval *j* reflects release by convection and decrease of mass within the waste form. The rate of flow of water through the waste form is equal to the rate of infiltration at the ground surface, which is represented as a series of pulses defined for a set of time intervals (see Figure M–1). The mass balance formed around the waste form is as follows:

$$\partial \, AT/\partial t = -\, A_{wf} \, q_{inf,j} \, C_l - \lambda_i \, AT$$

$$(1/AT) \, \partial \, AT/\partial t = -\, q_{inf,j} \, / \, (\varepsilon_s \, H_{wf} \, R_d) - \lambda_i$$

$$= -\, (f_j + \lambda_i) \tag{M–6}$$

where:

AT	=	total mass at a given time, grams
t	=	time, years
A_{wf}	=	cross-sectional area of the waste form perpendicular to flow, square meters
$q_{inf,j}$	=	rate of infiltration during time period *j*, meters per year
C_l	=	concentration of the constituent in the liquid phase, grams per cubic meter
λ_i	=	decay constant, 1 per year
ε_s	=	saturated porosity of the waste form, unitless
H_{wf}	=	height of the waste form parallel to flow, meters
R_d	=	retardation factor for the constituent in the waste form, unitless

The total mass remaining in the waste form at any time in the time interval *j*, *AT* (grams), is as follows:

$$AT = AT_{s,j} \, \exp\,[\,-(f_j + \lambda_i)\,(t - t_{s,j})] \tag{M–7}$$

where:

$AT_{s,j}$	=	mass in the waste form at the start of time interval *j*, grams
t	=	time, years
$t_{s,j}$	=	time at the start of time interval *j*, years

The release rate of the constituent during time interval *j*, R_{wfj} (grams per year) is as follows:

$$R_{wfj} = f_j \, AT_{s,j} \, \exp\,[\,-(f_j + \lambda_i)\,(t - t_{s,j})] \tag{M–8}$$

where:

$AT_{s,j}$	=	mass in the waste form at the start of time interval *j*, grams
t	=	time, years
$t_{s,j}$	=	time at the start of time interval *j*, years

The partitioning-limited, convective-flow release model is applicable for contaminated soil sources and grouted waste forms that have degraded over hundreds of years. Primary parameters of the model are rate of infiltration, dimensions of the waste form, and distribution coefficient of constituents.

M.2.2.2   Matrix Solubility–Limited Release Model

In the matrix solubility–limited release model, hazardous constituents are assumed to be uniformly distributed throughout a much larger mass of soluble material, such as salt cake. The matrix is porous and water flowing through the waste form dissolves the matrix and releases encapsulated constituents. The

waste form is in the unsaturated zone with a downward flow, as depicted in Figure M–3. The time variation of infiltration is represented as a series of step functions, as shown in Figure M–1. A mass balance formed on the matrix is as follows:

$$\partial\, M_{sc} / \partial t = -\, A_{wf}\, q_{inf,j}\, C_{s,sc} \tag{M–9}$$

where:

M_{sc} =   mass of matrix, grams
t =   time, years
A_{wf} =   cross-sectional area of the waste matrix for flow, square meters
$q_{inf,j}$ =   rate of infiltration, meters per year
$C_{s,sc}$ =   solubility of waste matrix, grams per cubic meter

The mass of waste matrix present at any time during a time period is as follows:

$$M_{sc} = M_{sc,j} - [(A_{wf}\, q_{inf,j}\, C_{s,sc})\, (t - t_{s,j})] \tag{M–10}$$

where:

M_{sc} =   mass of waste matrix at time t, grams
$M_{sc,j}$ =   mass of waste matrix at start of time period j, grams
A_{wf} =   cross-sectional area of the waste matrix for flow, square meters
$q_{inf,j}$ =   rate of infiltration, meters per year
$C_{s,sc}$ =   solubility of waste matrix, grams per cubic meter
t =   time, years
$t_{s,j}$ =   time at start of time period j, years

During any interval, the rate of loss of waste matrix given by the second term on the right-hand side of Equation M–10 cannot exceed the amount of waste matrix present at the start of the time interval. When the waste matrix is completely removed by dissolution, the release is terminated. A mass balance on a constituent encapsulated in the waste matrix can be expressed as follows:

$$\partial\, AT / \partial t = -\, A_{wf}\, q_{inf,j}\, C_{s,sc}\, (AT / M_{sc}) - \lambda_i\, AT \tag{M–11}$$

where:

AT   =   total amount of constituent, grams
t =   time, years
A_{wf} =   cross-sectional area of the waste matrix for flow, square meters
$q_{inf,j}$ =   rate of infiltration, meters per year
$C_{s,sc}$ =   solubility of waste matrix, grams per cubic meter
M_{sc} =   mass of waste matrix at time t, grams
λ_i =   decay constant for the constituent i, 1 per year

The release of hazardous constituent during time interval j (Rwfj), taking into account dissolution of the matrix and decay of the constituent, is expressed as follows:

$$Rwf_j = [(A_{wf}\, q_{inf,j}\, C_{s,sc})/\, \lambda_i]\, [AT_{s,j}/M_{sc,j}]\, \{1 - \exp\,[-\lambda_i\, (t - t_{s,j})]\} \tag{M–12}$$

The primary application of the matrix solubility limited-release model is for releases from salt cake in high-level radioactive waste (HLW) tanks under Tank Closure Alternatives 1 and 2A and from steam reforming waste under Tank Closure Alternative 3C. Primary parameters of the model are rate of

infiltration, mass of the waste matrix, solubility of the waste matrix, and concentration of hazardous constituents in the waste matrix.

M.2.2.3 Fractional-Release-Rate Model

In chemical reactions where reactants and products are present in excess or where complex chemical and physical processes produce a constant rate of degradation of the waste form, the release rate is linearly proportional to the amount of hazardous constituent remaining at the source. The physical configuration of the waste form is the same as that represented in Figure M–3. A mass balance on the hazardous constituent at the source is as follows:

$$\partial M / \partial t = -(f_{wf} + \lambda_i)\, M \tag{M–13}$$

where:

M = mass of hazardous constituent at the source, grams
t = time, years
f_{wf} = fractional rate of degradation of the waste form, grams per gram per year
λ_i = decay constant, 1 per year

The amount of hazardous constituent present at the source at any time is as follows:

$$M = M_j\, exp\, [-(f_{wf} + \lambda_i)\, (t - t_s)] \tag{M–14}$$

where:

M = mass of hazardous constituent at the source, grams
M_j = mass of hazardous constituent present at the source at the beginning of the time period j, grams
f_{wf} = fractional rate of degradation of the waste form, grams per gram per year
λ_i = decay constant, 1 per year
t = time, years
t_s = time at start of time period j, years

The release rate of the constituent from the waste form at any time is as follows:

$$R_{wf} = f_{wf}\, M_j\, exp\, [-(f_{wf} + \lambda_i)\, (t - t_s)] \tag{M–15}$$

where:

R_{wf} = rate of release of the constituent from the waste form, grams per year
f_{wf} = fractional rate of degradation of the waste form, grams per gram per year
M_j = mass of hazardous constituent present at the source at the beginning of the time period j, grams
λ_i = decay constant, 1 per year
t = time, years
t_s = time at start of time period j, years

The fractional-release-rate model is applicable for Waste Treatment Plant (WTP) immobilized low-activity waste (ILAW) glass, bulk vitrification glass, and glass in retired melters. Primary parameters of the model are the fractional-release-rate constant and the initial inventory of hazardous constituents.

M.2.2.4   Diffusion-Limited Release Models

If a waste form were to have a value of hydraulic conductivity much lower than that of the surrounding material, convective flow would be diverted around the waste form. In this case, diffusive transport of the hazardous constituent within the waste form would constitute the primary mechanism for constituent release to the environment. The boundary condition specified for the concentration of the constituent outside the waste form plays a role in determining the release rate. In a conservative approach to specification of this boundary condition, the convective flow outside the waste form is assumed to maintain the concentration of the constituent at a low value at the outside boundary of the form. This maximizes the release rate of the constituent diffusing out of the waste form. In a less conservative approach to specification of this boundary condition, the rate of convective flow can be used to establish the concentration of the constituent at the boundary of the waste form. In addition, the waste form may degrade over time, allowing an increase in the rate of release. In the diffusion-limited release models, transport of solute occurs only in the liquid-filled pore space of the waste form, and partitioning of constituents between the solid and liquid phases is included in the release model. The geometry of the waste form is a factor in determining transport distances and the area available for release. For this *TC & WM EIS*, diffusion-controlled release models have been developed for rectangular and cylindrical geometries. For both geometries, the rate of transport by diffusion is conservatively represented by a shrinking core model to simplify the mathematical form of the model (Levenspiel 1962; Sarkar, Chakrabarti, and Dutta 2009). Key assumptions of the shrinking core model are that the interface moves slowly in comparison with the time needed for a quasi–steady state profile to develop across the depleted shell and that the amount of the diffusing constituent in the depleted shell is negligibly small. Degradation of the waste form is represented as a time-dependent increase in the tortuosity of the waste form, producing an increase in the rate of diffusion toward the outer boundary of the waste form. Tortuosity is a measure of the length of the path traversed by a diffusing species as it moves through the waste matrix, with the length of the path decreasing as the waste matrix degrades.

A source with rectangular symmetry is shown in Figure M–4.
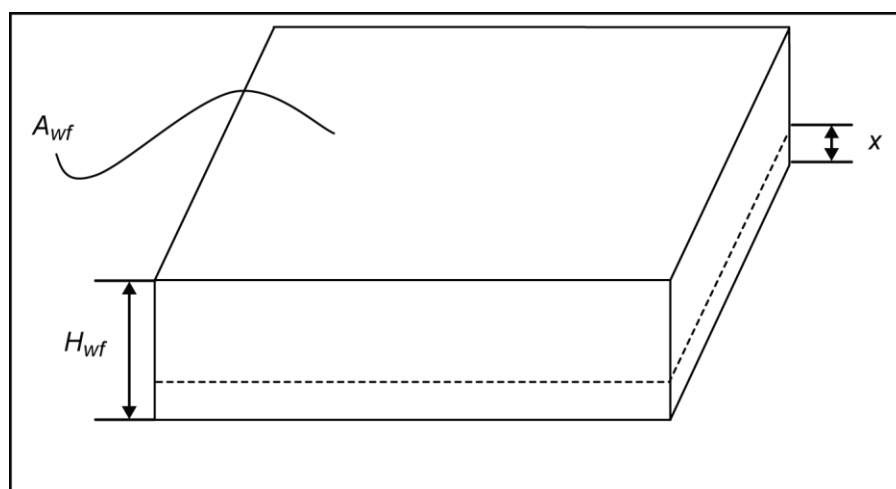
**Figure M–4. Schematic of Rectangular Waste Form with
Diffusion Release from Lower Surface**

Resistance to mass transfer is assumed to reside in a layer, with thickness designated as *x* in Figure M–4, that exists between the shrinking core and the environment. The concentration of the constituent outside the waste form is assumed to be negligible. A mass balance on the diffusing constituent formed in the waste form is as follows:

$$- \varepsilon \, A_{wf} \, T \, D_w \, [(C_l - C_{vz})/x] = \varepsilon_s \, A_{wf} \, R_d \, C_l \, \partial \, (H_{wf} - x)/ \, \partial t \qquad \text{(M–16)}$$

$$R_d = \varepsilon/\varepsilon_s + [(1 - \varepsilon_s)/\varepsilon_s] \, \rho_s \, K_d \qquad \text{(M–17)}$$

where:

ε = volumetric moisture content of the waste form, unitless
A_{wf} = diffusion release area of the waste form, square meters
T = tortuosity of the waste form, unitless
D_w = diffusivity of the constituent in water, square meters per year
C_l = concentration of the constituent in the liquid in the core portion of the waste form, grams per cubic meter
C_{vz} = concentration of constituent in vadose zone between waste packages, grams per cubic meter
x = thickness of transport layer, meters
ε_s = saturated porosity of the waste form, unitless
R_d = retardation factor for the constituent in the waste form, unitless
H_{wf} = thickness of waste form, meters
t = time, years
ρ_s = particle density of the solid in the waste form, grams per cubic centimeter
K_d = distribution coefficient for the constituent in the waste form, milliliters per gram

Assuming that the concentration of the diffusing constituent is maintained at a low level outside of the waste form, the cumulative release of the constituent from the form, $R_{wf\text{cum}}$ (grams), calculated from the mass balance is as follows:

$$R_{wf\text{cum}} = [AT_0/(H_{wf} - x_0)] \, \sqrt{\{ \, [(2 \, (\varepsilon/\varepsilon_s) \, T \, D_w \,)/ R_d \,] \, t + x_0^2 \, \} } -$$

$$[AT_0/(H_{wf} - x_0)] \, (\, x_0 \,) \qquad \text{(M–18)}$$

where:

AT_o = initial inventory of the constituent, grams
H_{wf} = thickness of waste form, meters
x_0 = initial thickness of the waste form layer outside the core, meters
ε = volumetric moisture content of the waste form, unitless
ε_s = saturated porosity of the waste form, unitless
T = tortuosity of the waste form, unitless
D_w = diffusivity of the constituent in water, square meters per year
R_d = retardation factor for the constituent in the waste form, unitless
t = time, years

This rectangular geometry model assumes that the release occurs from only the lower surface of the waste form.

If the release occurs from both the upper and lower surfaces, the waste form is represented as shown in the volume of Figure M–5. Using the same approach as for a release from a single surface, the cumulative release of the constituent from both surfaces is calculated as follows:

$$R_{wfcum} = [2\ AT_0/(H_{wf}/2 - x_0)]\ \sqrt{\{\ [(2\ T\ (\varepsilon/\varepsilon_s)\ D_w\ )/\ R_d\ ]\ t + x_0^{\ 2}\ \}} -$$

$$[2\ AT_0/(H_{wf}/2 - x_0)]\ (\ x_0\ ) \hspace{2cm} (M–19)$$

where:

R_{wfcum}	=	cumulative release of the constituent from the waste form, grams
AT_0	=	initial inventory of the constituent, grams
H_{wf}	=	thickness of waste form, meters
x_0	=	initial thickness of the waste form layer outside the core, meters
T	=	tortuosity of the waste form, unitless
ε	=	volumetric moisture content of the waste form, unitless
ε_s	=	saturated porosity of the waste form, unitless
D_w	=	diffusivity of the constituent in water, square meters per year
R_d	=	retardation factor for the constituent in the waste form, unitless
t	=	time, years
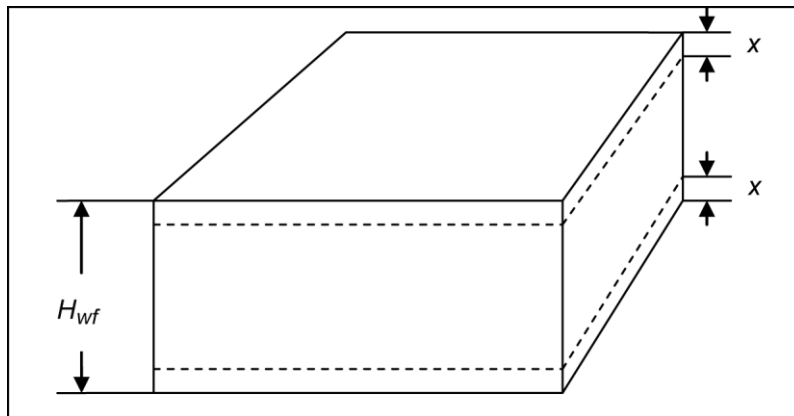
Figure M–5. Schematic of Rectangular Waste Form with Diffusion Release from Upper and Lower Surfaces

A source with cylindrical symmetry is shown in Figure M–6.
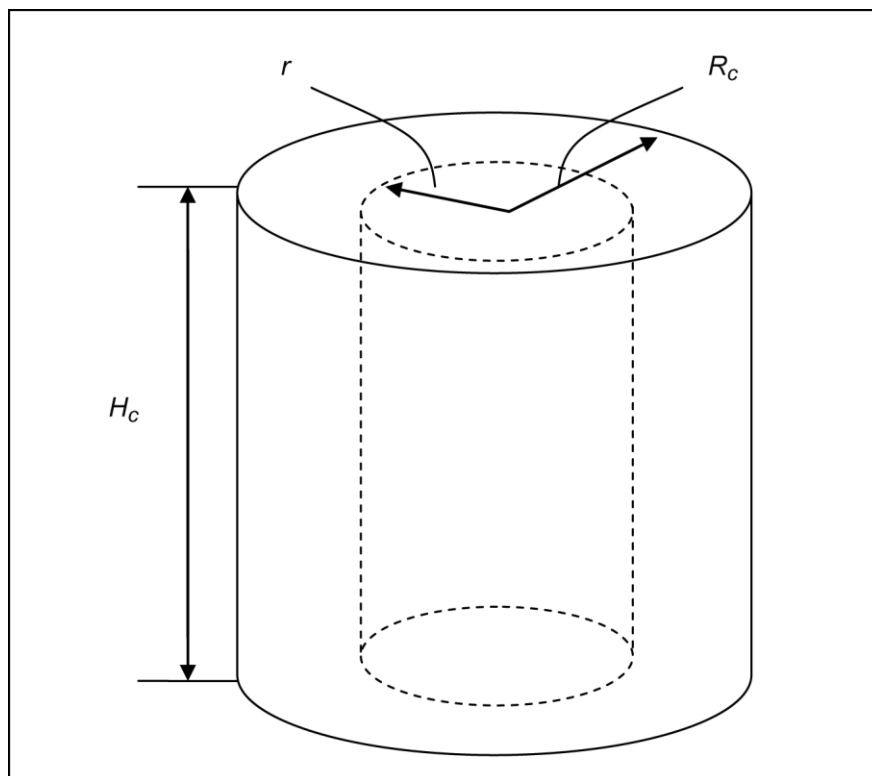
Figure M–6. Schematic of a Cylindrical Diffusion Release Model

Resistance to mass transfer is assumed to reside in an annular layer with thickness $R_c - r$ (see Figure M–6) that separates the core portion of the cylinder from the environment. Waste forms are assumed to be placed in a rectangular array, and infiltrating water flows downward through the space between waste packages. The constituent is released from the waste form by diffusion into the space between waste packages and then flows downward with the convective flow of infiltrating water. A mass balance formed on the diffusing constituent in the waste form is as follows:

$$(\varepsilon\,\pi\,H_c)\,R_d\,C_l\,\partial\,r^2\,/\,\partial t = -R_{wf} \tag{M–20}$$

$$R_{wf} = (\varepsilon\,2\,\pi\,r\,H_c)\,T\,D_w\,[(C_l - C_{vz})/(R_c - r)] \tag{M–21}$$

$$R_d = \varepsilon/\varepsilon_s + [(1 - \varepsilon_s)/\varepsilon_s]\,\rho_s\,K_d \tag{M–22}$$

where:

ε	=	volumetric moisture content of the waste form, unitless
H_c	=	height of the cylindrical waste form, meters
R_d	=	retardation factor (see Equation M–5) for the constituent in the waste form, unitless
C_l	=	concentration of the constituent in the pore space of the waste form, grams per cubic meter
r	=	radius of the shrinking core, meters
t	=	time, years
R_{wf}	=	rate of release of the constituent from the waste form, grams per year
T	=	tortuosity of the waste form, unitless
D_w	=	diffusion coefficient of the constituent in water, square meters per year

C_{vz} = concentration of the constituent in the vadose zone between the waste packages, grams per cubic meter

R_c = radius of the cylinder, meters

ε_s = saturated porosity of the waste form, unitless

ρ_s = particle density of the solid in the waste form, grams per cubic centimeter

K_d = distribution coefficient for the constituent and waste form, milliliters per gram

If the concentration of the diffusing constituent is maintained at a low level outside of the waste form ($C_{vz} = 0$), the cumulative release of the constituent from the form calculated using the mass balance is as follows:

$$R_{wf\mathrm{cum}} = (2\,[R_c / r_0{}^2]\,AT_0\,)\,\sqrt{\,\{[(2\,(\varepsilon/\varepsilon_s)\,T\,D_w\,)/\,R_d\,]\,t + (R_c - r_0)^2\,\} } - [\,R_c - r_0\,])$$

$$- ([\,AT_0 / r_0{}^2\,]\,[(2\,(\varepsilon/\varepsilon_s)\,T\,D_w\,)/\,R_d\,]\,t\,) \qquad\qquad (M–23)$$

where:

R_{wfcum} = cumulative release of the constituent from the waste form, grams

R_c = radius of the cylinder, meters

r_0 = initial radius of the core of the waste form, meters

AT_0 = initial inventory of the constituent in the waste form, grams

ε = volumetric moisture content of the waste form, unitless

ε_s = saturated porosity of the waste form, unitless

T = tortuosity of the waste form, unitless

D_w = diffusion coefficient of the constituent in water, square meters per year

R_d = retardation factor (see Equation M–5) for the constituent in the waste form, unitless

t = time, years

If the concentration of the constituent in the vadose zone between waste forms is not maintained at a low level, the solution procedure is extended to include a mass balance formed on the constituent in the volume of soil and water in the space between waste packages. This additional mass balance is expressed as follows:

$$(A_f - A_{wf}\,)\,H_{wf}\,\varepsilon_{svz}\,R_{d,vz}\,\partial\,C_{vz}\,/\,\partial t = R_{wf} - R_{vz} \qquad\qquad (M–24)$$

$$R_{vz} = A_f\,q_{\mathrm{inf,j}}\,C_{vz} \qquad\qquad (M–25)$$

$$R_{d,vz} = (\theta_{vz}\,/\,\varepsilon_{svz}) + [(1 - \varepsilon_{svz})/\,\varepsilon_{svz}\,]\,\rho_s\,K_{d,vz} \qquad\qquad (M–26)$$

where:

A_f = area in horizontal plane for infiltration of water, square meters

A_{wf} = area in horizontal plane intersected by stacks of waste packages, square meters

H_{wf} = height of a stack of waste packages, meters

ε_{svz} = saturated porosity of the vadose zone, unitless

$R_{d,vz}$ = retardation factor for the constituent in the vadose zone between waste packages, unitless

C_{vz} = concentration of the constituent in the water in the vadose zone between the waste packages, grams per cubic meter

t = time, years

R_{wf} = rate of release of the constituent from the waste form, grams per year

R_{vz} = rate of release of the constituent from the vadose zone between the waste packages to the vadose zone below the waste packages, grams per year

$q_{inf,j}$	=	rate of infiltration during time interval j, meters per year
θ_{vz}	=	moisture content of the vadose between the waste packages, unitless
ρ_s	=	particle density of the solid in the waste form, grams per cubic centimeter
$K_{d,vz}$	=	distribution coefficient for the constituent in the vadose zone between the waste packages, milliliters per gram

Mass balances of Equations M–20 and M–24 are solved simultaneously for the concentration of the constituent in the vadose zone between waste packages (C_{vz}) and the release rates to the vadose zone below waste packages (R_{vz}).

Diffusion-controlled release models are applicable for grout or cement waste forms, such as grouted HLW tanks or cast stone waste. Primary parameters of the model are dimensions and tortuosity of the waste form, and the diffusion coefficient, distribution coefficient, and initial inventory for the constituent.

M.3   TECHNICAL BASIS AND VALUES OF RELEASE MODEL PARAMETERS

Factors affecting release rates of constituents to the vadose zone include environmental factors, such as rate of infiltration, and factors specific to the nature of the source and the disposal system. Values of rate of infiltration adopted for use in this *TC & WM EIS* are those recommended in the *Technical Guidance Document for Tank Closure Environmental Impact Statement Vadose Zone and Groundwater Revised Analyses (Technical Guidance Document)* (DOE 2005). *Technical Guidance Document* values recommended for base case analysis are summarized in Table M–3. Post–design life conditions in Table M–3 correspond to the period of time labeled as "Degraded cap" in Figure M–2.

Table M–3. Rates of Infiltration for *TC & WM EIS*
Base Case Analysis

Location	Rate of Infiltration (millimeters per year)
Pre-Hanford Background	
IDF	0.9
Balance of site	3.5
Disturbed Conditions	
Gravel (HLW tanks)	100
Sand (cribs and trenches [ditches])	50
IDF Barrier	
Design life	0.5
Post–design life	0.9
Sitewide Barrier	
Design life	0.5
Post–design life	3.5

Key: HLW=high-level radioactive waste; IDF=Integrated Disposal Facility; *TC & WM EIS=Tank Closure and Waste Management Environmental Impact Statement for the Hanford Site, Richland, Washington*.

Values of parameters related to specific actions and types of sources are summarized in the following sections for the Tank Closure, FFTF Decommissioning, and Waste Management alternatives. Tank Closure alternatives evaluate impacts occurring in the long-term period following stabilization or closure of the HLW tanks.

Under Waste Management Alternative 2, waste disposal would occur in an Integrated Disposal Facility (IDF) in the 200-East Area (IDF-East); under Waste Management Alternative 3, waste disposal would occur in IDF-East and other facilities in the 200-East Area, as well as in an IDF in the 200-West Area (IDF-West).

M.3.1 Tank Closure Alternatives

Types of sources considered for Tank Closure alternatives include past leaks, retrieval leaks, tank residuals, and ancillary equipment at 18 tank farms and planned discharges at 6 sets of cribs and trenches (ditches) associated with tank farm operations. These facilities are all in the 200-East and 200-West Areas.

M.3.1.1 Tank Farm Sources

Liquid and solid sources are considered for release analysis at the 18 HLW tank farms. Descriptions of the dimensions, configuration and closure systems for tank farms are presented in the *Tank System Closure and Facility D&D* [decontamination and decommissioning] *Data Package* (DOE 2003a).

Primary liquid sources are past leaks and retrieval leaks from 100- and 200-series tanks located at single-shell tank farms for all Tank Closure alternatives, and ancillary equipment failure leaks at all tank farms and tank failure leaks at double-shell tank farms for Tank Closure Alternatives 1 and 2A, for which tank closure does not occur.

For past leaks, 67 tanks are included in the analysis, and model parameters include volume of liquid, inventory of constituents, and time of occurrence of the leak. Volumes of liquid assumed for analysis purposes are those presented in the Hanlon waste tank summary report (Hanlon 2003). If a volume estimate is missing from the Hanlon report for a specific tank, an estimate of the leak volume of 30 cubic meters (8,000 gallons) is assumed for that tank. Inventory estimates for past leaks are developed from field investigation reports (FIRs) for tank farms B, BX, and BY (Knepp 2002); S and SX (CH2M HILL 2002); and T, TX, and TY (Myers 2005). Subsurface conditions reports are used for estimates of inventory for tank farms A, AX, and C (Wood et al. 2003) and U (Wood and Jones 2003). If an inventory estimate for a specific tank included in the Hanlon list is not presented in an FIR or subsurface conditions report, the inventory for that tank is estimated using the average concentration for leaks from that tank farm presented in the FIR or subsurface conditions report and the leak volume from the Hanlon report. Estimates of volume of leak and date of occurrence for the 67 tanks are presented in Table M–4. Estimates of date of occurrence are adopted from the FIRs, subsurface conditions reports, and preliminary field studies (Jones et al. 2000, 2001). Estimates of quantities of constituents released with past leaks are presented in Appendix D of this environmental impact statement (EIS).

Table M–4. Summary of Estimates of Volumes and Dates for Past Leaks

Tank	Leak Volume[a] (gallons)	Date of Occurrence	Tank	Leak Volume[a] (gallons)	Date of Occurrence
241-A-103	5,500	1956[b]	241-SX-104	6,000	1954[b]
241-A-104	2,500	1975[c]	241-SX-107	5,000	1964[f]
241-A-105	277,000	1963[c]	241-SX-108	35,000	1965[f]
241-AX-102	3,000	1965[b]	241-SX-109	10,000	1964[f]
241-AX-104	8,000	1965[b]	241-SX-110	5,500	1974[f]
241-B-101	8,000	1974[d]	241-SX-111	2,000	1973[f]
241-B-103	8,000	1945[b]	241-SX-112	30,000	1969[f]
241-B-105	8,000	1968[d]	241-SX-113	15,000	1962[f]
241-B-107	8,000	1966[d]	241-SX-114	8,000	1972[f]
241-B-110	10,000	1970[d]	241-SX-115	50,000	1964[f]
241-B-111	8,000	1945[b]	241-T-101	7,500	1969[g]
241-B-112	2,000	1945[b]	241-T-103	1,000	1973[g]
241-B-201	1,200	1966[c]	241-T-106	115,000	1973[g]
241-B-203	300	1966[c]	241-T-107	8,000	1944[b]
241-B-204	400	1966[c]	241-T-108	1,000	1944[b]
241-BX-101	8,000	1968[e]	241-T-109	1,000	1944[b]
241-BX-102	70,000	1951[e]	241-T-111	1,000	1944[b]
241-BX-108	2,500	1948[b]	241-TX-105	8,000	1949[b]
241-BX-110	8,000	1948[b]	241-TX-107	2,500	1977[g]
241-BX-111	8,000	1965[d]	241-TX-110	8,000	1949[b]
241-BY-103	5,000	1950[b]	241-TX-113	8,000	1949[b]
241-BY-105	8,000	1950[b]	241-TX-114	8,000	1949[b]
241-BY-106	8,000	1950[b]	241-TX-115	8,000	1949[b]
241-BY-107	15,100	1950[b]	241-TX-116	8,000	1949[b]
241-BY-108	5,000	1950[b]	241-TX-117	8,000	1949[b]
241-C-101	20,000	1946[b]	241-TY-101	1,000	1953[b]
241-C-110	2,000	1946[b]	241-TY-103	3,000	1971[g]
241-C-111	5,500	1946[b]	241-TY-104	1,400	1953[b]
241-C-201	550	1946[b]	241-TY-105	35,000	1960[g]
241-C-202	450	1946[b]	241-TY-106	20,000	1957[g]
241-C-203	400	1946[b]	241-U-101	30,000	1946[b]
241-C-204	350	1946[b]	241-U-104	55,000	1956[h]
241-S-104	24,000	1965[f]	241-U-110	8,100	1975[h]
			241-U-112	8,500	1946[b]

[a] Hanlon 2003.
[b] Anderson 1990.
[c] Wood et al. 2003.
[d] Jones et al. 2001.
[e] Knepp 2002.
[f] CH2M HILL 2002.
[g] Jones et al. 2000.
[h] Wood and Jones 2003.

The DOE estimates that a volume of 15 cubic meters (4,000 gallons) would leak from each of the 149 single-shell tanks during waste retrieval (see Section E.1.2.2.5.2). For each tank farm and alternative, the retrieval leaks are assumed to occur simultaneously in calendar year 2018. Estimates of the inventory of constituents for retrieval leaks are developed by assuming that three volumes of sluicing liquid are required to entrain one volume of tank solids and that the solids have the composition of the December 2002 estimate of the Best-Basis Inventory (BBI). The BBI is documented in the *Inventory and Source Term Data Package* (DOE 2003b). Estimates of quantities of constituents released in retrieval leaks are presented in Appendix D of this EIS.

Primary solid sources at tank farms are salt cake remaining in single-shell tanks under Tank Closure Alternatives 1 and 2A and grouted residuals in tanks and ancillary equipment under Alternatives 2B, 3A, 3B, 3C, 4, 5, and 6C.

For releases from salt cake and sludge, the release model proposed is the matrix solubility-limited release model described in Section M.2.2.2. The proposed value of solubility for the matrix is a literature estimate of the solubility of sodium nitrate at 25 degrees Celsius (°C) (77 degrees Fahrenheit [°F]): 920,000 grams per cubic meter (Weast and Selby 1967). Although the solubility of sludge would be expected to be significantly lower than that of salt cake, detailed characterization of sludge is not available for all tanks; thus, for analysis purposes, the solubility of sludge is assumed equal to that of salt cake. The mass and volume of waste in each tank farm and inventory of constituents are those documented in the *Inventory and Source Term Data Package* (DOE 2003b). For Tank Closure Alternative 1, the residual inventory in each tank at the time of failure (time of loss of administrative or institutional control) is the total inventory of the BBI. For Tank Closure Alternative 2A, the inventory remaining in each tank at the time of failure is 1 percent of the BBI. The magnitude and timing of infiltration for Tank Closure Alternatives 1 and 2A are summarized in Table M–5.

Table M–5. Tank Closure Alternatives 1 and 2A Infiltration Sequence Description

Location Conditions	Tank Closure Alternative 1	Tank Closure Alternative 2A	Infiltration Value (millimeters per year)
	Year at Start of Infiltration		
Pre-Hanford	1940	1940	3.5
Disturbed conditions	1948	1948	100
Post–barrier design life	2108	2194	3.5

For releases from grouted residuals in HLW tanks and ancillary equipment, the proposed release model is the partition-limited, convective-flow release model described in Section M.2.2.1. The inventory is assumed to reside in the bottom of the tank, occupying a volume equal to that of the residuals remaining after retrieval with a short diffusion distance in the downward vertical direction and a long diffusion distance in the upward vertical direction. Dimensions of the tank are those described in the *Tank System Closure and Facility D&D Data Package* (DOE 2003a), and the constituent inventories are fractions of the BBI appropriate for each alternative with the BBI specified in the *Inventory and Source Term Data Package* (DOE 2003b).

Primary remaining parameters of the model are the rate of recharge and the retardation factor defined in conjunction with Equation M–5. The magnitude and timing of the sequence of infiltration for Tank Closure Alternatives 2B, 3A, 3B, 3C, 4, 5, and 6C are summarized in Table M–6. Under Alternatives 2B, 3A, 3B, 3C, 4, and 6C, modified Resource Conservation and Recovery Act (RCRA) Subtitle C barriers with a design life of 500 years would be placed over the tank farms. Hanford barriers with a design life of 1,000 years would be placed over the tank farms under Tank Closure Alternative 5. Distribution coefficient values used to calculate the retardation factor are presented in Tables M–7 (radioactive constituents) and M–8 (chemical constituents) and are those either recommended for grout (DOE 2005) or reported in nationwide surveys of soil (Beyeler et al. 1999; Sheppard and Thibault 1990).

**Table M–6. Tank Closure Alternatives 2B, 3A, 3B, 3C, 4, 5, and 6C
Infiltration Sequence Description**

Location Conditions	Tank Closure Alternatives 2B, 3A, 3B, 3C, 4, and 6C	Tank Closure Alternative 5	Infiltration Value (millimeters per year)
	Year at Start of Infiltration Value		
Pre-Hanford Site	1940	1940	3.5
Disturbed conditions	1948	1948	100
Barrier design life	2050	2050	0.5
Post–barrier design life	2550	3050	3.5

**Table M–7. Values of Distribution Coefficient for Radioactive Constituents
in Hanford Grout**

Constituent	Distribution Coefficient (milliliters per gram)	Source
Hydrogen	0	DOE 2005
Carbon	5	DOE 2005
Potassium	15	Sheppard and Thibault 1990
Strontium	15	DOE 2005
Zirconium	600	Sheppard and Thibault 1990
Technetium	1	DOE 2005
Iodine	50	DOE 2005
Cesium	280	DOE 2005
Gadolinium	5	Sheppard and Thibault 1990
Thorium	3,200	Beyeler et al. 1999
Uranium	35	DOE 2005
Neptunium	15	DOE 2005
Plutonium	550	DOE 2005
Americium	1,900	Beyeler et al. 1999

**Table M–8. Values of Distribution Coefficient for Chemical Constituents
in Hanford Grout**

Constituent	Distribution Coefficient (milliliters per gram)	Source
Arsenic	400	Sheppard and Thibault 1990
Boron	0	Sheppard and Thibault 1990
Cadmium	80	Sheppard and Thibault 1990
Chromium	0	DOE 2005
Fluoride	0	Sheppard and Thibault 1990
Lead	80	DOE 2005
Manganese	50	Beyeler et al. 1999
Mercury	10	DOE 2005
Molybdenum	10	Beyeler et al. 1999
Nickel	400	Beyeler et al. 1999
Nitrate	0	DOE 2005

Table M–8. Values of Distribution Coefficient for Chemical Constituents in Hanford Grout *(continued)*

Constituent	Distribution Coefficient (milliliters per gram)	Source
Silver	90	Beyeler et al. 1999
Strontium	10	Sheppard and Thibault 1990
Total uranium	0.6	Sheppard and Thibault 1990
Acetonitrile	0	DOE 2005
Benzene	1	DOE 2005
Butanol	3	DOE 2005
Polychlorinated biphenyls	170,000	DOE 2005
2,4,6-Trichlorophenol	0.38	DOE 2005
1,2-Dichloroethane	0	Sheppard and Thibault 1990
1,4-Dioxane	0	Sheppard and Thibault 1990
Carbon tetrachloride	0	Sheppard and Thibault 1990
Dichloromethane	0	Sheppard and Thibault 1990
Hydrazine	0	Sheppard and Thibault 1990
Vinyl chloride	0	Sheppard and Thibault 1990
Trichloroethylene	0	Sheppard and Thibault 1990

M.3.1.2 Tank Closure Waste Forms

The primary-waste form associated with tank farm closure is ILAW glass, while supplemental-waste forms produced to facilitate timely processing of tank waste are bulk vitrification glass, bulk vitrification castable refractory block, cast stone waste, and steam reforming waste. Secondary waste generated in the production of primary- and secondary-waste forms include Effluent Treatment Facility (ETF)–generated secondary waste, sulfate grout, retired melters, and contaminated soil. A primary constituent of ETF-generated secondary waste is iodine-129 recovered from offgasses emitted by thermal treatment processes (vitrification, bulk vitrification, and steam reforming).

Technical guidance developed for this EIS (DOE 2005) recommended use of data and analysis developed for selection of low-activity-waste supplemental technologies (Mann et al. 2003). For ILAW glass and glass in retired melters, the fractional-release-rate model is applied. The value of the fractional-release rate is 2.8×10^{-8} grams per gram per year based on analysis using the STORM [Subsurface Transport Over Reactive Multiphases] model (Mann et al. 2003). For bulk vitrification glass, the fractional-release-rate model is applied. The value of the fractional-release rate is 1.0×10^{-8} grams per gram per year based on analysis using the STORM model (Mann et al. 2003). The rate of recharge used in the STORM analysis to predict the rate of release from ILAW and bulk vitrification glass (4.2 millimeters per year) is higher than the *Technical Guidance Document* base case conditions for IDF-East (0.9 millimeters per year), a difference expected to provide conservatism in the estimate of rate of release. During the bulk vitrification process, a portion of the feed technetium is volatilized and trapped in refractory above the glass surface. For this material, the partition-limited, convective-flow release model with a value of zero for the distribution coefficient of technetium is applied. The refractory is porous ceramic material, and research has demonstrated that technetium volatilized during bulk vitrification collects in this material (Mann et al. 2003). The fraction of technetium present in the original melt that resides in the castable refractory block has been measured, and an upper limit of 6.5 percent has been established (Burandt 2006). For cast stone waste, ETF-generated secondary waste, and sulfate grouted waste forms, the cylindrical geometry, diffusion-limited release model described in Section M.2.2.4 is applied. Values of aqueous diffusivity are based on ion conductivity data (Weast and Selby 1966:5-111) with values for

key species iodate, pertechnetate, and nitrate of 1.1×10^{-5}, 1.5×10^{-5}, and 1.9×10^{-5} square centimeters per second, respectively, at 25 °C (77 °F). The porosity of grout is estimated to be 0.43, based on a crystal density of 2.65 grams per cubic centimeter for natural silicates (Freeze and Cherry 1979:337; Mason and Berry 1968) and a bulk density of 1.5 grams per cubic centimeter for grout (DOE 2003c:6-100). Because the value of effective porosity has not been established for site conditions, the value of total porosity is applied for effective porosity as a conservative limit of release rates. Site-specific tests of effective diffusivity of nitrate in grout are reported as 3×10^{-8} square centimeters per second (Lockrem 2005). Effective diffusivity is defined as the product of tortuosity and aqueous diffusivity divided by the retardation factor. Assuming that nitrate does not adsorb onto the grout, these data imply a site-specific value of tortuosity of 1.6×10^{-3}. Using the definition of effective diffusivity and *Technical Guidance Document*–recommended values of effective diffusivity (DOE 2005), the implied values of the distribution coefficient for technetium and iodine in grout are 1 and 50 milliliters per gram, respectively. Values of aqueous diffusivity and effective diffusivity for grout, consistent with the *Technical Guidance Document* (DOE 2005), are summarized in Tables M–9 and M–10 for radioactive and chemical constituents, respectively. The experimental program for characterization of steam reforming waste has established the operability of the solidification process (THORTT 2002), and characterization of release mechanisms and rates (Lorier, Pareizs, and Jantzen 2005; McGrail et al. 2003a, 2003b) is under way, but has not yielded a complete basis for long-term performance assessment. In addition, alternative forms of the final product are under investigation (Jantzen 2006). For the purpose of long-term performance assessment for this *TC & WM EIS*, steam reforming waste is assumed to have the form of a finely divided solid. In light of the above considerations, an estimate of the rate of release of constituents from steam reforming waste was developed based on the equilibrium solubility of steam reforming waste calculated using the PHREEQC [Ph, REDOX (Reduction-Oxidation), and Equilibrium – C Language] geochemical model (Parkhurst and Appelo 1999). Research has identified nepheline as the primary component of steam reforming waste (McGrail et al. 2003a). The equilibrium solubility of crystalline nepheline in the presence of potential alteration phases was estimated to be 1.75×10^{5} grams per cubic meter at 15 °C (59 °F). Additional details on this estimate and other bounding estimates of the rate of dissolution of steam reforming waste are presented in Section M.5, Sensitivity Analysis. For contaminated soil disposed of at the River Protection Project Disposal Facility (RPPDF), the partition-limited, convective-flow model is applied. Distribution factor values for soil are those recommended in the *Technical Guidance Document* (DOE 2005) for Hanford vadose zone sediments or in nationwide surveys of soil (Beyeler et al. 1999; Sheppard and Thibault 1990). These values are summarized in Tables M–11 and M–12 for radioactive and chemical constituents, respectively.

Table M–9. Values of Aqueous and Effective Diffusivity for
Radioactive Constituents in Hanford Grout

Constituent	Aqueous Diffusivity (square centimeters per second)	Effective Diffusivity (square centimeters per second)
Hydrogen	9.3×10^{-5}	1.5×10^{-7}
Carbon	9.2×10^{-6}	7.9×10^{-10}
Potassium	2.0×10^{-5}	5.8×10^{-10}
Strontium	7.9×10^{-6}	2.3×10^{-10}
Zirconium	2.0×10^{-5}	1.5×10^{-11}
Technetium	1.5×10^{-5}	5.2×10^{-9}
Iodine	1.1×10^{-5}	1.0×10^{-10}
Cesium	2.1×10^{-5}	3.3×10^{-11}
Gadolinium	6.0×10^{-6}	5.1×10^{-10}
Thorium	4.3×10^{-6}	6.0×10^{-13}

Table M–9. Values of Aqueous and Effective Diffusivity for Radioactive Constituents in Hanford Grout *(continued)*

Constituent	Aqueous Diffusivity (square centimeters per second)	Effective Diffusivity (square centimeters per second)
Uranium	4.3×10^{-6}	5.5×10^{-11}
Neptunium	4.3×10^{-6}	1.3×10^{-10}
Plutonium	4.3×10^{-6}	3.5×10^{-12}
Americium	4.3×10^{-6}	1.0×10^{-12}

Table M–10. Values of Aqueous and Effective Diffusivity for Chemical Constituents in Hanford Grout

Constituent	Aqueous Diffusivity (square centimeters per second)	Effective Diffusivity (square centimeters per second)
Arsenic	9.05×10^{-6}	1.03×10^{-11}
Boron	1.25×10^{-5}	2.00×10^{-8}
Cadmium	7.19×10^{-6}	4.08×10^{-11}
Chromium	1.13×10^{-5}	1.81×10^{-8}
Fluoride	1.48×10^{-5}	2.36×10^{-8}
Lead	9.45×10^{-6}	5.36×10^{-11}
Manganese	7.12×10^{-6}	6.45×10^{-11}
Mercury	8.47×10^{-6}	3.75×10^{-10}
Molybdenum	1.98×10^{-5}	8.79×10^{-10}
Nickel	6.66×10^{-7}	7.58×10^{-13}
Nitrate	1.90×10^{-5}	3.04×10^{-8}
Silver	1.65×10^{-5}	8.32×10^{-11}
Strontium	7.91×10^{-6}	3.50×10^{-10}
Total uranium	4.26×10^{-6}	2.19×10^{-9}
Acetonitrile	8.77×10^{-7}	1.40×10^{-9}
Benzene	6.38×10^{-6}	2.26×10^{-9}
Butanol	6.26×10^{-6}	8.69×10^{-10}
Polychlorinated biphenyls	3.71×10^{-6}	9.93×10^{-15}
2,4,6-Trichlorophenol	5.00×10^{-6}	3.43×10^{-9}
1,2-Dichloroethane	6.84×10^{-6}	1.09×10^{-8}
1,4-Dioxane	6.54×10^{-6}	1.05×10^{-8}
Carbon tetrachloride	6.06×10^{-6}	9.70×10^{-9}
Dichloromethane	7.75×10^{-6}	1.24×10^{-8}
Hydrazine	1.25×10^{-5}	1.99×10^{-8}
Vinyl chloride	7.48×10^{-6}	1.20×10^{-8}
Trichloroethylene	6.33×10^{-6}	1.01×10^{-8}

**Table M–11. Values of Distribution Coefficient for Radioactive Constituents
for Contaminated Soil**

Constituent	Distribution Coefficient (milliliters per gram)	Source
Hydrogen	0	DOE 2005
Carbon	4	DOE 2005
Potassium	15	Sheppard and Thibault 1990
Strontium	10	DOE 2005
Zirconium	600	Sheppard and Thibault 1990
Technetium	0	DOE 2005
Iodine	0	DOE 2005
Cesium	80	DOE 2005
Gadolinium	5	Sheppard and Thibault 1990
Thorium	3,200	Beyeler et al. 1999
Uranium	0.6	DOE 2005
Neptunium	2.5	DOE 2005
Plutonium	150	DOE 2005
Americium	1,900	Beyeler et al. 1999

**Table M–12. Values of Distribution Coefficient for Chemical Constituents
for Contaminated Soils**

Constituent	Distribution Coefficient (milliliters per gram)	Source
Arsenic	400	Sheppard and Thibault 1990
Boron	0	Sheppard and Thibault 1990
Cadmium	0.8	Sheppard and Thibault 1990
Chromium	0	DOE 2005
Fluoride	0	Sheppard and Thibault 1990
Lead	80	DOE 2005
Manganese	50	Beyeler et al. 1999
Mercury	10	DOE 2005
Molybdenum	10	Beyeler et al. 1999
Nickel	400	Beyeler et al. 1999
Nitrate	0	DOE 2005
Silver	90	Beyeler et al. 1999
Strontium	10	Sheppard and Thibault 1990
Total uranium	0.6	Sheppard and Thibault 1990
Acetonitrile	0	DOE 2005
Benzene	1	DOE 2005
Butanol	3	DOE 2005
Polychlorinated biphenols	170,000	DOE 2005
2,4,6-Trichlorophenol	0.38	Sheppard and Thibault 1990
1,2-Dichloroethane	0	Sheppard and Thibault 1990
1,4-Dioxane	0	Sheppard and Thibault 1990

**Table M–12. Values of Distribution Coefficient for Chemical Constituents
for Contaminated Soils** *(continued)*

Constituent	Distribution Coefficient (milliliters per gram)	Source
Carbon tetrachloride	0	Sheppard and Thibault 1990
Dichloromethane	0	Sheppard and Thibault 1990
Hydrazine	0	Sheppard and Thibault 1990
Vinyl chloride	0	Sheppard and Thibault 1990
Trichloroethylene	0	Sheppard and Thibault 1990

M.3.1.3   Cribs and Trenches (Ditches)

Sources at cribs and trenches (ditches) are liquid sources modeled as pulse releases characterized by liquid volume, source area, and time of occurrence. The values for these model parameters are those reported in the Hanford Soil Inventory Model (SIM) database and summarized in Appendix D of this EIS.

M.3.2   FFTF Decommissioning Alternatives

Under FFTF Decommissioning Alternative 1, the FFTF [Fast Flux Test Facility] Reactor Containment Building (RCB, Building 405), as well as the other buildings within the 400 Area Property Protected Area, would be maintained under administrative controls for 100 years through 2107. After 2107, remaining waste would be available for release to the environment.

FFTF Decommissioning Alternative 2 calls for in-place closure of FFTF. The main RCB, the two immediately adjacent support facilities (Buildings 491E and 491W), and all other above-grade structures would be dismantled. Demolition waste would be consolidated in the below-grade spaces or disposed of in an IDF. Below-grade spaces would be filled with demolition waste and stabilized with fill material (grout) to immobilize hazardous materials and minimize future subsidence. A modified RCRA Subtitle C barrier would be constructed over the filled area with a design life of 500 years.

FFTF Decommissioning Alternative 3 describes removal and clean closure of FFTF. All above-grade structures around the main RCB and the immediately adjacent support facilities would be dismantled, and the contaminated demolition debris would be disposed of at an IDF. All other radioactively contaminated equipment and hazardous materials (including asbestos and lead shielding) would be removed for disposal at an IDF. Contaminated demolition debris would be removed to an IDF, and the vacated spaces backfilled, compacted, contoured, and revegetated. All radioactive and/or hazardous material and wood and large steel components would be removed. The surface would be contoured and revegetated; no barrier would be required.

Consistent with this description of the three FFTF Decommissioning alternatives, the partition-limited, convective-flow model is applied. The magnitude and timing of infiltration sequences for FFTF Decommissioning Alternatives 1, 2, and 3 are presented in Tables M–13, M–14, and M–15, respectively. The values of infiltration rate are based on chloride mass balance and lysimeter tests[1] and are those recommended in the *Technical Guidance Document* (DOE 2005).

---

[1] A lysimeter is a device used to measure the rate of drainage of water through the lower boundary of a vertical column of soil subjected to a controlled rate of application of water at the upper boundary.

Table M–13. FFTF Decommissioning Alternative 1 Infiltration Sequence Description

Location Condition	Year at Start of Infiltration	Infiltration Value (millimeters per year)
Pre–Hanford Site	1940	3.5
Disturbed conditions	1980	50
End of institutional controls	2107	3.5

Note: Sites with sandy surfaces other than tank farms are assigned infiltration rates of 50 millimeters per year during disturbed conditions (DOE 2005).
Key: FFTF=Fast Flux Test Facility.

Table M–14. FFTF Decommissioning Alternative 2 Infiltration Sequence Description

Location Condition	Year at Start of Infiltration	Infiltration Value (millimeters per year)
Pre–Hanford Site	1940	3.5
Disturbed conditions	1980	50
Barrier design life	2022	0.5
Post–barrier design life	2522	3.5

Note: Sites with sandy surfaces other than tank farms are assigned infiltration rates of 50 millimeters per year during disturbed conditions (DOE 2005).
Key: FFTF=Fast Flux Test Facility.

Table M–15. FFTF Decommissioning Alternative 3 Infiltration Sequence Description

Location Condition	Year at Start of Infiltration	Infiltration Value (millimeters per year)
Pre–Hanford Site	1940	3.5
Disturbed conditions	1980	50
End of institutional controls	2107	3.5

Note: Sites with sandy surfaces other than tank farms are assigned infiltration rates of 50 millimeters per year during disturbed conditions (DOE 2005).
Key: FFTF=Fast Flux Test Facility.

M.3.3 Waste Management Alternatives

Primary facilities considered in Waste Management alternatives are one or two IDFs, the RPPDF, and trenches 31 and 34 at Low-Level Radioactive Waste Burial Ground (LLBG) 218-W-5.

M.3.3.1 Low-Level Radioactive Waste Burial Facilities

Sources at LLW disposal facilities, including LLBG 218-W-5, are modeled as contaminated soil and debris. For contaminated soil sources, the partitioning-limited, convective-flow model is applied with soil type distribution coefficients presented in Tables M–11 and M–12. For stabilized waste, the cylindrical diffusion-limited release model is applied with effective diffusivities, as summarized in Tables M–9 and M–10.

Under Waste Management Alternative 1**,** LLW, mixed low-level radioactive waste (MLLW), and transuranic waste would be processed at the Central Waste Complex for disposal in LLBG 218-W-5 (lined) trenches 31 and 34. These trenches would operationally close in 2035. As discussed in Appendices D and S of this EIS, a barrier would not be placed over LLBG 218-W-5, including trenches 31 and 34, in 2035. The infiltration sequence used in the modeling is described in Table M–16.

Table M–16. Waste Management Alternative 1 Infiltration Sequence Description for LLBG 218-W-5, Trenches 31 and 34

Location Condition	Year at Start of Infiltration	Infiltration Value (millimeters per year)
Pre–Hanford Site	1940	3.5
Disturbed conditions	1986	50
Post–barrier design life	2086	3.5

Key: LLBG=low-level radioactive waste burial ground.

M.3.3.2   Integrated Disposal Facility Waste Forms

Characteristics of the tank closure primary- and secondary-waste forms proposed for disposal at an IDF are those described in Section M.3.1.2. The onsite non–Comprehensive Environmental Response, Compensation, and Liability Act (non-CERCLA) and waste management secondary wastes are modeled as grouted waste forms with the characteristics described in Section M.3.1.2.

Waste Management Alternatives 2 and 3 include construction, operation, deactivation, closure, and postclosure care of IDF-East for tank, onsite non-CERCLA, FFTF decommissioning, waste management, and offsite LLW and MLLW. Under Waste Management Alternative 3, onsite non-CERCLA, FFTF decommissioning, waste management, and offsite LLW and MLLW would be disposed of in an IDF to be constructed in IDF-West, while tank LLW and MLLW would be disposed of in IDF-East. Three disposal groups were analyzed under these alternatives. Disposal Group 1 analyzes the operational completion date of 2050, with a barrier placed over the IDFs with a design life of 500 years. Disposal Group 2 analyzes the operational completion date of 2100, with a barrier placed over the IDFs with a design life of 500 years. Disposal Group 3 analyzes the operational completion date of 2165, with a barrier placed over the IDFs with a design life of 500 years. The magnitude and timing of the infiltration sequence for Waste Management Alternatives 2 and 3 are presented in Table M–17.

Table M–17. Waste Management Alternatives 2 and 3 Infiltration Sequence Description 200-East and 200-West Area Integrated Disposal Facilities

Location Condition	Disposal Group 1	Disposal Group 2	Disposal Group 3	IDF-East	IDF-West
	Year at Start of Infiltration			Infiltration Value (millimeters per year)	
Pre–Hanford Site	1940	1940	1940	0.9	3.5
Barrier design life	2050	2100	2165	0.5	0.5
Post–barrier design life	2550	2600	2665	0.9	3.5

Key: IDF-East=200-East Area Integrated Disposal Facility; IDF-West=200-West Area Integrated Disposal Facility.

M.4   RESULTS

M.4.1   Tank Closure Alternatives

M.4.1.1   Past Leaks from Cribs and Trenches (Ditches)

All Tank Closure alternatives are analyzed for the same constituent release to the vadose zone from past leaks from HLW tanks and discharges from cribs and trenches (ditches). Tables M–18 and M–19 and Figures M–7 through M–12 demonstrate the total release of radioactive and chemical constituents for the 10,000-year modeling period.

Table M–18. Radionuclide and Chemical Releases to the Vadose Zone from Tank Farm Past Leaks

Source	Radionuclide (curies)						Chemical (kilograms)					
	H-3	C-14	Tc-99	I-129	Np-237	U-238	1-Butanol	Cr	Hg	NO$_3$	Pb	Utot
A tank farm	4.43×10^{-1}	1.13×10^{-1}	1.24	1.46×10^{-3}	3.87×10^{-3}	5.02×10^{-3}	5.18×10^{-1}	8.44	3.53×10^{-2}	5.10×10^{3}	5.13×10^{-1}	4.52
AX tank farm	2.04×10^{-2}	4.40×10^{-3}	4.80×10^{-2}	5.64×10^{-5}	1.50×10^{-4}	1.94×10^{-4}	2.00×10^{-2}	3.26×10^{-1}	6.77×10^{-5}	2.00×10^{1}	1.98×10^{-2}	1.74×10^{-1}
B tank farm	2.86×10^{1}	3.10	2.18×10^{1}	4.20×10^{-2}	6.74×10^{-2}	2.34×10^{-1}	9.41×10^{1}	2.35×10^{2}	3.55×10^{-1}	3.35×10^{4}	5.10×10^{1}	2.44×10^{2}
BX tank farm	1.25×10^{1}	5.17×10^{-1}	4.92	9.35×10^{-3}	2.64×10^{-2}	7.16	6.56	4.97×10^{1}	3.40×10^{-2}	1.65×10^{4}	5.51	1.06×10^{4}
BY tank farm	6.49	2.20×10^{-1}	2.10	3.98×10^{-3}	1.13×10^{-2}	3.07	2.79	2.12×10^{1}	1.45×10^{-2}	7.04×10^{3}	2.35	4.52×10^{3}
C tank farm	2.68×10^{1}	1.48×10^{-1}	6.61	2.59×10^{-3}	2.30×10^{-2}	5.41×10^{-3}	1.89×10^{1}	4.15×10^{1}	2.12×10^{-2}	4.82×10^{3}	6.87	2.88
S tank farm	7.12	5.53×10^{-1}	3.87	7.44×10^{-3}	2.52×10^{-2}	8.22×10^{-2}	3.86×10^{-5}	7.81×10^{2}	6.49×10^{-2}	2.63×10^{4}	1.07×10^{1}	1.19×10^{2}
SX tank farm	9.24×10^{1}	4.79	3.75×10^{1}	7.10×10^{-2}	1.65×10^{-1}	4.21×10^{-1}	6.37×10^{-2}	3.89×10^{3}	3.57×10^{-2}	1.14×10^{5}	5.75×10^{1}	5.52×10^{2}
T tank farm	2.32×10^{2}	9.55	6.74×10^{1}	1.30×10^{-1}	2.33×10^{-1}	3.49×10^{-1}	3.78×10^{2}	1.10×10^{3}	2.35×10^{-1}	6.74×10^{4}	3.53×10^{1}	3.82×10^{2}
TX tank farm	1.30×10^{3}	1.51×10^{1}	1.07×10^{2}	2.06×10^{-1}	3.86×10^{-1}	3.16	6.13×10^{2}	3.06×10^{3}	1.34	2.44×10^{5}	1.29×10^{2}	1.29×10^{3}
TY tank farm	1.37×10^{1}	3.41×10^{-1}	2.40	4.59×10^{-3}	1.15×10^{-2}	1.33×10^{-1}	9.40	8.47×10^{1}	2.71×10^{-2}	4.19×10^{4}	2.49	1.04×10^{2}
U tank farm	8.96×10^{1}	1.61×10^{-1}	3.57	4.50×10^{-3}	2.13×10^{-2}	1.23×10^{-1}	1.77	1.61×10^{2}	7.16×10^{-2}	1.16×10^{4}	8.41×10^{-1}	1.81×10^{2}

**Note:** To convert kilograms to pounds, multiply by 2.2046.

Key: C-14=carbon-14; Cr=chromium; H-3=hydrogen-3 (tritium); Hg=mercury; I-129=iodine-129; NO$_3$=nitrate; Np-237=neptunium-237; Pb=lead; Tc-99=technetium-99; U-238=uranium-238; Utot=total uranium.
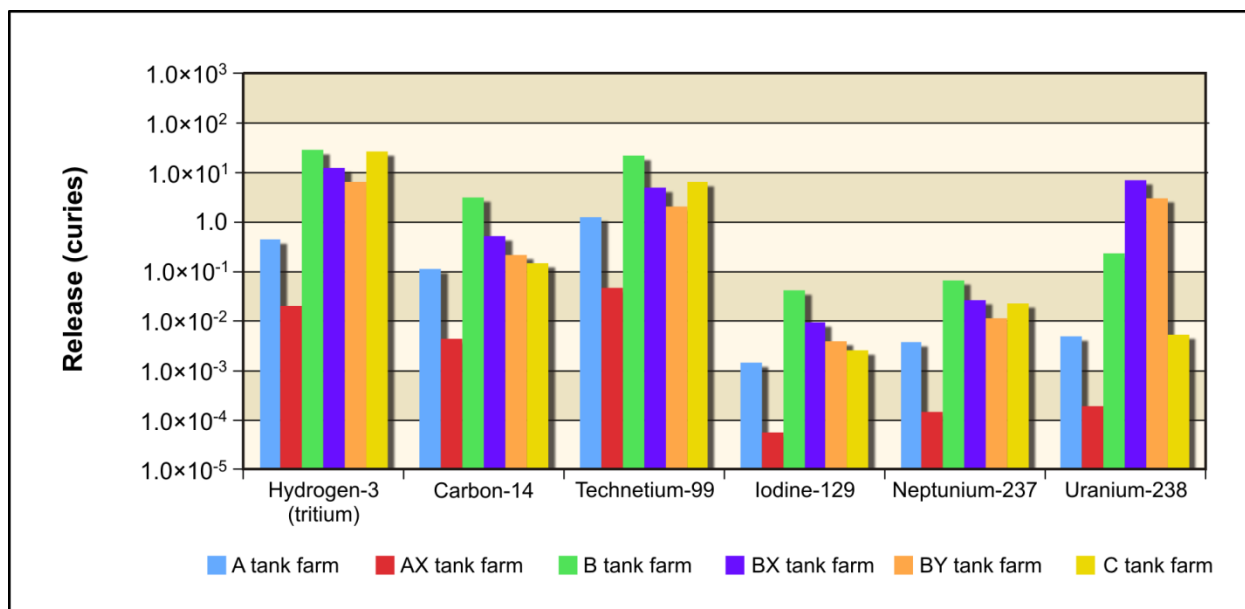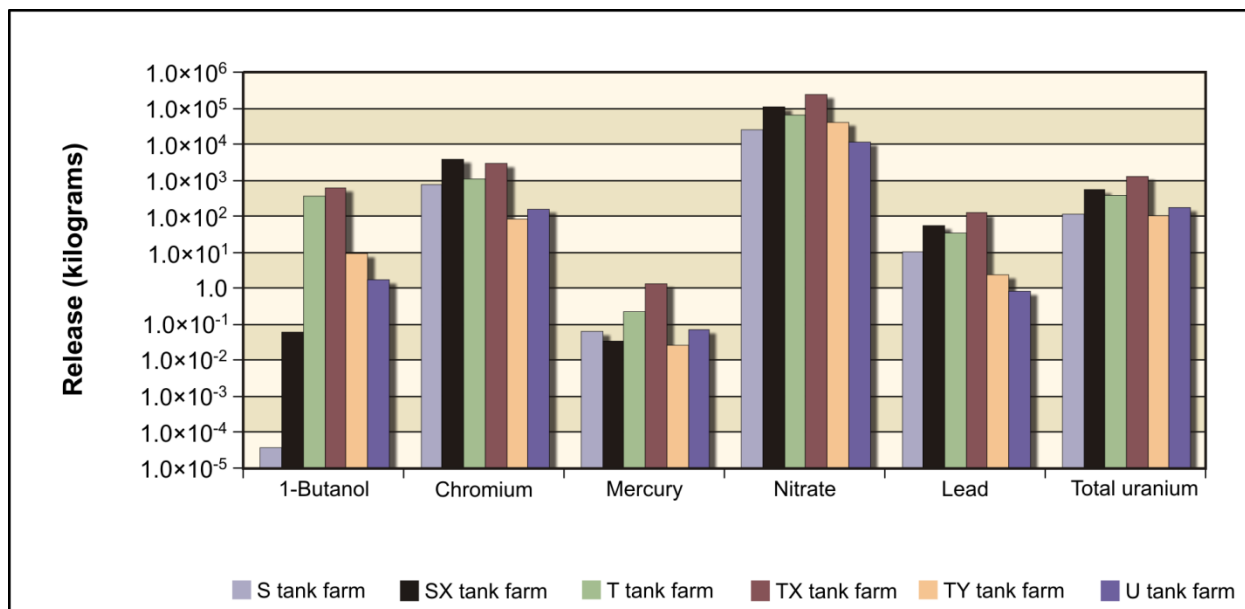
**Figure M–7. Radionuclide Releases to the Vadose Zone from
the 200-East Area Tank Farm Past Leaks**
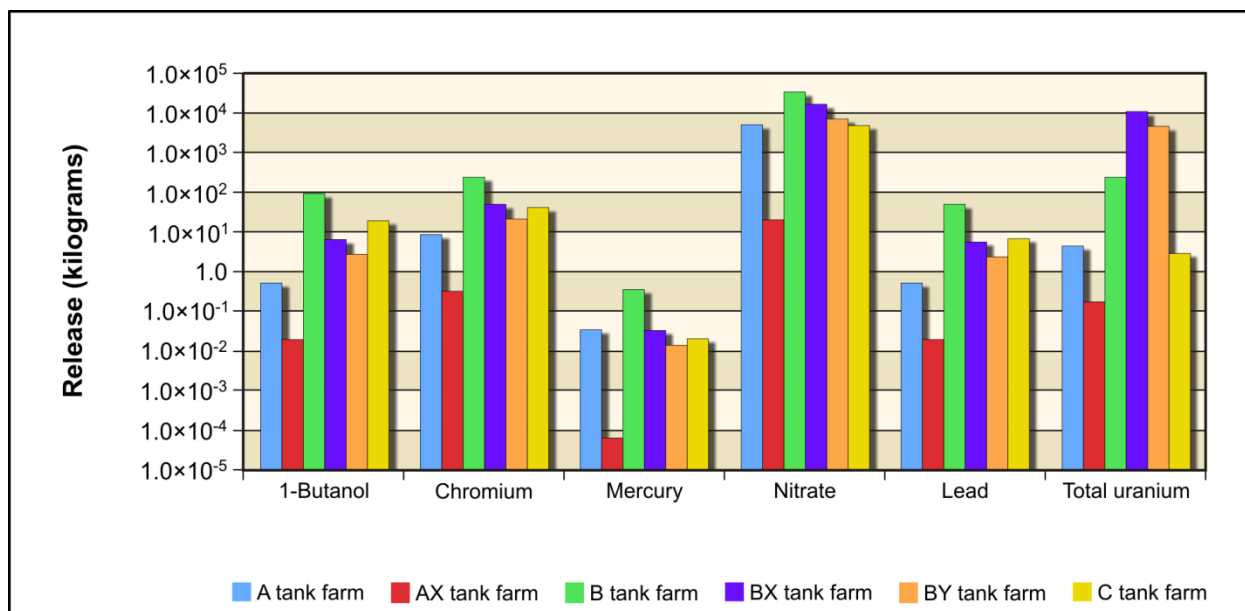
**Figure M–8. Chemical Releases to the Vadose Zone from
the 200-East Area Tank Farm Past Leaks**
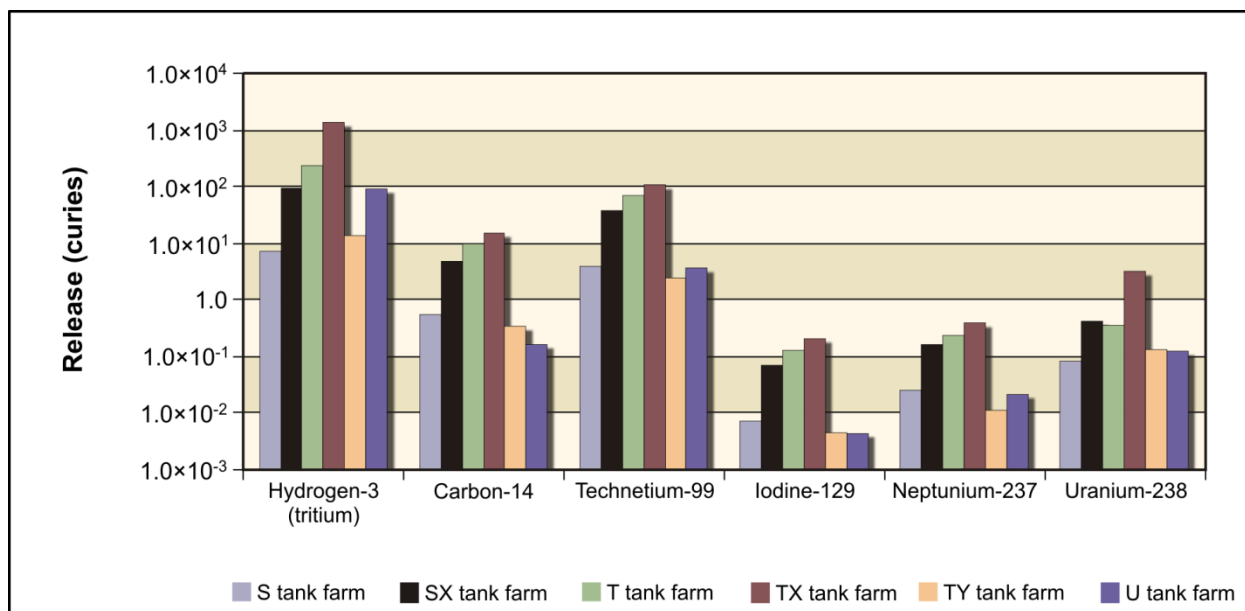
**Figure M–9. Radionuclide Releases to the Vadose Zone from
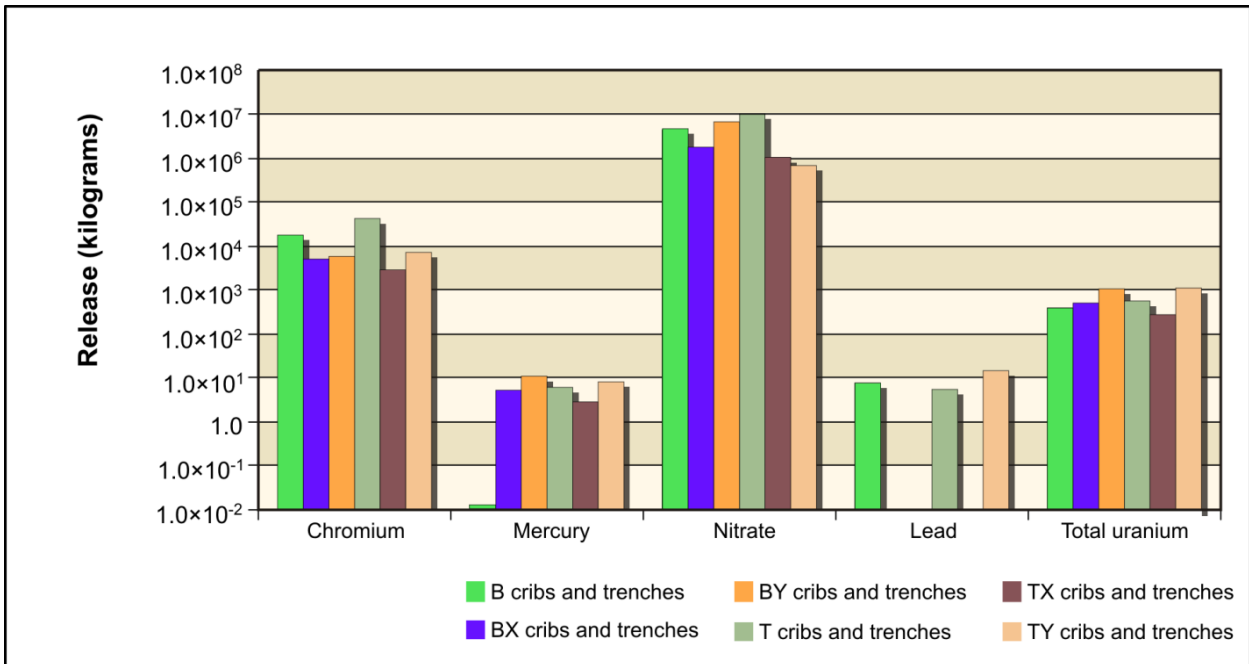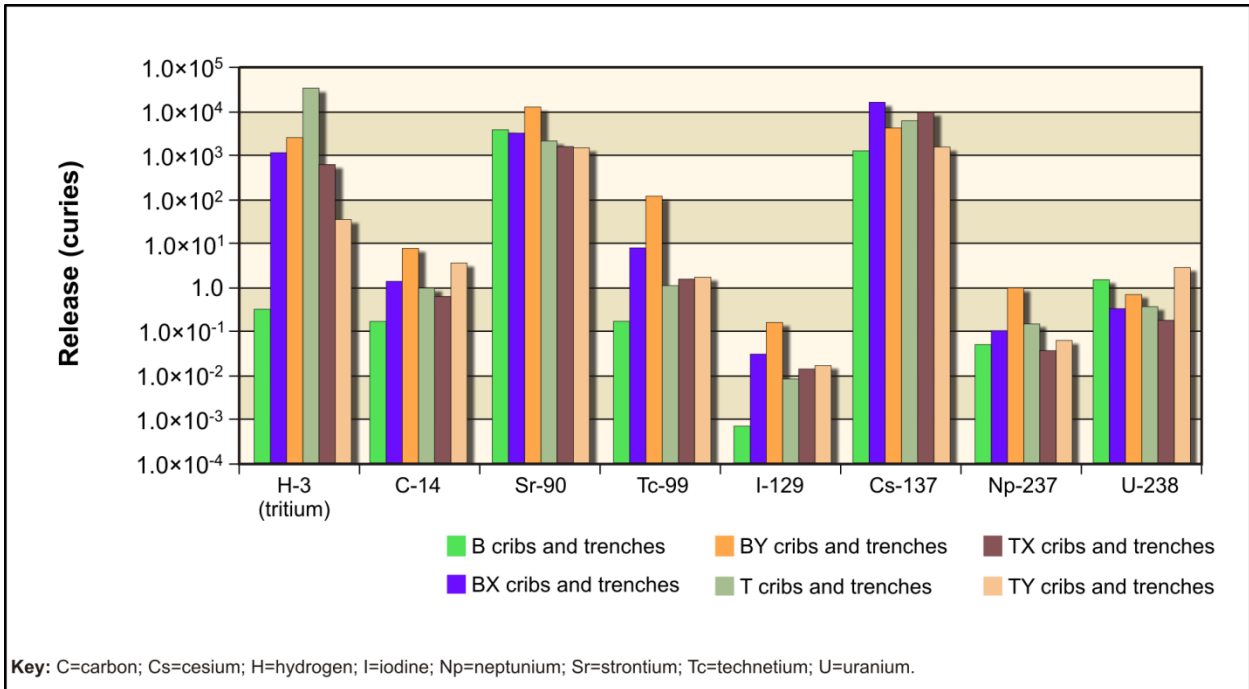the 200-West Area Tank Farm Past Leaks**

**Figure M–10. Chemical Releases to the Vadose Zone from
the 200-West Area Tank Farm Past Leaks**

Table M–19. Radionuclide and Chemical Releases to the Vadose Zone from Alternative Cribs and Trenches (Ditches)

Source	Radionuclide (curies)									Chemical (kilograms)				
	H-3	C-14	Sr-90	Tc-99	I-129	Cs-137	Np-237	U-238	Pu-239	Cr	Hg	NO$_3$	Pb	Utot
B cribs and trenches	3.29×10^{-1}	1.73×10^{-1}	4.29×10^3	1.75×10^{-1}	6.95×10^{-4}	1.42×10^3	5.12×10^{-2}	1.58	1.65×10^2	1.78×10^4	1.23×10^{-2}	4.65×10^6	7.69	3.88×10^2
BX cribs and trenches	1.28×10^3	1.45	3.57×10^3	8.40	3.09×10^{-2}	1.83×10^4	1.07×10^{-1}	3.40×10^{-1}	6.97	5.05×10^3	5.25	1.77×10^6	–	5.04×10^2
BY cribs and trenches	2.82×10^3	8.22	1.42×10^4	1.29×10^2	1.65×10^{-1}	4.71×10^3	1.02	7.15×10^{-1}	2.82×10^1	5.81×10^3	1.09×10^1	6.71×10^6	–	1.06×10^3
T cribs and trenches	3.89×10^4	1.01	2.39×10^3	1.15	8.31×10^{-3}	6.91×10^3	1.51×10^{-1}	3.80×10^{-1}	3.03×10^2	4.21×10^4	6.13	1.01×10^7	5.50	5.64×10^2
TX cribs and trenches	6.82×10^2	6.52×10^{-1}	1.76×10^3	1.62	1.41×10^{-2}	1.09×10^4	3.73×10^{-2}	1.85×10^{-1}	3.70	2.87×10^3	2.87	1.04×10^6	–	2.74×10^2
TY cribs and trenches	3.77×10^1	3.81	1.66×10^3	1.80	1.70×10^{-2}	1.73×10^3	6.40×10^{-2}	3.01	8.87×10^1	7.17×10^3	8.18	6.75×10^5	1.46×10^1	1.11×10^3

Note: To convert kilograms to pounds, multiply by 2.2046.

Key: C-14=carbon-14; Cr=chromium; Cs-137=cesium-137; H-3=hydrogen-3 (tritium); Hg=mercury; I-129=iodine-129; NO$_3$=nitrate; Np-237=neptunium-237; Pb=lead; Pu-239=plutonium-239; Sr-90=strontium-90; Tc-99=technetium-99; U-238=uranium-238; Utot=total uranium.

**Figure M–11. Radionuclide Releases to the Vadose Zone from
Alternative Cribs and Trenches (Ditches)**

**Figure M–12. Chemical Releases to the Vadose Zone from
Alternative Cribs and Trenches (Ditches)**

M.4.1.2   Releases from Other Sources in the Tank Farms

Releases from other sources related to the HLW tanks, including tank residuals, retrieval leaks, and ancillary equipment, were analyzed together. The amount of constituent released to the vadose zone is related to the activities under each Tank Closure alternative. Under Tank Closure Alternatives 6A and 6B, all tanks farms would be closed to a clean state by removing the tanks, ancillary equipment, and soil to a depth of 3 meters (10 feet) below the tank base. Where necessary, deep soil excavation would also be conducted to remove contamination plumes within the soil column. Therefore, releases from other sources related to the HLW tanks were not analyzed.

Under Tank Closure Alternative 1, tank farms would be maintained in the current condition indefinitely; however, for analysis purposes, they are assumed to fail after an institutional control period of 100 years. At this time, the salt cake in single-shell tanks is assumed available for leaching into the vadose zone, and the liquid contents of double-shell tanks are assumed to be discharged directly to the vadose zone. Table M–20 and Figures M–13 through M–18 indicate the constituent release estimated under Tank Closure Alternative 1.

Table M–20. Tank Closure Alternative 1 Radionuclide and Chemical Releases to the Vadose Zone from Other Sources in Tank Farms

| Source	Radionuclide (curies)						Chemical (kilograms)								
	H-3	C-14	Tc-99	I-129	Np-237	U-238	1-Butanol	Cr	Hg	NO$_3$	Pb	Utot	2,4,6-TCP	Benzene	PCBs
A tank farm	2.78	1.46	1.22×10^1	1.71×10^{-2}	3.98×10^{-2}	5.96×10^{-1}	–	1.63×10^4	1.60×10^2	1.42×10^6	4.05×10^3	1.11×10^4	–	–	3.05×10^1
AX tank farm	4.52	1.33	8.75	1.02×10^{-2}	1.66×10^{-2}	7.72×10^{-2}	–	7.96×10^3	4.32×10^1	7.72×10^5	1.27×10^3	1.50×10^3	–	–	1.47×10^1
B tank farm	3.99	7.63	2.19×10^2	8.46×10^{-2}	3.52×10^{-1}	2.11×10^1	3.86×10^{-4}	1.13×10^4	1.40×10^2	1.93×10^6	6.77×10^3	2.89×10^4	–	–	5.45×10^1
BX tank farm	3.71	4.06×10^1	3.74×10^2	4.54×10^{-1}	7.51×10^{-1}	5.15×10^1	–	2.23×10^4	2.30×10^2	1.75×10^6	3.70×10^3	7.44×10^4	–	–	4.18×10^1
BY tank farm	2.83×10^1	5.03×10^2	2.54×10^3	5.57	8.63	5.24×10^1	–	7.38×10^4	1.75×10^2	6.66×10^6	5.14×10^3	6.58×10^4	–	–	1.11×10^2
C tank farm	1.43×10^2	1.55×10^1	3.58×10^2	1.03	5.81	5.05×10^2	6.47×10^{-1}	5.72×10^3	3.99×10^2	6.75×10^5	2.35×10^4	1.15×10^5	–	–	4.68×10^1
S tank farm	2.15×10^1	4.41×10^2	2.74×10^3	5.95	1.12×10^1	5.20×10^1	–	1.20×10^5	7.18×10^1	1.10×10^7	2.24×10^3	5.21×10^4	–	–	1.39×10^2
SX tank farm	2.74×10^1	2.71×10^2	1.77×10^3	3.37	6.76	2.97×10^1	–	1.06×10^5	1.47×10^2	6.66×10^6	1.76×10^3	3.29×10^4	–	–	9.24×10^1
T tank farm	1.19	1.43×10^1	1.65×10^2	1.16×10^{-1}	2.82×10^{-1}	2.62×10^1	–	1.23×10^4	2.02×10^1	7.57×10^5	4.40×10^3	3.77×10^4	–	–	4.94×10^1
TX tank farm	2.92×10^1	5.79×10^2	3.91×10^2	7.18	1.33×10^1	4.81×10^1	1.15×10^{-5}	6.16×10^4	2.84×10^1	1.41×10^7	7.15×10^3	4.58×10^4	–	–	1.73×10^2
TY tank farm	1.59	7.48	1.04×10^2	1.31×10^{-1}	2.31×10^{-1}	2.26×10^1	–	8.07×10^3	2.60×10^2	8.49×10^5	1.41×10^3	3.29×10^4	–	–	1.68×10^1
U tank farm	2.97×10^1	3.30×10^2	2.44×10^3	4.73	9.01	3.93×10^1	–	5.15×10^4	2.57×10^1	5.50×10^6	1.09×10^4	5.01×10^4	–	–	8.54×10^1
AN tank farm	1.18×10^2	1.94×10^2	3.69×10^3	3.82	8.20	7.91	8.62×10^5	1.86×10^4	4.68	6.49×10^6	3.64×10^3	2.69×10^3	2.76×10^{-1}	5.99×10^{-1}	2.07×10^2
AP tank farm	1.53×10^3	1.98×10^2	4.08×10^3	7.71	1.43×10^1	2.86	1.13×10^6	1.03×10^4	–	5.67×10^6	9.04×10^2	1.23×10^3	3.63×10^{-1}	7.87×10^{-1}	2.71×10^2
AW tank farm	1.71×10^2	8.98×10^1	1.87×10^3	2.12	2.40×10^1	3.95×10^1	6.66×10^5	2.00×10^4	2.10×10^{-1}	3.48×10^6	1.52×10^3	3.97×10^4	2.14×10^{-1}	4.64×10^{-1}	1.60×10^2
AY tank farm	2.49×10^1	1.66	8.99×10^1	1.43×10^{-1}	5.06	3.22	1.33×10^5	2.81×10^3	1.27×10^2	1.71×10^5	4.51×10^3	3.54×10^3	4.26×10^{-2}	9.25×10^{-2}	3.18×10^1
AZ tank farm	1.88×10^2	1.04×10^1	2.05×10^3	1.92	2.71×10^1	5.69	3.07×10^5	5.10×10^3	4.16	7.76×10^5	4.04×10^2	5.20×10^3	9.84×10^{-2}	2.14×10^{-1}	7.36×10^1
SY tank farm	1.09×10^3	3.82×10^1	2.47×10^3	2.67	3.81	4.52	3.65×10^5	4.75×10^4	8.98	2.49×10^6	1.58×10^3	2.39×10^3	1.17×10^{-1}	2.54×10^{-1}	8.76×10^1

Note: To convert kilograms to pounds, multiply by 2.2046.

Key: 2,4,6-TCP=2,4,6-trichlorophenol; C-14=carbon-14; Cr=chromium; H-3=hydrogen-3 (tritium); Hg=mercury; I-129=iodine-129; NO$_3$=nitrate; Np-237=neptunium-237; Pb=lead; PCBs=polychlorinated biphenyls; Tc-99=technetium-99; U-238=uranium-238; Utot=total uranium.
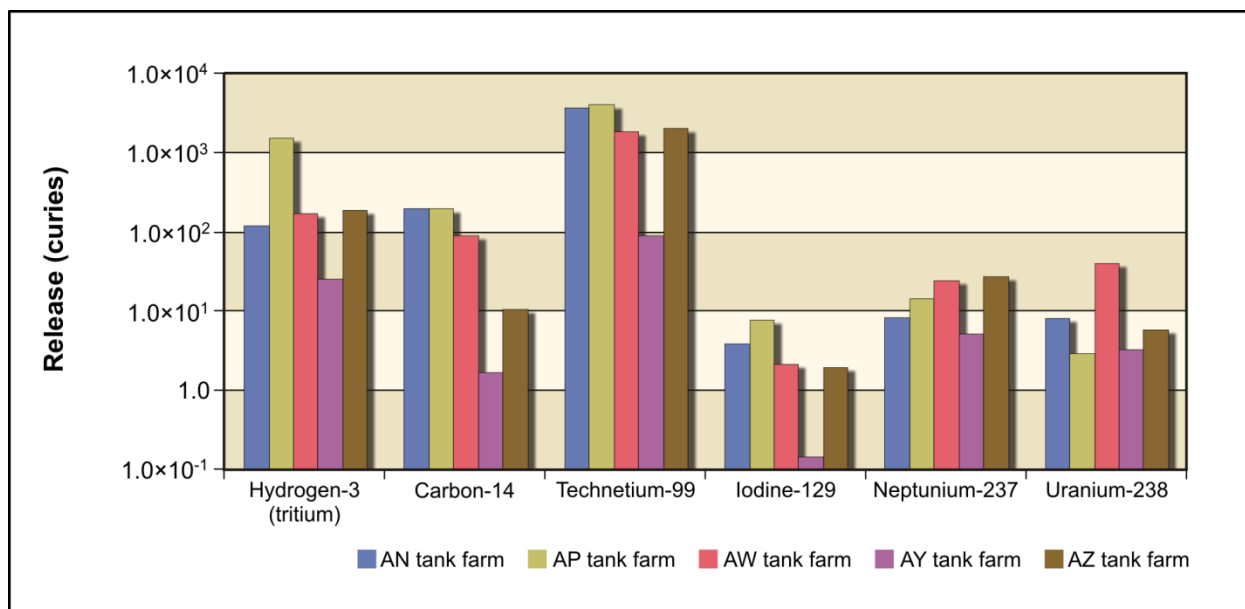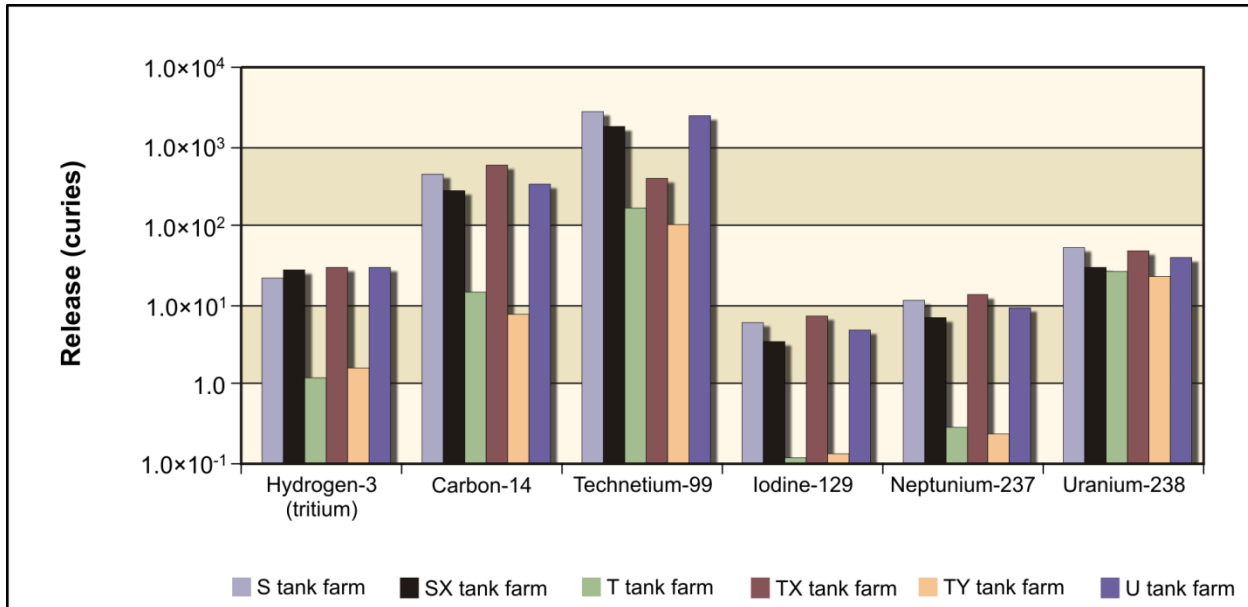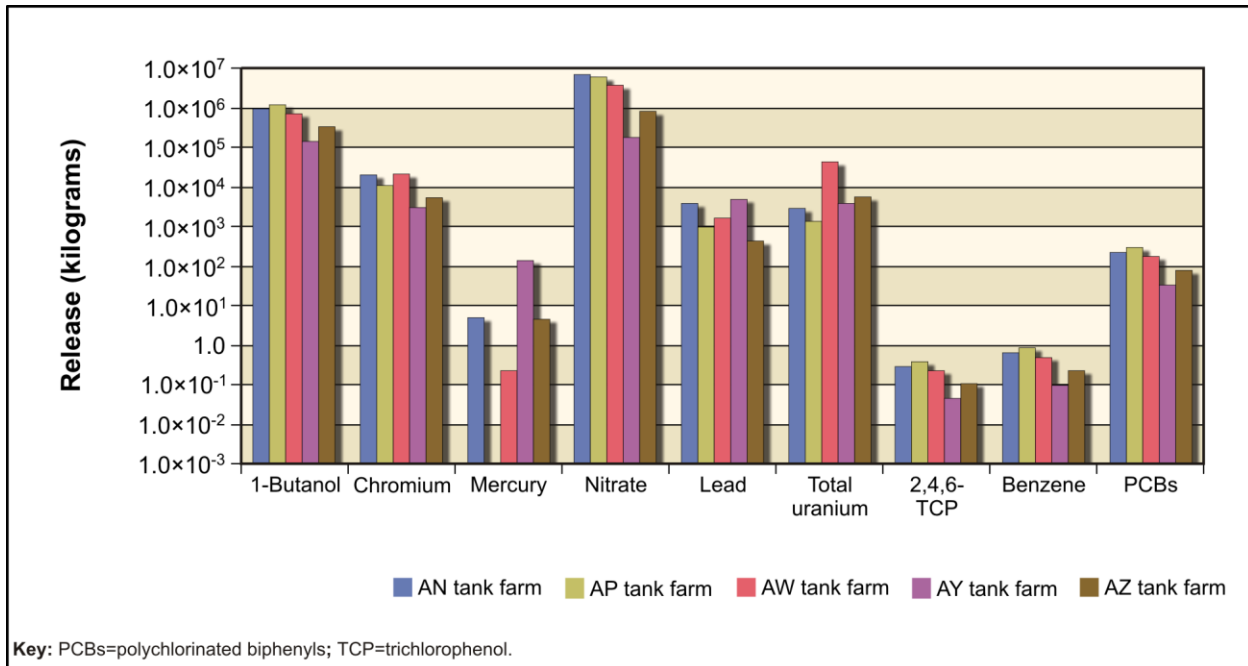
Figure M–13. Tank Closure Alternative 1 Radionuclide Releases to the Vadose Zone from Other Sources in Tank Farms AN, AP, AW, AY, and AZ
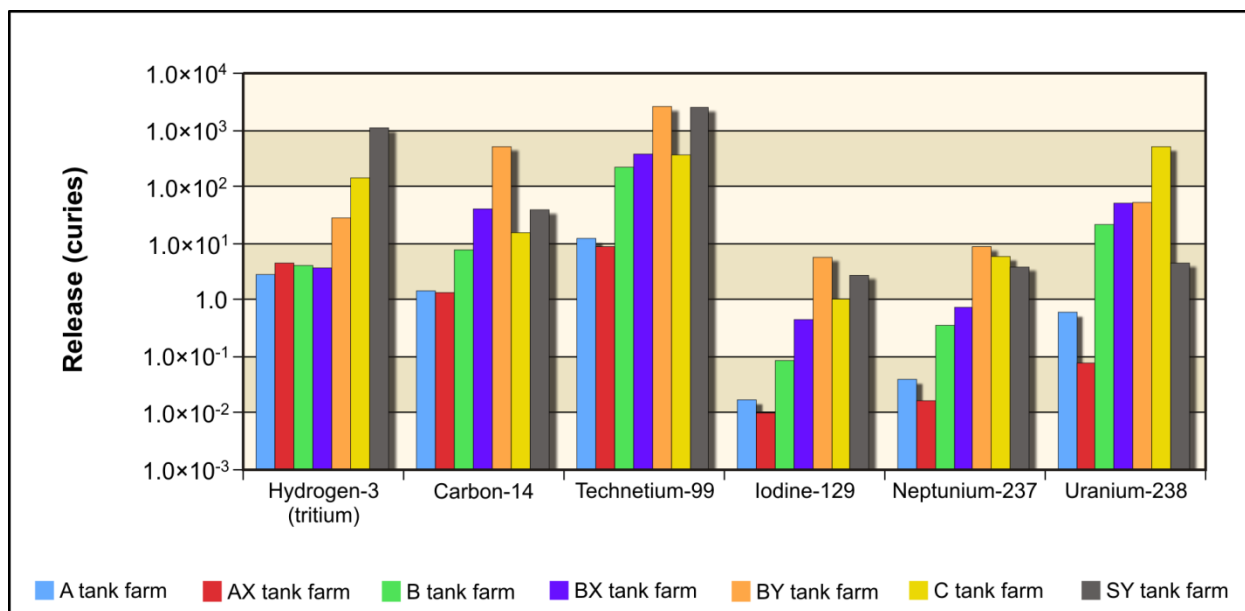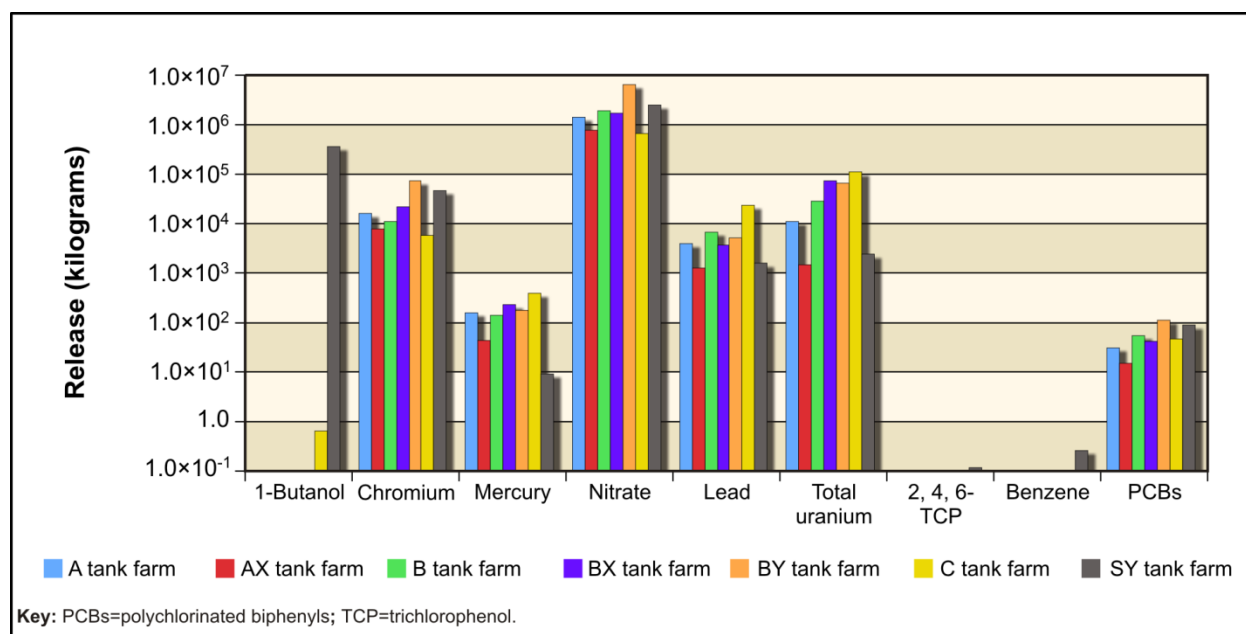

Figure M–14. Tank Closure Alternative 1 Radionuclide Releases to the Vadose Zone from Other Sources in Tank Farms A, AX, B, BX, BY, C, and SY
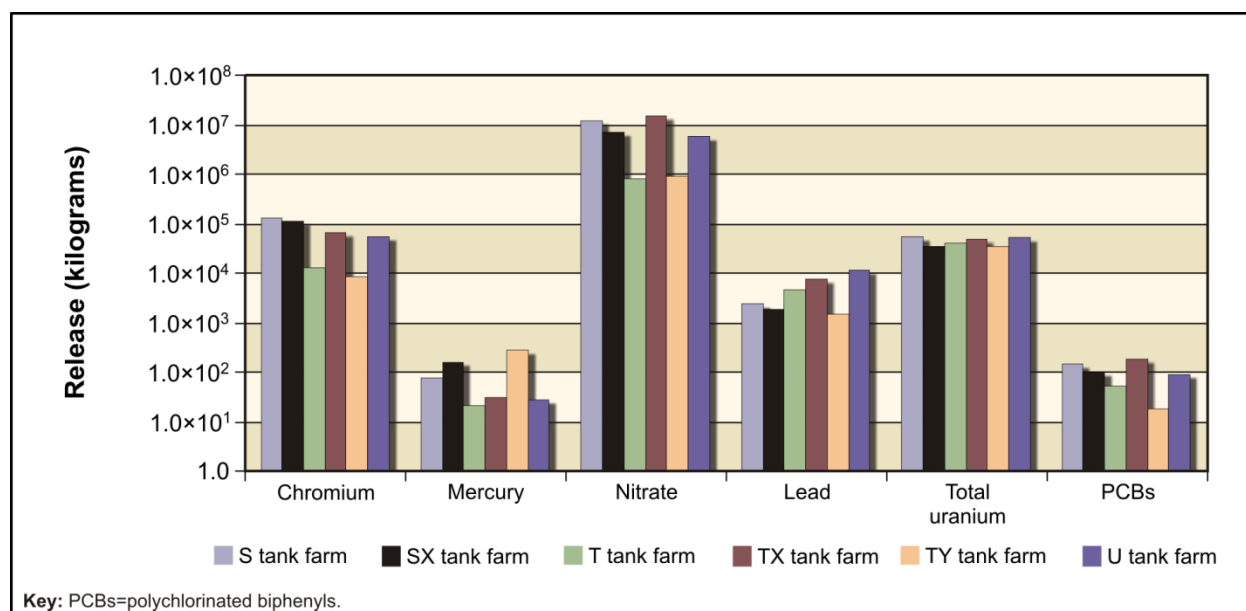
**Figure M–15. Tank Closure Alternative 1 Radionuclide Releases to the Vadose Zone from
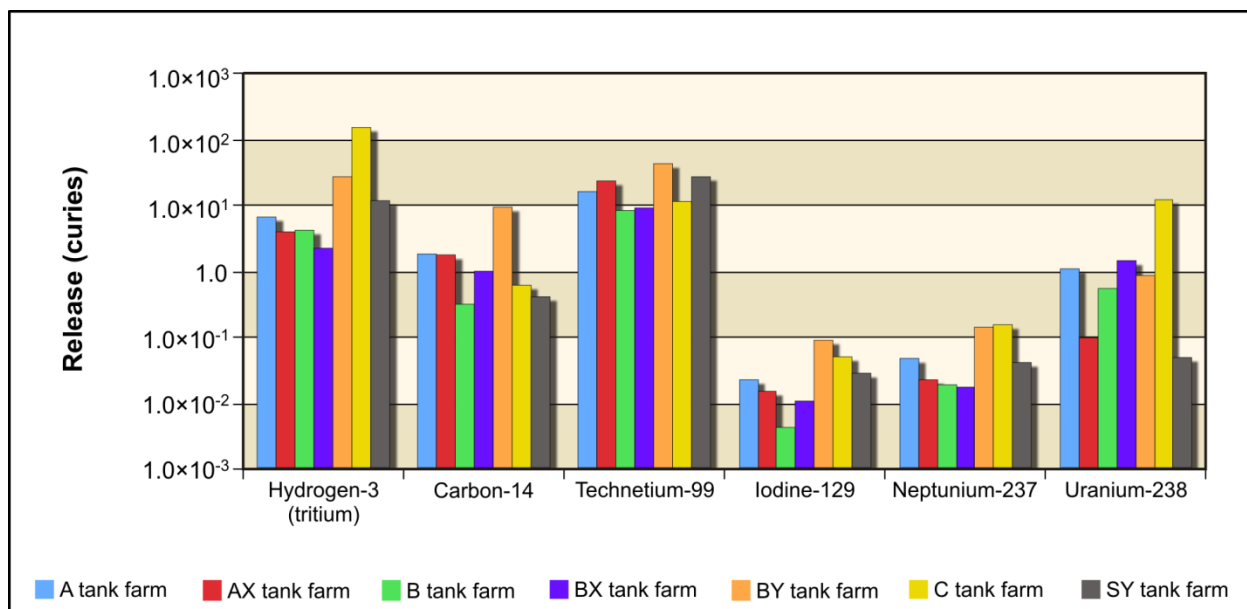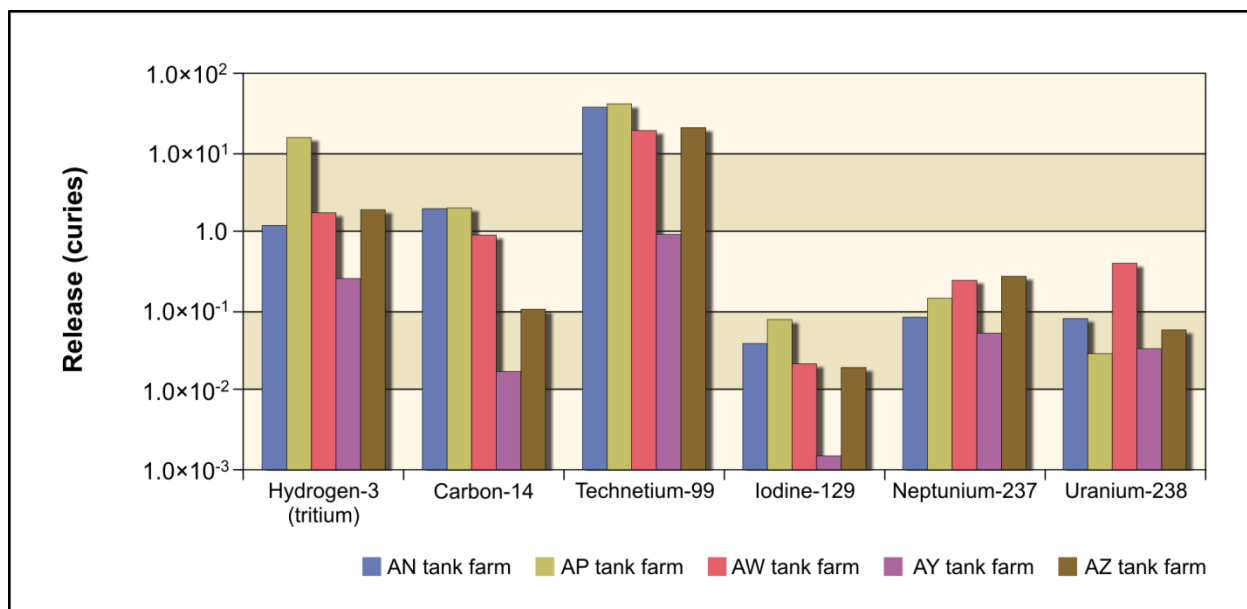Other Sources in Tank Farms S, SX, T, TX, TY, and U**

**Figure M–16. Tank Closure Alternative 1 Chemical Releases to the Vadose Zone from
Other Sources in Tank Farms AN, AP, AW, AY, and AZ**

Figure M–17. Tank Closure Alternative 1 Chemical Releases to the Vadose Zone from Other Sources in Tank Farms A, AX, B, BX, BY, C, and SY

Figure M–18. Tank Closure Alternative 1 Chemical Releases to the Vadose Zone from Other Sources in Tank Farms S, SX, T, TX, TY, and U

Under Tank Closure Alternative 2A, tank waste would be retrieved to a volume corresponding to 99 percent retrieval, but residual material in tanks would not be stabilized. After an institutional control period of 100 years, the salt cake in tanks is assumed available for dissolution in infiltrating water. Potential releases to the vadose zone under Tank Closure Alternative 2A are indicated in Table M–21 and Figures M–19 through M–24.

Table M–21. Tank Closure Alternative 2A Radionuclide and Chemical Releases to the Vadose Zone from Other Sources in Tank Farms

Source	Radionuclide (curies)						Chemical (kilograms)								
	H-3	C-14	Tc-99	I-129	Np-237	U-238	1-Butanol	Cr	Hg	NO$_3$	Pb	Utot	2,4,6-TCP	Benzene	PCBs
A tank farm	6.31	1.73	1.51×10^1	2.15×10^{-2}	4.52×10^{-2}	1.03	–	3.61×10^2	6.39	2.66×10^4	1.42×10^2	3.43×10^2	–	–	4.75×10^{-1}
AX tank farm	3.69	1.70	2.17×10^1	1.46×10^{-2}	2.16×10^{-2}	9.26×10^{-2}	–	1.76×10^2	3.26	1.15×10^5	9.10×10^1	5.41×10^1	–	–	2.60×10^{-1}
B tank farm	3.98	3.05×10^{-1}	7.92	4.16×10^{-3}	1.82×10^{-2}	5.21×10^{-1}	3.86×10^{-4}	3.48×10^2	3.59	1.09×10^5	1.62×10^2	7.13×10^2	–	–	1.00
BX tank farm	2.08	9.41×10^{-1}	8.66	1.02×10^{-2}	1.67×10^{-2}	1.37	–	6.09×10^2	6.61	5.86×10^4	1.06×10^2	1.99×10^3	–	–	7.62×10^{-1}
BY tank farm	2.54×10^1	8.70	3.98×10^1	8.64×10^{-2}	1.35×10^{-1}	8.20×10^{-1}	–	1.20×10^3	2.74	1.11×10^5	7.97×10^1	1.03×10^3	–	–	1.45
C tank farm	1.41×10^2	5.85×10^{-1}	1.09×10^1	4.81×10^{-2}	1.46×10^{-1}	1.14×10^1	6.47×10^{-1}	1.85×10^2	9.73	1.17×10^5	3.78×10^3	2.93×10^3	–	–	9.22×10^{-1}
S tank farm	1.93×10^1	7.28	3.97×10^1	8.56×10^{-2}	1.62×10^{-1}	6.60×10^{-1}	–	1.73×10^3	1.04	1.58×10^5	3.22×10^1	7.66×10^2	–	–	1.73
SX tank farm	1.91×10^1	4.84	3.03×10^1	5.64×10^{-2}	1.14×10^{-1}	5.98×10^{-1}	–	1.90×10^3	3.25	1.47×10^5	3.25×10^1	7.00×10^2	–	–	1.35
T tank farm	1.02	5.65×10^{-1}	4.66	3.65×10^{-3}	9.95×10^{-3}	6.64×10^{-1}	–	3.57×10^2	4.97×10^{-1}	7.54×10^4	1.28×10^2	9.52×10^2	–	–	9.49×10^{-1}
TX tank farm	2.51×10^1	9.85	5.75×10^1	1.09×10^{-1}	2.02×10^{-1}	7.60×10^{-1}	1.15×10^{-5}	9.81×10^2	6.13×10^{-1}	2.15×10^5	1.09×10^2	7.34×10^2	–	–	2.25
TY tank farm	9.68×10^{-1}	2.24×10^{-1}	3.29	3.35×10^{-3}	6.64×10^{-3}	6.43×10^{-1}	–	2.22×10^2	6.41	2.37×10^4	3.91×10^1	9.35×10^2	–	–	3.38×10^{-1}
U tank farm	2.15×10^1	6.24	4.27×10^1	8.21×10^{-2}	1.57×10^{-1}	7.57×10^{-1}	–	9.42×10^2	7.07×10^{-1}	1.77×10^5	2.57×10^2	9.82×10^2	–	–	1.31
AN tank farm	1.22	1.99	3.79×10^1	3.93×10^{-2}	8.42×10^{-2}	8.12×10^{-2}	8.85×10^3	1.91×10^2	4.80×10^{-2}	6.66×10^4	3.74×10^1	2.76×10^1	2.83×10^{-3}	6.15×10^{-3}	2.08
AP tank farm	1.57×10^1	2.02	4.18×10^1	7.89×10^{-2}	1.47×10^{-1}	2.92×10^{-2}	1.16×10^4	1.06×10^2	–	5.80×10^4	9.25	1.26×10^1	3.71×10^{-3}	8.06×10^{-3}	2.71
AW tank farm	1.76	9.25×10^{-1}	1.92×10^1	2.18×10^{-2}	2.47×10^{-1}	4.06×10^{-1}	6.85×10^3	2.06×10^2	2.16×10^{-3}	3.59×10^4	1.56×10^1	4.08×10^2	2.20×10^{-3}	4.77×10^{-3}	1.60
AY tank farm	2.60×10^{-1}	1.74×10^{-2}	9.43×10^{-1}	1.50×10^{-3}	5.31×10^{-2}	3.38×10^{-2}	1.39×10^3	2.95×10^1	1.33	1.80×10^3	4.73×10^1	3.72×10^1	4.47×10^{-4}	9.70×10^{-4}	3.18×10^{-1}
AZ tank farm	1.91	1.06×10^{-1}	2.09×10^1	1.96×10^{-2}	2.77×10^{-1}	5.81×10^{-2}	3.13×10^3	5.21×10^1	4.25×10^{-2}	7.93×10^3	4.13	5.32×10^1	1.00×10^{-3}	2.18×10^{-3}	7.37×10^{-1}
SY tank farm	1.12×10^1	3.93×10^{-1}	2.53×10^1	2.74×10^{-2}	3.92×10^{-2}	4.64×10^{-2}	3.75×10^3	4.87×10^2	9.22×10^{-2}	2.56×10^4	1.62×10^1	2.45×10^1	1.21×10^{-3}	2.61×10^{-3}	8.78×10^{-1}

**Note:** To convert kilograms to pounds, multiply by 2.2046.

Key: 2,4,6-TCP=2,4,6-trichlorophenol; C-14=carbon-14; Cr=chromium; H-3=hydrogen-3 (tritium); Hg=mercury; I-129=iodine-129; NO$_3$=nitrate; Np-237=neptunium-237; Pb=lead; PCBs=polychlorinated biphenyls; Tc-99=technetium-99; U-238=uranium-238; Utot=total uranium.
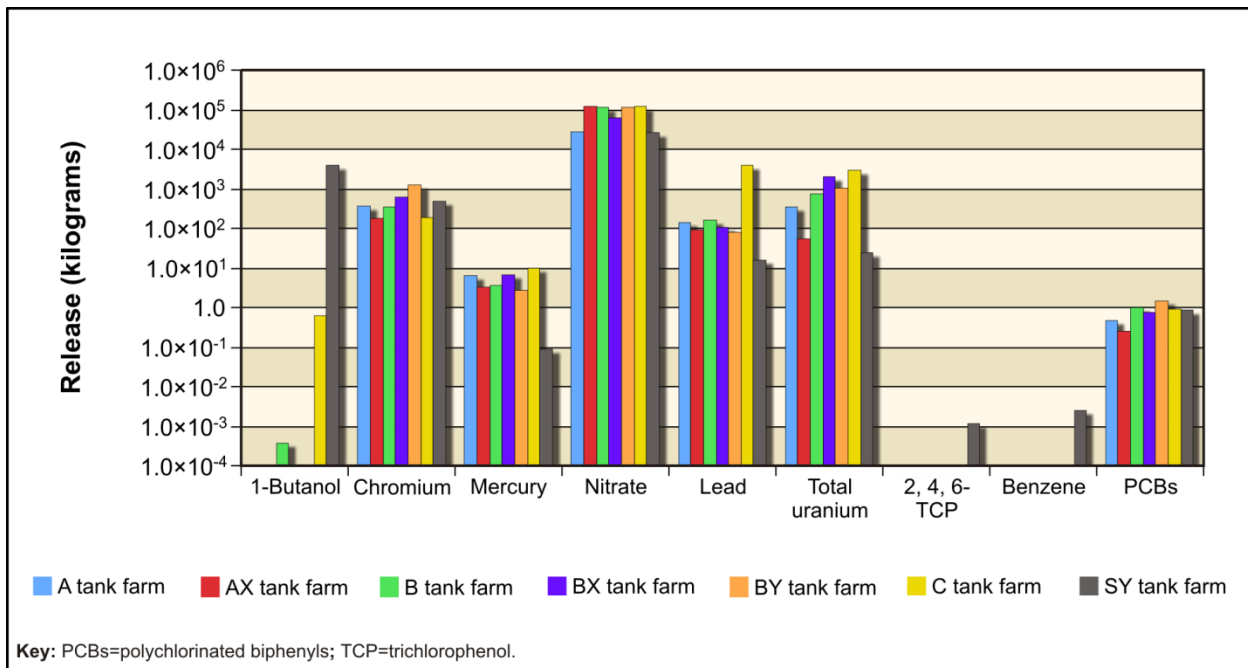
Figure M–19. Tank Closure Alternative 2A Radionuclide Releases to the Vadose Zone from Other Sources in Tank Farms A, AX, B, BX, BY, C, and SY
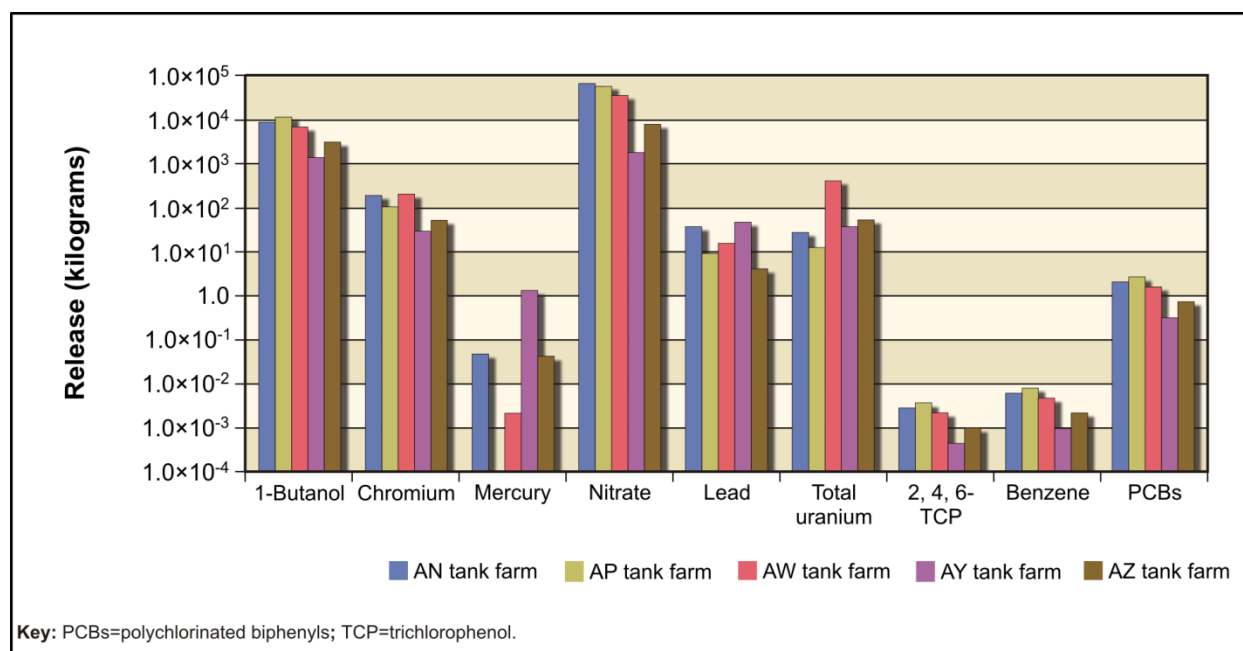

Figure M–20. Tank Closure Alternative 2A Radionuclide Releases to the Vadose Zone from Other Sources in Tank Farms AN, AP, AW, AY, and AZ
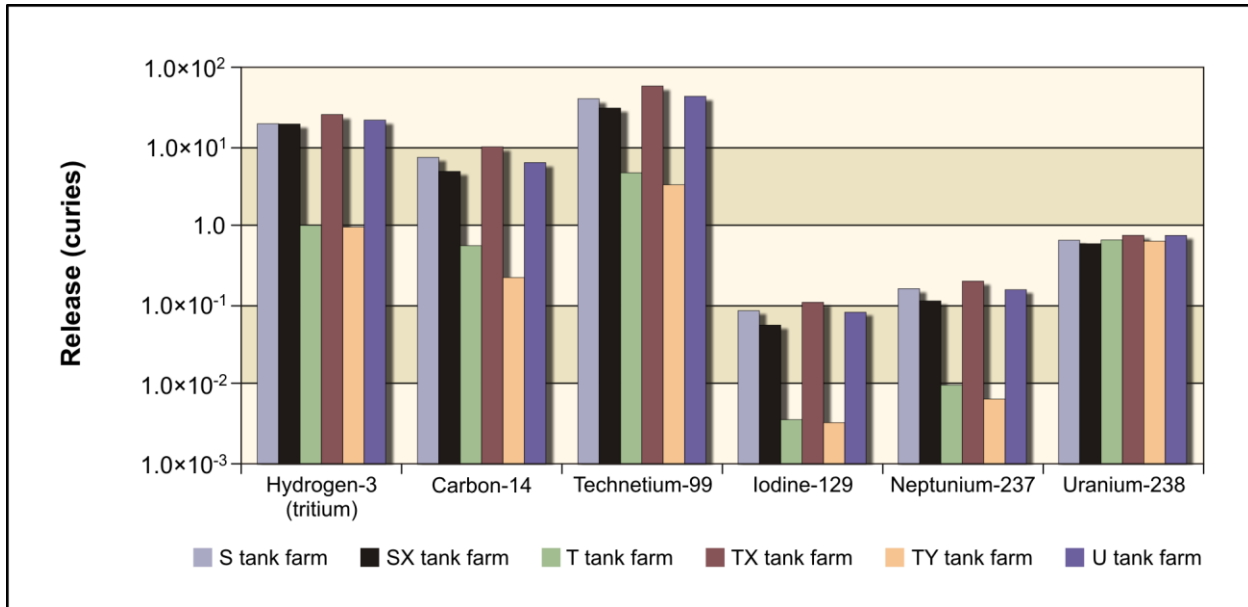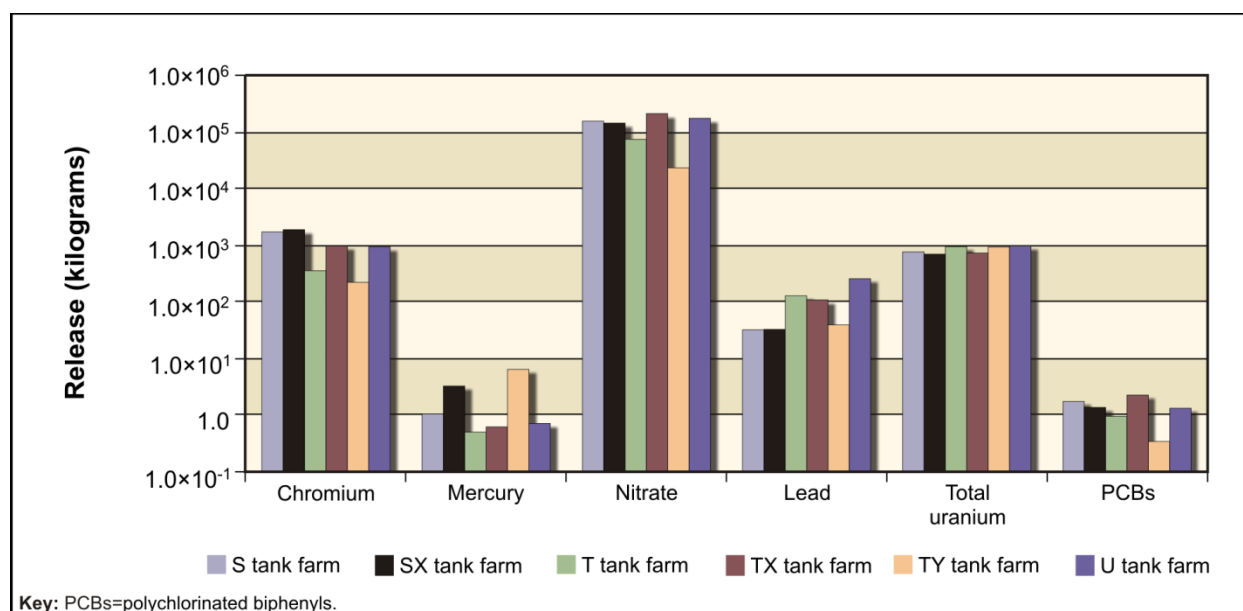
Figure M–21. Tank Closure Alternative 2A Radionuclide Releases to the Vadose Zone from Other Sources in Tank Farms S, SX, T, TX, TY, and U

Figure M–22. Tank Closure Alternative 2A Chemical Releases to the Vadose Zone from Other Sources in Tank Farms A, AX, B, BX, BY, C, and SY

Figure M–23. Tank Closure Alternative 2A Chemical Releases to the Vadose Zone from Other Sources in Tank Farms AN, AP, AW, and AZ

Figure M–24. Tank Closure Alternative 2A Chemical Releases to the Vadose Zone from Other Sources in Tank Farms S, SX, T, TX, TY, and U

Activities under Tank Closure Alternatives 2B, 3A, 3B, 3C, and 6C would be similar to those of Tank Closure Alternative 2A, except that residual material in tanks would be stabilized in place. Soil would be removed down to 4.6 meters (15 feet) for the BX and SX tank farms and replaced with clean soil from onsite sources. Potential releases to the vadose zone under Tank Closure Alternatives 2B, 3A, 3B, 3C, and 6C from tank residuals, ancillary equipment, retrieval losses, and unplanned releases are indicated in Tables M–22 through M–25 and Figures M–25 through M–42.

Table M–22. Tank Closure Alternatives 2B, 3A, 3B, 3C, and 6C Tank Farms Radionuclide and Chemical Releases to the Vadose Zone from Ancillary Equipment in Tank Farms

| Source	Radionuclide (curies)						Chemical (kilograms)								
	H-3	C-14	Tc-99	I-129	Np-237	U-238	1-Butanol	Cr	Hg	NO$_3$	Pb	Utot	2,4,6-TCP	Benzene	PCBs
A tank farm	1.18	4.04×10^{-1}	3.31	4.64×10^{-3}	1.08×10^{-2}	1.62×10^{-1}	–	7.97×10^1	7.83×10^{-1}	6.94×10^3	1.98×10^1	5.39×10^1	–	–	2.28×10^{-3}
AX tank farm	6.03×10^{-1}	4.29×10^{-1}	2.80	3.26×10^{-3}	5.31×10^{-3}	2.47×10^{-2}	–	5.33×10^1	2.90×10^{-1}	5.18×10^3	8.56	1.00×10^1	–	–	1.33×10^{-3}
B tank farm	1.10×10^{-1}	5.70×10^{-2}	1.57	6.01×10^{-4}	2.48×10^{-3}	1.53×10^{-1}	–	8.13×10^1	1.02	1.40×10^4	4.92×10^1	2.10×10^2	–	–	6.39×10^{-3}
BY tank farm	2.63	1.49	6.87	1.50×10^{-2}	2.32×10^{-2}	1.41×10^{-1}	–	1.98×10^2	4.69×10^{-1}	1.79×10^4	1.38×10^1	1.77×10^2	–	–	5.05×10^{-3}
C tank farm	6.71×10^{-1}	1.33×10^{-1}	3.00	8.49×10^{-3}	4.89×10^{-2}	4.26	–	4.78×10^1	3.36	5.60×10^3	1.98×10^2	9.64×10^2	–	–	6.16×10^{-3}
S tank farm	3.06	1.07	5.91	1.28×10^{-2}	2.42×10^{-2}	1.12×10^{-2}	–	2.60×10^2	1.54×10^{-1}	2.38×10^4	4.82	1.12×10^2	–	–	5.00×10^{-3}
T tank farm	1.99×10^{-1}	1.18×10^{-1}	1.32	9.22×10^{-4}	2.25×10^{-3}	2.10×10^{-1}	–	9.79×10^1	1.61×10^{-1}	6.04×10^3	3.51×10^1	3.01×10^2	–	–	6.33×10^{-3}
TX tank farm	4.23	1.66	9.80	1.86×10^{-2}	3.43×10^{-2}	1.25×10^{-1}	–	1.60×10^2	7.38×10^{-2}	3.65×10^4	1.85×10^1	1.19×10^2	–	–	8.83×10^{-3}
TY tank farm	2.22×10^{-1}	6.68×10^{-2}	9.09×10^{-1}	1.14×10^{-3}	2.03×10^{-3}	1.99×10^{-1}	–	7.07×10^1	2.28	7.45×10^3	1.24×10^1	2.88×10^2	–	–	2.28×10^{-3}
U tank farm	4.87	1.63	1.14×10^1	2.19×10^{-2}	4.19×10^{-2}	1.82×10^{-1}	–	2.39×10^2	1.19×10^{-1}	2.56×10^4	5.07×10^1	2.33×10^2	–	–	6.33×10^{-3}
AN tank farm	2.90×10^{-2}	5.74×10^{-2}	1.11	1.15×10^{-3}	2.46×10^{-3}	2.37×10^{-3}	2.58×10^2	5.57	1.40×10^{-3}	1.94×10^3	1.09	8.06×10^{-1}	8.28×10^{-5}	1.80×10^{-4}	1.73×10^{-3}
AP tank farm	2.77×10^{-1}	5.07×10^{-2}	1.06	2.01×10^{-3}	3.75×10^{-3}	7.44×10^{-4}	2.95×10^2	2.71	–	1.48×10^3	2.36×10^{-1}	3.22×10^{-1}	9.46×10^{-5}	2.05×10^{-4}	9.85×10^{-4}
AW tank farm	5.46×10^{-3}	2.70×10^{-2}	6.19×10^{-1}	6.28×10^{-4}	7.95×10^{-3}	1.26×10^{-2}	2.21×10^2	6.63	6.97×10^{-5}	1.16×10^3	5.05×10^{-1}	1.32×10^1	7.10×10^{-5}	1.54×10^{-4}	3.52×10^{-4}
AY tank farm	3.44×10^{-3}	8.70×10^{-4}	4.99×10^{-2}	7.90×10^{-5}	2.81×10^{-3}	1.79×10^{-3}	7.38×10^1	1.56	7.03×10^{-2}	9.51×10^1	2.47	1.96	2.37×10^{-5}	5.13×10^{-5}	3.66×10^{-5}
AZ tank farm	2.29×10^{-2}	2.42×10^{-3}	4.92×10^{-1}	4.60×10^{-4}	6.51×10^{-3}	1.37×10^{-3}	7.37×10^1	1.23	1.00×10^{-3}	1.86×10^2	9.71×10^{-2}	1.25	2.37×10^{-5}	5.13×10^{-5}	1.14×10^{-4}
SY tank farm	2.41×10^{-1}	1.14×10^{-2}	7.47×10^{-1}	8.10×10^{-4}	1.16×10^{-3}	1.37×10^{-3}	1.11×10^2	1.44×10^1	2.72×10^{-3}	7.55×10^2	4.76×10^{-1}	7.25×10^{-1}	3.55×10^{-5}	7.70×10^{-5}	4.34×10^{-4}

Note: To convert kilograms to pounds, multiply by 2.2046.

Key: 2,4,6-TCP=2,4,6-trichlorophenol; C-14=carbon-14; Cr=chromium; H-3=hydrogen-3 (tritium); Hg=mercury; I-129=iodine-129; NO$_3$=nitrate; Np-237=neptunium-237; Pb=lead; PCBs=polychlorinated biphenyls; Tc-99=technetium-99; U-238=uranium-238; Utot=total uranium.
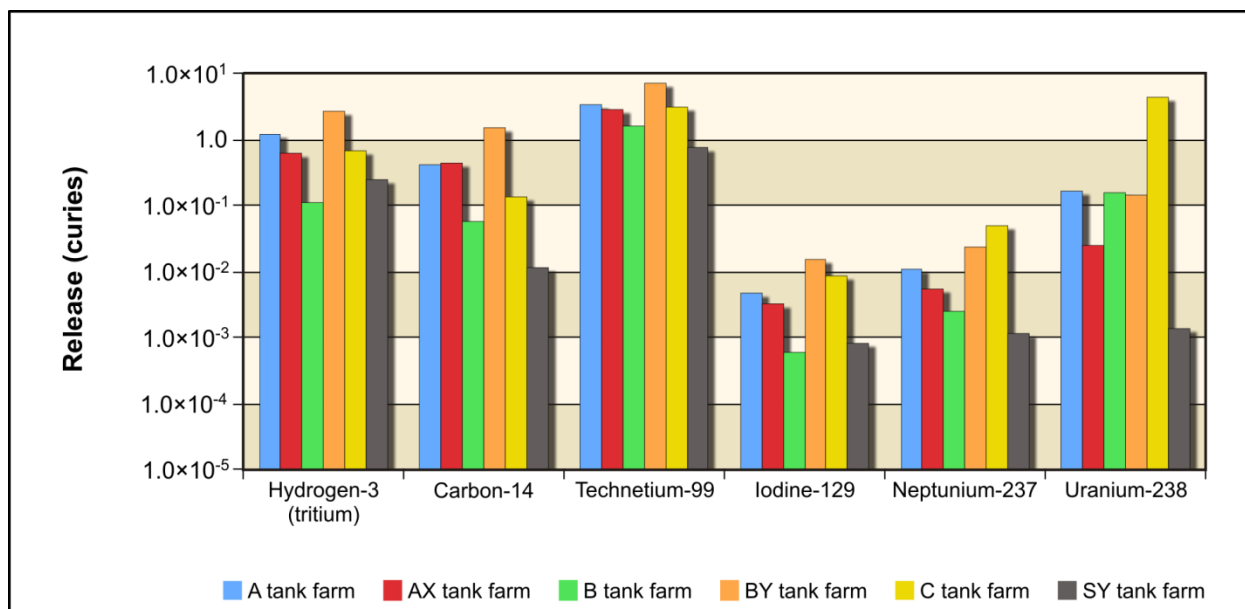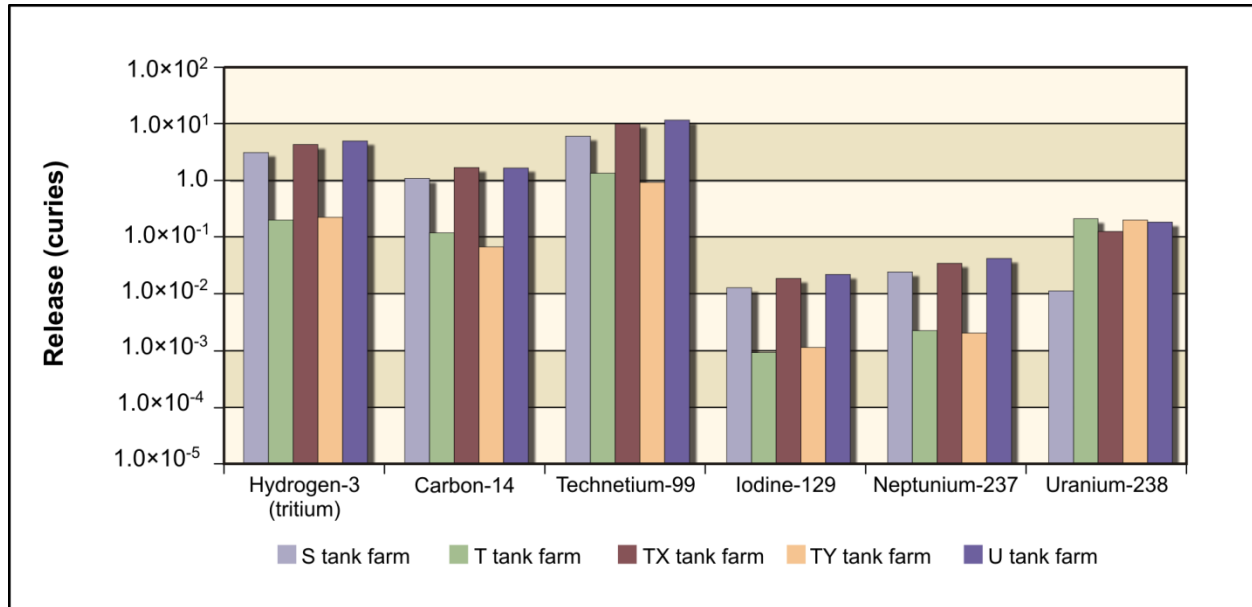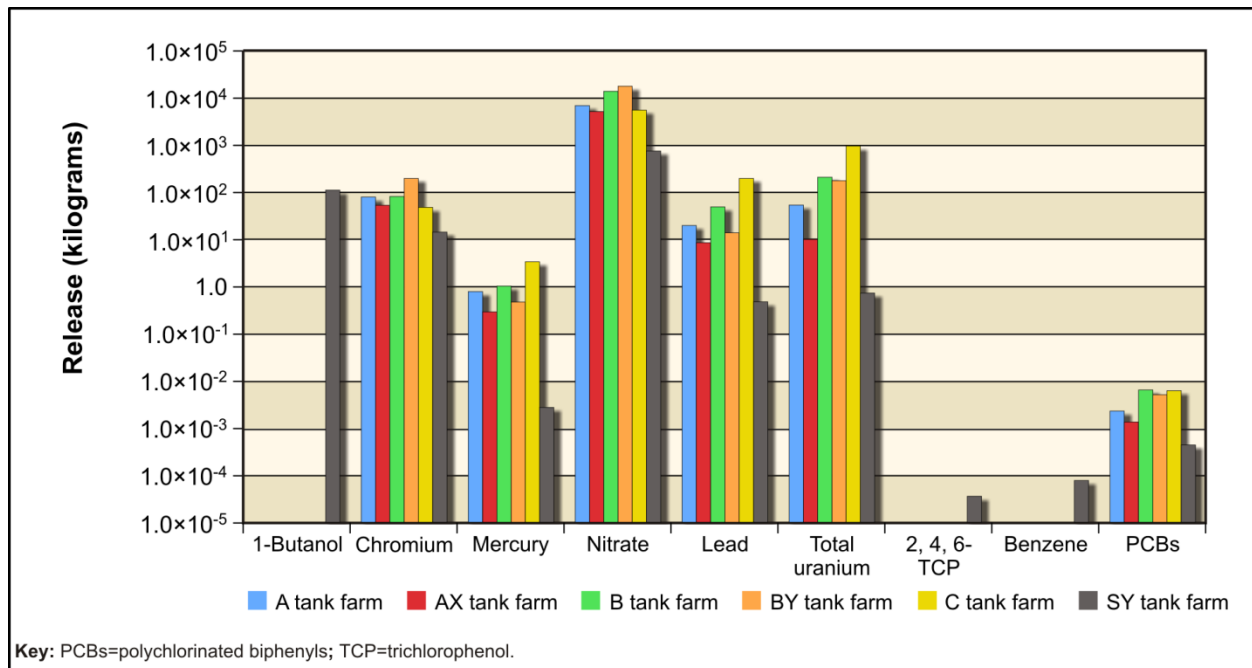
Figure M–25. Tank Closure Alternatives 2B, 3A, 3B, 3C, and 6C Radionuclide Releases to the Vadose Zone from Ancillary Equipment in Tank Farms A, AX, B, BX, BY, C, and SY
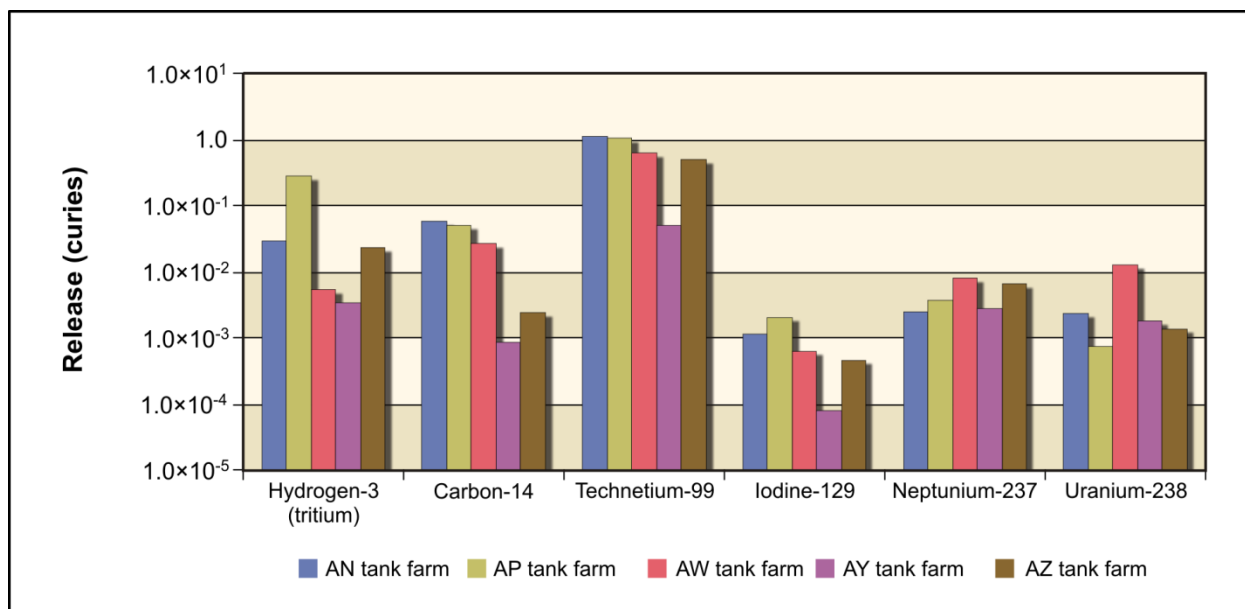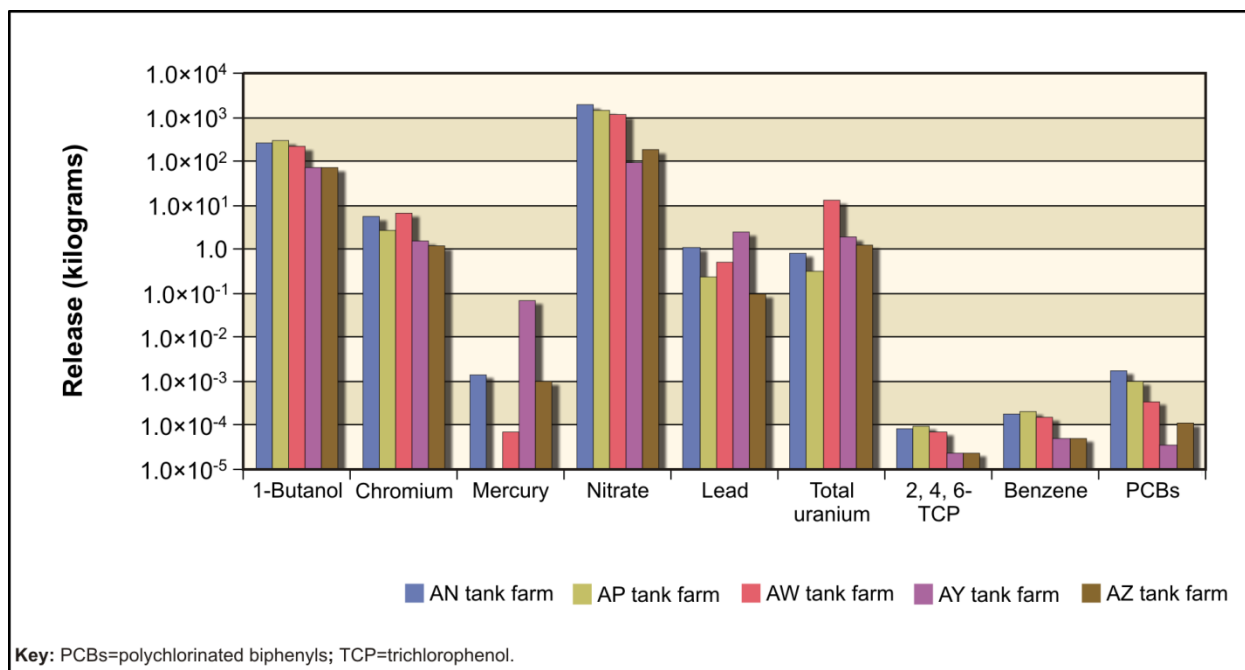

Figure M–26. Tank Closure Alternatives 2B, 3A, 3B, 3C, and 6C Radionuclide Releases to the Vadose Zone from Ancillary Equipment in Tank Farms AN, AP, AW, AY, and AZ
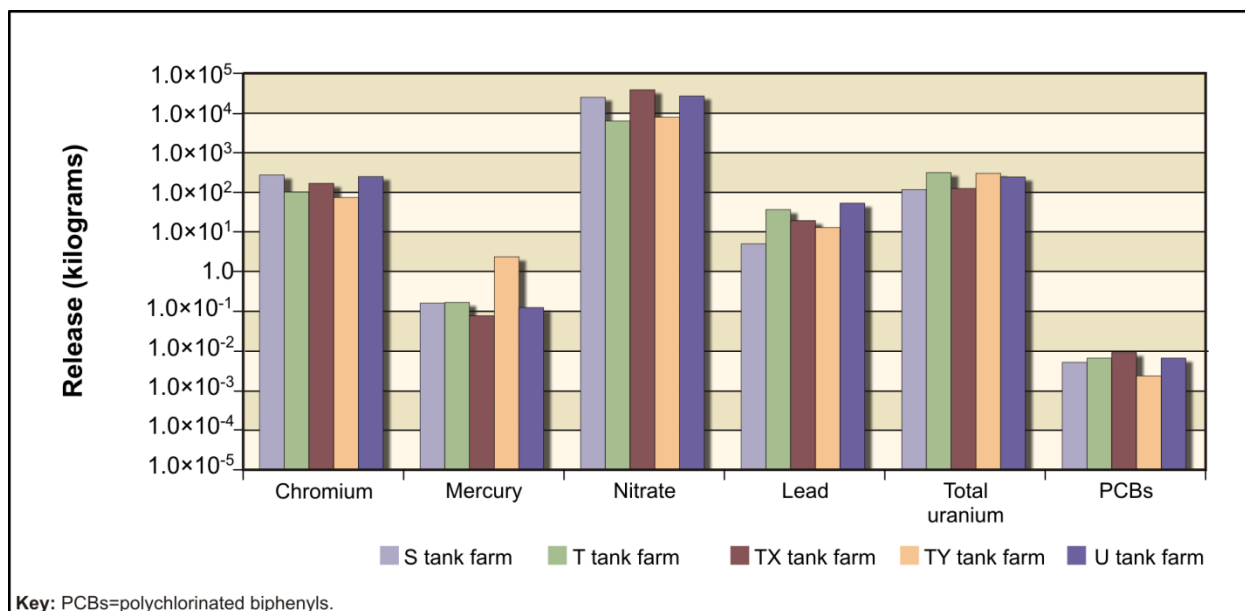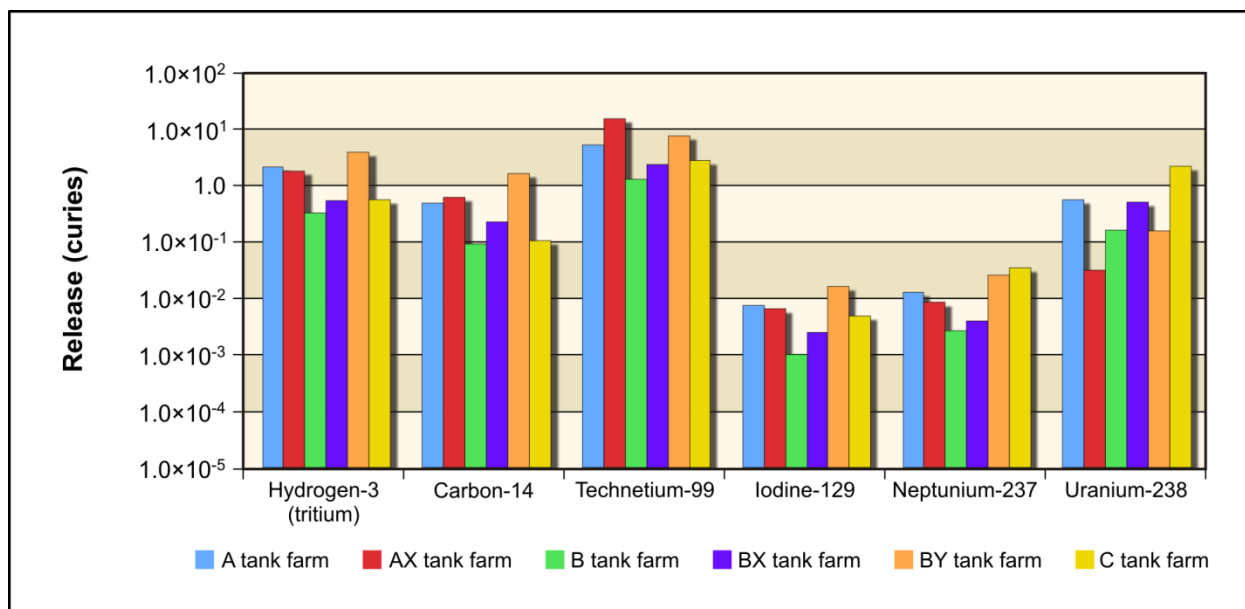
Figure M–27. Tank Closure Alternatives 2B, 3A, 3B, 3C, and 6C Radionuclide Releases to the Vadose Zone from Ancillary Equipment in Tank Farms S, SX, T, TX, TY, and U

Key: PCBs=polychlorinated biphenyls; TCP=trichlorophenol.

Figure M–28. Tank Closure Alternatives 2B, 3A, 3B, 3C, and 6C Chemical Releases to the Vadose Zone from Ancillary Equipment in Tank Farms A, AX, B, BX, BY, C, and SY

Figure M–29. Tank Closure Alternatives 2B, 3A, 3B, 3C, and 6C Chemical Releases to the Vadose Zone from Ancillary Equipment in Tank Farms AN, AP, AW, AY, and AZ

Figure M–30. Tank Closure Alternatives 2B, 3A, 3B, 3C, and 6C Chemical Releases to the Vadose Zone from Ancillary Equipment in Tank Farms S, SX, T, TX, TY, and U

Table M–23. Tank Closure Alternatives 2B, 3A, 3B, 3C, and 6C Radionuclide and Chemical Releases to the Vadose Zone from Retrieval Losses in Tank Farms

Source	Radionuclide (curies)						Chemical (kilograms)								
	H-3	C-14	Tc-99	I-129	Np-237	U-238	1-Butanol	Cr	Hg	NO$_3$	Pb	Utot	2,4,6-TCP	Benzene	PCBs
A tank farm	2.10	4.85×10^{-1}	5.06	7.38×10^{-3}	1.24×10^{-2}	5.43×10^{-1}	–	1.19×10^{2}	4.02	5.53×10^{3}	8.21×10^{1}	1.79×10^{2}	–	–	1.59×10^{-1}
AX tank farm	1.75	6.15×10^{-1}	1.48×10^{1}	6.54×10^{-3}	8.43×10^{-3}	3.15×10^{-2}	–	4.39×10^{1}	2.54	1.02×10^{5}	6.98×10^{1}	2.93×10^{1}	–	–	1.06×10^{-1}
B tank farm	3.22×10^{-1}	8.93×10^{-2}	1.26	9.81×10^{-4}	2.62×10^{-3}	1.58×10^{-1}	–	1.20×10^{2}	1.18	7.29×10^{4}	4.42×10^{1}	2.15×10^{2}	–	–	4.25×10^{-1}
BX tank farm	5.30×10^{-1}	2.23×10^{-1}	2.31	2.48×10^{-3}	3.94×10^{-3}	5.00×10^{-1}	–	2.31×10^{2}	2.71	2.89×10^{4}	4.26×10^{1}	7.25×10^{2}	–	–	3.19×10^{-1}
BY tank farm	3.78	1.59	7.46	1.57×10^{-2}	2.52×10^{-2}	1.55×10^{-1}	–	2.29×10^{2}	4.93×10^{-1}	1.55×10^{4}	1.47×10^{1}	1.95×10^{2}	–	–	3.19×10^{-1}
C tank farm	5.56×10^{-1}	1.02×10^{-1}	2.72	4.85×10^{-3}	3.42×10^{-2}	2.18	–	4.15×10^{1}	2.44	9.53×10^{4}	3.33×10^{3}	8.04×10^{2}	–	–	4.25×10^{-1}
S tank farm	4.39	1.15	6.36	1.35×10^{-2}	2.55×10^{-2}	1.31×10^{-1}	–	2.73×10^{2}	1.73×10^{-1}	2.40×10^{4}	5.05	1.35×10^{2}	–	–	3.19×10^{-1}
SX tank farm	4.33	7.71×10^{-1}	5.55	9.27×10^{-3}	1.96×10^{-2}	1.83×10^{-1}	–	4.21×10^{2}	1.20	5.35×10^{4}	7.89	2.40×10^{2}	–	–	3.99×10^{-1}
T tank farm	4.66×10^{-1}	2.97×10^{-1}	1.71	1.59×10^{-3}	4.92×10^{-3}	1.95×10^{-1}	–	1.38×10^{2}	1.37×10^{-1}	6.19×10^{4}	4.96×10^{1}	2.79×10^{2}	–	–	4.25×10^{-1}
TX tank farm	5.86	1.71	1.01×10^{1}	1.92×10^{-2}	3.56×10^{-2}	1.56×10^{-1}	–	2.05×10^{2}	2.53×10^{-1}	3.74×10^{4}	1.90×10^{1}	1.59×10^{2}	–	–	4.78×10^{-1}
TY tank farm	3.59×10^{-1}	8.03×10^{-2}	1.36	9.23×10^{-4}	2.33×10^{-3}	2.21×10^{-1}	–	7.17×10^{1}	1.57	7.84×10^{3}	1.28×10^{1}	3.23×10^{2}	–	–	1.59×10^{-1}
U tank farm	4.20	1.02	6.97	1.33×10^{-2}	2.59×10^{-2}	1.84×10^{-1}	–	1.92×10^{2}	3.32×10^{-1}	9.72×10^{4}	9.86×10^{1}	2.50×10^{2}	–	–	4.25×10^{-1}
A tank farm	1.81	8.09×10^{-1}	6.74	9.45×10^{-3}	2.20×10^{-2}	3.29×10^{-1}	–	1.62×10^{2}	1.59	1.41×10^{4}	4.02×10^{1}	1.10×10^{2}	–	–	2.17×10^{-3}

**Note:** To convert kilograms to pounds, multiply by 2.2046.

Key: 2,4,6-TCP=2,4,6-trichlorophenol; C-14=carbon-14; Cr=chromium; H-3=hydrogen-3 (tritium); Hg=mercury; I-129=iodine-129; NO$_3$=nitrate; Np-237=neptunium-237; Pb=lead; PCBs=polychlorinated biphenyls; Tc-99=technetium-99; U-238=uranium-238; Utot=total uranium.
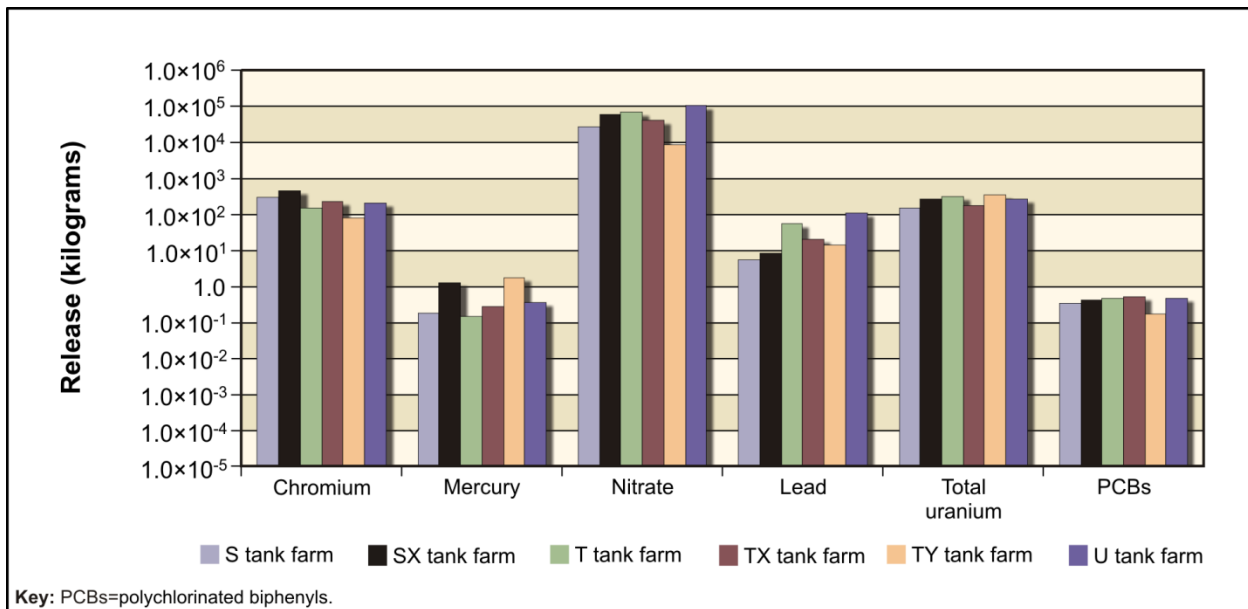
Figure M–31. Tank Closure Alternatives 2B, 3A, 3B, 3C, and 6C Radionuclide Releases to the Vadose Zone from Retrieval Losses in Tank Farms A, AX, B, BX, BY, and C
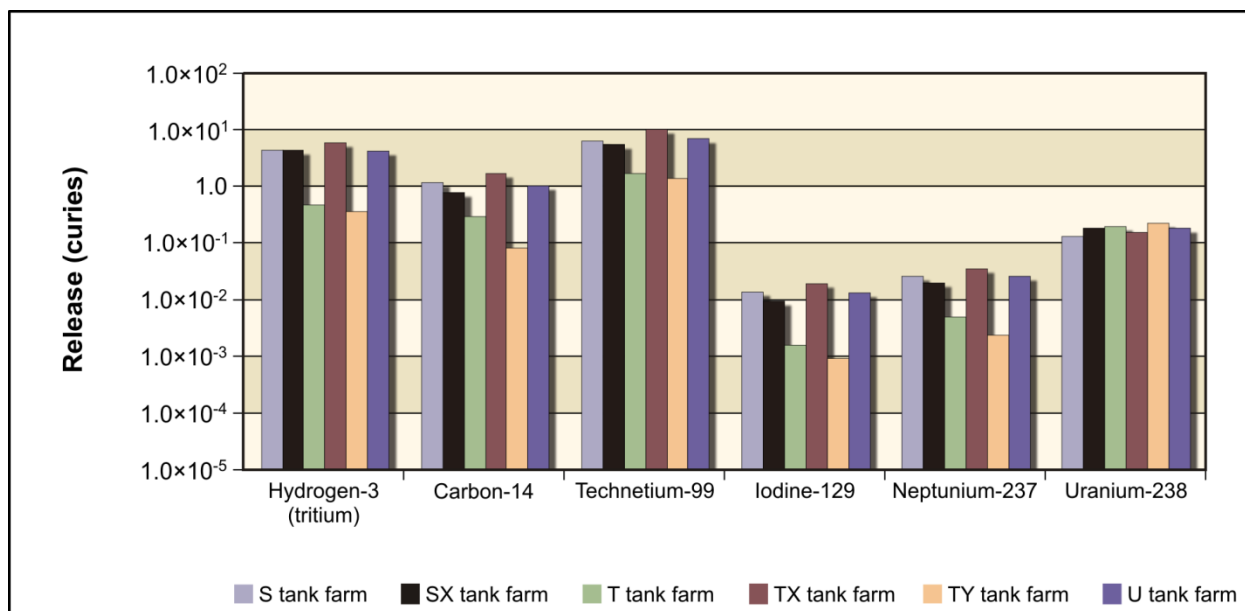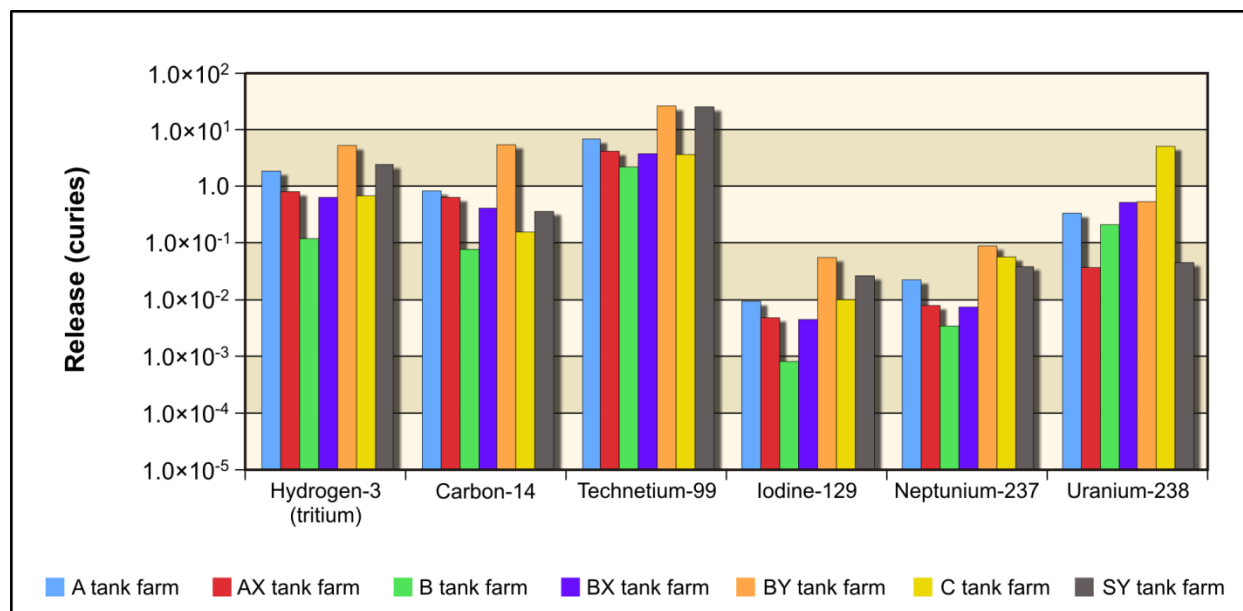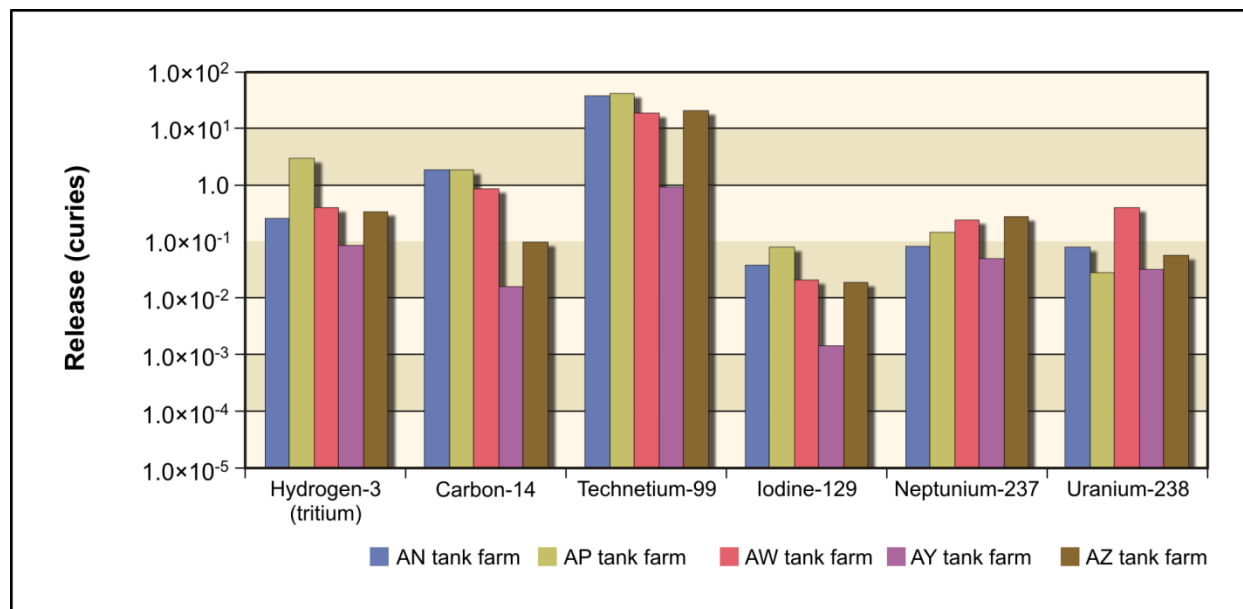

Figure M–32. Tank Closure Alternatives 2B, 3A, 3B, 3C, and 6C Radionuclide Releases to the Vadose Zone from Retrieval Losses in Tank Farms S, SX, T, TX, TY, and U
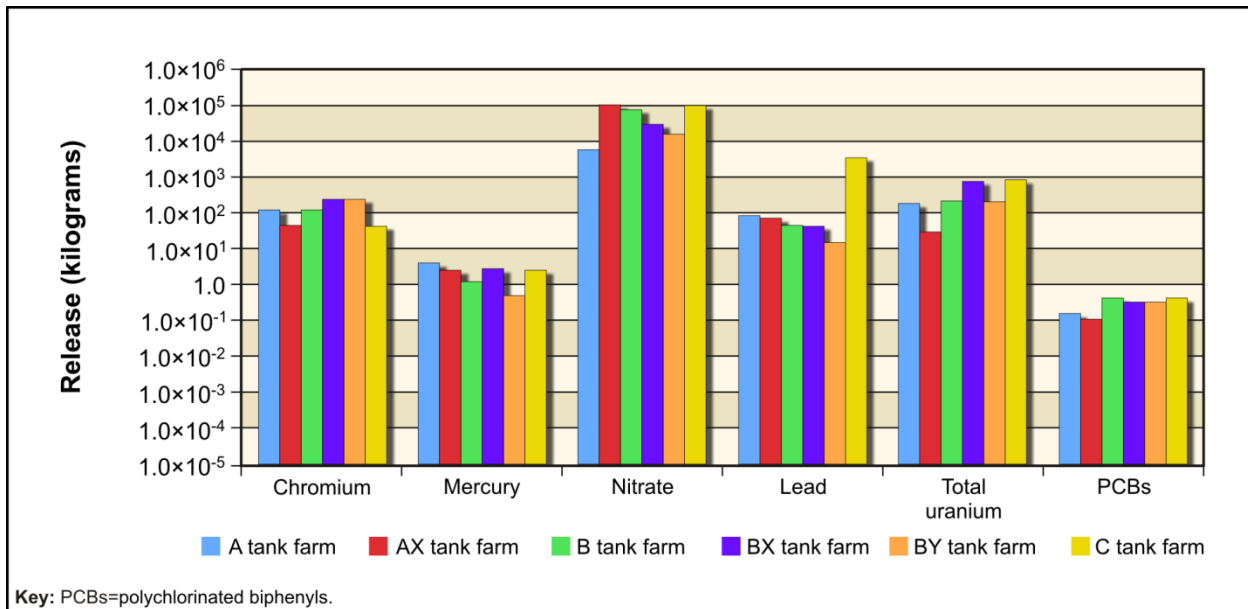
Figure M–33. Tank Closure Alternatives 2B, 3A, 3B, 3C, and 6C Chemical Releases to the Vadose Zone from Retrieval Losses in Tank Farms A, AX, B, BX, BY, and C

Figure M–34. Tank Closure Alternatives 2B, 3A, 3B, 3C, and 6C Chemical Releases to the Vadose Zone from Retrieval Losses in Tank Farms S, SX, T, TX, TY, and U

Table M–24. Tank Closure Alternatives 2B, 3A, 3B, 3C, and 6C Radionuclide and Chemical Releases to the Vadose Zone from Tank Residuals in Tank Farms

Source	Radionuclide (curies)						Chemical (kilograms)								
	H-3	C-14	Tc-99	I-129	Np-237	U-238	1-Butanol	Cr	Hg	NO₃	Pb	Utot	2,4,6-TCP	Benzene	PCBs
A tank farm	1.81	8.09×10^{-1}	6.74	9.45×10^{-3}	2.20×10^{-2}	3.29×10^{-1}	–	1.62×10^{2}	1.59	1.41×10^{4}	4.02×10^{1}	1.10×10^{2}	–	–	2.17×10^{-3}
AX tank farm	7.96×10^{-1}	6.29×10^{-1}	4.13	4.81×10^{-3}	7.83×10^{-3}	3.64×10^{-2}	–	7.87×10^{1}	4.27×10^{-1}	7.63×10^{3}	1.26×10^{1}	1.48×10^{1}	–	–	1.44×10^{-3}
B tank farm	1.17×10^{-1}	7.67×10^{-2}	2.13	8.18×10^{-4}	3.38×10^{-3}	2.08×10^{-1}	–	1.11×10^{2}	1.38	1.90×10^{4}	6.69×10^{1}	2.86×10^{2}	–	–	4.42×10^{-3}
BX tank farm	6.32×10^{-1}	4.10×10^{-1}	3.70	4.49×10^{-3}	7.42×10^{-3}	5.09×10^{-1}	–	2.20×10^{2}	2.27	1.73×10^{4}	3.66×10^{1}	7.35×10^{2}	–	–	4.33×10^{-3}
BY tank farm	5.14	5.37	2.54×10^{1}	5.55×10^{-2}	8.59×10^{-2}	5.22×10^{-1}	–	7.34×10^{2}	1.74	6.62×10^{4}	5.12×10^{1}	6.55×10^{2}	–	–	4.34×10^{-3}
C tank farm	6.64×10^{-1}	1.54×10^{-1}	3.51	9.93×10^{-3}	5.72×10^{-2}	4.98	–	5.60×10^{1}	3.93	6.56×10^{3}	2.32×10^{2}	1.13×10^{3}	–	–	4.41×10^{-3}
S tank farm	6.49	4.82	2.74×10^{1}	5.93×10^{-2}	1.12×10^{-1}	5.18×10^{-1}	–	1.20×10^{3}	7.15×10^{-1}	1.10×10^{5}	2.23×10^{1}	5.19×10^{2}	–	–	4.34×10^{-3}
SX tank farm	6.42	2.80	1.76×10^{1}	3.35×10^{-2}	6.71×10^{-2}	2.95×10^{-1}	–	1.05×10^{3}	1.46	6.62×10^{4}	1.75×10^{1}	3.27×10^{2}	–	–	5.42×10^{-3}
T tank farm	2.02×10^{-1}	1.44×10^{-1}	1.63	1.14×10^{-3}	2.78×10^{-3}	2.59×10^{-1}	–	1.21×10^{2}	1.99×10^{-1}	7.47×10^{3}	4.34×10^{1}	3.72×10^{2}	–	–	4.41×10^{-3}
TX tank farm	8.05	6.20	3.76×10^{1}	7.15×10^{-2}	1.32×10^{-1}	4.79×10^{-1}	–	6.13×10^{2}	2.83×10^{-1}	1.40×10^{5}	7.12×10^{1}	4.56×10^{2}	–	–	6.53×10^{-3}
TY tank farm	2.36×10^{-1}	7.49×10^{-2}	1.02	1.29×10^{-3}	2.28×10^{-3}	2.23×10^{-1}	–	7.95×10^{1}	2.56	8.37×10^{3}	1.39×10^{1}	3.24×10^{2}	–	–	2.15×10^{-3}
U tank farm	6.55	3.43	2.43×10^{1}	4.69×10^{-2}	8.94×10^{-2}	3.90×10^{-1}	–	5.11×10^{2}	2.55×10^{-1}	5.46×10^{4}	1.08×10^{2}	4.97×10^{2}	–	–	4.42×10^{-3}
AN tank farm	2.54×10^{-1}	1.81	3.68×10^{1}	3.80×10^{-2}	8.17×10^{-2}	7.88×10^{-2}	8.59×10^{3}	1.85×10^{2}	4.66×10^{-2}	6.47×10^{4}	3.53×10^{1}	2.68×10^{1}	2.75×10^{-3}	5.97×10^{-3}	3.53×10^{-3}
AP tank farm	2.94	1.84	4.07×10^{1}	7.91×10^{-2}	1.43×10^{-1}	2.85×10^{-2}	1.13×10^{4}	1.03×10^{2}	–	5.65×10^{4}	8.62	1.23×10^{1}	3.62×10^{-3}	7.85×10^{-3}	4.02×10^{-3}
AW tank farm	3.96×10^{-1}	8.43×10^{-1}	1.86×10^{1}	2.11×10^{-2}	2.39×10^{-1}	3.93×10^{-1}	6.63×10^{3}	1.99×10^{2}	2.09×10^{-3}	3.47×10^{4}	1.48×10^{1}	3.95×10^{2}	2.13×10^{-3}	4.62×10^{-3}	3.02×10^{-3}
AY tank farm	8.33×10^{-2}	1.57×10^{-2}	8.93×10^{-1}	1.42×10^{-3}	5.03×10^{-2}	3.20×10^{-2}	1.32×10^{3}	2.79×10^{1}	1.26	1.70×10^{3}	4.47×10^{1}	3.52×10^{1}	4.23×10^{-4}	9.19×10^{-4}	1.01×10^{-3}
AZ tank farm	3.37×10^{-1}	9.70×10^{-2}	2.04×10^{1}	1.89×10^{-2}	2.70×10^{-1}	5.66×10^{-2}	3.06×10^{3}	5.09×10^{1}	4.15×10^{-2}	7.74×10^{3}	3.81	5.18×10^{1}	9.81×10^{-4}	2.13×10^{-3}	1.01×10^{-3}
SY tank farm	2.36	3.58×10^{-1}	2.46×10^{1}	2.65×10^{-2}	3.80×10^{-2}	4.50×10^{-2}	3.64×10^{3}	4.73×10^{2}	8.95×10^{-2}	2.48×10^{4}	1.53×10^{1}	2.38×10^{1}	1.17×10^{-3}	2.53×10^{-3}	1.51×10^{-3}

Note: To convert kilograms to pounds, multiply by 2.2046.

Key: 2,4,6-TCP=2,4,6-trichlorophenol; C-14=carbon-14; Cr=chromium; H-3=hydrogen-3 (tritium); Hg=mercury; I-129=iodine-129; NO₃=nitrate; Np-237=neptunium-237; Pb=lead; PCBs=polychlorinated biphenyls; Tc-99=technetium-99; U-238=uranium-238; Utot=total uranium.
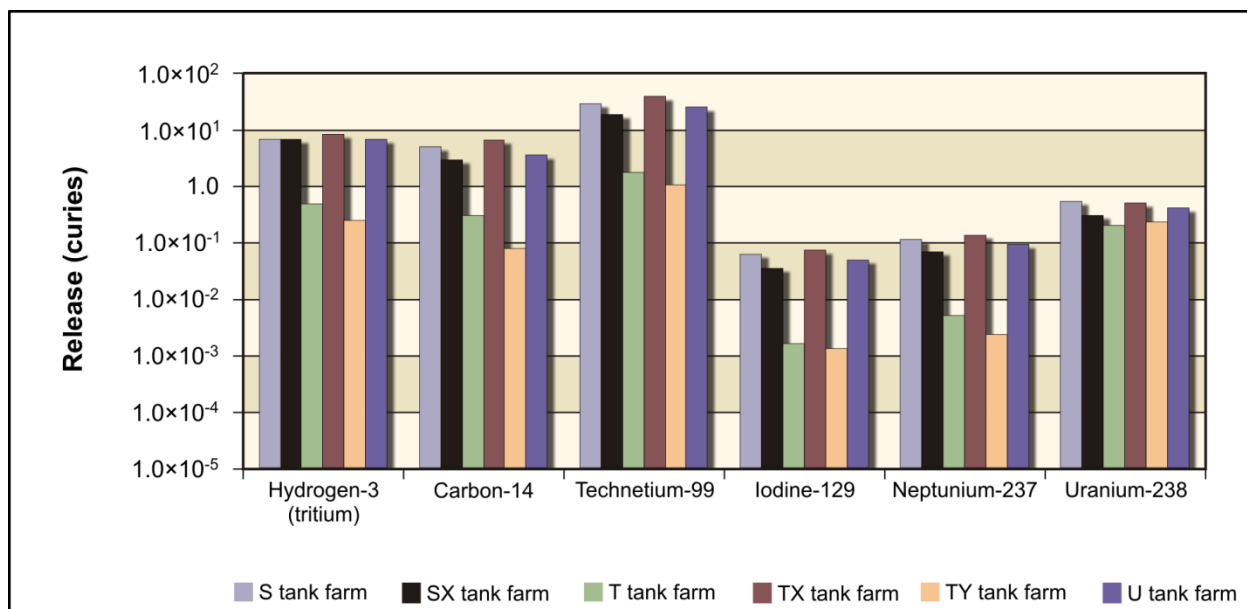
Figure M–35. Tank Closure Alternatives 2B, 3A, 3B, 3C, and 6C Radionuclide Releases to the Vadose Zone from Tank Residuals in Tank Farms A, AX, B, BX, BY, C, and SY
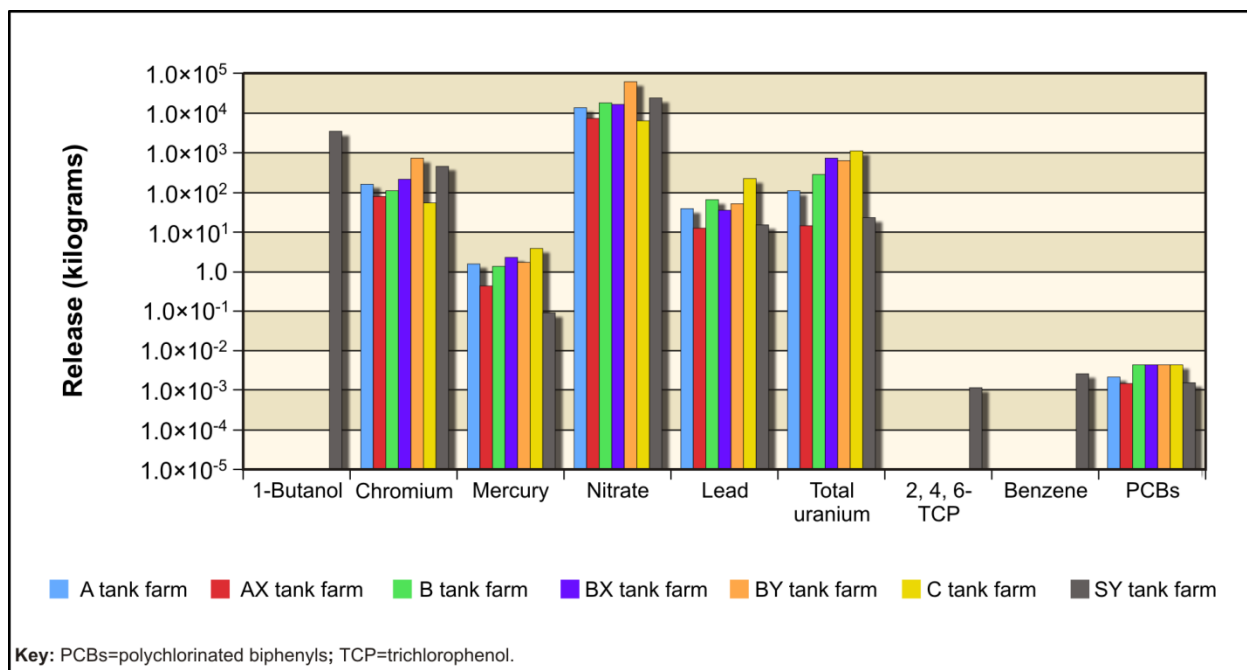

Figure M–36. Tank Closure Alternatives 2B, 3A, 3B, 3C, and 6C Radionuclide Releases to the Vadose Zone from Tank Residuals in Tank Farms AN, AP, AW, AY, and AZ
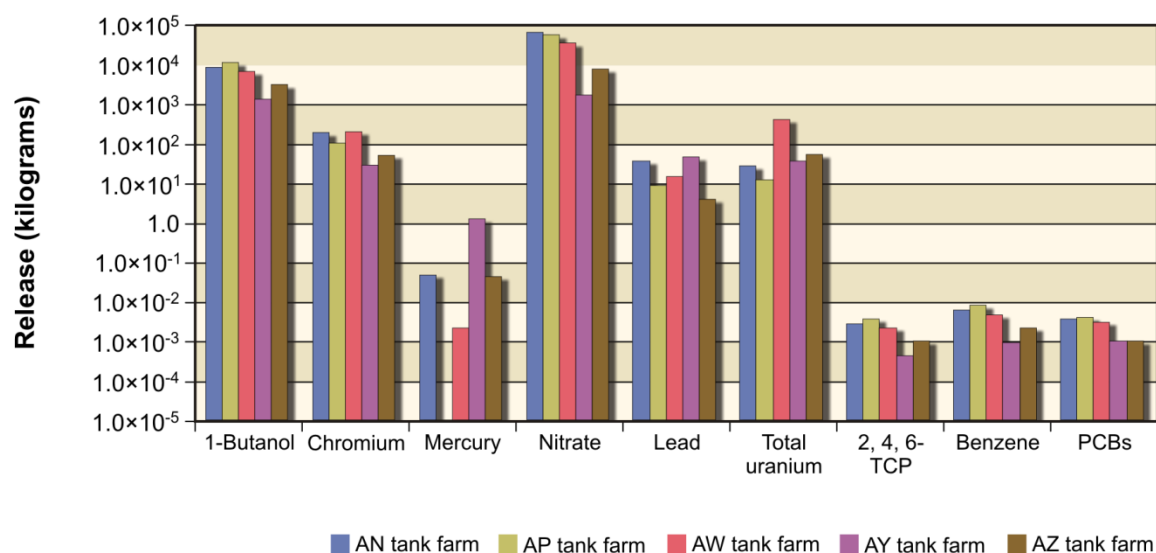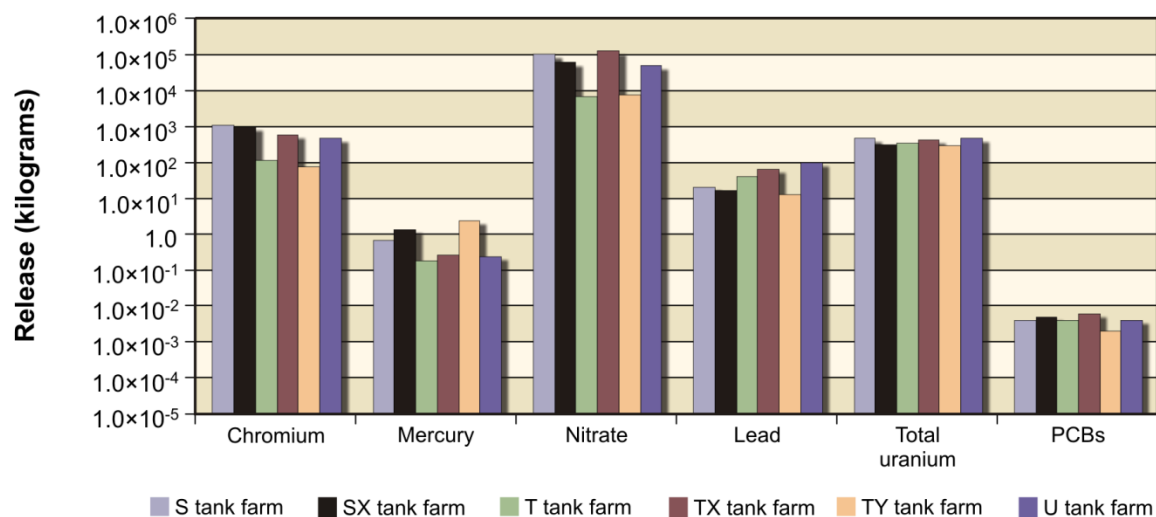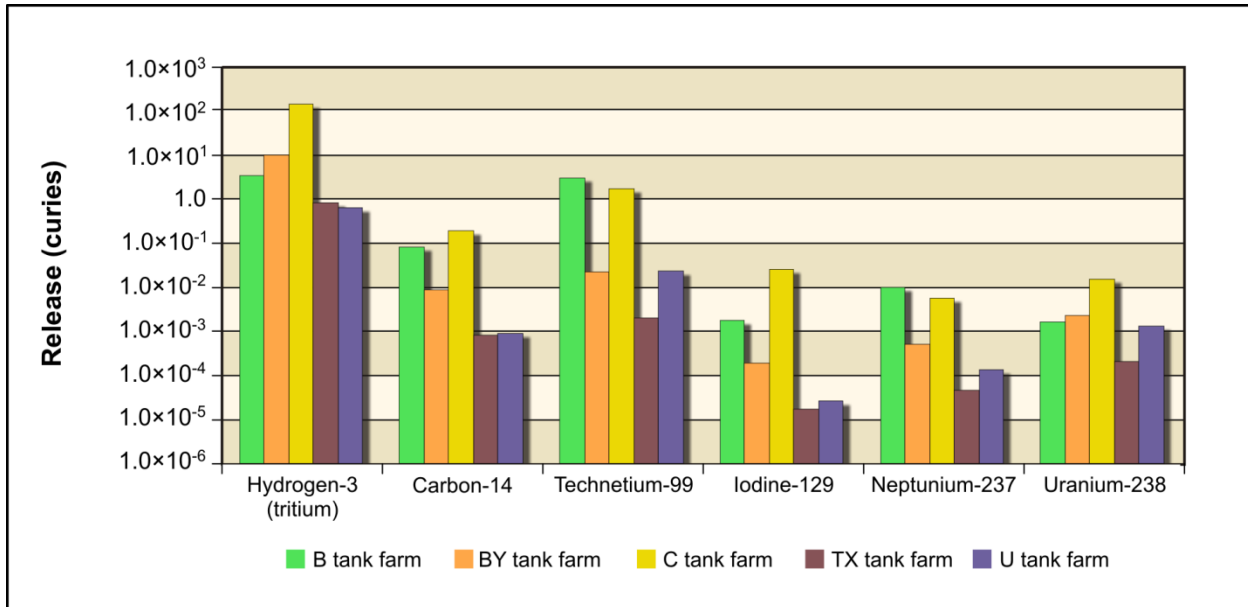
Figure M–37. Tank Closure Alternatives 2B, 3A, 3B, 3C, and 6C Radionuclide Releases to the Vadose Zone from Tank Residuals in Tank Farms S, SX, T, TX, TY, and U

Figure M–38. Tank Closure Alternatives 2B, 3A, 3B, 3C, and 6C Chemical Releases to the Vadose Zone from Tank Residuals in Tank Farms A, AX, B, BX, BY, C, and SY

Figure M–39. Tank Closure Alternatives 2B, 3A, 3B, 3C, and 6C Chemical Releases to the Vadose Zone from Tank Residuals in Tank Farms AN, AP, AW, AY, and AZ

Figure M–40. Tank Closure Alternatives 2B, 3A, 3B, 3C, and 6C Chemical Releases to the Vadose Zone from Tank Residuals in Tank Farms S, SX, T, TX, TY, and U

Table M–25. Tank Closure Alternatives 2B, 3A, 3B, 3C, and 6C Radionuclide and Chemical Releases to the Vadose Zone from Unplanned Releases in Tank Farms B, BY, C, TX, and U

Source	Radionuclide (curies)						Chemical (kilograms)								
	H-3	C-14	Tc-99	I-129	Np-237	U-238	1-Butanol	Cr	Hg	NO$_3$	Pb	Utot	2,4,6-TCP	Benzene	PCBs
B tank farm	3.34	7.87×10^{-2}	2.96	1.76×10^{-3}	9.69×10^{-3}	1.57×10^{-3}	3.86×10^{-4}	3.53×10^{1}	8.41×10^{-3}	3.24×10^{3}	2.07	1.81	–	–	–
BY tank farm	9.86	8.65×10^{-3}	2.15×10^{-2}	1.88×10^{-4}	4.95×10^{-4}	2.22×10^{-3}	–	3.81×10^{1}	3.44×10^{-2}	1.17×10^{4}	–	3.30	–	–	–
C tank farm	1.39×10^{2}	1.90×10^{-1}	1.67	2.48×10^{-2}	5.58×10^{-3}	1.49×10^{-2}	6.47×10^{-1}	3.94×10^{1}	3.92×10^{-3}	9.68×10^{3}	2.16×10^{1}	3.47×10^{1}	–	–	–
TX tank farm	8.21×10^{-1}	7.88×10^{-4}	2.01×10^{-3}	1.71×10^{-5}	4.52×10^{-5}	2.02×10^{-4}	1.15×10^{-5}	3.47	3.13×10^{-3}	1.06×10^{3}	–	3.00×10^{-1}	–	–	–
U tank farm	6.36×10^{-1}	8.63×10^{-4}	2.27×10^{-2}	2.53×10^{-5}	1.30×10^{-4}	1.31×10^{-3}	–	3.76×10^{-1}	6.14×10^{-4}	2.59×10^{1}	–	1.93	–	–	–

Note: To convert kilograms to pounds, multiply by 2.2046.

Key: 2,4,6-TCP=2,4,6-trichlorophenol; C-14=carbon-14; Cr=chromium; H-3=hydrogen-3 (tritium); Hg=mercury; I-129=iodine-129; NO$_3$=nitrate; Np-237=neptunium-237; Pb=lead; PCBs=polychlorinated biphenyls; Tc-99=technetium-99; U-238=uranium-238; Utot=total uranium.

Figure M–41. Tank Closure Alternatives 2B, 3A, 3B, 3C, and 6C Radionuclide Releases to the Vadose Zone from Unplanned Releases in Tank Farms B, BY, C, TX, and U
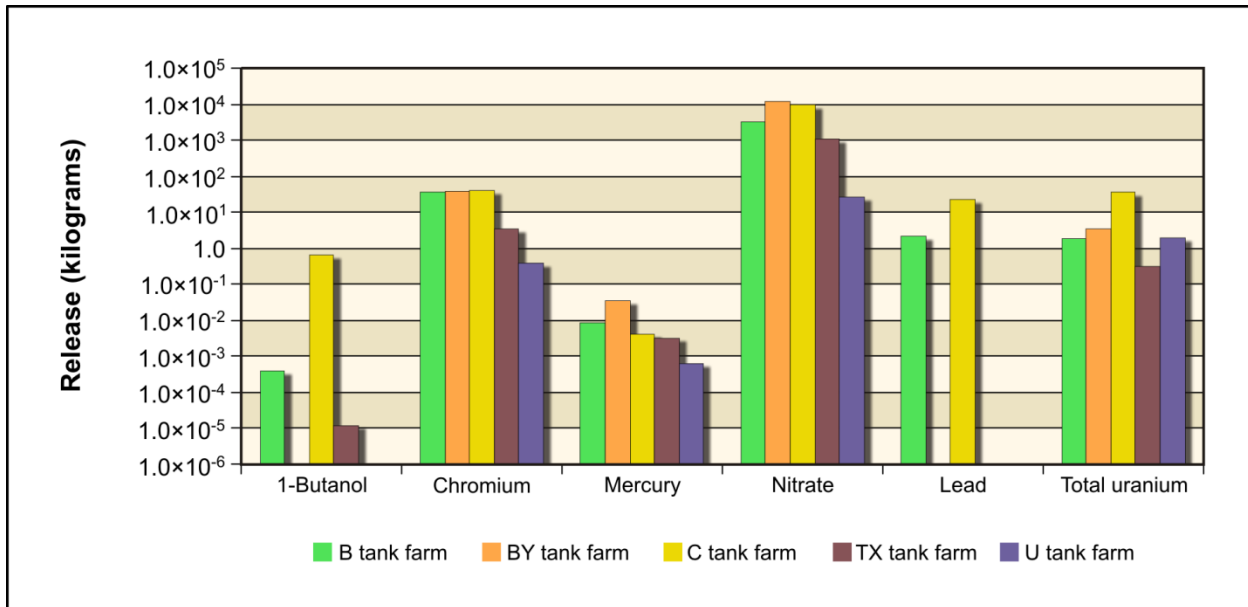
Figure M–42. Tank Closure Alternatives 2B, 3A, 3B, 3C, and 6C Chemical Releases to the Vadose Zone from Unplanned Releases in Tank Farms B, BY, C, TX, and U

Under Tank Closure Alternative 4, tank waste would be retrieved to a volume corresponding to 99.9 percent retrieval. Except for the BX and SX tank farms, residual material in tanks would be stabilized in place, and the tank farms and adjacent cribs and trenches (ditches) would be covered with an engineered modified RCRA Subtitle C barrier. The BX and SX tank farms would be closed to a clean state by removing the tanks, ancillary equipment, and soils to a depth of 3 meters (10 feet) below the tank base. Where necessary, deep soil excavation would also be conducted to remove contamination plumes within the soil column. Potential releases to the vadose zone under Tank Closure Alternative 4 are indicated in Table M–26 and Figures M–43 through M–48.

Table M–26. Tank Closure Alternative 4 Radionuclide and Chemical Releases to the Vadose Zone from Other Sources in Tank Farms

Source	Radionuclide (curies)						Chemical (kilograms)								
	H-3	C-14	Tc-99	I-129	Np-237	U-238	1-Butanol	Cr	Hg	NO$_3$	Pb	Utot	2,4,6-TCP	Benzene	PCBs
A tank farm	3.58	9.69×10^{-1}	9.02	1.29×10^{-2}	2.53×10^{-2}	7.37×10^{-1}	–	2.15×10^{2}	4.96	1.38×10^{4}	1.06×10^{2}	2.44×10^{2}	–	–	1.63×10^{-1}
AX tank farm	2.47	1.11	1.80×10^{1}	1.03×10^{-2}	1.45×10^{-2}	5.96×10^{-2}	–	1.05×10^{2}	2.87	1.08×10^{5}	7.96×10^{1}	4.08×10^{1}	–	–	1.09×10^{-1}
B tank farm	3.79	2.25×10^{-1}	5.79	3.34×10^{-3}	1.48×10^{-2}	3.12×10^{-1}	3.86×10^{-4}	2.47×10^{2}	2.34	9.19×10^{4}	1.02×10^{2}	4.54×10^{2}	–	–	4.36×10^{-1}
BY tank farm	1.74×10^{1}	3.63	1.69×10^{1}	3.63×10^{-2}	5.74×10^{-2}	3.49×10^{-1}	–	5.38×10^{2}	1.17	5.16×10^{4}	3.35×10^{1}	4.40×10^{2}	–	–	3.28×10^{-1}
C tank farm	1.40×10^{2}	4.40×10^{-1}	7.72	3.91×10^{-2}	9.41×10^{-2}	6.92	6.47×10^{-1}	1.34×10^{2}	6.18	1.11×10^{5}	3.57×10^{3}	1.91×10^{3}	–	–	4.35×10^{-1}
S tank farm	9.05	2.71	1.50×10^{1}	3.21×10^{-2}	6.07×10^{-2}	2.94×10^{-1}	–	6.51×10^{2}	3.98×10^{-1}	5.87×10^{4}	1.21×10^{1}	2.98×10^{2}	–	–	3.28×10^{-1}
T tank farm	6.97×10^{-1}	4.30×10^{-1}	3.18	2.62×10^{-3}	7.44×10^{-3}	4.30×10^{-1}	–	2.47×10^{2}	3.17×10^{-1}	6.87×10^{4}	8.88×10^{1}	6.15×10^{2}	–	–	4.36×10^{-1}
TX tank farm	1.27×10^{1}	4.00	2.36×10^{1}	4.49×10^{-2}	8.29×10^{-2}	3.28×10^{-1}	1.15×10^{-5}	4.29×10^{2}	3.58×10^{-1}	8.88×10^{4}	4.45×10^{1}	3.23×10^{2}	–	–	4.93×10^{-1}
TY tank farm	6.12×10^{-1}	1.54×10^{-1}	2.37	2.19×10^{-3}	4.58×10^{-3}	4.40×10^{-1}	–	1.50×10^{2}	4.09	1.61×10^{4}	2.65×10^{1}	6.41×10^{2}	–	–	1.63×10^{-1}
U tank farm	1.10×10^{1}	3.00	2.07×10^{1}	3.98×10^{-2}	7.66×10^{-2}	4.05×10^{-1}	–	4.81×10^{2}	4.77×10^{-1}	1.28×10^{5}	1.60×10^{2}	5.33×10^{2}	–	–	4.36×10^{-1}
AN tank farm	1.13×10^{-1}	2.42×10^{-1}	4.68	4.84×10^{-3}	1.04×10^{-2}	1.00×10^{-2}	1.09×10^{3}	2.35×10^{1}	5.92×10^{-3}	8.22×10^{3}	4.62	3.41	3.50×10^{-4}	7.59×10^{-4}	5.06×10^{-3}
AP tank farm	1.33	2.40×10^{-1}	5.03	9.50×10^{-3}	1.77×10^{-2}	3.52×10^{-3}	1.40×10^{3}	1.27×10^{1}	–	6.98×10^{3}	1.11	1.52	4.47×10^{-4}	9.70×10^{-4}	4.88×10^{-3}
AW tank farm	1.54×10^{-1}	1.14×10^{-1}	2.42	2.74×10^{-3}	3.11×10^{-2}	5.11×10^{-2}	8.63×10^{2}	2.59×10^{1}	2.72×10^{-4}	4.51×10^{3}	1.97	5.14×10^{1}	2.77×10^{-4}	6.01×10^{-4}	3.32×10^{-3}
AY tank farm	2.37×10^{-2}	2.43×10^{-3}	1.34×10^{-1}	2.13×10^{-4}	7.57×10^{-3}	4.81×10^{-3}	1.99×10^{2}	4.20	1.90×10^{-1}	2.56×10^{2}	6.71	5.29	6.36×10^{-5}	1.38×10^{-4}	1.02×10^{-3}
AZ tank farm	1.49×10^{-1}	1.24×10^{-2}	2.48	2.33×10^{-3}	3.29×10^{-2}	6.90×10^{-3}	3.73×10^{2}	6.20	5.05×10^{-3}	9.42×10^{2}	4.91×10^{-1}	6.32	1.19×10^{-4}	2.59×10^{-4}	1.10×10^{-3}
SY tank farm	1.02	4.78×10^{-2}	3.13	3.39×10^{-3}	4.84×10^{-3}	5.73×10^{-3}	4.64×10^{2}	6.03×10^{1}	1.14×10^{-2}	3.16×10^{3}	2.00	3.03	1.49×10^{-4}	3.23×10^{-4}	1.89×10^{-3}

**Note:** To convert kilograms to pounds, multiply by 2.2046.

Key: 2,4,6-TCP=2,4,6-trichlorophenol; C-14=carbon-14; Cr=chromium; H-3=hydrogen-3 (tritium); Hg=mercury; I-129=iodine-129; NO$_3$=nitrate; Np-237=neptunium-237; Pb=lead; PCBs=polychlorinated biphenyls; Tc-99=technetium-99; U-238=uranium-238; Utot=total uranium.
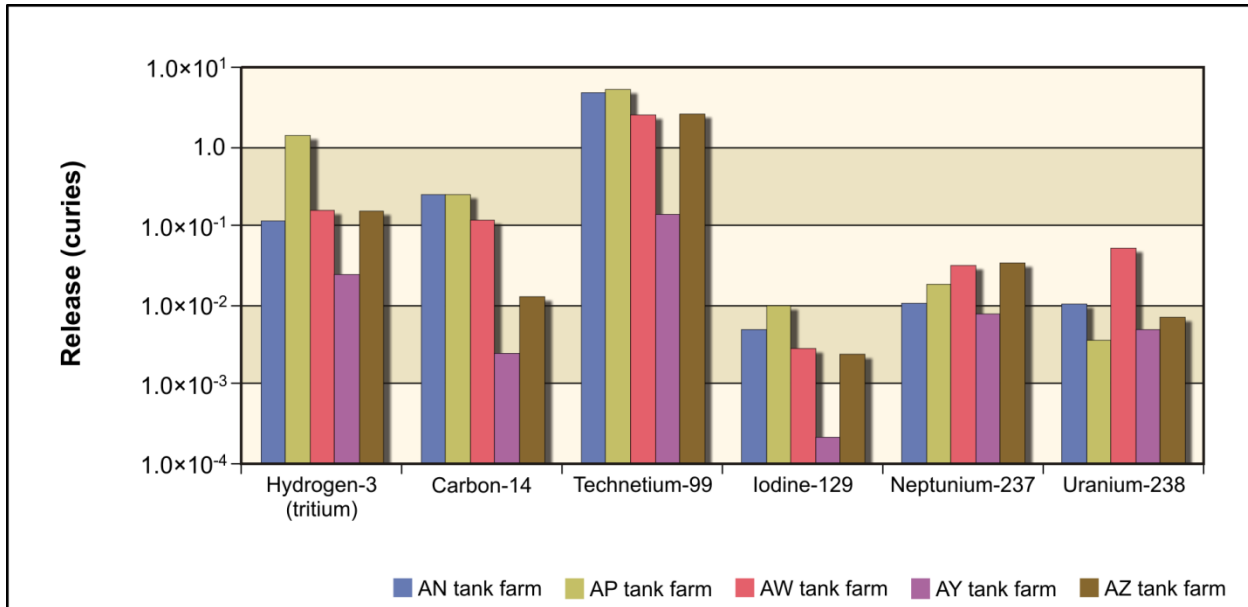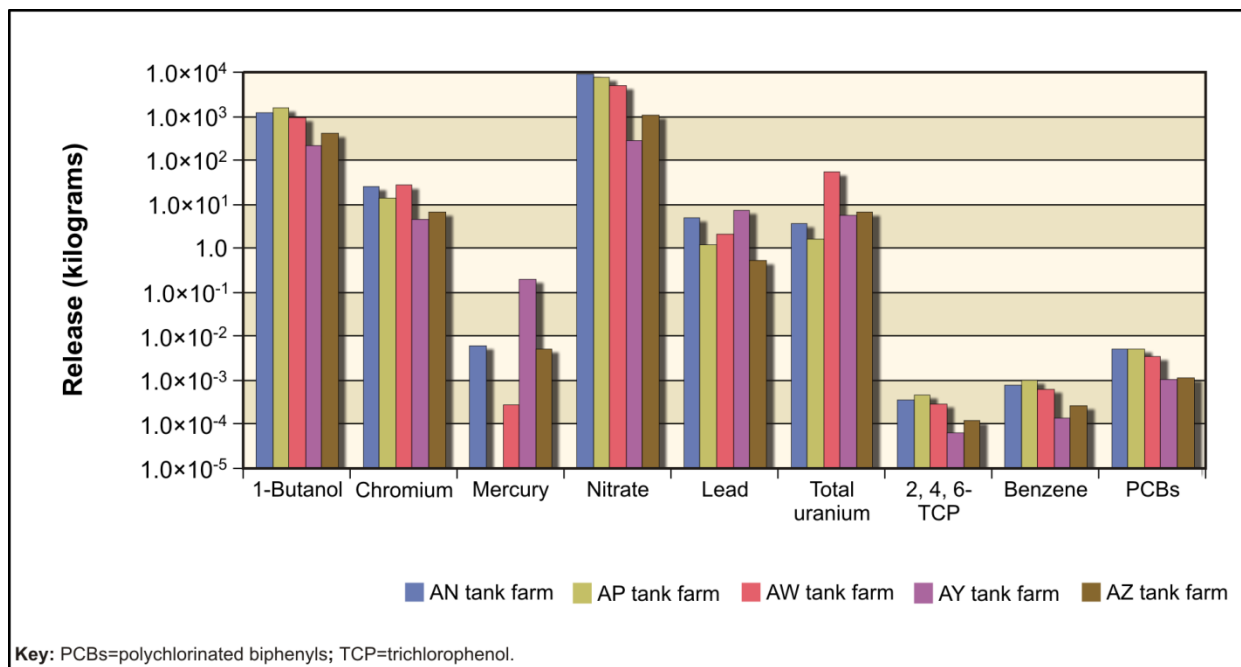
**Figure M–43. Tank Closure Alternative 4 Radionuclide Releases to the Vadose Zone from
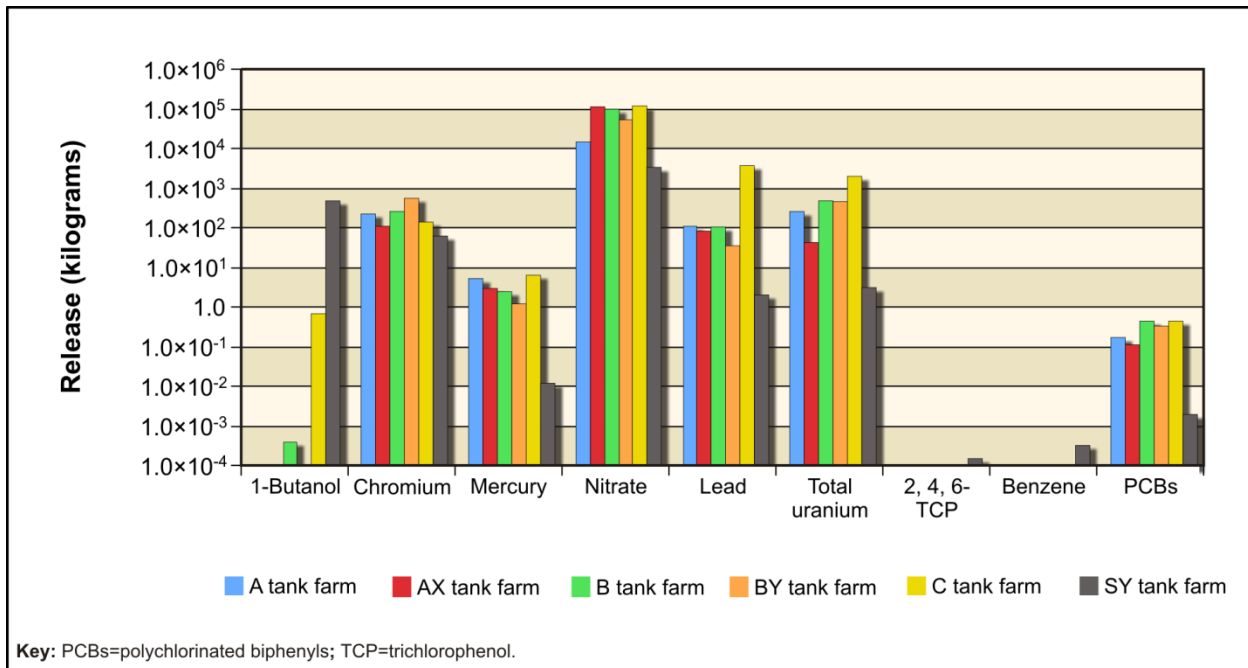Other Sources in Tank Farms AN, AP, AW, AY, and AZ**
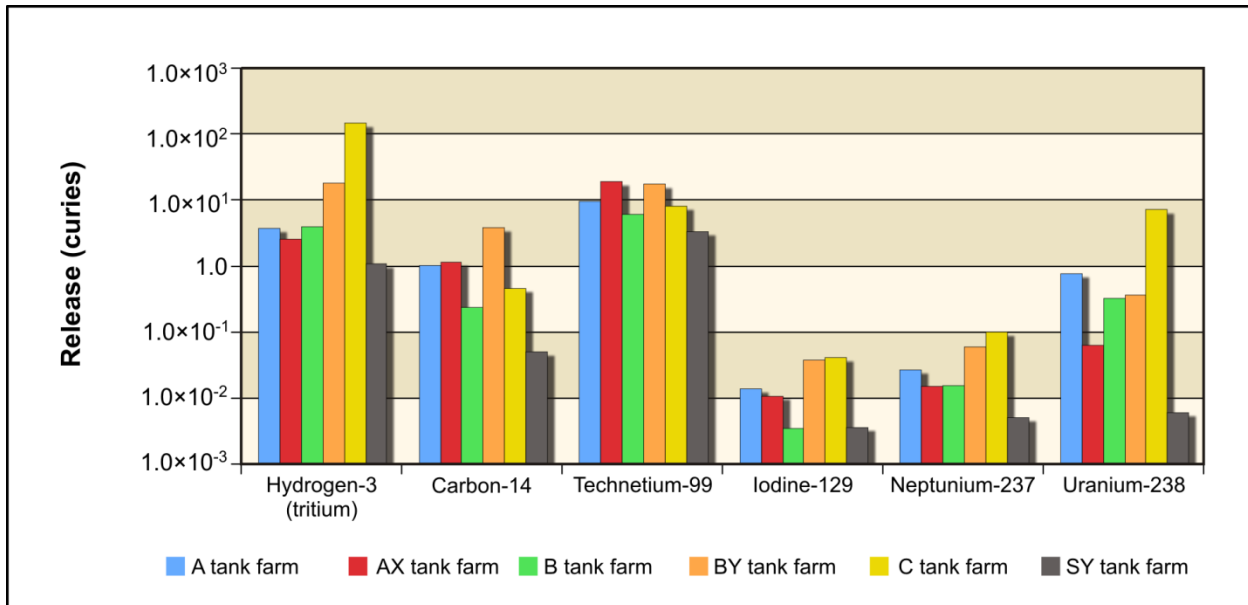
**Figure M–44. Tank Closure Alternative 4 Radionuclide Releases to the Vadose Zone from
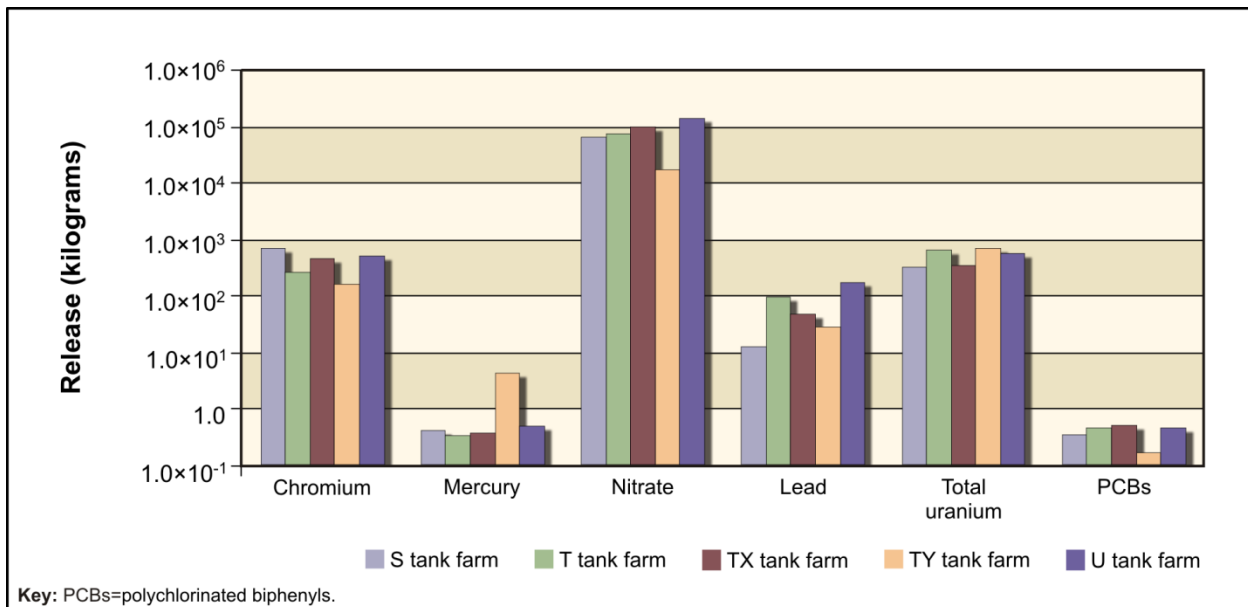Other Sources in Tank Farms A, AX, B, BY, C and SY**
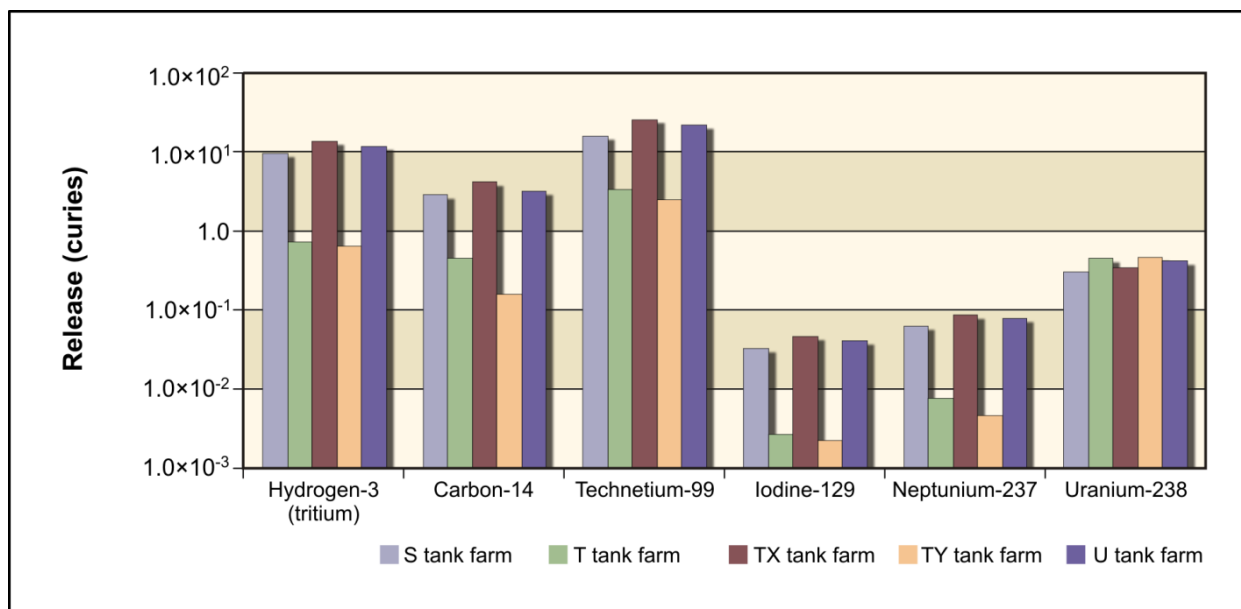
Figure M–45. Tank Closure Alternative 4 Radionuclide Releases to the Vadose Zone from Other Sources in Tank Farms S, T, TX, TY, and U

Figure M–46. Tank Closure Alternative 4 Chemical Releases to the Vadose Zone from Other Sources in Tank Farms AN, AP, AW, AY, and AZ

Figure M–47. Tank Closure Alternative 4 Chemical Releases to the Vadose Zone from Other Sources in Tank Farms A, AX, B, BY, C, and SY

Figure M–48. Tank Closure Alternative 4 Chemical Releases to the Vadose Zone from Other Sources in Tank Farms S, T, TX, TY, and U

Under Tank Closure Alternative 5, tank waste would be retrieved to a volume corresponding to 90 percent retrieval, residual material in tanks would be stabilized in place, and the tank farms and adjacent cribs and trenches (ditches) would be covered with a Hanford barrier. Potential releases to the vadose zone under Tank Closure Alternative 5 are indicated in Table M–27 and Figures M–49 through M–54.

Table M–27. Tank Closure Alternative 5 Radionuclide and Chemical Releases to the Vadose Zone from Other Sources in Tank Farms

Source	Radionuclide (curies)						Chemical (kilograms)								
	H-3	C-14	Tc-99	I-129	Np-237	U-238	1-Butanol	Cr	Hg	NO$_3$	Pb	Utot	2,4,6-TCP	Benzene	PCBs
A tank farm	6.83	8.19	7.59×10^1	9.73×10^{-2}	2.44×10^{-1}	3.88	–	1.82×10^3	2.07×10^1	1.54×10^5	4.10×10^2	1.30×10^3	–	–	1.63×10^{-1}
AX tank farm	4.16	6.80	5.90×10^1	5.61×10^{-2}	9.24×10^{-2}	4.18×10^{-1}	–	8.87×10^2	7.12	1.84×10^5	1.88×10^2	1.86×10^2	–	–	1.09×10^{-1}
B tank farm	6.78×10^{-1}	8.44×10^{-1}	2.42×10^1	9.21×10^{-3}	3.91×10^{-2}	2.35	–	1.32×10^3	1.61×10^1	2.78×10^5	6.36×10^2	3.23×10^3	–	–	4.36×10^{-1}
BX tank farm	2.54	4.28	4.20×10^1	4.92×10^{-2}	8.38×10^{-2}	5.94	–	2.60×10^3	2.71×10^1	2.15×10^5	3.91×10^2	8.57×10^3	–	–	3.28×10^{-1}
BY tank farm	2.43×10^1	5.00×10^1	2.68×10^2	4.30×10^{-1}	8.95×10^{-1}	4.67	–	7.82×10^3	1.84×10^1	7.08×10^5	3.09×10^2	5.86×10^3	–	–	3.28×10^{-1}
C tank farm	1.42×10^2	1.83	4.26×10^1	1.33×10^{-1}	6.64×10^{-1}	5.59×10^1	6.47×10^{-1}	6.92×10^2	4.53×10^1	1.77×10^5	5.54×10^3	1.31×10^4	–	–	4.35×10^{-1}
S tank farm	1.69×10^1	4.35×10^1	2.86×10^2	4.04×10^{-1}	1.13	4.20	–	1.25×10^4	7.44	1.15×10^6	1.15×10^2	4.21×10^3	–	–	3.28×10^{-1}
SX tank farm	1.99×10^1	2.70×10^1	1.89×10^2	3.09×10^{-1}	7.17×10^{-1}	3.06	–	1.14×10^4	1.64×10^1	7.44×10^5	1.37×10^2	3.43×10^3	–	–	4.11×10^{-1}
T tank farm	1.11	1.73	1.94×10^1	1.34×10^{-2}	3.51×10^{-2}	2.97	–	1.45×10^3	2.30	1.43×10^5	4.51×10^2	4.26×10^3	–	–	4.36×10^{-1}
TX tank farm	2.34×10^1	5.73×10^1	3.96×10^2	5.43×10^{-1}	1.36	4.24	1.15×10^{-5}	6.51×10^3	3.15	1.48×10^6	4.19×10^2	4.05×10^3	–	–	4.93×10^{-1}
TY tank farm	1.20	8.39×10^{-1}	1.25×10^1	1.48×10^{-2}	2.73×10^{-2}	2.65	–	9.42×10^2	2.96×10^1	9.94×10^4	1.55×10^2	3.86×10^3	–	–	1.63×10^{-1}
U tank farm	2.11×10^1	3.32×10^1	2.61×10^2	4.18×10^{-1}	9.60×10^{-1}	3.92	–	5.56×10^3	3.01	6.70×10^5	8.55×10^2	5.02×10^3	–	–	4.36×10^{-1}
AN tank farm	3.72×10^{-1}	1.45×10^1	3.69×10^2	1.63×10^{-1}	6.87×10^{-1}	4.33×10^{-1}	8.64×10^4	1.86×10^3	4.37×10^{-1}	6.51×10^5	1.08×10^2	1.48×10^2	2.77×10^{-2}	6.01×10^{-2}	6.64×10^{-3}
AP tank farm	4.11	1.44×10^1	4.07×10^2	2.96×10^{-1}	1.14	1.42×10^{-1}	1.14×10^5	1.04×10^3	–	5.68×10^5	2.38×10^1	6.14×10^1	3.64×10^{-2}	7.89×10^{-2}	5.70×10^{-3}
AW tank farm	5.59×10^{-1}	6.88	1.86×10^2	9.78×10^{-2}	2.09	2.31	6.67×10^4	2.00×10^3	1.99×10^{-2}	3.49×10^5	4.90×10^1	2.32×10^3	2.14×10^{-2}	4.65×10^{-2}	3.55×10^{-3}
AY tank farm	1.27×10^{-1}	1.37×10^{-1}	9.01	9.25×10^{-3}	4.91×10^{-1}	2.49×10^{-1}	1.33×10^4	2.82×10^2	1.26×10^1	1.72×10^4	2.17×10^2	2.74×10^2	4.28×10^{-3}	9.29×10^{-3}	1.03×10^{-3}
AZ tank farm	4.47×10^{-1}	7.48×10^{-1}	2.04×10^2	6.90×10^{-2}	2.07	2.68×10^{-1}	3.07×10^4	5.11×10^2	3.69×10^{-1}	7.78×10^4	9.92	2.44×10^2	9.86×10^{-3}	2.14×10^{-2}	1.18×10^{-3}
SY tank farm	3.42	2.88	2.46×10^2	1.15×10^{-1}	3.21×10^{-1}	2.49×10^{-1}	3.66×10^4	4.76×10^3	8.41×10^{-1}	2.49×10^5	4.71×10^1	1.31×10^2	1.18×10^{-2}	2.55×10^{-2}	2.26×10^{-3}

**Note:** To convert kilograms to pounds, multiply by 2.2046.

Key: 2,4,6-TCP=2,4,6-trichlorophenol; C-14=carbon-14; Cr=chromium; H-3=hydrogen-3 (tritium); Hg=mercury; I-129=iodine-129; NO$_3$=nitrate; Np-237=neptunium-237; Pb=lead; PCBs=polychlorinated biphenyls; Tc-99=technetium-99; U-238=uranium-238; Utot=total uranium.
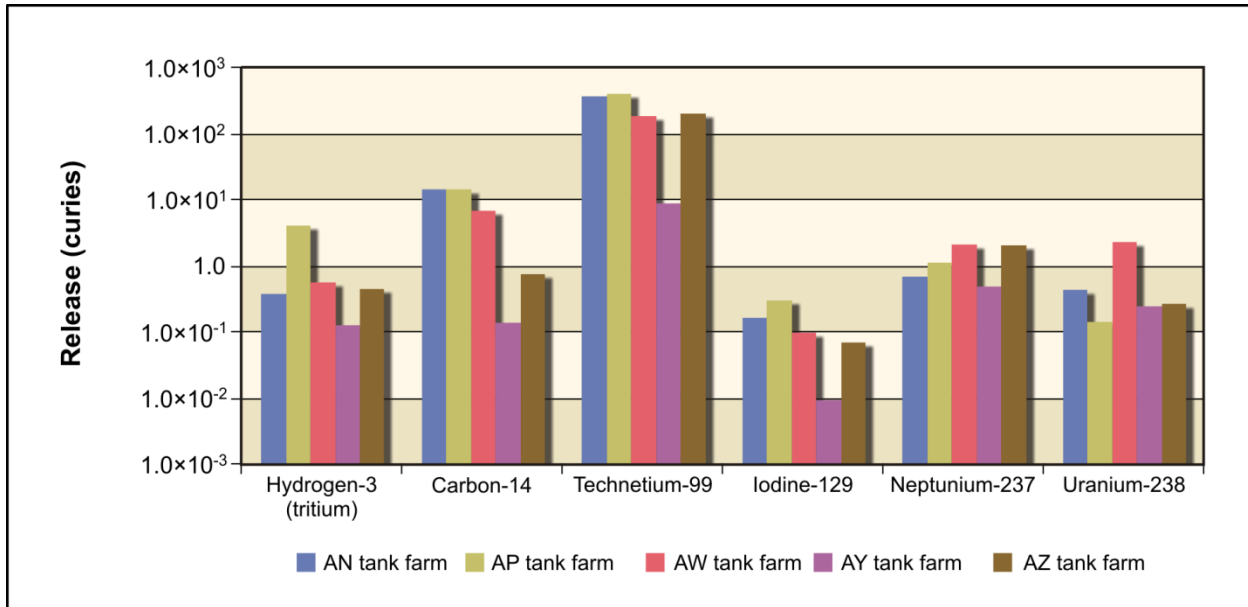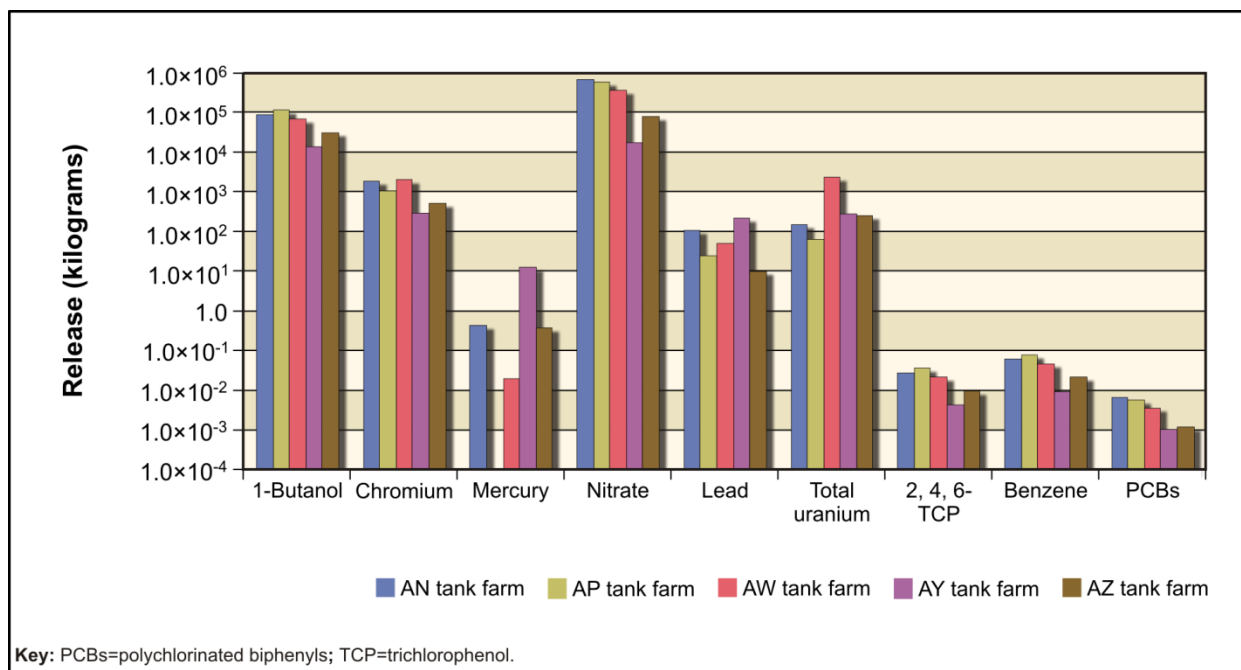
Figure M–49. Tank Closure Alternative 5 Radionuclide Releases to the Vadose Zone from Other Sources in Tank Farms AN, AP, AW, AY, and AZ
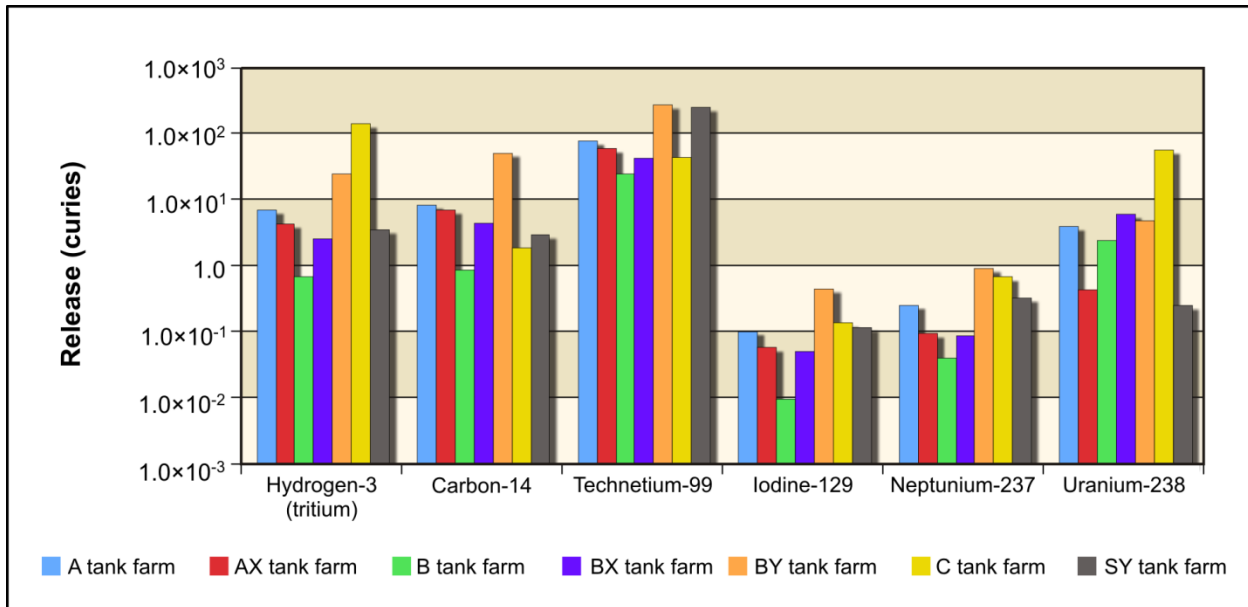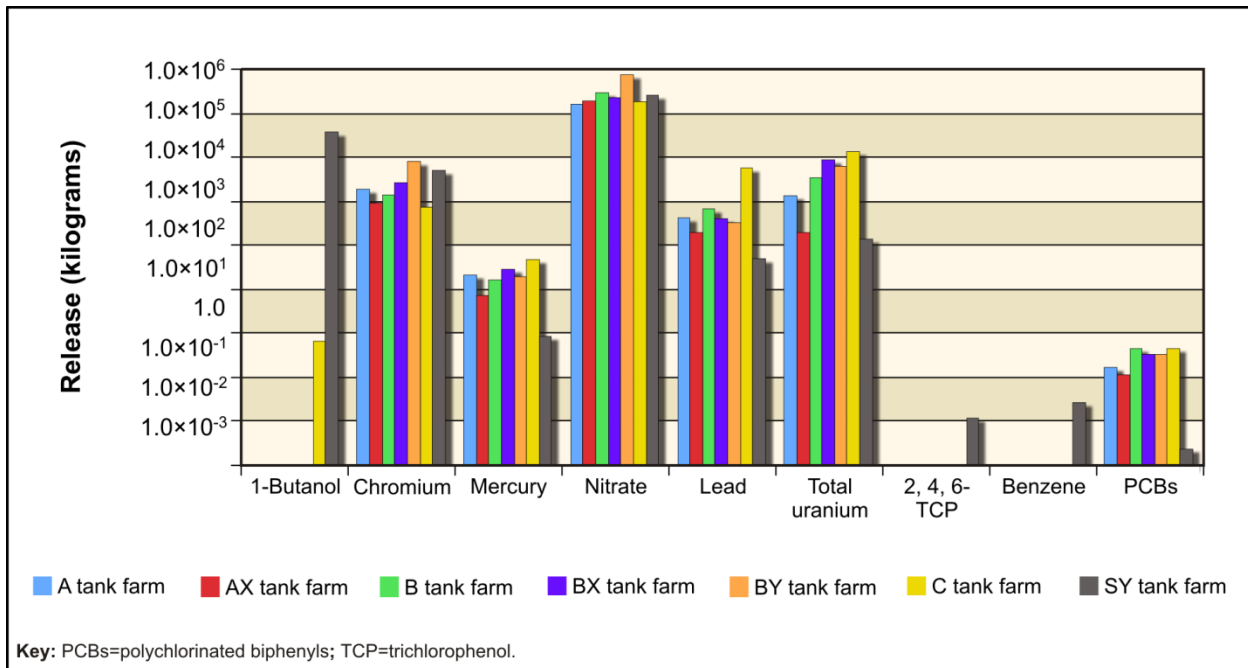

Figure M–50. Tank Closure Alternative 5 Radionuclide Releases to the Vadose Zone from Other Sources in Tank Farms A, AX, B, BX, BY, C, and SY
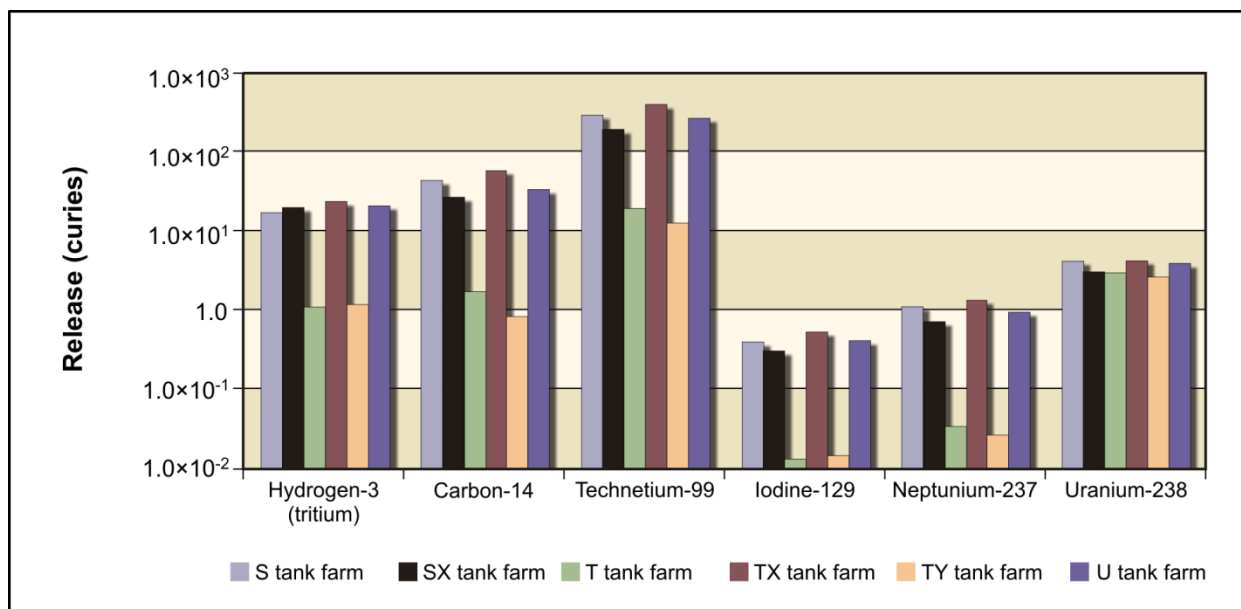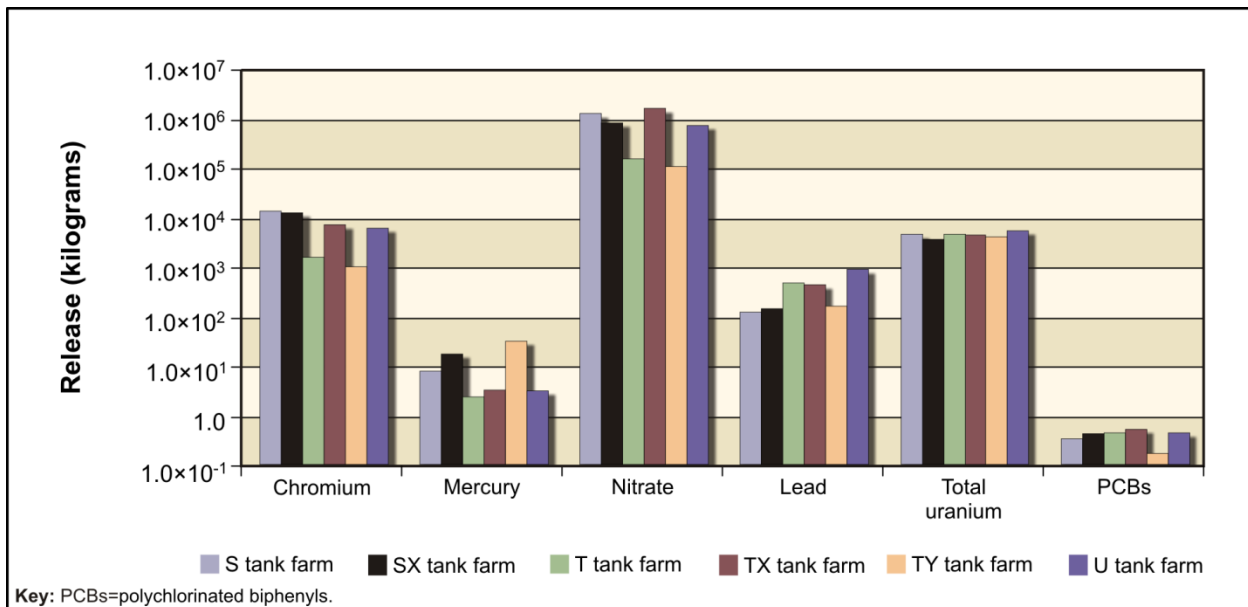
Figure M–51. Tank Closure Alternative 5 Radionuclide Releases to the Vadose Zone from Other Sources in Tank Farms S, SX, T, TX, TY, and U

Key: PCBs=polychlorinated biphenyls; TCP=trichlorophenol.

Figure M–52. Tank Closure Alternative 5 Chemical Releases to the Vadose Zone from Other Sources in Tank Farms AN, AP, AW, AY, and AZ

Figure M–53. Tank Closure Alternative 5 Chemical Releases to the Vadose Zone from Other Sources in Tank Farms A, AX, B, BX, BY, C, and SY

Figure M–54. Tank Closure Alternative 5 Chemical Releases to the Vadose Zone from Other Sources in Tank Farms S, SX, T, TX, TY, and U

Under Tank Closure Alternative 6A, Base Case, tank waste would be retrieved to a volume corresponding to 99.9 percent retrieval, and all tank farms would be clean-closed by removing the tanks, ancillary equipment, and soils to a depth of 3 meters (10 feet) below the tank base. Where necessary, deep soil excavation would also be conducted to remove contamination plumes within the soil column. The adjacent cribs and trenches (ditches) would be covered with an engineered modified RCRA Subtitle C barrier. The potential releases from other sources in tank farms under Alternative 6A, Base Case, originate from unplanned releases within the tank farm boundaries.

Under Tank Closure Alternative 6A, Option Case, tank waste would be retrieved to a volume corresponding to 99.9 percent retrieval, and all tank farms would be clean-closed by removing the tanks, ancillary equipment, and soils to a depth of 3 meters (10 feet) below the tank base. Where necessary, deep soil excavation would also be conducted to remove contamination plumes within the soil column. In addition, the adjacent cribs and trenches (ditches) would be clean-closed. The potential releases from other sources in tank farms under Alternative 6A, Option Case, originate from unplanned releases within the tank farm boundaries. Potential releases to the aquifer under Tank Closure Alternative 6A, Base and Option Cases, are indicated in Table M–28 and Figures M–55 and M–56.

Under Tank Closure Alternative 6B, Base Case, tank waste would be retrieved to a volume corresponding to 99.9 percent retrieval, and all tank farms would be clean-closed by removing the tanks, ancillary equipment, and soils to a depth of 3 meters (10 feet) below the tank base. Where necessary, deep soil excavation would also be conducted to remove contamination plumes within the soil column. The adjacent cribs and trenches (ditches) would be covered with an engineered modified RCRA Subtitle C barrier. The potential releases from other sources in tank farms under Alternative 6B, Base Case, originate from unplanned releases within the tank farm boundaries.

Under Tank Closure Alternative 6B, Option Case, tank waste would be retrieved to a volume corresponding to 99.9 percent retrieval, and all tank farms would be clean-closed by removing the tanks, ancillary equipment, and soils to a depth of 3 meters (10 feet) below the tank base. Where necessary, deep soil excavation would also be conducted to remove contamination plumes within the soil column. In addition, the adjacent cribs and trenches (ditches) would be clean-closed. The potential releases from other sources in tank farms under Alternative 6B, Option Case, originate from unplanned releases within the tank farm boundaries. Potential releases to the aquifer under Tank Closure Alternative 6B, Base and Option Cases, are indicated in Table M–29 and Figures M–57 and M–58.

Table M–28. Tank Closure Alternative 6A, Base and Option Cases, Radionuclide and Chemical Releases to the Vadose Zone from Other Sources in Tank Farms

Source	Radionuclide (curies)						Chemical (kilograms)								
	H-3	C-14	Tc-99	I-129	Np-237	U-238	1-Butanol	Cr	Hg	NO$_3$	Pb	Utot	2,4,6-TCP	Benzene	PCBs
B tank farm	3.34	7.87×10^{-2}	2.96	1.76×10^{-3}	9.69×10^{-3}	1.57×10^{-3}	3.86×10^{-4}	3.53×10^{1}	8.41×10^{-3}	3.24×10^{3}	2.07	1.81	–	–	–
BY tank farm	9.86	8.65×10^{-3}	2.15×10^{-2}	1.88×10^{-4}	4.95×10^{-4}	2.22×10^{-3}	–	3.81×10^{1}	3.44×10^{-2}	1.17×10^{4}	–	3.30	–	–	–
C tank farm	1.39×10^{2}	1.90×10^{-1}	1.67	2.48×10^{-2}	5.58×10^{-3}	1.49×10^{-2}	6.47×10^{-1}	3.94×10^{1}	3.92×10^{-3}	9.68×10^{3}	2.16×10^{1}	3.47×10^{1}	–	–	–
TX tank farm	8.21×10^{-1}	7.88×10^{-4}	2.01×10^{-3}	1.71×10^{-5}	4.52×10^{-5}	2.02×10^{-4}	1.15×10^{-5}	3.47	3.13×10^{-3}	1.06×10^{3}	–	3.00×10^{-1}	–	–	–
U tank farm	6.36×10^{-1}	8.63×10^{-4}	2.27×10^{-2}	2.53×10^{-5}	1.30×10^{-4}	1.31×10^{-3}	–	3.76×10^{-1}	6.14×10^{-4}	2.59×10^{1}	–	1.93	–	–	–

Note: To convert kilograms to pounds, multiply by 2.2046.
Key: 2,4,6-TCP=2,4,6-trichlorophenol; C-14=carbon-14; Cr=chromium; H-3=hydrogen-3 (tritium); Hg=mercury; I-129=iodine-129; NO$_3$=nitrate; Np-237=neptunium-237; Pb=lead; PCBs=polychlorinated biphenyls; Tc-99=technetium-99; U-238=uranium-238; Utot=total uranium.

Table M–29. Tank Closure Alternative 6B, Base and Option Cases, Radionuclide and Chemical Releases to the Vadose Zone from Other Sources in Tank Farms

Source	Radionuclide (curies)						Chemical (kilograms)								
	H-3	C-14	Tc-99	I-129	Np-237	U-238	1-Butanol	Cr	Hg	NO$_3$	Pb	Utot	2,4,6-TCP	Benzene	PCBs
B tank farm	3.34	7.87×10^{-2}	2.96	1.76×10^{-3}	9.69×10^{-3}	1.57×10^{-3}	3.86×10^{-4}	3.53×10^{1}	8.41×10^{-3}	3.24×10^{3}	2.07	1.81	–	–	–
BY tank farm	9.86	8.65×10^{-3}	2.15×10^{-2}	1.88×10^{-4}	4.95×10^{-4}	2.22×10^{-3}	–	3.81×10^{1}	3.44×10^{-2}	1.17×10^{4}	–	3.30	–	–	–
C tank farm	1.39×10^{2}	1.90×10^{-1}	1.67	2.48×10^{-2}	5.58×10^{-3}	1.49×10^{-2}	6.47×10^{-1}	3.94×10^{1}	3.92×10^{-3}	9.68×10^{3}	2.16×10^{1}	3.47×10^{1}	–	–	–
TX tank farm	8.21×10^{-1}	7.88×10^{-4}	2.01×10^{-3}	1.71×10^{-5}	4.52×10^{-5}	2.02×10^{-4}	1.15×10^{-5}	3.47	3.13×10^{-3}	1.06×10^{3}	–	3.00×10^{-1}	–	–	–
U tank farm	6.36×10^{-1}	8.63×10^{-4}	2.27×10^{-2}	2.53×10^{-5}	1.30×10^{-4}	1.31×10^{-3}	–	3.76×10^{-1}	6.14×10^{-4}	2.59×10^{1}	–	1.93	–	–	–

Note: To convert kilograms to pounds, multiply by 2.2046.
Key: 2,4,6-TCP=2,4,6-trichlorophenol; C-14=carbon-14; Cr=chromium; H-3=hydrogen-3 (tritium); Hg=mercury; I-129=iodine-129; NO$_3$=nitrate; Np-237=neptunium-237; Pb=lead; PCBs=polychlorinated biphenyls; Tc-99=technetium-99; U-238=uranium-238; Utot=total uranium.
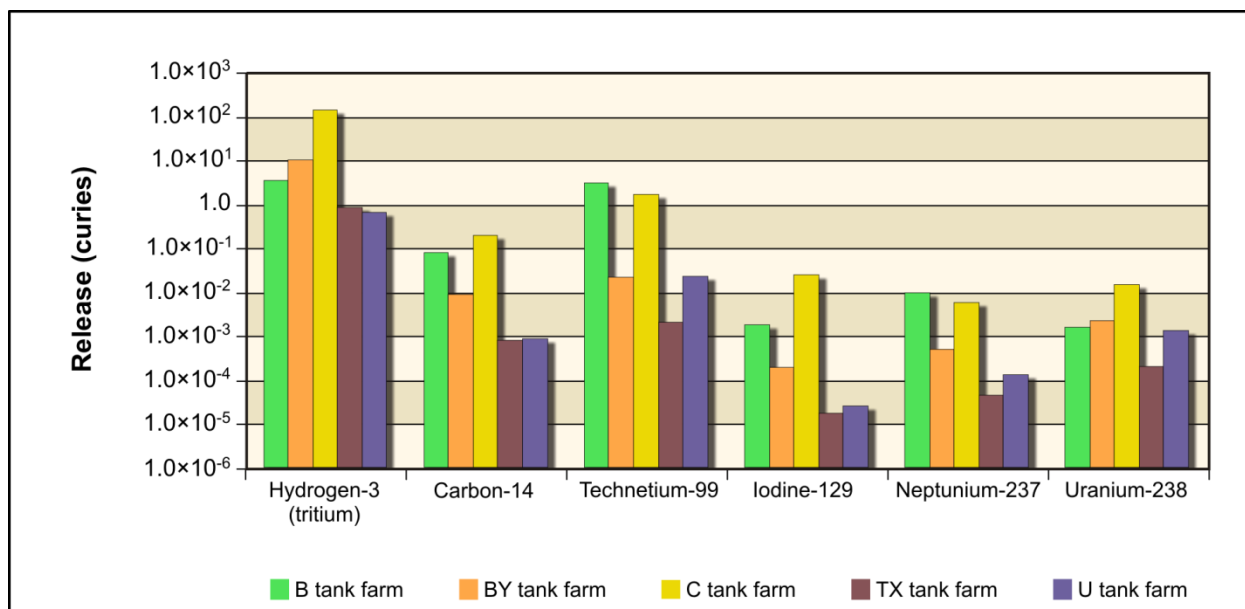
Figure M–55. Tank Closure Alternative 6A, Base and Option Cases, Radionuclide Releases to the Vadose Zone from Other Sources in Tank Farms B, BY, C, TX, and U
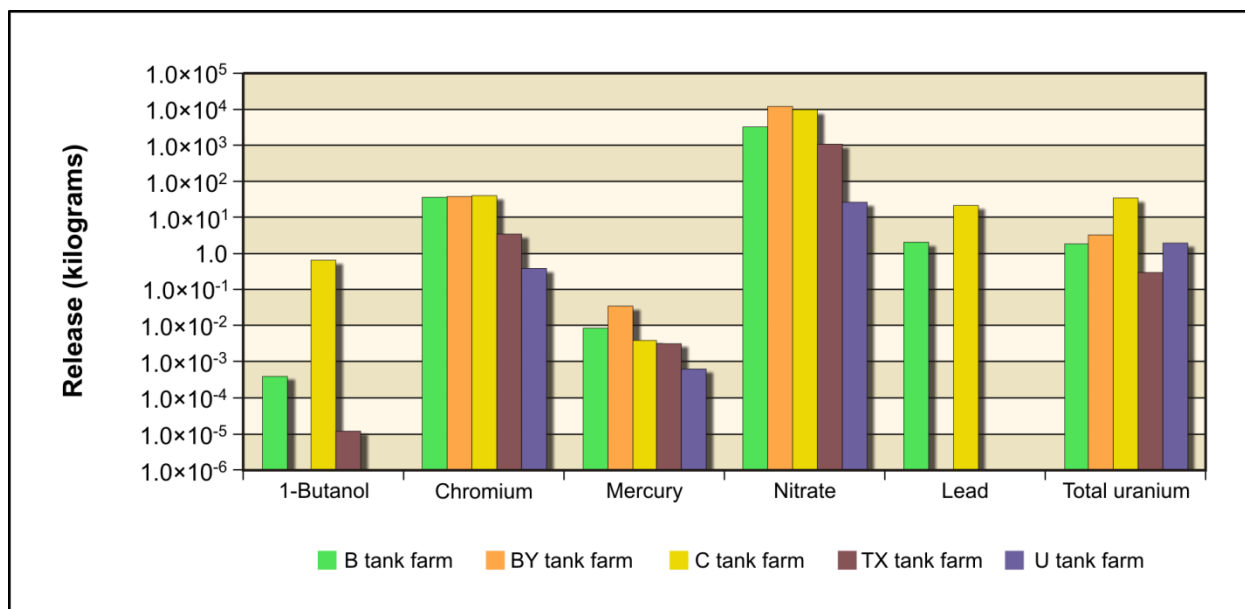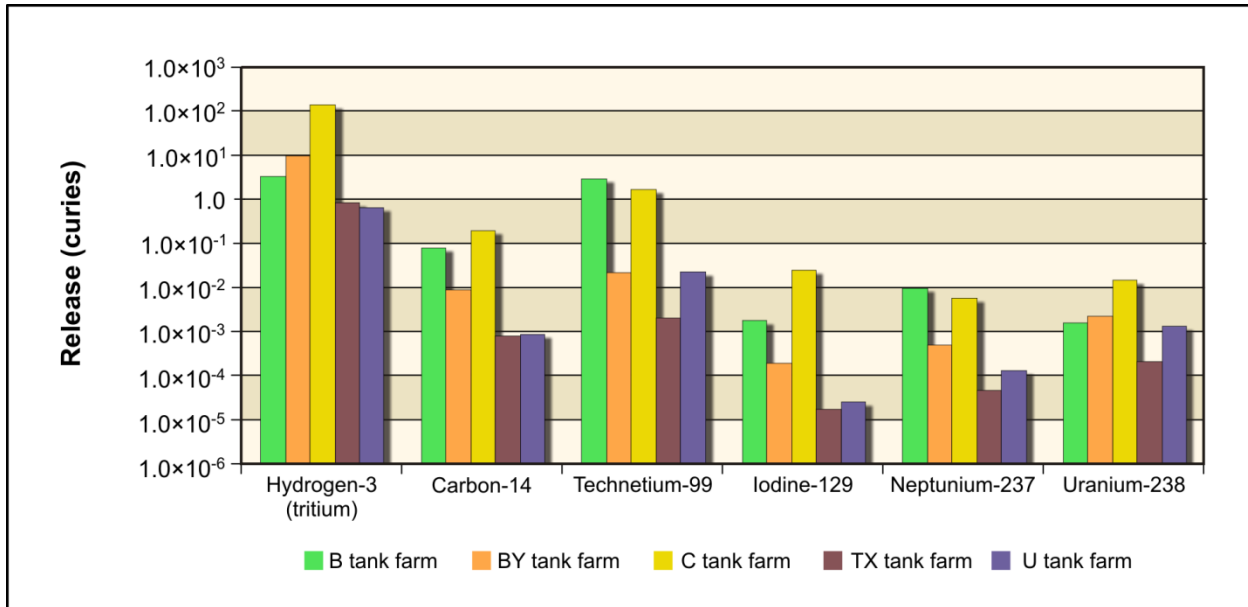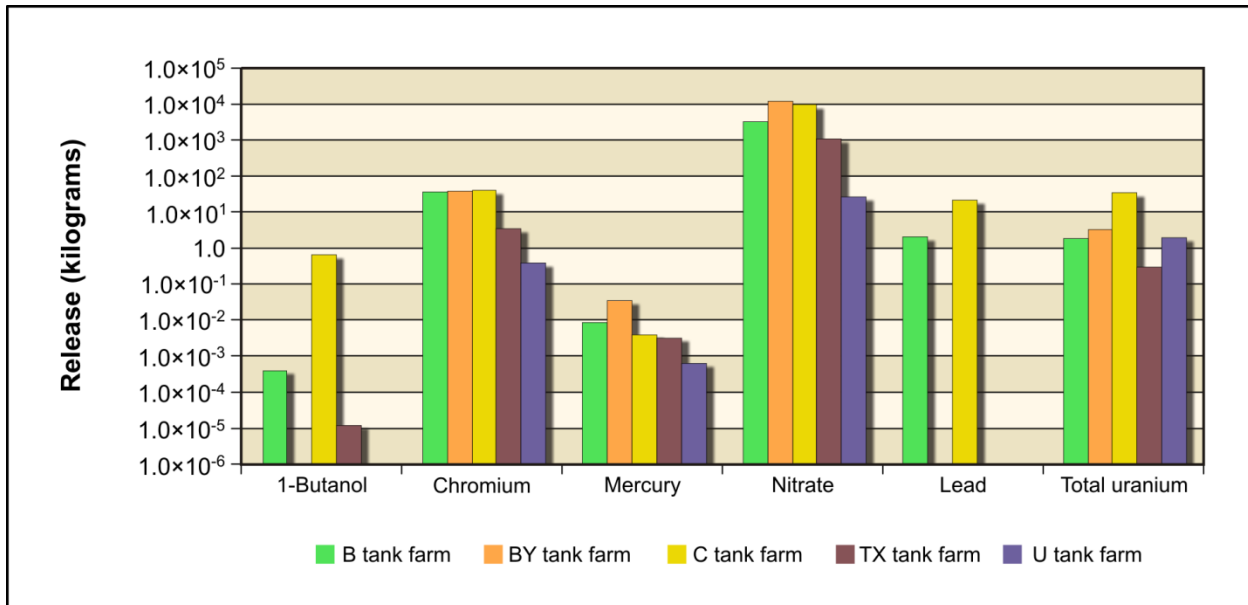

Figure M–56. Tank Closure Alternative 6A, Base and Option Cases, Chemical Releases to the Vadose Zone from Other Sources in Tank Farms B, BY, C, TX, and U

Figure M–57. Tank Closure Alternative 6B, Base and Option Cases, Radionuclide Releases to the Vadose Zone from Other Sources in Tank Farms B, BY, C, TX, and U

Figure M–58. Tank Closure Alternative 6B, Base and Option Cases, Chemical Releases to the Vadose Zone from Other Sources in Tank Farms B, BY, C, TX, and U

M.4.2   FFTF Decommissioning Alternatives

M.4.2.1   FFTF Decommissioning Alternative 1: No Action

Under FFTF Decommissioning Alternative 1, only those actions consistent with previous DOE National Environmental Policy Act actions would be completed. Final decommissioning of FFTF would not occur. For analysis purposes, the remaining waste would be available for release to the environment after an institutional control period of 100 years. Results for potential releases under all FFTF Decommissioning alternatives are shown in Table M–30. Potential releases to the vadose zone under FFTF Decommissioning Alternative 1 are indicated in Figure M–59.

**Table M–30. FFTF Decommissioning Alternatives 1, 2, and 3
Radionuclide Releases to the Vadose Zone (curies)**

| Alternative	H-3	C-14	K-40	Tc-99	Cs-137
Alternative 1	3.72×10^{-1}	1.68×10^{1}	2.16×10^{-9}	2.72×10^{1}	2.27×10^{-7}
Alternative 2	4.66×10^{-7}	1.57×10^{1}	2.10×10^{-9}	2.72×10^{1}	–
Alternative 3	2.96×10^{-6}	2.57×10^{-4}	2.31×10^{-9}	4.52×10^{-6}	–

Key: C-14=carbon-14; Cs-137=cesium-137; FFTF=Fast Flux Test Facility; H-3=hydrogen-3 (tritium); K-40=potassium-40; Tc-99=technetium-99.
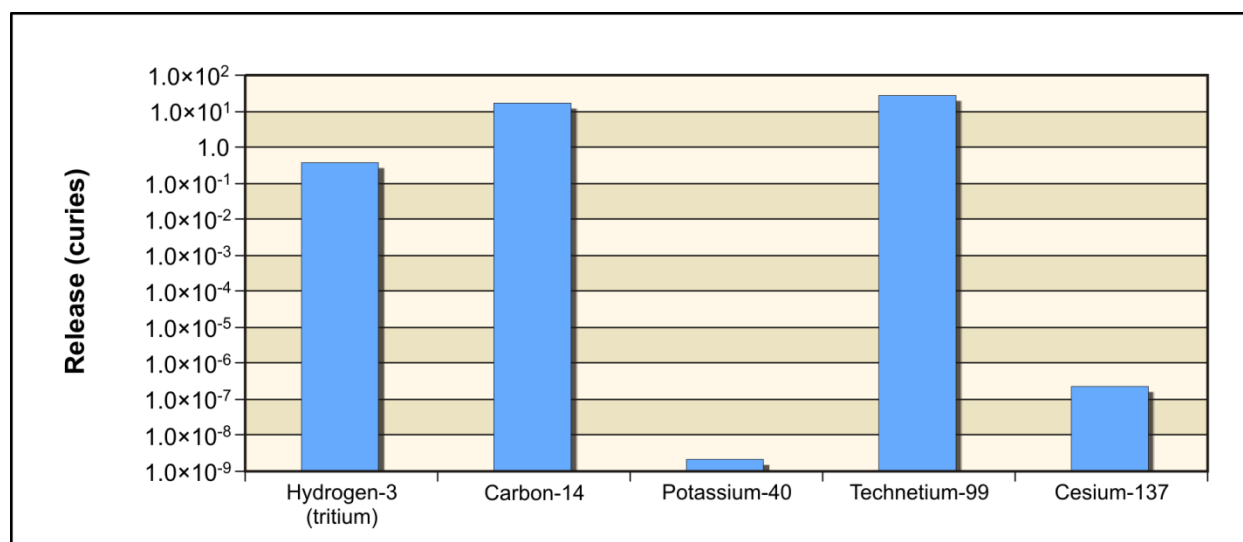
Figure M–59. FFTF Decommissioning Alternative 1 Radionuclide Releases to the Vadose Zone

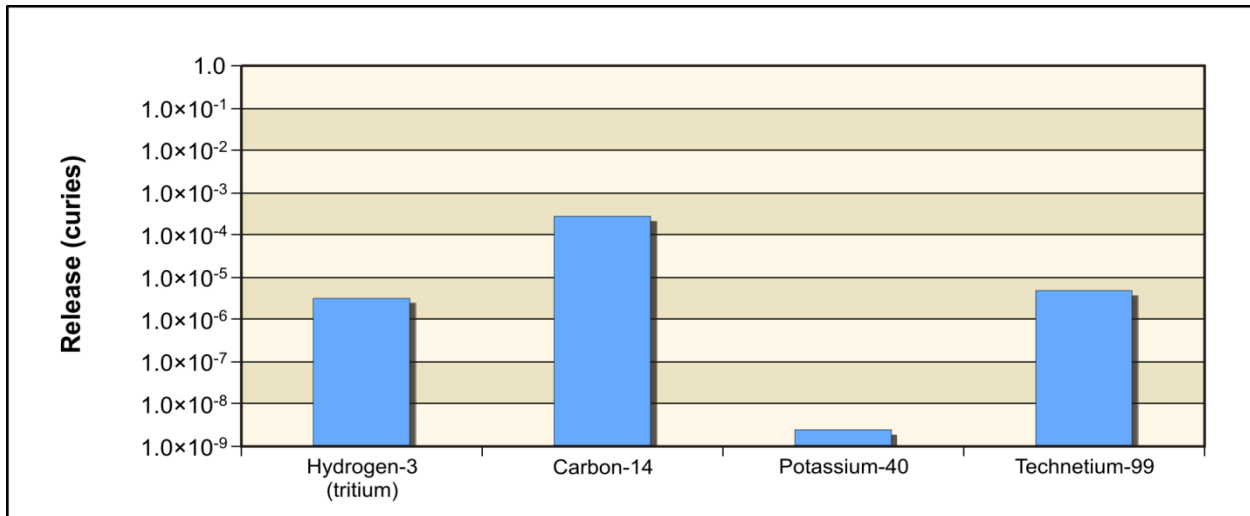### M.4.2.2   FFTF Decommissioning Alternative 2: Entombment

Under FFTF Decommissioning Alternative 2, all aboveground structures and minimal below-grade structures, equipment, and materials would be removed. An RCRA-compliant barrier would be constructed over the RCB and any other remaining below-grade structures (including the reactor vessel). Potential releases to the vadose zone under FFTF Decommissioning Alternative 2 are indicated in Figure M–60.
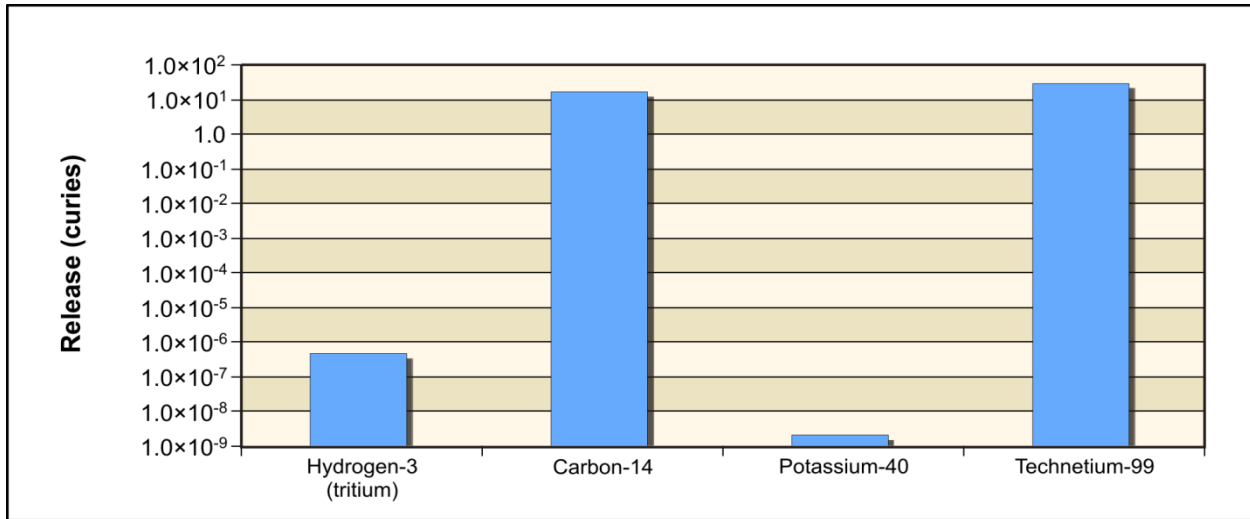
Figure M–60. FFTF Decommissioning Alternative 2 Radionuclide Releases to the Vadose Zone

M.4.2.3 FFTF Decommissioning Alternative 3: Removal

Under FFTF Decommissioning Alternative 3, all aboveground structures and contaminated below-grade structures, equipment, and materials would be removed. Potential releases to the vadose zone under FFTF Decommissioning Alternative 3 are indicated in Figure M–61.

Figure M–61. FFTF Decommissioning Alternative 3 Radionuclide Releases to the Vadose Zone

M.4.3 Waste Management Alternatives

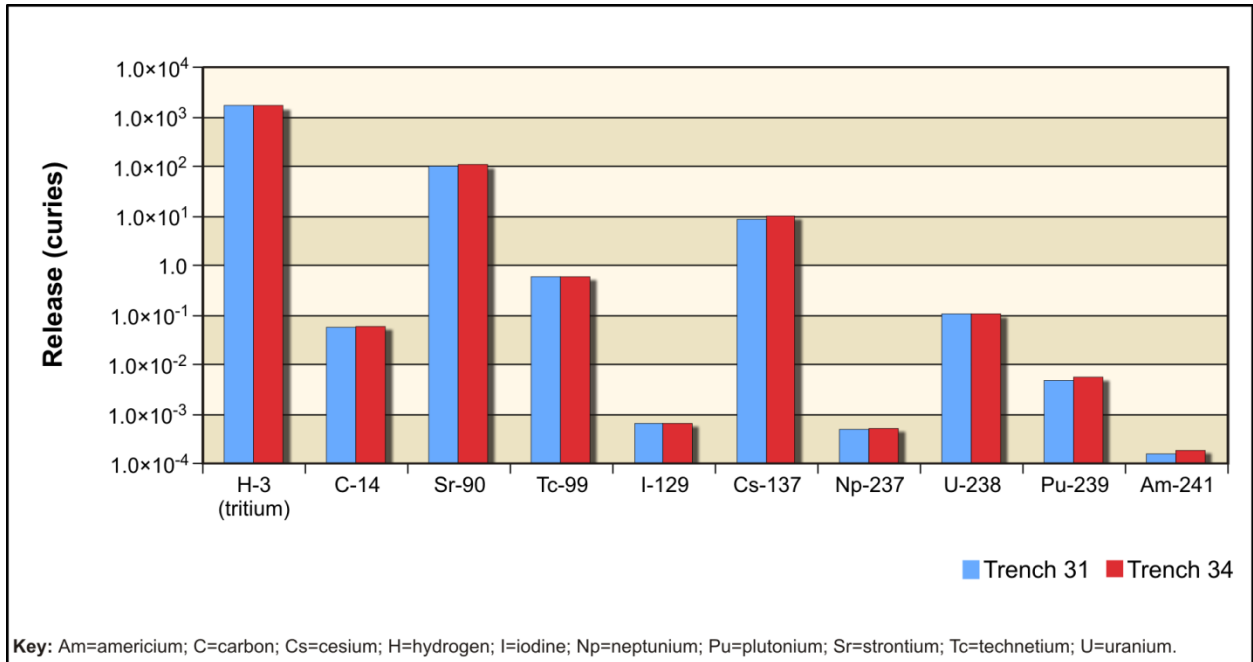### M.4.3.1 Waste Management Alternative 1

Under Waste Management Alternative 1, only the waste currently generated on site at Hanford from non-CERCLA actions would continue to be disposed of in LLBG 218-W-5, trenches 31 and 34. Although short-term impacts do not address impacts associated with closure activities for this site, for the purpose of analyzing long-term impacts, it is assumed that these trenches would be closed using an RCRA-compliant barrier consistent with the closure plans for these burial grounds. As a result, the non-CERCLA waste disposed of in these trenches from 2008 to 2035 would become available for release to the environment. Potential releases to the vadose zone under Waste Management Alternative 1 are indicated in Table M–31 and Figures M–62 and M–63.

Table M–31. Waste Management Alternative 1 Radionuclide and Chemical Releases to the Vadose Zone

Source	Radionuclide (curies)										Chemical (kilograms)					
	H-3	**C-14**	**Sr-90**	**Tc-99**	**I-129**	**Cs-137**	**Np-237**	**U-238**	**Pu-239**	**Am-241**	**Cr**	**F**	**Hg**	**NO$_3$**	**Pb**	**Utot**
Trench 31	1.75×10^3	5.84×10^{-2}	1.02×10^2	6.04×10^{-1}	6.56×10^{-4}	8.84	5.02×10^{-4}	1.06×10^{-1}	4.92×10^{-3}	1.62×10^{-4}	8.96×10^1	1.37×10^2	2.72	1.49×10^3	5.77×10^1	1.37×10^{-1}
Trench 34	1.75×10^3	6.07×10^{-2}	1.10×10^2	6.04×10^{-1}	6.56×10^{-4}	1.02×10^1	5.12×10^{-4}	1.07×10^{-1}	5.68×10^{-3}	1.88×10^{-4}	8.96×10^1	1.37×10^2	2.72	1.49×10^3	5.77×10^1	1.37×10^{-1}

Note: To convert kilograms to pounds, multiply by 2.2046.

Key: Am-241=americium-241; C-14=carbon-14; Cr=chromium; Cs-137=cesium-137; F=fluoride; H-3=hydrogen-3 (tritium); Hg=mercury; I-129=iodine-129; NO$_3$=nitrate; Np-237=neptunium-237; Pb=lead; Pu-239=plutonium-239; Sr-90=strontium-90; Tc-99=technetium-99; U-238=uranium-238; Utot=total uranium.

Figure M–62. Waste Management Alternative 1 Radionuclide Releases to the Vadose Zone
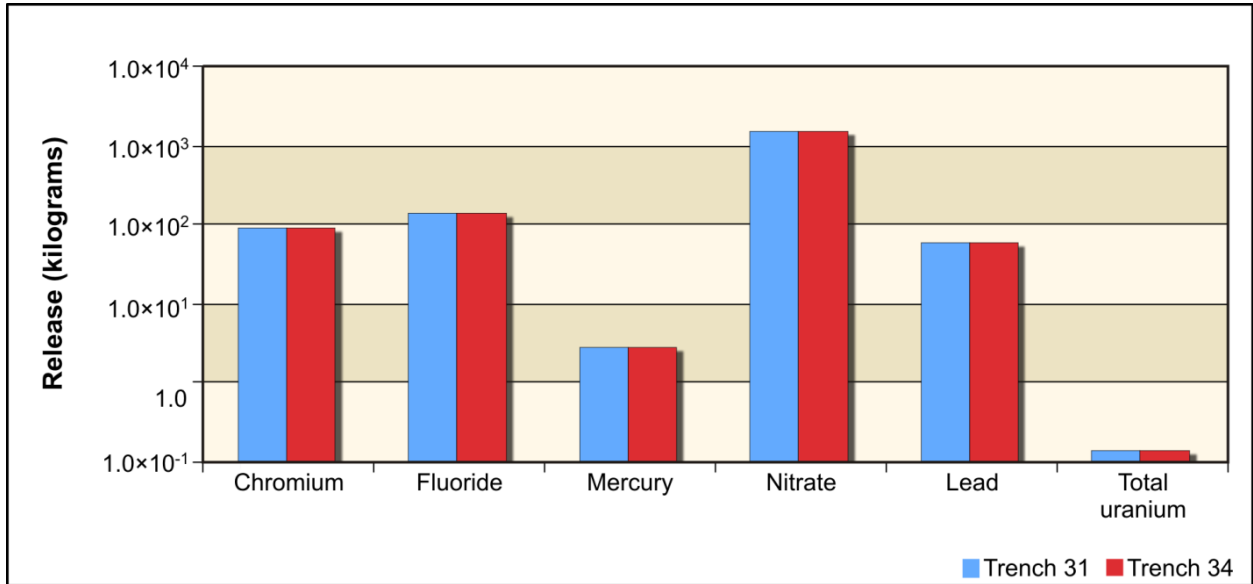
Figure M–63. Waste Management Alternative 1 Chemical Releases to the Vadose Zone

M.4.3.2   Waste Management Alternative 2

Under Waste Management Alternative 2, waste from tank treatment operations, onsite non-CERCLA sources, FFTF decommissioning, waste management, and other DOE sites would be disposed of in IDF-East. Waste from tank farm cleanup activities would be disposed of in the RPPDF. As a result, the waste disposed of in these two facilities would become available for release to the environment. Because different waste types would result from the Tank Closure action alternatives, three disposal groups were considered to account for the different IDF-East sizes and operational time periods. In addition, within these three disposal groups, subgroups were identified to allow for consideration of the different waste types resulting from the Tank Closure alternatives.

M.4.3.2.1   Waste Management Alternative 2: Disposal in IDF, 200-East Area Only, Disposal Group 1, Subgroup 1-A

Disposal Group 1, Subgroup 1-A, addresses the waste resulting from Tank Closure Alternative 2B, onsite non-CERCLA sources, FFTF decommissioning, waste management, and other DOE sites. Waste forms for IDF-East include the following:

- ILAW glass
- LAW melters
- Tank closure secondary waste
- FFTF decommissioning secondary waste
- Waste management secondary waste
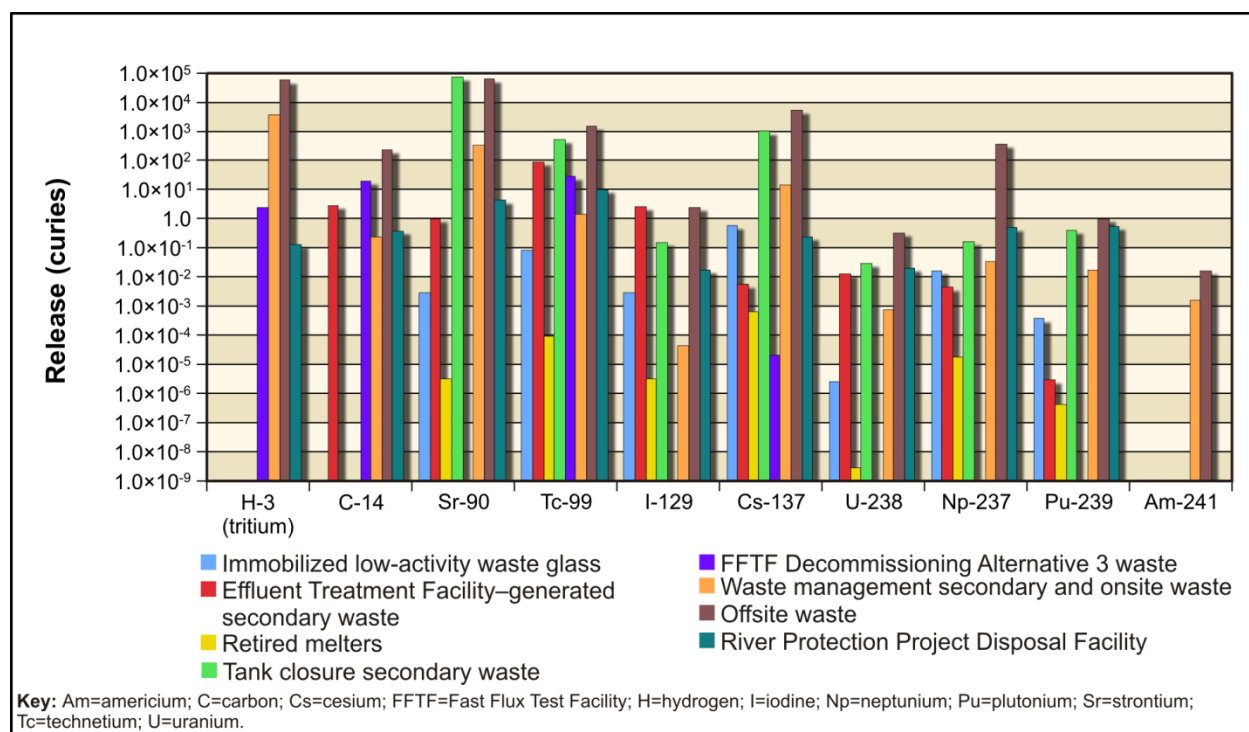- Offsite waste
- Onsite non-CERCLA waste

Waste forms for the RPPDF include those resulting from tank closure cleanup activities under Tank Closure Alternative 2B. Potential releases to the vadose zone under Waste Management Alternative 2, Disposal Group 1, Subgroup 1-A, are indicated in Table M–32 and Figures M–64 and M–65.

Table M–32. Waste Management Alternative 2, Disposal Group 1, Subgroup 1-A, Radionuclide and Chemical Releases to the Vadose Zone

Source	Radionuclide (curies)										Chemical (kilograms)					
	H-3	C-14	Sr-90	Tc-99	I-129	Cs-137	Np-237	U-238	Pu-239	Am-241	Cr	F	Hg	NO$_3$	Pb	Utot
ILAW glass	–	-	2.71×10^{-3}	7.85×10^{-2}	2.64×10^{-3}	5.38×10^{-1}	2.31×10^{-6}	1.51×10^{-2}	3.49×10^{-4}	–	1.26×10^{2}	–	–	–	2.46	1.04×10^{1}
ETF-generated secondary waste	–	2.77	9.24×10^{-1}	8.62×10^{1}	2.50	5.44×10^{-3}	1.20×10^{-2}	4.24×10^{-3}	2.76×10^{-6}	–	4.43×10^{1}	–	8.07×10^{-1}	9.01×10^{6}	8.36×10^{-2}	4.21
Retired melters	–	–	3.02×10^{-6}	8.75×10^{-5}	2.96×10^{-6}	6.01×10^{-4}	2.58×10^{-9}	1.69×10^{-5}	3.90×10^{-7}	–	1.41×10^{-1}	–	–	–	2.74×10^{-3}	1.15×10^{-2}
TC secondary waste	–	–	7.36×10^{4}	4.92×10^{2}	1.45×10^{-1}	1.02×10^{3}	2.81×10^{-2}	1.61×10^{-1}	3.95×10^{-1}	–	1.94×10^{3}	–	2.40×10^{2}	–	3.29	1.03×10^{2}
FFTF Decommissioning Alternative 3 waste	2.29	1.86×10^{1}	–	2.72×10^{1}	–	1.94×10^{-5}	–	–	–	–	7.51×10^{-3}	–	–	–	9.74×10^{-5}	2.16×10^{3}
FFTF Decommissioning Alternative 2 waste	2.29	2.18×10^{-4}	–	1.48×10^{-2}	–	1.88×10^{-5}	–	–	–	–	7.49×10^{-3}	–	–	–	9.41×10^{-5}	1.82×10^{-3}
WM secondary and onsite waste	3.66×10^{3}	2.29×10^{-1}	3.31×10^{2}	1.35	4.19×10^{-5}	1.42×10^{1}	7.33×10^{-4}	3.26×10^{-2}	1.62×10^{-2}	1.46×10^{-3}	1.83×10^{2}	2.74×10^{2}	1.23×10^{1}	2.97×10^{3}	3.45×10^{2}	4.20×10^{-2}
Offsite waste	5.57×10^{4}	2.25×10^{2}	6.05×10^{4}	1.46×10^{3}	2.26	5.16×10^{3}	3.07×10^{-1}	3.48×10^{2}	9.20×10^{-1}	1.50×10^{-2}	8.05×10^{1}	–	2.53	–	8.70×10^{-1}	–
RPPDF	1.27×10^{-1}	3.61×10^{-1}	4.15	9.71	1.67×10^{-2}	2.30×10^{-1}	1.85×10^{-2}	4.66×10^{-1}	5.31×10^{-1}	–	5.86×10^{2}	–	1.61	3.93×10^{4}	4.97	6.60×10^{2}

Note: To convert kilograms to pounds, multiply by 2.2046.

Key: Am-241=americium-241; C-14=carbon-14; Cr=chromium; Cs-137=cesium-137; ETF=Effluent Treatment Facility; F=fluoride; FFTF=Fast Flux Test Facility; H-3=hydrogen-3 (tritium); Hg=mercury; I-129=iodine-129; ILAW=immobilized low-activity waste; NO$_3$=nitrate; Np-237=neptunium-237; Pb=lead; Pu-239=plutonium-239; RPPDF=River Protection Project Disposal Facility; Sr-90=strontium-90; TC=tank closure; Tc-99=technetium-99; U-238=uranium-238; Utot=total uranium; WM=waste management.

**Figure M–64. Waste Management Alternative 2, Disposal Group 1, Subgroup 1-A,
Radionuclide Releases to the Vadose Zone**
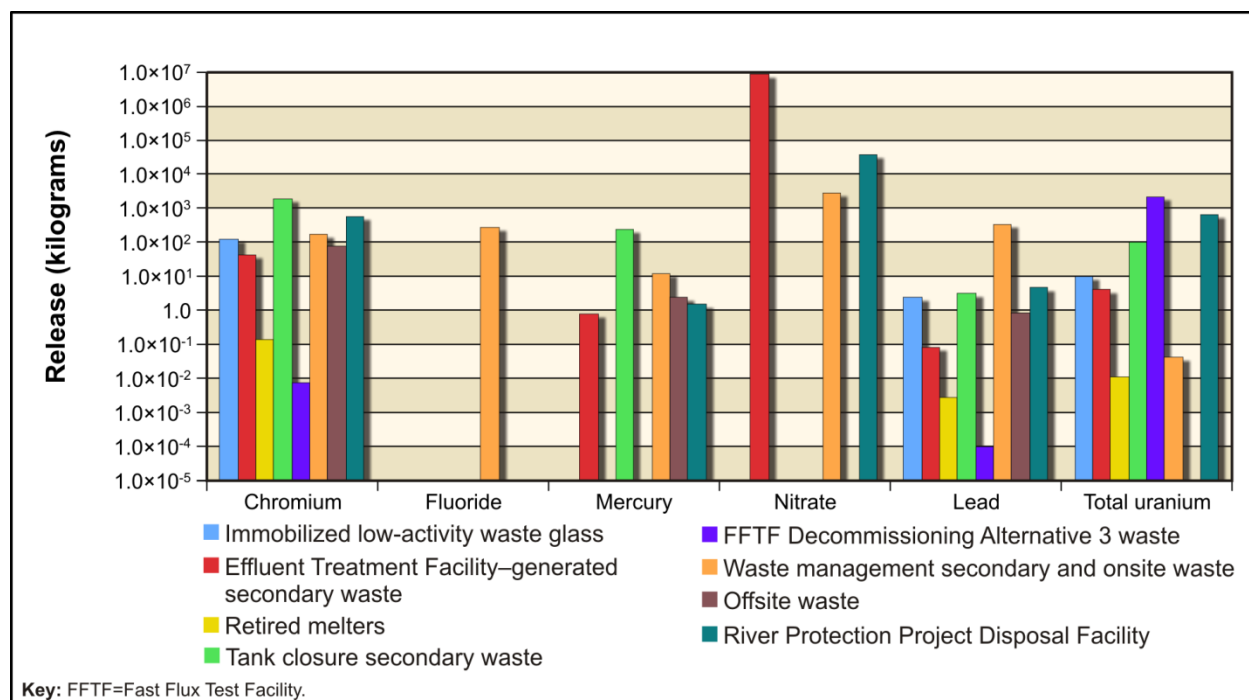
**Figure M–65. Waste Management Alternative 2, Disposal Group 1, Subgroup 1-A,
Chemical Releases to the Vadose Zone**

M.4.3.2.2   Waste Management Alternative 2: Disposal in IDF, 200-East Area Only, Disposal Group 1, Subgroup 1-B

Disposal Group 1, Subgroup 1-B, addresses the waste resulting from Tank Closure Alternative 3A, onsite non-CERCLA sources, FFTF decommissioning, waste management, and other DOE sites. Waste forms for IDF-East include the following:

- ILAW glass
- LAW melters
- bulk vitrification glass
- Tank closure secondary waste
- FFTF decommissioning secondary waste
- Waste management secondary waste
- Offsite waste
- Onsite non-CERCLA waste

Waste forms for the RPPDF include those resulting from tank closure cleanup activities under Tank Closure Alternative 3A. Potential releases to the vadose zone under Waste Management Alternative 2, Disposal Group 1, Subgroup 1-B, are indicated in Table M–33 and Figures M–66 and M–67.
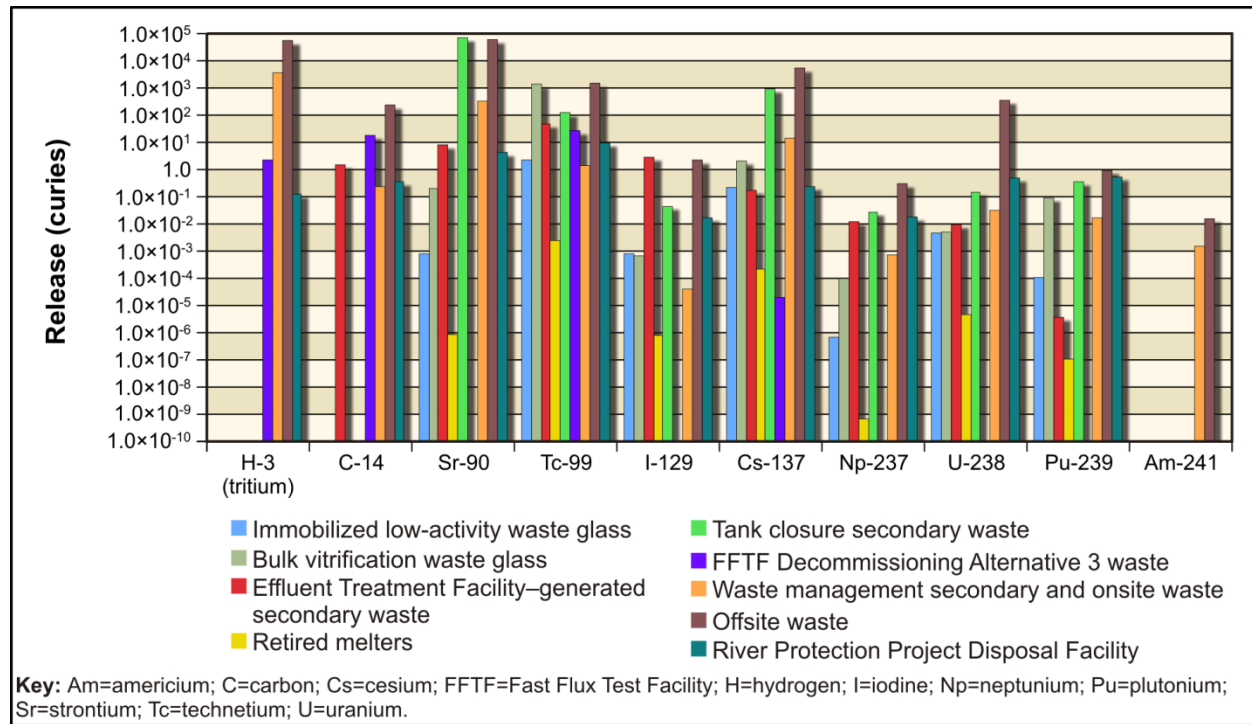
Table M–33. Waste Management Alternative 2, Disposal Group 1, Subgroup 1-B, Radionuclide and Chemical Releases to the Vadose Zone

Source	Radionuclide (curies)										Chemical (kilograms)					
	H-3	C-14	Sr-90	Tc-99	I-129	Cs-137	Np-237	U-238	Pu-239	Am-241	Cr	F	Hg	NO$_3$	Pb	Utot
ILAW glass	–	–	8.12×10^{-4}	2.30	7.75×10^{-4}	2.10×10^{-1}	6.86×10^{-7}	4.49×10^{-3}	1.04×10^{-4}	–	3.71×10^{1}	–	–	–	7.39×10^{-1}	3.13
BV waste glass	–	–	1.94×10^{-1}	1.34×10^{3}	6.67×10^{-4}	2.00	9.49×10^{-5}	5.08×10^{-3}	8.95×10^{-2}	–	3.18×10^{1}	–	–	–	6.62×10^{-1}	3.41
ETF-generated secondary waste	–	1.54	7.84	4.63×10^{1}	2.74	1.69×10^{-1}	1.21×10^{-2}	9.18×10^{-3}	3.75×10^{-6}	–	2.76×10^{1}	–	8.05×10^{-1}	8.14×10^{6}	1.38×10^{1}	7.37
Retired melters	–	–	8.27×10^{-7}	2.34×10^{-3}	7.89×10^{-7}	2.13×10^{-4}	6.97×10^{-10}	4.57×10^{-6}	1.06×10^{-7}	–	3.77×10^{-2}	–	–	–	7.53×10^{-4}	3.18×10^{-3}
TC secondary waste	–	–	7.27×10^{4}	1.28×10^{2}	4.25×10^{-2}	9.16×10^{2}	2.77×10^{-2}	1.47×10^{-1}	3.59×10^{-1}	–	8.02×10^{2}	–	2.38×10^{2}	–	2.89	9.08×10^{1}
FFTF Decommissioning Alternative 3 waste	2.29	1.86×10^{1}	–	2.72×10^{1}	–	1.94×10^{-5}	–	–	–	–	7.51×10^{-3}	–	–	–	9.74×10^{-5}	2.16×10^{3}
FFTF Decommissioning Alternative 2 waste	2.29	2.18×10^{-4}	–	1.48×10^{-2}	–	1.88×10^{-5}	–	–	–	–	7.49×10^{-3}	–	–	–	9.41×10^{-5}	1.82×10^{-3}
WM secondary and onsite waste	3.66×10^{3}	2.29×10^{-1}	3.31×10^{2}	1.35	4.19×10^{-5}	1.42×10^{1}	7.33×10^{-4}	3.26×10^{-2}	1.62×10^{-2}	1.46×10^{-3}	1.83×10^{2}	2.74×10^{2}	1.23×10^{1}	2.97×10^{3}	3.45×10^{2}	4.20×10^{-2}
Offsite waste	5.57×10^{4}	2.25×10^{2}	6.05×10^{4}	1.46×10^{3}	2.26	5.16×10^{3}	3.07×10^{-1}	3.48×10^{2}	9.20×10^{-1}	1.50×10^{-2}	8.05×10^{1}	–	2.53	–	8.70×10^{-1}	–
RPPDF	1.27×10^{-1}	3.61×10^{-1}	4.15	9.71	1.67×10^{-2}	2.30×10^{-1}	1.85×10^{-2}	4.66×10^{-1}	5.31×10^{-1}	–	5.86×10^{2}	–	1.61	3.93×10^{4}	4.97	6.60×10^{2}

Note: To convert kilograms to pounds, multiply by 2.2046.

Key: Am-241=americium-241; BV=bulk vitrification; C-14=carbon-14; Cr=chromium; Cs-137=cesium-137; ETF=Effluent Treatment Facility; F=fluoride; FFTF=Fast Flux Test Facility; H-3=hydrogen-3 (tritium); Hg=mercury; I-129=iodine-129; ILAW=immobilized low-activity waste; NO$_3$=nitrate; Np-237=neptunium-237; Pb=lead; Pu-239=plutonium-239; RPPDF=River Protection Project Disposal Facility; Sr-90=strontium-90; TC=tank closure; Tc-99=technetium-99; U-238=uranium-238; Utot=total uranium; WM=waste management.

**Figure M–66. Waste Management Alternative 2, Disposal Group 1, Subgroup 1-B,
Radionuclide Releases to the Vadose Zone**
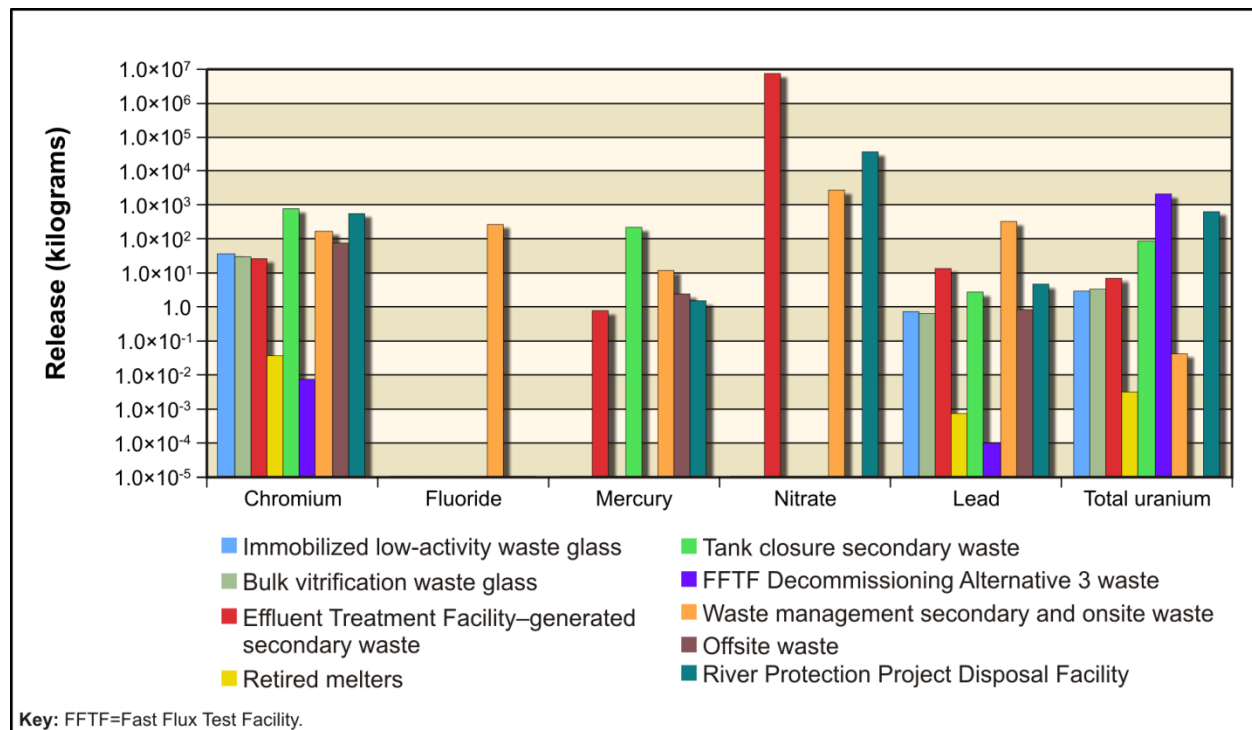
**Figure M–67. Waste Management Alternative 2, Disposal Group 1, Subgroup 1-B,
Chemical Releases to the Vadose Zone**

M.4.3.2.3   Waste Management Alternative 2: Disposal in IDF, 200-East Area Only, Disposal Group 1, Subgroup 1-C

Disposal Group 1, Subgroup 1-C, addresses the waste resulting from Tank Closure Alternative 3B, onsite non-CERCLA sources, FFTF decommissioning, waste management, and other DOE sites. Waste forms for IDF-East include the following:

- ILAW glass
- LAW melters
- Cast stone waste
- Tank closure secondary waste
- FFTF decommissioning secondary waste
- Waste management secondary waste
- Offsite waste
- Onsite non-CERCLA waste

Waste forms for the RPPDF include those resulting from tank closure cleanup activities under Tank Closure Alternative 3B. Potential releases to the vadose zone under Waste Management Alternative 2, Disposal Group 1, Subgroup 1-C, are indicated in Table M–34 and Figures M–68 and M–69.

Table M–34. Waste Management Alternative 2, Disposal Group 1, Subgroup 1-C, Radionuclide and Chemical Releases to the Vadose Zone
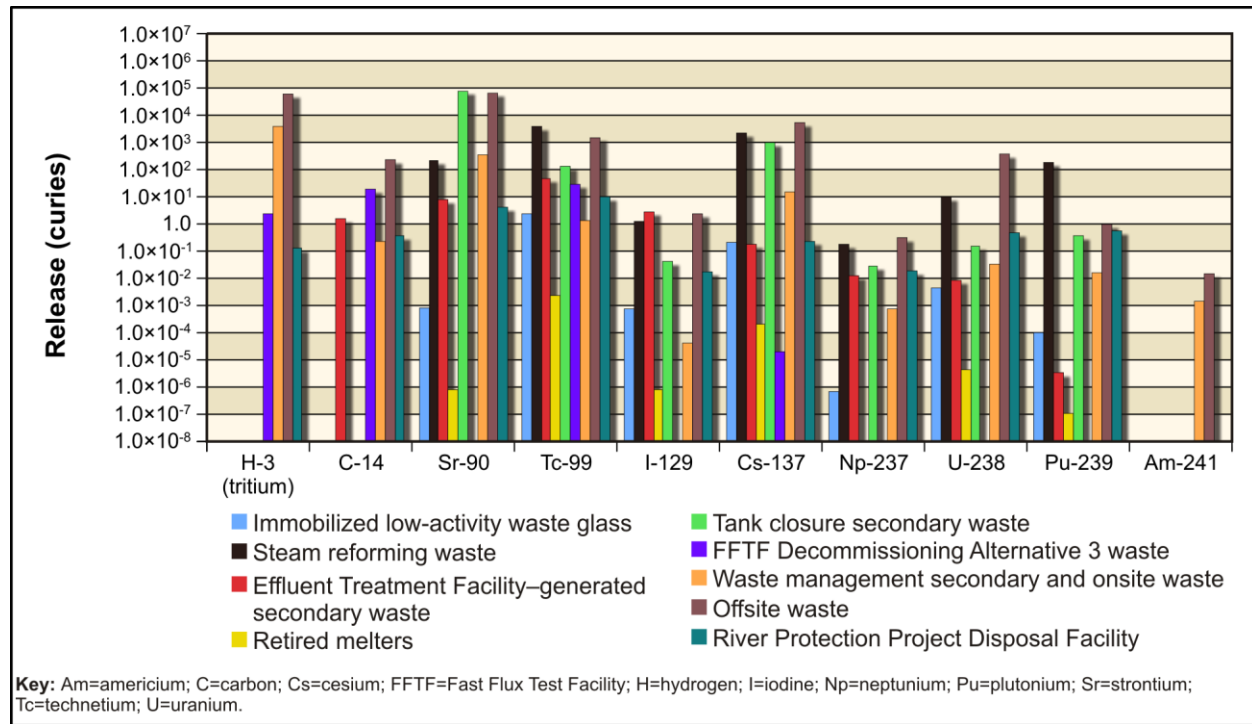
Source	Radionuclide (curies)										Chemical (kilograms)					
	H-3	C-14	Sr-90	Tc-99	I-129	Cs-137	Np-237	U-238	Pu-239	Am-241	Cr	F	Hg	NO₃	Pb	Utot
ILAW glass	–	–	8.12×10^{-4}	2.30×10^{-2}	7.75×10^{-4}	2.10×10^{-1}	6.86×10^{-7}	4.49×10^{-3}	1.04×10^{-4}	–	3.71×10^{1}	–	-	-	7.39×10^{-1}	3.13
Cast stone waste	8.44×10^{3}	5.03×10^{2}	3.73×10^{4}	9.14×10^{3}	8.98×10^{-1}	2.08×10^{4}	8.07×10^{-2}	1.93	1.84	–	3.25×10^{5}	–	5.39×10^{1}	4.95×10^{7}	9.08×10^{1}	1.31×10^{3}
ETF-generated secondary waste	–	8.54×10^{-1}	9.13×10^{-1}	5.81×10^{1}	7.32×10^{-1}	4.87×10^{-3}	1.19×10^{-2}	3.84×10^{-3}	2.53×10^{-6}	–	1.84×10^{1}	–	6.00×10^{-1}	2.63×10^{6}	1.06×10^{-1}	3.76
Retired melters	–	–	8.27×10^{-7}	2.34×10^{-5}	7.89×10^{-7}	2.13×10^{-4}	6.97×10^{-10}	4.57×10^{-6}	1.06×10^{-7}	–	3.77×10^{-2}	–	–	–	7.53×10^{-4}	3.18×10^{-3}
TC secondary waste	–	–	7.27×10^{4}	3.33×10^{2}	4.25×10^{-2}	9.16×10^{2}	2.77×10^{-2}	1.47×10^{-1}	3.59×10^{-1}	–	8.02×10^{2}	–	1.78×10^{2}	–	2.89	9.08×10^{1}
FFTF Decommissioning Alternative 3 waste	2.29	1.86×10^{1}	–	2.72×10^{1}	–	1.94×10^{-5}	–	–	–	–	7.51×10^{-3}	–	–	–	9.74×10^{-5}	2.16×10^{3}
FFTF Decommissioning Alternative 2 waste	2.29	2.18×10^{-4}	–	1.48×10^{-2}	–	1.88×10^{-5}	–	–	–	–	7.49×10^{-3}	–	–	–	9.41×10^{-5}	1.82×10^{-3}
WM secondary and onsite waste	3.66×10^{3}	2.29×10^{-1}	3.31×10^{2}	1.35	4.19×10^{-5}	1.42×10^{1}	7.33×10^{-4}	3.26×10^{-2}	1.62×10^{-2}	1.46×10^{-3}	1.83×10^{2}	2.74×10^{2}	1.23×10^{1}	2.97×10^{3}	3.45×10^{2}	4.20×10^{-2}
Offsite waste	5.57×10^{4}	2.25×10^{2}	6.05×10^{4}	1.46×10^{3}	2.26	5.16×10^{3}	3.07×10^{-1}	3.48×10^{2}	9.20×10^{-1}	1.50×10^{-2}	8.05×10^{1}	–	2.53	–	8.70×10^{-1}	–
RPPDF	1.27×10^{-1}	3.61×10^{-1}	4.15	9.71	1.67×10^{-2}	2.30×10^{-1}	1.85×10^{-2}	4.66×10^{-1}	5.31×10^{-1}	–	5.86×10^{2}	–	1.61	3.93×10^{4}	4.97	6.60×10^{2}

Note: To convert kilograms to pounds, multiply by 2.2046.

Key: Am-241=americium-241; C-14=carbon-14; Cr=chromium; Cs-137=cesium-137; ETF=Effluent Treatment Facility; F=fluoride; FFTF=Fast Flux Test Facility; H-3=hydrogen-3 (tritium); Hg=mercury; I-129=iodine-129; ILAW=immobilized low-activity waste; NO₃=nitrate; Np-237=neptunium-237; Pb=lead; Pu-239=plutonium-239; RPPDF=River Protection Project Disposal Facility; Sr-90=strontium-90; TC=tank closure; Tc-99=technetium-99; U-238=uranium-238; Utot=total uranium; WM=waste management.

Figure M–68. Waste Management Alternative 2, Disposal Group 1, Subgroup 1-C, Radionuclide Releases to the Vadose Zone
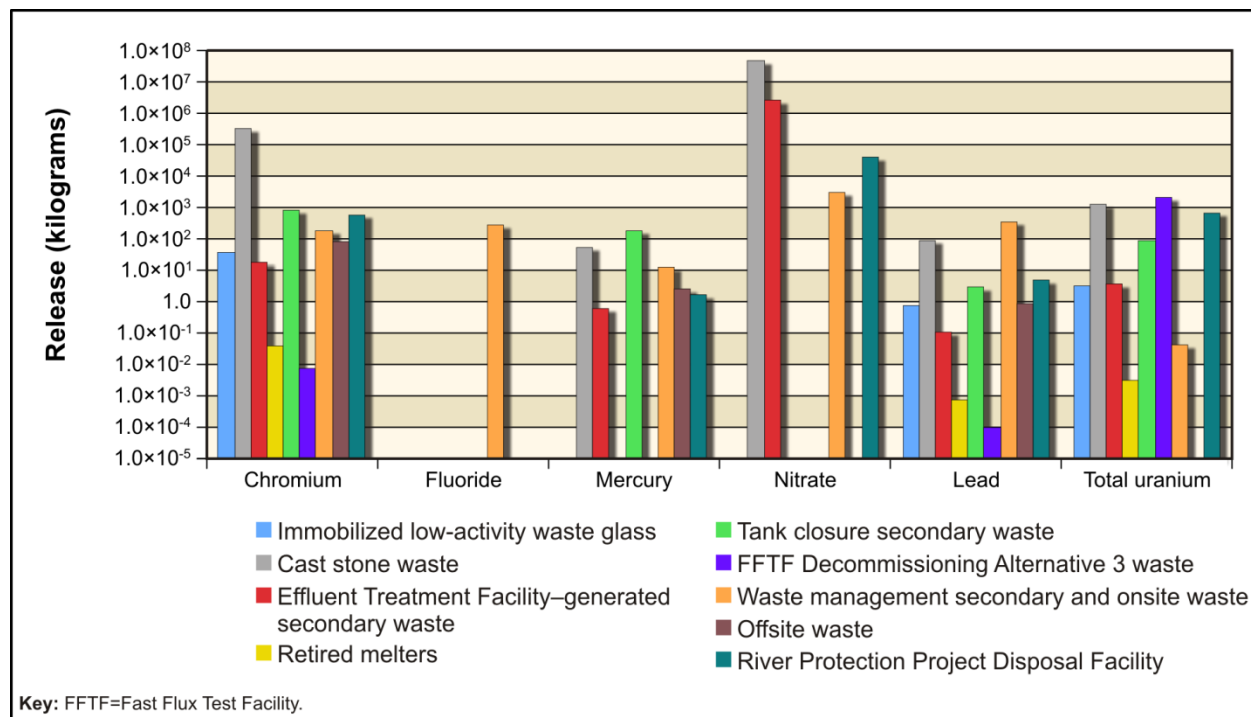
Figure M–69. Waste Management Alternative 2, Disposal Group 1, Subgroup 1-C, Chemical Releases to the Vadose Zone

M.4.3.2.4   Waste Management Alternative 2: Disposal in IDF, 200-East Area Only, Disposal Group 1, Subgroup 1-D

Disposal Group 1, Subgroup 1-D, addresses the waste resulting from Tank Closure Alternative 3C, onsite non-CERCLA sources, FFTF decommissioning, waste management, and other DOE sites. Waste forms for IDF-East include the following:

- ILAW glass
- LAW melters
- Steam reforming waste
- Tank closure secondary waste
- FFTF decommissioning secondary waste
- Waste management secondary waste
- Offsite waste
- Onsite non-CERCLA waste

Waste forms for the RPPDF include those resulting from tank closure cleanup activities under Tank Closure Alternative 3C. Potential releases to the vadose zone under Waste Management Alternative 2, Disposal Group 1, Subgroup 1-D, are indicated in Table M–35 and Figures M–70 and M–71.

Table M–35. Waste Management Alternative 2, Disposal Group 1, Subgroup 1-D, Radionuclide and Chemical Releases to the Vadose Zone

Source	Radionuclide (curies)										Chemical (kilograms)					
	H-3	C-14	Sr-90	Tc-99	I-129	Cs-137	Np-237	U-238	Pu-239	Am-241	Cr	F	Hg	NO$_3$	Pb	Utot
ILAW glass	–	–	8.12×10^{-4}	2.30	7.75×10^{-4}	2.10×10^{-1}	6.86×10^{-7}	4.49×10^{-3}	1.04×10^{-4}	–	3.71×10^{1}	–	–	–	7.39×10^{-1}	3.13
Steam Reforming waste	–	–	2.07×10^{2}	3.76×10^{3}	1.25	2.14×10^{3}	1.78×10^{-1}	9.54	1.69×10^{2}	–	6.01×10^{4}	–	–	–	1.25×10^{3}	6.44×10^{3}
ETF-generated secondary waste	–	1.54	7.69	4.63×10^{1}	2.74	1.71×10^{-1}	1.20×10^{-2}	8.33×10^{-3}	3.36×10^{-6}	–	2.72×10^{1}	–	8.05×10^{-1}	9.17×10^{6}	1.38×10^{1}	6.72
Retired melters	–	–	8.27×10^{-7}	2.34×10^{-3}	7.89×10^{-7}	2.13×10^{-4}	6.97×10^{-10}	4.57×10^{-6}	1.06×10^{-7}	–	3.77×10^{-2}	–	–	–	7.53×10^{-4}	3.18×10^{-3}
TC secondary waste	–	–	7.28×10^{4}	1.28×10^{2}	4.25×10^{-2}	9.17×10^{2}	2.77×10^{-2}	1.48×10^{-1}	3.59×10^{-1}	–	8.02×10^{2}	–	2.38×10^{2}	–	2.89	9.08×10^{1}
FFTF Decommissioning Alternative 3 waste	2.29	1.86×10^{1}	–	2.72×10^{1}	–	1.94×10^{-5}	–	–	–	–	7.51×10^{-3}	–	–	–	9.74×10^{-5}	2.16×10^{3}
FFTF Decommissioning Alternative 2 waste	2.29	2.18×10^{-4}	–	1.48×10^{-2}	–	1.88×10^{-5}	–	–	–	–	7.49×10^{-3}	–	–	–	9.41×10^{-5}	1.82×10^{-3}
WM secondary and onsite waste	3.66×10^{3}	2.29×10^{-1}	3.31×10^{2}	1.35	4.19×10^{-5}	1.42×10^{1}	7.33×10^{-4}	3.26×10^{-2}	1.62×10^{-2}	1.46×10^{-3}	1.83×10^{2}	2.74×10^{2}	1.23×10^{1}	2.97×10^{3}	3.45×10^{2}	4.20×10^{-2}
Offsite waste	5.57×10^{4}	2.25×10^{2}	6.05×10^{4}	1.46×10^{3}	2.26	5.16×10^{3}	3.07×10^{-1}	3.48×10^{2}	9.20×10^{-1}	1.50×10^{-2}	8.05×10^{1}	–	2.53	–	8.70×10^{-1}	–
RPPDF	1.27×10^{-1}	3.61×10^{-1}	4.15	9.71	1.67×10^{-2}	2.30×10^{-1}	1.85×10^{-2}	4.66×10^{-1}	5.31×10^{-1}	–	5.86×10^{2}	–	1.61	3.93×10^{4}	4.97	6.60×10^{2}

Note: To convert kilograms to pounds, multiply by 2.2046.

Key: Am-241=americium-241; C-14=carbon-14; Cr=chromium; Cs-137=cesium-137; ETF=Effluent Treatment Facility; F=fluoride; FFTF=Fast Flux Test Facility; H-3=hydrogen-3 (tritium); Hg=mercury; I-129=iodine-129; ILAW=immobilized low-activity waste; NO$_3$=nitrate; Np-237=neptunium-237; Pb=lead; Pu-239=plutonium-239; RPPDF=River Protection Project Disposal Facility; Sr-90=strontium-90; TC=tank closure; Tc-99=technetium-99; U-238=uranium-238; Utot=total uranium; WM=waste management.

Figure M–70. Waste Management Alternative 2, Disposal Group 1, Subgroup 1-D, Radionuclide Releases to the Vadose Zone
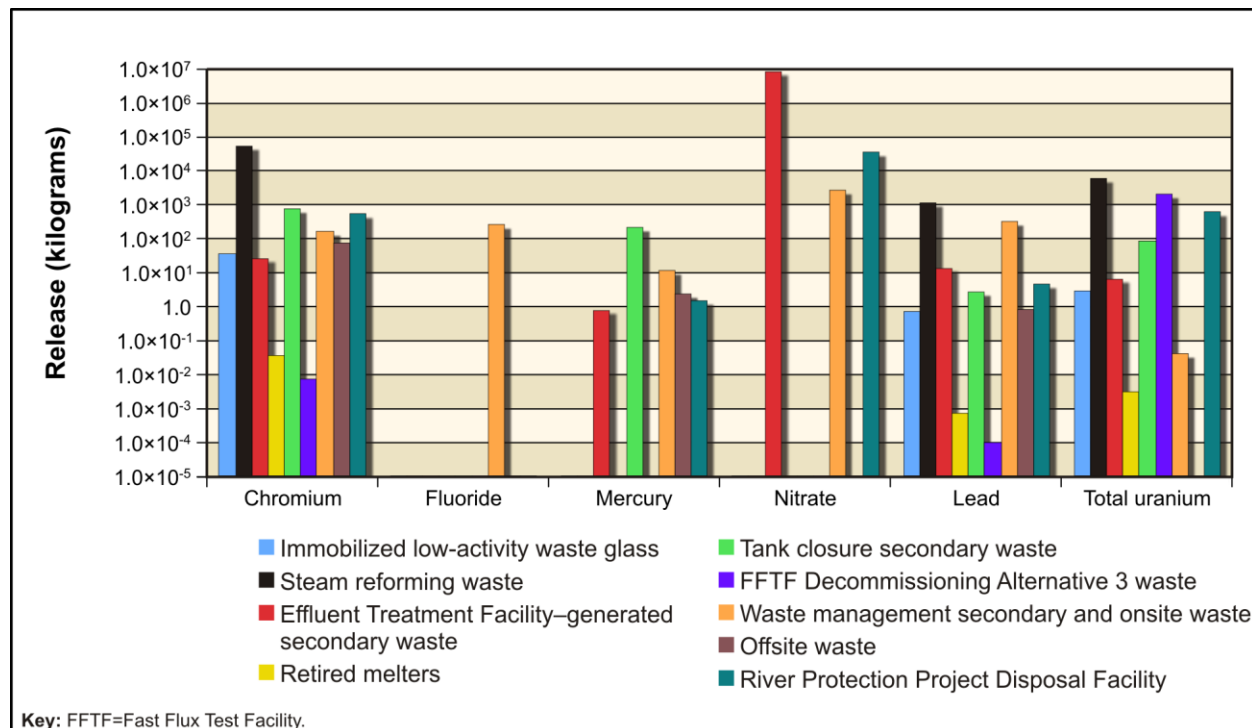
Figure M–71. Waste Management Alternative 2, Disposal Group 1, Subgroup 1-D, Chemical Releases to the Vadose Zone

M.4.3.2.5   Waste Management Alternative 2: Disposal in IDF, 200-East Area Only, Disposal Group 1, Subgroup 1-E

Disposal Group 1, Subgroup 1-E, addresses the waste resulting from Tank Closure Alternative 4, onsite non-CERCLA sources, FFTF decommissioning, waste management, and other DOE sites. Waste forms for IDF-East include the following:

- ILAW glass
- LAW melters
- bulk vitrification glass
- Cast stone waste
- Tank closure secondary waste
- FFTF decommissioning secondary waste
- Waste management secondary waste
- Offsite waste
- Onsite non-CERCLA waste

Waste forms for the RPPDF include those resulting from tank closure cleanup activities under Tank Closure Alternative 4. Potential releases to the vadose zone under Waste Management Alternative 2, Disposal Group 1, Subgroup 1-E, are indicated in Table M–36 and Figures M–72 and M–73.

Table M–36. Waste Management Alternative 2, Disposal Group 1, Subgroup 1-E, Radionuclide and Chemical Releases to the Vadose Zone

Source	Radionuclide (curies)										Chemical (kilograms)					
	H-3	C-14	Sr-90	Tc-99	I-129	Cs-137	Np-237	U-238	Pu-239	Am-241	Cr	F	Hg	NO$_3$	Pb	Utot
ILAW glass	–	–	1.66×10^{-2}	2.31	7.78×10^{-4}	2.90×10^{-1}	2.51×10^{-5}	5.57×10^{-3}	1.49×10^{-3}	–	3.74×10^{1}	–	–	–	7.67×10^{-1}	3.63
BV waste glass	–	–	1.95×10^{-1}	6.18×10^{2}	3.08×10^{-4}	1.90	9.54×10^{-5}	3.00×10^{-3}	9.04×10^{-2}	–	1.47×10^{1}	–	–	–	3.55×10^{-1}	1.97
Cast stone waste	4.66×10^{3}	2.77×10^{2}	7.46×10^{1}	1.09×10^{4}	4.94×10^{-1}	1.04×10^{3}	2.77×10^{-4}	8.16×10^{-1}	1.02×10^{-3}	–	1.78×10^{5}	–	2.86×10^{1}	2.73×10^{7}	4.33×10^{1}	5.64×10^{2}
ETF-generated secondary waste	–	1.18	7.88	3.53×10^{1}	1.66	1.61×10^{-1}	1.22×10^{-2}	7.05×10^{-3}	3.79×10^{-6}	–	2.31×10^{1}	–	7.05×10^{-1}	5.20×10^{6}	7.43	5.89
Retired melters	–	–	1.92×10^{-5}	2.65×10^{-3}	8.94×10^{-7}	3.32×10^{-4}	3.12×10^{-8}	6.40×10^{-6}	1.71×10^{-6}	–	4.32×10^{-2}	–	–	–	8.80×10^{-4}	4.15×10^{-3}
TC secondary waste	–	–	7.36×10^{4}	1.28×10^{2}	4.28×10^{-2}	9.27×10^{2}	2.80×10^{-2}	1.50×10^{-1}	3.63×10^{-1}	–	8.21×10^{2}	–	2.10×10^{2}	–	2.93	9.22×10^{1}
FFTF Decommissioning Alternative 3 waste	2.29	1.86×10^{1}	–	2.72×10^{1}	–	1.94×10^{-5}	–	–	–	–	7.51×10^{-3}	–	–	–	9.74×10^{-5}	2.16×10^{3}
FFTF Decommissioning Alternative 2 waste	2.29	2.18×10^{-4}	–	1.48×10^{-2}	–	1.88×10^{-5}	–	–	–	–	7.49×10^{-3}	–	–	–	9.41×10^{-5}	1.82×10^{-3}
WM secondary and onsite waste	3.66×10^{3}	2.29×10^{-1}	3.31×10^{2}	1.35	4.19×10^{-5}	1.42×10^{1}	7.33×10^{-4}	3.26×10^{-2}	1.62×10^{-2}	1.46×10^{-3}	1.83×10^{2}	2.74×10^{2}	1.23×10^{1}	2.97×10^{3}	3.45×10^{2}	4.20×10^{-2}
Offsite waste	5.57×10^{4}	2.25×10^{2}	6.05×10^{4}	1.46×10^{3}	2.26	5.16×10^{3}	3.07×10^{-1}	3.48×10^{2}	9.20×10^{-1}	1.50×10^{-2}	8.05×10^{1}	–	2.53	–	8.70×10^{-1}	–
RPPDF	1.50	2.61	7.31	3.14×10^{1}	5.84×10^{-2}	1.57	7.75×10^{-2}	4.99	6.83×10^{-1}	–	1.86×10^{3}	–	9.23×10^{-1}	7.78×10^{4}	6.31	4.85×10^{3}

Note: To convert kilograms to pounds, multiply by 2.2046.

Key: Am-241=americium-241; BV=bulk vitrification; C-14=carbon-14; Cr=chromium; Cs-137=cesium-137; ETF=Effluent Treatment Facility; F=fluoride; FFTF=Fast Flux Test Facility; H-3=hydrogen-3 (tritium); Hg=mercury; I-129=iodine-129; ILAW=immobilized low-activity waste; NO$_3$=nitrate; Np-237=neptunium-237; Pb=lead; Pu-239=plutonium-239; RPPDF=River Protection Project Disposal Facility; Sr-90=strontium-90; TC=tank closure; Tc-99=technetium-99; U-238=uranium-238; Utot=total uranium; WM=waste management.
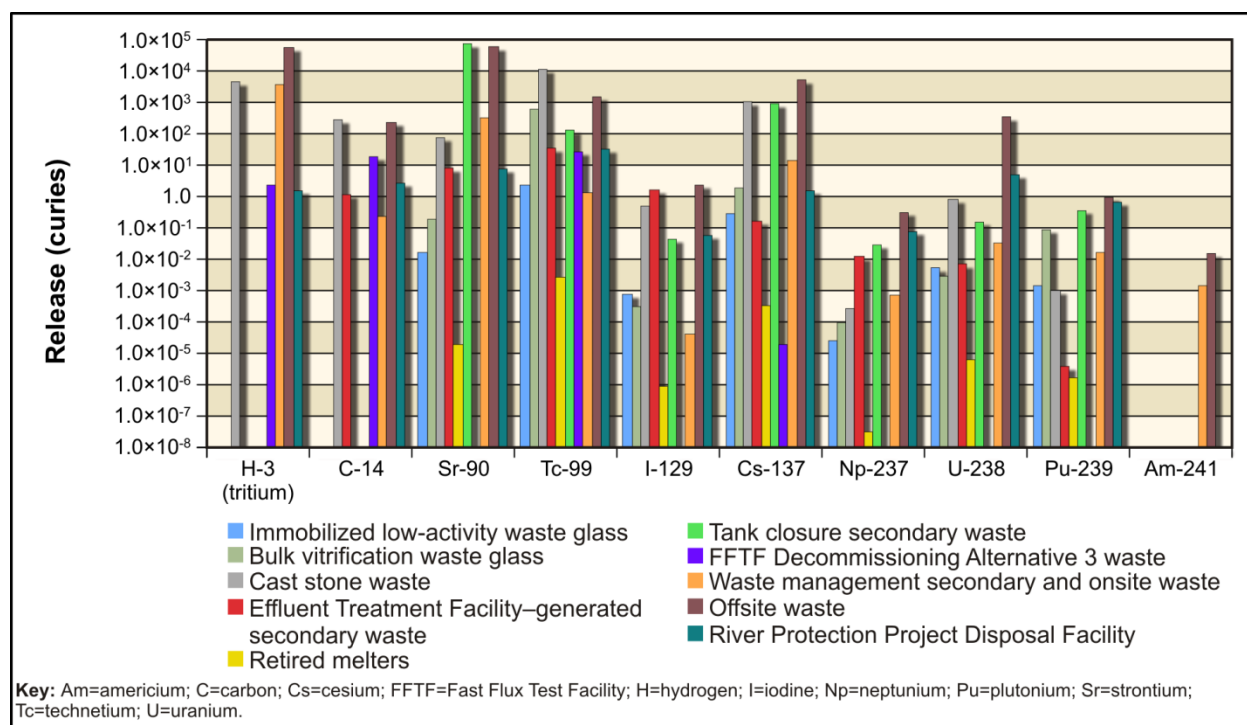
Figure M–72. Waste Management Alternative 2, Disposal Group 1, Subgroup 1-E, Radionuclide Releases to the Vadose Zone
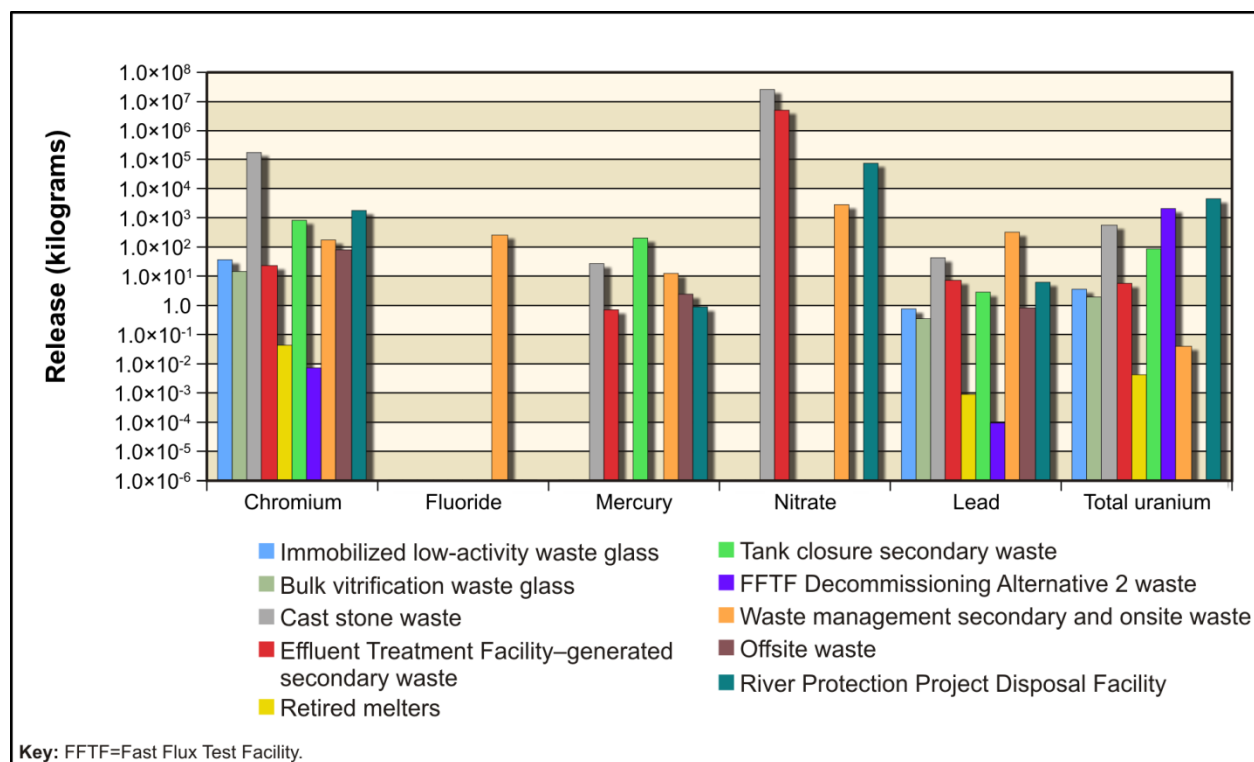
Figure M–73. Waste Management Alternative 2, Disposal Group 1, Subgroup 1-E, Chemical Releases to the Vadose Zone

M.4.3.2.6 **Waste Management Alternative 2: Disposal in IDF, 200-East Area Only, Disposal Group 1, Subgroup 1-F**

Disposal Group 1, Subgroup 1-F, addresses the waste resulting from Tank Closure Alternative 5, onsite non-CERCLA sources, FFTF decommissioning, waste management, and other DOE sites. Waste forms for IDF-East include the following:

- ILAW glass
- LAW melters
- bulk vitrification glass
- Cast stone waste
- Sulfate grout
- Tank closure secondary waste
- FFTF decommissioning secondary waste
- Waste management secondary waste
- Offsite waste
- Onsite non-CERCLA waste

The RPPDF would not be constructed or operated under Tank Closure Alternative 5 because tank closure cleanup activities would not be conducted. Potential releases to the vadose zone under Waste Management Alternative 2, Disposal Group 1, Subgroup 1-F, are indicated in Table M–37 and Figures M–74 and M–75.

Table M–37. Waste Management Alternative 2, Disposal Group 1, Subgroup 1-F, Radionuclide and Chemical Releases to the Vadose Zone
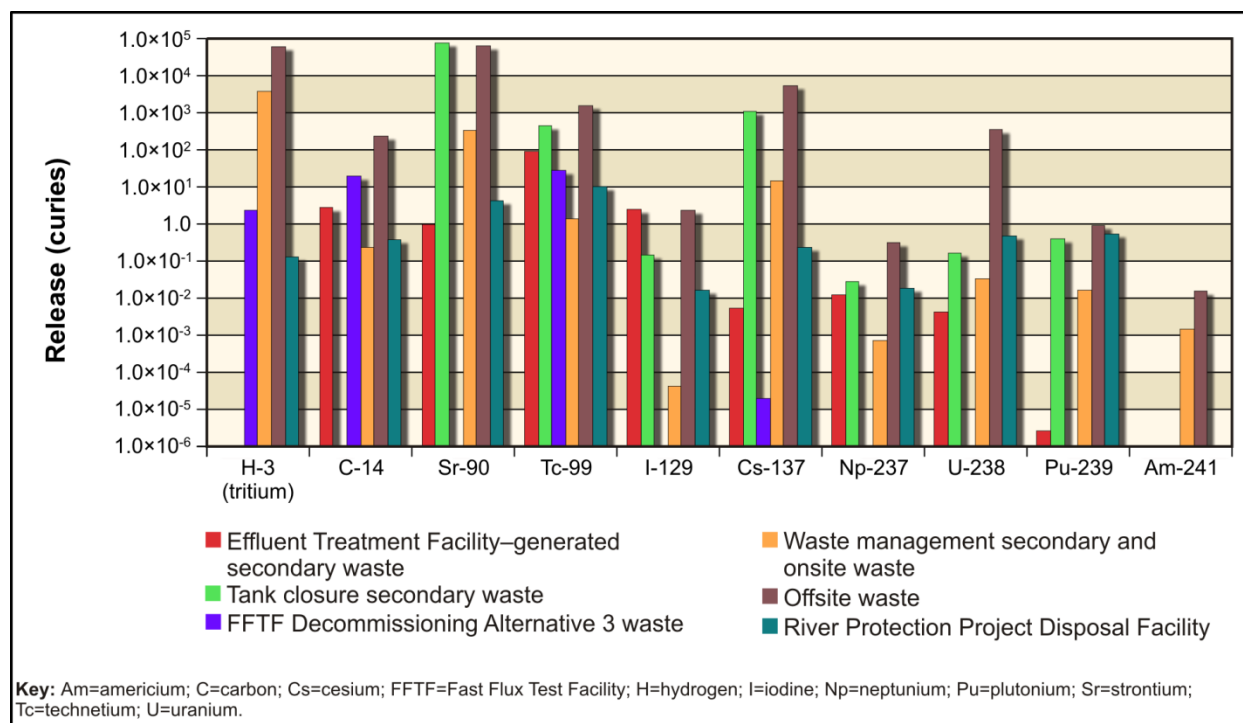
Source	Radionuclide (curies)										Chemical (kilograms)					
	H-3	**C-14**	**Sr-90**	**Tc-99**	**I-129**	**Cs-137**	**Np-237**	**U-238**	**Pu-239**	**Am-241**	**Cr**	**F**	**Hg**	**NO$_3$**	**Pb**	**Utot**
ILAW glass	–	–	1.34×10^{-7}	3.79	1.28×10^{-3}	3.04×10^{-1}	1.08×10^{-6}	7.39×10^{-3}	1.47×10^{-4}	–	6.09×10^{-3}	–	–	–	1.22×10^{-4}	5.15
BV waste glass	–	–	1.76×10^{-1}	5.57×10^{2}	2.77×10^{-4}	1.90	8.60×10^{-5}	2.70×10^{-3}	8.17×10^{-2}	–	1.34×10^{1}	–	–	–	3.19×10^{-1}	1.78
Cast stone waste	1.60×10^{3}	9.53×10^{1}	2.56×10^{1}	3.74×10^{3}	1.70×10^{-1}	3.51×10^{2}	9.50×10^{-5}	2.79×10^{-1}	3.49×10^{-4}	–	6.10×10^{4}	–	9.80	9.34×10^{6}	1.48×10^{1}	1.94×10^{2}
ETF-generated secondary waste	–	3.37×10^{-1}	7.09	5.03×10^{1}	2.06	1.62×10^{-1}	1.11×10^{-2}	6.47×10^{-3}	3.41×10^{-6}	–	1.15×10^{1}	–	6.90×10^{-1}	1.20×10^{7}	6.66	5.42
Retired melters	–	–	1.36×10^{-10}	3.84×10^{-3}	1.30×10^{-6}	3.10×10^{-4}	1.10×10^{-9}	7.53×10^{-6}	1.50×10^{-7}	–	6.20×10^{-6}	–	–	–	1.24×10^{-7}	5.23×10^{-3}
Sulfate grout	–	–	1.05×10^{2}	–	–	1.57×10^{2}	1.54×10^{-5}	–	2.17×10^{-4}	–	2.21×10^{5}	–	–	–	6.46×10^{1}	–
TC secondary waste	–	–	7.05×10^{4}	2.08×10^{2}	7.48×10^{-2}	8.84×10^{2}	2.69×10^{-2}	1.45×10^{-1}	3.49×10^{-1}	–	3.32×10^{2}	–	2.19×10^{2}	–	2.70	8.99×10^{1}
FFTF Decommissioning Alternative 3 waste	2.29	1.86×10^{1}	–	2.72×10^{1}	–	1.94×10^{-5}	–	–	–	–	7.51×10^{-3}	–	–	–	9.74×10^{-5}	2.16×10^{3}
FFTF Decommissioning Alternative 2 waste	2.29	2.18×10^{-4}	–	1.48×10^{-2}	–	1.88×10^{-5}	–	–	–	–	7.49×10^{-3}	–	–	–	9.41×10^{-5}	1.82×10^{-3}
WM secondary and onsite waste	3.66×10^{3}	2.29×10^{-1}	3.31×10^{2}	1.35	4.19×10^{-5}	1.42×10^{1}	7.33×10^{-4}	3.26×10^{-2}	1.62×10^{-2}	1.46×10^{-3}	1.83×10^{2}	2.74×10^{2}	1.23×10^{1}	2.97×10^{3}	3.45×10^{2}	4.20×10^{-2}
Offsite waste	5.57×10^{4}	2.25×10^{2}	6.05×10^{4}	1.46×10^{3}	2.26	5.16×10^{3}	3.07×10^{-1}	3.48×10^{2}	9.20×10^{-1}	1.50×10^{-2}	8.05×10^{1}	–	2.53	–	8.70×10^{-1}	–

Note: To convert kilograms to pounds, multiply by 2.2046.
Key: Am-241=americium-241; BV=bulk vitrification; C-14=carbon-14; Cr=chromium; Cs-137=cesium-137; ETF=Effluent Treatment Facility; F=fluoride; FFTF=Fast Flux Test Facility; H-3=hydrogen-3 (tritium); Hg=mercury; I-129=iodine-129; ILAW=immobilized low-activity waste; NO$_3$=nitrate; Np-237=neptunium-237; Pb=lead; Pu-239=plutonium-239; Sr-90=strontium-90; TC=tank closure; Tc-99=technetium-99; U-238=uranium-238; Utot=total uranium; WM=waste management.
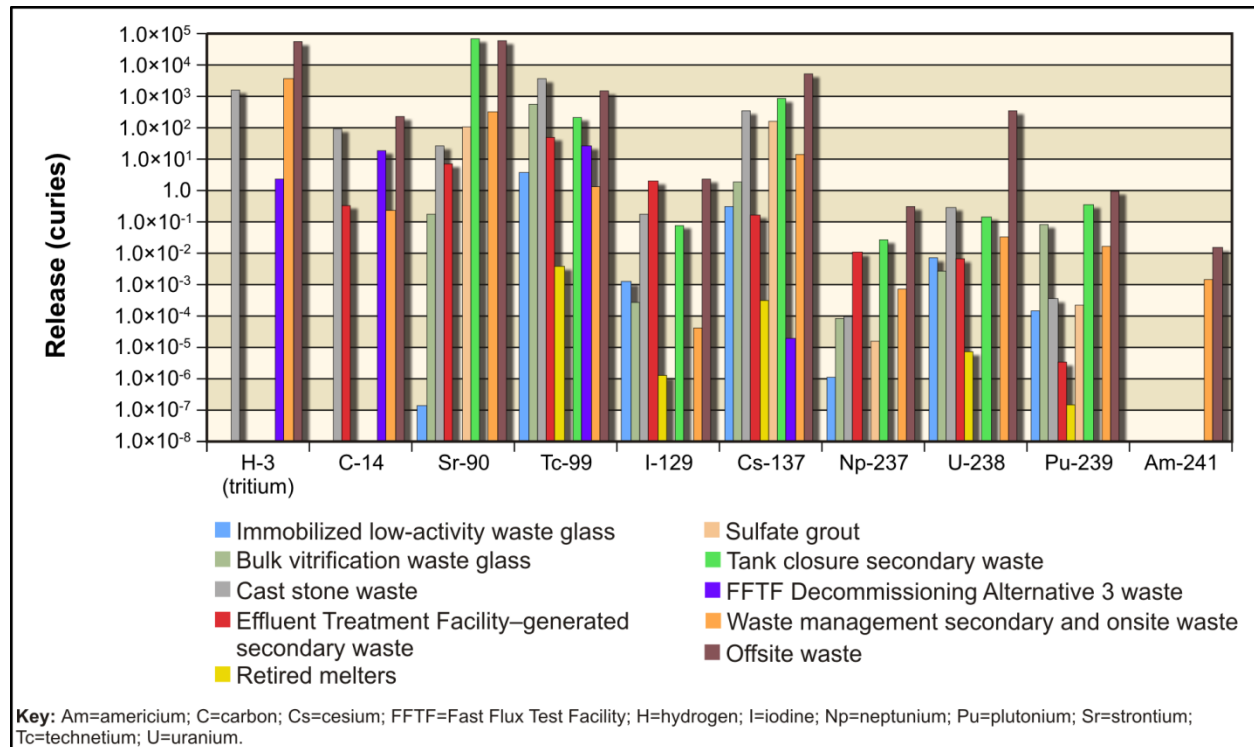
Figure M–74. Waste Management Alternative 2, Disposal Group 1, Subgroup 1-F,
Radionuclide Releases to the Vadose Zone
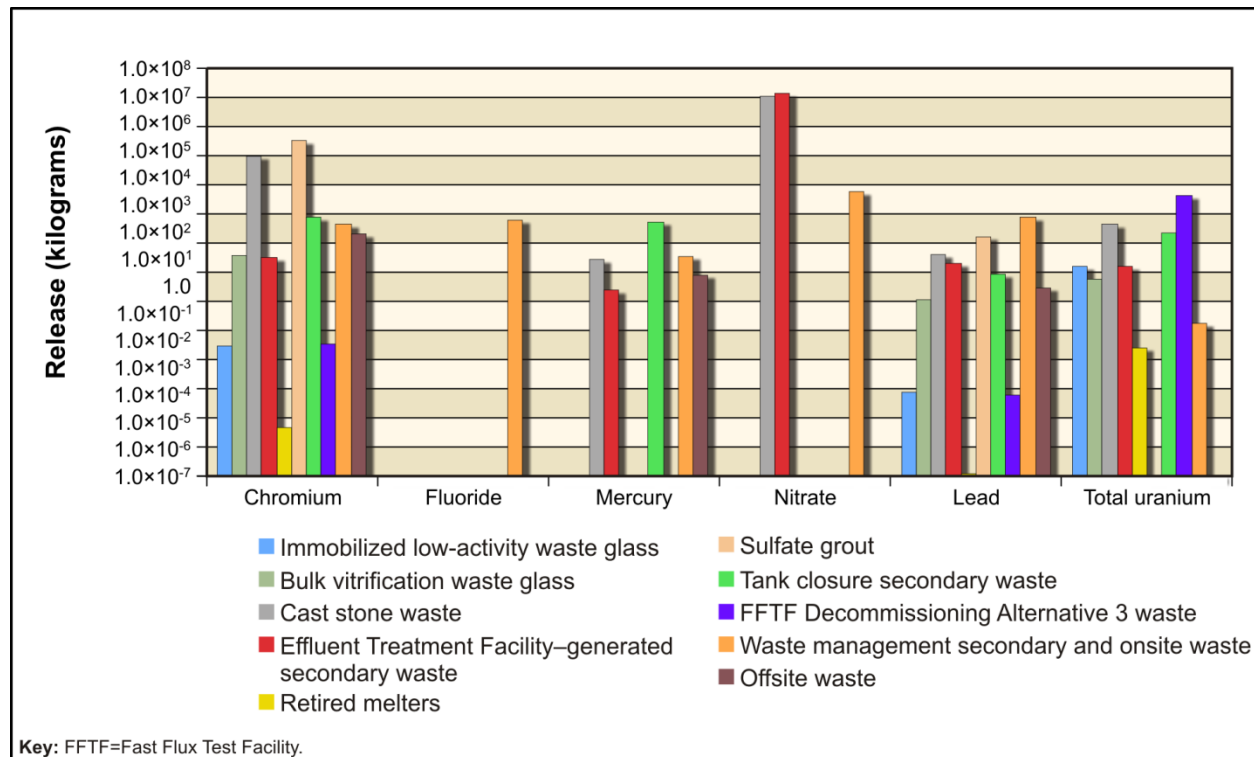
Figure M–75. Waste Management Alternative 2, Disposal Group 1, Subgroup 1-F,
Chemical Releases to the Vadose Zone

M.4.3.2.7   Waste Management Alternative 2: Disposal in IDF, 200-East Area Only, Disposal Group 1, Subgroup 1-G

Disposal Group 1, Subgroup 1-G, addresses the waste resulting from Tank Closure Alternative 6C, onsite non-CERCLA sources, FFTF decommissioning, waste management, and other DOE sites. Waste forms for IDF-East include the following:

- Tank closure secondary waste
- FFTF decommissioning secondary waste
- Waste management secondary waste
- Offsite waste
- Onsite non-CERCLA waste

Waste forms for the RPPDF include those resulting from tank closure cleanup activities under Tank Closure Alternative 6C. Potential releases to the vadose zone under Waste Management Alternative 2, Disposal Group 1, Subgroup 1-G, are indicated in Table M–38 and Figures M–76 and M–77.

Table M–38. Waste Management Alternative 2, Disposal Group 1, Subgroup 1-G, Radionuclide and Chemical Releases to the Vadose Zone

| Source	Radionuclide (curies)										Chemical (kilograms)					
	H-3	**C-14**	**Sr-90**	**Tc-99**	**I-129**	**Cs-137**	**Np-237**	**U-238**	**Pu-239**	**Am-241**	**Cr**	**F**	**Hg**	**NO$_3$**	**Pb**	**Utot**
ETF-generated secondary waste	–	2.77	9.24×10^{-1}	8.62×10^{1}	2.50	5.44×10^{-3}	1.20×10^{-2}	4.24×10^{-3}	2.76×10^{-6}	–	4.43×10^{1}	–	8.07×10^{-1}	9.01×10^{6}	8.36×10^{-2}	4.21
TC secondary waste	–	–	7.35×10^{4}	4.31×10^{2}	1.45×10^{-1}	1.02×10^{3}	2.81×10^{-2}	1.61×10^{-1}	3.95×10^{-1}	–	1.94×10^{3}	–	2.39×10^{2}	–	3.29	1.03×10^{2}
FFTF Decommissioning Alternative 3 waste	2.29	1.86×10^{1}	–	2.72×10^{1}	–	1.94×10^{-5}	–	–	–	–	7.51×10^{-3}	–	–	–	9.74×10^{-5}	2.16×10^{3}
FFTF Decommissioning Alternative 2 waste	2.29	2.18×10^{-4}	–	1.48×10^{-2}	–	1.88×10^{-5}	–	–	–	–	7.49×10^{-3}	–	–	–	9.41×10^{-5}	1.82×10^{-3}
WM secondary and onsite waste	3.66×10^{3}	2.29×10^{-1}	3.31×10^{2}	1.35	4.19×10^{-5}	1.42×10^{1}	7.33×10^{-4}	3.26×10^{-2}	1.62×10^{-2}	1.46×10^{-3}	1.83×10^{2}	2.74×10^{2}	1.23×10^{1}	2.97×10^{3}	3.45×10^{2}	4.20×10^{-2}
Offsite waste	5.57×10^{4}	2.25×10^{2}	6.05×10^{4}	1.46×10^{3}	2.26	5.16×10^{3}	3.07×10^{-1}	3.48×10^{2}	9.20×10^{-1}	1.50×10^{-2}	8.05×10^{1}	–	2.53	–	8.70×10^{-1}	–
RPPDF	1.27×10^{-1}	3.61×10^{-1}	4.15	9.71	1.67×10^{-2}	2.30×10^{-1}	1.85×10^{-2}	4.66×10^{-1}	5.31×10^{-1}	–	5.86×10^{2}	–	1.61	3.93×10^{4}	4.97	6.60×10^{2}

Note: To convert kilograms to pounds, multiply by 2.2046.

Key: Am-241=americium-241; C-14=carbon-14; Cr=chromium; Cs-137=cesium-137; ETF=Effluent Treatment Facility; F=fluoride; FFTF=Fast Flux Test Facility; H-3=hydrogen-3 (tritium); Hg=mercury; I-129=iodine-129; ILAW=immobilized low-activity waste; NO$_3$=nitrate; Np-237=neptunium-237; Pb=lead; Pu-239=plutonium-239; RPPDF=River Protection Project Disposal Facility; Sr-90=strontium-90; TC=tank closure; Tc-99=technetium-99; U-238=uranium-238; Utot=total uranium; WM=waste management.

Figure M–76. Waste Management Alternative 2, Disposal Group 1, Subgroup 1-G, Radionuclide Releases to the Vadose Zone
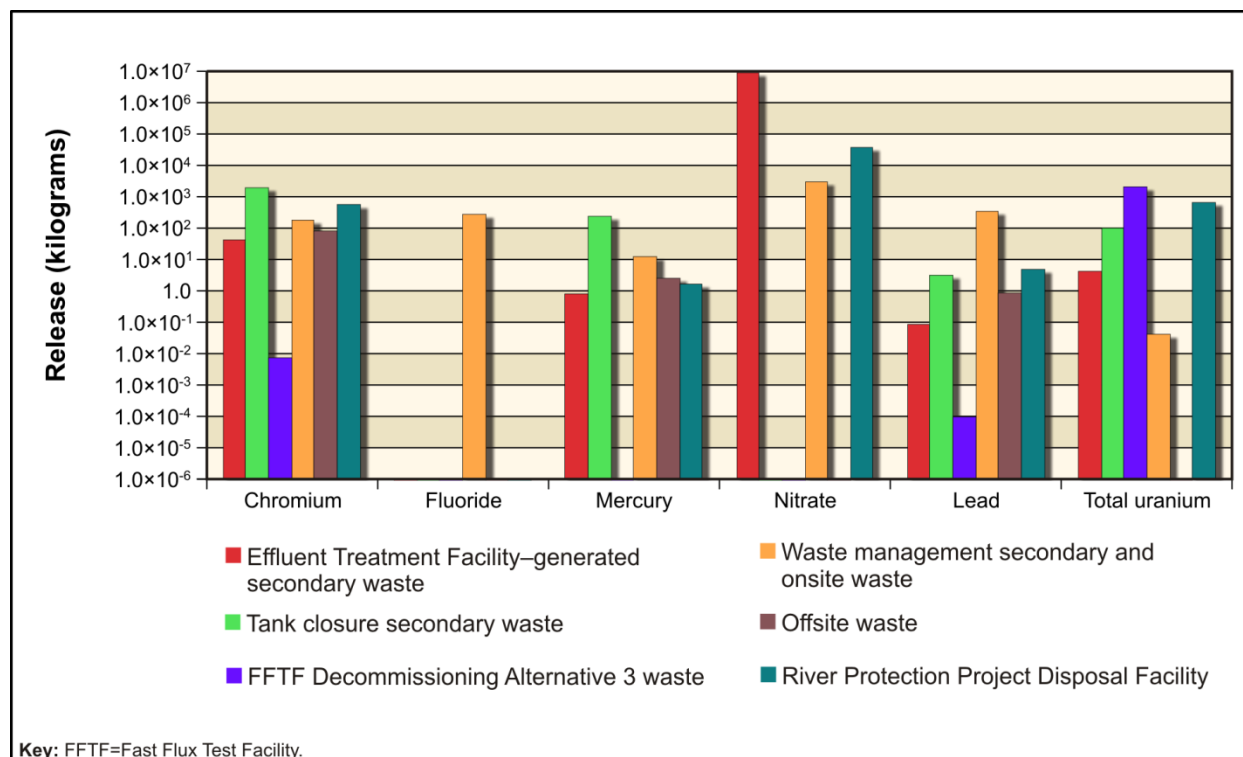
Figure M–77. Waste Management Alternative 2, Disposal Group 1, Subgroup 1-G, Chemical Releases to the Vadose Zone

M.4.3.2.8   Waste Management Alternative 2: Disposal in IDF, 200-East Area Only, Disposal Group 2, Subgroup 2-A

Disposal Group 2, Subgroup 2-A, addresses the waste resulting from Tank Closure Alternative 2A, onsite non-CERCLA sources, FFTF decommissioning, waste management, and other DOE sites. Waste forms for IDF-East include the following:

- ILAW glass
- LAW melters
- Tank closure secondary waste
- FFTF decommissioning secondary waste
- Waste management secondary waste
- Offsite waste
- Onsite non-CERCLA waste

The RPPDF would not be constructed or operated under Tank Closure Alternative 2A because tank closure cleanup activities would not be conducted. Potential releases to the vadose zone under Waste Management Alternative 2, Disposal Group 2, Subgroup 2-A, are indicated in Table M–39 and Figures M–78 and M–79.

Table M–39. Waste Management Alternative 2, Disposal Group 2, Subgroup 2-A, Radionuclide and Chemical Releases to the Vadose Zone

| Source	Radionuclide (curies)										Chemical (kilograms)					
	H-3	C-14	Sr-90	Tc-99	I-129	Cs-137	Np-237	U-238	Pu-239	Am-241	Cr	F	Hg	NO$_3$	Pb	Utot
ILAW glass	–	–	2.71×10^{-3}	7.81	2.63×10^{-3}	5.38×10^{-1}	2.30×10^{-6}	1.51×10^{-2}	3.48×10^{-4}	–	1.26×10^{2}	–	–	–	2.46	1.04×10^{1}
ETF-generated secondary waste	–	2.76	9.19×10^{-1}	8.62×10^{1}	2.48	5.41×10^{-3}	1.19×10^{-2}	4.22×10^{-3}	2.74×10^{-6}	–	4.43×10^{1}	–	8.03×10^{-1}	9.01×10^{6}	8.31×10^{-2}	4.19
Retired melters	–	–	2.91×10^{-6}	8.38×10^{-3}	2.84×10^{-6}	5.78×10^{-4}	2.46×10^{-9}	1.62×10^{-5}	3.74×10^{-7}	–	1.35×10^{-1}	–	–	–	2.62×10^{-3}	1.10×10^{-2}
TC secondary waste	–	–	7.32×10^{4}	4.31×10^{2}	1.45×10^{-1}	1.02×10^{3}	2.80×10^{-2}	1.60×10^{-1}	3.92×10^{-1}	–	1.94×10^{3}	–	2.38×10^{2}	–	3.27	1.02×10^{2}
FFTF Decommissioning Alternative 3 waste	2.29	1.85×10^{1}	–	2.72×10^{1}	–	1.93×10^{-5}	–	–	–	–	7.51×10^{-3}	–	–	–	9.67×10^{-5}	2.15×10^{3}
FFTF Decommissioning Alternative 2 waste	2.29	2.16×10^{-4}	–	1.48×10^{-2}	–	1.87×10^{-5}	–	–	–	–	7.49×10^{-3}	–	–	–	9.34×10^{-5}	1.81×10^{-3}
WM secondary and onsite waste	3.66×10^{3}	2.27×10^{-1}	3.29×10^{2}	1.35	4.17×10^{-5}	1.41×10^{1}	7.29×10^{-4}	3.24×10^{-2}	1.61×10^{-2}	1.44×10^{-3}	1.83×10^{2}	2.74×10^{2}	1.22×10^{1}	2.97×10^{3}	3.43×10^{2}	4.17×10^{-2}
Offsite waste	5.57×10^{4}	2.24×10^{2}	6.01×10^{4}	1.46×10^{3}	2.26	5.12×10^{3}	3.05×10^{-1}	3.48×10^{2}	9.13×10^{-1}	1.49×10^{-2}	8.05×10^{1}	–	2.52	–	8.63×10^{-1}	–

Note: To convert kilograms to pounds, multiply by 2.2046.

Key: Am-241=americium-241; C-14=carbon-14; Cr=chromium; Cs-137=cesium-137; ETF=Effluent Treatment Facility; F=fluoride; FFTF=Fast Flux Test Facility; H-3=hydrogen-3 (tritium); Hg=mercury; I-129=iodine-129; ILAW=immobilized low-activity waste; NO$_3$=nitrate; Np-237=neptunium-237; Pb=lead; Pu-239=plutonium-239; Sr-90=strontium-90; TC=tank closure; Tc-99=technetium-99; U-238=uranium-238; Utot=total uranium; WM=waste management.
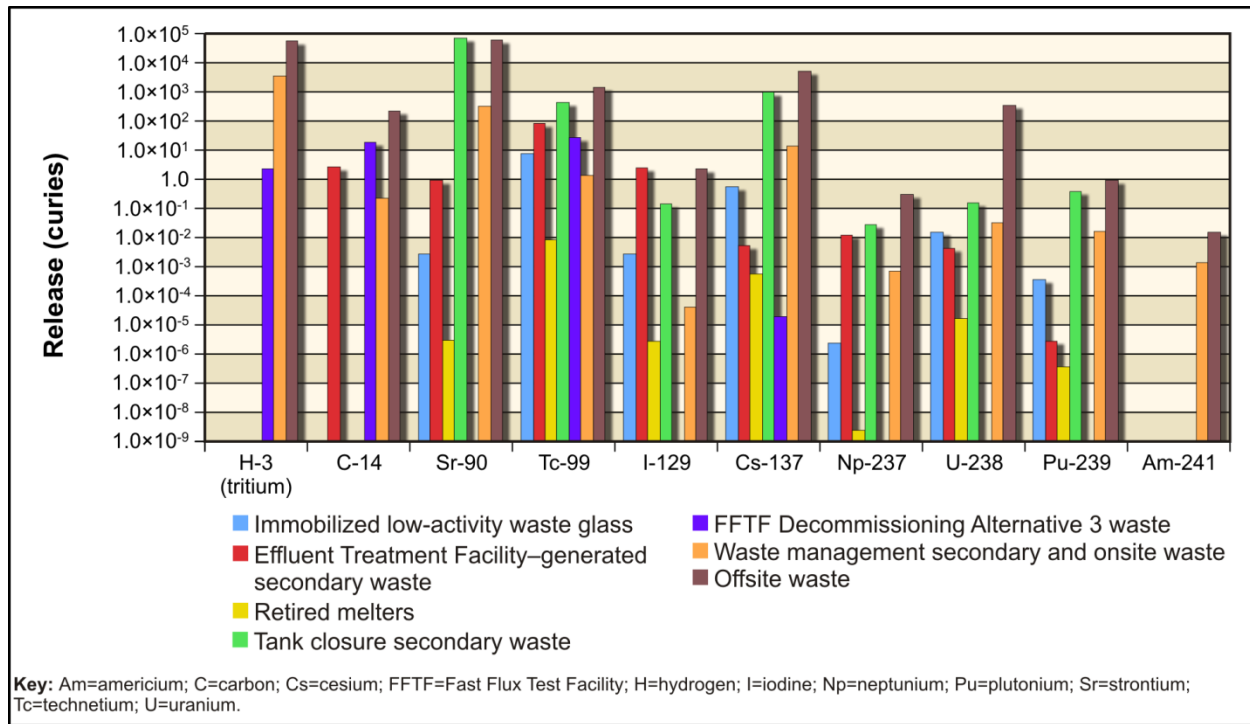
**Figure M–78. Waste Management Alternative 2, Disposal Group 2, Subgroup 2-A,
Radionuclide Releases to the Vadose Zone**
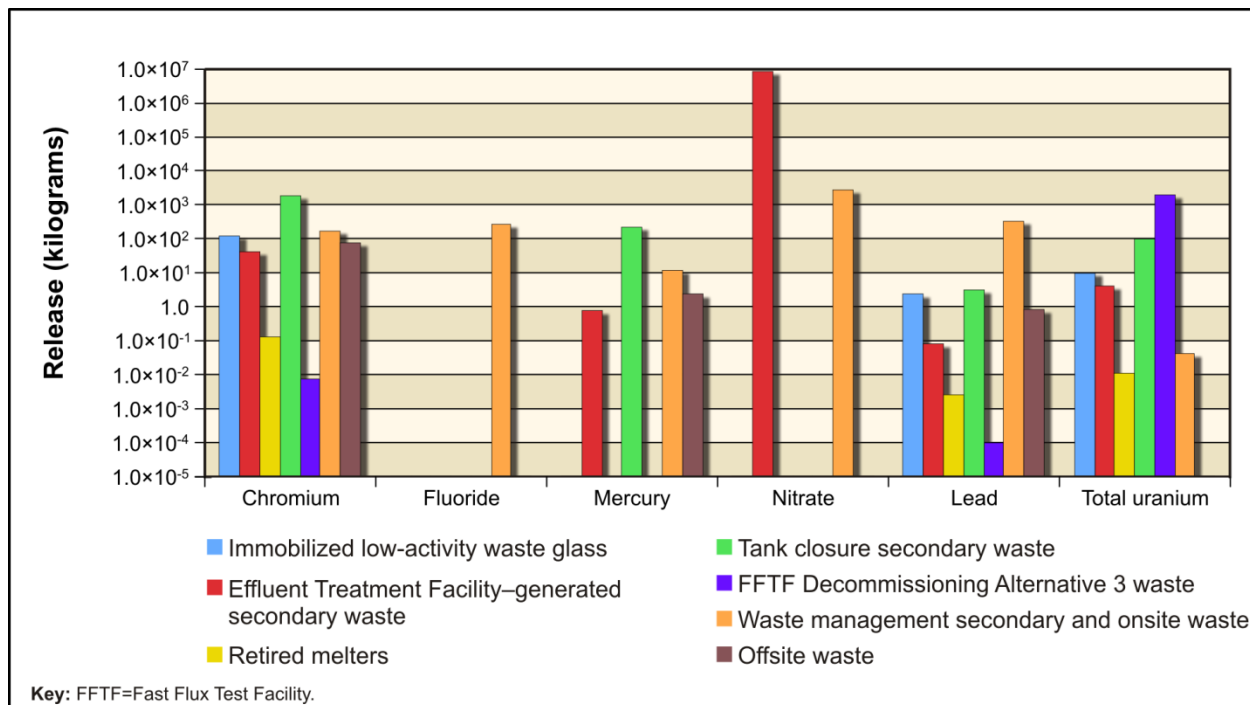
**Figure M–79. Waste Management Alternative 2, Disposal Group 2, Subgroup 2-A,
Chemical Releases to the Vadose Zone**

M.4.3.2.9   Waste Management Alternative 2: Disposal in IDF, 200-East Area Only, Disposal Group 2, Subgroup 2-B

Disposal Group 2, Subgroup 2-B, addresses the waste resulting from Tank Closure Alternative 6B, Base and Option Cases; onsite non-CERCLA sources; FFTF decommissioning; waste management; and other DOE sites. Waste forms for IDF-East include the following:

- Preprocessing Facility (PPF) glass
- PPF melters
- Tank closure secondary waste
- FFTF decommissioning secondary waste
- Waste management secondary waste
- Offsite waste
- Onsite non-CERCLA waste

Waste forms for the RPPDF include those resulting from tank closure cleanup activities under Tank Closure Alternative 6B, Base and Option Cases. Potential releases to the vadose zone under Waste Management Alternative 2, Disposal Group 2, Subgroup 2-B, Base and Option Cases, are indicated in Tables M–40 and M–41 and Figures M–80 through M–83.

Table M–40. Waste Management Alternative 2, Disposal Group 2, Subgroup 2-B, Base Case, Radionuclide and Chemical Releases to the Vadose Zone

Source	Radionuclide (curies)										Chemical (kilograms)					
	H-3	**C-14**	**Sr-90**	**Tc-99**	**I-129**	**Cs-137**	**Np-237**	**U-238**	**Pu-239**	**Am-241**	**Cr**	**F**	**Hg**	**NO$_3$**	**Pb**	**Utot**
ETF-generated secondary waste	–	2.78	9.24×10^{-1}	8.73×10^{1}	2.51	5.44×10^{-3}	1.20×10^{-2}	4.28×10^{-3}	2.75×10^{-6}	–	4.53×10^{1}	–	8.06×10^{-1}	9.16×10^{6}	8.37×10^{-2}	4.31
PPF glass	–	–	7.42×10^{-2}	3.52×10^{-2}	1.40×10^{-5}	2.36×10^{-1}	1.36×10^{-4}	2.03×10^{-3}	7.96×10^{-3}	–	2.20	–	–	–	7.05×10^{-2}	4.21
Retired melters	–	–	3.07×10^{-3}	1.46×10^{-3}	5.81×10^{-7}	9.80×10^{-3}	5.64×10^{-6}	8.40×10^{-5}	3.29×10^{-4}	–	9.12×10^{-2}	–	–	–	2.92×10^{-3}	1.74×10^{-1}
TC secondary waste	–	–	7.01×10^{4}	4.37×10^{2}	1.38×10^{-1}	9.77×10^{2}	2.68×10^{-2}	1.55×10^{-1}	3.75×10^{-1}	–	1.98×10^{3}	–	2.29×10^{2}	–	3.13	1.00×10^{2}
FFTF Decommissioning Alternative 3 waste	2.29	1.85×10^{1}	–	2.72×10^{1}	–	1.93×10^{-5}	–	–	–	–	7.51×10^{-3}	–	–	–	9.67×10^{-5}	2.15×10^{3}
FFTF Decommissioning Alternative 2 waste	2.29	2.16×10^{-4}	–	1.48×10^{-2}	–	1.87×10^{-5}	–	–	–	–	7.49×10^{-3}	–	–	–	9.34×10^{-5}	1.81×10^{-3}
WM secondary and onsite waste	3.66×10^{3}	2.27×10^{-1}	3.29×10^{2}	1.35	4.17×10^{-5}	1.41×10^{1}	7.29×10^{-4}	3.24×10^{-2}	1.61×10^{-2}	1.44×10^{-3}	1.83×10^{2}	2.74×10^{2}	1.22×10^{1}	2.97×10^{3}	3.43×10^{2}	4.17×10^{-2}
Offsite waste	5.57×10^{4}	2.24×10^{2}	6.01×10^{4}	1.46×10^{3}	2.26	5.12×10^{3}	3.05×10^{-1}	3.48×10^{2}	9.13×10^{-1}	1.49×10^{-2}	8.05×10^{1}	–	2.52	–	8.63×10^{-1}	–
RPPDF	4.57	5.80	1.80×10^{1}	1.78×10^{2}	3.43×10^{-1}	4.61	3.81×10^{-1}	9.87	1.22	–	4.10×10^{3}	–	1.73	2.83×10^{5}	5.15×10^{1}	7.66×10^{3}

Note: To convert kilograms to pounds, multiply by 2.2046.

Key: Am-241=americium-241; C-14=carbon-14; Cr=chromium; Cs-137=cesium-137; ETF=Effluent Treatment Facility; F=fluoride; FFTF=Fast Flux Test Facility; H-3=hydrogen-3 (tritium); Hg=mercury; I-129=iodine-129; NO$_3$=nitrate; Np-237=neptunium-237; Pb=lead; PPF=Preprocessing Facility; Pu-239=plutonium-239; RPPDF=River Protection Project Disposal Facility; Sr-90=strontium-90; TC=tank closure; Tc-99=technetium-99; U-238=uranium-238; Utot=total uranium; WM=waste management.
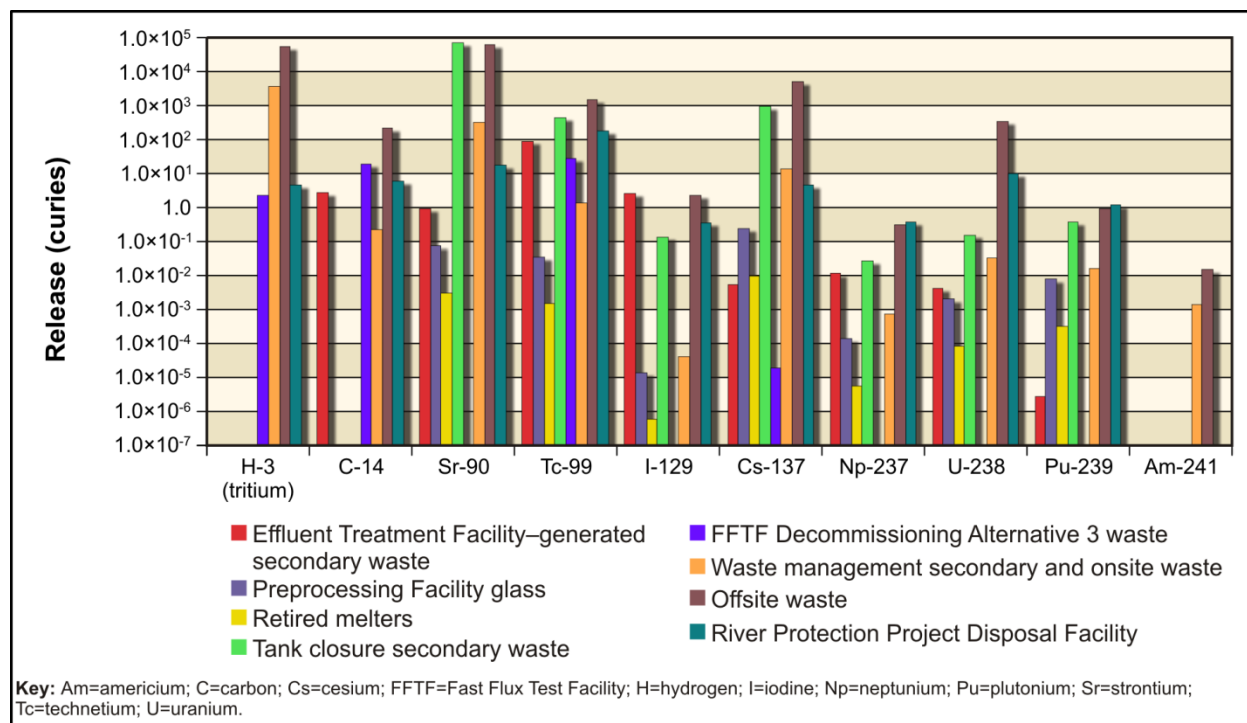
Figure M–80. Waste Management Alternative 2, Disposal Group 2, Subgroup 2-B, Base Case, Radionuclide Releases to the Vadose Zone
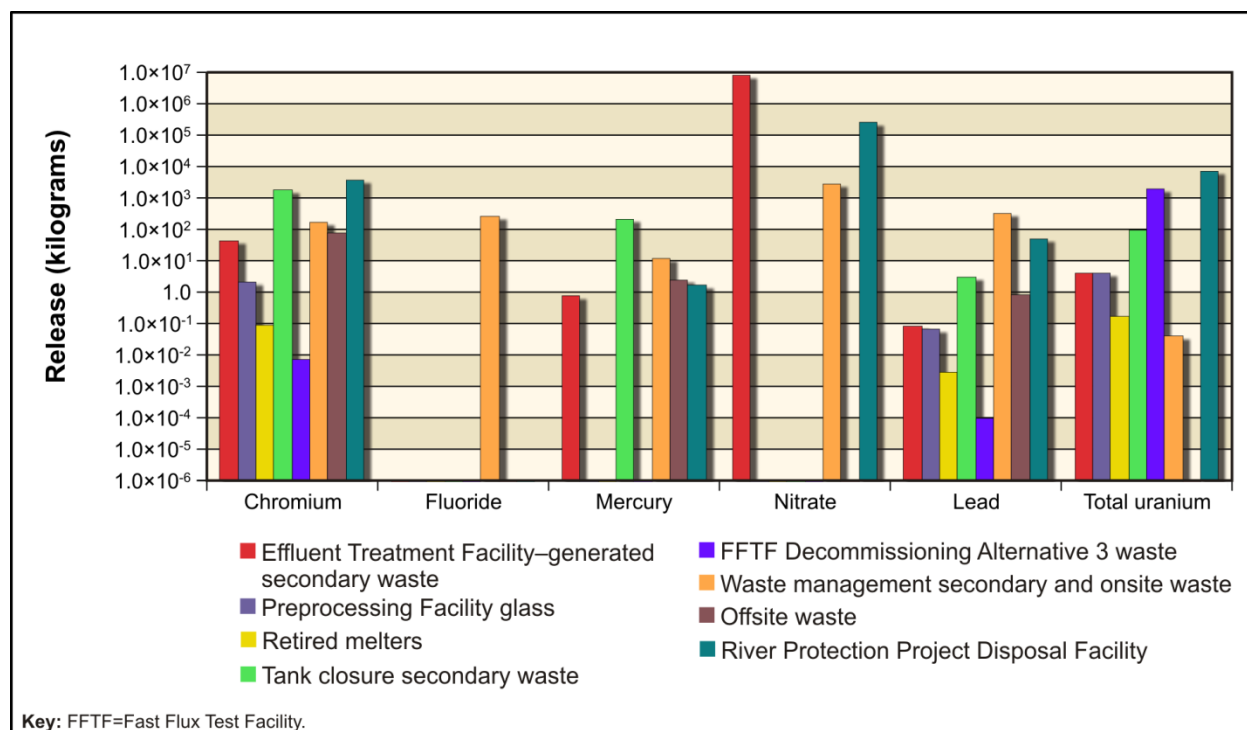
Figure M–81. Waste Management Alternative 2, Disposal Group 2, Subgroup 2-B, Base Case, Chemical Releases to the Vadose Zone
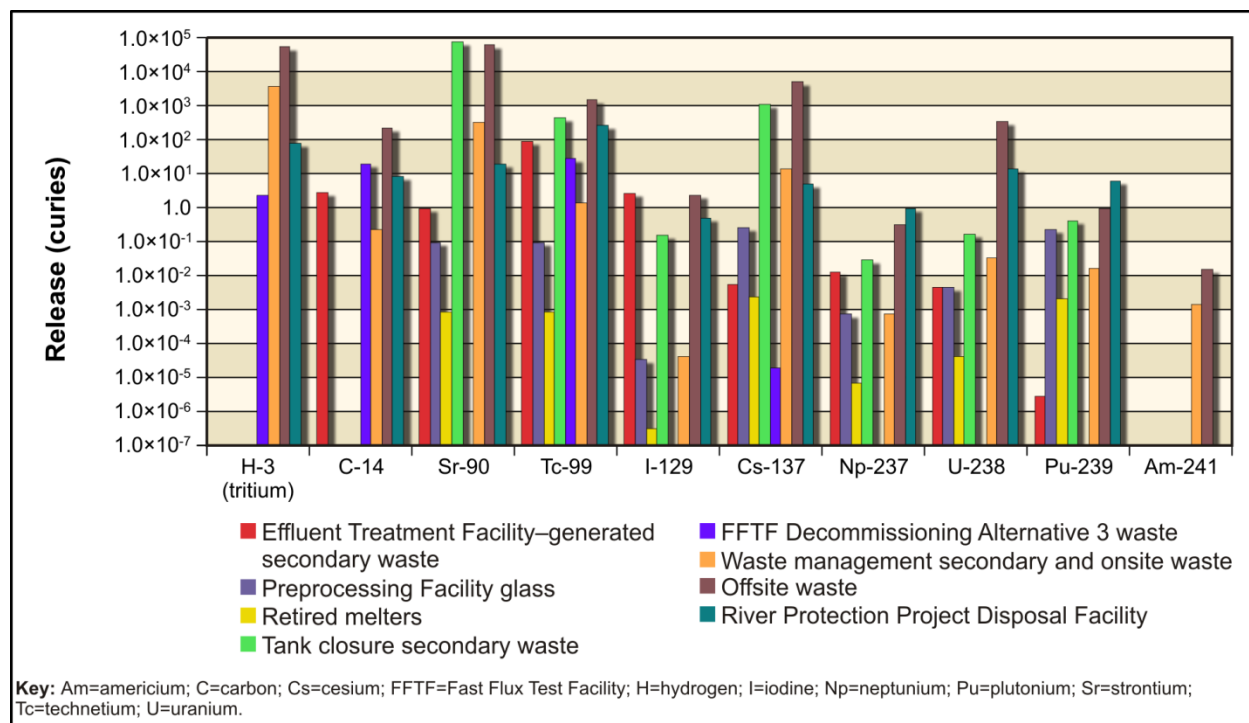
Table M–41. Waste Management Alternative 2, Disposal Group 2, Subgroup 2-B, Option Case, Radionuclide and Chemical Releases to the Vadose Zone

| Source	Radionuclide (curies)										Chemical (kilograms)					
	H-3	C-14	Sr-90	Tc-99	I-129	Cs-137	Np-237	U-238	Pu-239	Am-241	Cr	F	Hg	NO$_3$	Pb	Utot
ETF-generated secondary waste	–	2.82	9.29×10^{-1}	8.79×10^{1}	2.53	5.48×10^{-3}	1.23×10^{-2}	4.35×10^{-3}	2.80×10^{-6}	–	5.65×10^{1}	–	8.38×10^{-1}	1.51×10^{7}	8.41×10^{-2}	4.38
PPF glass	–	–	9.09×10^{-2}	9.19×10^{-2}	3.36×10^{-5}	2.63×10^{-1}	7.26×10^{-4}	4.57×10^{-3}	2.22×10^{-1}	–	4.32×10^{1}	–	–	–	8.45×10^{-2}	6.20
Retired melters	–	–	8.33×10^{-4}	8.40×10^{-4}	3.06×10^{-7}	2.41×10^{-3}	6.63×10^{-6}	4.19×10^{-5}	2.03×10^{-3}	–	1.93×10^{-1}	–	–	–	7.02×10^{-4}	4.68×10^{-2}
TC secondary waste	–	–	7.54×10^{4}	4.40×10^{2}	1.51×10^{-1}	1.05×10^{3}	2.92×10^{-2}	1.68×10^{-1}	4.10×10^{-1}	–	2.47×10^{3}	–	2.54×10^{2}	–	3.37	1.09×10^{2}
FFTF Decommissioning Alternative 3 waste	2.29	1.85×10^{1}	–	2.72×10^{1}	–	1.93×10^{-5}	–	–	–	–	7.51×10^{-3}	–	–	–	9.67×10^{-5}	2.15×10^{3}
FFTF Decommissioning Alternative 2 waste	2.29	2.16×10^{-4}	–	1.48×10^{-2}	–	1.87×10^{-5}	–	–	–	–	7.49×10^{-3}	–	–	–	9.34×10^{-5}	1.81×10^{-3}
WM secondary and onsite waste	3.66×10^{3}	2.27×10^{-1}	3.29×10^{2}	1.35	4.17×10^{-5}	1.41×10^{1}	7.29×10^{-4}	3.24×10^{-2}	1.61×10^{-2}	1.44×10^{-3}	1.83×10^{2}	2.74×10^{2}	1.22×10^{1}	2.97×10^{3}	3.43×10^{2}	4.17×10^{-2}
Offsite waste	5.57×10^{4}	2.24×10^{2}	6.01×10^{4}	1.46×10^{3}	2.26	5.12×10^{3}	3.05×10^{-1}	3.48×10^{2}	9.13×10^{-1}	1.49×10^{-2}	8.05×10^{1}	–	2.52	–	8.63×10^{-1}	–
RPPDF	7.95×10^{1}	8.26	1.89×10^{1}	2.70×10^{2}	4.96×10^{-1}	4.77	9.11×10^{-1}	1.37×10^{1}	5.94	–	3.69×10^{4}	–	1.15×10^{1}	1.04×10^{7}	5.29×10^{1}	9.24×10^{3}

Note: To convert kilograms to pounds, multiply by 2.2046.

Key: Am-241=americium-241; C-14=carbon-14; Cr=chromium; Cs-137=cesium-137; ETF=Effluent Treatment Facility; F=fluoride; FFTF=Fast Flux Test Facility; H-3=hydrogen-3 (tritium); Hg=mercury; I-129=iodine-129; NO$_3$=nitrate; Np-237=neptunium-237; Pb=lead; PPF=Preprocessing Facility; Pu-239=plutonium-239; RPPDF=River Protection Project Disposal Facility; Sr-90=strontium-90; TC=tank closure; Tc-99=technetium-99; U-238=uranium-238; Utot=total uranium; WM=waste management.

Figure M–82. Waste Management Alternative 2, Disposal Group 2, Subgroup 2-B, Option Case, Radionuclide Releases to the Vadose Zone
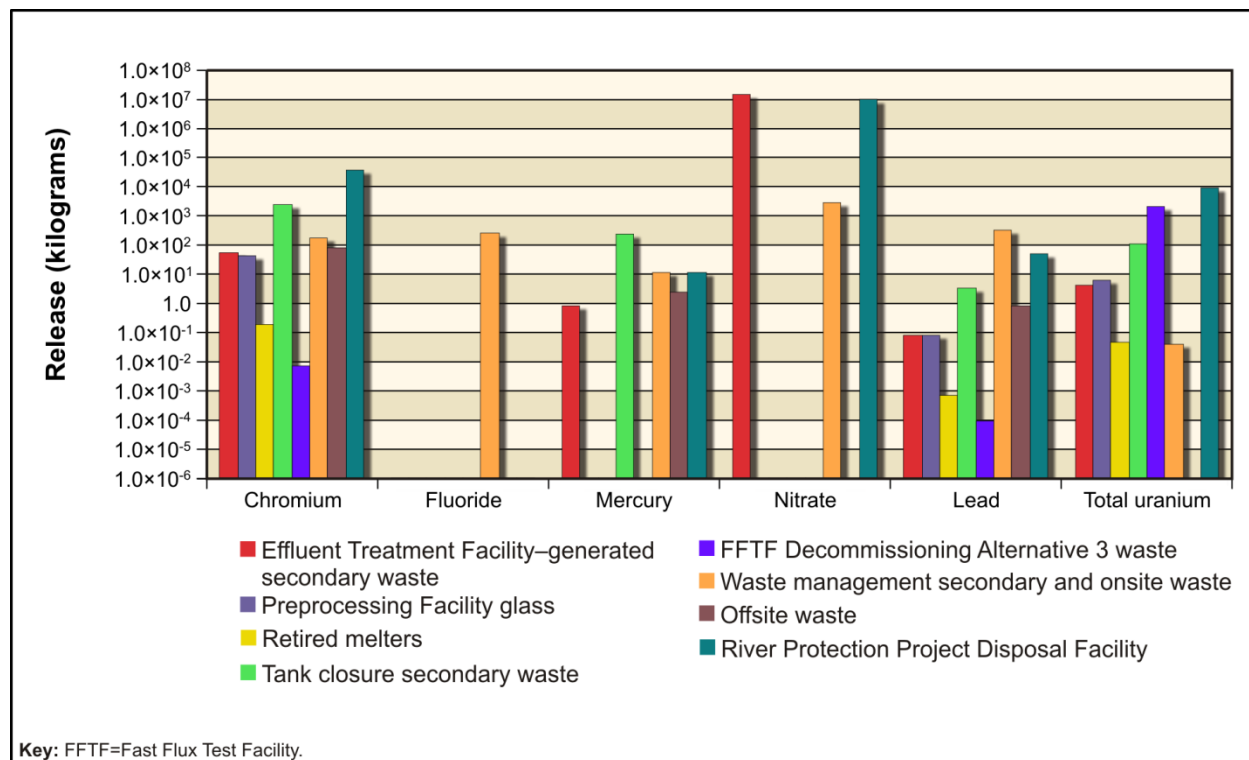
Figure M–83. Waste Management Alternative 2, Disposal Group 2, Subgroup 2-B, Option Case, Chemical Releases to the Vadose Zone

M.4.3.2.10   Waste Management Alternative 2: Disposal in IDF, 200-East Area Only, Disposal Group 3

Disposal Group 3 addresses the waste resulting from Tank Closure Alternative 6A, Base and Option Cases; onsite non-CERCLA sources; FFTF decommissioning; waste management; and other DOE sites. Waste forms for IDF-East include the following:

- PPF glass
- PPF melters
- Tank closure secondary waste
- FFTF decommissioning secondary waste
- Waste management secondary waste
- Offsite waste
- Onsite non-CERCLA waste

Waste forms for the RPPDF include those resulting from tank closure cleanup activities under Tank Closure Alternative 6A, Base and Option Cases. Potential releases to the vadose zone under Waste Management Alternative 2, Disposal Group 3, Base and Option Cases, are indicated in Tables M–42 and M–43 and Figures M–84 through M–87.

Table M–42. Waste Management Alternative 2, Disposal Group 3, Base Case, Radionuclide and Chemical Releases to the Vadose Zone

Source	Radionuclide (curies)										Chemical (kilograms)					
	H-3	**C-14**	**Sr-90**	**Tc-99**	**I-129**	**Cs-137**	**Np-237**	**U-238**	**Pu-239**	**Am-241**	**Cr**	**F**	**Hg**	**NO₃**	**Pb**	**Utot**
ETF-generated secondary waste	–	2.78	9.24×10^{-1}	8.73×10^{1}	2.51	5.44×10^{-3}	1.20×10^{-2}	4.28×10^{-3}	2.75×10^{-6}	–	4.53×10^{1}	–	8.06×10^{-1}	9.16×10^{6}	8.37×10^{-2}	4.31
PPF glass	–	–	7.42×10^{-2}	3.50×10^{-2}	1.39×10^{-5}	2.36×10^{-1}	1.35×10^{-4}	2.01×10^{-3}	7.92×10^{-3}	–	2.19	–	–	–	7.00×10^{-2}	4.19
Retired melters	–	–	4.80×10^{-3}	2.26×10^{-3}	9.03×10^{-7}	1.53×10^{-2}	8.74×10^{-6}	1.30×10^{-4}	5.13×10^{-4}	–	1.42×10^{-1}	–	–	–	4.51×10^{-3}	2.70×10^{-1}
TC secondary waste	–	–	7.01×10^{4}	4.37×10^{2}	1.38×10^{-1}	9.77×10^{2}	2.68×10^{-2}	1.55×10^{-1}	3.75×10^{-1}	–	1.98×10^{3}	–	2.29×10^{2}	–	3.13	1.00×10^{2}
FFTF Decommissioning Alternative 3 waste	2.29	1.84×10^{1}	–	2.72×10^{1}	–	1.92×10^{-5}	–	–	–	–	7.51×10^{-3}	–	–	–	9.59×10^{-5}	2.14×10^{3}
FFTF Decommissioning Alternative 2 waste	2.29	2.15×10^{-4}	–	1.48×10^{-2}	–	1.86×10^{-5}	–	–	–	–	7.49×10^{-3}	–	–	–	9.26×10^{-5}	1.79×10^{-3}
WM secondary and onsite waste	3.66×10^{3}	2.26×10^{-1}	3.27×10^{2}	1.35	4.14×10^{-5}	1.40×10^{1}	7.24×10^{-4}	3.22×10^{-2}	1.59×10^{-2}	1.43×10^{-3}	1.83×10^{2}	2.74×10^{2}	1.21×10^{1}	2.97×10^{3}	3.40×10^{2}	4.15×10^{-2}
Offsite waste	5.57×10^{4}	2.22×10^{2}	5.96×10^{4}	1.46×10^{3}	2.26	5.08×10^{3}	3.04×10^{-1}	3.47×10^{2}	9.04×10^{-1}	1.47×10^{-2}	8.05×10^{1}	–	2.50	–	8.55×10^{-1}	–
RPPDF	4.57	5.78	1.80×10^{1}	1.78×10^{2}	3.43×10^{-1}	4.61	3.80×10^{-1}	9.86	1.21	–	4.10×10^{3}	–	1.73	2.83×10^{5}	5.12×10^{1}	7.66×10^{3}

Note: To convert kilograms to pounds, multiply by 2.2046.

Key: Am-241=americium-241; C-14=carbon-14; Cr=chromium; Cs-137=cesium-137; ETF=Effluent Treatment Facility; F=fluoride; FFTF=Fast Flux Test Facility; H-3=hydrogen-3 (tritium); Hg=mercury; I-129=iodine-129; NO₃=nitrate; Np-237=neptunium-237; Pb=lead; PPF=Preprocessing Facility; Pu-239=plutonium-239; RPPDF=River Protection Project Disposal Facility; Sr-90=strontium-90; TC=tank closure; Tc-99=technetium-99; U-238=uranium-238; Utot=total uranium; WM=waste management.
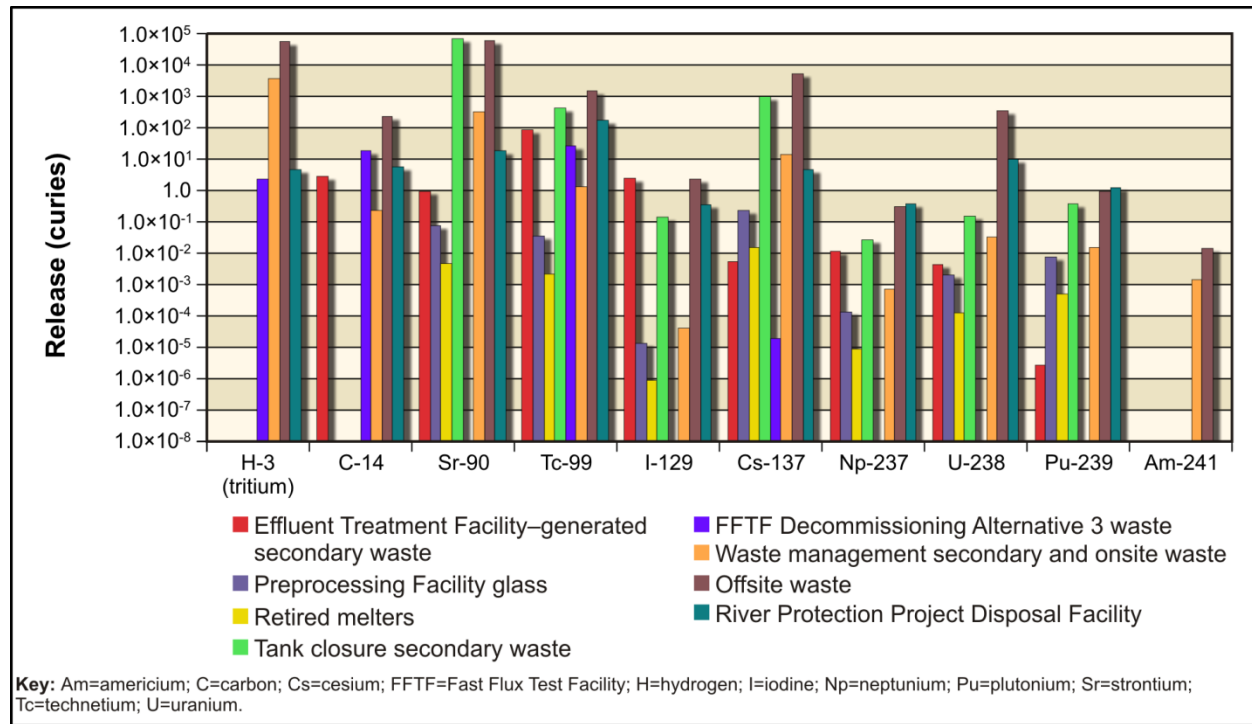
Figure M–84. Waste Management Alternative 2, Disposal Group 3,
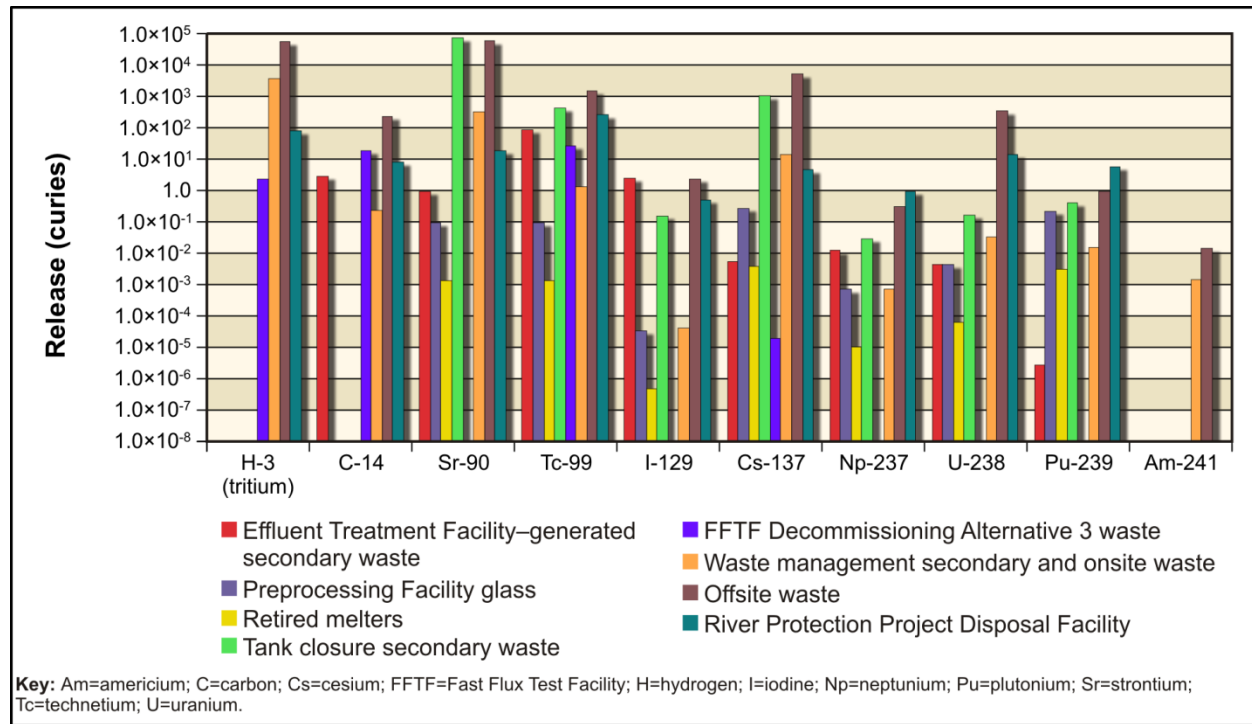**Base Case, Radionuclide Releases to the Vadose Zone**
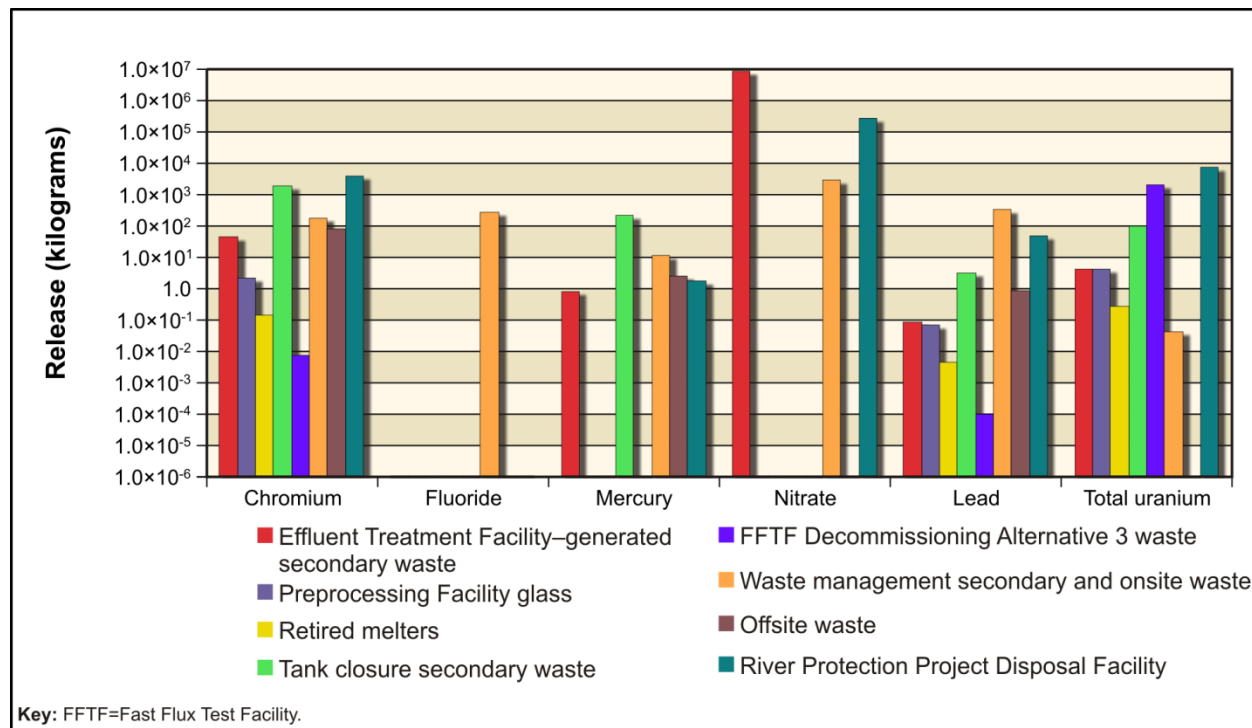
Figure M–85. Waste Management Alternative 2, Disposal Group 3,
Base Case, Chemical Releases to the Vadose Zone

Table M–43. Waste Management Alternative 2, Disposal Group 3, Option Case, Radionuclide and Chemical Releases to the Vadose Zone

Source	Radionuclide (curies)										Chemical (kilograms)					
	H-3	**C-14**	**Sr-90**	**Tc-99**	**I-129**	**Cs-137**	**Np-237**	**U-238**	**Pu-239**	**Am-241**	**Cr**	**F**	**Hg**	**NO$_3$**	**Pb**	**Utot**
ETF-generated secondary waste	–	2.82	9.29×10^{-1}	8.79×10^{1}	2.53	5.48×10^{-3}	1.23×10^{-2}	4.35×10^{-3}	2.80×10^{-6}	–	5.65×10^{1}	–	8.38×10^{-1}	1.51×10^{7}	8.41×10^{-2}	4.38
PPF glass	–	–	9.09×10^{-2}	9.13×10^{-2}	3.34×10^{-5}	2.63×10^{-1}	7.21×10^{-4}	4.54×10^{-3}	2.21×10^{-1}	–	4.30×10^{1}	–	–	–	8.40×10^{-2}	6.16
Retired melters	–	–	1.31×10^{-3}	1.31×10^{-3}	4.79×10^{-7}	3.78×10^{-3}	1.04×10^{-5}	6.54×10^{-5}	3.17×10^{-3}	–	6.18×10^{-1}	–	–	–	1.21×10^{-3}	8.84×10^{-2}
TC secondary waste	–	–	7.54×10^{4}	4.40×10^{2}	1.51×10^{-1}	1.05×10^{3}	2.92×10^{-2}	1.68×10^{-1}	4.10×10^{-1}	–	2.47×10^{3}	–	2.54×10^{2}	–	3.37	1.09×10^{2}
FFTF Decommissioning Alternative 3 waste	2.29	1.84×10^{1}	–	2.72×10^{1}	–	1.92×10^{-5}	–	–	–	–	7.51×10^{-3}	–	–	–	9.59×10^{-5}	2.14×10^{3}
FFTF Decommissioning Alternative 2 waste	2.29	2.15×10^{-4}	–	1.48×10^{-2}	–	1.86×10^{-5}	–	–	–	–	7.49×10^{-3}	–	–	–	9.26×10^{-5}	1.79×10^{-3}
WM secondary and onsite waste	3.66×10^{3}	2.26×10^{-1}	3.27×10^{2}	1.35	4.14×10^{-5}	1.40×10^{1}	7.24×10^{-4}	3.22×10^{-2}	1.59×10^{-2}	1.43×10^{-3}	1.83×10^{2}	2.74×10^{2}	1.21×10^{1}	2.97×10^{3}	3.40×10^{2}	4.15×10^{-2}
Offsite waste	5.57×10^{4}	2.22×10^{2}	5.96×10^{4}	1.46×10^{3}	2.26	5.08×10^{3}	3.04×10^{-1}	3.47×10^{2}	9.04×10^{-1}	1.47×10^{-2}	8.05×10^{1}	–	2.50	–	8.55×10^{-1}	–
RPPDF	7.95×10^{1}	8.18	1.89×10^{1}	2.70×10^{2}	4.96×10^{-1}	4.77	9.07×10^{-1}	1.37×10^{1}	5.90	–	3.69×10^{4}	–	1.14×10^{1}	1.04×10^{7}	5.26×10^{1}	9.24×10^{3}

Note: To convert kilograms to pounds, multiply by 2.2046.

Key: Am-241=americium-241; C-14=carbon-14; Cr=chromium; Cs-137=cesium-137; ETF=Effluent Treatment Facility; F=fluoride; FFTF=Fast Flux Test Facility; H-3=hydrogen-3 (tritium); Hg=mercury; I-129=iodine-129; NO$_3$=nitrate; Np-237=neptunium-237; Pb=lead; PPF=Preprocessing Facility; Pu-239=plutonium-239; RPPDF=River Protection Project Disposal Facility; Sr-90=strontium-90; TC=tank closure; Tc-99=technetium-99; U-238=uranium-238; Utot=total uranium; WM=waste management.

**Figure M–86. Waste Management Alternative 2, Disposal Group 3,
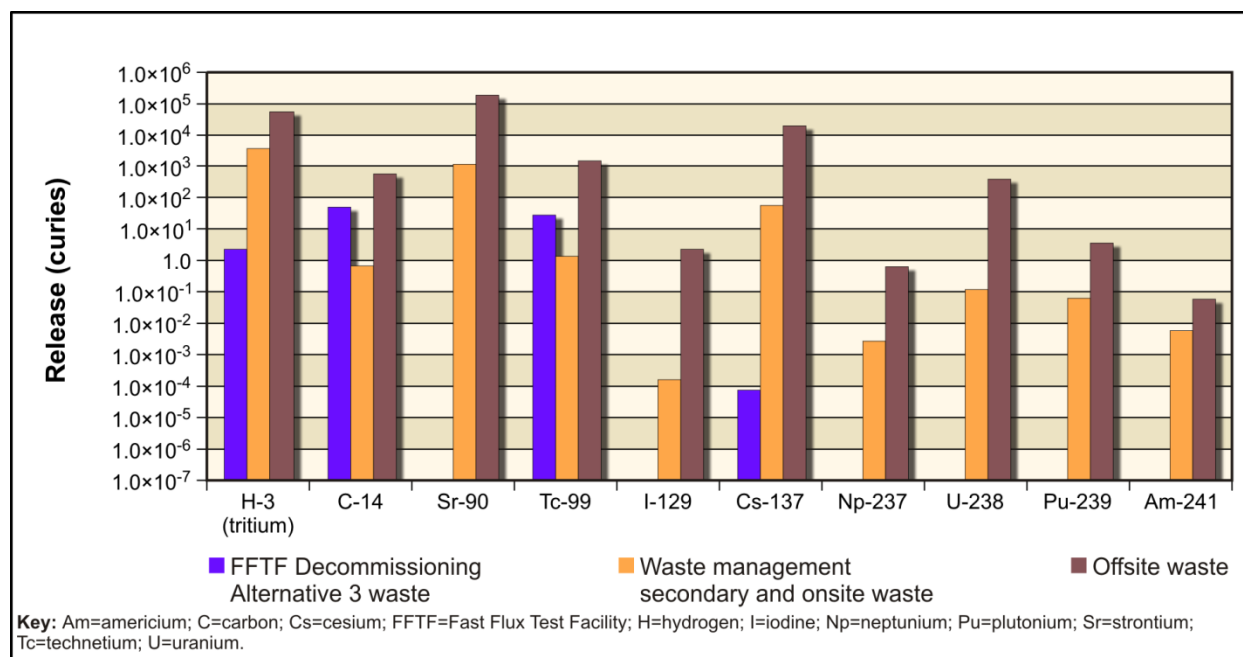Option Case, Radionuclide Releases to the Vadose Zone**
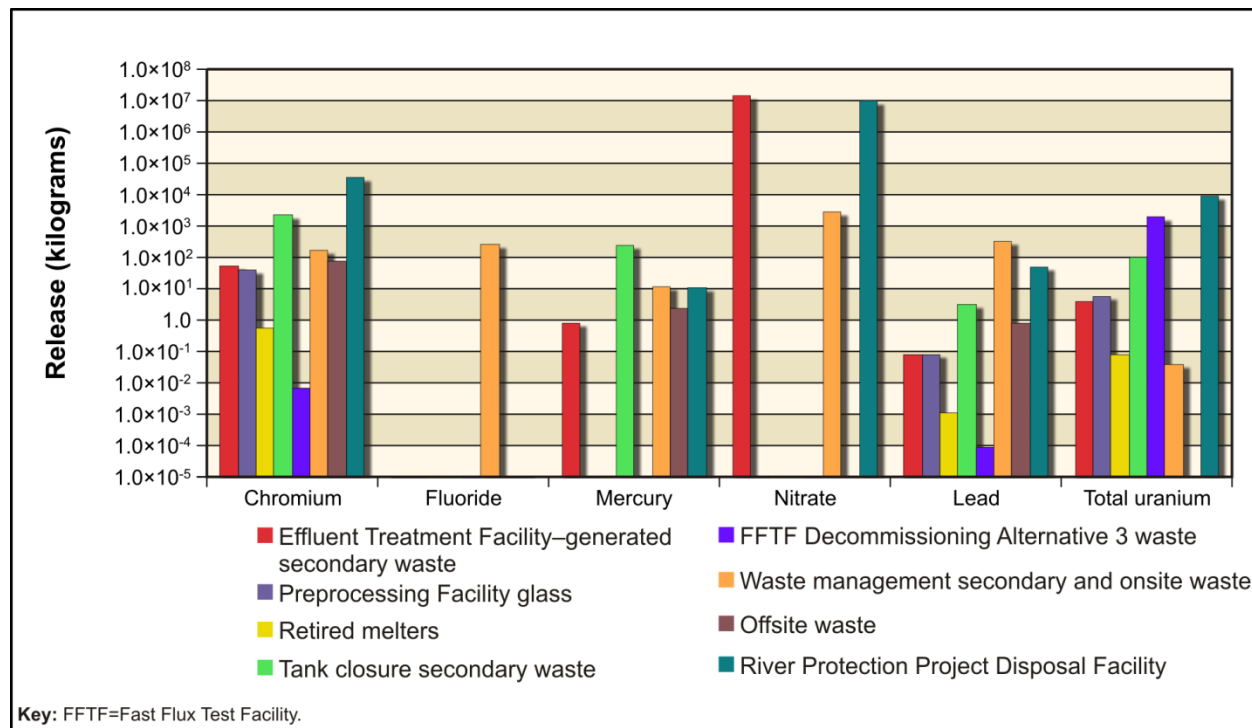
**Figure M–87. Waste Management Alternative 2, Disposal Group 3,
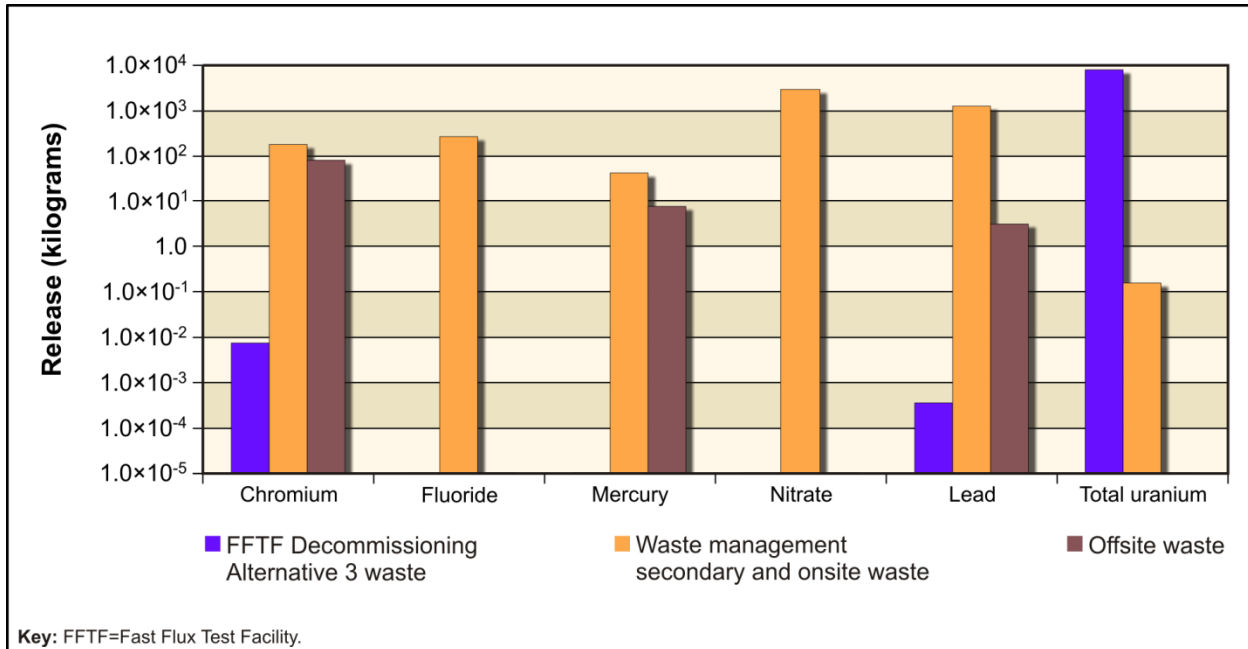Option Case, Chemical Releases to the Vadose Zone**

M.4.3.2.11 Waste Management Alternative 3: Disposal in IDF, 200-East and 200-West Areas

Under Waste Management Alternative 3, the waste from tank treatment operations would be disposed of in IDF-East, and that from onsite non-CERCLA sources, FFTF decommissioning, waste management, and other DOE sites would be disposed of in IDF-West. Waste from tank farm cleanup operations would be disposed of in the RPPDF. As a result, the waste disposed of in these three facilities would become available for release to the environment. Because of the different waste types that result from the Tank Closure action alternatives, three disposal groups were considered to account for the different IDF-East sizes and operational time periods. In addition, within these three disposal groups, subgroups were identified to allow consideration of the different waste types resulting from the Tank Closure alternatives.

The amount of waste disposed of at IDF-West under each subgroup is identical. Potential releases to the vadose zone from IDF-West under Waste Management Alternative 3 are indicated in Figures M–88 and M–89 (presented only once for all disposal groups under Waste Management Alternative 3).

Figure M–88. Waste Management Alternative 3, All Disposal Groups, Radionuclide Releases to the Vadose Zone from the 200-West Area Integrated Disposal Facility

Figure M–89. Waste Management Alternative 3, All Disposal Groups, Chemical Releases to the Vadose Zone from the 200-West Area Integrated Disposal Facility

Potential releases from IDF-East and the RPPDF are discussed in the following sections.

M.4.3.2.12 Waste Management Alternative 3: Disposal in IDF, 200-East and 200-West Areas, Disposal Group 1, Subgroup 1-A

Disposal Group 1, Subgroup 1-A, addresses the waste resulting from Tank Closure Alternative 2B, onsite non-CERCLA sources, FFTF decommissioning, waste management, and other DOE sites. Waste forms for IDF-East include the following:

- ILAW glass
- LAW melters
- Tank closure secondary waste

Waste forms for IDF-West include the following:

- FFTF decommissioning secondary waste
- Waste management secondary waste
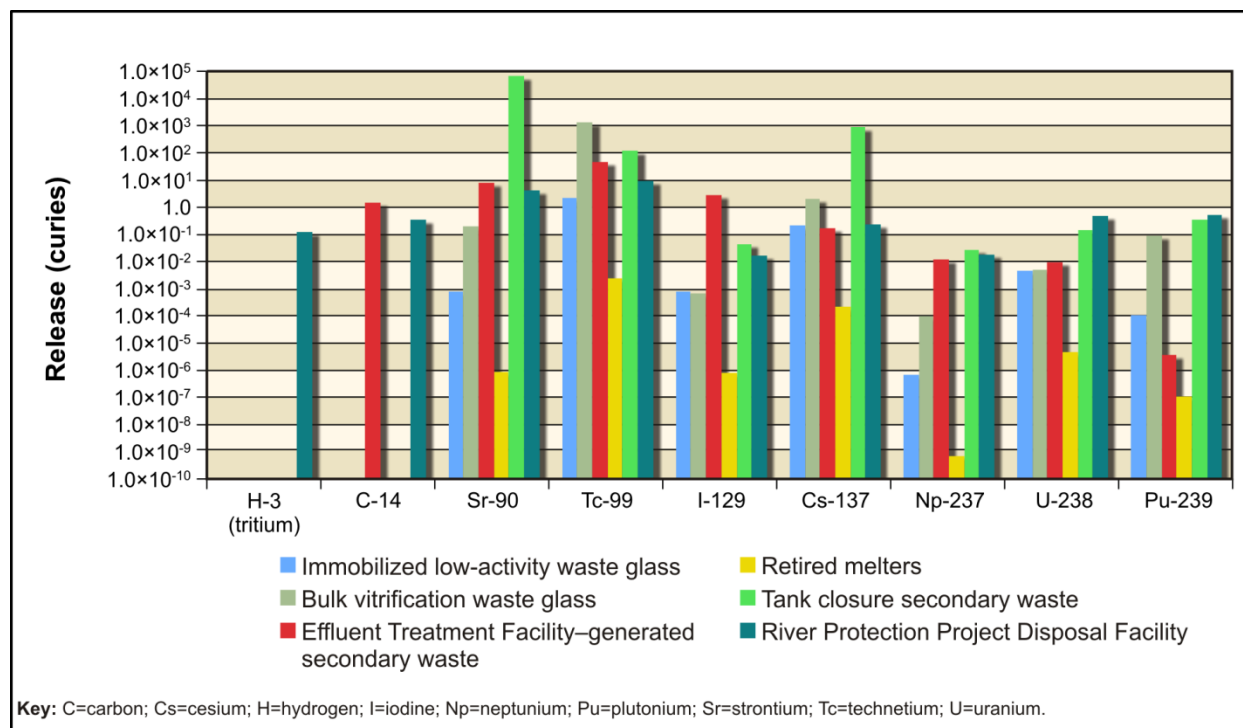- Offsite waste
- Onsite non-CERCLA waste

Waste forms for the RPPDF include those resulting from tank closure cleanup activities under Tank Closure Alternative 2B. Potential releases to the vadose zone under Waste Management Alternative 3, Disposal Group 1, Subgroup 1-A, are indicated in Table M–44 and Figures M–90 and M–91.

Table M–44. Waste Management Alternative 3, Disposal Group 1, Subgroup 1-A, Radionuclide and Chemical Releases to the Vadose Zone

Source	Radionuclide (curies)										Chemical (kilograms)					
	H-3	C-14	Sr-90	Tc-99	I-129	Cs-137	Np-237	U-238	Pu-239	Am-241	Cr	F	Hg	NO$_3$	Pb	Utot
IDF-East																
ILAW glass	–	–	2.71×10^{-3}	7.85×10^{-2}	2.64×10^{-3}	5.38×10^{-1}	2.31×10^{-6}	1.51×10^{-2}	3.49×10^{-4}	–	1.26×10^{2}	–	–	–	2.46	1.04×10^{1}
ETF-generated secondary waste	–	2.77	9.24×10^{-1}	8.62×10^{1}	2.50	5.44×10^{-3}	1.20×10^{-2}	4.24×10^{-3}	2.76×10^{-6}	–	4.43×10^{1}	–	8.07×10^{-1}	9.01×10^{6}	8.36×10^{-2}	4.21
Retired melters	–	–	3.02×10^{-6}	8.75×10^{-5}	2.96×10^{-6}	6.01×10^{-4}	2.58×10^{-9}	1.69×10^{-5}	3.90×10^{-7}	–	1.41×10^{-1}	–	–	–	2.74×10^{-3}	1.15×10^{-2}
TC secondary waste	–	–	7.36×10^{4}	4.92×10^{2}	1.45×10^{-1}	1.02×10^{3}	2.81×10^{-2}	1.61×10^{-1}	3.95×10^{-1}	–	1.94×10^{3}	–	2.40×10^{2}	–	3.29	1.03×10^{2}
RPPDF	1.27×10^{-1}	3.61×10^{-1}	4.15	9.71	1.67×10^{-2}	2.30×10^{-1}	1.85×10^{-2}	4.66×10^{-1}	5.31×10^{-1}	–	5.86×10^{2}	–	1.61	3.93×10^{4}	4.97	6.60×10^{2}
IDF-West																
FFTF Decommissioning Alternative 3 waste	2.29	4.78×10^{1}	–	2.72×10^{1}	–	7.46×10^{-5}	–	–	–	–	7.51×10^{-3}	–	–	–	3.64×10^{-4}	7.91×10^{3}
WM secondary and onsite waste	3.66×10^{3}	6.82×10^{-1}	1.18×10^{3}	1.35	1.58×10^{-4}	5.47×10^{1}	2.62×10^{-3}	1.21×10^{-1}	6.20×10^{-2}	5.65×10^{-3}	1.83×10^{2}	2.74×10^{2}	4.16×10^{1}	2.97×10^{3}	1.30×10^{3}	1.56×10^{-1}
Offsite waste	5.57×10^{4}	5.68×10^{2}	1.87×10^{5}	1.46×10^{3}	2.26	1.93×10^{4}	6.28×10^{-1}	3.77×10^{2}	3.49	5.80×10^{-2}	8.05×10^{1}	–	7.85	–	3.24	–

Note: To convert kilograms to pounds, multiply by 2.2046.

Key: Am-241=americium-241; C-14=carbon-14; Cr=chromium; Cs-137=cesium-137; ETF=Effluent Treatment Facility; F=fluoride; FFTF=Fast Flux Test Facility; H-3=hydrogen-3 (tritium); Hg=mercury; I-129=iodine-129; IDF-East=200-East Area Integrated Disposal Facility; IDF-West=200-West Area Integrated Disposal Facility; ILAW=immobilized low-activity waste; NO$_3$=nitrate; Np-237=neptunium-237; Pb=lead; Pu-239=plutonium-239; RPPDF=River Protection Project Disposal Facility; Sr-90=strontium-90; TC=tank closure; Tc-99=technetium-99; U-238=uranium-238; Utot=total uranium; WM=waste management.

**Figure M–90. Waste Management Alternative 3, Disposal Group 1, Subgroup 1-A,
Radionuclide Releases to the Vadose Zone from the 200-East Area Integrated Disposal Facility**
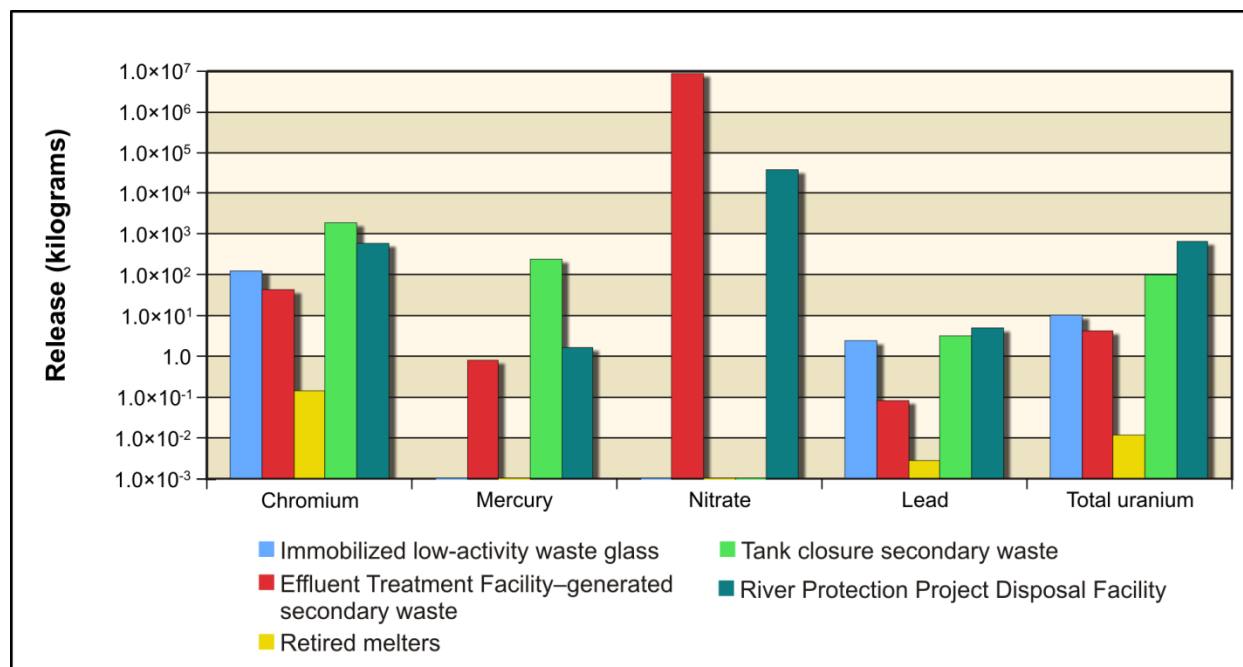
**Figure M–91. Waste Management Alternative 3, Disposal Group 1, Subgroup 1-A,
Chemical Releases to the Vadose Zone from the 200-East Area Integrated Disposal Facility**

M.4.3.2.13   Waste Management Alternative 3: Disposal in IDF, 200-East and 200-West Areas, Disposal Group 1, Subgroup 1-B

Disposal Group 1, Subgroup 1-B, addresses the waste resulting from Tank Closure Alternative 3A, onsite non-CERCLA sources, FFTF decommissioning, waste management, and other DOE sites. Waste forms for IDF-East include the following:

- ILAW glass
- LAW melters
- bulk vitrification glass
- Tank closure secondary waste

Waste forms for IDF-West include the following:

- FFTF decommissioning secondary waste
- Waste management secondary waste
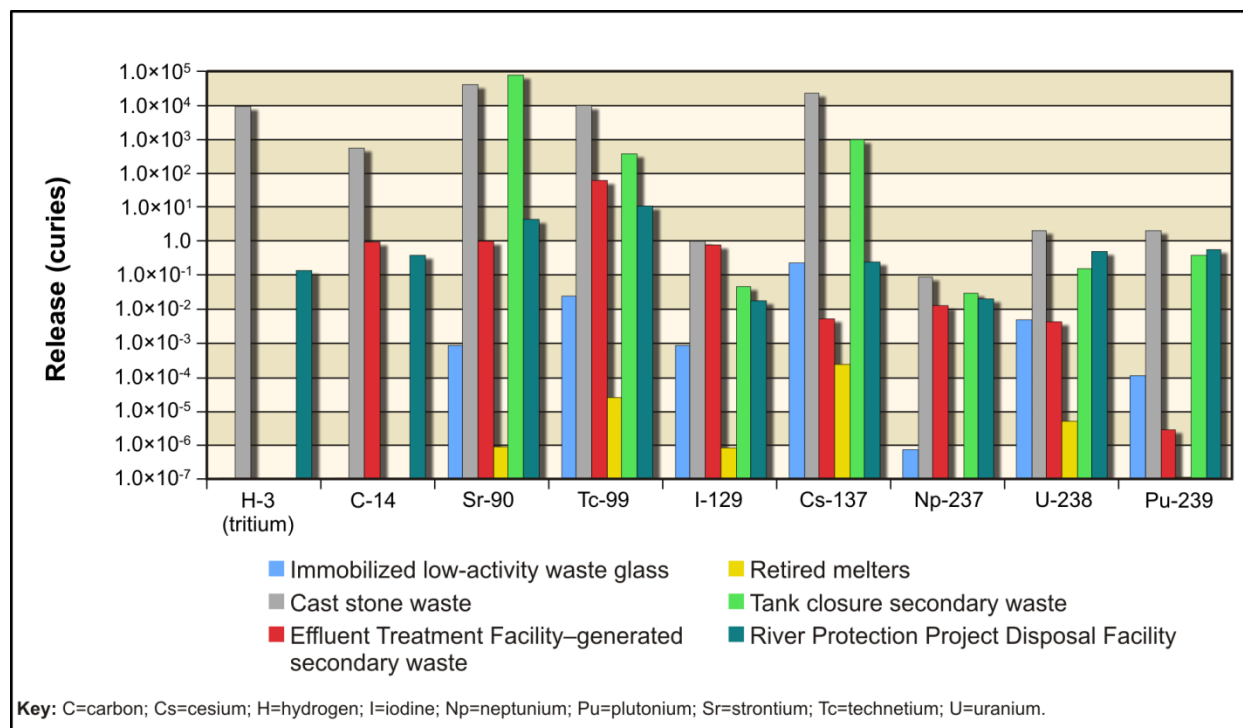- Offsite waste
- Onsite non-CERCLA waste

Waste forms for the RPPDF include those resulting from tank closure cleanup activities under Tank Closure Alternative 3A. Potential releases to the vadose zone under Waste Management Alternative 3, Disposal Group 1, Subgroup 1-B, are indicated in Table M–45 and Figures M–92 and M–93.

Table M–45. Waste Management Alternative 3, Disposal Group 1, Subgroup 1-B, Radionuclide and Chemical Releases to the Vadose Zone

Source	Radionuclide (curies)										Chemical (kilograms)					
	H-3	**C-14**	**Sr-90**	**Tc-99**	**I-129**	**Cs-137**	**Np-237**	**U-238**	**Pu-239**	**Am-241**	**Cr**	**F**	**Hg**	**NO$_3$**	**Pb**	**Utot**
IDF-East																
ILAW glass	–	–	8.12×10^{-4}	2.30	7.75×10^{-4}	2.10×10^{-1}	6.86×10^{-7}	4.49×10^{-3}	1.04×10^{-4}	–	3.71×10^{1}	–	–	–	7.39×10^{-1}	3.13
BV waste glass	–	–	1.94×10^{-1}	1.34×10^{3}	6.67×10^{-4}	2.00	9.49×10^{-5}	5.08×10^{-3}	8.95×10^{-2}	–	3.18×10^{1}	–	–	–	6.62×10^{-1}	3.41
ETF-generated secondary waste	–	1.54	7.84	4.63×10^{1}	2.74	1.69×10^{-1}	1.21×10^{-2}	9.18×10^{-3}	3.75×10^{-6}	–	2.76×10^{1}	–	8.05×10^{-1}	8.14×10^{6}	1.38×10^{1}	7.37
Retired melters	–	–	8.27×10^{-7}	2.34×10^{-3}	7.89×10^{-7}	2.13×10^{-4}	6.97×10^{-10}	4.57×10^{-6}	1.06×10^{-7}	–	3.77×10^{-2}	–	–	–	7.53×10^{-4}	3.18×10^{-3}
TC secondary waste	–	–	7.27×10^{4}	1.28×10^{2}	4.25×10^{-2}	9.16×10^{2}	2.77×10^{-2}	1.47×10^{-1}	3.59×10^{-1}	–	8.02×10^{2}	–	2.38×10^{2}	–	2.89	9.08×10^{1}
RPPDF	1.27×10^{-1}	3.61×10^{-1}	4.15	9.71	1.67×10^{-2}	2.30×10^{-1}	1.85×10^{-2}	4.66×10^{-1}	5.31×10^{-1}	–	5.86×10^{2}	–	1.61	3.93×10^{4}	4.97	6.60×10^{2}
IDF-West																
FFTF Decommissioning Alternative 3 waste	2.29	5.72×10^{-4}	–	1.48×10^{-2}	–	7.22×10^{-5}	–	–	–	–	7.49×10^{-3}	–	–	–	3.52×10^{-4}	6.66×10^{-3}
WM secondary and onsite waste	3.66×10^{3}	6.82×10^{-1}	1.18×10^{3}	1.35	1.58×10^{-4}	5.47×10^{1}	2.62×10^{-3}	1.21×10^{-1}	6.20×10^{-2}	5.65×10^{-3}	1.83×10^{2}	2.74×10^{2}	4.16×10^{1}	2.97×10^{3}	1.30×10^{3}	1.56×10^{-1}
Offsite waste	5.57×10^{4}	5.68×10^{2}	1.87×10^{5}	1.46×10^{3}	2.26	1.93×10^{4}	6.28×10^{-1}	3.77×10^{2}	3.49	5.80×10^{-2}	8.05×10^{1}	–	7.85	–	3.24	–

Note: To convert kilograms to pounds, multiply by 2.2046.
Key: Am-241=americium-241; BV=bulk vitrification; C-14=carbon-14; Cr=chromium; Cs-137=cesium-137; ETF=Effluent Treatment Facility; F=fluoride; FFTF=Fast Flux Test Facility; H-3=hydrogen-3 (tritium); Hg=mercury; I-129=iodine-129; IDF-East=200-East Area Integrated Disposal Facility; IDF-West=200-West Area Integrated Disposal Facility; ILAW=immobilized low-activity waste; NO$_3$=nitrate; Np-237=neptunium-237; Pb=lead; Pu-239=plutonium-239; RPPDF=River Protection Project Disposal Facility; Sr-90=strontium-90; TC=tank closure; Tc-99=technetium-99; U-238=uranium-238; Utot=total uranium; WM=waste management.

Figure M–92. Waste Management Alternative 3, Disposal Group 1, Subgroup 1-B, Radionuclide Releases to the Vadose Zone from the 200-East Area Integrated Disposal Facility
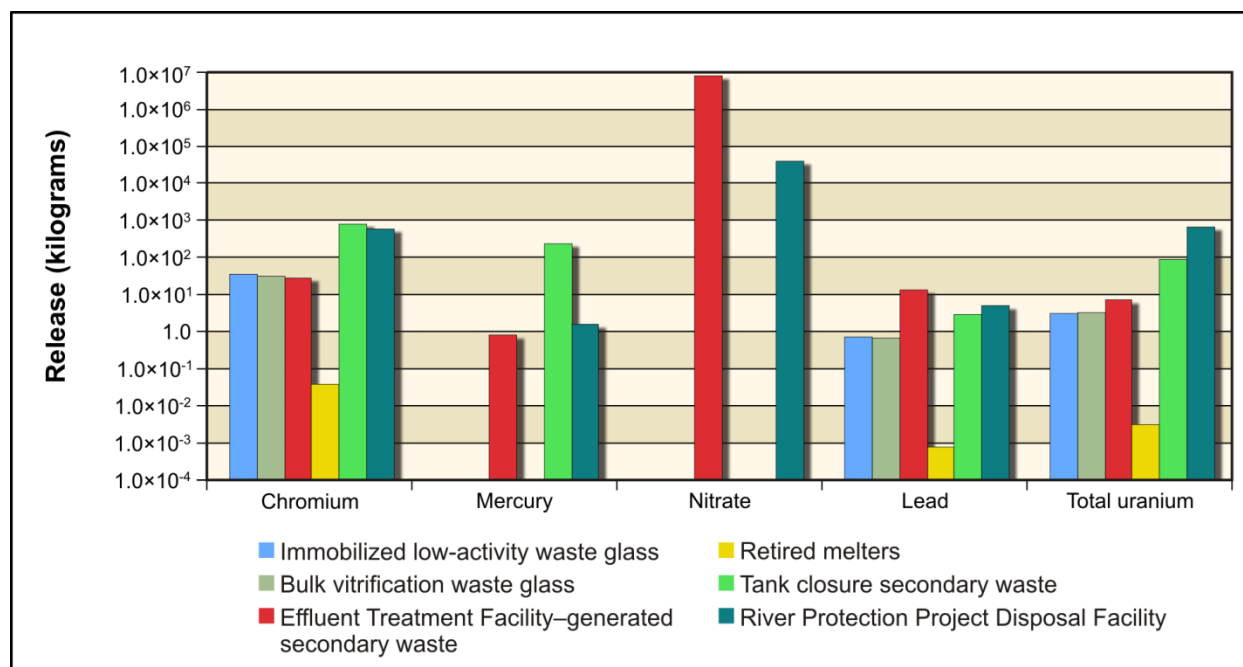
Figure M–93. Waste Management Alternative 3, Disposal Group 1, Subgroup 1-B, Chemical Releases to the Vadose Zone from the 200-East Area Integrated Disposal Facility

M.4.3.2.14   Waste Management Alternative 3: Disposal in IDF, 200-East and 200-West Areas, Disposal Group 1, Subgroup 1-C

Disposal Group 1, Subgroup 1-C, addresses the waste resulting from Tank Closure Alternative 3B, onsite non-CERCLA sources, FFTF decommissioning, waste management, and other DOE sites. Waste forms for IDF-East include the following:

- ILAW glass
- LAW melters
- Cast stone waste
- Tank closure secondary waste

Waste forms for IDF-West include the following:

- FFTF decommissioning secondary waste
- Waste management secondary waste
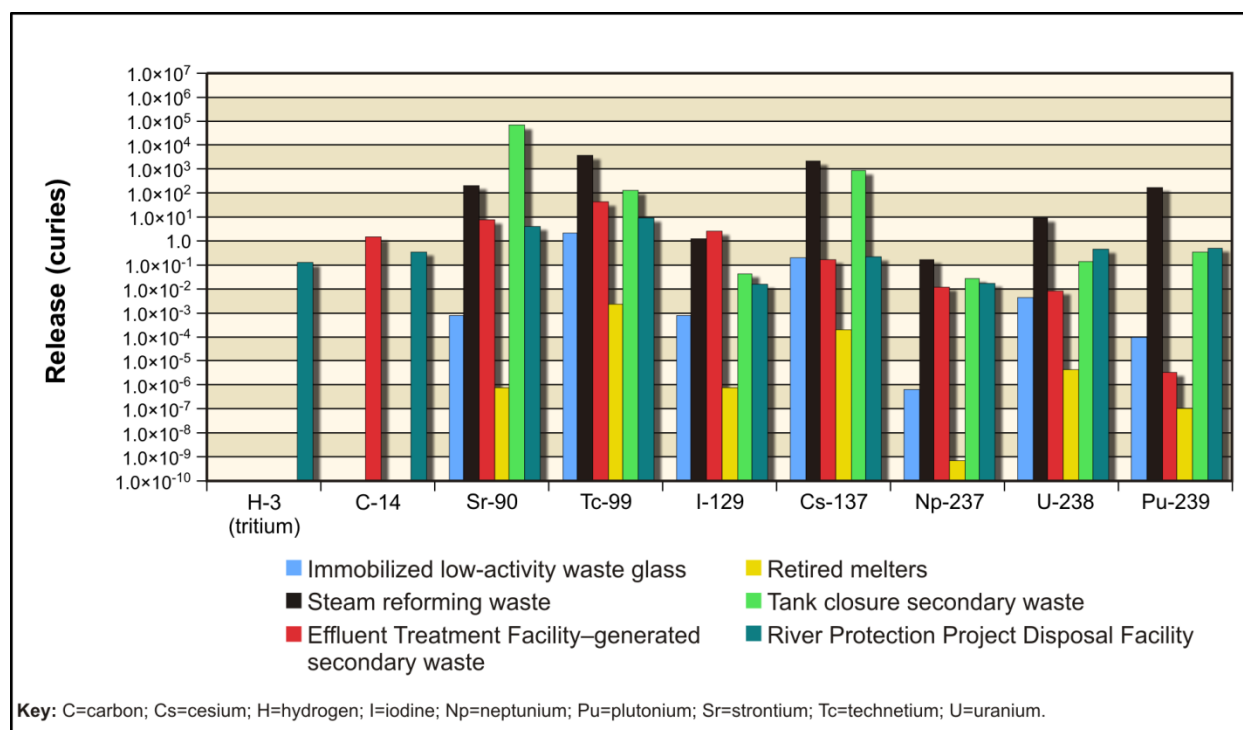- Offsite waste
- Onsite non-CERCLA waste

Waste forms for the RPPDF include those resulting from tank closure cleanup activities under Tank Closure Alternative 3B. Potential releases to the vadose zone under Waste Management Alternative 3, Disposal Group 1, Subgroup 1-C, are indicated in Table M–46 and Figures M–94 and M–95.

Table M–46. Waste Management Alternative 3, Disposal Group 1, Subgroup 1-C, Radionuclide and Chemical Releases to the Vadose Zone

Source	Radionuclide (curies)										Chemical (kilograms)					
	H-3	C-14	Sr-90	Tc-99	I-129	Cs-137	Np-237	U-238	Pu-239	Am-241	Cr	F	Hg	NO₃	Pb	Utot
IDF-East																
ILAW glass	–	–	8.12×10^{-4}	2.30×10^{-2}	7.75×10^{-4}	2.10×10^{-1}	6.86×10^{-7}	4.49×10^{-3}	1.04×10^{-4}	–	3.71×10^{1}	–	–	–	7.39×10^{-1}	3.13
Cast stone waste	8.44×10^{3}	5.03×10^{2}	3.73×10^{4}	9.14×10^{3}	8.98×10^{-1}	2.08×10^{4}	8.07×10^{-2}	1.93	1.84	–	3.25×10^{5}	–	5.39×10^{1}	4.95×10^{7}	9.08×10^{1}	1.31×10^{3}
ETF-generated secondary waste	–	8.54×10^{-1}	9.13×10^{-1}	5.81×10^{1}	7.32×10^{-1}	4.87×10^{-3}	1.19×10^{-2}	3.84×10^{-3}	2.53×10^{-6}	–	1.84×10^{1}	–	6.00×10^{-1}	2.63×10^{6}	1.06×10^{-1}	3.76
Retired melters	–	–	8.27×10^{-7}	2.34×10^{-5}	7.89×10^{-7}	2.13×10^{-4}	6.97×10^{-10}	4.57×10^{-6}	1.06×10^{-7}	–	3.77×10^{-2}	–	–	–	7.53×10^{-4}	3.18×10^{-3}
TC secondary waste	–	–	7.27×10^{4}	3.33×10^{2}	4.25×10^{-2}	9.16×10^{2}	2.77×10^{-2}	1.47×10^{-1}	3.59×10^{-1}	–	8.02×10^{2}	–	1.78×10^{2}	–	2.89	9.08×10^{1}
RPPDF	1.27×10^{-1}	3.61×10^{-1}	4.15	9.71	1.67×10^{-2}	2.30×10^{-1}	1.85×10^{-2}	4.66×10^{-1}	5.31×10^{-1}	–	5.86×10^{2}	–	1.61	3.93×10^{4}	4.97	6.60×10^{2}
IDF-West																
FFTF Decommissioning Alternative 3 waste	2.29	4.78×10^{1}	–	2.72×10^{1}	–	7.46×10^{-5}	–	–	–	–	7.51×10^{-3}	–	–	–	3.64×10^{-4}	7.91×10^{3}
WM secondary and onsite waste	3.66×10^{3}	6.82×10^{-1}	1.18×10^{3}	1.35	1.58×10^{-4}	5.47×10^{1}	2.62×10^{-3}	1.21×10^{-1}	6.20×10^{-2}	5.65×10^{-3}	1.83×10^{2}	2.74×10^{2}	4.16×10^{1}	2.97×10^{3}	1.30×10^{3}	1.56×10^{-1}
Offsite waste	5.57×10^{4}	5.68×10^{2}	1.87×10^{5}	1.46×10^{3}	2.26	1.93×10^{4}	6.28×10^{-1}	3.77×10^{2}	3.49	5.80×10^{-2}	8.05×10^{1}	–	7.85	–	3.24	–

Note: To convert kilograms to pounds, multiply by 2.2046.

Key: Am-241=americium-241; C-14=carbon-14; Cr=chromium; Cs-137=cesium-137; ETF=Effluent Treatment Facility; F=fluoride; FFTF=Fast Flux Test Facility; H-3=hydrogen-3 (tritium); Hg=mercury; I-129=iodine-129; IDF-East=200-East Area Integrated Disposal Facility; IDF-West=200-West Area Integrated Disposal Facility; ILAW=immobilized low-activity waste; NO₃=nitrate; Np-237=neptunium-237; Pb=lead; Pu-239=plutonium-239; RPPDF=River Protection Project Disposal Facility; Sr-90=strontium-90; TC=tank closure; Tc-99=technetium-99; U-238=uranium-238; Utot=total uranium; WM=waste management.

Figure M–94. Waste Management Alternative 3, Disposal Group 1, Subgroup 1-C, Radionuclide Releases to the Vadose Zone from the 200-East Area Integrated Disposal Facility
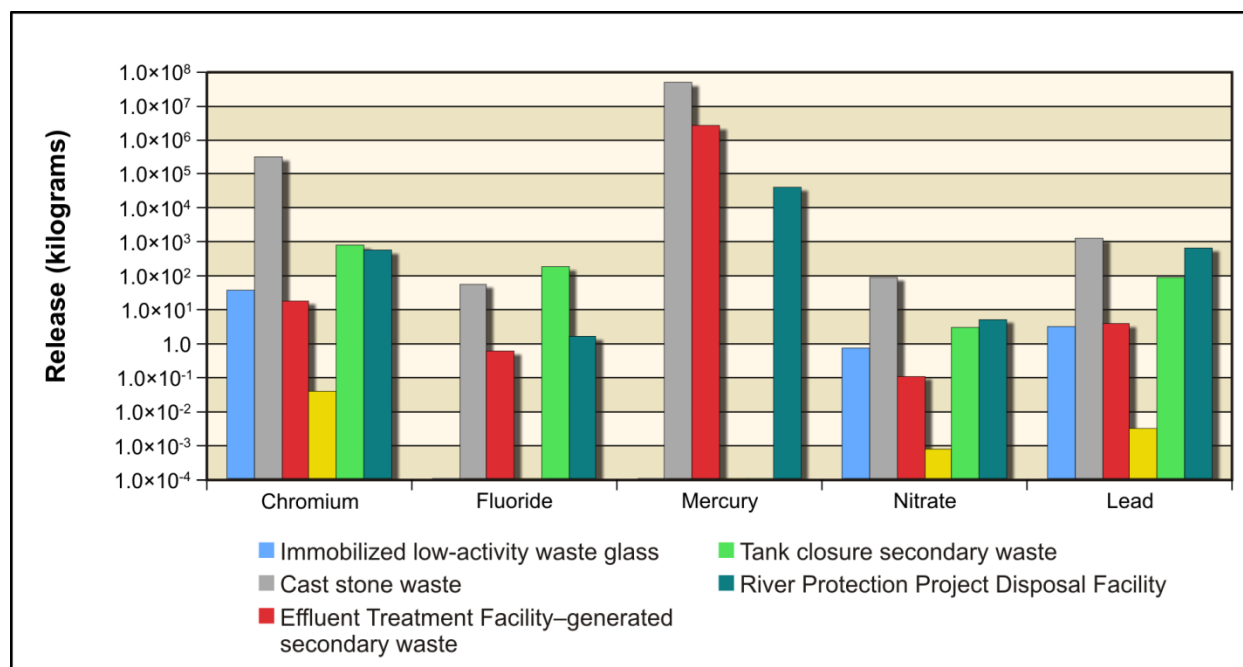
Figure M–95. Waste Management Alternative 3, Disposal Group 1, Subgroup 1-C, Chemical Releases to the Vadose Zone from the 200-East Area Integrated Disposal Facility

M.4.3.2.15   Waste Management Alternative 3: Disposal in IDF, 200-East and 200 West Areas, Disposal Group 1, Subgroup 1-D

Disposal Group 1, Subgroup 1-D, addresses the waste resulting from Tank Closure Alternative 3C, onsite non-CERCLA sources, FFTF decommissioning, waste management, and other DOE sites. Waste forms for IDF-East include the following:

- ILAW glass
- LAW melters
- Steam reforming waste
- Tank closure secondary waste

Waste forms for IDF-West include the following:

- FFTF decommissioning secondary waste
- Waste management secondary waste
- Offsite waste
- Onsite non-CERCLA waste

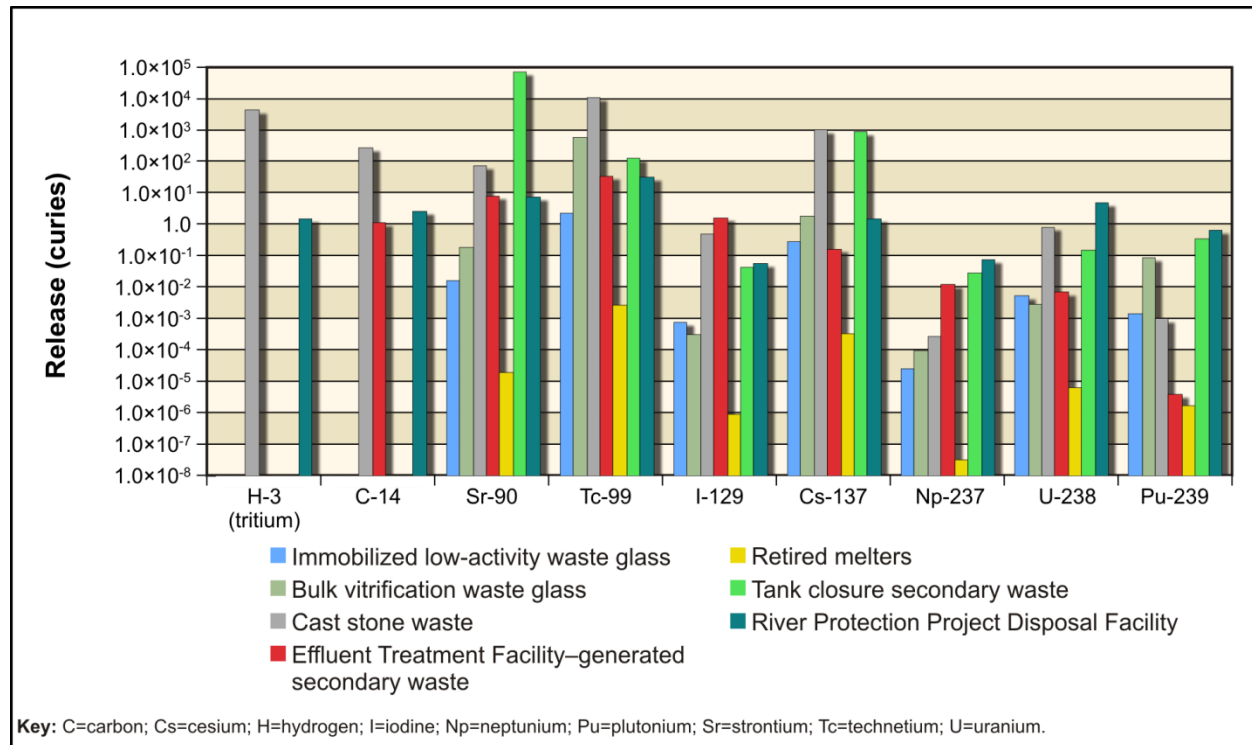Waste forms for the RPPDF include those resulting from tank closure cleanup activities under Tank Closure Alternative 3C. Potential releases to the vadose zone under Waste Management Alternative 3, Disposal Group 1, Subgroup 1-D, are indicated in Table M–47 and Figures M–96 and M–97.

Table M–47. Waste Management Alternative 3, Disposal Group 1, Subgroup 1-D, Radionuclide and Chemical Releases to the Vadose Zone

Source	Radionuclide (curies)										Chemical (kilograms)					
	H-3	C-14	Sr-90	Tc-99	I-129	Cs-137	Np-237	U-238	Pu-239	Am-241	Cr	F	Hg	NO$_3$	Pb	Utot
IDF-East																
ILAW glass	–	–	8.12×10^{-4}	2.30	7.75×10^{-4}	2.10×10^{-1}	6.86×10^{-7}	4.49×10^{-3}	1.04×10^{-4}	–	3.71×10^{1}	–	–	–	7.39×10^{-1}	3.13
Steam reforming waste	–	–	2.07×10^{2}	3.76×10^{3}	1.25	2.14×10^{3}	1.78×10^{-1}	9.54	1.69×10^{2}	–	6.01×10^{4}	–	–	–	1.25×10^{3}	6.44×10^{3}
ETF-generated secondary waste	–	1.54	7.69	4.63×10^{1}	2.74	1.71×10^{-1}	1.20×10^{-2}	8.33×10^{-3}	3.36×10^{-6}	–	2.72×10^{1}	–	8.05×10^{-1}	9.17×10^{6}	1.38×10^{1}	6.72
Retired melters	–	–	8.27×10^{-7}	2.34×10^{-3}	7.89×10^{-7}	2.13×10^{-4}	6.97×10^{-10}	4.57×10^{-6}	1.06×10^{-7}	–	3.77×10^{-2}	–	–	–	7.53×10^{-4}	3.18×10^{-3}
TC secondary waste	–	–	7.28×10^{4}	1.28×10^{2}	4.25×10^{-2}	9.17×10^{2}	2.77×10^{-2}	1.48×10^{-1}	3.59×10^{-1}	–	8.02×10^{2}	–	2.38×10^{2}	–	2.89	9.08×10^{1}
RPPDF	1.27×10^{-1}	3.61×10^{-1}	4.15	9.71	1.67×10^{-2}	2.30×10^{-1}	1.85×10^{-2}	4.66×10^{-1}	5.31×10^{-1}	–	5.86×10^{2}	–	1.61	3.93×10^{4}	4.97	6.60×10^{2}
IDF-West																
FFTF Decommissioning Alternative 3 waste	2.29	4.78×10^{1}	–	2.72×10^{1}	–	7.46×10^{-5}	–	–	–	–	7.51×10^{-3}	–	–	–	3.64×10^{-4}	7.91×10^{3}
WM secondary and onsite waste	3.66×10^{3}	6.82×10^{-1}	1.18×10^{3}	1.35	1.58×10^{-4}	5.47×10^{1}	2.62×10^{-3}	1.21×10^{-1}	6.20×10^{-2}	5.65×10^{-3}	1.83×10^{2}	2.74×10^{2}	4.16×10^{1}	2.97×10^{3}	1.30×10^{3}	1.56×10^{-1}
Offsite waste	5.57×10^{4}	5.68×10^{2}	1.87×10^{5}	1.46×10^{3}	2.26	1.93×10^{4}	6.28×10^{-1}	3.77×10^{2}	3.49	5.80×10^{-2}	8.05×10^{1}	–	7.85	–	3.24	–

Note: To convert kilograms to pounds, multiply by 2.2046.

Key: Am-241=americium-241; C-14=carbon-14; Cr=chromium; Cs-137=cesium-137; ETF=Effluent Treatment Facility; F=fluoride; FFTF=Fast Flux Test Facility; H-3=hydrogen-3 (tritium); Hg=mercury; I-129=iodine-129; IDF-East=200-East Area Integrated Disposal Facility; IDF-West=200-West Area Integrated Disposal Facility; ILAW=immobilized low-activity waste; NO$_3$=nitrate; Np-237=neptunium-237; Pb=lead; Pu-239=plutonium-239; RPPDF=River Protection Project Disposal Facility; Sr-90=strontium-90; TC=tank closure; Tc-99=technetium-99; U-238=uranium-238; Utot=total uranium; WM=waste management.

Figure M–96. Waste Management Alternative 3, Disposal Group 1, Subgroup 1-D, Radionuclide Releases to the Vadose Zone from the 200-East Area Integrated Disposal Facility
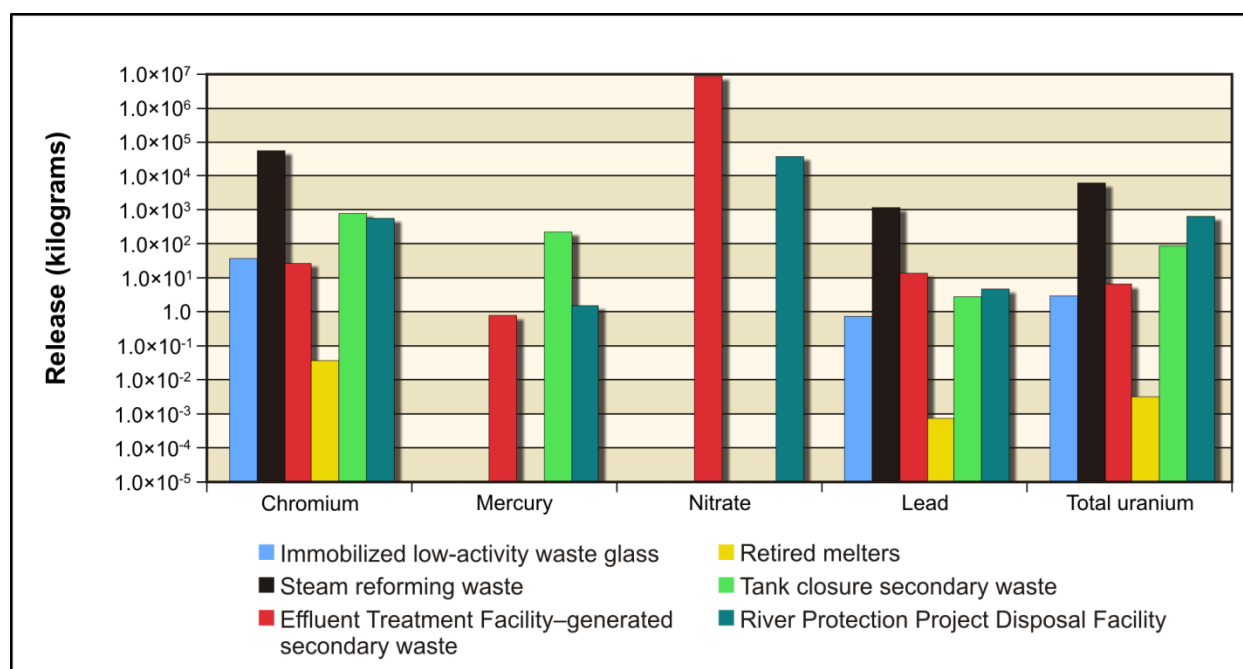
Figure M–97. Waste Management Alternative 3, Disposal Group 1, Subgroup 1-D, Chemical Releases to the Vadose Zone from the 200-East Area Integrated Disposal Facility

M.4.3.2.16 **Waste Management Alternative 3: Disposal in IDF, 200-East and 200-West Areas, Disposal Group 1, Subgroup 1-E**

Disposal Group 1, Subgroup 1-E, addresses the waste resulting from Tank Closure Alternative 4, onsite non-CERCLA sources, FFTF decommissioning, waste management, and other DOE sites. Waste forms for IDF-East include the following:

- ILAW glass
- LAW melters
- bulk vitrification glass
- Cast stone waste
- ETF-generated secondary solid waste
- Tank closure secondary waste

Waste forms for IDF-West include the following:

- FFTF decommissioning secondary waste
- Waste management secondary waste
- Offsite waste
- Onsite non-CERCLA waste

The RPPDF would not be constructed or operated under Tank Closure Alternative 4 because tank closure cleanup activities would not be conducted. Potential releases to the vadose zone under Waste Management Alternative 3, Disposal Group 1, Subgroup 1-E, are indicated in Table M–48 and Figures M–98 and M–99.
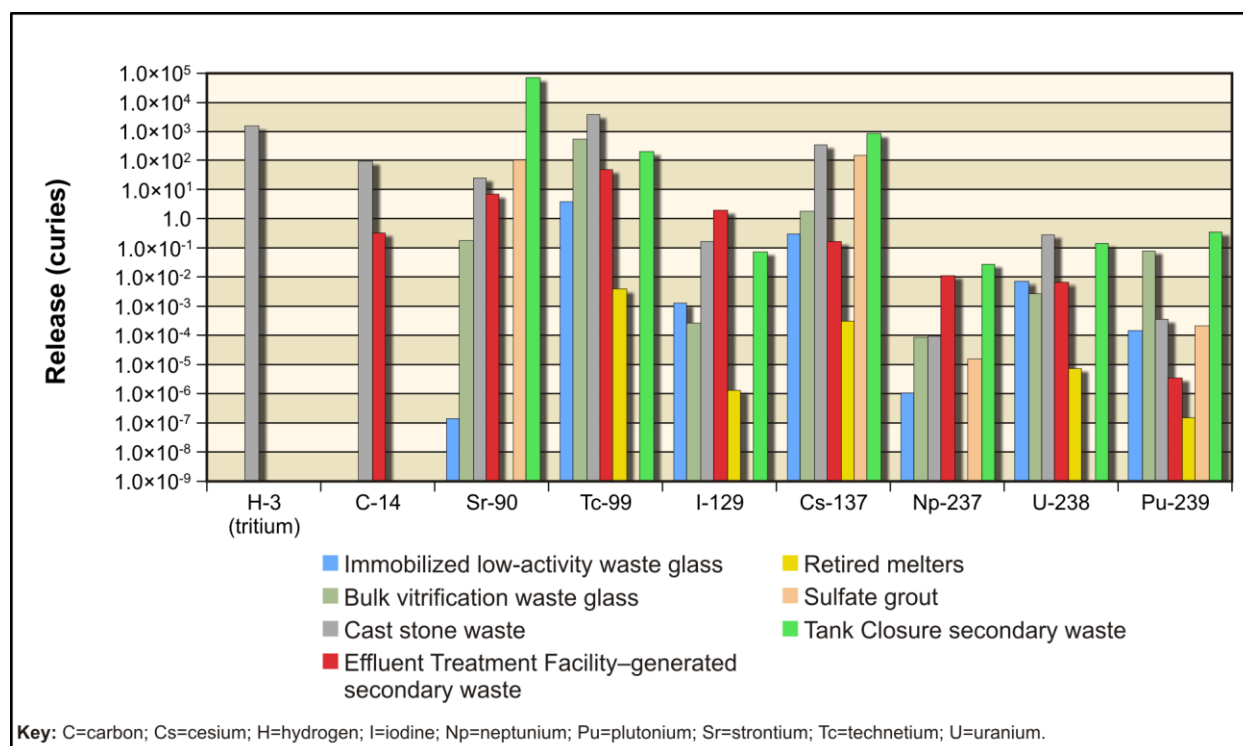
Table M–48. Waste Management Alternative 3, Disposal Group 1, Subgroup 1-E, Radionuclide and Chemical Releases to the Vadose Zone

Source	Radionuclide (curies)										Chemical (kilograms)					
	H-3	C-14	Sr-90	Tc-99	I-129	Cs-137	Np-237	U-238	Pu-239	Am-241	Cr	F	Hg	NO₃	Pb	Utot
IDF-East																
ILAW glass	–	–	1.66×10^{-2}	2.31	7.78×10^{-4}	2.90×10^{-1}	2.51×10^{-5}	5.57×10^{-3}	1.49×10^{-3}	–	3.74×10^{1}	–	–	–	7.67×10^{-1}	3.63
BV waste glass	–	–	1.95×10^{-1}	6.18×10^{2}	3.08×10^{-4}	1.90	9.54×10^{-5}	3.00×10^{-3}	9.04×10^{-2}	–	1.47×10^{1}	–	–	–	3.55×10^{-1}	1.97
Cast stone waste	4.66×10^{3}	2.77×10^{2}	7.46×10^{1}	1.09×10^{4}	4.94×10^{-1}	1.04×10^{3}	2.77×10^{-4}	8.16×10^{-1}	1.02×10^{-3}	–	1.78×10^{5}	–	2.86×10^{1}	2.73×10^{7}	4.33×10^{1}	5.64×10^{2}
ETF-generated secondary waste	–	1.18	7.88	3.53×10^{1}	1.66	1.61×10^{-1}	1.22×10^{-2}	7.05×10^{-3}	3.79×10^{-6}	–	2.31×10^{1}	–	7.05×10^{-1}	5.20×10^{6}	7.43	5.89
Retired melters	–	–	1.92×10^{-5}	2.65×10^{-3}	8.94×10^{-7}	3.32×10^{-4}	3.12×10^{-8}	6.40×10^{-6}	1.71×10^{-6}	–	4.32×10^{-2}	–	–	–	8.80×10^{-4}	4.15×10^{-3}
TC secondary waste	–	–	7.36×10^{4}	1.28×10^{2}	4.28×10^{-2}	9.27×10^{2}	2.80×10^{-2}	1.50×10^{-1}	3.63×10^{-1}	–	8.21×10^{2}	–	2.10×10^{2}	–	2.93	9.22×10^{1}
RPPDF	1.50	2.61	7.31	3.14×10^{1}	5.84×10^{-2}	1.57	7.75×10^{-2}	4.99	6.83×10^{-1}	–	1.86×10^{3}	–	9.23×10^{-1}	7.78×10^{4}	6.31	4.85×10^{3}
IDF-West																
FFTF Decommissioning Alternative 3 waste	2.29	4.78×10^{1}	–	2.72×10^{1}	–	7.46×10^{-5}	–	–	–	–	7.51×10^{-3}	–	–	–	3.64×10^{-4}	7.91×10^{3}
WM secondary and onsite waste	3.66×10^{3}	6.82×10^{-1}	1.18×10^{3}	1.35	1.58×10^{-4}	5.47×10^{1}	2.62×10^{-3}	1.21×10^{-1}	6.20×10^{-2}	5.65×10^{-3}	1.83×10^{2}	2.74×10^{2}	4.16×10^{1}	2.97×10^{3}	1.30×10^{3}	1.56×10^{-1}
Offsite waste	5.57×10^{4}	5.68×10^{2}	1.87×10^{5}	1.46×10^{3}	2.26	1.93×10^{4}	6.28×10^{-1}	3.77×10^{2}	3.49	5.80×10^{-2}	8.05×10^{1}	–	7.85	–	3.24	–

Note: To convert kilograms to pounds, multiply by 2.2046.

Key: Am-241=americium-241; BV=bulk vitrification; C-14=carbon-14; Cr=chromium; Cs-137=cesium-137; ETF=Effluent Treatment Facility; F=fluoride; FFTF=Fast Flux Test Facility; H-3=hydrogen-3 (tritium); Hg=mercury; I-129=iodine-129; IDF-East=200-East Area Integrated Disposal Facility; IDF-West=200-West Area Integrated Disposal Facility; ILAW=immobilized low-activity waste; NO₃=nitrate; Np-237=neptunium-237; Pb=lead; Pu-239=plutonium-239; RPPDF=River Protection Project Disposal Facility; Sr-90=strontium-90; TC=tank closure; Tc-99=technetium-99; U-238=uranium-238; Utot=total uranium; WM=waste management.

**Figure M–98. Waste Management Alternative 3, Disposal Group 1, Subgroup 1-E,
Radionuclide Releases to the Vadose Zone from the 200-East Area Integrated Disposal Facility**
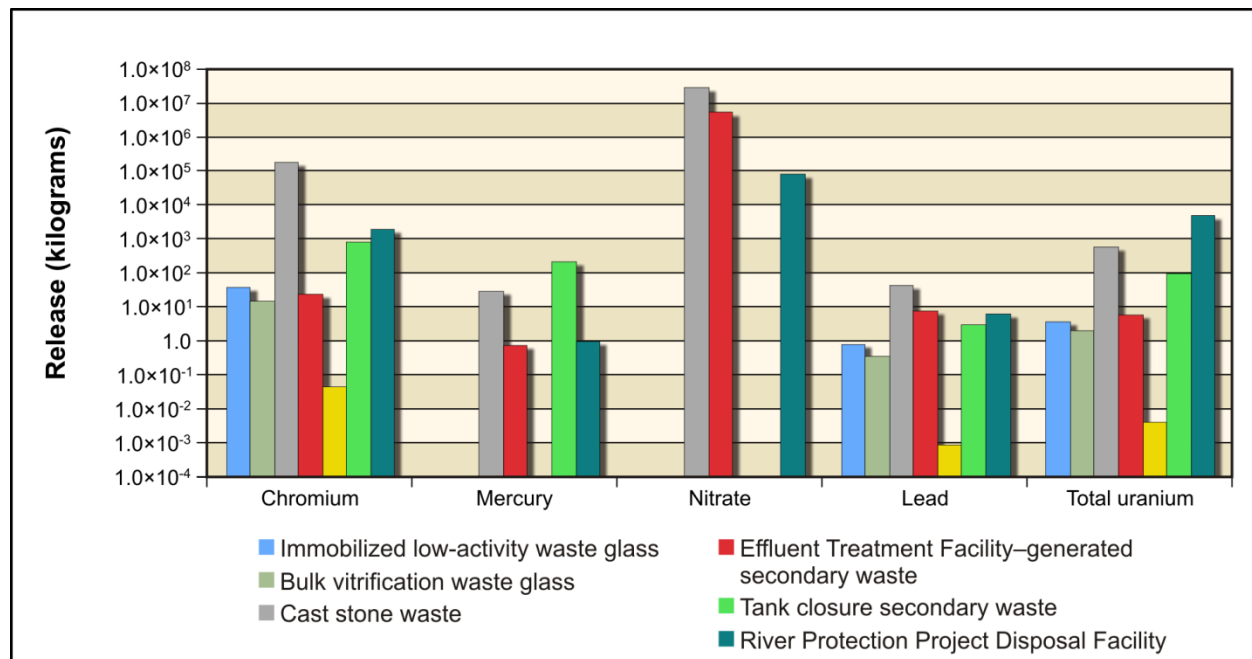
**Figure M–99. Waste Management Alternative 3, Disposal Group 1, Subgroup 1-E,
Chemical Releases to the Vadose Zone from the 200-East Area Integrated Disposal Facility**

M.4.3.2.17   Waste Management Alternative 3: Disposal in IDF, 200-East and 200-West Areas, Disposal Group 1, Subgroup 1-F

Disposal Group 1, Subgroup 1-F, addresses the waste resulting from Tank Closure Alternative 5, onsite non-CERCLA sources, FFTF decommissioning, waste management, and other DOE sites. Waste forms for IDF-East include the following:

- ILAW glass
- LAW melters
- bulk vitrification glass
- Cast stone waste
- Sulfate grout
- Tank closure secondary waste

Waste forms for IDF-West include the following:

- FFTF decommissioning secondary waste
- Waste management secondary waste
- Offsite waste
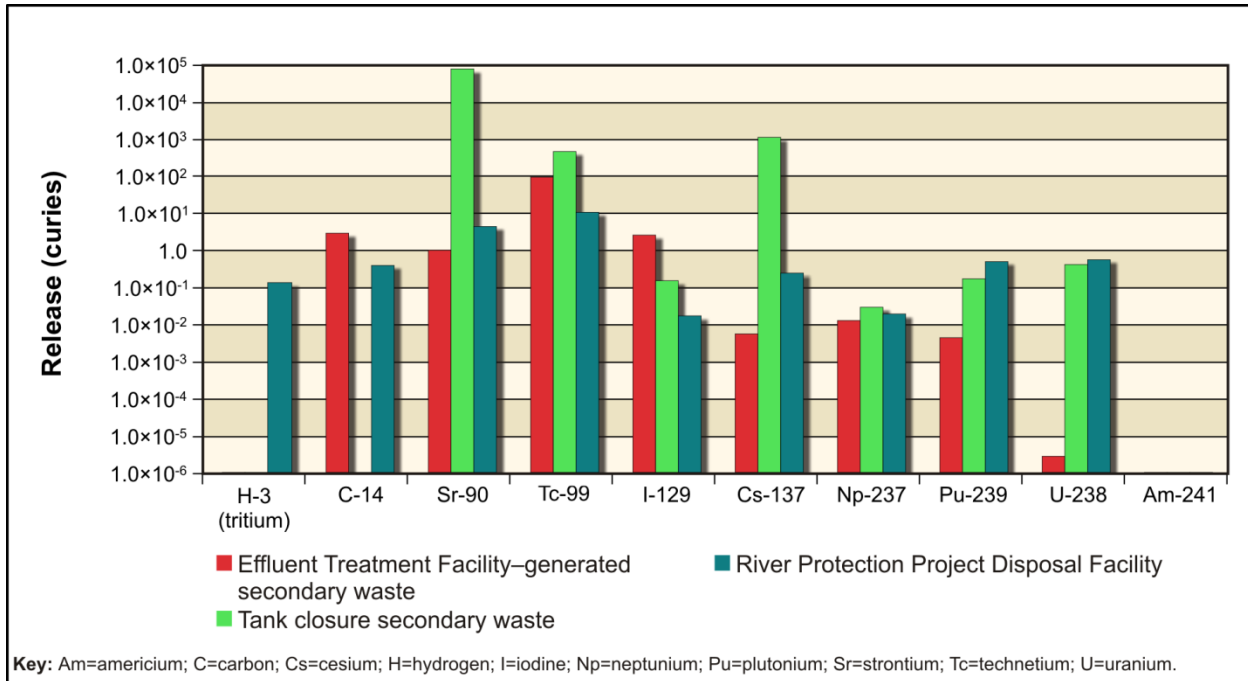- Onsite non-CERCLA waste

Potential releases to the vadose zone under Waste Management Alternative 3, Disposal Group 1, Subgroup 1-F, are indicated in Table M–49 and Figures M–100 and M–101.

Table M–49. Waste Management Alternative 3, Disposal Group 1, Subgroup 1-F, Radionuclide and Chemical Releases to the Vadose Zone

Source	Radionuclide (curies)										Chemical (kilograms)					
	H-3	C-14	Sr-90	Tc-99	I-129	Cs-137	Np-237	U-238	Pu-239	Am-241	Cr	F	Hg	NO$_3$	Pb	Utot
IDF-East																
ILAW glass	–	–	1.34×10^{-7}	3.79	1.28×10^{-3}	3.04×10^{-1}	1.08×10^{-6}	7.39×10^{-3}	1.47×10^{-4}	–	6.09×10^{-3}	–	–	–	1.22×10^{-4}	5.15
BV waste glass	–	–	1.76×10^{-1}	5.57×10^{2}	2.77×10^{-4}	1.90	8.60×10^{-5}	2.70×10^{-3}	8.17×10^{-2}	–	1.34×10^{1}	–	–	–	3.19×10^{-1}	1.78
Cast stone waste	1.60×10^{3}	9.53×10^{1}	2.56×10^{1}	3.74×10^{3}	1.70×10^{-1}	3.51×10^{2}	9.50×10^{-5}	2.79×10^{-1}	3.49×10^{-4}	–	6.10×10^{4}	–	9.80	9.34×10^{6}	1.48×10^{1}	1.94×10^{2}
ETF-generated secondary waste	–	3.37×10^{-1}	7.09	5.03×10^{1}	2.06	1.62×10^{-1}	1.11×10^{-2}	6.47×10^{-3}	3.41×10^{-6}	–	1.15×10^{1}	–	6.90×10^{-1}	1.20×10^{7}	6.66	5.42
Retired melters	–	–	1.36×10^{-10}	3.84×10^{-3}	1.30×10^{-6}	3.10×10^{-4}	1.10×10^{-9}	7.53×10^{-6}	1.50×10^{-7}	–	6.20×10^{-6}	–	–	–	1.24×10^{-7}	5.23×10^{-3}
Sulfate grout	–	–	1.05×10^{2}	–	–	1.57×10^{2}	1.54×10^{-5}	–	2.17×10^{-4}	–	2.21×10^{5}	–	–	–	6.46×10^{1}	–
TC secondary waste	–	–	7.05×10^{4}	2.08×10^{2}	7.48×10^{-2}	8.84×10^{2}	2.69×10^{-2}	1.45×10^{-1}	3.49×10^{-1}	–	3.32×10^{2}	–	2.19×10^{2}	–	2.70	8.99×10^{1}
IDF-West																
FFTF Decommissioning Alternative 3 waste	2.29	4.78×10^{1}	–	2.72×10^{1}	–	7.46×10^{-5}	–	–	–	–	7.51×10^{-3}	–	–	–	3.64×10^{-4}	7.91×10^{3}
WM secondary and onsite waste	3.66×10^{3}	6.82×10^{-1}	1.18×10^{3}	1.35	1.58×10^{-4}	5.47×10^{1}	2.62×10^{-3}	1.21×10^{-1}	6.20×10^{-2}	5.65×10^{-3}	1.83×10^{2}	2.74×10^{2}	4.16×10^{1}	2.97×10^{3}	1.30×10^{3}	1.56×10^{-1}
Offsite waste	5.57×10^{4}	5.68×10^{2}	1.87×10^{5}	1.46×10^{3}	2.26	1.93×10^{4}	6.28×10^{-1}	3.77×10^{2}	3.49	5.80×10^{-2}	8.05×10^{1}	–	7.85	–	3.24	–

Note: To convert kilograms to pounds, multiply by 2.2046.

Key: Am-241=americium-241; BV=bulk vitrification; C-14=carbon-14; Cr=chromium; Cs-137=cesium-137; ETF=Effluent Treatment Facility; F=fluoride; FFTF=Fast Flux Test Facility; H-3=hydrogen-3 (tritium); Hg=mercury; I-129=iodine-129; IDF-East=200-East Area Integrated Disposal Facility; IDF-West=200-West Area Integrated Disposal Facility; ILAW=immobilized low-activity waste; NO$_3$=nitrate; Np-237=neptunium-237; Pb=lead; Pu-239=plutonium-239; Sr-90=strontium-90; TC=tank closure; Tc-99=technetium-99; U-238=uranium-238; Utot=total uranium; WM=waste management.

Figure M–100. Waste Management Alternative 3, Disposal Group 1, Subgroup 1-F, Radionuclide Releases to the Vadose Zone from the 200-East Area Integrated Disposal Facility
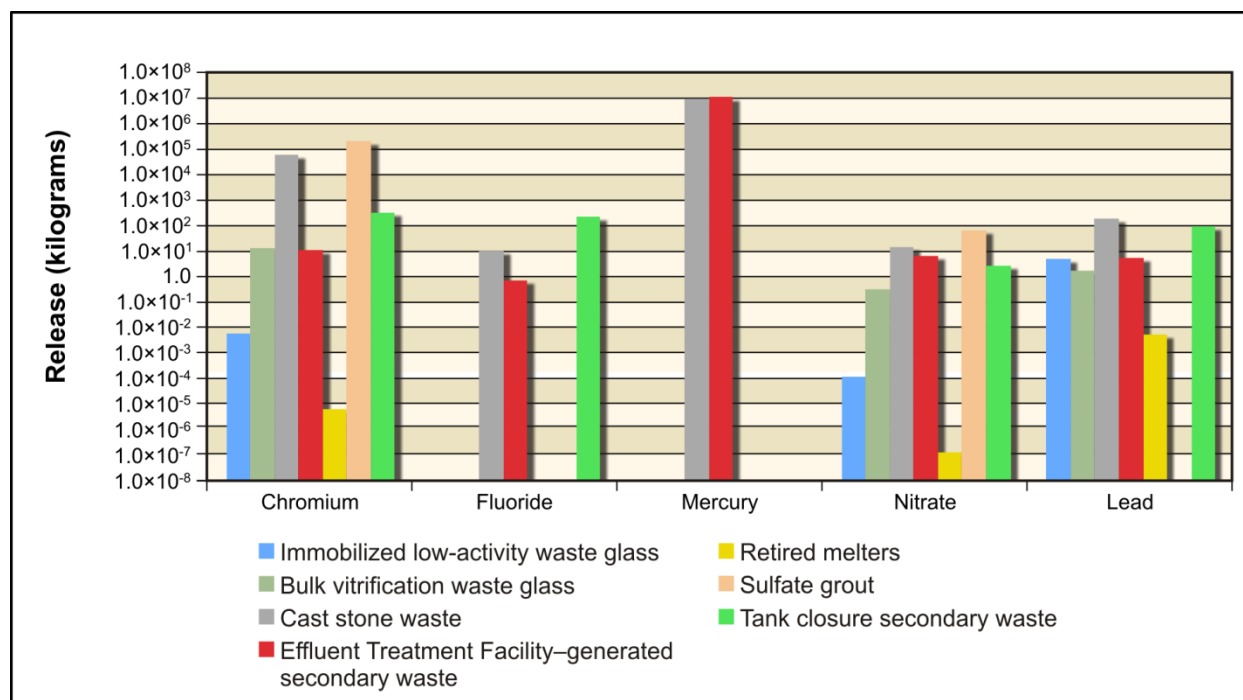
Figure M–101. Waste Management Alternative 3, Disposal Group 1, Subgroup 1-F, Chemical Releases to the Vadose Zone from the 200-East Area Integrated Disposal Facility

M.4.3.2.18   Waste Management Alternative 3: Disposal in IDF, 200-East and 200-West Areas, Disposal Group 1, Subgroup 1-G

Disposal Group 1, Subgroup 1-G, addresses the waste resulting from Tank Closure Alternative 6C, onsite non-CERCLA sources, FFTF decommissioning, waste management, and other DOE sites. Waste forms for IDF-East include the following:

- Tank closure secondary waste

The waste forms for IDF-West include the following:

- FFTF decommissioning secondary waste
- Waste management secondary waste
- Offsite waste
- Onsite non-CERCLA waste

Waste forms for the RPPDF include those resulting from tank closure cleanup activities under Tank Closure Alternative 6C. Potential releases to the vadose zone under Waste Management Alternative 3, Disposal Group 1, Subgroup 1-G, are indicated in Table M–50 and Figures M–102 and M–103.

Table M–50. Waste Management Alternative 3, Disposal Group 1, Subgroup 1-G, Radionuclide and Chemical Releases to the Vadose Zone

Source	Radionuclide (curies)										Chemical (kilograms)					
	H-3	C-14	Sr-90	Tc-99	I-129	Cs-137	Np-237	U-238	Pu-239	Am-241	Cr	F	Hg	NO$_3$	Pb	Utot
IDF-East																
ETF-generated secondary waste	–	2.77	9.24×10^{-1}	8.62×10^{1}	2.50	5.44×10^{-3}	1.20×10^{-2}	4.24×10^{-3}	2.76×10^{-6}	–	4.43×10^{1}	–	8.07×10^{-1}	9.01×10^{6}	8.36×10^{-2}	4.21
TC secondary waste	–	–	7.35×10^{4}	4.31×10^{2}	1.45×10^{-1}	1.02×10^{3}	2.81×10^{-2}	1.61×10^{-1}	3.95×10^{-1}	–	1.94×10^{3}	–	2.39×10^{2}	–	3.29	1.03×10^{2}
RPPDF	1.27×10^{-1}	3.61×10^{-1}	4.15	9.71	1.67×10^{-2}	2.30×10^{-1}	1.85×10^{-2}	4.66×10^{-1}	5.31×10^{-1}	–	5.86×10^{2}	–	1.61	3.93×10^{4}	4.97	6.60×10^{2}
IDF-West																
FFTF Decommissioning Alternative 3 waste	2.29	4.78×10^{1}	–	2.72×10^{1}	–	7.46×10^{-5}	–	–	–	–	7.51×10^{-3}	–	–	–	3.64×10^{-4}	7.91×10^{3}
WM secondary and onsite waste	3.66×10^{3}	6.82×10^{-1}	1.18×10^{3}	1.35	1.58×10^{-4}	5.47×10^{1}	2.62×10^{-3}	1.21×10^{-1}	6.20×10^{-2}	5.65×10^{-3}	1.83×10^{2}	2.74×10^{2}	4.16×10^{1}	2.97×10^{3}	1.30×10^{3}	1.56×10^{-1}
Offsite waste	5.57×10^{4}	5.68×10^{2}	1.87×10^{5}	1.46×10^{3}	2.26	1.93×10^{4}	6.28×10^{-1}	3.77×10^{2}	3.49	5.80×10^{-2}	8.05×10^{1}	–	7.85	–	3.24	–

Note: To convert kilograms to pounds, multiply by 2.2046.

Key: Am-241=americium-241; C-14=carbon-14; Cr=chromium; Cs-137=cesium-137; ETF=Effluent Treatment Facility; F=fluoride; FFTF=Fast Flux Test Facility; H-3=hydrogen-3 (tritium); Hg=mercury; I-129=iodine-129; IDF-East=200-East Area Integrated Disposal Facility; IDF-West=200-West Area Integrated Disposal Facility; NO$_3$=nitrate; Np-237=neptunium-237; Pb=lead; Pu-239=plutonium-239; RPPDF=River Protection Project Disposal Facility; Sr-90=strontium-90; TC=tank closure; Tc-99=technetium-99; U-238=uranium-238; Utot=total uranium; WM=waste management.

Figure M–102. Waste Management Alternative 3, Disposal Group 1, Subgroup 1-G, Radionuclide Releases to the Vadose Zone from the 200-East Area Integrated Disposal Facility
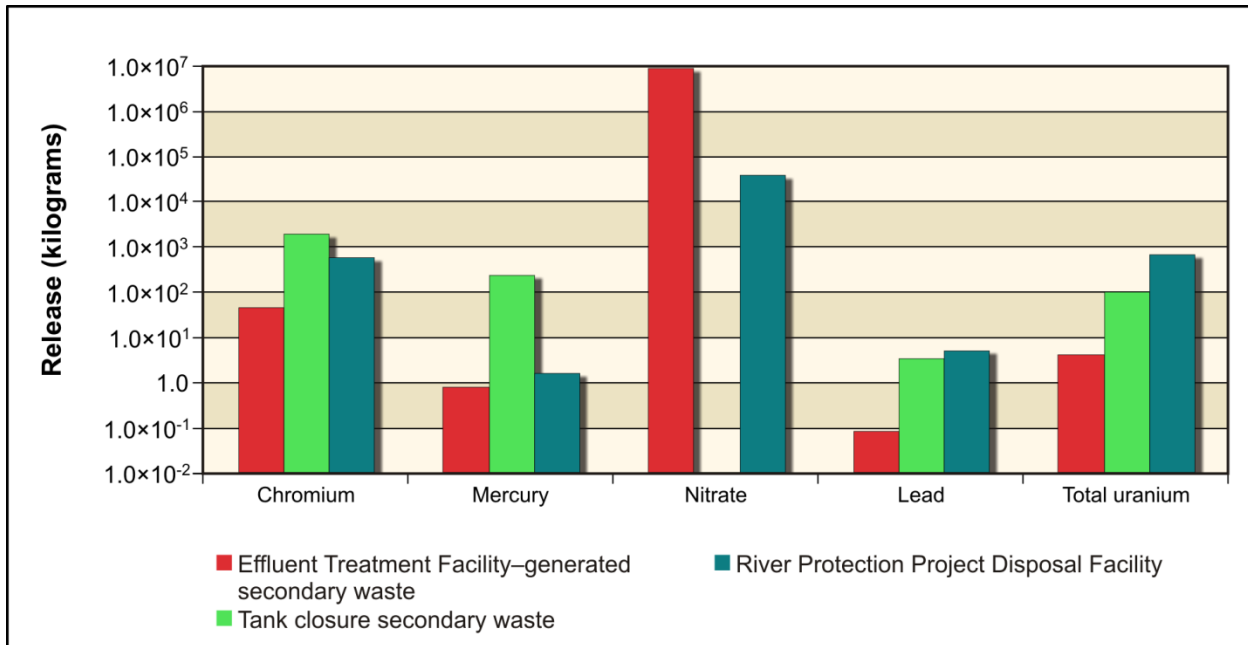
Figure M–103. Waste Management Alternative 3, Disposal Group 1, Subgroup 1-G, Chemical Releases to the Vadose Zone from the 200-East Area Integrated Disposal Facility

M.4.3.2.19 Waste Management Alternative 3: Disposal in IDF, 200-East and 200-West Areas, Disposal Group 2, Subgroup 2-A

Disposal Group 2, Subgroup 2-A, addresses the waste resulting from Tank Closure Alternative 2A, onsite non-CERCLA sources, FFTF decommissioning, waste management, and other DOE sites. Waste forms for IDF-East include the following:

- ILAW glass
- LAW melters
- Tank closure secondary waste

The waste forms for IDF-West include the following:

- FFTF decommissioning secondary waste
- Waste management secondary waste
- Offsite waste
- Onsite non-CERCLA waste

The RPPDF would not be constructed or operated under Tank Closure Alternative 2A because tank closure cleanup activities would not be conducted. Potential releases to the vadose zone under Waste Management Alternative 3, Disposal Group 2, Subgroup 2-A, are indicated in Table M–51 and Figures M–104 and M–105.
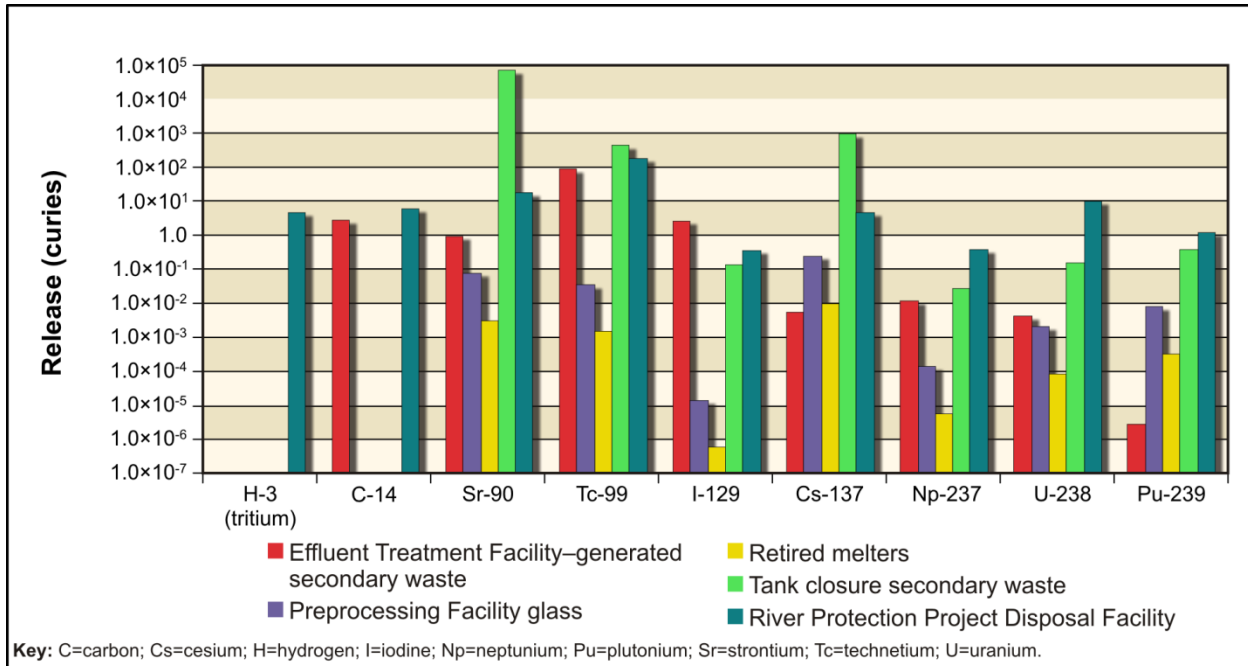
Table M–51. Waste Management Alternative 3, Disposal Group 2, Subgroup 2-A, Radionuclide and Chemical Releases to the Vadose Zone

| Source	Radionuclide (curies)										Chemical (kilograms)					
	H-3	C-14	Sr-90	Tc-99	I-129	Cs-137	Np-237	U-238	Pu-239	Am-241	Cr	F	Hg	NO$_3$	Pb	Utot
IDF-East																
ILAW glass	–	–	2.71×10^{-3}	7.81	2.63×10^{-3}	5.38×10^{-1}	2.30×10^{-6}	1.51×10^{-2}	3.48×10^{-4}	–	1.26×10^{2}	–	–	–	2.46	1.04×10^{1}
ETF-generated secondary waste	–	2.76	9.19×10^{-1}	8.62×10^{1}	2.48	5.41×10^{-3}	1.19×10^{-2}	4.22×10^{-3}	2.74×10^{-6}	–	4.43×10^{1}	–	8.03×10^{-1}	9.01×10^{6}	8.31×10^{-2}	4.19
Retired melters	–	–	2.91×10^{-6}	8.38×10^{-3}	2.84×10^{-6}	5.78×10^{-4}	2.46×10^{-9}	1.62×10^{-5}	3.74×10^{-7}	–	1.35×10^{-1}	–	–	–	2.62×10^{-3}	1.10×10^{-2}
TC secondary waste	–	–	7.32×10^{4}	4.31×10^{2}	1.45×10^{-1}	1.02×10^{3}	2.80×10^{-2}	1.60×10^{-1}	3.92×10^{-1}	–	1.94×10^{3}	–	2.38×10^{2}	–	3.27	1.02×10^{2}
IDF-West																
FFTF Decommis-sioning Alternative 3 waste	2.29	4.78×10^{1}	–	2.72×10^{1}	–	7.46×10^{-5}	–	–	–	–	7.51×10^{-3}	–	–	–	3.64×10^{-4}	7.91×10^{3}
WM secondary and onsite waste	3.66×10^{3}	6.82×10^{-1}	1.18×10^{3}	1.35	1.58×10^{-4}	5.47×10^{1}	2.62×10^{-3}	1.21×10^{-1}	6.20×10^{-2}	5.65×10^{-3}	1.83×10^{2}	2.74×10^{2}	4.16×10^{1}	2.97×10^{3}	1.30×10^{3}	1.56×10^{-1}
Offsite waste	5.57×10^{4}	5.68×10^{2}	1.87×10^{5}	1.46×10^{3}	2.26	1.93×10^{4}	6.28×10^{-1}	3.77×10^{2}	3.49	5.80×10^{-2}	8.05×10^{1}	–	7.85	–	3.24	–

Note: To convert kilograms to pounds, multiply by 2.2046.

Key: Am-241=americium-241; C-14=carbon-14; Cr=chromium; Cs-137=cesium-137; ETF=Effluent Treatment Facility; F=fluoride; FFTF=Fast Flux Test Facility; H-3=hydrogen-3 (tritium); Hg=mercury; I-129=iodine-129; IDF-East=200-East Area Integrated Disposal Facility; IDF-West=200-West Area Integrated Disposal Facility; ILAW=immobilized low-activity waste; NO$_3$=nitrate; Np-237=neptunium-237; Pb=lead; Pu-239=plutonium-239; Sr-90=strontium-90; TC=tank closure; Tc-99=technetium-99; U-238=uranium-238; Utot=total uranium; WM=waste management.

Figure M–104. Waste Management Alternative 3, Disposal Group 2, Subgroup 2-A, Radionuclide Releases to the Vadose Zone from the 200-East Area Integrated Disposal Facility
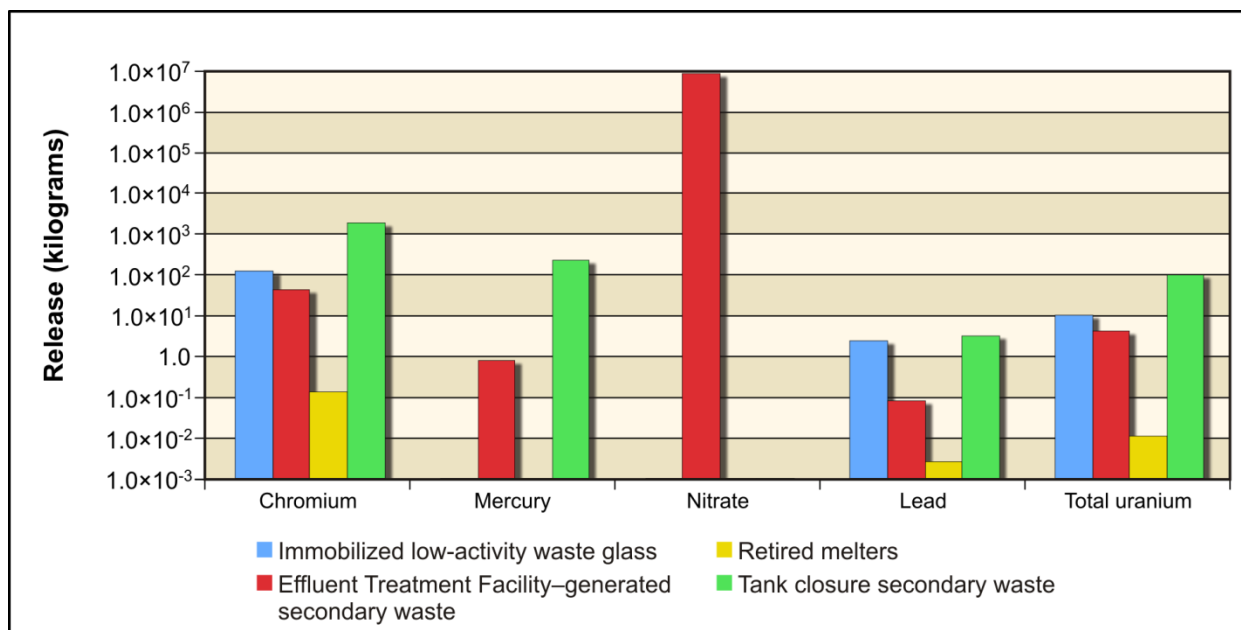
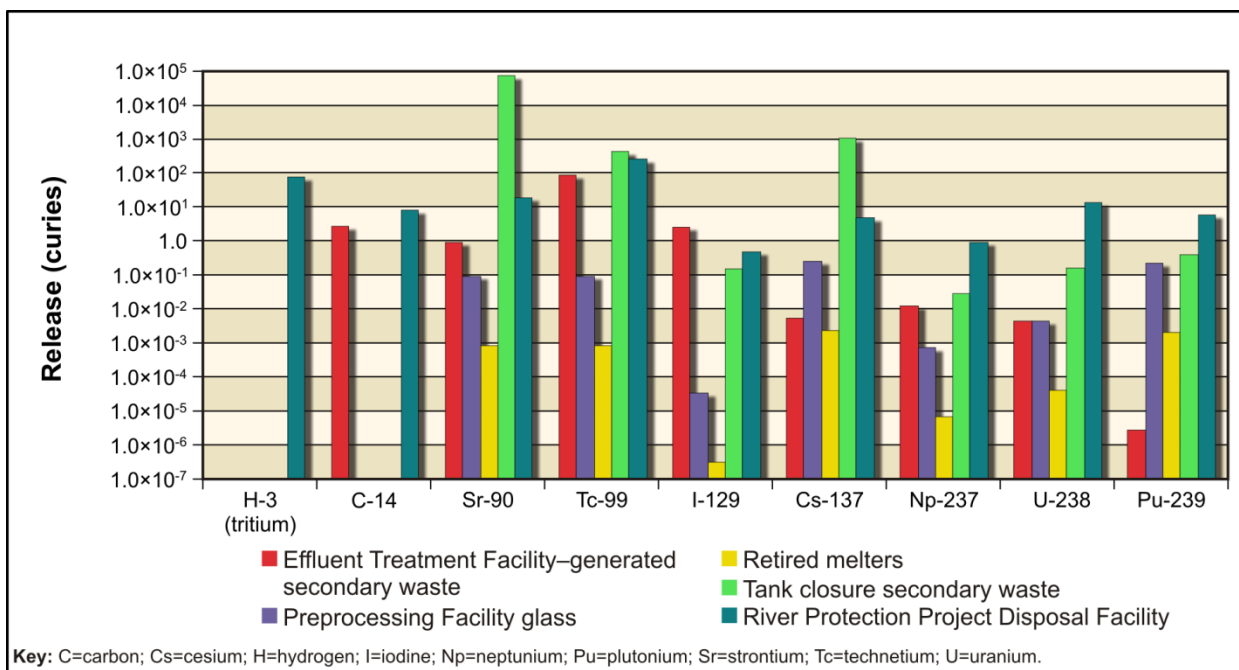**Figure M–105. Waste Management Alternative 3, Disposal Group 2, Subgroup 2-A, Chemical Releases to the Vadose Zone from the 200-East Area Integrated Disposal Facility**

M.4.3.2.20   Waste Management Alternative 3: Disposal in IDF, 200-East and 200-West Areas, Disposal Group 2, Subgroup 2-B

Disposal Group 2, Subgroup 2-B, addresses the waste resulting from Tank Closure Alternative 6B, Base and Option Cases; onsite non-CERCLA sources; FFTF decommissioning; waste management; and other DOE sites. Waste forms for IDF-East include the following:

- PPF glass
- PPF melters
- Tank closure secondary waste

The waste forms for IDF-West include the following:

- FFTF decommissioning secondary waste
- Waste management secondary waste
- Offsite waste
- Onsite non-CERCLA waste

Waste forms for the RPPDF include those resulting from tank closure cleanup activities under Tank Closure Alternative 6B, Base and Option Cases. Potential releases to the vadose zone under Waste Management Alternative 3, Disposal Group 2, Subgroup 2-B, Base and Option Cases, are indicated in Tables M–52 and M–53 and Figures M–106 through M–109.

Table M–52. Waste Management Alternative 3, Disposal Group 2, Subgroup 2-B, Base Case, Radionuclide and Chemical Releases to the Vadose Zone

Source	Radionuclide (curies)										Chemical (kilograms)					
	H-3	C-14	Sr-90	Tc-99	I-129	Cs-137	Np-237	U-238	Pu-239	Am-241	Cr	F	Hg	NO₃	Pb	Utot
IDF-East																
ETF-generated secondary waste	–	2.78	9.24×10^{-1}	8.73×10^{1}	2.51	5.44×10^{-3}	1.20×10^{-2}	4.28×10^{-3}	2.75×10^{-6}	–	4.53×10^{1}	–	8.06×10^{-1}	9.16×10^{6}	8.37×10^{-2}	4.31
PPF glass	–	–	7.42×10^{-2}	3.52×10^{-2}	1.40×10^{-5}	2.36×10^{-1}	1.36×10^{-4}	2.03×10^{-3}	7.96×10^{-3}	–	2.20	–	–	–	7.05×10^{-2}	4.21
Retired melters	–	–	3.07×10^{-3}	1.46×10^{-3}	5.81×10^{-7}	9.80×10^{-3}	5.64×10^{-6}	8.40×10^{-5}	3.29×10^{-4}	–	9.12×10^{-2}	–	–	–	2.92×10^{-3}	1.74×10^{-1}
TC secondary waste	–	–	7.01×10^{4}	4.37×10^{2}	1.38×10^{-1}	9.77×10^{2}	2.68×10^{-2}	1.55×10^{-1}	3.75×10^{-1}	–	1.98×10^{3}	–	2.29×10^{2}	–	3.13	1.00×10^{2}
RPPDF	4.57	5.80	1.80×10^{1}	1.78×10^{2}	3.43×10^{-1}	4.61	3.81×10^{-1}	9.87	1.22	–	4.10×10^{3}	–	1.73	2.83×10^{5}	5.15×10^{1}	7.66×10^{3}
IDF-West																
FFTF Decommissioning Alternative 3 waste	2.29	4.78×10^{1}	–	2.72×10^{1}	–	7.46×10^{-5}	–	–	–	–	7.51×10^{-3}	–	–	–	3.64×10^{-4}	7.91×10^{3}
WM secondary and onsite waste	3.66×10^{3}	6.82×10^{-1}	1.18×10^{3}	1.35	1.58×10^{-4}	5.47×10^{1}	2.62×10^{-3}	1.21×10^{-1}	6.20×10^{-2}	5.65×10^{-3}	1.83×10^{2}	2.74×10^{2}	4.16×10^{1}	2.97×10^{3}	1.30×10^{3}	1.56×10^{-1}
Offsite waste	5.57×10^{4}	5.68×10^{2}	1.87×10^{5}	1.46×10^{3}	2.26	1.93×10^{4}	6.28×10^{-1}	3.77×10^{2}	3.49	5.80×10^{-2}	8.05×10^{1}	–	7.85	–	3.24	–

Note: To convert kilograms to pounds, multiply by 2.2046.

Key: Am-241=americium-241; C-14=carbon-14; Cr=chromium; Cs-137=cesium-137; ETF=Effluent Treatment Facility; F=fluoride; FFTF=Fast Flux Test Facility; H-3=hydrogen-3 (tritium); Hg=mercury; I-129=iodine-129; IDF-East=200-East Area Integrated Disposal Facility; IDF-West=200-West Area Integrated Disposal Facility; NO₃=nitrate; Np-237=neptunium-237; Pb=lead; PPF=Preprocessing Facility; Pu-239=plutonium-239; RPPDF=River Protection Project Disposal Facility; Sr-90=strontium-90; TC=tank closure; Tc-99=technetium-99; U-238=uranium-238; Utot=total uranium; WM=waste management.

Figure M–106. Waste Management Alternative 3, Disposal Group 2, Subgroup 2-B, Base Case, Radionuclide Releases to the Vadose Zone from the 200-East Area Integrated Disposal Facility
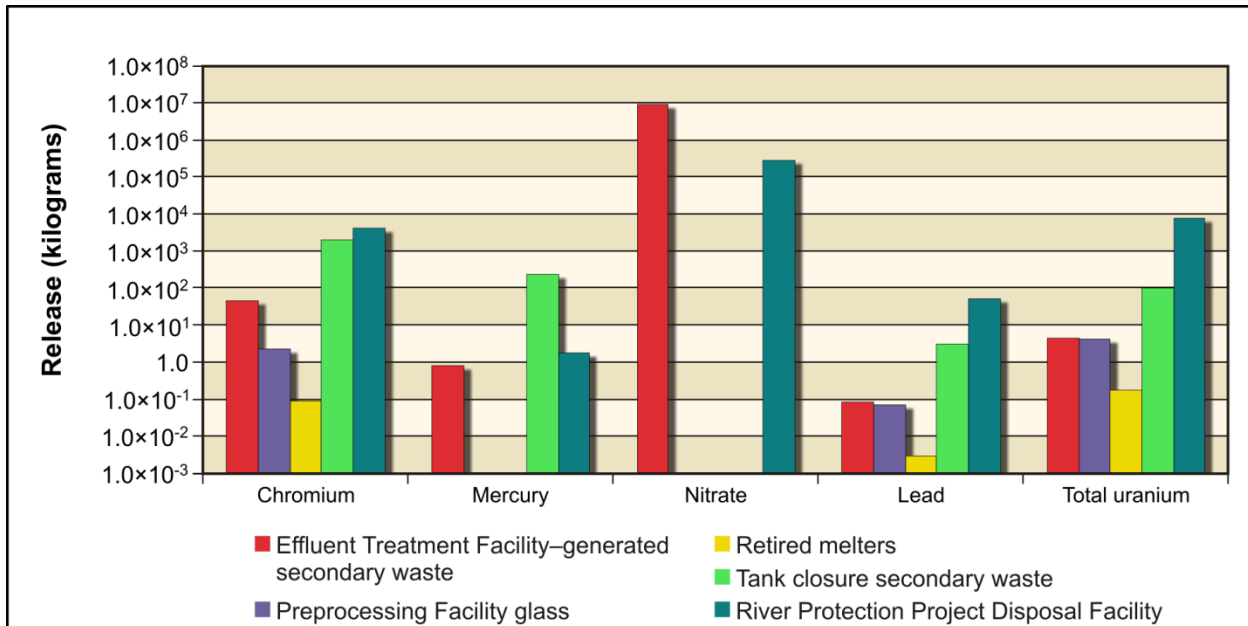
Figure M–107. Waste Management Alternative 3, Disposal Group 2, Subgroup 2-B, Base Case, Chemical Releases to the Vadose Zone from the 200-East Area Integrated Disposal Facility

Table M–53. Waste Management Alternative 3, Disposal Group 2, Subgroup 2-B, Option Case, Radionuclide and Chemical Releases to the Vadose Zone

Source	Radionuclide (curies)										Chemical (kilograms)					
	H-3	C-14	Sr-90	Tc-99	I-129	Cs-137	Np-237	U-238	Pu-239	Am-241	Cr	F	Hg	NO$_3$	Pb	Utot
IDF-East																
ETF-generated secondary waste	–	2.82	9.29×10^{-1}	8.79×10^{1}	2.53	5.48×10^{-3}	1.23×10^{-2}	4.35×10^{-3}	2.80×10^{-6}	–	5.65×10^{1}	–	8.38×10^{-1}	1.51×10^{7}	8.41×10^{-2}	4.38
PPF glass	–	–	9.09×10^{-2}	9.19×10^{-2}	3.36×10^{-5}	2.63×10^{-1}	7.26×10^{-4}	4.57×10^{-3}	2.22×10^{-1}	–	4.32×10^{1}	–	–	–	8.45×10^{-2}	6.20
Retired melters	–	–	8.33×10^{-4}	8.40×10^{-4}	3.06×10^{-7}	2.41×10^{-3}	6.63×10^{-6}	4.19×10^{-5}	2.03×10^{-3}	–	1.93×10^{-1}	–	–	–	7.02×10^{-4}	4.68×10^{-2}
TC secondary waste	–	–	7.54×10^{4}	4.40×10^{2}	1.51×10^{-1}	1.05×10^{3}	2.92×10^{-2}	1.68×10^{-1}	4.10×10^{-1}	–	2.47×10^{3}	–	2.54×10^{2}	–	3.37	1.09×10^{2}
RPPDF	7.95×10^{1}	8.26	1.89×10^{1}	2.70×10^{2}	4.96×10^{-1}	4.77	9.11×10^{-1}	1.37×10^{1}	5.94	–	3.69×10^{4}	–	1.15×10^{1}	1.04×10^{7}	5.29×10^{1}	9.24×10^{3}
IDF-West																
FFTF Decommissioning Alternative 3 waste	2.29	4.78×10^{1}	–	2.72×10^{1}	–	7.46×10^{-5}	–	–	–	–	7.51×10^{-3}	–	–	–	3.64×10^{-4}	7.91×10^{3}
WM secondary and onsite waste	3.66×10^{3}	6.82×10^{-1}	1.18×10^{3}	1.35	1.58×10^{-4}	5.47×10^{1}	2.62×10^{-3}	1.21×10^{-1}	6.20×10^{-2}	5.65×10^{-3}	1.83×10^{2}	2.74×10^{2}	4.16×10^{1}	2.97×10^{3}	1.30×10^{3}	1.56×10^{-1}
Offsite waste	5.57×10^{4}	5.68×10^{2}	1.87×10^{5}	1.46×10^{3}	2.26	1.93×10^{4}	6.28×10^{-1}	3.77×10^{2}	3.49	5.80×10^{-2}	8.05×10^{1}	–	7.85	–	3.24	–

Note: To convert kilograms to pounds, multiply by 2.2046.

Key: Am-241=americium-241; C-14=carbon-14; Cr=chromium; Cs-137=cesium-137; ETF=Effluent Treatment Facility; F=fluoride; FFTF=Fast Flux Test Facility; H-3=hydrogen-3 (tritium); Hg=mercury; I-129=iodine-129; IDF-East=200-East Area Integrated Disposal Facility; IDF-West=200-West Area Integrated Disposal Facility; NO$_3$=nitrate; Np-237=neptunium-237; Pb=lead; PPF=Preprocessing Facility; Pu-239=plutonium-239; RPPDF=River Protection Project Disposal Facility; Sr-90=strontium-90; TC=tank closure; Tc-99=technetium-99; U-238=uranium-238; Utot=total uranium; WM=waste management.

Figure M–108. Waste Management Alternative 3, Disposal Group 2, Subgroup 2-B, Option Case, Radionuclide Releases to the Vadose Zone from the 200-East Area Integrated Disposal Facility
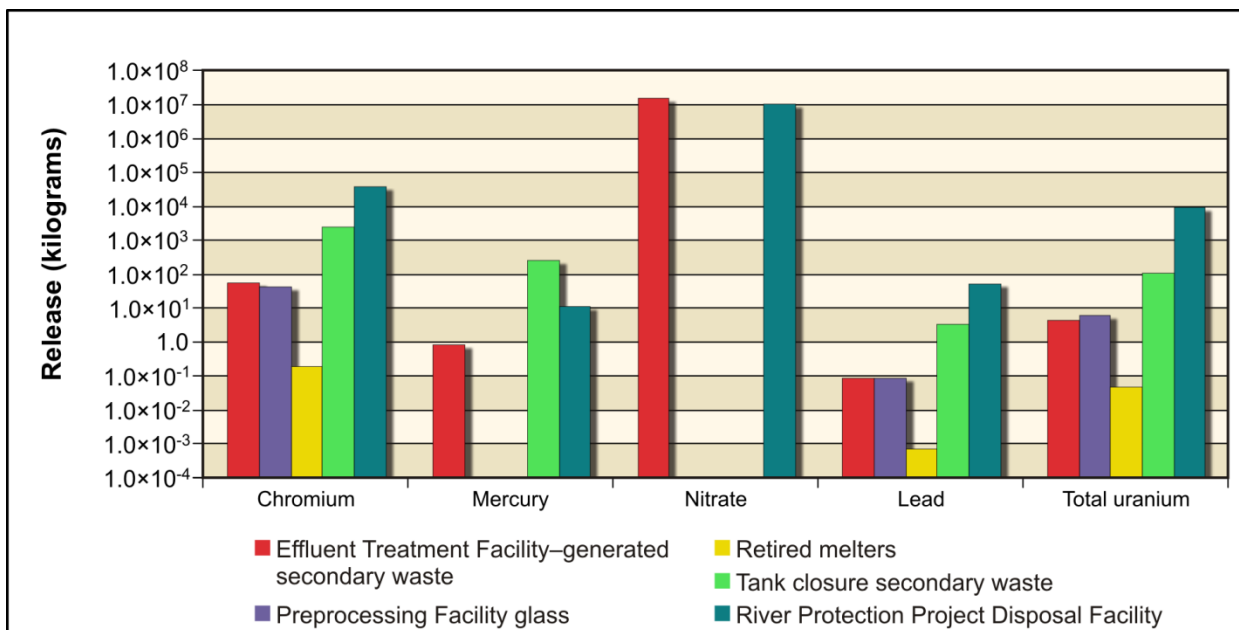
Figure M–109. Waste Management Alternative 3, Disposal Group 2, Subgroup 2-B, Option Case, Chemical Releases to the Vadose Zone from the 200-East Area Integrated Disposal Facility

M.4.3.2.21   Waste Management Alternative 3: Disposal in IDF, 200-East and 200-West Areas, Disposal Group 3

Disposal Group 3 addresses the waste resulting from Tank Closure Alternative 6A, Base and Option Cases; onsite non-CERCLA sources; FFTF decommissioning; waste management; and other DOE sites. Waste forms for IDF-East include the following:

- PPF glass
- PPF melters
- Tank closure secondary waste

The waste forms for IDF-West include the following:

- FFTF decommissioning secondary waste
- Waste management secondary waste
- Offsite waste
- Onsite non-CERCLA waste

Waste forms for the RPPDF include those resulting from tank closure cleanup activities under Tank Closure Alternative 6A, Base and Option Cases. Potential releases to the vadose zone under Waste Management Alternative 3,Disposal Group 3, Base and Option Cases, are indicated in Tables M–54 and M–55 and Figures M–110 through M–113.
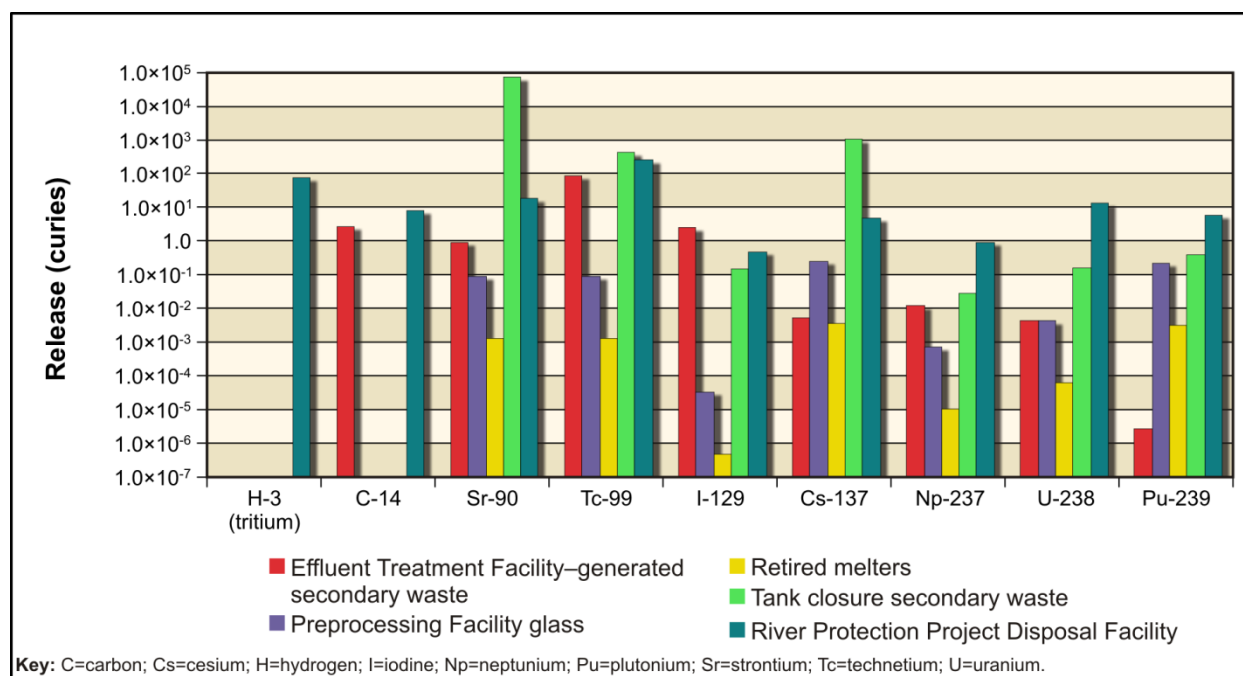
Table M–54. Waste Management Alternative 3, Disposal Group 3, Base Case, Radionuclide and Chemical Releases to the Vadose Zone

| Source	Radionuclide (curies)										Chemical (kilograms)					
	H-3	**C-14**	**Sr-90**	**Tc-99**	**I-129**	**Cs-137**	**Np-237**	**U-238**	**Pu-239**	**Am-241**	**Cr**	**F**	**Hg**	**NO$_3$**	**Pb**	**Utot**
IDF-East																
ETF-generated secondary waste	–	2.78	9.24×10^{-1}	8.73×10^{1}	2.51	5.44×10^{-3}	1.20×10^{-2}	4.28×10^{-3}	2.75×10^{-6}	–	4.53×10^{1}	–	8.06×10^{-1}	9.16×10^{6}	8.37×10^{-2}	4.31
PPF glass	–	–	7.42×10^{-2}	3.50×10^{-2}	1.39×10^{-5}	2.36×10^{-1}	1.35×10^{-4}	2.01×10^{-3}	7.92×10^{-3}	–	2.19	–	–	–	7.00×10^{-2}	4.19
Retired melters	–	–	4.80×10^{-3}	2.26×10^{-3}	9.03×10^{-7}	1.53×10^{-2}	8.74×10^{-6}	1.30×10^{-4}	5.13×10^{-4}	–	1.42×10^{-1}	–	–	–	4.51×10^{-3}	2.70×10^{-1}
TC secondary waste	–	–	7.01×10^{4}	4.37×10^{2}	1.38×10^{-1}	9.77×10^{2}	2.68×10^{-2}	1.55×10^{-1}	3.75×10^{-1}	–	1.98×10^{3}	–	2.29×10^{2}	–	3.13	1.00×10^{2}
RPPDF	4.57	5.78	1.80×10^{1}	1.78×10^{2}	3.43×10^{-1}	4.61	3.80×10^{-1}	9.86	1.21	–	4.10×10^{3}	–	1.73	2.83×10^{5}	5.12×10^{1}	7.66×10^{3}
IDF-West																
FFTF Decommissioning Alternative 3 waste	2.29	4.78×10^{1}	–	2.72×10^{1}	–	7.46×10^{-5}	–	–	–	–	7.51×10^{-3}	–	–	–	3.64×10^{-4}	7.91×10^{3}
WM secondary and onsite waste	3.66×10^{3}	6.82×10^{-1}	1.18×10^{3}	1.35	1.58×10^{-4}	5.47×10^{1}	2.62×10^{-3}	1.21×10^{-1}	6.20×10^{-2}	5.65×10^{-3}	1.83×10^{2}	2.74×10^{2}	4.16×10^{1}	2.97×10^{3}	1.30×10^{3}	1.56×10^{-1}
Offsite waste	5.57×10^{4}	5.68×10^{2}	1.87×10^{5}	1.46×10^{3}	2.26	1.93×10^{4}	6.28×10^{-1}	3.77×10^{2}	3.49	5.80×10^{-2}	8.05×10^{1}	–	7.85	–	3.24	–

Note: To convert kilograms to pounds, multiply by 2.2046.
Key: Am-241=americium-241; C-14=carbon-14; Cr=chromium; Cs-137=cesium-137; ETF=Effluent Treatment Facility; F=fluoride; FFTF=Fast Flux Test Facility; H-3=hydrogen-3 (tritium); Hg=mercury; I-129=iodine-129; IDF-East=200-East Area Integrated Disposal Facility; IDF-West=200-West Area Integrated Disposal Facility; NO$_3$=nitrate; Np-237=neptunium-237; PPF=Preprocessing Facility; Pu-239=plutonium-239; RPPDF=River Protection Project Disposal Facility; Sr-90=strontium-90; TC=tank closure; Tc-99=technetium-99; U-238=uranium-238; Utot=total uranium; WM=waste management.

Figure M–110. Waste Management Alternative 3, Disposal Group 3, Base Case, Radionuclide Releases to the Vadose Zone from the 200-East Area Integrated Disposal Facility
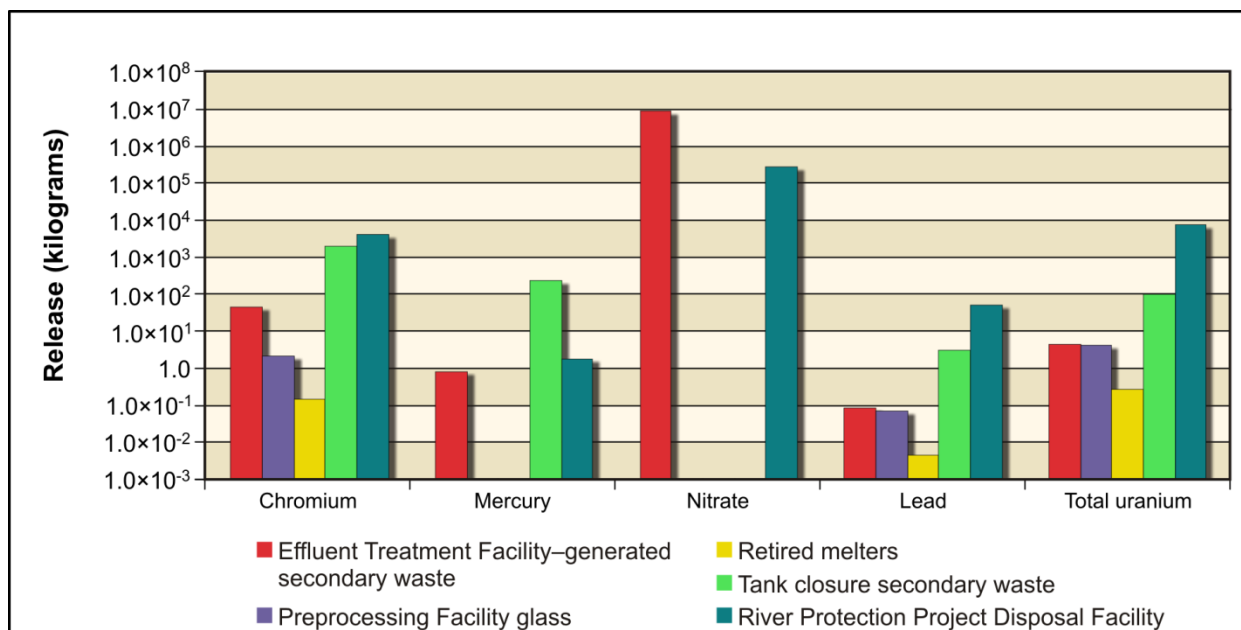
Figure M–111. Waste Management Alternative 3, Disposal Group 3, Base Case, Chemical Releases to the Vadose Zone from the 200-East Area Integrated Disposal Facility

Table M–55. Waste Management Alternative 3, Disposal Group 3, Option Case, Radionuclide and Chemical Releases to the Vadose Zone

Source	Radionuclide (curies)										Chemical (kilograms)					
	H-3	C-14	Sr-90	Tc-99	I-129	Cs-137	Np-237	U-238	Pu-239	Am-241	Cr	F	Hg	NO$_3$	Pb	Utot
IDF-East																
ETF-generated secondary waste	–	2.82	9.29×10^{-1}	8.79×10^{1}	2.53	5.48×10^{-3}	1.23×10^{-2}	4.35×10^{-3}	2.80×10^{-6}	–	5.65×10^{1}	–	8.38×10^{-1}	1.51×10^{7}	8.41×10^{-2}	4.38
PPF glass	–	–	9.09×10^{-2}	9.13×10^{-2}	3.34×10^{-5}	2.63×10^{-1}	7.21×10^{-4}	4.54×10^{-3}	2.21×10^{-1}	–	4.30×10^{1}	–	–	–	8.40×10^{-2}	6.16
Retired melters	–	–	1.31×10^{-3}	1.31×10^{-3}	4.79×10^{-7}	3.78×10^{-3}	1.04×10^{-5}	6.54×10^{-5}	3.17×10^{-3}	–	6.18×10^{-1}	–	–	–	1.21×10^{-3}	8.84×10^{-2}
TC secondary waste	–	–	7.54×10^{4}	4.40×10^{2}	1.51×10^{-1}	1.05×10^{3}	2.92×10^{-2}	1.68×10^{-1}	4.10×10^{-1}	–	2.47×10^{3}	–	2.54×10^{2}	–	3.37	1.09×10^{2}
RPPDF	7.95×10^{1}	8.18	1.89×10^{1}	2.70×10^{2}	4.96×10^{-1}	4.77	9.07×10^{-1}	1.37×10^{1}	5.90	–	3.69×10^{4}	–	1.14×10^{1}	1.04×10^{7}	5.26×10^{1}	9.24×10^{3}
IDF-West																
FFTF Decommissioning Alternative 3 waste	2.29	4.78×10^{1}	–	2.72×10^{1}	–	7.46×10^{-5}	–	–	–	–	7.51×10^{-3}	–	–	–	3.64×10^{-4}	7.91×10^{3}
WM secondary and onsite waste	3.66×10^{3}	6.82×10^{-1}	1.18×10^{3}	1.35	1.58×10^{-4}	5.47×10^{1}	2.62×10^{-3}	1.21×10^{-1}	6.20×10^{-2}	5.65×10^{-3}	1.83×10^{2}	2.74×10^{2}	4.16×10^{1}	2.97×10^{3}	1.30×10^{3}	1.56×10^{-1}
Offsite waste	5.57×10^{4}	5.68×10^{2}	1.87×10^{5}	1.46×10^{3}	2.26	1.93×10^{4}	6.28×10^{-1}	3.77×10^{2}	3.49	5.80×10^{-2}	8.05×10^{1}	–	7.85	–	3.24	–

Note: To convert kilograms to pounds, multiply by 2.2046.

Key: Am-241=americium-241; C-14=carbon-14; Cr=chromium; Cs-137=cesium-137; ETF=Effluent Treatment Facility; F=fluoride; FFTF=Fast Flux Test Facility; H-3=hydrogen-3 (tritium); Hg=mercury; I-129=iodine-129; IDF-East=200-East Area Integrated Disposal Facility; IDF-West=200-West Area Integrated Disposal Facility; NO$_3$=nitrate; Np-237=neptunium-237; Pb=lead; PPF=Preprocessing Facility; Pu-239=plutonium-239; RPPDF=River Protection Project Disposal Facility; Sr-90=strontium-90; TC=tank closure; Tc-99=technetium-99; U-238=uranium-238; Utot=total uranium; WM=waste management.

Figure M–112. Waste Management Alternative 3, Disposal Group 3, Option Case, Radionuclide Releases to the Vadose Zone from the 200-East Area Integrated Disposal Facility
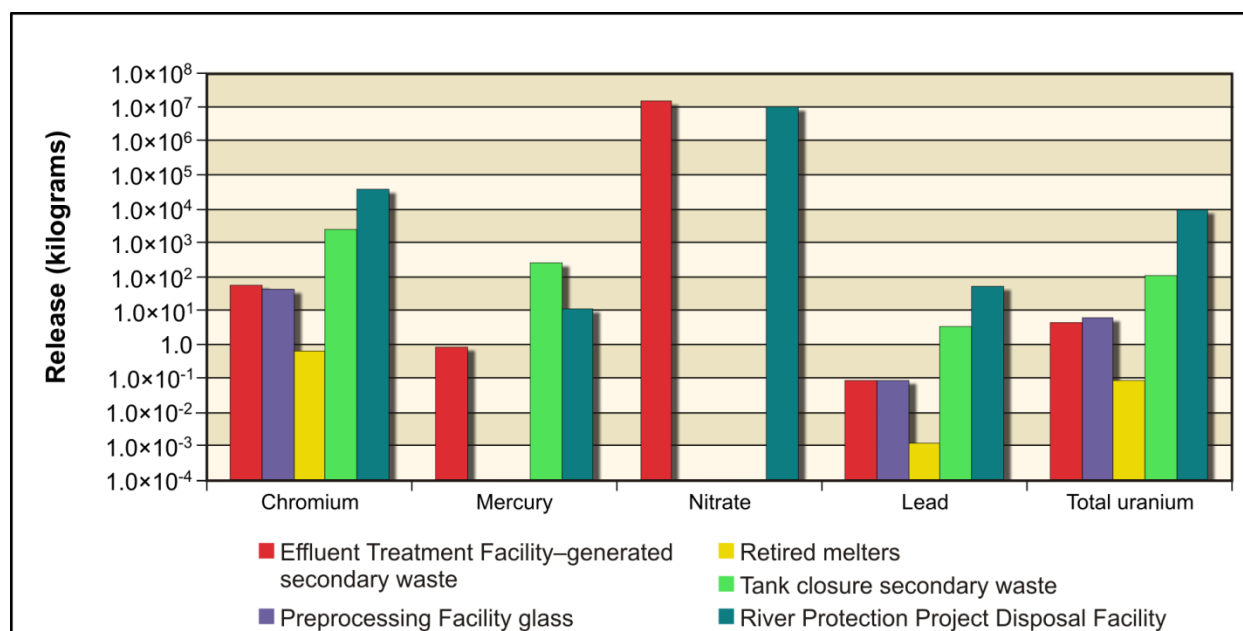
Figure M–113. Waste Management Alternative 3, Disposal Group 3, Option Case, Chemical Releases to the Vadose Zone from the 200-East Area Integrated Disposal Facility

M.5   SENSITIVITY ANALYSIS

Because of the long-term nature of processes expected to occur at Hanford, direct observation of potential impacts is not possible and mathematical models were developed to estimate the rate of release of constituents to the vadose zone. Estimates thus depend on the description of the release incorporated into the model and on values of parameters that quantify rates of physical and chemical processes constituting the model. The objective of this section is to investigate the sensitivity of the estimates of rate of release

to the vadose zone to elements of the model concepts and to values of parameters used in the models. Three cases are considered: discharge of liquid and solute representing a past leak at a tank farm, leaching from supplemental-waste forms in the 200-East Area, and diffusive release from a grouted waste form. The three cases illustrate the range of sensitivities for liquid and solid sources. The constituents technetium-99 and iodine-129 were selected for this sensitivity analysis because they move at the velocity of groundwater and have been observed in Hanford groundwater near known sources of contamination.

M.5.1 Aqueous Volumetric Release

During tank farm operations, aqueous liquids and solutes were discharged to the vadose zone in uncontrolled leakage events. The magnitude, duration, and timing of the leaks and the spatial distribution of recharge at the tank farms are not well characterized. Studies have determined that the volume of leaks may be on the order of 400 cubic meters (100,000 gallons) (Hanlon 2003) and that recharge at the tank farms may be high relative to Hanford background conditions (DOE 2005). To investigate the sensitivity of potential impacts on conditions affecting an aqueous discharge at a tank farm, two cases were evaluated. In the first case, an isolated tank in the center of a tank farm was surrounded by an area of elevated recharge, and the release duration and timing were varied. In the second case, the area of an isolated tank was subject to excess recharge while the surrounding area experienced recharge at a normal background rate, and the leak duration and timing were varied. A plan view of the configuration is presented in Figure M–114. The inner source area representing the tank is a square with sides equal to 20 meters (66 feet). In the first case, the dashed rectangle representing the tank farm area experienced recharge at 100 millimeters per year and the balance of the study area experienced recharge at 3.5 millimeters per year. In the second case, only the area of the source experienced recharge at 100 millimeters per year and the balance of the study area experienced recharge at 3.5 millimeters per year. The initial moisture profile was established as the steady state condition at a recharge rate of 3.5 millimeters per year, and elevated recharge was assumed to begin at the start time of tank farm operations. In both cases, the site geology corresponded to 200-West Area conditions with Hanford gravel, Hanford sand, Plio-Pleistocene silt, and Ringold gravel layered from the ground surface downward to the water table at a depth of 70 meters (230 feet).
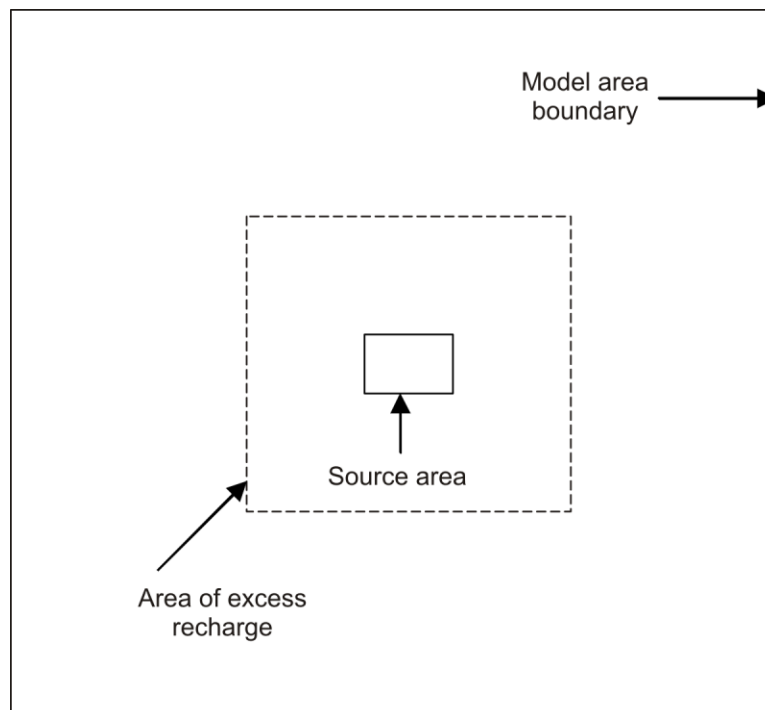
Figure M–114. Plan View of Aqueous Discharge Study Area

M.5.1.1 Extended Area of Elevated Recharge

In this first case, elevated recharge was assumed to occur over the area of a tank farm, approximately 10,000 square meters (110,000 square feet), and the leak duration and timing were varied. For a leak beginning at the start time of tank operations, rate of arrival of solute at the water table for leaks of duration of 1 year, 1 month, 1 week, and 1 day are presented in Figure M–115. The four curves plotted on this figure coincide at nearly all points in time and therefore may not be separately distinguished. Releases of relatively short duration are considered because these have the greatest potential to produce high flux of solute at the water table. Results show only a small dependence of solute flux at the water table on duration of release. For this case of extended area of elevated recharge, approximately 60 percent of the release reached the water table in the 400-square-meter (4,305-square-foot) area directly below the source, while nearly the entirety of the release reached the water table in a 1,600-square-meter (17,222-square-foot) area centered below the source. For a 1-year release duration, rate of arrival of solute at the water table for releases beginning at the start of tank farm operations and at 15 and 30 years after start are presented in Figure M–116. Results indicate that the transition from background to elevated recharge moisture conditions did not have a significant effect on the time profile of solute flux. The magnitude of peak solute flux varied by approximately 5 percent as release timing changed from start of operations to 30 years after start of operations. Results reflect the delay in arrival due to the delay in beginning of release, but the interval of time from release to peak dose decreased by approximately 1 percent as time of release changed from start of operations to 30 years after start of operations.
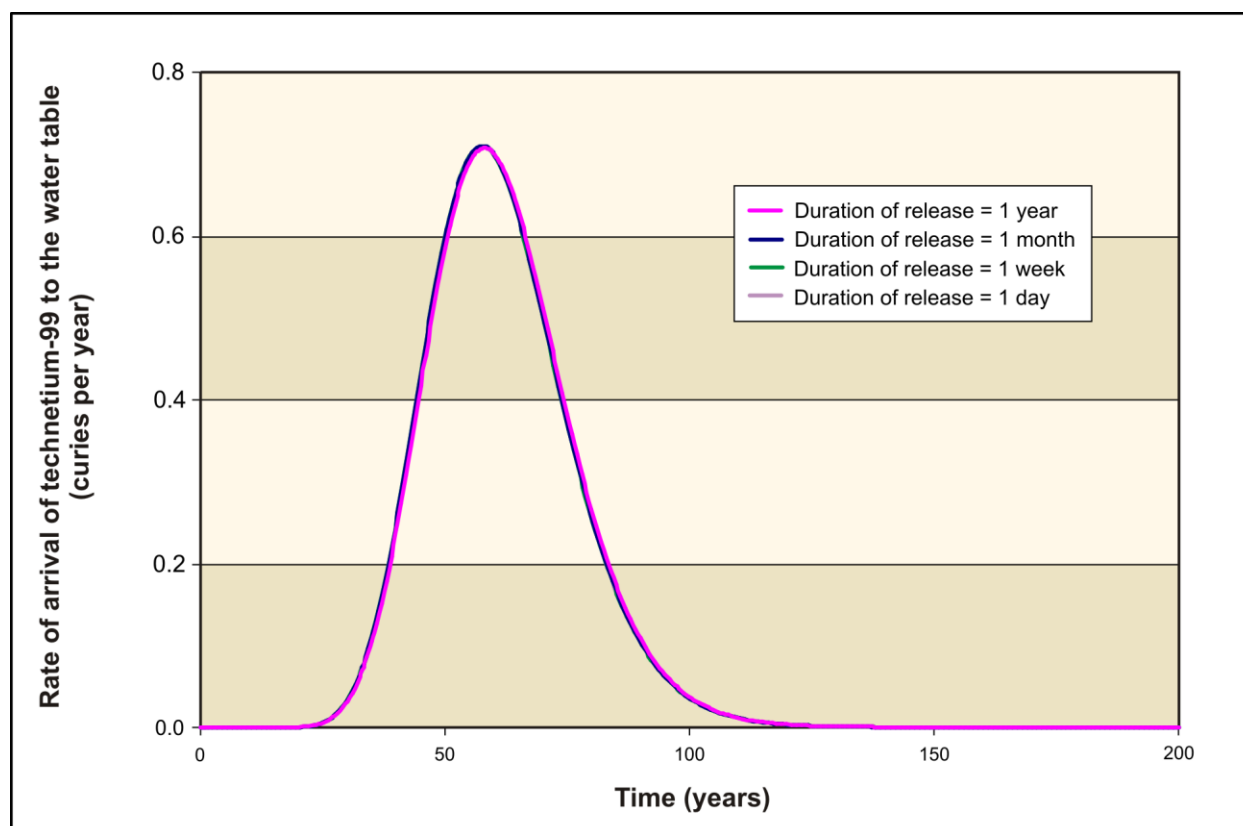
Figure M–115. Variation of Rate of Arrival of Solute at the Water Table with Release Duration for Extended Area of Elevated Recharge
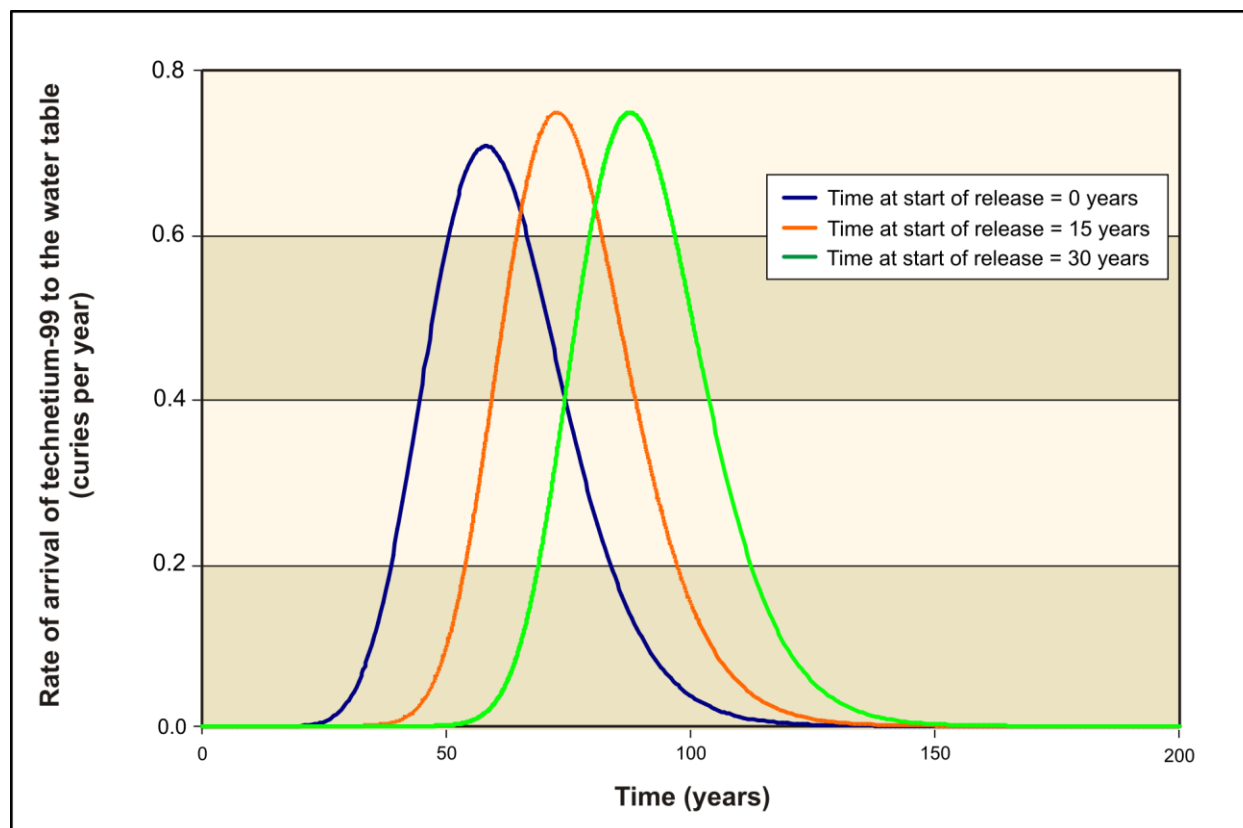
**Figure M–116. Variation of Rate of Arrival of Solute at the Water Table with
Release Timing for Extended Area of Elevated Recharge**

M.5.1.2   Local Area of Elevated Recharge

In this second case, elevated recharge was assumed to occur only over the area of a tank, approximately 400 square meters (4,300 square feet), and the leak duration and timing were varied. For a leak beginning at the start time of tank operations, the rate of arrival of solute at the water table for leaks of duration of 1 year, 1 month, 1 week, and 1 day are presented in Figure M–117. The four curves plotted on this figure coincide at nearly all points in time and, therefore, may not be separately distinguished. Results show only a small dependence of solute flux at the water table on duration of release. For this case of local area of elevated recharge, approximately 9 percent of the release reached the water table in the 400-square-meter (4,305-square-foot) area directly below the source, approximately 30 percent of the release reached the water table in the 1,600-square-meter (17,222-square-foot) area centered below the source, and nearly the entirety of the release reached the water table in the 6,400-square-meter (68,889-square-foot) area centered below the source. Due to the restriction of elevated recharge to the area of the source and the low rate of recharge outside of the source area, horizontal spreading of water and solute reduces the flux of solute at the water table and extends the period of time during which the release reaches the water table. For a 1-year release duration, rate of arrival of solute at the water table for releases beginning at the start of tank farm operations and at 15 and 30 years after start are presented in Figure M–118. Results indicate that the transition from background to elevated recharge moisture conditions did not have a significant effect on the time profile of solute flux. The magnitude of peak solute flux varied by approximately 2 percent as release timing changed from start of operations to 30 years after start of operations. Results reflect the delay in arrival due to the delay in beginning of release, but the interval of time from release to peak dose remained approximately constant as time of release changed from start of operations to 30 years after start of operations.
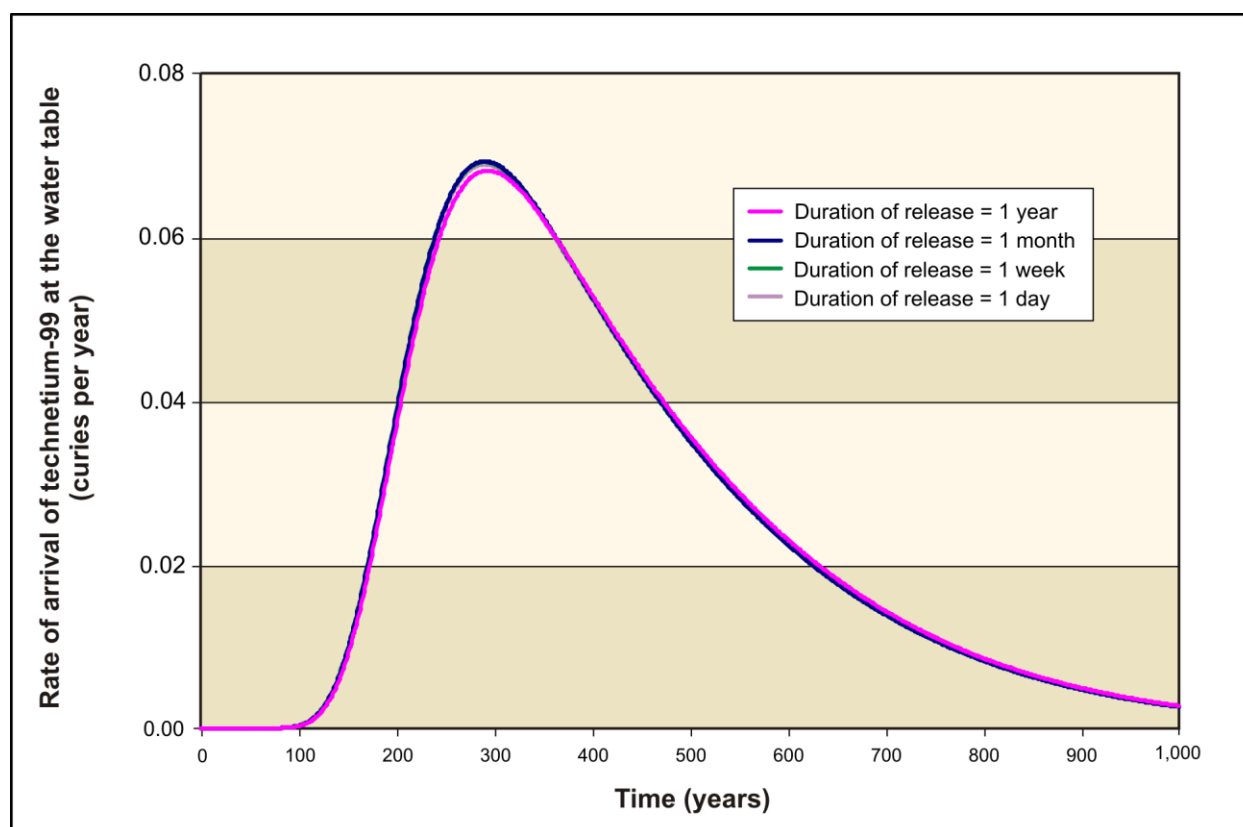
Figure M–117. Variation of Rate of Arrival of Solute at the Water Table with Release Duration for Local Area of Elevated Recharge
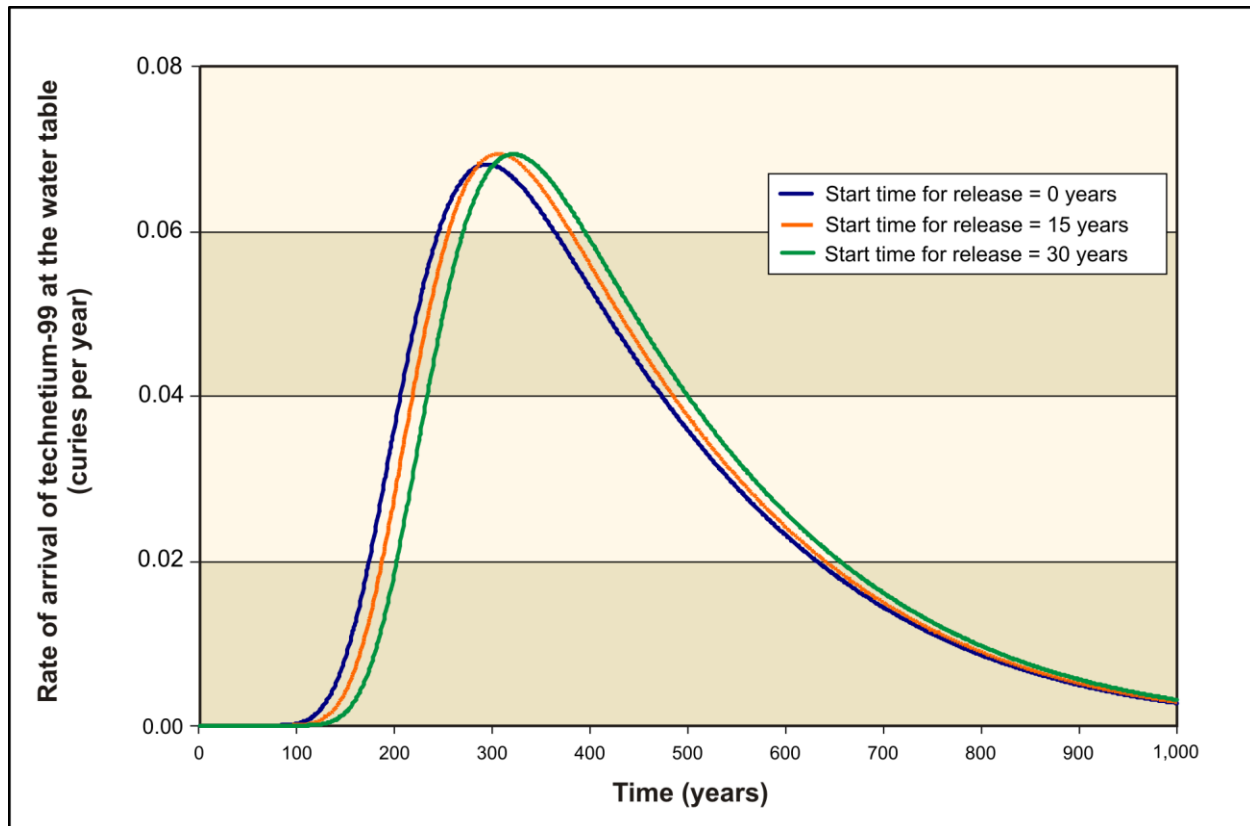
**Figure M–118. Variation of Rate of Arrival of Solute at the Water Table with
Release Timing for Local Area of Elevated Recharge**

M.5.1.3   Conclusions

For cases of both extended and local areas of elevated recharge, solute flux at the water table showed low sensitivity to change in release duration and timing. Results show sensitivity to moisture conditions as the average travel time for the case of extended area of elevated recharge was approximately one-quarter the average travel time for the case of local area of elevated recharge.

M.5.2   Leaching from Supplemental-Waste Forms

Activities under consideration for this *TC & WM EIS* include solidification of hazardous constituents currently stored in belowground tanks in the 200-East and 200-West Areas. The primary-waste form proposed is ILAW glass. Three additional waste forms under consideration to supplement management capacity for tank constituents are bulk vitrification glass, cast stone waste, and steam reforming waste. Analysis completed for Tank Closure Alternatives 3A, 3B, and 3C provides a basis for comparative evaluation of these three waste forms. Additional details on the nature of these waste forms are provided in Appendix D of this EIS, while estimates of the inventory of technetium-99 and iodine-129 for the set of waste forms for the three variants of Tank Closure Alternative 3 are summarized in Table M–56. The balance of this section presents details on the sensitivity of estimates of the rates of release to the vadose zone of two select radionuclides to changes in the type of waste form. The background and engineered-cap-design recharge rates, selected as the basis for estimating release rates, were 0.9 and 0.5 millimeters per year, respectively, values recommended for the proposed IDF-East (DOE 2005). Depending on the type of release model applied, transition from the engineered-cap-design recharge rate to the background recharge rate at the end of the 500-year design life of the cap may produce an increase

in the rate of release from the waste form. This effect is observed in results presented in the following subsections.

Table M–56. Tank Closure Alternatives 3A, 3B, and 3C Summary of
Waste Form Inventories of Technetium-99 and Iodine-129

Waste Form	Technetium-99 (curies)			Iodine-129 (curies)		
	Alt. 3A	Alt. 3B	Alt. 3C	Alt. 3A	Alt. 3B	Alt. 3C
Immobilized high-level radioactive waste	150	19,600	150	0	0	0
ILAW glass	8,440	84	8,440	2.8	2.8	2.8
Bulk vitrification glass	20,600[a]	N/A[b]	N/A[b]	6.8	N/A[b]	N/A[b]
Cast stone waste	N/A[b]	9,540	N/A[b]	N/A[b]	33.8	N/A[b]
Steam reforming waste	N/A[b]	N/A[b]	20,600	N/A[b]	N/A[b]	6.8
ETF-generated secondary waste	50	60	46	36.9	9.9	36.9

[a] The inventory of technetium-99 in the castable refractory block is 1,340 curies with the balance of the technetium-99 in intact bulk vitrification glass.
[b] Waste form not used under this alternative.
Key: Alt.=Alternative; ETF=Effluent Treatment Facility; ILAW=immobilized low-activity waste; N/A= not applicable.

M.5.3   Supplemental Waste Forms Leaching Behavior

M.5.3.1   Tank Closure Alternative 3A

For Tank Closure Alternative 3A, the inventory of technetium-99 is largely divided between ILAW glass and bulk vitrification glass, while the inventory of iodine-129 is divided between ILAW glass, bulk vitrification glass, and ETF-generated secondary waste (a grouted waste form). Release rate estimates for technetium-99 and iodine-129 under this alternative are presented in Figures M–119 and M–120, respectively. Low rates of release are predicted for the intact glass of the ILAW and bulk vitrification glass waste forms. However, the portion of technetium-99 transferred to castable refractory block in the bulk vitrification container is projected to release at a much higher rate upon placement in the vadose zone. The peak in the release rate for technetium-99 from castable refractory block reflects the increase in infiltration that is specified to occur at the end of the design life of the engineered barrier. For iodine-129, the glass waste forms release iodine at very low rates, while the ETF-generated secondary waste releases it at a higher (but still low) rate.
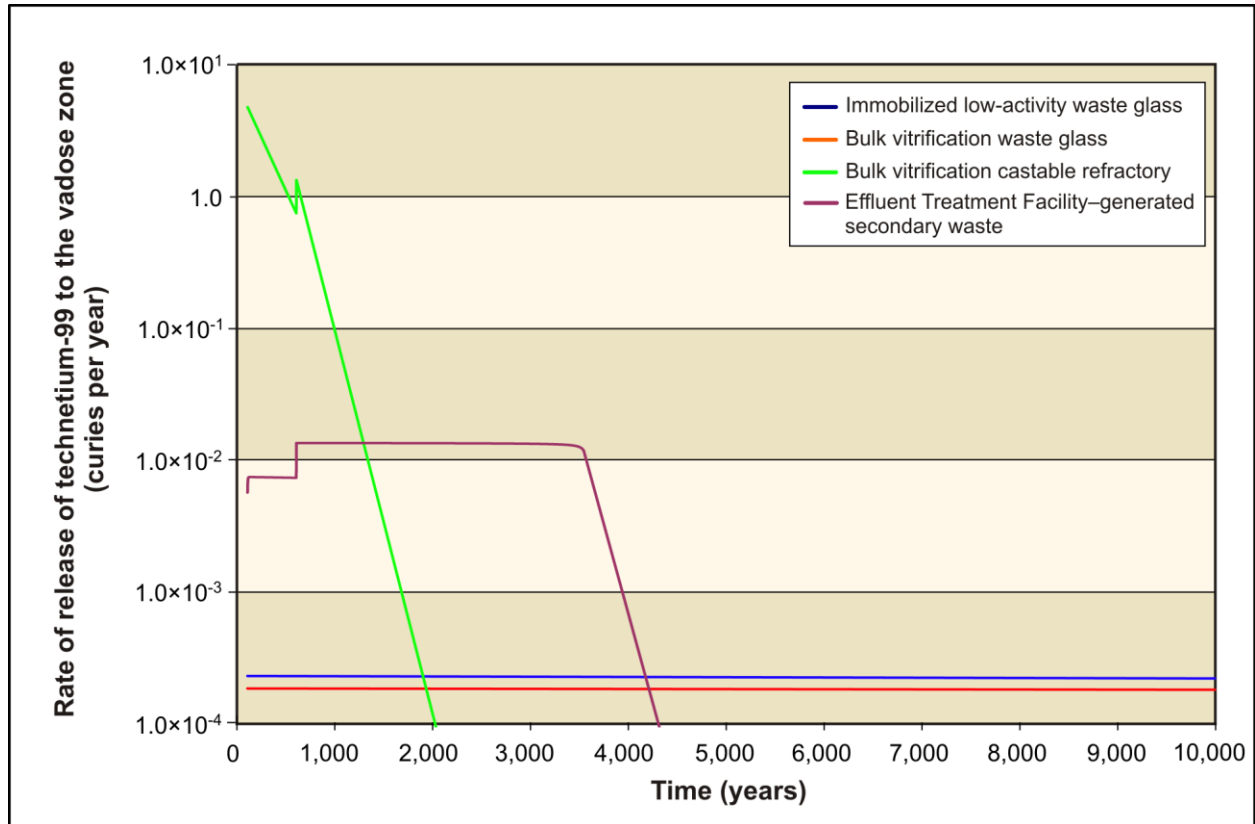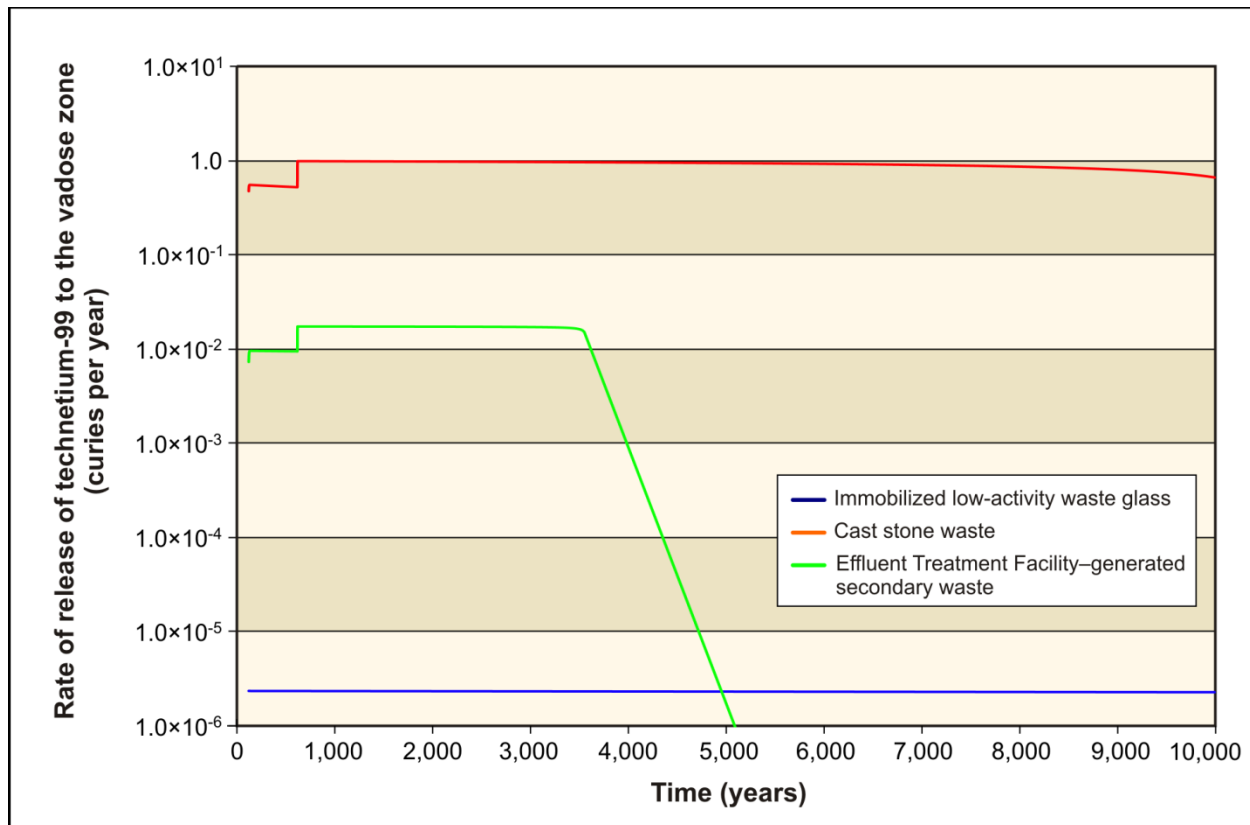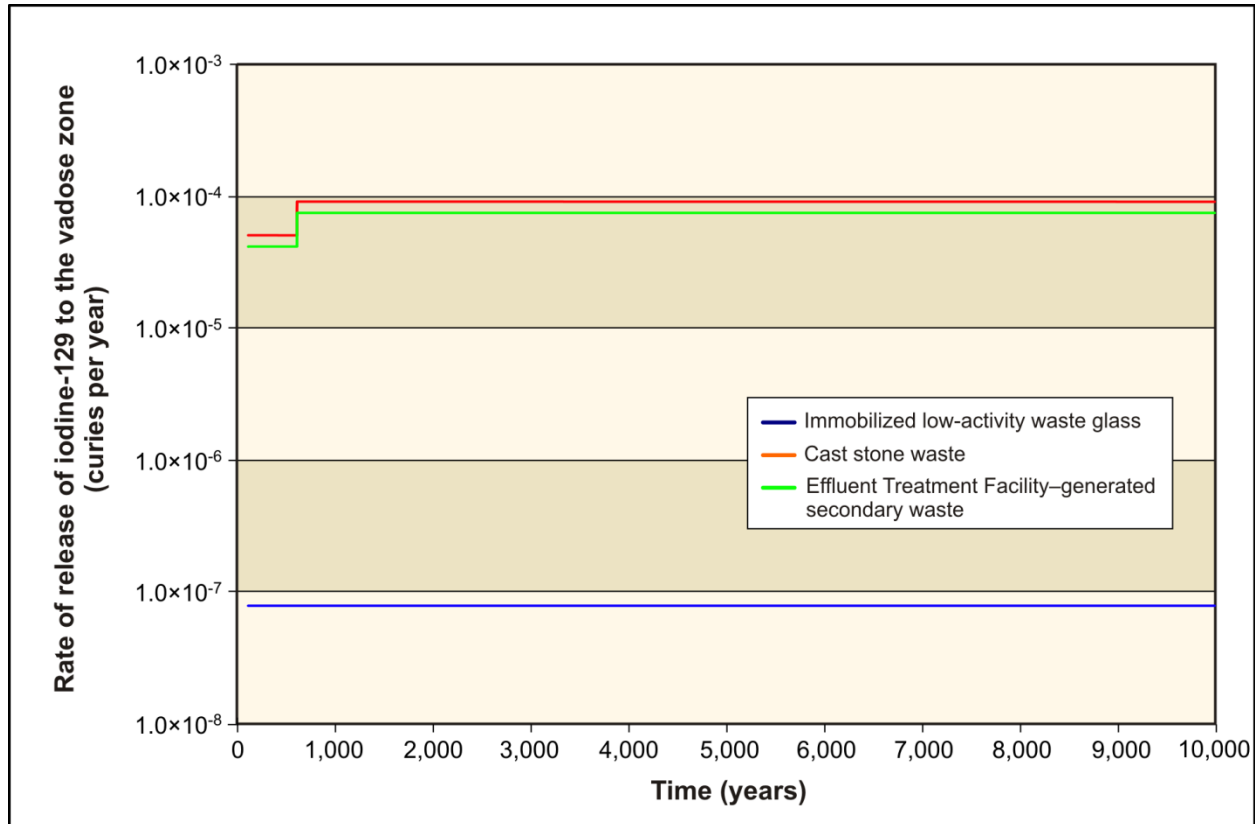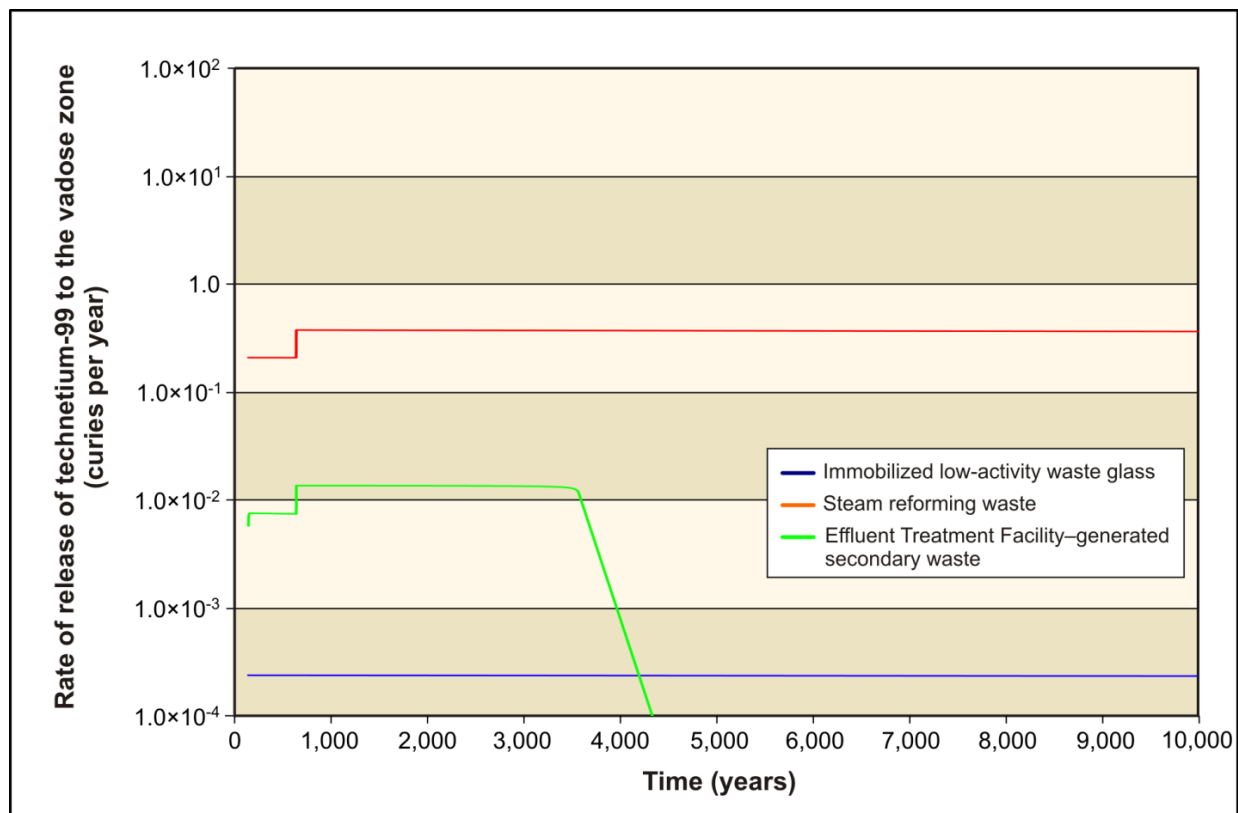
Figure M–119. Tank Closure Alternative 3A Waste Form Rates of Release of Technetium-99
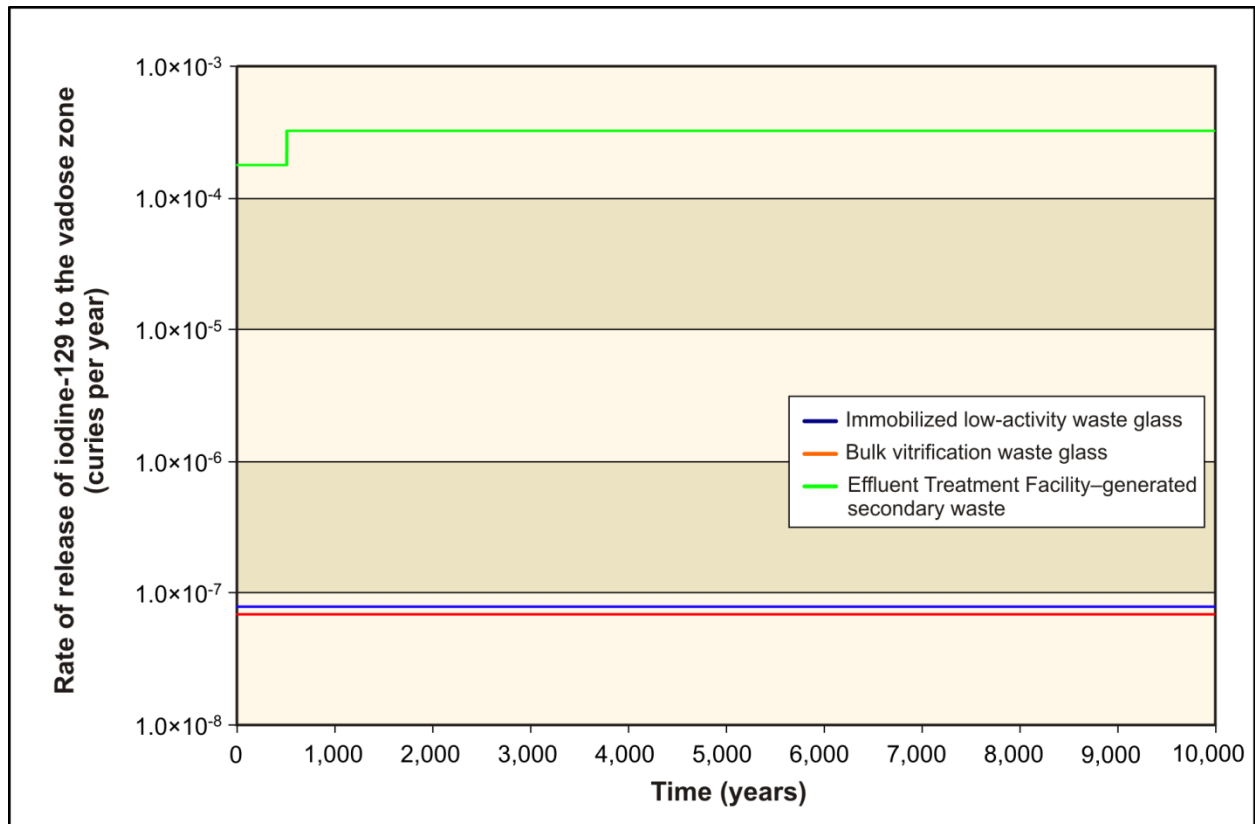
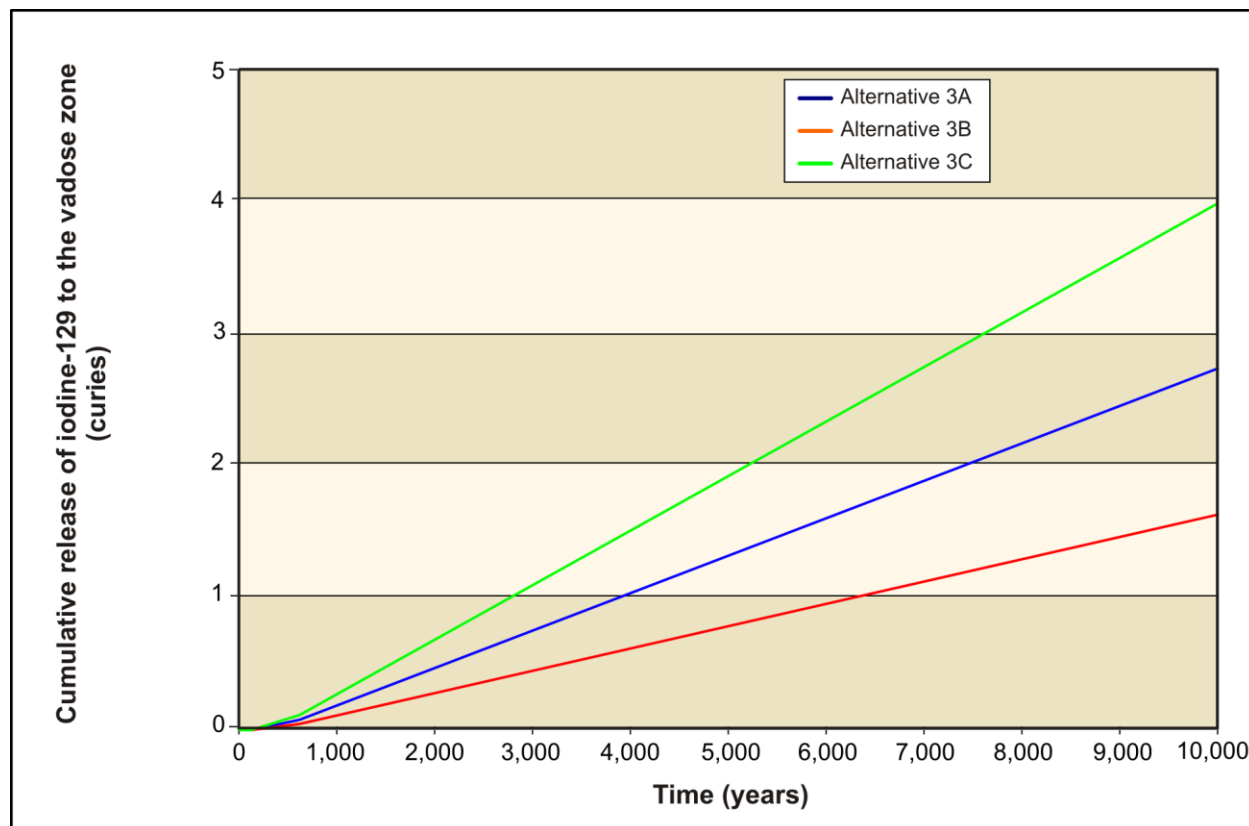**Figure M–120. Tank Closure Alternative 3A Waste Form Rates of Release of Iodine-129**

M.5.3.2 Tank Closure Alternative 3B

For Tank Closure Alternative 3B, the inventory of technetium-99 is largely divided between immobilized high-level radioactive waste glass and cast stone waste, while the inventory of iodine-129 is divided between ILAW glass, cast stone waste, and ETF-generated secondary waste. Estimates of the rate of release of technetium-99 and iodine-129 under this alternative are presented in Figures M–121 and M–122, respectively. The small amount of technetium-99 present in the ILAW glass is estimated to release at a low rate, while the cast stone waste is projected to release technetium-99 at a higher rate. Nearly the entire inventory of technetium-99 in the cast stone waste form is released during the 10,000-year period of analysis. The smaller inventory of technetium-99 (60 curies) in the ETF-generated secondary waste is released over a period of approximately 3,500 years. For iodine-129, the combined rate of release from cast stone waste and ETF-generated secondary waste is comparable to that of ETF-generated secondary waste with comparable inventory under Tank Closure Alternative 3A.

Figure M–121. Tank Closure Alternative 3B Waste Form Rates of Release of Technetium-99

Figure M–122. Tank Closure Alternative 3B Waste Form Rates of Release of Iodine-129

M.5.3.3   Tank Closure Alternative 3C

For Tank Closure Alternative 3C, the inventory of technetium-99 is largely divided between ILAW glass and steam reforming waste, while the inventory of iodine-129 is divided between ILAW glass, steam reforming waste, and ETF-generated secondary waste. Release rate estimates of technetium-99 and iodine-129 under this alternative are presented in Figures M–123 and M–124, respectively. The estimated rate of release of both technetium-99 and iodine-129 is higher for steam reforming waste than for the ILAW glass waste form.

Figure M–123. Tank Closure Alternative 3C Waste Form Rates of Release of Technetium-99
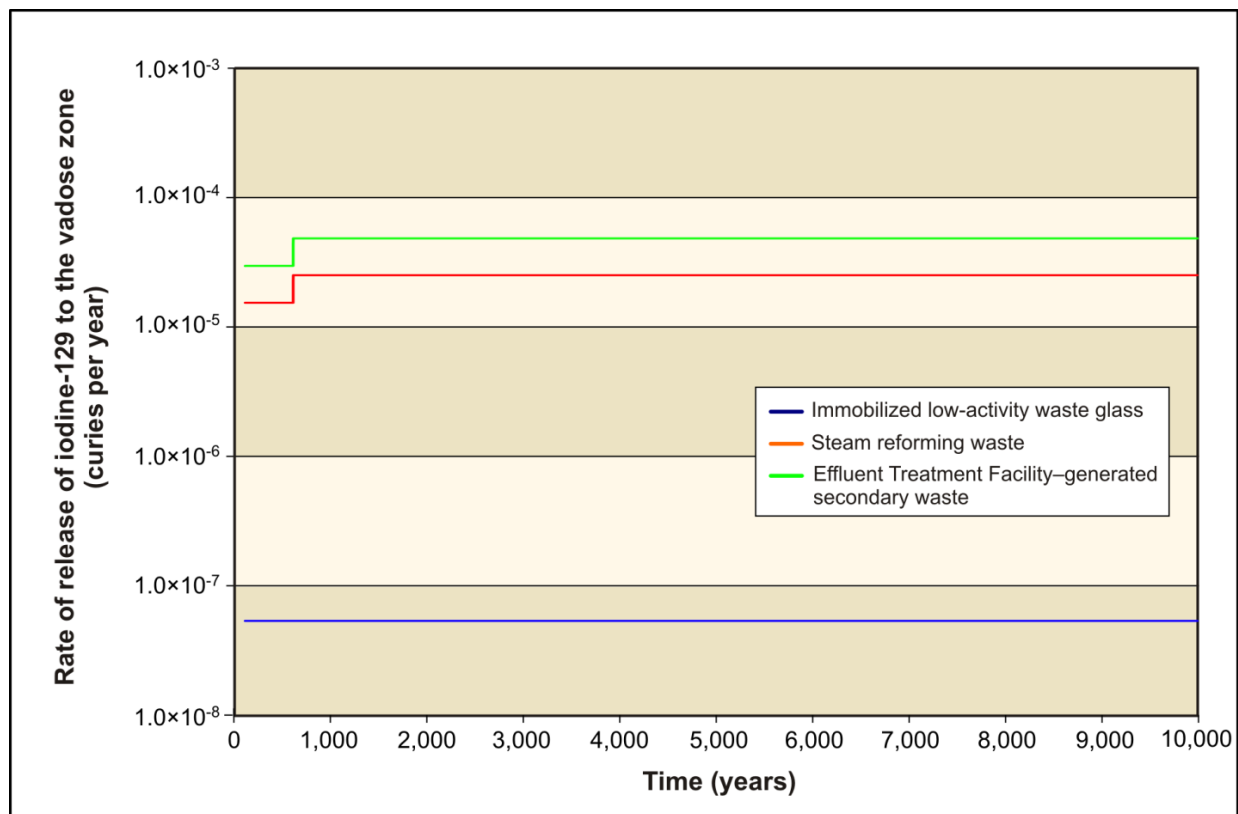
Figure M–124. Tank Closure Alternative 3C Waste Form Rates of Release of Iodine-129

M.5.3.4   Conclusions

Cumulative releases of technetium-99 and iodine-129 from the combined waste forms for Tank Closure Alternatives 3A, 3B, and 3C are presented in Figures M–125 and M–126, respectively. For technetium-99 under Alternative 3A, the majority of release is due to the castable refractory block portion of the bulk vitrification inventory, and the entirety of that inventory is released in approximately 2,000 years. For technetium-99, cumulative release from cast stone waste under Tank Closure Alternative 3B is higher than that from steam reforming waste under Tank Closure Alternative 3C or bulk vitrification glass and castable refractory block under Tank Closure Alternative 3B. For iodine-129, cumulative releases from steam reforming waste and ETF-generated secondary waste under Alternative 3C exceed the cumulative release estimated for the combined waste forms under Tank Closure Alternative 3A or 3B.
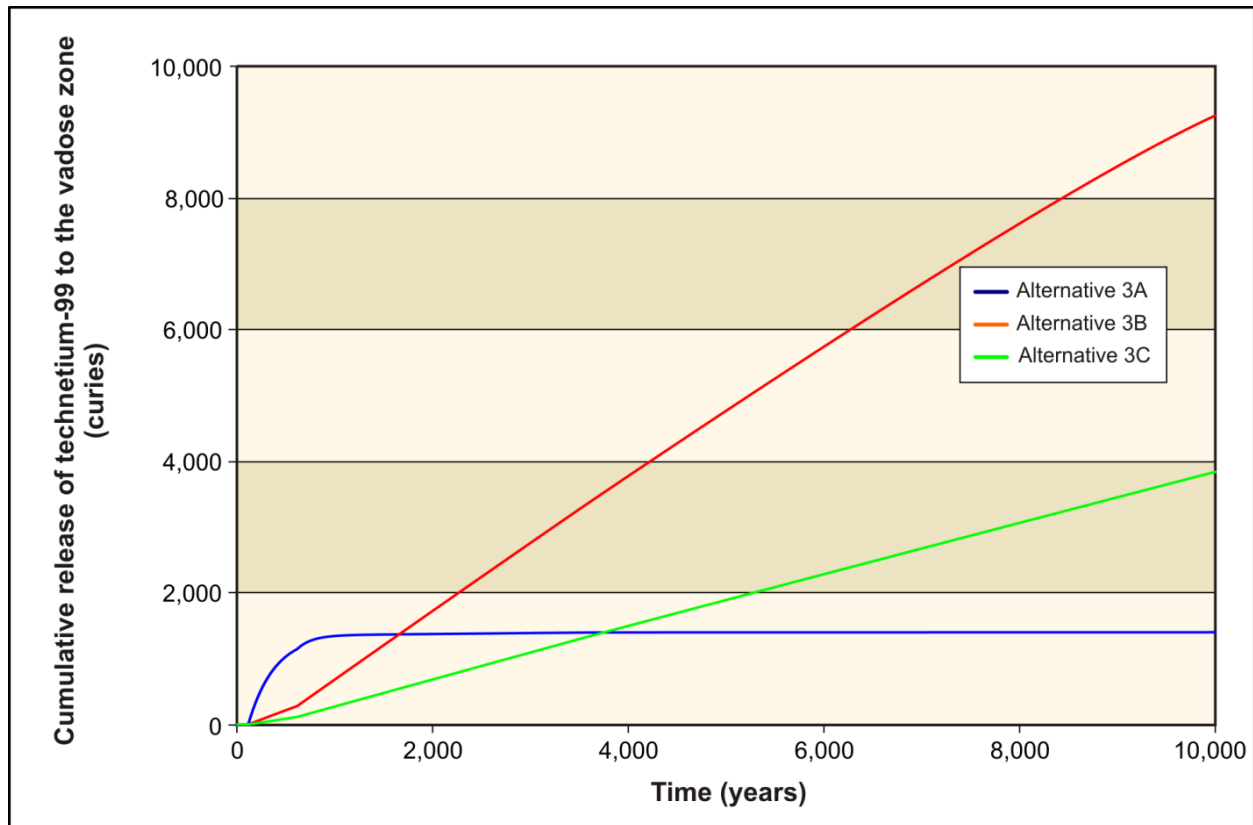
**Figure M–125. Tank Closure Alternatives 3A, 3B, and 3C Waste Form
Combined Cumulative Release of Technetium-99**

**Figure M–126. Tank Closure Alternatives 3A, 3B, and 3C Waste Form
Combined Cumulative Release of Iodine-129**

M.5.4 Rate of Recharge and Diffusion Release

Grouted waste forms are proposed for both primary- and secondary-waste categories under the Tank Closure and Waste Management alternatives. For these waste forms and the low rates of recharge projected for the waste disposal locations, release rates under the diffusion mechanism are greater than those under the convective mechanism. In addition, for the diffusion-limited release model described in Section M.2.2.4, the release rate from the waste package would be limited by the accumulation of the released constituent in the vicinity of the waste form. This section investigates the dependence of the release rate to the vadose zone underlying the waste packages on the recharge rate in the vicinity of the waste form. In this example calculation, an inventory of 9,500 curies of technetium-99 is encapsulated in 233,000 cubic meters (8,230,000 cubic feet) of grout. Stacks of packages 5.3 meters (17.4 feet) high with a package radius of 1.55 meters (5.1 feet) are placed in a rectangular array. The constituent is released by diffusion into the vadose zone adjacent to the packages and transported downward in the convective flow due to recharge. The release rates to the underlying vadose zone for varying recharge rates are presented in Figure M–127. In the limit of very high values of recharge, the initial rate of release would be independent of the rate of recharge, indicating that the constituent rapidly transports downward and that the rate of release is controlled by diffusion within the waste form. For lower rates of recharge, the constituent concentration increases adjacent to the waste package, decreasing the rate of diffusive release from the package, and the rate of downward movement is more dependent on the rate of recharge. For the diffusion-limited release model, degradation of the waste form at the end of the 500-year design life is represented as an increase in the tortuosity of the waste form and the related effective diffusivity of the waste form–constituent pair. The results also indicate that the effect of degradation of the package is more pronounced at higher rates of recharge. The significant increase in rate of release at the time of 500 years for the 50- and 100-millimeter-per-year recharge rates is due to increase of tortuosity and

supports the premise that diffusion within the waste form is a controlled rate of release to the vadose zone below the waste form. The minor increase in rate of release for the 0.9-millimeter-per-year recharge rate indicates that diffusion release from the waste package is suppressed at a low rate of recharge.
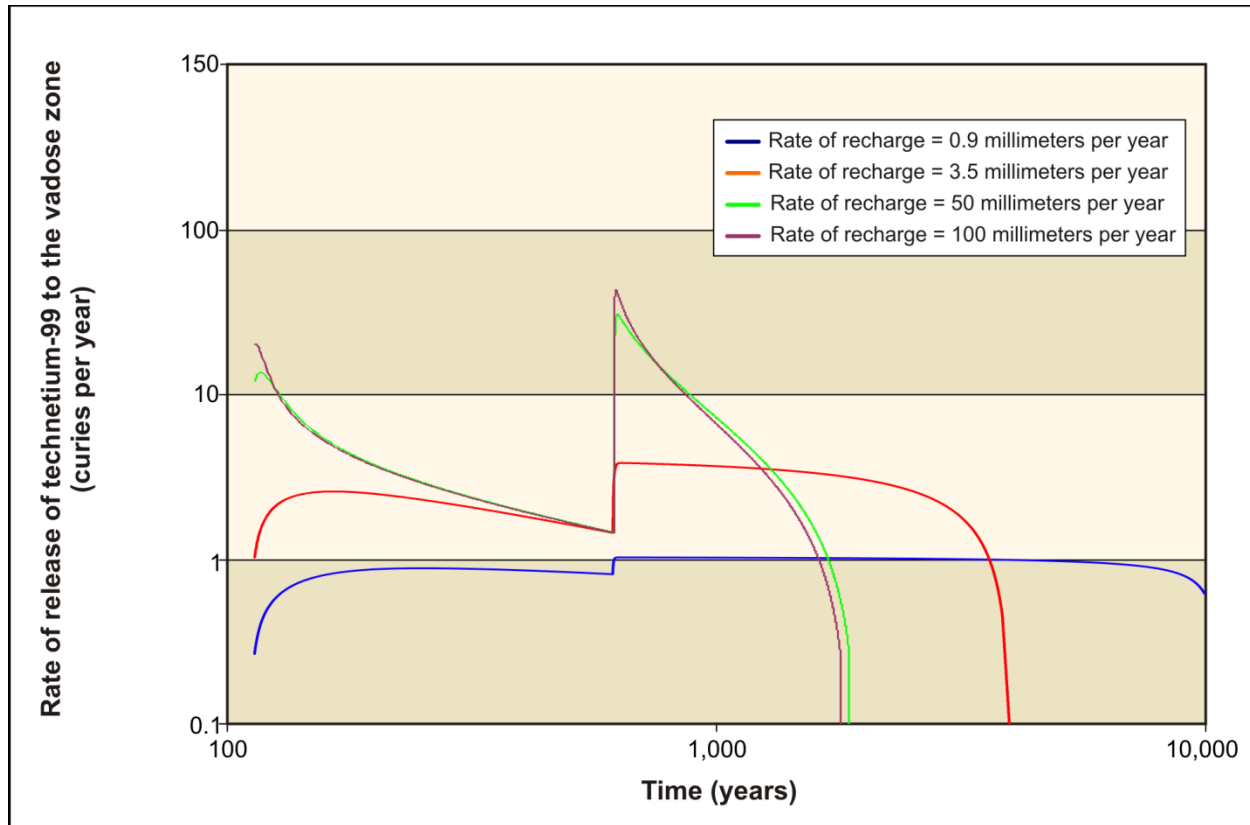
Figure M–127. Dependence of Rate of Release of Technetium-99 on Rate of Recharge
for Diffusion-Limited Release Model

M.5.5   Release Mechanisms for Steam Reforming Waste

A fluidized-bed steam reformer combines a waste stream containing organics, nitrates, and dissolved solids with a carbonaceous or clay co-reactant in a reducing steam environment to produce a mineralized waste form product. Organics in the feed stream are destroyed and nitrates are converted to nitrogen gas. The solid product is produced by the drainage of small particles from the reformer bed and by capture in offgas equipment of finer particles removed from the reformer by the fluidizing gas. Depending on the fluidized-bed steam reforming (FBSR) operating conditions and the nature of the co-reactant, the solid product may adopt amorphous, glassy, or crystalline structures exhibiting a range of matrix solubility and constituent retention properties. Potential mineral phases include nepheline, carnegieite, and nosean (Olson et al. 2004a).

Approaches available for estimation of rates of release from waste forms considered in this *TC & WM EIS* include direct utilization of release rate data for disposal conditions and application of mathematical models whose parameters are derived from experimental data. Because release rate data for disposal conditions are not available, mathematical models are required to estimate rates of release from waste packages. Mass conservation and thermodynamic constraint models are applicable to the *TC & WM EIS* analysis and provide conservative upper bound estimates of performance. Mass transfer–based models consider external film resistance, diffusion through alteration layers developed on the reacting surface, and transport through the pore structure of the reacting particle. These models require knowledge of

product particle and alteration product structure and parameters such as mass transfer coefficients and effective diffusivities that have not been investigated for the current FBSR waste forms. The detailed models incorporating mass transfer, alteration and precipitation product effects, and kinetic rate forms also require data that are not currently available. While complex models are applicable with adequate data support, and use of such models provides understanding of the role of contributing physical and chemical processes, their use in the absence of complete data support is not recommended (NCRP 2005:95).

Consistent with the above discussion, release models considered in detail include a reactant (water)–limited release model supported by surface reaction rate data and a chemical reaction equilibrium–limited release model. Based on analysis of pilot plant data (Olson et al. 2004a, 2004b), the primary matrix of the FBSR product is taken to be nepheline, and constituents (e.g., silicon, sulfur, rhenium) distributed throughout the matrix are released upon dissolution of the nepheline matrix. Details of each model are presented in the following paragraphs.

M.5.5.1 Reactant-Limited Release Model

The rate of release of a constituent from a surface reaction rate–limited model does not take account of mass transfer processes involving reactants or products, the effect of alteration products on the rate of reaction, or limitations imposed by the availability of reactants. Two approaches were implemented: first, the rate of dissolution was calculated directly from experimental data; and second, the rate of reaction was calculated from the empirical expression using parameter values derived from experimental data.

In the first approach, the average fractional release rate was calculated directly from several sets of reported Single Pass Flow Through and Pressurized Unsaturated Flow test data (McGrail et al. 2003a:Appendices A and B). Fractional release rates were calculated using concentrations of silicon, sulfur, and rhenium measured in the dissolution reactor effluent in conjunction with information about sample size and chemical composition.

Based on measurements of the concentration of silicon, the daily fractional release rate ranged from 4×10^{-5} to 7×10^{-3}, with the lower values associated with the Pressurized Unsaturated Flow experiments. For sulfur, the daily fractional release rate ranged from 9×10^{-4} to 2×10^{-2}, with estimates from the Pressurized Unsaturated Flow experiments in the central region of the range. For rhenium, the daily fractional release rate ranged from 7×10^{-4} to 4×10^{-2}, with the lower values associated with the Pressurized Unsaturated Flow experiments (McGrail et al. 2003a:Appendices A and B).

These estimates are for an elevated temperature (90 °C [194 °F]) and for values of pH (acidity/alkalinity) between 7 and 9. In these calculations, the fractional release rates for sulfur and rhenium, components that were expected to be incorporated into a sodalite "cage," were not always lower than the fractional release rate for silicon, which is expected to be dissolved primarily from the nepheline mineral.

Using the results of the Single Pass Flow Through testing, parameters of a kinetic rate law were estimated by regression on the data sets for both nepheline and nosean (McGrail et al. 2003b). The kinetic law was as follows:

$$J = k_0 \, 10^{\eta \, pH} \exp\left(-E_a / RT\right) \tag{M–27}$$

where:

J	=	normalized dissolution rate, moles per square meter per second
k_0	=	intrinsic rate constant, moles per square meter per second
η	=	pH power law coefficient, dimensionless
pH	=	negative logarithm of the molar concentration of dissolved hydrogen ions
E_a	=	activation energy, kilojoules per mole
R	=	ideal gas constant, 0.008314 kilojoules per mole per kelvin
T	=	temperature, kelvins

The values of the parameters determined from the regression of the data are presented in Table M–57. This kinetic law model can be incorporated into a more detailed flow, reaction, and transport model to develop estimates of waste form performance under disposal conditions.

Table M–57. Kinetic Rate Law Parameters for Hanford FBSR Product[a]

Parameter	Symbol	Units	Value	
			Nepheline	**Nosean**
Intrinsic rate constant	k_0	g-mole m^{-2} s^{-1}	2.0×10^{-9}	0.25
Activation energy	E_a	kJ mol^{-1}	16.6	48.6
pH power law coefficient	η	dimensionless	0.25	1

[a] McGrail et al. 2003b:26, 27.
Key: FBSR=fluidized-bed steam reforming; kJ=kilojoule.

The rate of dissolution in the absence of influence of mass transfer, alteration products, and precipitation effects can be estimated using the rate form of Equation M–27 and the rate parameters presented in Table M–57. At the expected disposal temperature of approximately 15 °C (59 °F) and a pH of 7, the rates of dissolution are estimated to be 0.032 and 0.0013 grams per square meter per day (6.56×10^{-6} and 2.66×10^{-7} pounds per square foot per day) for nosean and nepheline, respectively. Using a surface area per unit mass of 2.37 square meters per gram (1.16×10^4 square feet per pound) reported for granular FBSR product (McGrail et al. 2003a:3.2), the estimate of the daily fractional rate of dissolution for nepheline would be approximately 0.003, in agreement with the values calculated directly from experimental data for comparable conditions.

While the rates of release estimated in the preceding paragraphs are high, they apply primarily to the intrinsic rate of dissolution and can be reduced by consideration of both mass transfer limitations and the effects of alteration and precipitation products on the rate of reaction. At the present time, data needed to quantify the additional processes have not been collected. In addition, a major factor in estimating the high rate of dissolution of FBSR product is the high surface area per unit mass of the granular form of the product.

The dissolution of the FBSR product matrix is likely initiated by the reaction of infiltrating water with the nepheline glass or crystal. The reaction can be expressed as follows:

$$NaAlSiO_4 + 2H_2O = Na^{+1} + Al^{+3} + SiO_2(aq) + 4(OH^{-1}) \qquad (M–28)$$
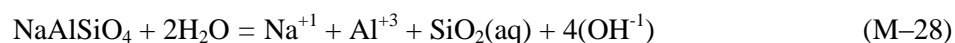
The stoichiometry of the reaction dictates that 1 mole (142 grams) of nepheline is dissolved for each 2-mole (36-gram) quantity of water. On a mass-to-volume basis, this is equivalent to approximately 3.94×10^6 grams of nepheline dissolved per cubic meter of water. In the concept developed for a reactant-limited release, the amount of water available for dissolution is the amount that would flow through the cross-sectional area of waste packages perpendicular to the vertical flow of the water that would flow between the stacks of packages carrying the dissolution products downward into the vadose zone underlying the stacks of packages.

For the IDF conceptual design, the cross-sectional area of flow for a stack is approximately 2.31 square meters (24.86 square feet) and the cross-sectional area of flow for a waste package is 1.17 square meters (9.59 square feet). With an FBSR product bulk density of 1 gram per cubic centimeter (THORTT and WGI 2006:7-56) and a waste package volume of 2.25 cubic meters (594.38 gallons), a stack of four packages contains 9.0×10^6 grams of waste matrix. For IDF-East, the rate of recharge through the cap would be 0.5 millimeters per year for the first 500 years and 0.9 millimeters per year for all subsequent time. The rate of flow through the cross-sectional area of the waste packages in a stack would be 5.845×10^{-4} and 1.052×10^{-3} cubic meters per year for the first 500 and subsequent years, respectively. The rate of dissolution of the waste matrix would be calculated as follows:

$$R_{diss} = [(\rho w \ R_{inf} \ A_{inf})/ \ MW_w] \ \nu_{n-w} \ MW_n \qquad (M–29)$$

where:

R_{diss} = rate of dissolution of the waste matrix, grams per year
ρ_w = density of water (1×10^6), grams per cubic meter
R_{inf} = rate of recharge, meters per year
A_{inf} = area of recharge, square meters
MW_w = molecular weight of water (180), grams per gram-mole
ν_{n-w} = moles of nepheline dissolved per mole of water reacted (0.5), gram-moles per gram-mole
MW_n = molecular weight of nepheline (142), grams per gram-mole

The related rates of dissolution of nepheline are 2,305.5 and 4,150 grams per year for the first 500 and subsequent years, respectively. The time required for complete dissolution of the waste matrix would be 2,390 years, with average fractional release rates of 2.6×10^{-4} and 5.3×10^{-4} per year for the first 500 and subsequent years, respectively.

The *TC & WM EIS* release model that fits the constant release rate estimated above is the matrix solubility model (see Section M.2.2.2). In this model, the rate of dissolution of the waste matrix is calculated as follows:

$$R_{diss} = R_{inf} \ A_{inf} \ Cs_{WM} \qquad (M–30)$$

where:

R_{diss} = rate of dissolution of the waste matrix, grams per year
R_{inf} = rate of recharge, meters per year
A_{inf} = flow area of the stack of packages, square meters
Cs_{WM} = solubility of the waste matrix (grams per cubic meter)

With a flow area of 2.31 square meters (24.86 square feet) per stack and the matrix dissolution rates estimated above, the solubility for use in the *TC & WM EIS* matrix solubility release model is approximately 2.0×10^6 grams per cubic meter.

M.5.5.2   Solubility-Limited Release Model

The concept of chemical equilibrium can be used to place constraints on the aqueous-phase concentrations of constituents constituting a system for specified values of intensive variables. In addition, the effect of changes in intensive variables, such as temperature, can be established. The approach is limited by the need for identification and characterization of aqueous- and solid-phase constituents present in the system, including specification of stoichiometric relations and the values of thermodynamic functions (free energies of formation and enthalpy change for reactions) for all

constituents. The particular application for FBSR product release modeling is estimation of the equilibrium solubility of the material. Steps in the analysis include the following:

- Specification of constraints (e.g., temperature, pressure, pH)

- Identification of aqueous-phase constituents and complexes

- Identification of solid-phase constituents

- Calculation of the distribution of aqueous-phase constituents for the vadose zone water contacting the FBSR product

- Calculation of aqueous-phase constituents for aqueous solutions in equilibrium with the FBSR product

The conceptual model for the system is the portion of the vadose zone inside the IDF under an engineered cap in which stacks of packages containing FBSR product are in contact with vadose zone water. The chemical composition of precipitation infiltrating into the cap may be altered when in contact with material composing the cap. Within the disposal horizon, the infiltrating water is in contact with both the IDF backfill material and the FBSR product and is presumed to reach a state of chemical-thermodynamic equilibrium prior to downward movement into the vadose zone underlying the facility. The role of the package material is not included in the conceptual model. For analysis purposes, the cap and backfill are represented as sand, either quartz or amorphous silica, and the FBSR product is represented as crystalline nepheline.

The objective of the analysis is determination of the equilibrium solubility of nepheline under potential IDF disposal conditions, including consideration of conditions that cannot be known with certainty prior to operation of the facility. Conditions considered variable are temperature, gas phase composition, chemical composition of water entering the disposal horizon, and precipitation of alteration phases during dissolution of nepheline.

The geochemical model adopted for the analysis was the PHREEQC computer code (Parkhurst and Appelo 1999) developed at the U.S. Geological Survey. PHREEQC uses an ion-association aqueous model to simulate speciation and saturation, batch reaction, one-dimensional transport, or inverse modeling. Only the speciation and saturation capabilities were used in this analysis. The geochemical database, MINTEQ.DAT, supplied with the code was used in the analysis. Aqueous-phase constituents included hydrogen, hydroxide, sodium, and aluminum ions; hydroxides of aluminum; carbonate, bicarbonate, and carbonic acid; sodium carbonate and bicarbonate; and silicic acid and dissociated silicic acid. Solid-phase species included quartz, amorphous silica, gibbsite, kaolinite, analcime, and nepheline.

The conceptual model for determination of the composition of water entering the disposal horizon prior to contacting the FBSR product was movement of precipitation through the cap material at a temperature of 15 °C (59 °F). The water entering the disposal horizon was assumed in equilibrium with the ambient atmosphere at oxygen and carbon dioxide partial pressures of 0.2 and 0.03 atmospheres, respectively.

The first case determined the solubility in the absence of alteration phases or the potential for precipitation of quartz or amorphous silica. In the final solution for each of these cases, the aqueous phase was slightly oversaturated with respect to quartz and slightly undersaturated with respect to amorphous silica, and the solubility of nepheline was estimated to be 118.2 grams per cubic meter.

The second case determined the solubility of nepheline with the potential for precipitation of alteration phases (gibbsite, kaolinite, and analcime) at a temperature of 15 °C (59 °F). The final solution was undersaturated with respect to both quartz and amorphous silica, and the solubility of nepheline was

estimated to be 175,000 grams per cubic meter. The results indicated that the precipitation of alteration phases has the effect of significantly increasing the solubility of nepheline, especially for the cases involving analcime.

M.5.5.3   Conclusion

Estimates of rates of release based solely on dissolution reaction rate models not limited by reactant availability, mass transfer limitation, or alteration and precipitation product effects produce high estimates. However, data justifying incorporation of the contributing physical and chemical processes into a detailed flow and reaction model are not available at the current time. Estimates of rates of release based on the availability of water reactant are also high, but place an upper limit on potential rates of dissolution. Estimates of rates of release based on predictions of the equilibrium solubility of nepheline cover a wide range, depending on the types of alteration phases that may precipitate as nepheline dissolves. A lower-end range of estimates of the equilibrium solubility of nepheline, approximately 120 grams per cubic meter, was estimated using the PHREEQC geochemical model based on the assumption that alteration phases do not precipitate. This value is consistent with that proposed, 105 to 430 grams per cubic meter, in an evaluation of FBSR product solubility and dissolution (CEES 2010). An upper-end estimate of the equilibrium solubility of nepheline, approximately 1.75×10^5 grams per cubic meter, was estimated using the PHREEQC geochemical model based on the assumption that the alteration phases of gibbsite, kaolinite, or analcime could precipitate.

Based on observation of the formation of alteration phases in dissolution of nepheline (Tole et al. 1986), it is concluded that the upper-limit estimate of solubility, 1.75×10^5 grams per cubic meter, is reasonably conservative and is the value recommended for use in the *TC & WM EIS* impacts analysis. The lower end of the range of solubility, 120 grams per cubic meter, and the limit based on availability of water reactant, 2.01×10^6 grams per cubic meter, are recommended as a reasonable range for sensitivity analysis. Estimates of the rate of release of technetium-99 from FBSR solids to the vadose zone and of rate of arrival at the water table using these three values of release rate are presented in Figures M–128 and M–129, respectively. Consistent with the values of solubility, the peak rate of arrival at the water table is approximately a factor of 10 higher than the upper-limit solubility estimate. The flux at the water table for the lower-limit solubility case is approximately a factor of 1,000 lower than the flux at the water table for the upper-limit solubility case.
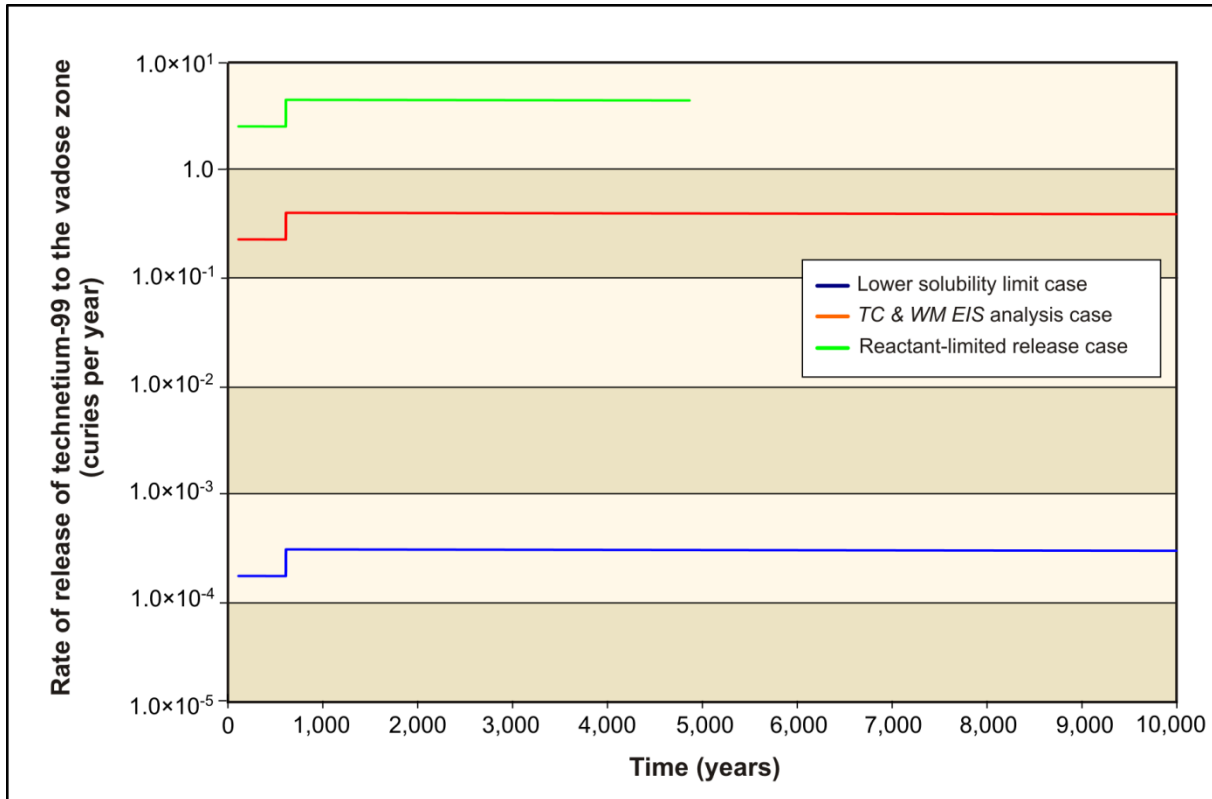
Figure M–128. Dependence of Rate of Release of Technetium-99 to the Vadose Zone on Steam Reforming Waste Release Model
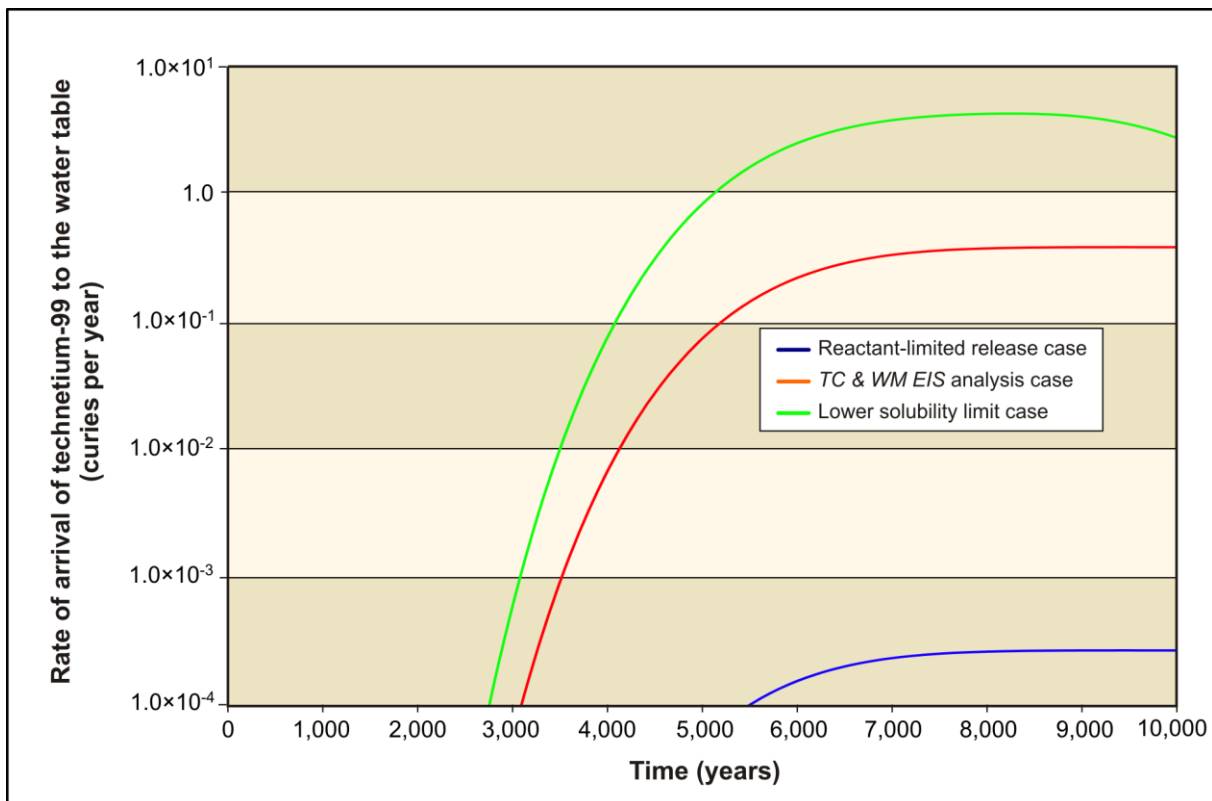

Figure M–129. Dependence of Rate of Arrival of Technetium-99 at the Water Table on Steam Reforming Waste Release Model
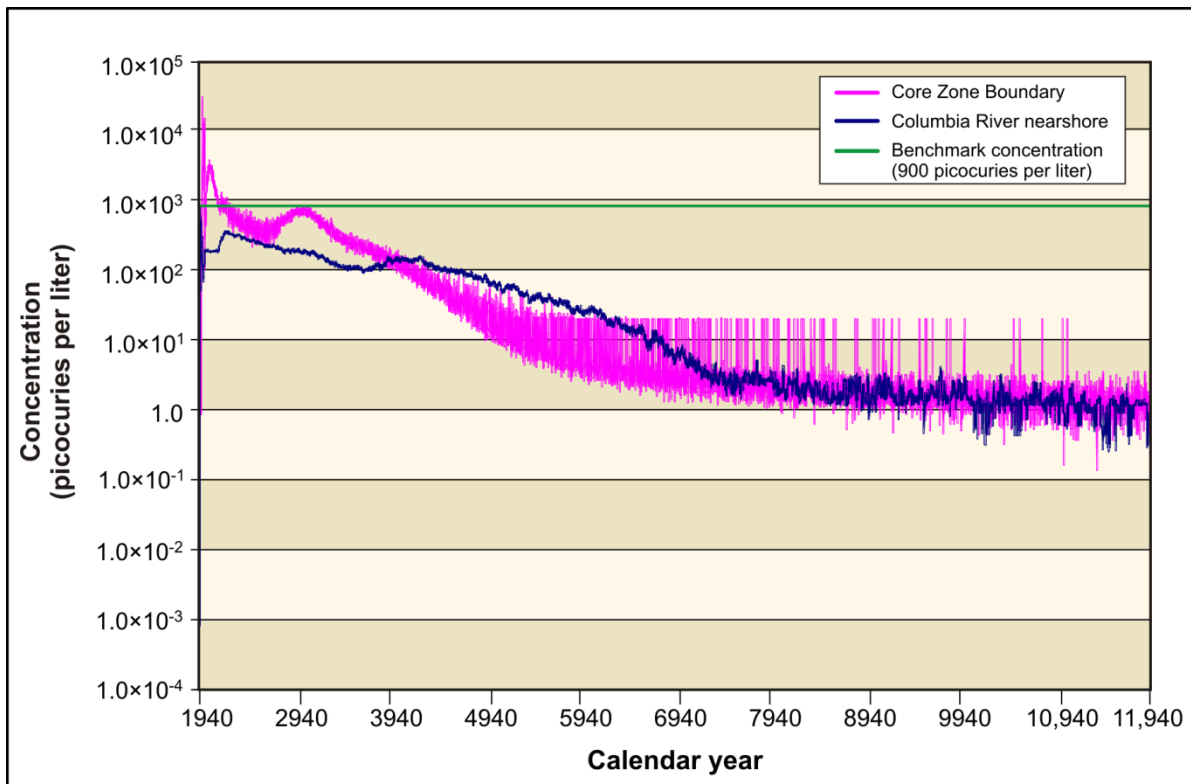
M.5.6   No-Retrieval-Losses Sensitivity Case

This *TC & WM EIS* evaluates the releases from other sources related to the HLW tanks, including tank residuals, retrieval leaks, ancillary equipment, and unplanned releases within the tank farm boundary that were analyzed together. The amount of constituent released to the aquifer is related to the activities under each Tank Closure alternative. The objective of this sensitivity analysis is to examine the effect on the concentrations of constituents in the groundwater of the removal of the retrieval leaks from the other sources. Figure M–130 reports the predicted flux of technetium-99 to the vadose zone for the C tank farm under Tank Closure Alternative 2B. The figure reports a release of a liquid source of technetium-99 from retrieval leaks in 2018. The timing of the release due to retrieval losses is the same for each affected tank farm, and the inventories for the HLW tanks vary between tank farms. The figure reports predicted releases of technetium-99 to the vadose zone for 1940 to 2440, so single-year releases are visible on the graph. Ancillary equipment and tank residual sources would continue to release indefinitely as the source is depleted. The sensitivity case analyzes the removal of that source from the alternative. Figure M–131 reports the predicted concentration of technetium-99 versus time for all sources under Tank Closure Alternative 2B. Figure M–132 reports the predicted concentration of technetium-99 versus time when the retrieval losses source is removed from the alternative. The benchmark value was derived from relevant regulatory standards as a means of assessing long-term human health impacts.
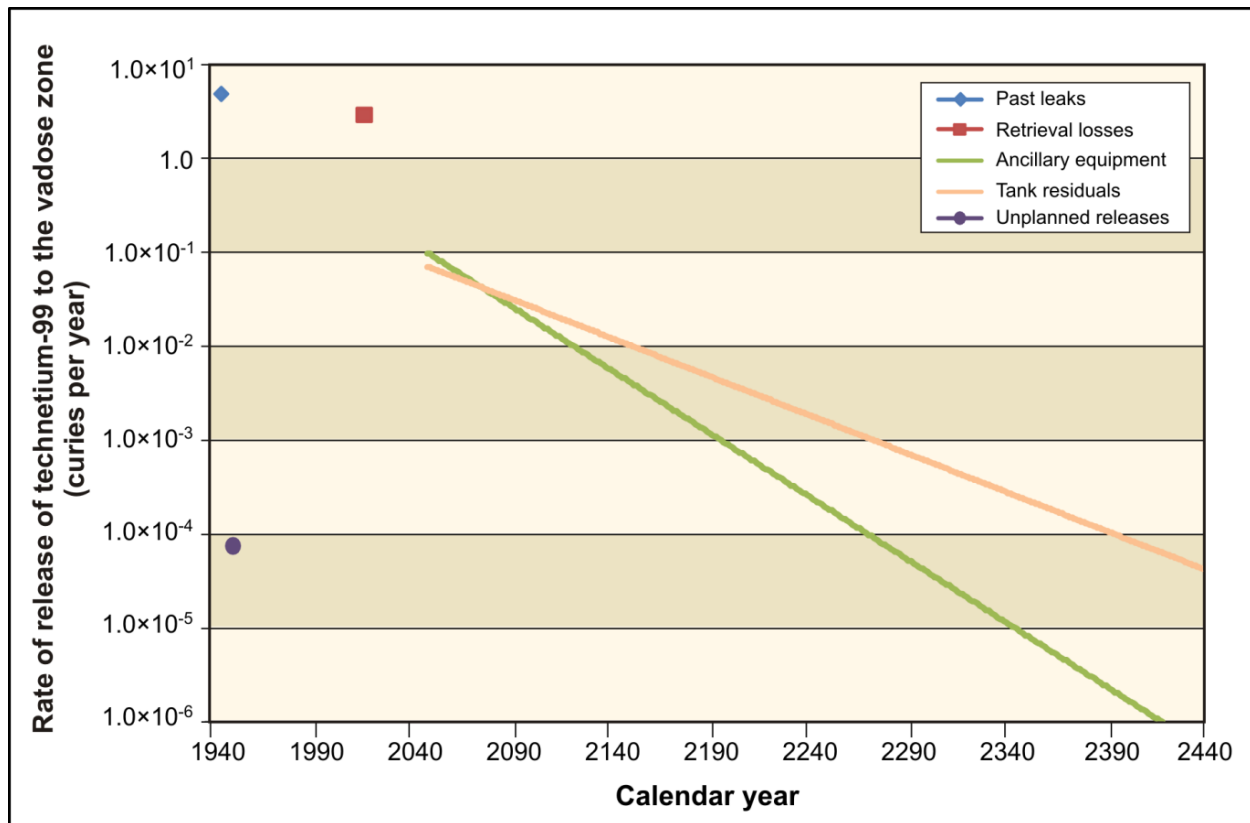
Figure M–130. Tank Closure Alternative 2B Release of Technetium-99 to the Vadose Zone from Tank Farm C
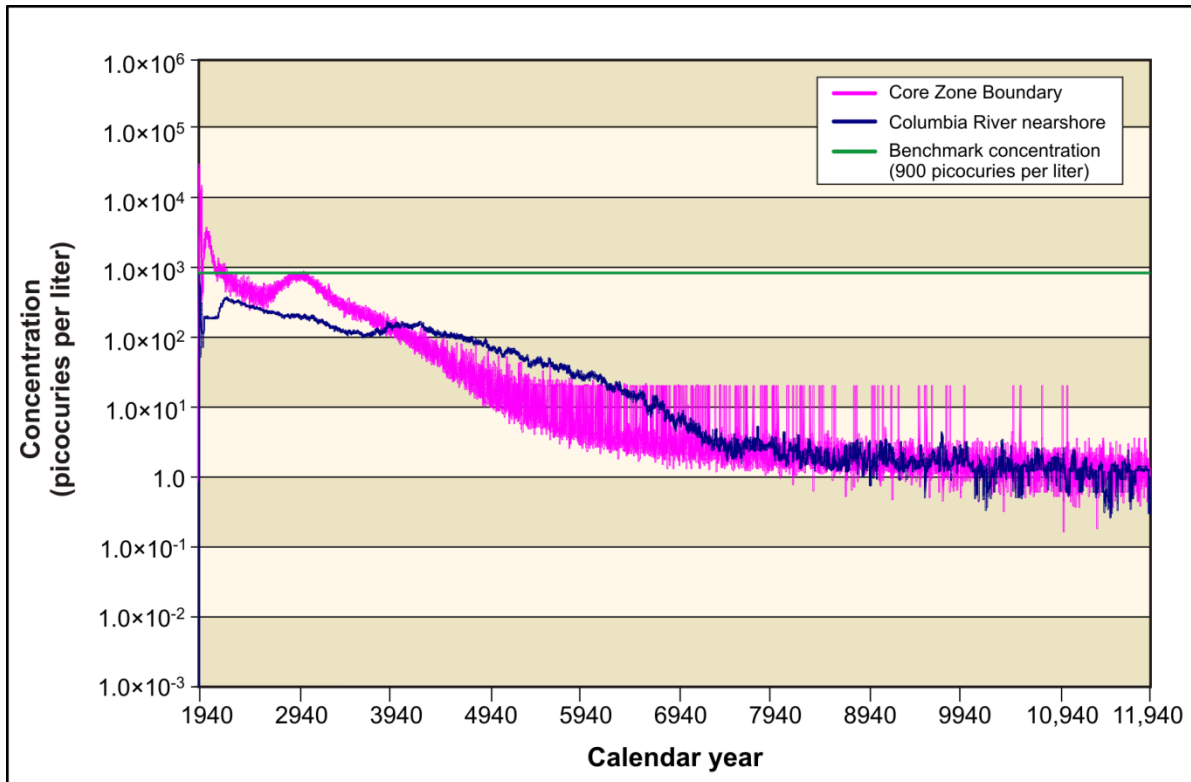
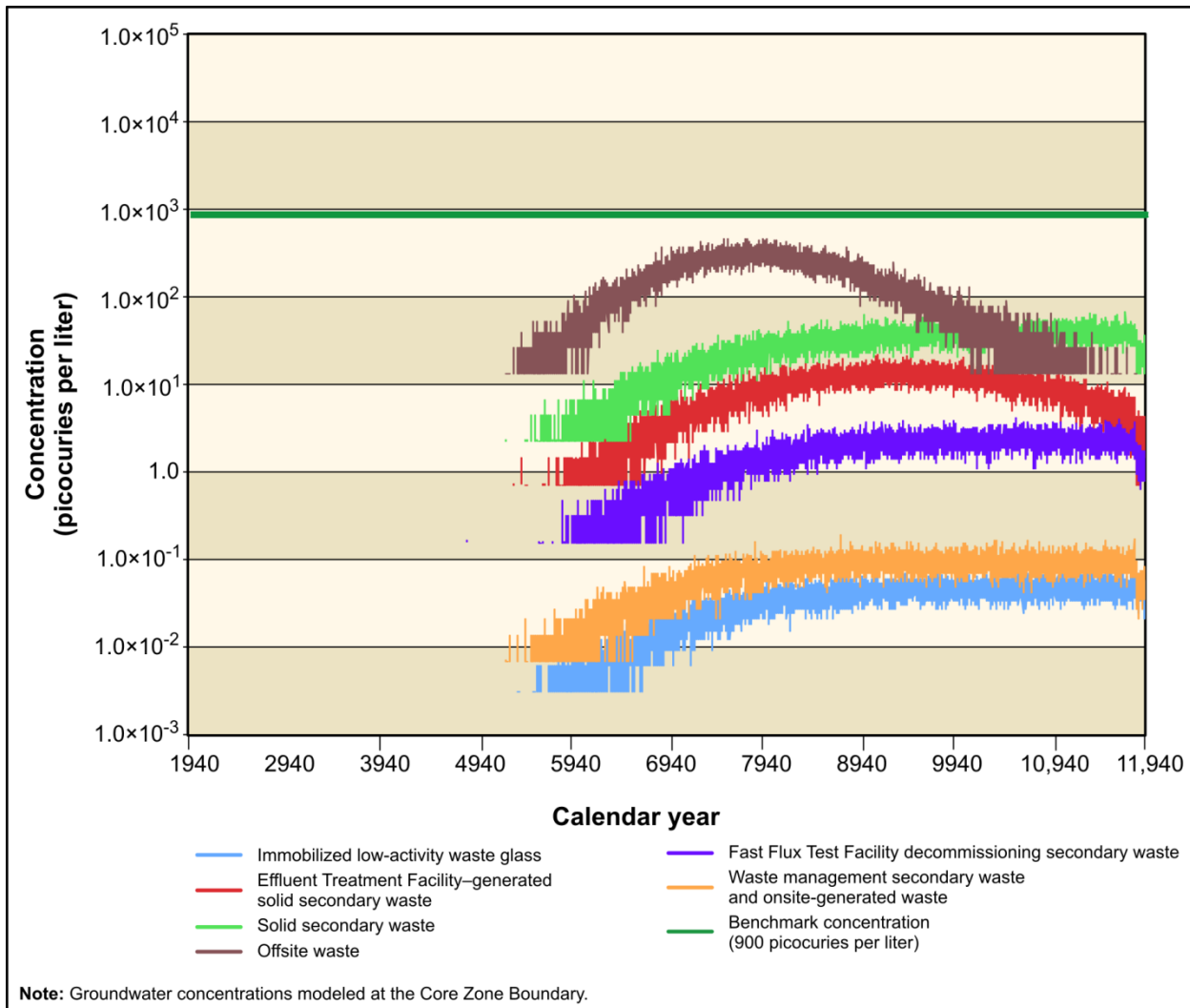**Figure M–131. Tank Closure Alternative 2B Groundwater Technetium-99 Concentration at the Core Zone Boundary and the Columbia River, Retrieval Loss Sensitivity Case**

Figure M–132. Tank Closure Alternative 2B Groundwater Technetium-99 Concentration at the Core Zone Boundary and the Columbia River, No-Retrieval-Losses Sensitivity Case

M.5.7　　IDF-East Sensitivity Analyses

M.5.7.1　　Immobilized Low-Activity Waste Glass Sensitivity Analysis

This *TC & WM EIS* models ILAW glass using the fractional release model. In the EIS analysis, the fractional release rate is 2.80×10^{-8} grams per gram per year. The objective of this sensitivity analysis is to examine the effect of increasing and decreasing the fractional release rate on the predicted concentration in the aquifer. The sensitivity analysis examined the ILAW glass under Tank Closure Alternative 2B. Table M–58 summarizes the values of fractional release rates for the three cases analyzed. Figure M–133 reports the predicted release of technetium-99 to the vadose zone under each case.

Table M–58. Immobilized Low-Activity Waste Glass Sensitivity Analysis Cases

Sensitivity Analysis Case	Fractional Release Rate (grams per gram per year)
EIS Case	2.80×10^{-8}
Sensitivity Case 1	2.80×10^{-7}
Sensitivity Case 2	2.80×10^{-9}

Key: EIS=environmental impact statement.
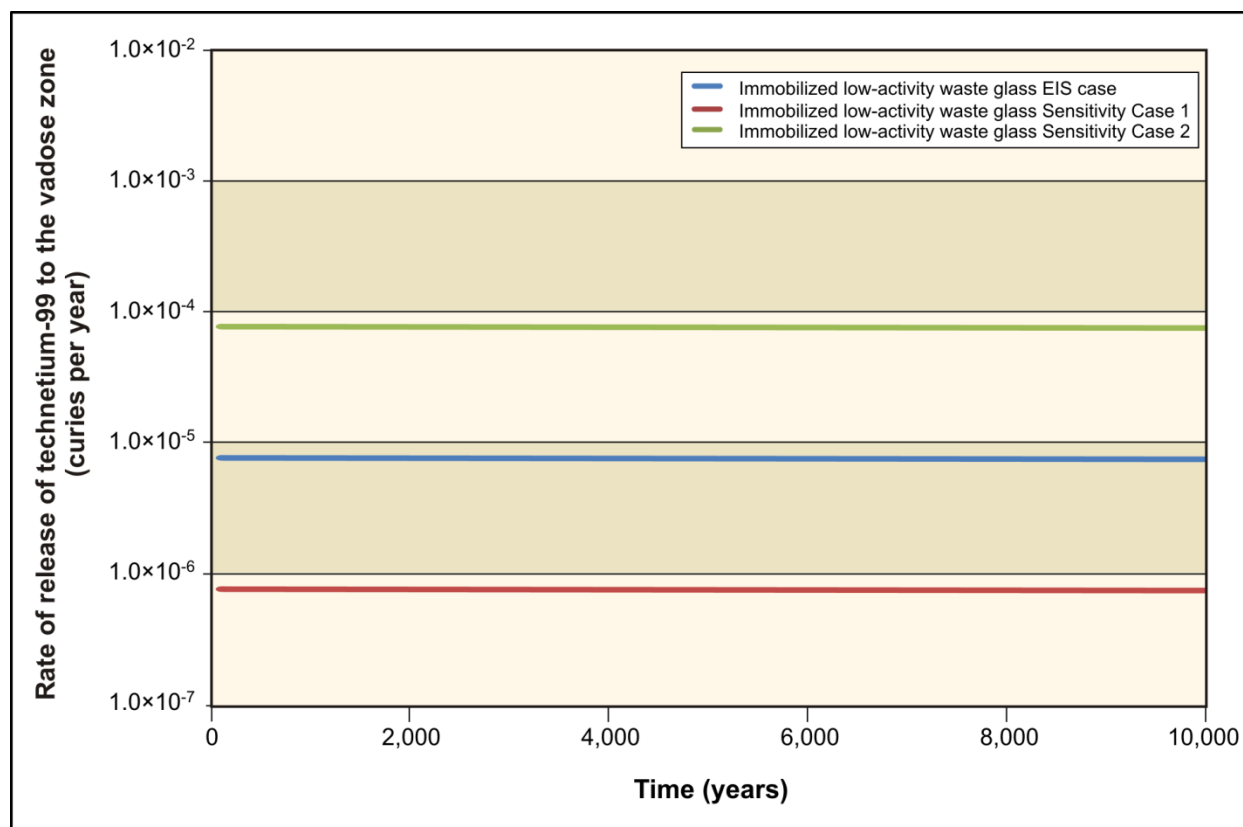
Figure M–133. Release of Technetium-99 to the Vadose Zone from Immobilized Low-Activity Waste Glass for Sensitivity Analysis

Figures M–134 through M–136 indicate the predicted concentrations of technetium-99 in groundwater versus time for the sensitivity analysis cases. Decreases in concentration after a peak reflect depletion of inventory at the source, while constant concentrations generally reflect release at the source that is a small fraction of inventory at the source.
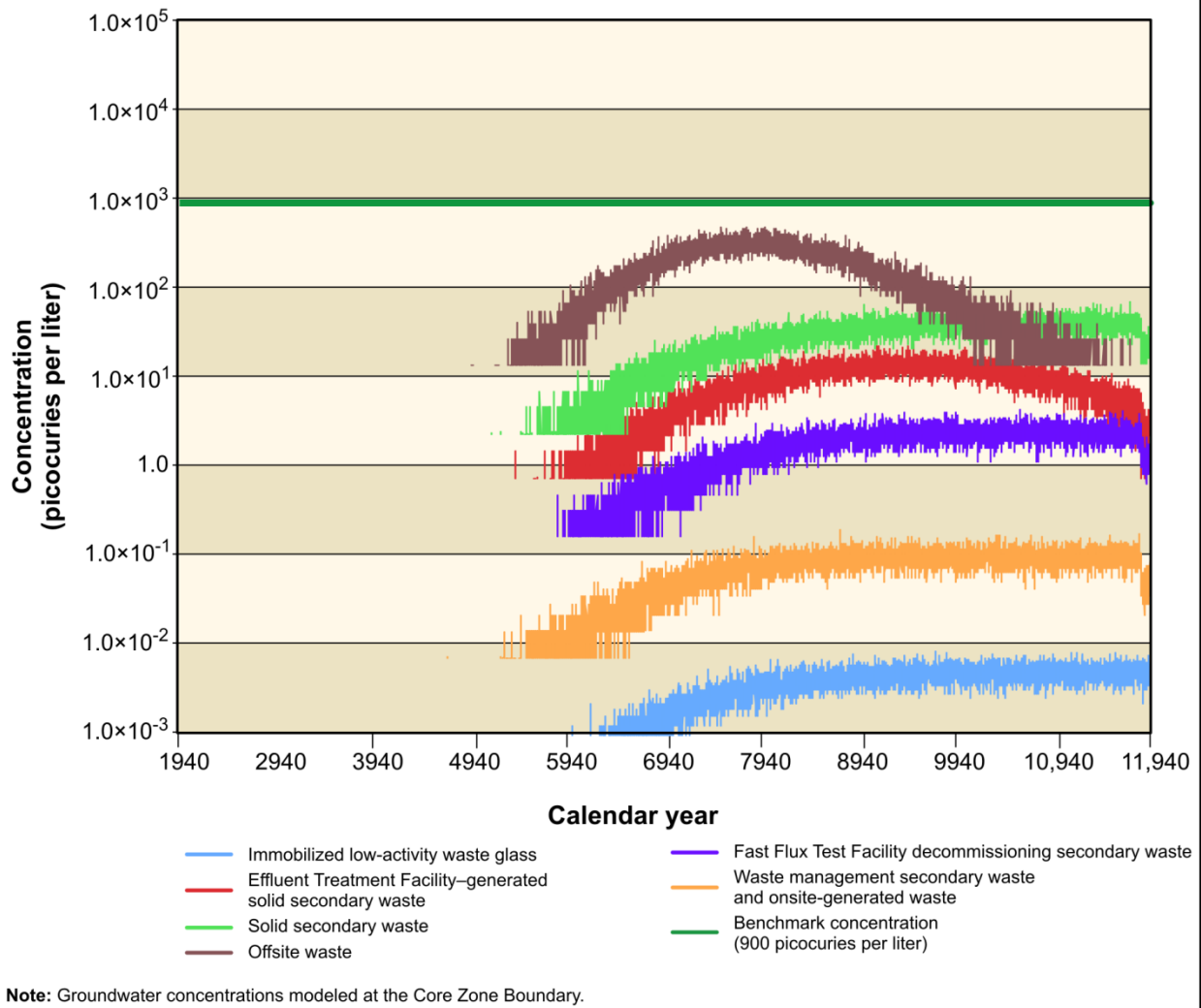
Figure M–134. Tank Closure Alternative 2B
Groundwater Technetium-99 Concentration at the Core Zone Boundary
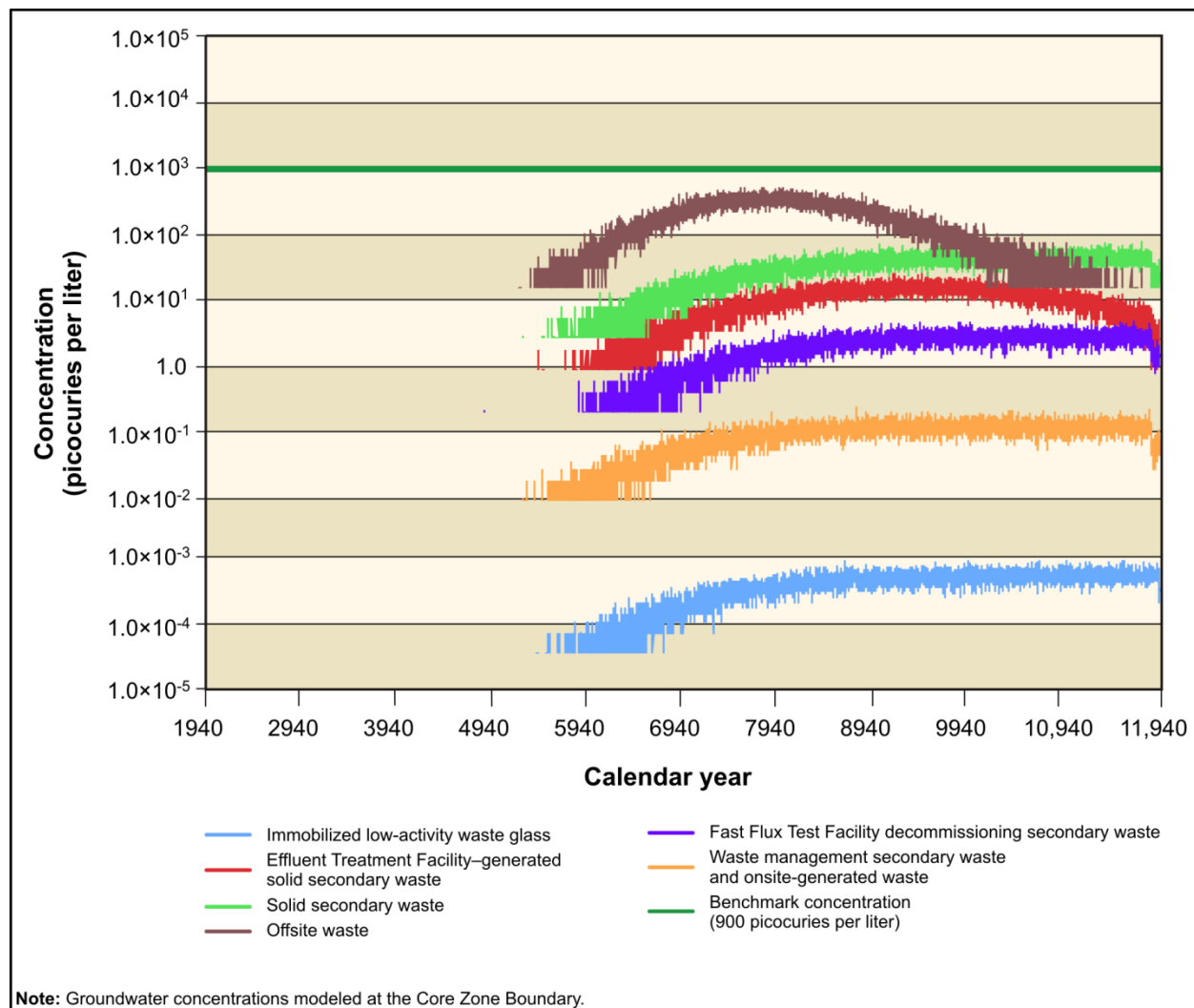
**Figure M–135. Groundwater Technetium-99 Concentration at
the Core Zone Boundary, Sensitivity Case 1**

**Figure M–136. Groundwater Technetium-99 Concentration at
the Core Zone Boundary, Sensitivity Case 2**

The results of the sensitivity analysis indicate that increasing the fractional release rate of ILAW glass by an order of magnitude increases the predicted release of technetium-99 to the vadose zone by an order of magnitude. The predicted concentration of technetium-99 in groundwater at the Core Zone Boundary follows a similar pattern. However, the contribution of ILAW glass remains a small fraction of the combined impacts for each of the analysis cases.

M.5.7.2   Iodine Recycle Sensitivity Analysis

Under Tank Closure Alternative 2B, tank closure waste would be treated in the WTP and the treated waste would be disposed of in IDF-East. Two waste forms that would result from this treatment are ILAW glass and ETF-generated secondary waste. This *Final TC & WM EIS* assumes that process flow around the melter and the melter's offgas system are such that iodine-129 would partition 20 percent into ILAW glass and 80 percent into a grouted secondary-waste form (Whyatt, Shade, and Stegen 1996). The objective of the iodine-recycle sensitivity analyses is to evaluate changes in the concentration of iodine in groundwater due to variations in the WTP process flows that increase the portion of iodine partitioned into ILAW glass. The sensitivity case evaluates the effect of partitioning 70 percent iodine-129 into ILAW glass and 30 percent into secondary grout. The distribution of inventory of iodine-129 across the waste forms for each case is presented in Table M–59. Figure M–137 reports the estimated rate of release

of iodine-129 to the vadose zone for the ILAW glass and ETF-generated secondary-waste forms. The results indicate that the rate of release from the grouted waste form is a factor of approximately 200 higher than the rate of release from the glass waste form. For the grouted waste form, the rate of release decreases in proportion to the decrease in inventory in grout by approximately a factor of three as the WTP process recycle directs iodine to the ILAW glass waste form.

Table M–59. Iodine-129 Inventory for Effluent Treatment Facility–Generated Secondary Waste and ILAW Glass for *TC & WM EIS* and Iodine-Recycle Sensitivity Analysis Cases

Waste Form	Iodine -129 (curies)	
	EIS Case	Iodine-Recycle Sensitivity Case
ETF-generated secondary waste	3.36×10^1	1.26×10^1
ILAW glass	9.55	3.35×10^1
ILAW melter offgas secondary waste	4.65	1.90

Key: EIS=environmental impact statement; ETF=Effluent Treatment Facility; ILAW=Immobilized Low-Activity Waste; *TC & WM EIS=Tank Closure and Waste Management Environmental Impact Statement for the Hanford Site, Richland, Washington.*
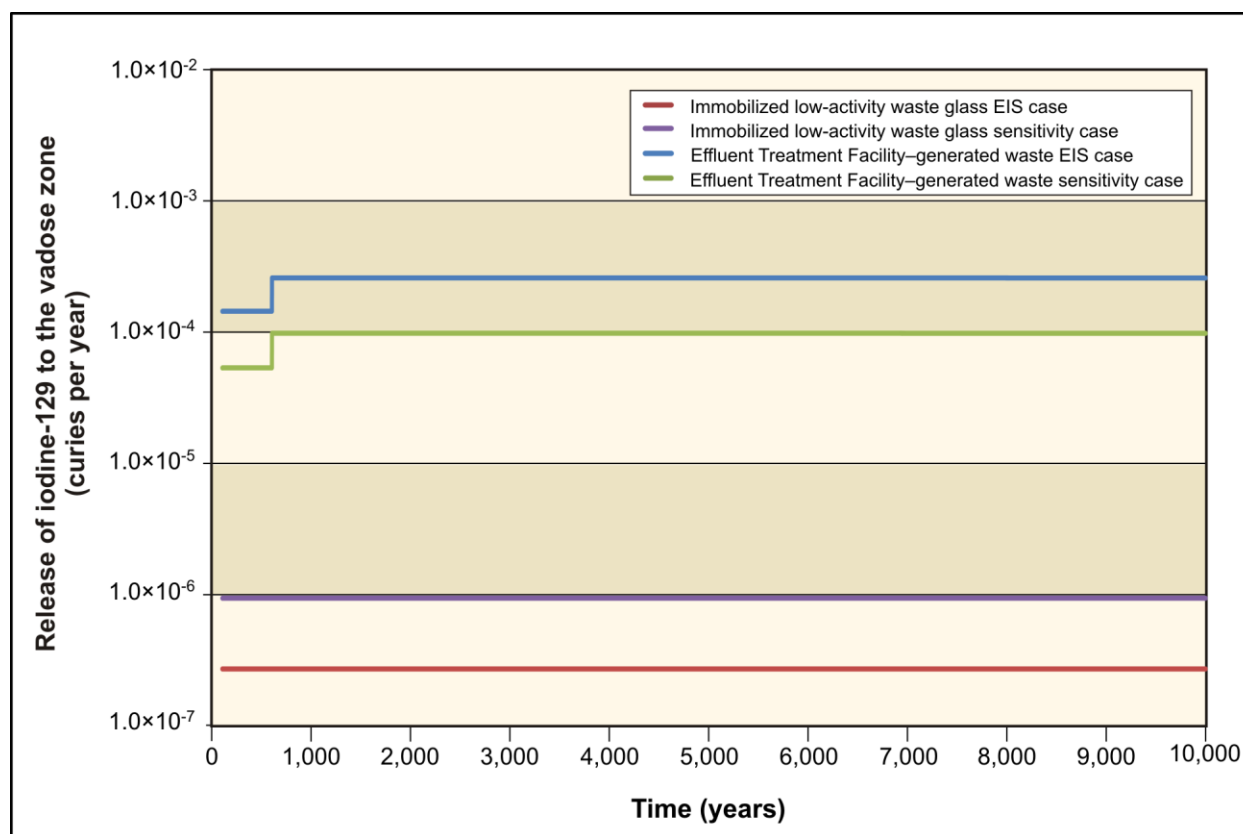
Figure M–137. Release of Iodine-129 to the Vadose Zone from Effluent Treatment Facility–Generated Secondary Waste and Immobilized Low-Activity Waste Glass for *TC & WM EIS* and Iodine-Recycle Sensitivity Cases

Figures M–138 and M–139 report the concentration of iodine-129 in the groundwater at the Core Zone Boundary for all waste forms, including those not directly affected by changes in WTP recycle flows for both the *TC & WM EIS* and iodine-recycle sensitivity cases.

Note: Groundwater concentrations modeled at the Core Zone Boundary.
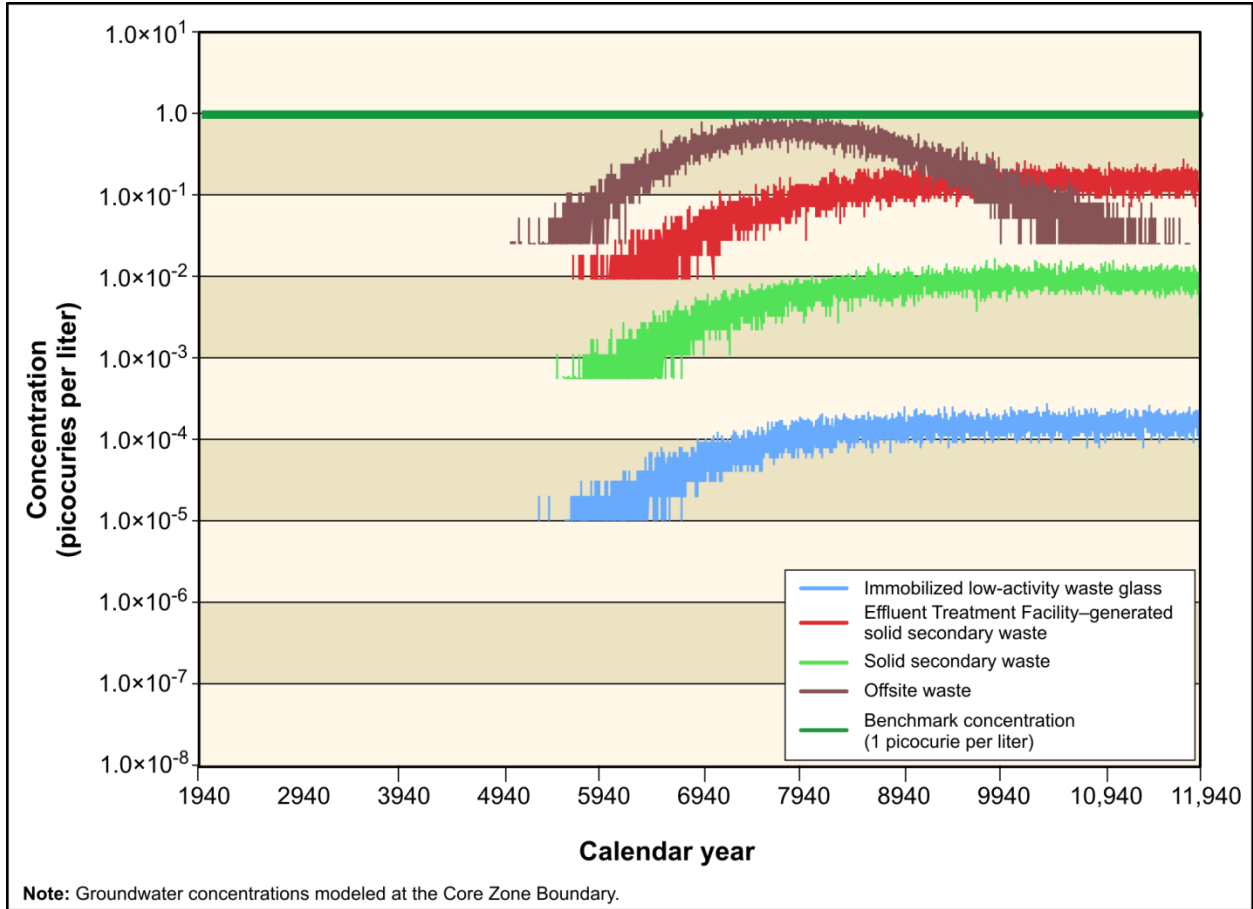
Figure M–138. Waste Management Alternative 2, Tank Closure Alternative 2B, Groundwater Iodine-129 Concentrations at the Core Zone Boundary, *TC & WM EIS* **Case**

Note: Groundwater concentrations modeled at the Core Zone Boundary.
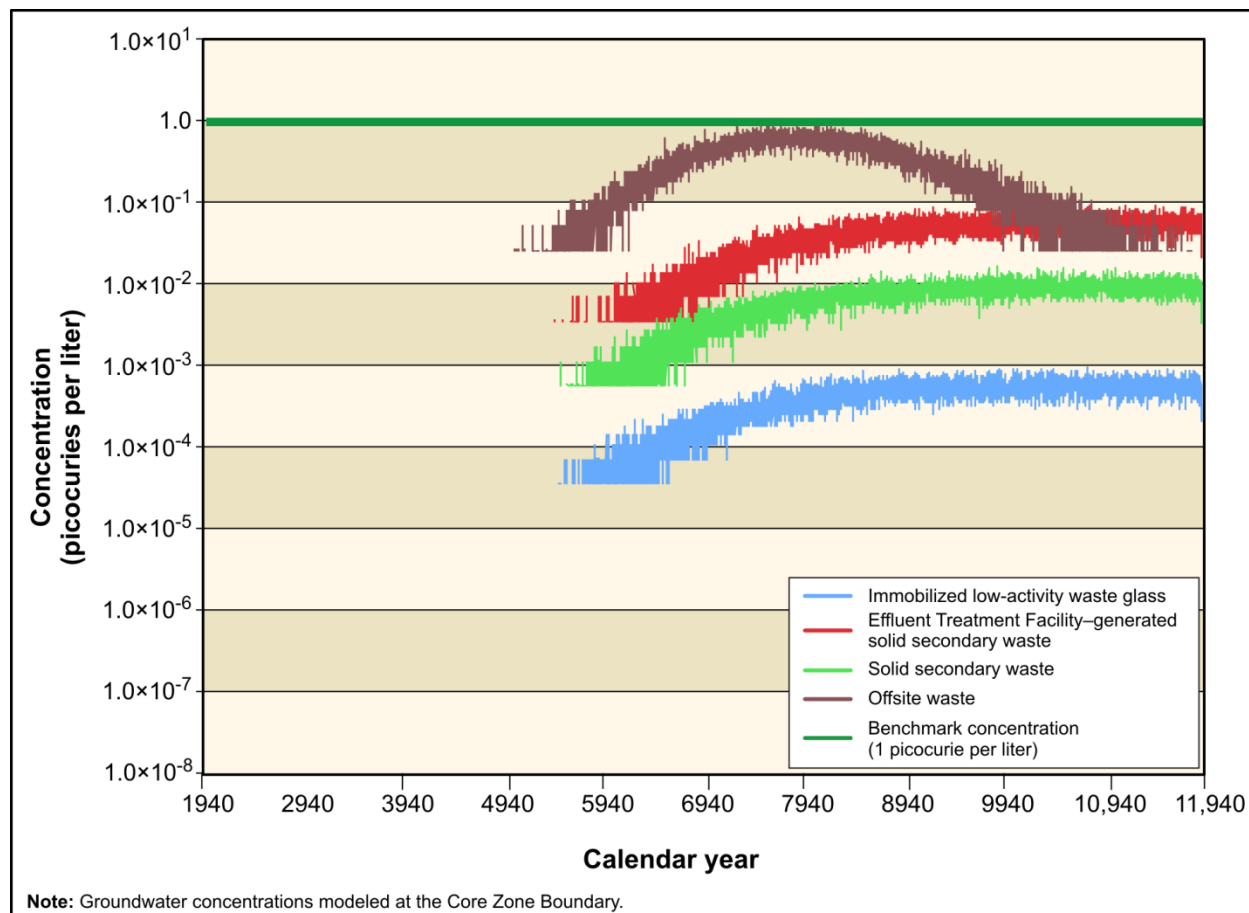
**Figure M–139. Waste Management Alternative 2, Tank Closure Alternative 2B,
Groundwater Iodine-129 Concentrations at the Core Zone Boundary
Iodine-Recycle Sensitivity Case**

The decrease of iodine-129 inventory in the ETF-generated secondary waste in the iodine-recycle sensitivity case produces a decrease in the predicted groundwater concentration at the Core Zone Boundary due to this single source by a factor of approximately 2.5. This release to the vadose zone produces a similar decrease in the flux of iodine-129 to the water table due to this single source. The increase of iodine-129 in ILAW glass under the iodine-recycle sensitivity case resulted in a 3.5 times greater predicted release to the vadose zone and concentration in the groundwater at the Core Zone Boundary, but the contribution of this source to combined impacts remains a small fraction of the impacts due to grouted secondary-waste forms.

M.5.7.3   No-Technetium-99-Removal Sensitivity Analysis

Under Tank Closure Alternative 2B, this *Final TC & WM EIS* assumes that technetium-99 would be selectively removed from the LAW waste stream as a pretreatment step within the WTP and captured in IHLW glass, which would be disposed of off site. The objective of this sensitivity analysis is to examine the predicted impacts on groundwater if the technetium-99 were not selectively removed from the LAW stream, but rather was processed through the WTP and encapsulated in ILAW glass. Table M–60 reports the technetium-99 inventory for the waste forms evaluated for this sensitivity analysis. Figure M–140 reports the predicted release of technetium-99 to the vadose zone from the affected sources. The results indicate that the rates of release from ETF-generated secondary waste and WTP secondary solid waste are similar. The *TC & WM EIS* case predicts a slightly higher rate of release from WTP secondary solid waste due to the larger technetium-99 inventory. The estimated rate of release for

the ILAW glass in the no-technetium-99-removal case is greater than three orders of magnitude higher due to the larger technetium-99 inventory that remains on site. However, the rate of release from ILAW glass remains small in absolute terms and is relative to the releases from other waste forms included under this alternative.

**Table M–60. Initial Inventory for No-Technetium-99-Removal Sensitivity Analysis**

	Technetium-99 Inventory (curies)	
Waste Form	***TC & WM EIS* Case**	**No-Technetium-99-Removal Sensitivity Case**
IHLW glass	2.90×10^4	2.47×10^2
ILAW glass and retired melters	2.88×10^2	2.88×10^4
ETF-generated secondary waste	8.63×10^1	8.63×10^1
WTP secondary solid waste	4.92×10^2	4.31×10^2

Key: ETF=Effluent Treatment Facility; IHLW=immobilized high-level radioactive waste; ILAW=immobilized low-activity waste; *TC & WM EIS=Tank Closure and Waste Management Environmental Impact Statement for the Hanford Site, Richland, Washington*; WTP=Waste Treatment Plant.
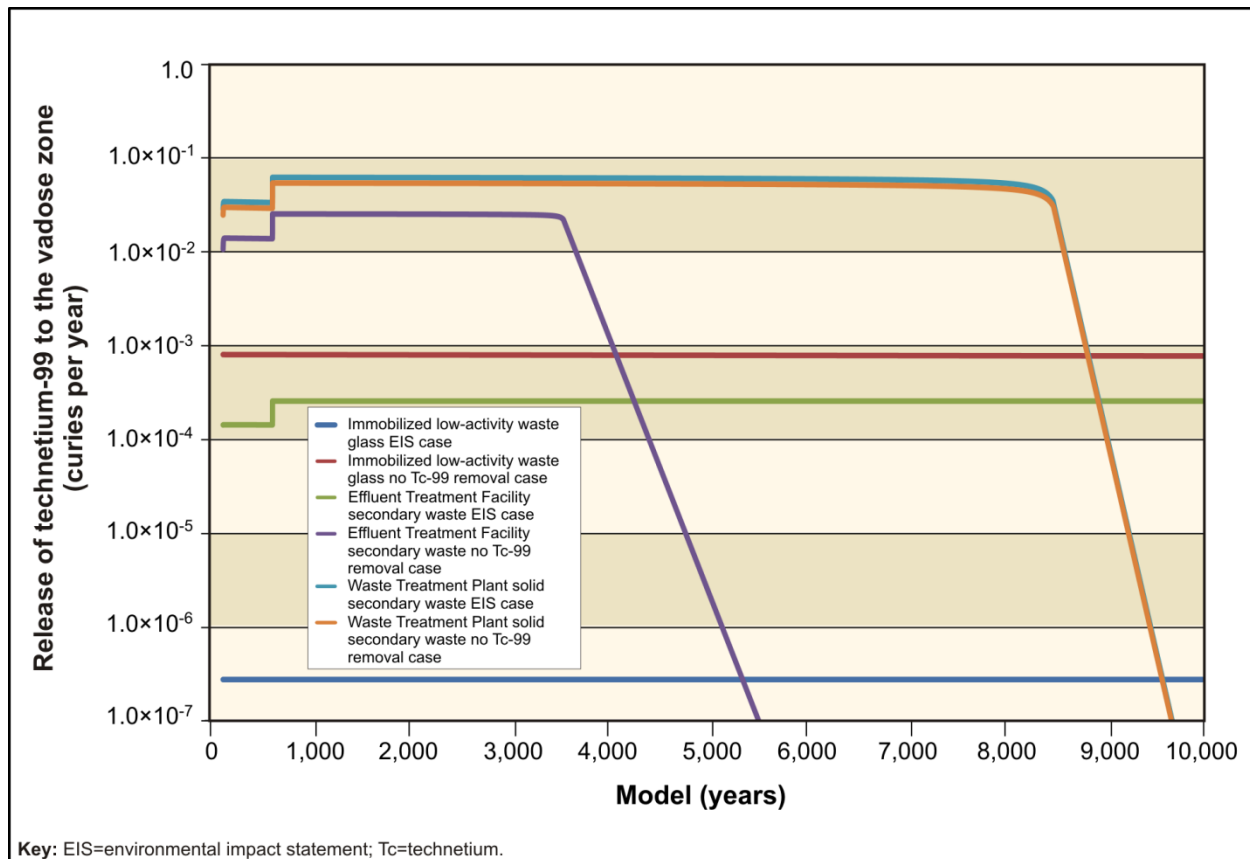
Figure M–140. Release of Technetium-99 to the Vadose Zone, *TC & WM EIS* and No-Technetium-99-Removal Sensitivity Cases

Figures M–141 and M–142 report the concentration of technetium-99 in the groundwater at the Core Zone Boundary for all waste forms, including those not directly affected by change in the technetium-99 flow.
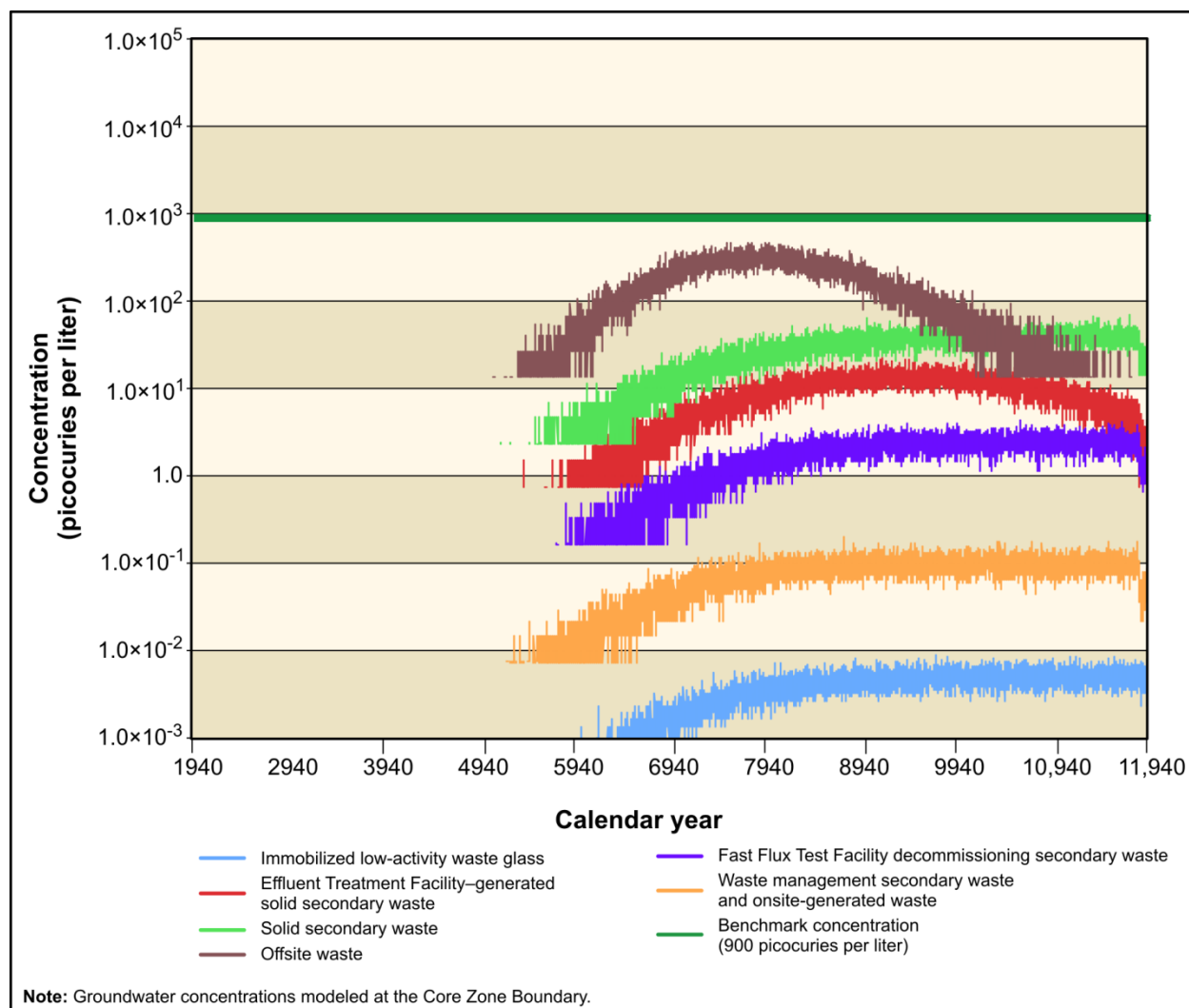
Figure M–141. Waste Management Alternative 2, Disposal Group 1, Subgroup 1-A, Groundwater Technetium-99 Concentration at the Core Zone Boundary
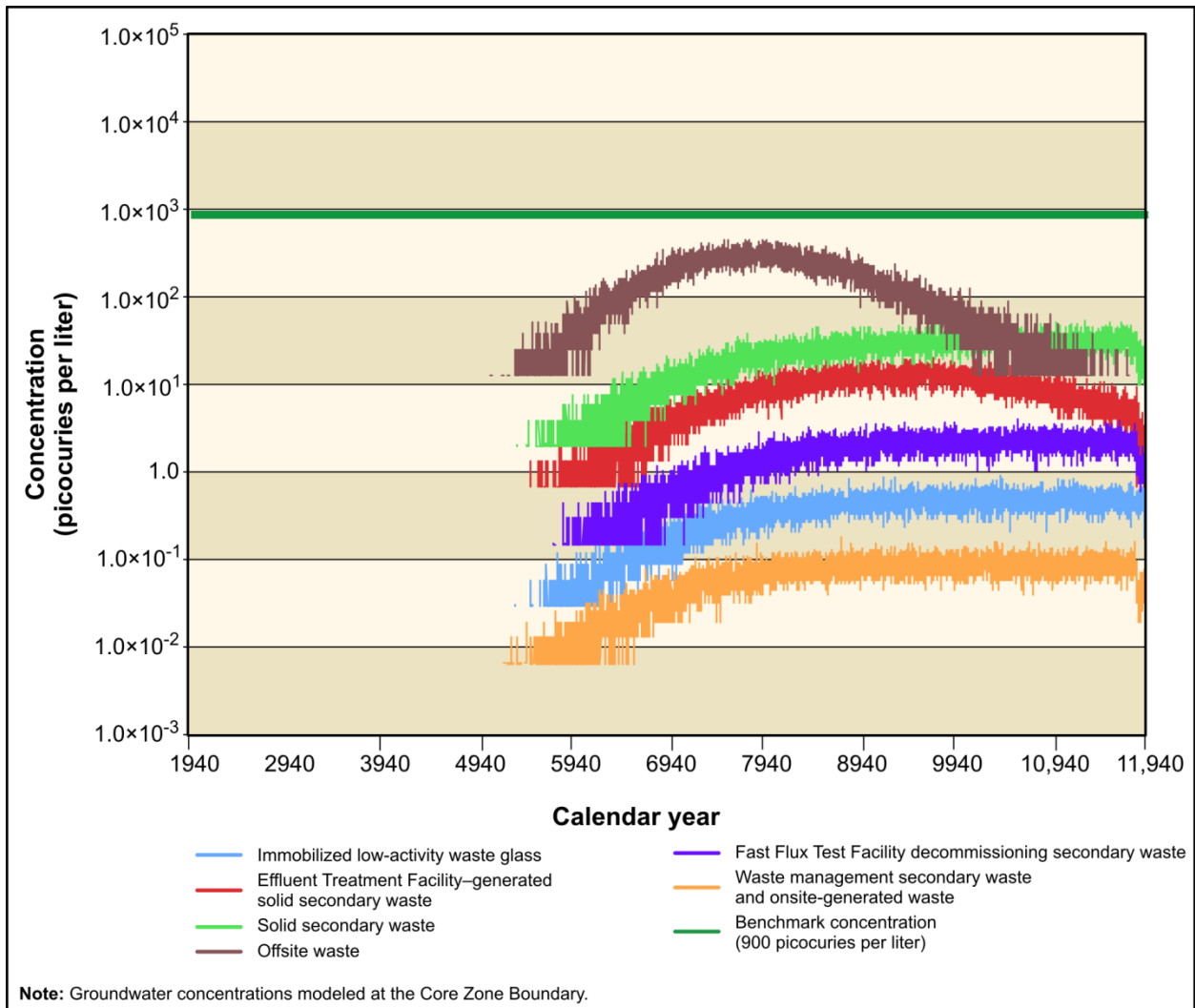
**Figure M–142. Groundwater Technetium-99 Concentration at the Core Zone Boundary,
No-Technetium-99-Removal Case**

The increase in technetium-99 inventory in ILAW glass in the no-technetium-99-removal sensitivity case produces an increase in the predicted groundwater concentration at the Core Zone Boundary due to this single source by two orders of magnitude. The increase in technetium-99 in ILAW glass in the no-technetium-99-removal case does not make it a primary contributor to the combined impacts in this case, and the predicted groundwater concentration from this source at the Core Zone Boundary is approximately three orders of magnitude below the benchmark.

M.5.7.4   Bulk Vitrification Sensitivity Analysis

As described in Appendix E, Section E.1.2.3.6, during engineering-scale and large-scale testing, results suggested that technetium-99 might present itself in a more soluble form deposited as a vesicular glass layer on top of the bulk vitrification melt (Pierce et al. 2005). This would affect the release rates from the final waste form in an IDF. The very high temperatures associated with bulk vitrification volatilize and drive off technetium-99 from the waste feed prior to its incorporation into the vitrified glass matrix. The volatilized technetium-99 then condenses on the surface of the castable refractory block as the offgas flows out of the vitrification container (Pierce et al. 2005). The *TC & WM EIS* models the technetium-99 in the bulk vitrification supplemental-waste form with 93.5 percent of the inventory in the glass and 6.5 percent in the castable refractory block. The *TC & WM EIS* release model for bulk vitrification glass

waste form is a fractional release model, with a fractional release rate of 1.00×10^{-8} grams per gram per year. The castable refractory block is modeled using the partitioning-limited, convective-flow model.

The objective of this sensitivity analysis is to analyze the effect of optimizing the bulk vitrification system for Tank Closure Alternative 3A using the two cases described below and in Table M–61:

- Reducing the technetium-99 inventory in the castable refractory block to 0.3 percent, with 99.7 percent in the bulk vitrification performance glass

- Keeping the technetium-99 inventory in the castable refractory block at 6.5 percent, with 93.5 percent in glass with a reduced fractional release rate

Table M–61. Bulk Vitrification Sensitivity Analysis Cases

Sensitivity Cases	Technetium-99 Inventory (curies)		Fractional Release Rate
	Bulk Vitrification Glass	Castable Refractory Block	
EIS Case	1.93×10^4	1.34×10^3	1.00×10^{-8}
Sensitivity Case 1	2.06×10^4	6.20×10^1	1.00×10^{-8}
Sensitivity Case 2	1.93×10^4	1.34×10^3	1.00×10^{-9}

Key: EIS=environmental impact statement.

Figure M–143 reports the release to the vadose zone for each of the cases listed above. The short spike in release of technetium-99 from castable refractory block is due to the increased infiltration rate after the barrier lifetime.

Key: EIS=environmental impact statement.
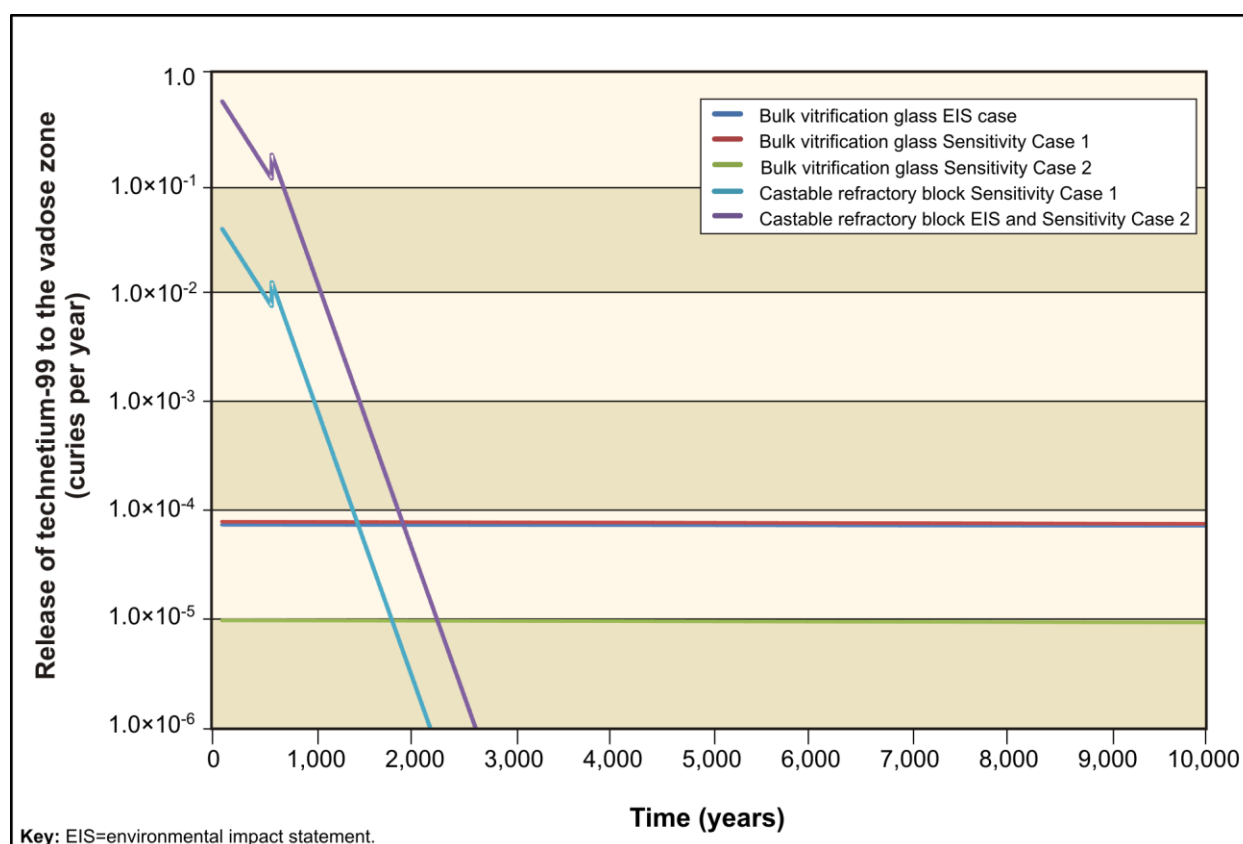
**Figure M–143. Release of Technetium-99 to the Vadose Zone,
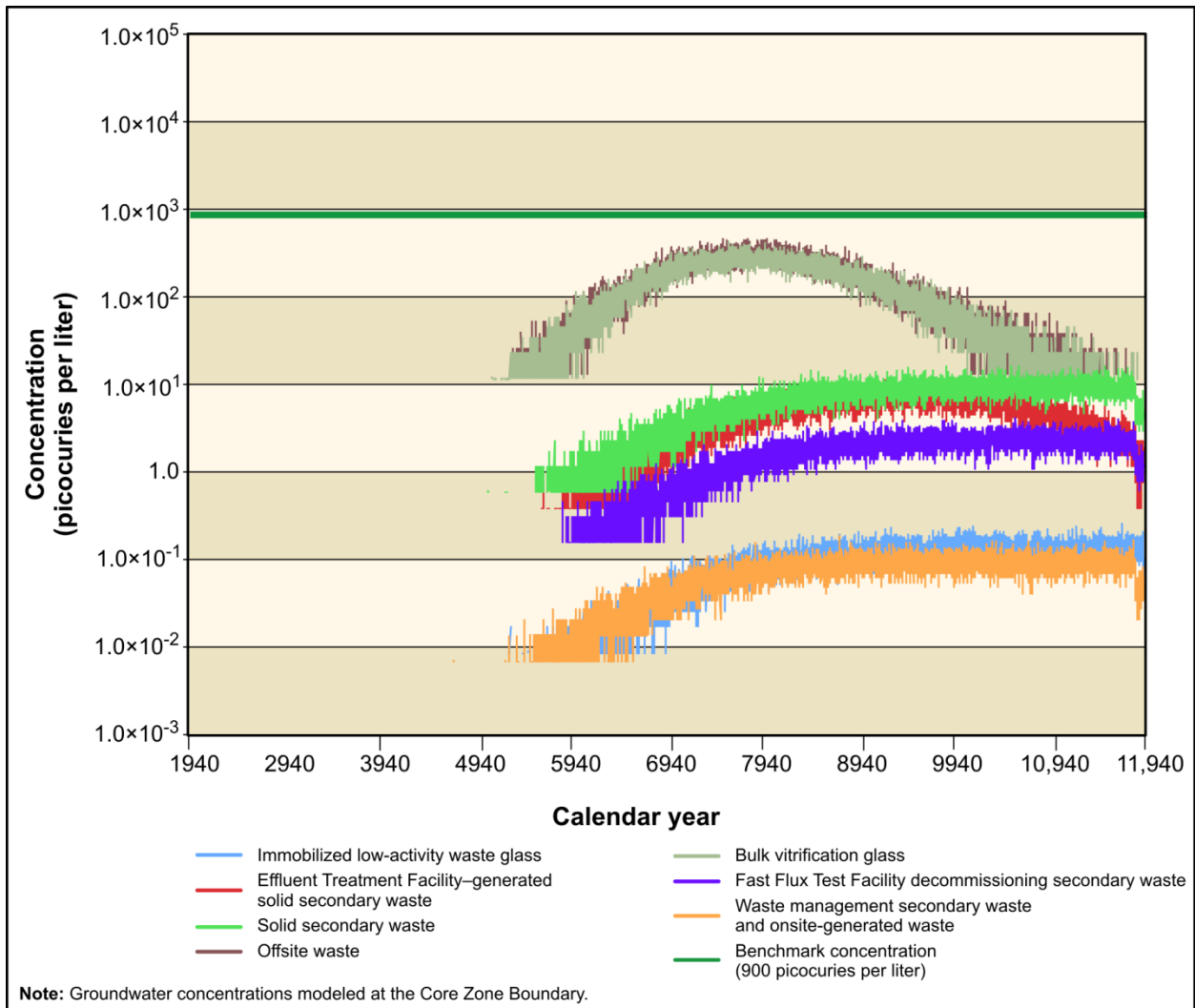Bulk Vitrification Glass Sensitivity Analysis**

Predicted concentrations of technetium-99 in groundwater at the Core Zone Boundary for the *TC & WM EIS* and Sensitivity Cases 1 and 2 for all waste forms under Tank Closure Alternative 3A are presented in Figures M–144, M–145, and M–146, respectively.

Note: Groundwater concentrations modeled at the Core Zone Boundary.
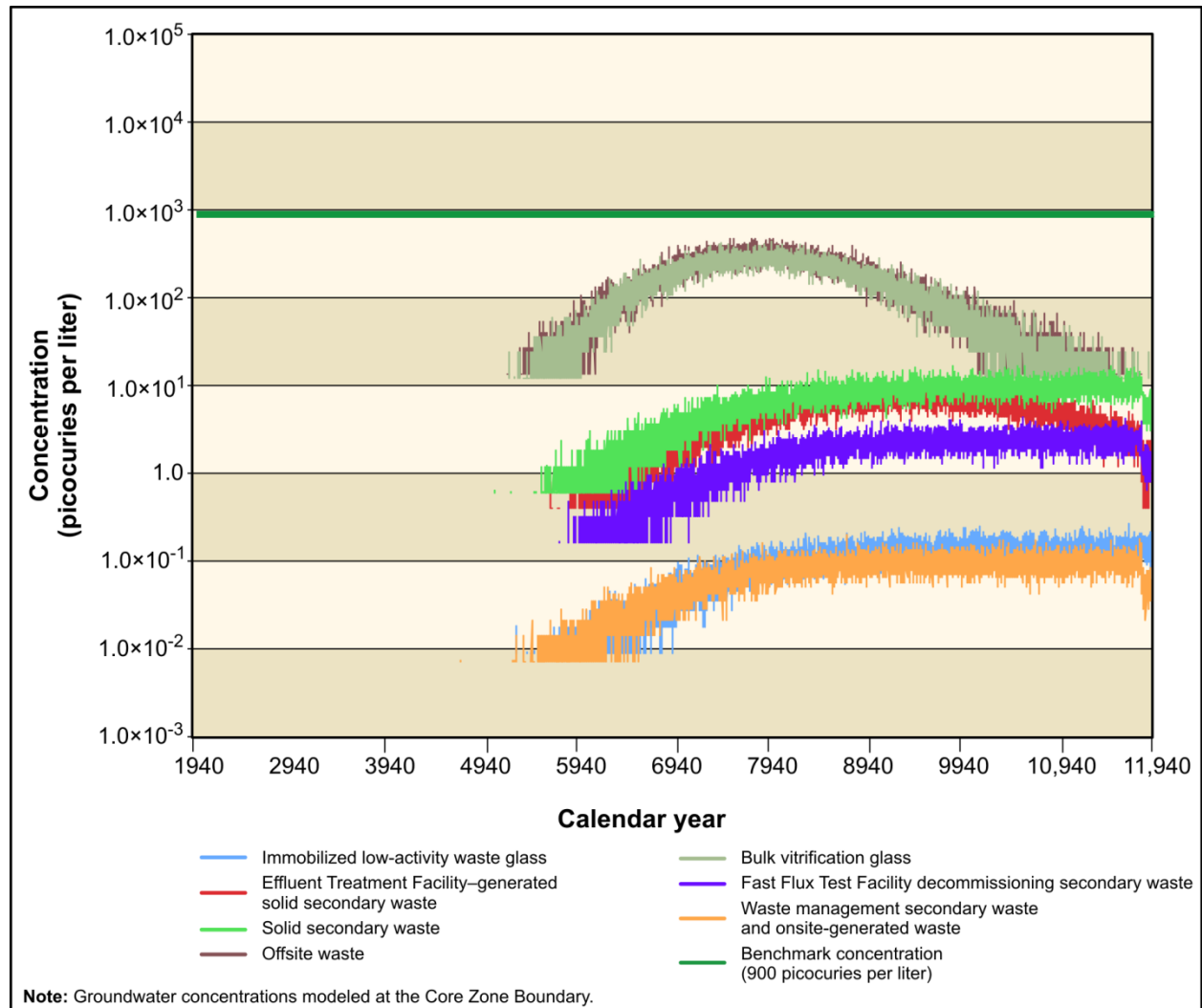
Figure M–144. Tank Closure Alternative 3A, Groundwater Technetium-99 Concentrations at the Core Zone Boundary, Bulk Vitrification EIS Case
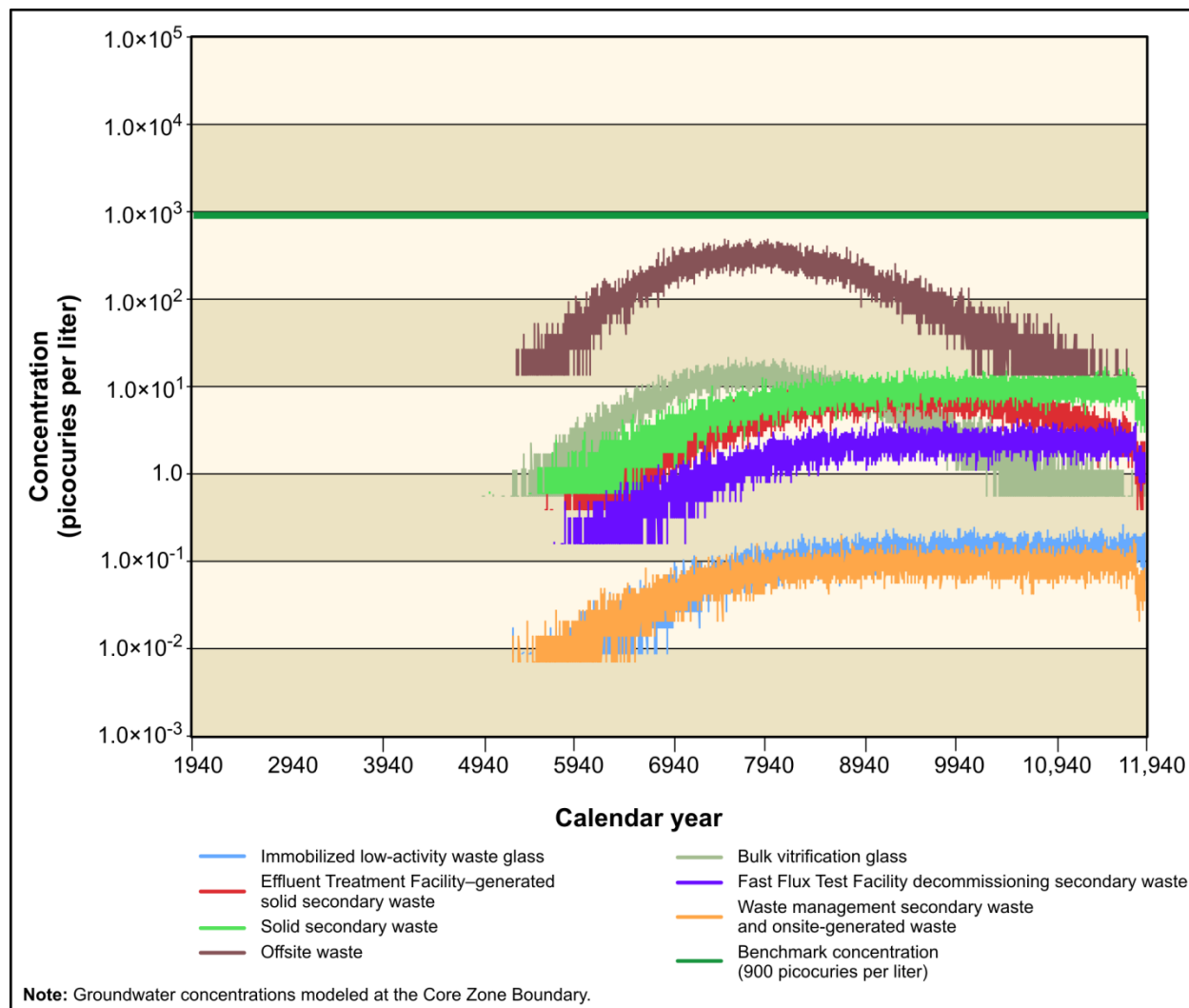
Figure M–145. Groundwater Technetium-99 Concentrations at the Core Zone Boundary, Bulk Vitrification Sensitivity Case 1

Figure M–146. Groundwater Technetium-99 Concentrations at the Core Zone Boundary, Bulk Vitrification Sensitivity Case 2

The analysis indicates that, for waste forms directly related to bulk vitrification, the release from castable refractory block is the primary source for the predicted concentrations of technetium-99 in the groundwater. Reducing the fractional release rate in the bulk vitrification glass does not result in a noticeable difference in the predicted concentrations of technetium-99 in the groundwater. The predicted concentrations of technetium-99 in bulk vitrification glass for Sensitivity Case 1 indicate that reducing the inventory in the castable refractory block provides the greatest effect in reducing the estimated concentration in the aquifer.

M.5.7.5   Grout Performance

The assessment of the long-term performance of grout to be disposed of in IDF-East assumes the waste form is saturated. The effective diffusion coefficients for iodine-129 and technetium-99 used in this EIS were 1.0×10^{-10} and 5.0×10^{-9} square centimeters per second, respectively (DOE 2005). The distribution coefficient (K_d) values that can be inferred from these effective diffusion coefficients for iodine-129 and technetium-99 are 50 milliliters per gram and 1.1 milliliters per gram, respectively.

Documentation for the Hanford site indicates that the moisture content for the waste form may be below saturated conditions, ranging from 4 percent and 7 percent moisture content (Mattigod et al. 2001). As the moisture content decreases, the aqueous diffusion coefficient decreases, leading to a smaller effective diffusion coefficient. *Diffusion and Leaching of Selected Radionuclides (Iodine-129, Technetium-99, and Uranium) Through Category 3 Waste Encasement Concrete and Soil Fill Material* (Mattigod et al. 2001) indicates that the grout effective diffusion coefficient for iodine-129 could range between 2.07×10^{-14} square centimeters per second (approximately 4 percent soil moisture content) and 1.31×10^{-12} square centimeters per second (7 percent soil moisture content) and for technetium-99, between 6.22×10^{-12} square centimeters per second (approximately 4 percent soil moisture content) and 4.24×10^{-11} square centimeters per second (7 percent soil moisture content).

The objective of this sensitivity assessment is to evaluate the effect of the suggested decrease in effective diffusion coefficient in iodine-129 and technetium-99 on the grouted waste forms disposed of at IDF-East. This sensitivity analysis for grout examined the 7 percent moisture content indicated in Mattigod et al. (2001).

The grouted waste forms considered in this analysis include ETF-generated secondary waste, solid secondary waste, FFTF Decommissioning (Alternative 3) secondary waste, waste management secondary waste, onsite non-CERCLA waste, and cast stone waste (Tank Closure Alternative 3B). These waste forms are portions of the proposed action for four Waste Management alternatives:

- Waste Management Alternative 2, Disposal Group 1, Subgroup 1-A, addresses the waste from Tank Closure Alternative 2B.

- Waste Management Alternative 2, Disposal Group 1, Subgroup 1-B, addresses the waste from Tank Closure Alternative 3A.
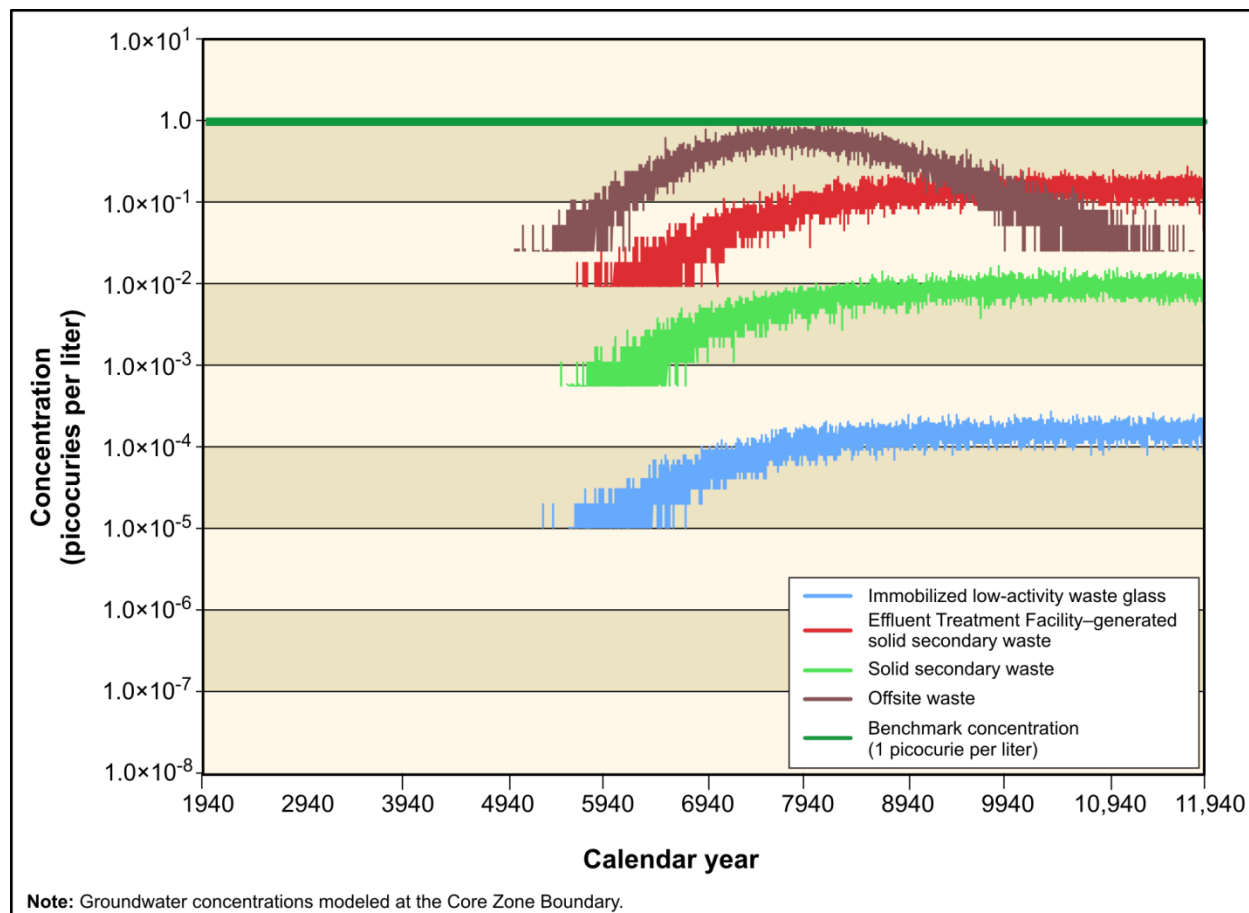
- Waste Management Alternative 2, Disposal Group 1, Subgroup 1-C, addresses the waste from Tank Closure Alternative 3B.

- Waste Management Alternative 2, Disposal Group 1, Subgroup 1-D, addresses the waste from Tank Closure Alternative 3C.

Waste Management Alternative 2, Disposal Group 1, Subgroup 1-A, Addresses the Waste from Tank Closure Alternative 2B

Waste Management Alternative 2, Disposal Group 1, Subgroup 1-A, addresses disposal in IDF-East of the waste from Tank Closure Alternative 2B, onsite non-CERCLA sources, FFTF decommissioning, waste management, and other DOE sites. Waste forms for IDF-East include ILAW glass, LAW melters, tank closure secondary waste, FFTF decommissioning secondary waste, waste management secondary waste, offsite waste, and onsite non-CERCLA waste. The grouted waste forms under this alternative are ETF-generated secondary waste and tank closure solid secondary waste. The waste packages are cylindrical with radii of 0.25 and 0.83 meters for ETF-generated secondary waste and tank closure solid secondary waste, respectively. Figure M–147 compares the releases of iodine-129 to the vadose zone for the grouted waste forms for both ETF-generated secondary waste and tank closure solid secondary waste. The releases to the vadose zone in curies per year decrease by approximately two orders of magnitude as the effective diffusivity decreases from the EIS case value to the sensitivity case value.
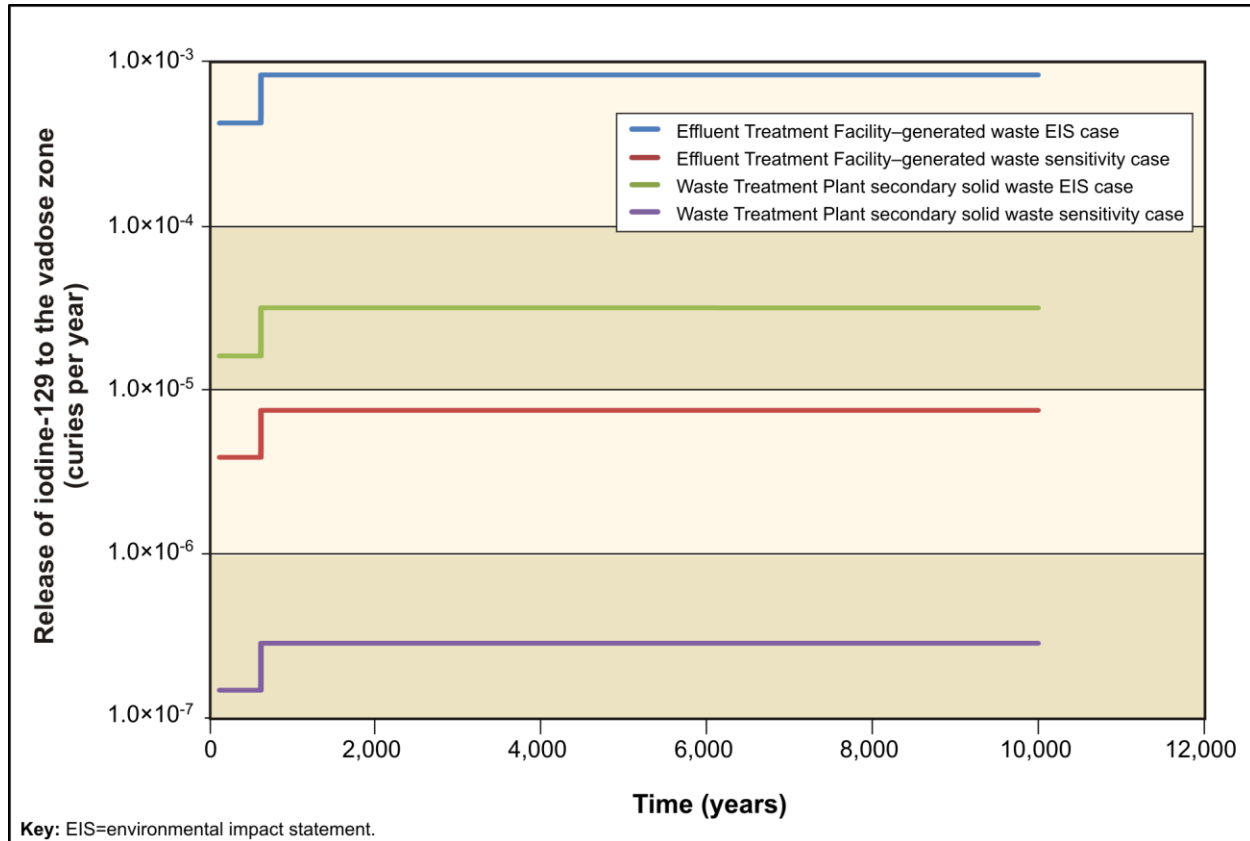
Figure M–147. Rate of Release of Iodine-129 to the Vadose Zone,
Grout Performance Sensitivity Analysis

Figures M–148 and M–149 report estimated groundwater concentrations at the Core Zone Boundary resulting from each of the waste forms under this alternative. Groundwater concentrations predicted for the LAW melter, FFTF decommissioning secondary waste, waste management secondary waste, and onsite non-CERCLA waste are below 1.0×10^{-8} picocuries per liter at the Core Zone Boundary. As indicated in Figure M–149, the sensitivity case, projected concentrations of iodine-129 in the groundwater for the grouted waste forms (ETF-generated and tank closure solid secondary wastes) are decreased by approximately two orders of magnitude relative to the EIS case.

Figure M–148. Waste Management Alternative 2, Tank Closure Alternative 2B, Groundwater Iodine-129 Concentrations at the Core Zone Boundary, EIS Performance
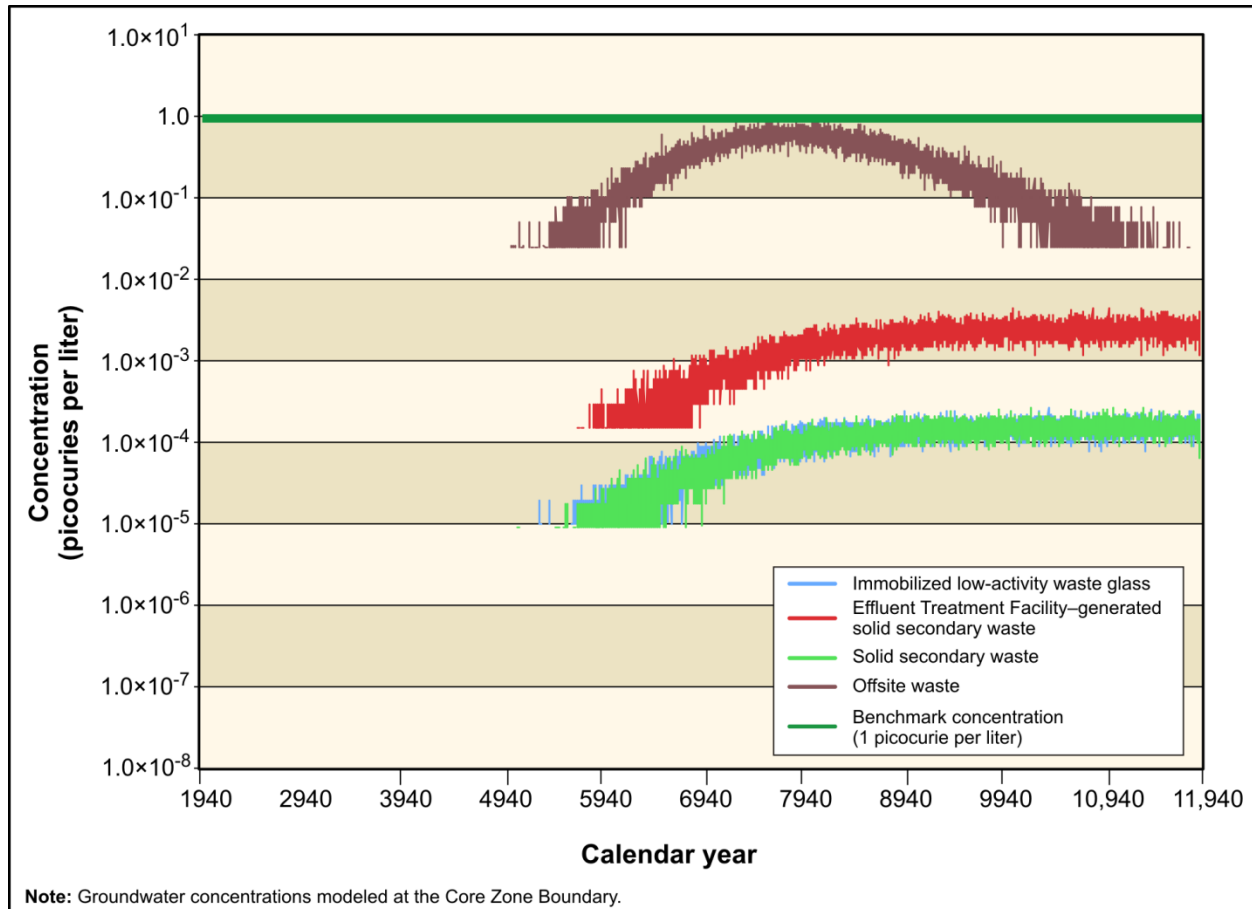
**Figure M–149. Waste Management Alternative 2, Tank Closure Alternative 2B,
Groundwater Iodine-129 Concentrations at the Core Zone Boundary, Grout Sensitivity Case**
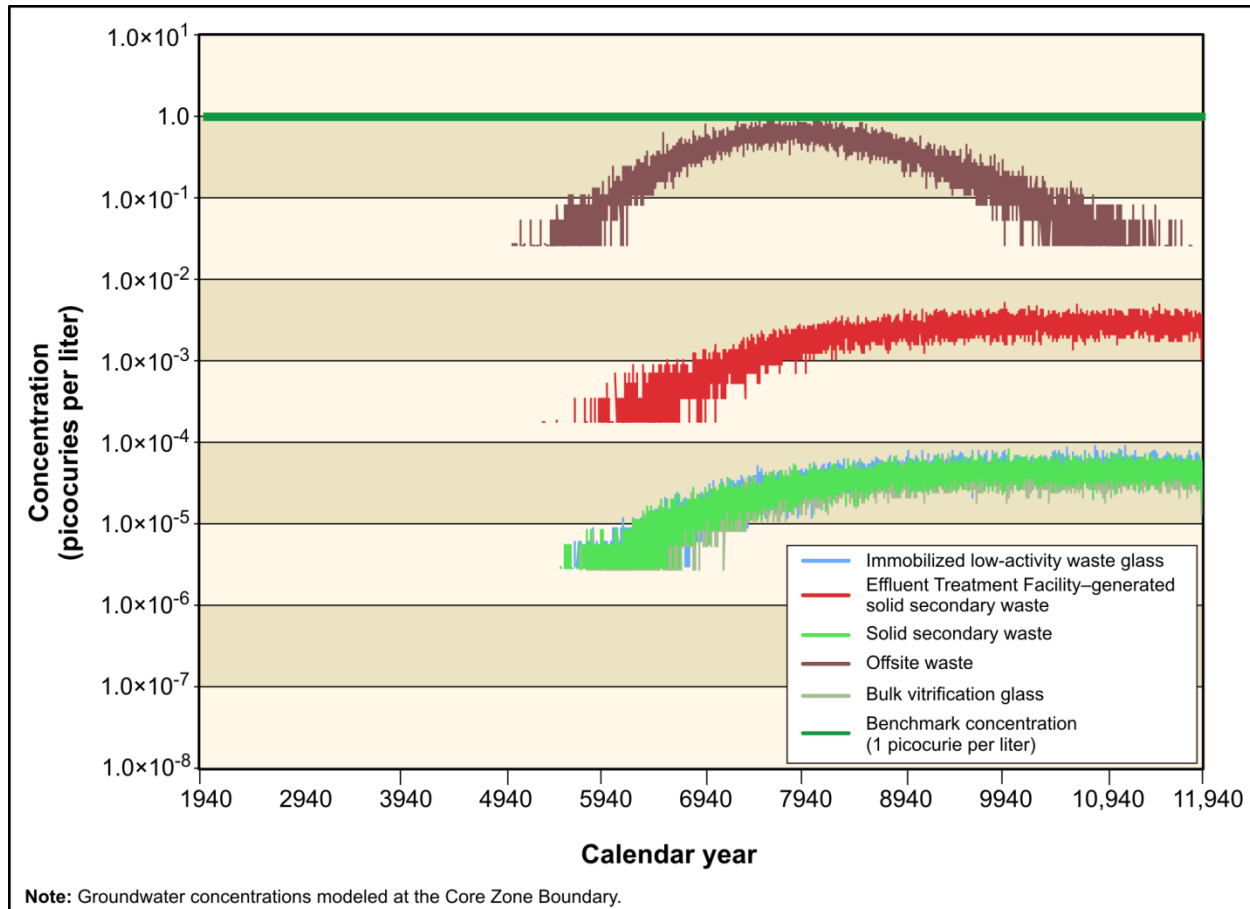
Waste Management Alternative 2, Disposal Group 1, Subgroup 1-B, Addresses the Waste from Tank Closure Alternative 3A

Waste Management Alternative 2, Disposal Group 1, Subgroup 1-B, addresses the waste from *TC & WM EIS* Tank Closure Alternative 3A, onsite non-CERCLA sources, FFTF decommissioning, waste management, and other DOE sites. Waste forms for IDF-East include ILAW glass, LAW melters, bulk vitrification glass, tank closure secondary waste, FFTF decommissioning secondary waste, waste management secondary waste, offsite waste, and onsite non-CERCLA waste. Figures M–150 and M–151 report projected groundwater concentrations at the Core Zone Boundary resulting from each of the waste forms under this alternative. Groundwater concentrations predicted for LAW melters, FFTF decommissioning secondary waste, waste management secondary waste, and onsite non-CERCLA waste are below 1.0×10^{-8} picocuries per liter at the Core Zone Boundary. The grouted waste forms under this alternative are ETF-generated secondary waste and tank closure solid secondary waste. As indicated in Figure M–151, the sensitivity case, the concentration of iodine-129 for the grouted waste forms in the groundwater decreased by approximately two orders of magnitude relative to the EIS case.
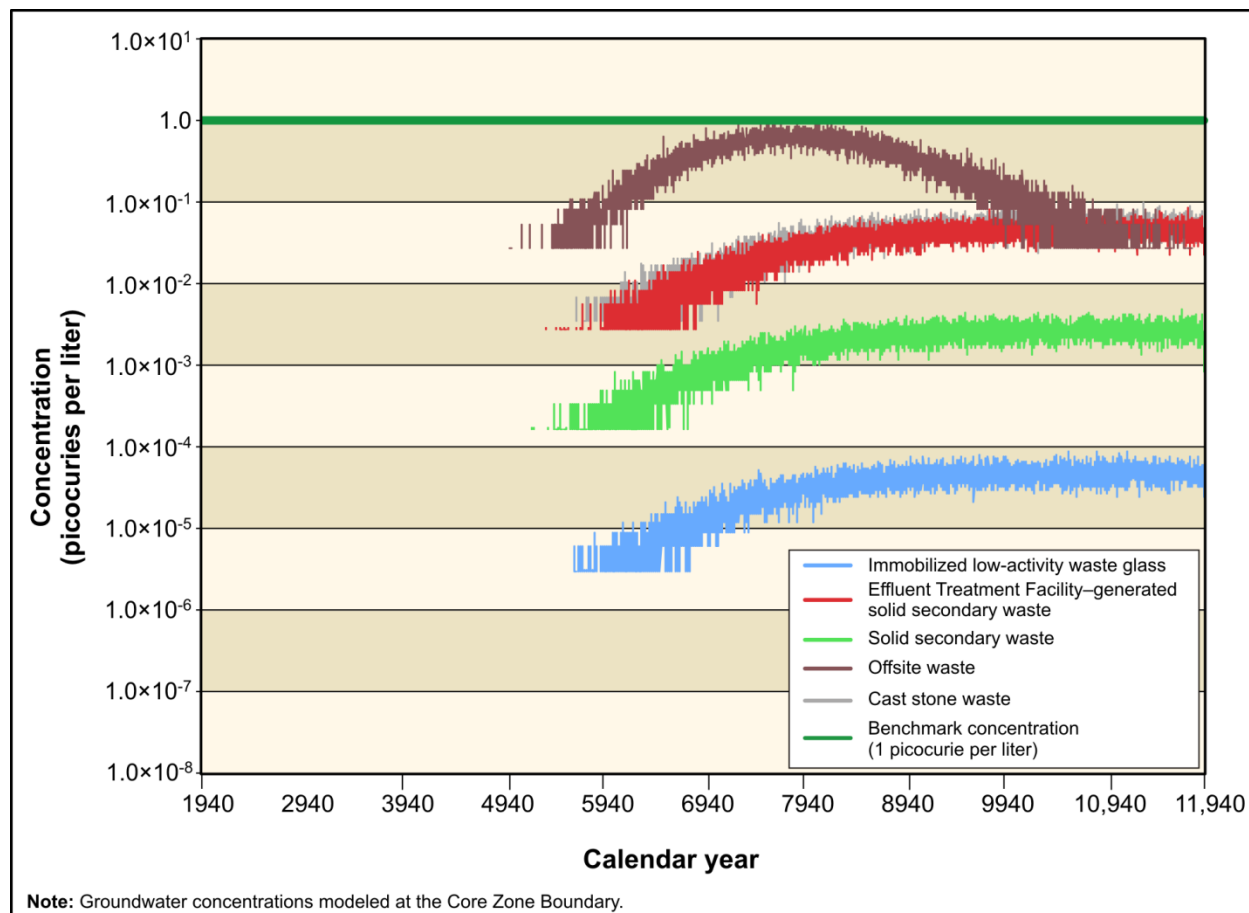
Note: Groundwater concentrations modeled at the Core Zone Boundary.
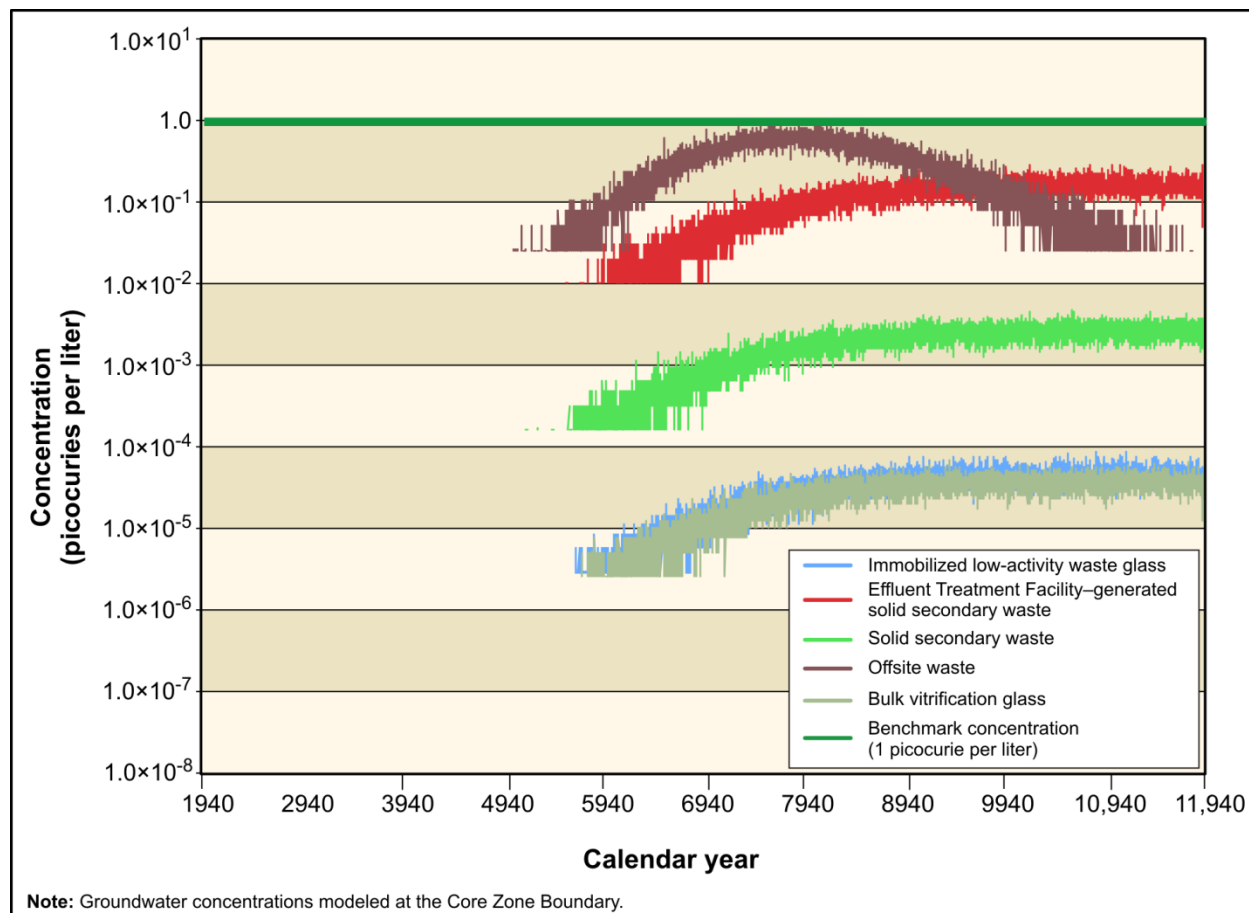
Figure M–150. Waste Management Alternative 2, Tank Closure Alternative 3A, Groundwater Iodine-129 Concentrations at the Core Zone Boundary, EIS Performance
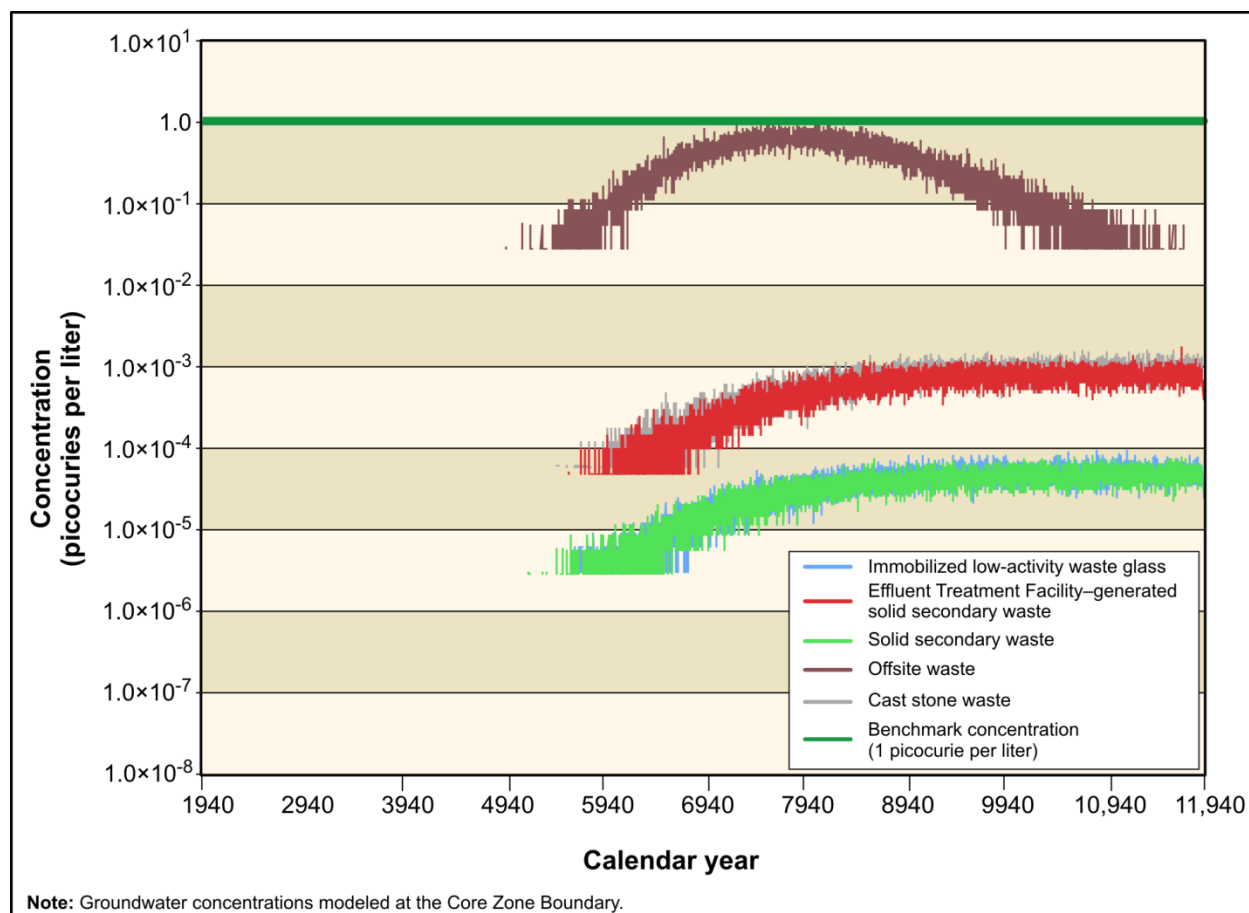
Figure M–151. Waste Management Alternative 2, Tank Closure Alternative 3A, Groundwater Iodine-129 Concentrations at the Core Zone Boundary, Grout Sensitivity Case

Waste Management Alternative 2, Disposal Group 1, Subgroup 1-C, Addresses the Waste from Tank Closure Alternative 3B

Waste Management Alternative 2, Disposal Group 1, Subgroup 1-C, addresses the waste from Tank Closure Alternative 3B, onsite non-CERCLA sources, FFTF decommissioning, waste management, and other DOE sites. Waste forms for IDF-East include ILAW glass, LAW melters, cast stone waste, tank closure secondary waste, FFTF decommissioning secondary waste, waste management secondary waste, offsite waste, and onsite non-CERCLA waste. Figures M–152 and M–153 indicate the groundwater concentration at the Core Zone Boundary resulting from each of the waste forms under this alternative. Groundwater concentrations predicted for LAW melters, FFTF decommissioning secondary waste, waste management secondary waste, and onsite non-CERCLA waste are below 1.0×10^{-8} picocuries per liter at the Core Zone Boundary. The grouted waste forms under this alternative are ETF-generated secondary waste, tank closure solid secondary waste, and cast stone waste. As indicated in Figure M–153, the sensitivity case, the concentration of iodine-129 in the grouted waste forms in the groundwater decreased by approximately two orders of magnitude relative to the EIS case.
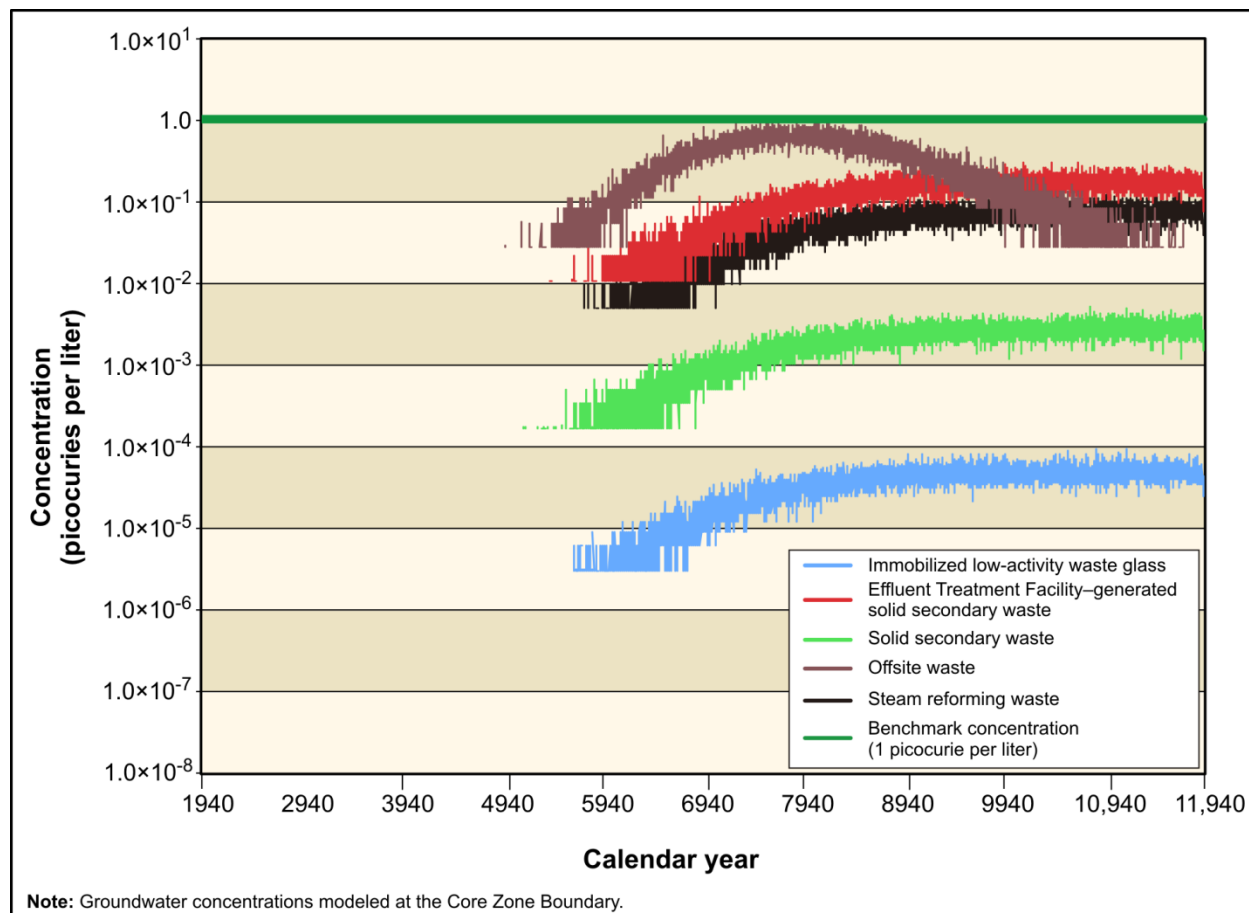
Figure M–152. Waste Management Alternative 2, Tank Closure Alternative 3B, Groundwater Iodine-129 Concentrations at the Core Zone Boundary, EIS Performance

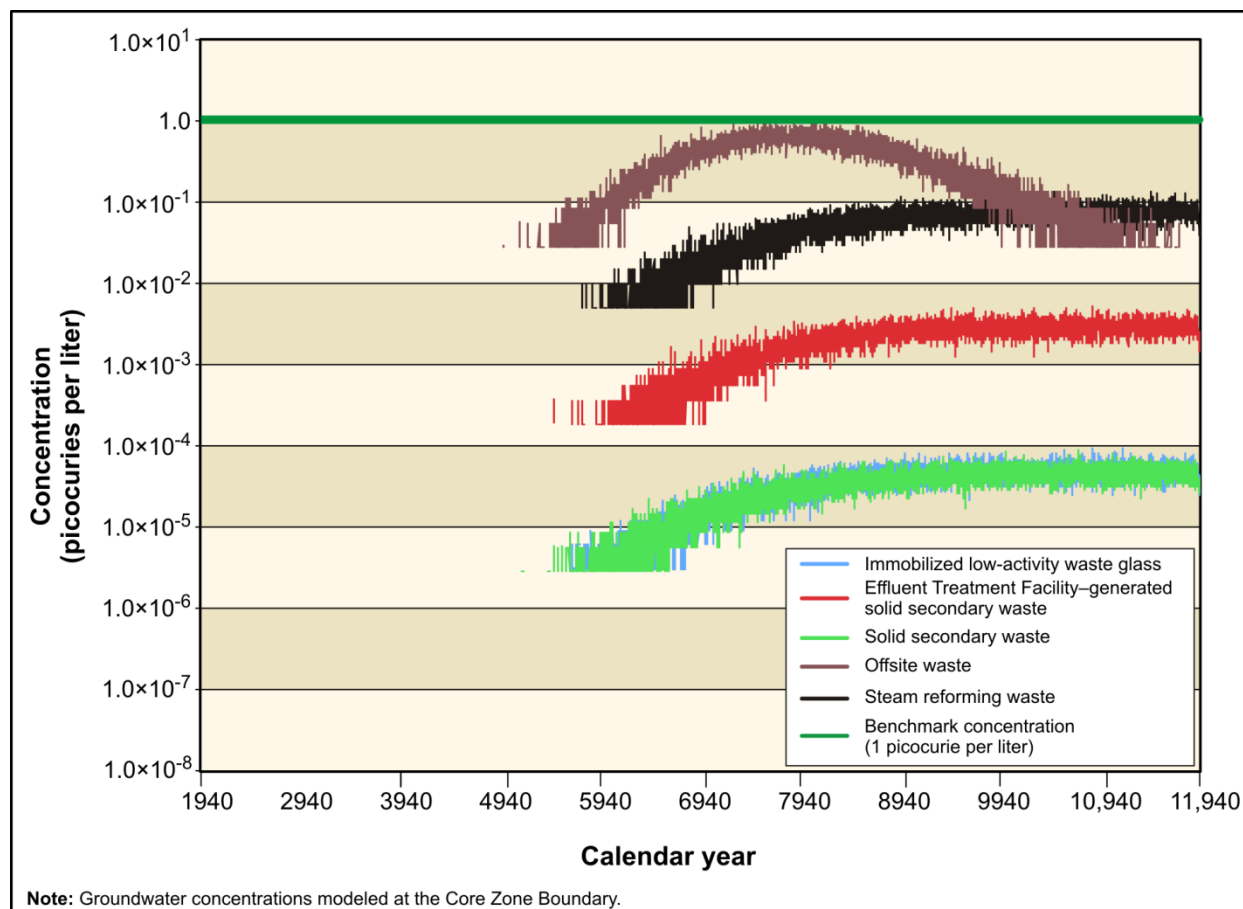**Note:** Groundwater concentrations modeled at the Core Zone Boundary.

**Figure M–153. Waste Management Alternative 2, Tank Closure Alternative 3B,
Groundwater Iodine-129 Concentrations at the Core Zone Boundary, Grout Sensitivity Case**

**Waste Management Alternative 2, Disposal Group 1, Subgroup 1-D, Addresses the Waste from
Tank Closure Alternative 3C**

Waste Management Alternative 2, Disposal Group 1, Subgroup 1-D, addresses the waste from Tank
Closure Alternative 3C, onsite non-CERCLA sources, FFTF decommissioning, waste management, and
other DOE sites. Waste forms for IDF-East include ILAW glass, LAW melters, steam reforming waste,
tank closure secondary waste, FFTF decommissioning secondary waste, waste management secondary
waste, offsite waste, and onsite non-CERCLA waste. Figures M–154 and M–155 indicate the
groundwater concentration at the Core Zone Boundary resulting from each of the waste forms under this
alternative. Groundwater concentrations predicted for LAW melters, FFTF decommissioning
secondary waste, waste management secondary waste, and onsite non-CERCLA waste are below
1.0×10^{-8} picocuries per liter at the Core Zone Boundary. The grouted waste forms under this alternative
are ETF-generated secondary waste and tank closure solid secondary waste. As indicated in
Figure M–155, the sensitivity case, the concentration of iodine-129 for the grouted waste forms in the
groundwater decreased by approximately two orders of magnitude relative to the EIS case.

Note: Groundwater concentrations modeled at the Core Zone Boundary.

Figure M–154. Waste Management Alternative 2, Tank Closure Alternative 3C, Groundwater Iodine-129 Concentrations at the Core Zone Boundary, EIS Performance

Figure M–155. Waste Management Alternative 2, Tank Closure Alternative 3C,
Groundwater Iodine-129 Concentrations at the Core Zone Boundary, Grout Sensitivity Case

Conclusions:

- The decrease in effective diffusion coefficient results in a lower flux of iodine-129 from grouted waste forms to the aquifer.

- The decrease in effective diffusion coefficient results in lower estimated groundwater concentrations.

- Similar results are projected for all alternatives.

M.5.7.6   Offsite Waste

DOE has taken the mitigating action of eliminating the INL remote-handled LLW resin waste from the inventory of offsite waste considered for disposal at Hanford in this *Final TC & WM EIS*. This single waste stream removes approximately 13 curies of iodine-129 (a reduction of almost 85 percent) and 438 curies of technetium-99 (a reduction of almost 25 percent) from the offsite inventory that was considered for disposal at Hanford in the *Draft TC & WM EIS*. With the removal of the INL remote-handled LLW resins, this *Final TC & WM EIS* considers the receipt of offsite waste containing 2.3 curies of iodine-129 and 1,460 curies of technetium-99.

The objective of this sensitivity analysis is to evaluate the potential contribution to predicted long-term groundwater impacts at Hanford that are attributed to varying inventories of offsite waste. The analysis evaluates Waste Management Alternative 2, Disposal Group 1, Subgroup 1-A, which addresses the waste resulting from Tank Closure Alternative 2B. The analysis evaluated the four cases of varying inventories of iodine-129 and technetium-99 in offsite waste described in Table M–62.

Table M–62. Offsite Waste Sensitivity Cases

| Offsite Sensitivity Case	Iodine-129 Inventory (curies)	Technetium-99 (curies)
Case A	0	0
Case B	1	500
Case C	2	1,000
Case D	3	1,500

Figures M–156 through M–159 report the predicted concentrations of iodine-129 in groundwater at the Core Zone Boundary and the Columbia River, with inventories ranging between 0 and 3 curies. Figures M–160 through M–163 report the predicted concentrations of technetium-99 in groundwater at the Core Zone Boundary and the Columbia River, with inventories ranging between 0 and 1,500 curies.
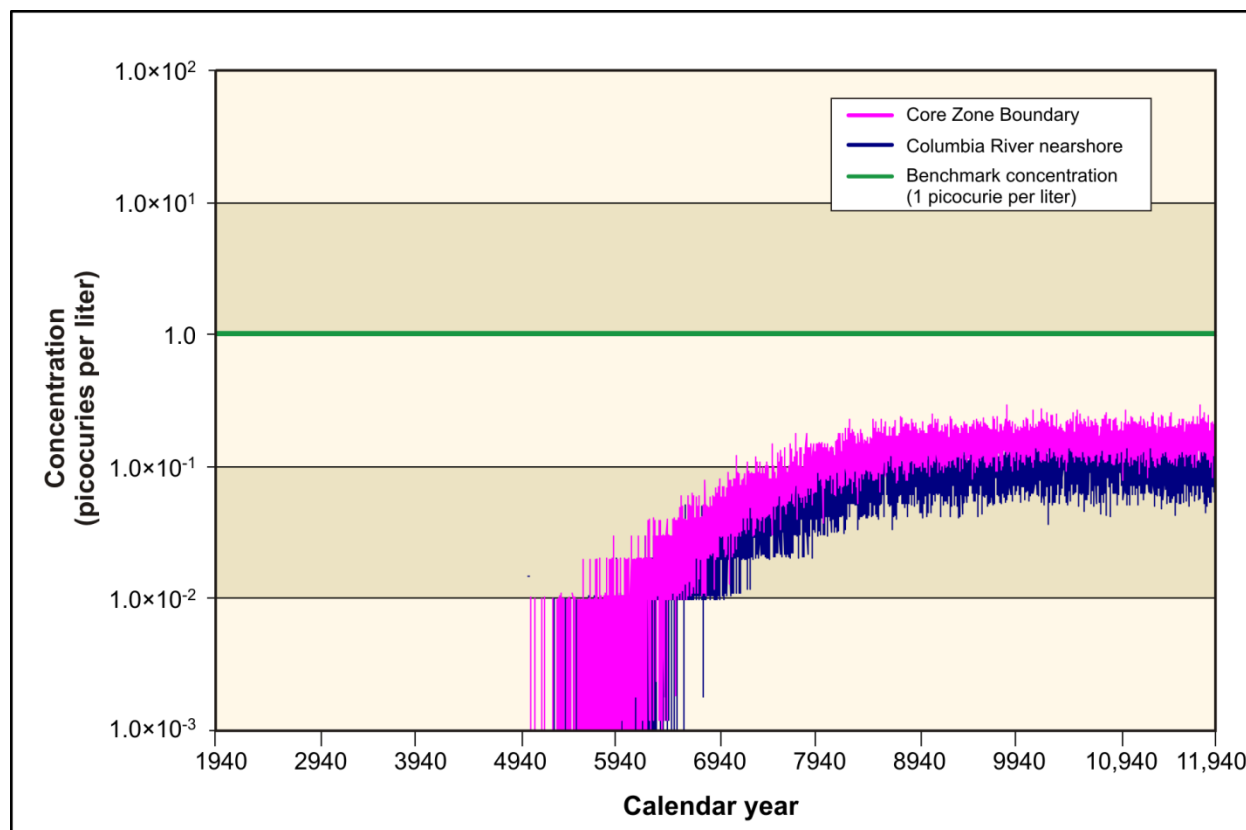
**Figure M–156. Tank Closure Alternative 2B,
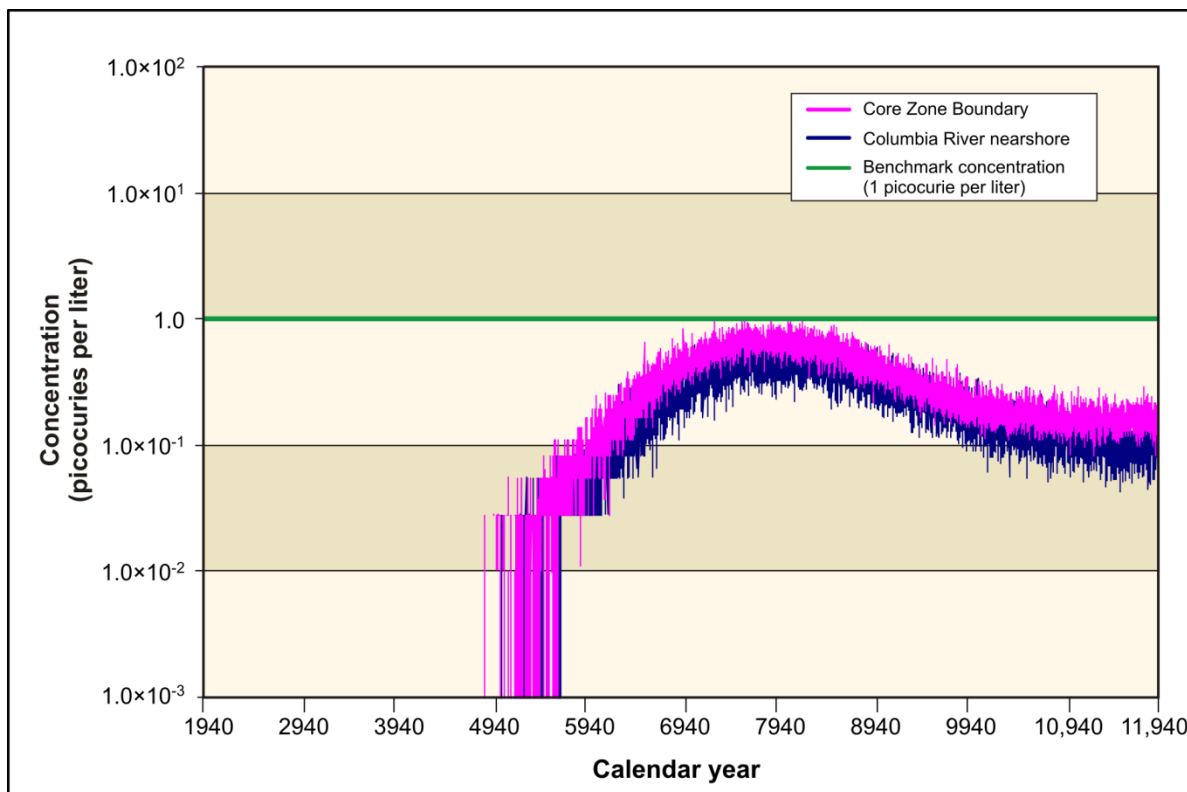Groundwater Iodine-129 Concentration Without Offsite Waste**
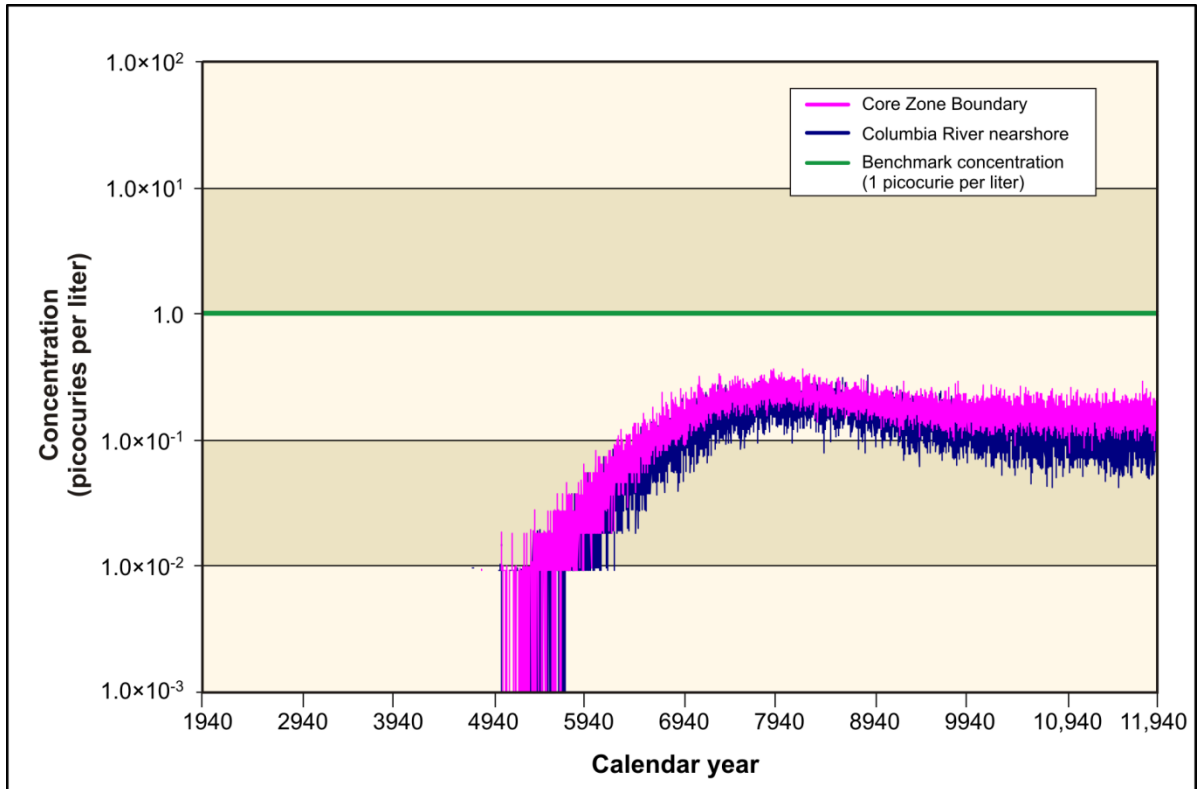
Figure M–157. Tank Closure Alternative 2B,
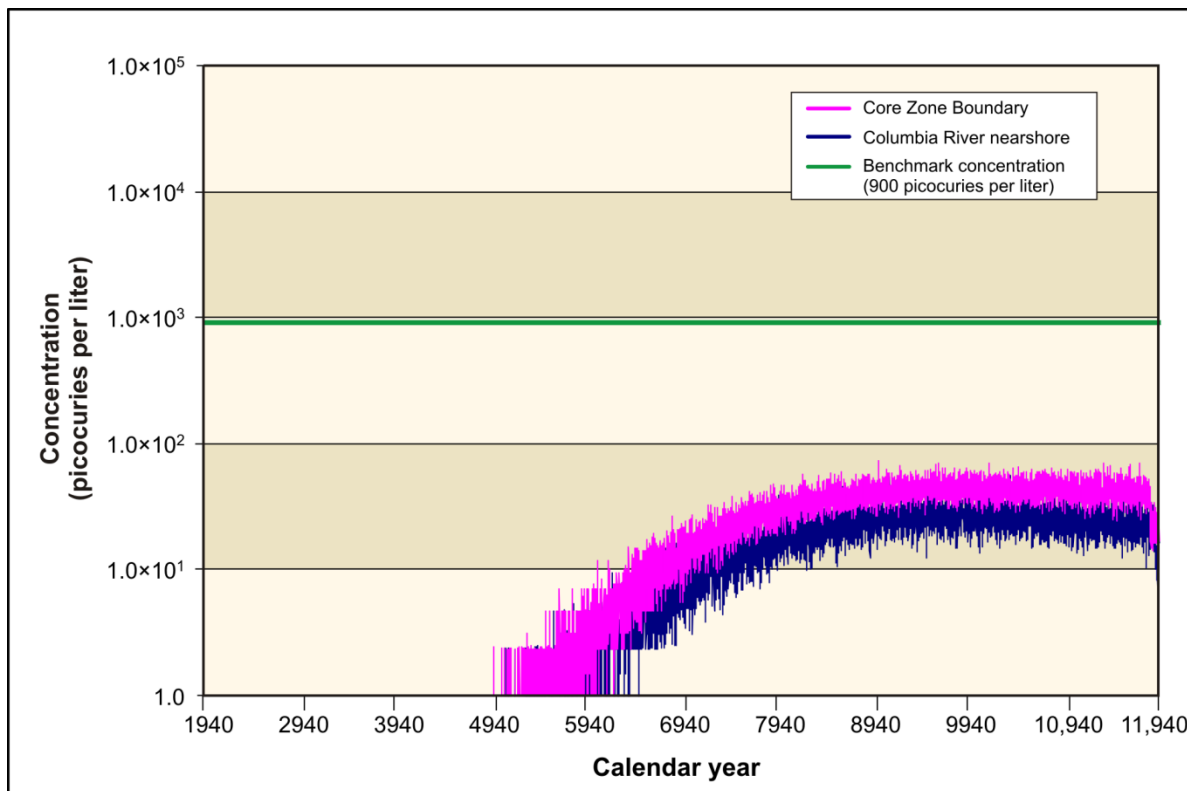**Groundwater Iodine-129 Concentration with 1 Curie of Iodine in Offsite Waste**
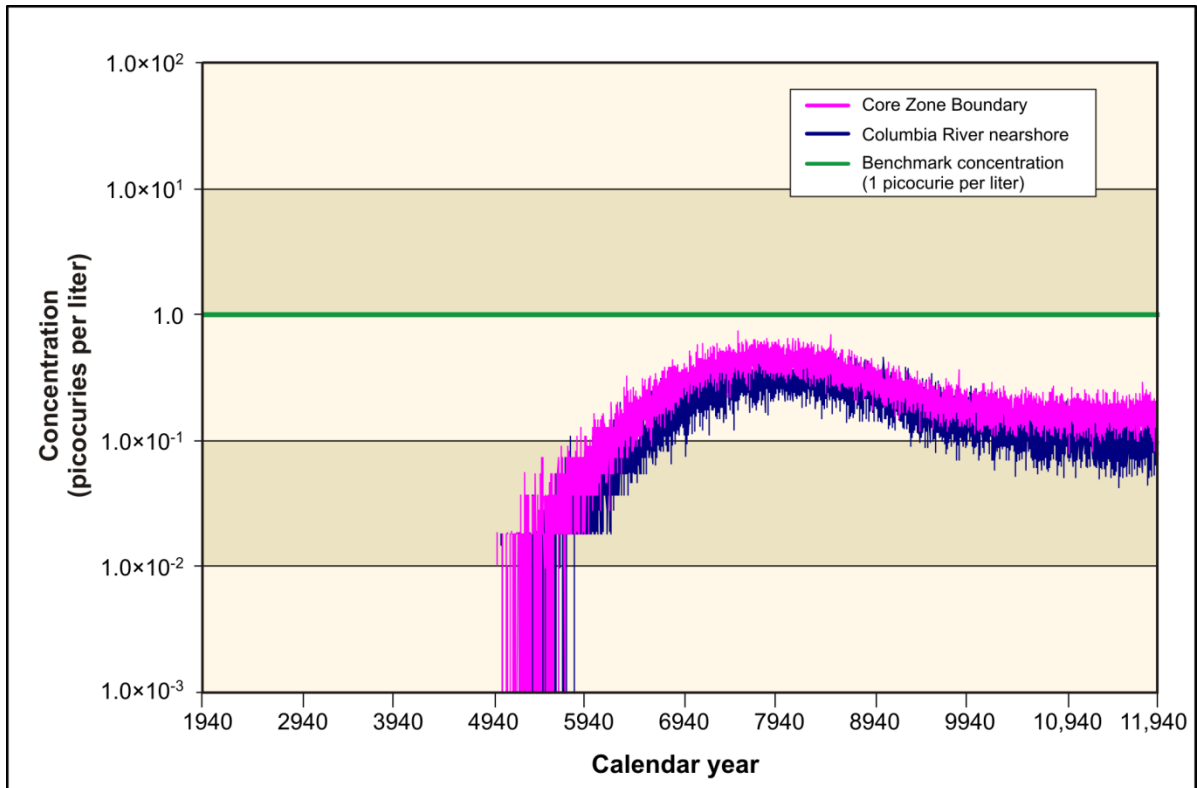
Figure M–158. Tank Closure Alternative 2B,
Groundwater Iodine-129 Concentration with 2 Curies of Iodine in Offsite Waste
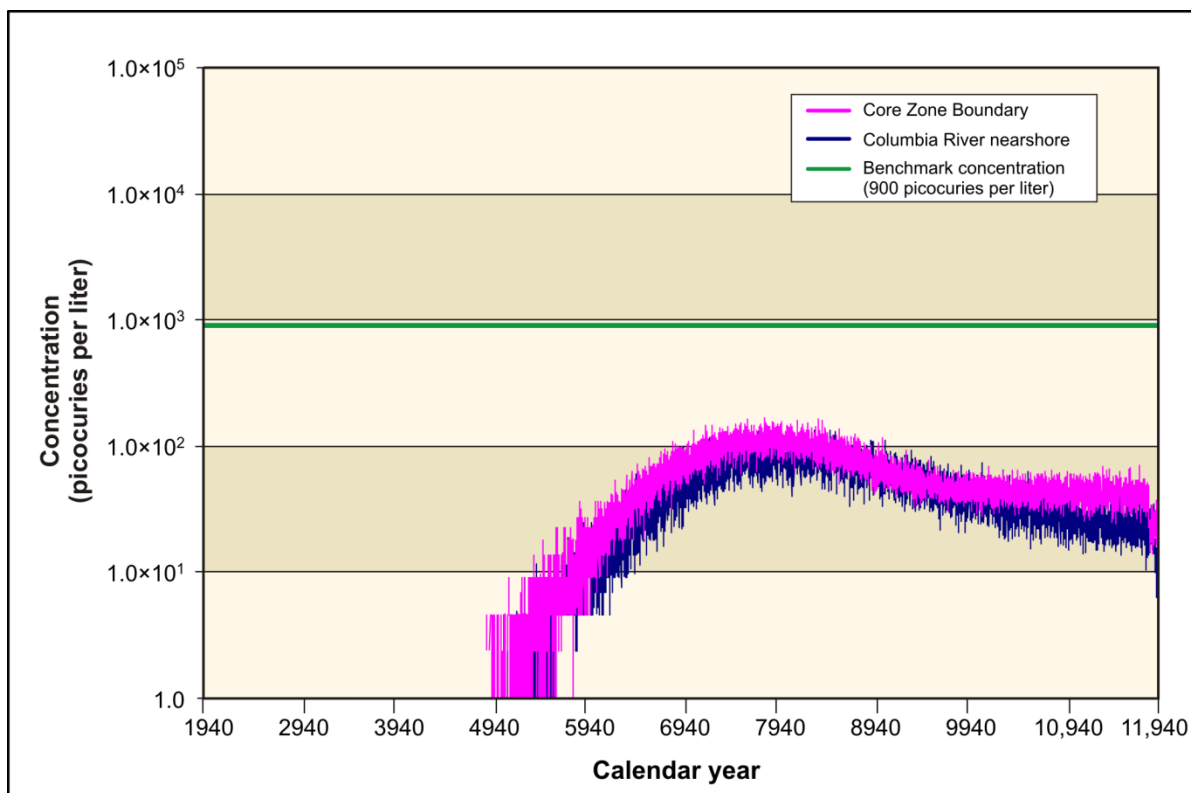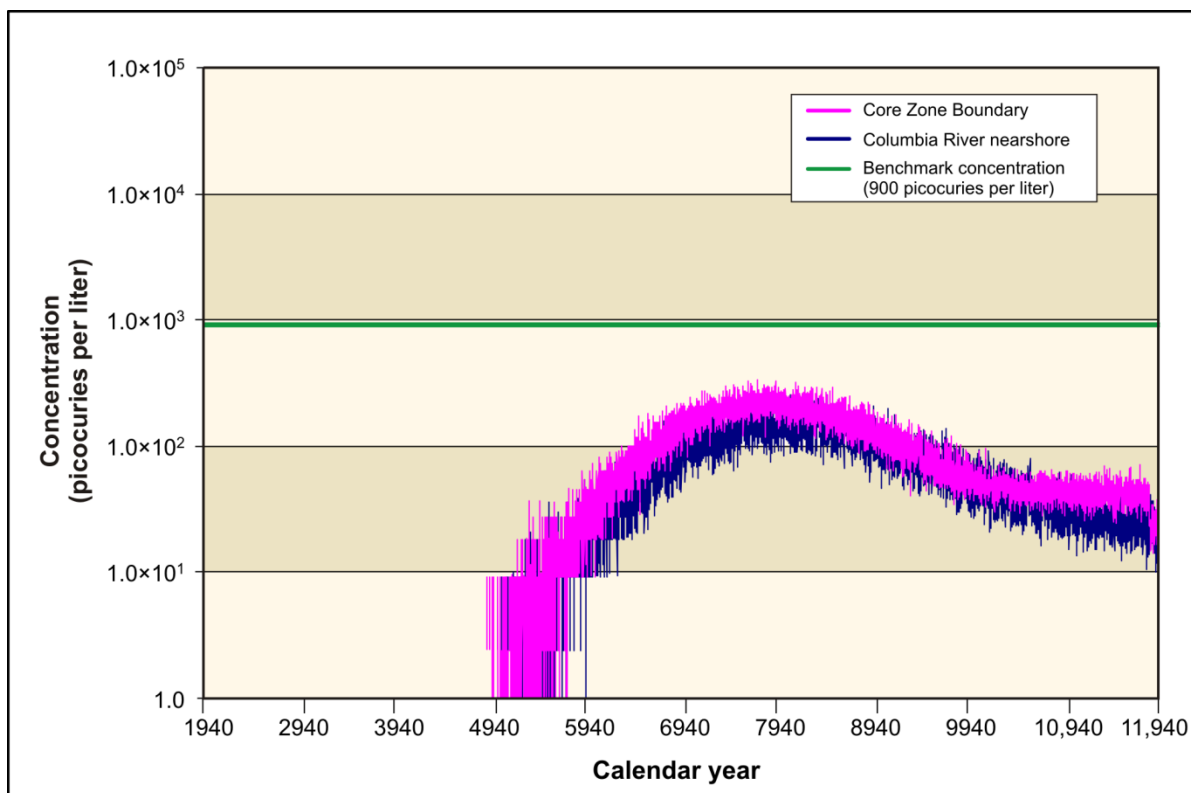
**Figure M–159. Tank Closure Alternative 2B,
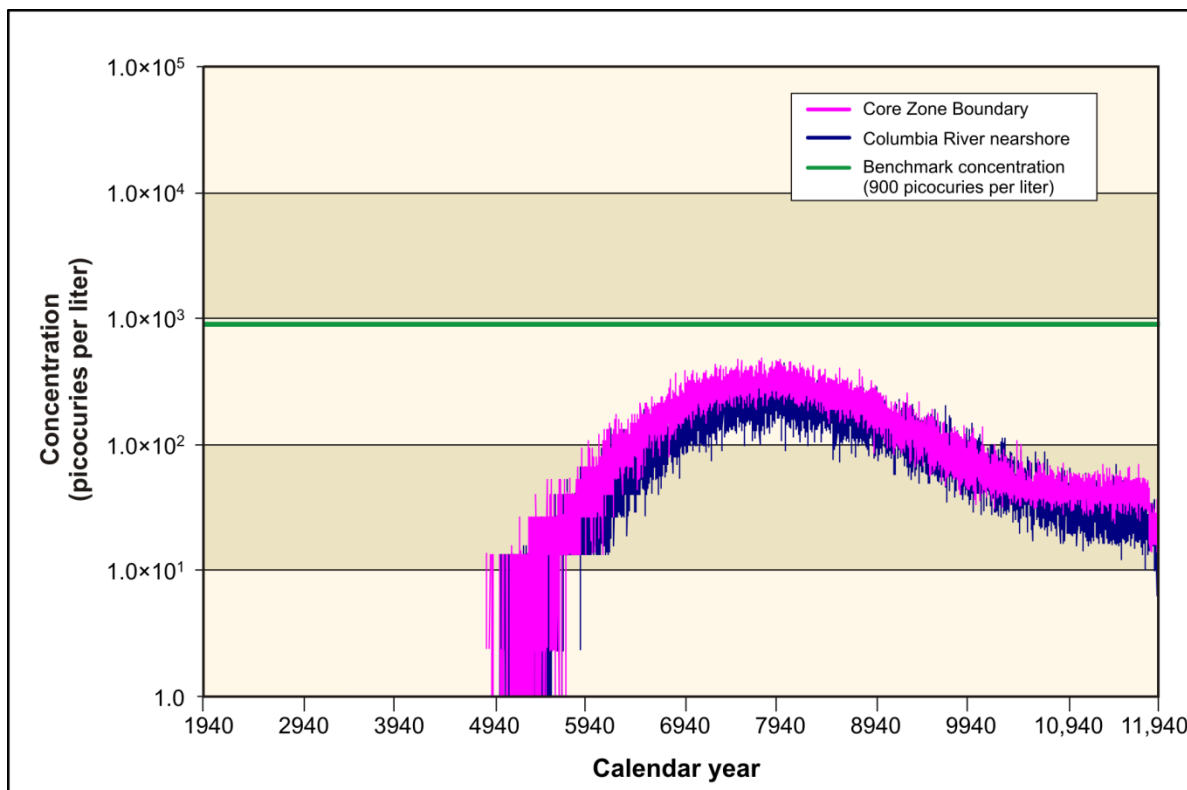Groundwater Iodine-129 Concentration with 3 Curies of Iodine in Offsite Waste**

**Figure M–160. Tank Closure Alternative 2B,
Groundwater Technetium-99 Concentration Without Offsite Waste**

Figure M–161. Tank Closure Alternative 2B,
Groundwater Technetium-99 Concentration with 500 Curies Offsite Waste

Figure M–162. Tank Closure Alternative 2B,
Groundwater Technetium-99 Concentration with 1,000 Curies Offsite Waste

**Figure M–163. Tank Closure Alternative 2B,
Groundwater Technetium-99 Concentration with 1,500 Curies Offsite Waste**

The predicted groundwater concentrations for the varying inventories of iodine-129 and technetium-99 show similar dependence on time, rate of recharge, and magnitude of inventory. The increase of inventory produces a proportional increase in concentration in the aquifer. The shape of the time-series of concentrations in Figures M–156 through M–163 is due to a combination of releases from six sources. Releases of technetium-99 and iodine-129 from offsite waste occur rapidly, and the inventory of these constituents from this source is depleted within approximately 2,000 years. This release accounts for the curved early maximum portion of the graph. The latter plateau extending out for a longer period of time is due to gradual releases from other waste forms (e.g., ILAW glass). A discussion regarding the method of calculating the maximum concentration at lines of analysis (such as the Columbia River nearshore) is provided in Appendix O, Section O.2.5.

M.6 REFERENCES

Anderson, J.D., 1990, *A History of the 200 Area Tank Farms*, WHC-MR-0132, Westinghouse Hanford Company, Richland, Washington, June.

Beyeler, W.E., W.A. Hareland, F.A. Durán, T.J. Brown, E. Kalinina, D.P. Gallegos, and P.A. Davis, 1999, *Residual Radioactive Contamination from Decommissioning, Parameter Analysis, Draft Report for Comment*, NUREG/CR-5512, Vol. 3, U.S. Nuclear Regulatory Commission, Washington, D.C., October.

Burandt, M., 2006, U.S. Department of Energy, Office of River Protection, Richland, Washington, personal communication (email) to L.B. Gannon, Science Applications International Corporation, Germantown, Maryland, (and others), "RE: BV Partioning (*sic:* Partitioning) Information," July 20.

CEES (Columbia Energy & Environmental Services, Inc.), 2010, *Evaluation of Fluidized Bed Steam Reforming Product Solubility and Dissolution*, RPP-RPT-47374, Rev. 0, Richland, Washington, September 8.

CH2M HILL (CH2M HILL Hanford Group, Inc.), 2002, *Field Investigation Report for Waste Management Area S-SX*, RPP-7884, Rev. 0, Richland, Washington, January 31.

DOE (U.S. Department of Energy), 2003a, *Environmental Impact Statement for Retrieval, Treatment, and Disposal of Tank Waste and Closure of Single-Shell Tanks at the Hanford Site, Richland, WA: Tank System Closure and Facility D&D Data Package*, DOE/ORP-2003-05, Rev. 0, Office of River Protection, Richland, Washington, April 17.

DOE (U.S. Department of Energy), 2003b, *Environmental Impact Statement for Retrieval, Treatment, and Disposal of Tank Waste and Closure of Single-Shell Tanks at the Hanford Site, Richland, WA: Inventory and Source Term Data Package*, DOE/ORP-2003-02, Rev. 0, Office of River Protection, Richland, Washington, April 17.

DOE (U.S. Department of Energy), 2003c, *Environmental Impact Statement for Retrieval, Treatment, and Disposal of Tank Waste and Closure of Single-Shell Tanks at the Hanford Site, Richland, WA: Waste Treatment and Supplemental Technology Data Package*, DOE/ORP-2003-07, Rev. 0, Office of River Protection, Richland, Washington, April 17.

DOE (U.S. Department of Energy), 2005, *Technical Guidance Document for Tank Closure Environmental Impact Statement Vadose Zone and Groundwater Revised Analyses*, Final Rev. 0, Office of River Protection, Richland, Washington, March 25.

Freeze, R.A., and J.A. Cherry, 1979, *Groundwater*, Prentice-Hall Inc., Englewood Cliffs, New Jersey.

Hanlon, B.M., 2003, *Waste Tank Summary Report for Month Ending August 31, 2003*, HNF-EP-0182, Rev. 185, CH2M HILL Hanford Group Inc., Richland, Washington, October.

Jantzen, C.M., 2006, *Fluidized Bed Steam Reformer (FBSR) Product: Monolith Formation and Characterization*, WSRC-STI-2006-00033, Rev. 0, Savannah River National Laboratory, Aiken, South Carolina, June.

Jones, T.E., B.C. Simpson, M.I. Wood, and R.A. Corbin, 2000, *Preliminary Inventory Estimates for Single-Shell Tank Leaks in T, TX, and TY Tank Farms*, RPP-7218, Rev. 0, CH2M HILL Hanford Group, Inc., Richland, Washington, November.

Jones, T.E., B.C. Simpson, M.I. Wood, and R.A. Corbin, 2001, *Preliminary Inventory Estimates for Single-Shell Tank Leaks in B, BX, and BY Tank Farms*, RPP-7389, Rev. 0, CH2M HILL Hanford Group, Inc., Richland, Washington, February.

Knepp, A.J., 2002, *Field Investigation Report for Waste Management Area B-BX-BY*, RPP-10098, Rev. 0, CH2M HILL Hanford Group, Inc., Richland, Washington, December 13.

Levenspiel, O., 1962, *Chemical Reaction Engineering*, John Wiley and Sons, Inc., New York, New York.

Lockrem, L.L., 2005, *Hanford Containerized Cast Stone Facility Task 1 – Process Testing and Development Final Test Report*, RPP-RPT-26742, Rev. 0, CH2M HILL Hanford Group, Inc., Richland, Washington, July 15.

Lorier, T.H., J.M. Pareizs, and C.M. Jantzen, 2005, *Single-Pass Flow Through (SPFT) Testing of Fluidized-Bed Steam Reforming (FBSR) Waste Forms*, WSRC-TR-2005-00124, Rev. 0, Savannah River National Laboratory, Aiken, South Carolina, August.

Mann, F.M., R.J. Puigh, R. Khaleel, S. Finfrock, B.P. McGrail, D.H. Bacon, and R.J. Serne, 2003, *Risk Assessment Supporting the Decision on the Initial Selection of Supplemental ILAW Technologies*, RPP-17675, Rev. 0, CH2M HILL Hanford Group, Inc., Richland, Washington, September 29.

Mason, B., and L.G. Berry, 1968, *Elements of Mineralogy*, W.H. Freeman and Co., San Francisco, California.

Mattigod, S.V., G.A. Whyatt, R.J. Serne, P.F. Martin, K.E. Schwab, and M.L. Wood, 2001, *Diffusion and Leaching of Selected Radionuclides (Iodine-129, Technetium-99, and Uranium) Through Category 3 Waste Encasement Concrete and Soil Fill Material*, PNNL-13639, Pacific Northwest National Laboratory, Richland, Washington, September.

McGrail, B.P., H.T. Schaef, P.F. Martin, D.H. Bacon, E.A. Rodriguez, D.E. McCready, A.N. Primak, and R.D. Orr, 2003a, *Initial Suitability Evaluation of Steam-Reformed Low Activity Waste for Direct Land Disposal*, WTP-RPT-097, Rev. 0, Bechtel National, Inc., Richland, Washington, January.

McGrail, B.P., E.M. Pierce, H.T. Schaef, E.A. Rodriguez, J.L. Steele, A.T. Owen, and D.M. Wellman, 2003b, *Laboratory Testing of Bulk Vitrified and Steam Reformed Low-Activity Waste Forms to Support a Preliminary Risk Assessment for an Integrated Disposal Facility*, PNNL-14414, Pacific Northwest National Laboratory, Richland, Washington, September.

Myers, D.A., 2005, *Field Investigation Report for Waste Management Areas T and TX-TY*, RPP-23752, Rev. 0, CH2M HILL Hanford Group, Inc., Richland, Washington, June.

NCRP (National Council on Radiation Protection and Measurements), 2005, *Performance Assessment of Near-Surface Facilities for Disposal of Low-Level Radioactive Waste*, NCRP Report No. 152, Bethesda, Maryland, December 31.

Olson, A.L., N.R. Soelberg, D.W. Marshall, and G.L. Anderson, 2004a, *Fluidized Bed Steam Reforming of Hanford LAW Using THOR^{sm} Mineralizing Technology*, INEEL/EXT-04-02492, Idaho National Engineering and Environmental Laboratory, Idaho Falls, Idaho, November.

Olson, A.L., N.R. Soelberg, D.W. Marshall, and G.L. Anderson, 2004b, *Fluidized Bed Steam Reforming of INEEL SBW Using THOR^{sm} Mineralizing Technology*, INEEL/EXT-04-02564, Idaho National Engineering and Environmental Laboratory, Idaho Falls, Idaho, December.

Parkhurst, D.L., and C.A.J. Appelo, 1999, *User's Guide to PHREEQC (Version 2) – A Computer Program for Speciation, Batch-Reaction, One-Dimensional Transport, and Inverse Geochemical Calculations*, Water-Resources Investigations Report 99-4259, U.S. Geological Survey, Denver, Colorado.

Pierce, E.M., B.P. McGrail, L.M. Bagaasen, E.A. Rodriguez, D.M. Wellman, K.N. Geiszler, S.R. Baum, L.R. Reed, J.V. Crum, and H.T. Schaef, 2005, *Laboratory Testing of Bulk Vitrified Low-Activity Waste Forms to Support the 2005 Integrated Disposal Facility Performance Assessment*, PNNL-15126, Rev. 1, Pacific Northwest National Laboratory, Richland, Washington, June.

Riley, R.G., and C.A. Lo Presti, 2004, *Release Data Package for the 2004 Composite Analysis*, PNNL-14760, Rev. 0, Pacific Northwest National Laboratory, Richland, Washington, August.

Sarkar, D., S. Chakrabarti, and B.K. Dutta, 2009, "Diffusion of Methylene Blue in Glass Fibers – Application of the Shrinking Core Model," *Applied Mathematical Modeling*, Vol. 33, pp. 2874–2881.

Sheppard, M.I., and D.H. Thibault, 1990, "Default Soil Solid/Liquid Partition Coefficients, K_ds, for Four Major Soil Types: A Compendium," *Health Physics*, Vol. 59, No. 4, pp. 471–482, October.

THORTT (THOR Treatment Technologies, LLC), 2002, *THOR^SM Steam Reforming Process for Hazardous and Radioactive Wastes, Technology Report*, TR-SR02-1, Rev. 1, Richland, Washington.

THORTT and WGI (THOR Treatment Technologies, LLC, and Washington Group International), 2006, *Pilot Plant Report for Treating Sodium-Bearing Waste Surrogates Carbonate Flowsheet*, RT-ESTD-PMR-001, Rev. 0, Denver, Colorado, October.

Tole, M.P., A.C. Lasaga, C. Pantano, and W.B. White, 1986, "The Kinetics of Dissolution of Nepheline $(NaAlSiO_4)$," *Geochimica et Cosmochimica Acta*, Vol. 50, pp. 379–392.

Weast, R.C., and S.M. Selby, eds., 1966, *CRC Handbook of Chemistry and Physics*, 47th ed., The Chemical Rubber Company, Cleveland, Ohio.

Weast, R.C., and S.M. Selby, eds., 1967, *CRC Handbook of Chemistry and Physics*, 48th ed., The Chemical Rubber Company, Cleveland, Ohio.

Whyatt, G.A., J.W. Shade, G.E. Stegen, 1996, *Volatility and Entrainment of Feed Components and Product Glass Characteristics During Pilot-Scale Vitrification of Simulated Hanford Site Low-Level Waste*, WHC-SA-3093-FP, Westinghouse Hanford Company, Richland, Washington, April.

Wood, M.I., and T.E. Jones, 2003, *Subsurface Conditions Description of the U Waste Management Areas*, RPP-15808, Rev. 0, CH2M HILL Hanford Group, Inc., Richland, Washington, April.

Wood, M.I., T.E. Jones, B.N. Bjornstad, D.G. Horton, S.M. Narbutovskih, and R. Schalla, 2003, *Subsurface Conditions Description of the C and A-AX Waste Management Areas*, RPP-14430, Rev. 0, CH2M HILL Hanford Group, Inc., Richland, Washington, April.

U.S. Department of Energy Manual

DOE Manual 435.1-1, *Radioactive Waste Management Manual*, Change 2, June 8, 2011.